



Novel methods for stereocontrolled cycloaddition/dearomatization reactions under catalytic conditions

Aitor Lacambra

► To cite this version:

Aitor Lacambra. Novel methods for stereocontrolled cycloaddition/dearomatization reactions under catalytic conditions. Organic chemistry. Université de Bordeaux, 2017. English. NNT : 2017BORD0576 . tel-02160811

HAL Id: tel-02160811

<https://theses.hal.science/tel-02160811>

Submitted on 20 Jun 2019

HAL is a multi-disciplinary open access archive for the deposit and dissemination of scientific research documents, whether they are published or not. The documents may come from teaching and research institutions in France or abroad, or from public or private research centers.

L'archive ouverte pluridisciplinaire **HAL**, est destinée au dépôt et à la diffusion de documents scientifiques de niveau recherche, publiés ou non, émanant des établissements d'enseignement et de recherche français ou étrangers, des laboratoires publics ou privés.

THÈSE EN COTUTELLE PRÉSENTÉE
POUR OBTENIR LE GRADE DE
DOCTEUR DE
L'UNIVERSITÉ DE BORDEAUX
ET DE L'UNIVERSITÉ DE PAYS BASQUE

ÉCOLE DOCTORALE SCIENCES CHIMIQUES
ÉCOLE DOCTORALE DU UNIVERSITÉ DU PAYS BASQUE
SPÉCIALITÉ CHIMIE ORGANIQUE

Par Aitor LACAMBRA

**NOVEL METHODS FOR STEREOCONTROLLED
CYCLOADDITION/DEAROMATIZATION REACTIONS
UNDER CATALYTIC CONDITIONS**

Sous la direction de Stéphane QUIDEAU (ISM, ORGA)
et de Fernando P. COSSÍO (UPV/EHU, Dept. Chimie Organique I)

Soutenue le 28/04/2017

Membres du jury :

M. AIZPURUA, Jesús María
Mme MIELGO, María Antonia
Mme. De la Torre, María del Carmen
M. BACEIREDO, J. Antoine
M. FREDERIC, Robert

Prof., University of the Basque Country	Président
Prof., University of the Basque Country	Examinateur
Dr., IQOG-CSIC	Examinateur
Dr., Université Paul Sabatier	Examinateur
Dr., Université de Bordeaux	Rapporteur

Titre : Nouvelle Methode pour des Réactions de Cycloaddition/Dearomatization Stéréocontrôlées sous Conditions Catalytiques

Résumé :

Les alcaloïdes sont, en général, une famille de composés hétérocycliques d'origine végétale qui intègrent des atomes d'azote dans leur structure complexe. Leur intérêt réside dans les activités biologiques intéressantes qu'ils présentent, et pour cette raison, ils sont largement utilisés par l'industrie pharmaceutique. En particulier, les anneaux de pyrrolidine et de pipéridine se trouvent comme base fondamentale dans un grand nombre de telles structures. D'autre part, l'un des principaux objectifs de la chimie synthétique est d'obtenir ces types de molécules d'une manière asymétrique. Entre autres, la catalyse métallique s'est révélée très utile à cet effet. Par exemple, les ligands de type ferrocényle précédemment développés dans notre groupe donnent naissance à des pyrrolidines énantio-purées densément substituées. De même, ces types de ligands ont été évalués dans différents types de réactions de cycloaddition, ce qui a entraîné la formation asymétrique de structures tricycliques d'intérêt biologique. D'autre part, une synthèse racémique collective de composés tétracycliques de la famille *Securinega* a été développée. Cette synthèse permet d'accéder à différents produits naturels de la famille en raison de la polyvalence de l'intermédiaire lactone bicyclique.

Mots clés : [3 minimum]

Produit Naturels, Ferrocényle Prolines, Réactions de Cycloaddition

Title : NOVEL METHODS FOR STEREOCONTROLLED CYCLOADDITION/DEAROMATIZATION REACTIONS UNDER CATALYTIC CONDITIONS

Abstract :

Alkaloids are, in general, a family of heterocyclic compounds of vegetal origin that incorporate nitrogen atoms in their complex structure. Their interest lies in the outstanding biological activities they present, and for this reason they are widely used by the pharmaceutical industry. In particular, pyrrolidine and piperidine rings are fundamental scaffolds found in a large number of such structures. On the other hand, one of the main objectives of synthetic chemistry is to obtain these types of molecules in an asymmetric way. Among others, metal catalysis has proven to be very useful for this purpose. For example, ferrocenyl proline ligands previously developed in our group gave rise to densely substituted enantiopure pyrrolidines. Likewise, these types of ligands have been evaluated in different types of cycloaddition reactions, which have resulted in the asymmetric formation of tricyclic structures of biological interest. In contrast, a collective racemic synthesis of tetracyclic compounds of the *Securinega* family has been developed. This synthesis provides an access to different natural products of the family due to the divergence given by a bicyclic lactone intermediate.

Keywords :

Natural Products, Ferrocenyl Prolines, Cycloaddition Reactions

Unité de recherche

ISM, UMR 5255 CNRS, ORGA, Talence (Université de Bordeaux)

Bâtiment Joxe Mari Korta, Departement de Chimie Organique I, Donostia/ San
Sebastian (Université du Pays Basque)



Unibertsitatea
Euskal Herriko Unibertsitatea
The University of the Basque Country

université
de BORDEAUX

Novel Methods for Stereocontrolled Cycloaddition/Dearomatization Reactions Under Catalytic Conditions

Doctoral Thesis

Aitor Lacambra Galain

Donostia-San Sebastián, 2017

ACKNOWLEDGEMENTS

First of all, I would like to thank *Fernando* and *Ana*, and *Stéphane* for giving me the opportunity to carry out my research in your groups. This three years and a half were intense and full of knowledge. Thank you *Philippe* because of the project of the *Securinega* alkaloids and for all the knowledge shared with me about Chemistry. *Ivan*, gracias por la paciencia y los conocimientos en técnicas organometálicas que has compartido conmigo.

I would like to thank my colleagues from Bordeaux for their help during my stay there, especially to *Antoine*, *Nicoletta* and *Richard* for their patience and great kindness. *Antoine*, I will always thank you for the help at the beginning and for all the support. *Nicoletta*, finally I can say that ``here comes the sun'', soon I will be in Italy visiting you, ti voglio bene. *Richard*, my mate, I appreciate you so much! You were a great lab mate and a better friend, thank you for helping me during my last days. Remember bro, we need to form our boy band when I visit you in London.

Shortly I would like to thank to everybody in IECB, starting from Huc team and Guichard group. I would like to thank particularly to *Christoph*, *Steph* and *Maïalen* at the beginning of my stay there. I will also remember moments with *Diane*, *Simon*, *Maëlle*, *Caro*, *Joan*, *Camille* and the other PhD students.

Pero los que personalmente han marcado la diferencia en el trabajo han sido dos personitas con un gran corazón. Gracias *Albano*, por todo. Por los dramas, por las cervezas, por las risas y por los llantos y gracias por ser esa personita que me daba conversación en esos pasillos a veces tan oscuros, te quiero mucho. Que voy a decir de mi Guichard (jajajajaj) favorita, *Anita*. Gracias por darme la vida en aquellos últimos meses, por mostrarme que cada uno tiene que ser como es. Por hacerme ver que nadie puede dictarnos el que hacer y por todo el marujeo. Siempre recordaré que *lo contrario de vivir es no arriesgarse*. Te quiero muchísimo.

Sois muchos los que he conocido en mi estancia en Burdeos. Entre los diferentes grupos, gracias a *Victor*, *Ignacio*, *Cata*, *Roberto* y *Julen* por ser parte de este grupo tan grande. *Ana* (Rosario), *Noe* (Sueca) y *Noelia* (Mostoles) no os imagináis lo especial que fue conocerlos y compartir experiencias tanto como emociones con vosotras (cumple de Hugo, *here comes the sun*). Gracias *Antonet* por ser tan buena persona, y gracias a *Ángela* (mi amol) por presentarnos. *Ángela*, fue intensa la experiencia durante la Eurocopa y triste tu despedida, siempre estarás en mi corazón. Gracias *Antonio* por ser mi maestro en Burdeos y por presentarme a gente como *Julián* y al grupo de Erasmus! Que experiencia con *Carlota*, *Arrate* y compañía. *Julián*, siempre tendrás un lugar en donde yo viva, creo que no he conocido persona más generosa que tú.

Aquí viene la parte más delicada, a mis tres amores. *Hugo*, me alegro tanto de haberte conocido...no te lo imaginas. A veces he sido muy duro contigo, pero es porque te quiero mucho. Siempre que necesites cualquier cosa allí estaré (beti nire bihotzean egongo zara). *Mikelon*, te quiero tanto, algún día te lo demostraré. Gracias por presentarme a tanta gente, por todas esas birras en el trou y por ser como eres.

Acknowledgements

He aprendido muchísimo de ti y Burdeos no hubiese sido igual sin ti. Y finalmente, mi pichilla, mi otra mitad, mi cómplice. Gracias *Mario* por existir, por ser pura ternura, sensibilidad y demostrarme que se pueden hacer cosas increíbles con la voz y una guitarra. Nunca podré agradecerte lo suficiente aquel *entre la espada y la pared* que me dedicaste, ni el hecho de que me trajeras hasta Donostia desde Burdeos. Desde el primer día supe que eres alguien que quiero en mi vida para siempre.

Por otro lado, esa cuadrilla de Burdeos!!! *Ana Sevilla*, gracias por tu gracia! *María* (manchega) gracias por acercarme más a Hugo y por ser tan sensible y especial. *Enea* ta *Maria*, asko maite zaituztet, ea azkar ikusten garen! *Ane*, I really, really, really...jajaja (gracias por todos los consejos de cotutela). Y que voy a decir de mi grupo de hombres! Ese *Pablo*, *Xabi* y *Sufi*, increíbles experiencias, birras y risas. Nunca podré olvidar los ataques de risas provocadas por nuestras propias risas. *Sufi*, nunca te perdonaré aquel abandono cuando llevaba la maleta, jajajaja. Fuera coñas has sido una de las mejores cosas que me han pasado en Burdeos. Siempre fiel, riéndote de mí pero a la vez apoyándome incondicionalmente. Eres un crack, siempre tendrás un amigo en mí, y un apoyo incondicional. Gracias por creer en mí antes de que yo lo hiciera.

Marta, *Agustín*, *Ana* y *Ester* me lo pase pipa con vosotros de picnics, ojala hubiésemos tenido más tiempo para coincidir todos. *Ana*, fuiste un gran apoyo al principio de mi etapa en Burdeos, llegué destrozado por razones personales y aun así hacías que me meara de risa. Estoy seguro que eres una gran madre y eres una excelente persona. *Marta*, tú y yo tendremos siempre una conexión por ser los pringados de la cotutela. Gracias por escucharme, ayudarme y explicarme cuando no entendía algo. Dentro de todos estos problemas de cotutelados entre dos universidades, quisiera agradecer a los CONFUSION. *Olaia*, *Ane*, *Ana*, *Ainara*, *Oihana* y *Marta*, estaremos siempre marcados a fuego con la maldita burocracia francesa pero siempre saldremos adelante juntos, os quiero chicas.

I would like to thank my Czech people, *Ondřej*, *Kateřina* and *Marketa* for making me feel so loved by you three. Děkuji! Thank you very much *Andreas* for being the perfect flatmate. If it was not for you I do not know if I would have handled the situation. En los 18 meses de estancia en Burdeos conocí muchísima gente y solo he podido nombrar por encima a muchas personas. Gracias a *Dominik*, *Boris*, *Hugo* (Madrid), *Jerôme*...gente increíble que he conocido y que aprecio, merci a tous.

Ioritz, eskerrik asko beti hor egotegatik. Naiz eta 11 urteko adiskidetasuna izan, beti zaude prest entzuteko eta gomendioak emateko. Agian ezagutzen dudana pertsonarik onena zara, eta bakarra etorri zaidana bisitan hainbeste aldiz. Barkatu batzutan ez badizut nahikoa baloratu. Baino bukaeran, piraten errege izango gara!

Erkuden, *Asier*, *Heidi*, *Iñaki*, *Joel*, *Kintano*, *Dani*, *Ainhoa*, gracias por siempre ponerme una sonrisa y acogerme como uno más. Iker, ze in dit nik hiri!!! *Peronie*, musika asko egin behar dugu batera e! Eskerrik asko abestera animatzegatik.

Ainhoa (lilu) te quiero mucho. Sé que no nos vemos tanto pero me parece que tienes tanta bondad dentro de ti que siempre me mantendré como amigo y puedes

Acknowledgements

contar conmigo para lo que necesites. Eres mi peluquera favorita y eso no cambiará nunca.

Roxi, gracias por estar ahí, por apoyarme cuando más bajo estuve por saber sacarme cuando lo necesitaba, te quiero loca. Gracias a ti también *Silvia* por ser una de mis personas favoritas en Donostia. *María* (marmota) hace mucho que no quedamos pero no me olvido de todas esas salidas nocturnas y conversaciones profundas. *Maialen* (Lujambio) gracias por ser un amor de persona siempre que me has visto y por darme tan buena energía. Gracias *Martin* por apoyarme en esta última etapa de mi vida.

Eskerrik asko unibertsitateko koadrilari: *Xabi*, *Garazi*, *Unai*, *Lore*, *Iñaki* eta *Maddalen*. Gogo asko dauzkat berriz denak batera egoteko eta oso ondo pasatzeko. A parte quisiera agradecer a toda esa gente que me ha hecho el día a día más agradable, la gente de Polymat, los técnicos de SGiker y sobre todo las que para mí son unas de las personas más importantes: las limpiadoras. Gracias *Arancha* por todas las conversaciones durante las comidas que hacían todo más ameno. Muchísimas gracias *Celsi* por ser una de las mejores personas que me he encontrado en estos cuatro últimos años, nunca cambies y te deseo lo mejor.

También agradecer a mi grupo de laboratorio en Donostia por el apoyo que he recibido, sobretudo en la recta final. Muchas gracias *Iosune* por ayudarme con el francés cuando lo he necesitado y gracias *Abel* tu ayuda con los cálculos. En especial agradecer a *Miquel*, por la conversaciones que me han ayudado a ver todas las perspectivas posibles y racionalizar mis decisiones. Gracias *Tamara* por la ayuda en el laboratorio, y compartir tus conocimientos conmigo. También agradecer las experiencias vividas con *Aitziber*, *Xabi*, *Arkaitz*, *Zaira*, *Nerea* y *Elena*.

Pero sin duda las personitas que más se merecen mis agradecimientos son aquellos que han compartido el día a día conmigo. *Javi*, muchas gracias por hacerme reír aunque a la vez te estabas metiendo conmigo, y por escucharme en algunos momentos difíciles. Eskerrik asko *Mikel* laguntzagatik eta batzutan nire ideiak kontrajartzegatik, pentsarazten utzi nauzu askotan, ze badakigu egiak ez direla absolutoak.

Maddalen, eskerrik asko denagatik, irrifarregatik, bazkari guztiengatik, konbertsazioengatik, Gaztelo guztiengatik, noblezia momentuengatik, eta zure originaltasun eta inozentziagatik. Badakizu hemen lagun bat daukazula bizi guztirako, eta zu zarela hurrengoa, oso gutxi falta da! Askok maite zaitut, asko poztzen naiz esperientzia hau zurekin pasa izana eta barkamena eskatzen dizut gaizki sentiarazi dizudan momentuengatik, Enantioma (te lo dice Pita)...ajajaja.

Por último, quería agradecer a toda mi familia en general. *Eli* gracias por ser lo más especial cuando vuelvo a casa, siempre te voy a querer como si fueras un hermana/hija. Gracias *Ainara* por demostrarme que hay que luchar por lo que uno quiere hacer, estoy muy orgulloso de que seas mi hermana, te quiero. Ama, no puedo decirte nada más que gracias. Gracias por estar ahí siempre, por llevar adelante la familia, y por seguir con nosotros cada día aunque no estemos en el mismo lugar. Si no fuera por ti no estaría donde estoy, y nunca podré agradecerte todas las

Acknowledgements

conversaciones y apoyo incondicional que me has dado. Te quiero. Y pase lo que pase siempre te voy a querer.

A modo de reflexión, quisiera decir que cada persona que ha pasado en mi vida me ha dejado una parte de ella. Gracias a esa gente que ha hecho de esta experiencia maravillosa, y son la razón de que me mantenga en pie a día de hoy. Por todo eso, gracias, un gracias eterno.

This thesis dissertation was carried out in the framework of collaboration between the University of the Basque Country and the Université de Bordeaux, under the supervision of Prof. Fernando P. Cossío and Prof. Stéphane Quideau, respectively.

The numbering of the tables, figures, schemes and references on this manuscript are independent for each chapter. In addition, the numbering of molecules is written in Roman numerals for the first Introduction Chapter. On the contrary, molecule numbering within the content of Chapter two and Chapter three is written consecutively in Arabic numerals.

TABLE OF CONTENTS

Spanish Summary	1
French Summary	7
Acronyms and Abbreviations	13

1. Introduction 17

1.1 Chirality.....	19
1.2 Strategies for the obtention of enantiomerically pure compounds (EPC).....	20
1.2.1 Resolution of racemates	20
1.2.2 <i>Chiral Pool</i>	21
1.2.3 Asymmetric Synthesis.....	21
1.2.3.1 Chiral Auxiliaries and chiral reagents.....	21
1.2.3.2 Asymmetric catalysis	21
1.3 Chiral ligands in organometallic catalysis.....	23
1.3.1 Bidentate ligands including C_2 symmetry	23
1.3.2 Bidentate ligands presenting absence of C_2 symmetry.....	24
1.3.3 Chiral ligands containing a ferrocene structure	25
1.4 Nitrogen Containing Heteromolecules.....	27
1.4.1 Pyrrolidine and Piperidine scaffolds	27
1.4.2 <i>Securinega</i> alkaloids	30
1.4.2.1 <i>Securinega</i> alkaloids: structural classification	31
1.4.2.2 Occurrence and biological activity of <i>Securinega</i> alkaloids.....	34
1.4.2.3 Biosynthesis of <i>Securinega</i> alkaloids.....	38
1.5 Cannabinoid receptors and Cannabinoid ligands	40

2. Synthesis of Tricyclic Molecules by Ferrocenyl-Proline Catalyzed Enantioselective (2+1) and (3+2) Cycloaddition

Reactions	45
2.1 Cycloaddition reactions	47
2.1.1 (2+1) Cycloaddition Reactions	49
2.1.1.1 Importance of cyclopropanes in nature and chemistry	49
2.1.2.2 Metal catalyzed cyclopropanation reactions between alkenes and diazocompounds	50
2.1.2.3 Chiral ligands and transition metals in enantioselective cyclopropanation	52
2.1.2 1,3-Dipolar Cycloaddition Reactions.....	58
2.1.2.1 Azomethine ylides in 1,3-dipolar cycloadditions	59
2.1.3 Asymmetric 1,3-dipolar cycloadditions of azomethine ylides	61
2.1.3.1 Diastereoselective reactions	61
2.1.3.2 Enantioselective 1,3-dipolar cycloaddition reactions	62
2.2 Objectives	70
2.3 Novel Ferrocenyl-proline ligand derivatives.....	71
2.4 (2+1) cycloaddition reactions catalyzed by ferrocenyl proline ligands and transition metals	74
2.5 Ferrocenyl-proline ligand catalyzed intramolecular (3+2) cycloaddition reactions.....	79
2.5.1 Synthesis of the precursor for the access to tricyclic compounds	79
2.5.2 Intramolecular enantioselective (3+2) cycloaddition reaction and proposed reaction mechanism.....	80
2.5.3 Optimization of enantioselective intramolecular reaction conditions	82
2.6 Intermolecular enantioselective (3+2) cycloadditions catalyzed by ferrocenyl-proline ligands and transition metals.....	85
2.6.1 Synthesis of 3-nitrochromene and optimization of reaction conditions	85
2.6.2 Relative and absolute configuration of diastereoisomers.....	87
2.6.3 Synthesis of α-iminoesters 88a-i and aryl chromene derivative 135.....	90
2.6.4 Scope of the reaction: chromeno[3,4-c]pyrrolidine derivatives.....	91
2.6.5 Cannabinoid receptor affinity of chromeno[3,4-c]pyrrolidines	93

2.6.6 Preliminary experimental and computational studies on the configuration of chromene stereogenic center for 130 and 130' cycloadducts.....	95
2.7 Conclusions	99
2.8 Experimental part.....	100
3. Total Synthesis of <i>Securinega</i> alkaloids	137
3.1. Organocatalysis	139
3.1.1 Covalent activation.....	139
3.1.1.1 Enamine catalysis.....	140
3.1.1.2 Catalysis via ion iminium.....	141
3.1.2 Non-Covalent activation	142
3.1.2.1 Thiourea catalysts.....	143
3.1.2.2 Phosphoric acid catalysts	143
3.1.2 Enantioselective oxa-Michael reactions.....	144
3.1.4 Enantioselective desymmetrization reactions	149
3.2 Precedents in the total synthesis of <i>Securinega</i> alkaloids	153
3.3 Hypervalent iodine reagents and enantioselective oxidative dearomatization reactions	161
3.3.1 Chiral hypervalent iodine reagents	162
3.3.2 Dearomatization reactions.....	163
3.4 Objectives	170
3.5 Retrosynthetic analysis of <i>Securinega</i> natural products	171
3.6 Total Synthesis of <i>Securinega</i> Alkaloids	172
3.6.1 Racemic synthesis of lactone intermediate 328	172
3.6.2 Asymmetric direct approach through oxa-Michael desymmetrization	176
3.6.3 Asymmetric alternative strategy in oxa-Michael desymmetrization	180
3.6.4 Development of Aldol reaction and Swern oxidation.....	188
3.6.5 Synthesis of neosecurinine-type natural products	191

3.6.6 Synthesis of neonorsecurinine-type natural products	195
3.7 Synthesis of Ferrocenyl Iodanes and their applications.....	200
3.8 Conclusions	206
3.9 Experimental Part	207

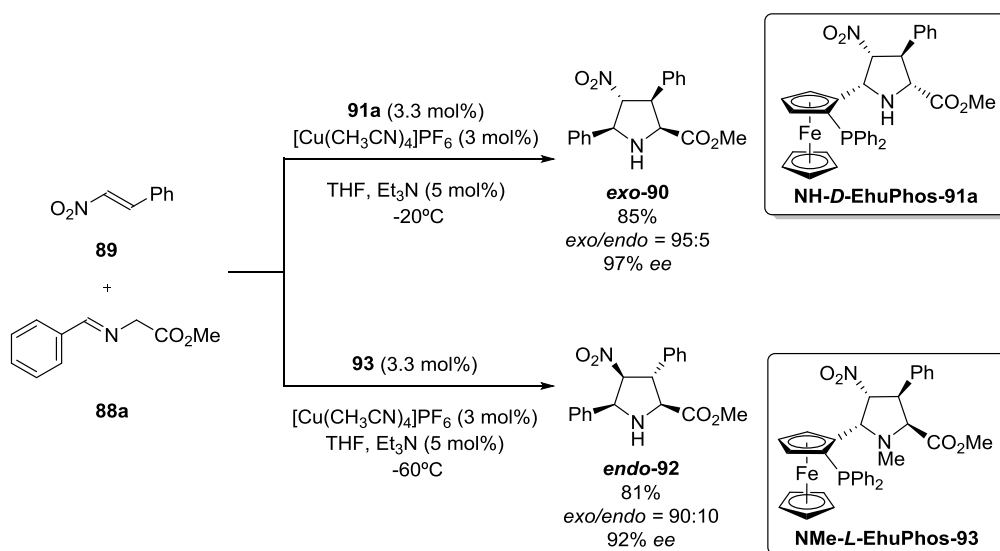
ANNEXES 241

ANNEX I. ^1H NMR and ^{13}C NMR Spectra of Chapter 2.....	243
ANNEX II. ^1H NMR and ^{13}C NMR Spectra of Chapter 3.....	268
ANNEX III. X-ray analysis	286

Los alcaloides constituyen una importante familia de compuestos de origen natural que poseen, entre otros, átomos de nitrógeno en su esqueleto hidrocarbonado. Muchos de los componentes de esta extensa familia se han empleado por la industria farmacéutica debido a sus excelentes propiedades y características, siendo utilizados en campos tan diversos como la lucha contra la malaria, analgésicos, sedantes e incluso como agentes anticancerígenos. Un elevado porcentaje de estas moléculas poseen anillos o unidades de pirrolidina o piperidina como base fundamental de su estructura. Un ejemplo lo constituyen los alcaloides de la familia *Securinega* (pertenecientes a la familia Euphorbiaceae), los cuales se han empleado para el tratamiento de enfermedades tales como la poliomielitis o la esclerosis lateral amiotrófica, entre otras.

Uno de los principales objetivos de la química sintética es el de intentar sintetizar compuestos naturales como los descritos anteriormente. En las últimas décadas, la catálisis organometálica ha demostrado ser una poderosa y versátil herramienta para lograr tal objetivo, utilizando para ello una gran variedad de complejos organometálicos. En concreto, los ligandos tipo ferrocenilo han demostrado una gran versatilidad como catalizadores en reacciones asimétricas.

Nuestro grupo de investigación tiene una amplia experiencia en el ámbito de ligandos ferrocenilo, habiendo sintetizado los ligandos de ferrocenil prolina **NH-D-EhuPhos-91a** y **NMe-L-EhuPhos-93**. Estos compuestos han resultado ser eficientes en reacciones de cicloadición (3+2) entre α -iminoésteres y nitroalquenos para generar los cicloaductos **exo-90** y **endo-92** con excelentes excesos enantioméricos (ver **Esquema 1**). De este modo, se han sintetizado derivados de prolina no-naturales densamente sustituidas con un elevado enantiocontrol.



Esquema 1. Síntesis enantioselectiva de los cicloaductos **endo-92** y **exo-90** mediante el empleo de los ligandos ferrocenil prolina **93** y **91a**.

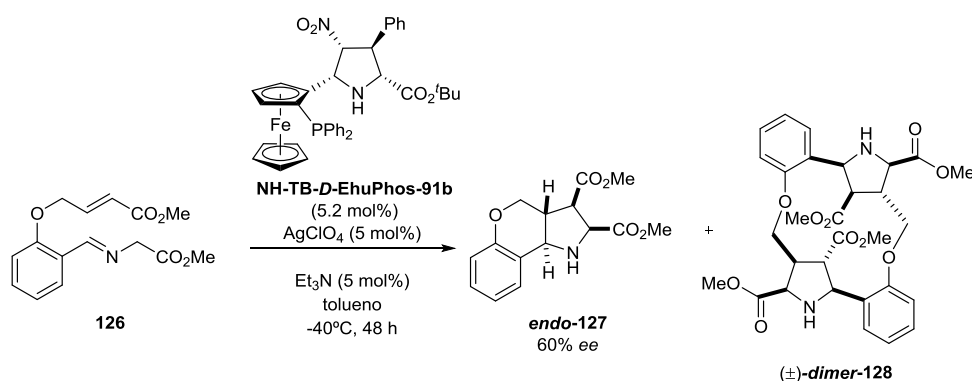
Resumen de la Tesis Doctoral

En vista de estos resultados, en el segundo capítulo de esta tesis se ha ampliado la familia de ligandos tipo ferrocenil prolina realizando variaciones estructurales frente a los ligandos previamente descritos. Adicionalmente, se ha llevado a cabo la preparación de los correspondientes complejos de Au(I).

Las reacciones de cicloadición representan una ruta versátil para la síntesis de compuestos cíclicos con un alto grado de estereoselectividad. Por ello, se planteó como objetivo principal de este segundo capítulo la evaluación de la versatilidad de los ligandos y complejos de tipo ferrocenil pirrolidina en reacciones de cicloadición (2+1) y en reacciones inter- e intramoleculares de cicloadición (3+2) enantioselectivas.

Las reacciones de cicloadición (2+1) dan lugar principalmente a ciclopropanos que pueden ser empleados como *building blocks* en la síntesis de productos naturales, y además pueden presentar diversas aplicaciones farmacéuticas. Dentro de la síntesis de ciclopropanos, la estrategia más utilizada ha sido la reacción entre alquenos y diazocompuestos catalizada por metales de transición. Los ligandos de tipo ferrocenilo **NH-D-EhuPhos-91a** y **NMe-L-EhuPhos-93** fueron utilizados en combinación con una variedad de sales metálicas en la reacción entre los diazo compuestos (EDA y MEDA) y alquenos heterocíclicos (tales como indeno o 2.3-benzofurano). Aunque el uso de sales de rodio(II) produjese únicamente la síntesis de *trans*-ciclopropanos solo se pudieron obtener los productos racémicos.

Por otro lado, el interés para sintetizar de compuestos tricíclicos que contienen un anillo pirrolidina unido a un cromeno nos condujo a la evaluación de nuestros ligandos en reacciones intramoleculares de cicloadición (3+2) enantioselectiva. Las estructuras de tipo cromeno[4,3-*b*]pirrol constituyen un objetivo particularmente interesante debido a sus propiedades biológicas. Por ello, la reacción intramolecular de la imina **126** fue evaluada en diferentes condiciones de reacción, observándose un exceso enantiomérico máximo de un 60% para el producto **endo-127** cuando se empleó el ligando **NH-TB-D-EhuPhos-91b** en combinación con la sal AgClO_4 bajo las condiciones descritas en el **Esquema 2**. La libertad conformacional que presenta la imina **126** puede explicar la presencia del **dimero-121** al producirse un procesos competitivo ente una cicloadición de tipo intramolecular o intermolecular.

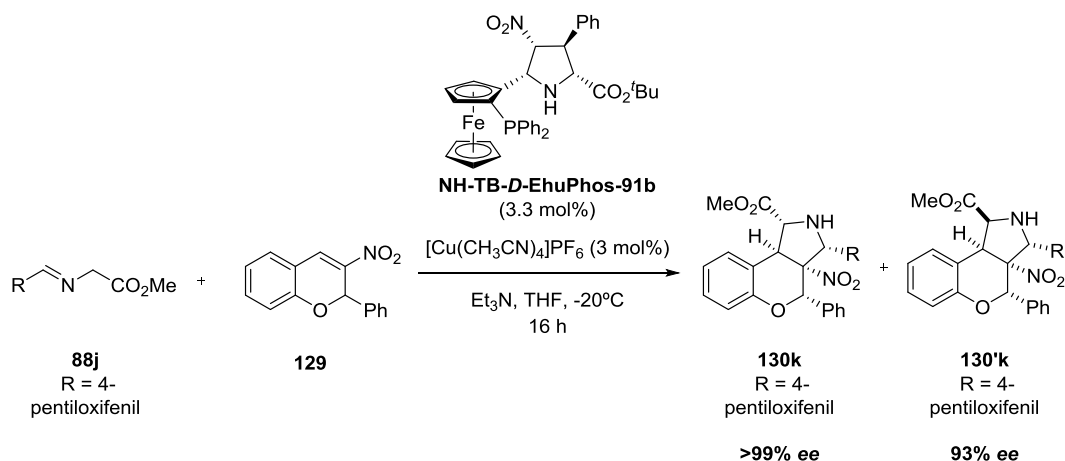


Esquema 2. Reacción de cicloadición intramolecular (3+2) enantioselectiva que permite las síntesis de los productos **endo-127** y **dimero-128**.

En vista de los resultados obtenidos para la versión intramolecular, se diseñó una nueva estrategia para la síntesis asimétrica de compuestos tricíclicos que

incorporan una estructura tipo cromenopirrolidina. De este modo, el empleo como dipolarófilo del compuesto 3-nitro-2*H*-cromeno-**129** en la reacción intermolecular de cicloadición (3+2) enantioselectiva con diferentes α -iminoésteres dio lugar en presencia del ligando **NH-TB-D-EhuPhos-91b** a los cromeno[3,4-*c*]pirrolidinas **130** y **130'** con un elevado enantiocontrol (hasta 97% ee). La configuración absoluta para los compuestos enantiopuros se estudio mediante el análisis por difracción de rayos-X de los cristales correspondientes. Además, se demostró el alcance de la reacción mediante variaciones estructurales generando así compuestos con excelentes valores de ee.

Dado que los compuestos sintetizados **130** y **130'** guardan cierta analogía con los cromenopirazoles desarrollados por Jagerovic *et al.*, los cuales presentan actividad cuando se unen a los receptores cannabinoides CB1 y CB2, se testó la afinidad de los cicloaductos **130a** y **130'a**. Desafortunadamente, no se alcanzó el mínimo de desplazamiento de radioligando que mide la afinidad requerido para pasar a siguientes evaluaciones. Posteriormente, se consideró incrementar la lipofilicidad de los incorporando una cadena alifática en los cicloaductos para mejorar la afinidad con los receptores cannabinoides (ver **Esquema 3**). Los resultados de afinidad hacia los receptores CB1 y CB2 de estos compuestos están siendo evaluados en la actualidad por el grupo de Jagerovic.

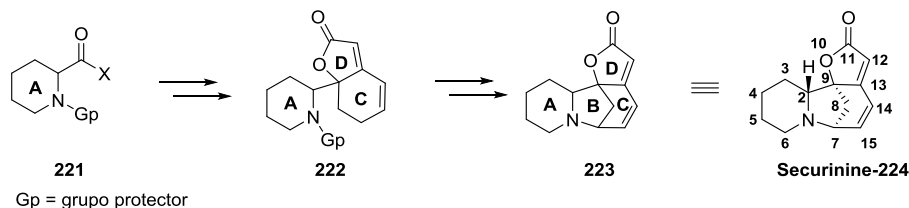


Esquema 3. Reacción de cicloadición intermolecular (3+2) enantioselectiva que permite las síntesis de los productos **130k** y **130'k**.

La configuración absoluta de los cicloaductos enantiopuros obtenidos dio lugar a la necesidad de realizar un análisis tanto computacional como experimental del mecanismo de esta reacción. Los estudios preliminares indican que se trata de una reacción por etapas. Además de la adición de Michael y la posterior reacción de aza-Henry, que suelen mostrar las cicloadiciones de este tipo, la inversión de configuración del carbono asimétrico del cromeno en α al grupo fenilo podría ocurrir mediante un proceso de isomerización mediado por el grupo nitronato del intermedio Michael. El estudio computacional del mecanismo unimolecular de isomerización postulado hasta la fecha ha demostrado la inviabilidad de este proceso, debido a las altas energías de activación observadas. En la actualidad, se están estudiando computacionalmente otros posibles mecanismos que puedan explicar dicho proceso de isomerización.

Resumen de la Tesis Doctoral

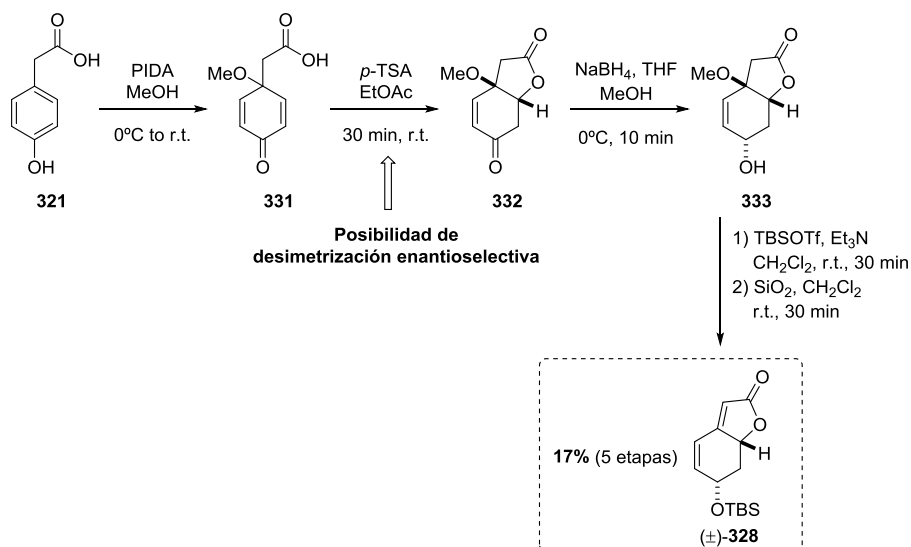
El tercer capítulo de esta tesis tiene como objetivo la síntesis total de alcaloides de la familia de *Securinega*. Generalmente, las estrategias empleadas se basan en el uso de derivados de piperidina o pirrolidina (anillo A) como reactivos de partida, seguidos de la formación del anillo butenolida (anillos CD) y la posterior ciclización intramolecular para dar lugar a la formación de sistemas azabicclo[3.2.1]octano.



Esquema 4. Estrategia general descrita para la síntesis total de alcaloides de *Securinega*.

La síntesis total de los alcaloides de la familia *Securinega* se propuso de una manera colectiva y divergente teniendo como intermediario clave una lactona bicíclica. Previamente se ha descrito una lactona similar como intermediario en varias síntesis totales, además de haber sido propuesta como posible intermediario en la biosíntesis de la Securinina.

La estrategia a seguir propuesta por nuestro grupo parte de la desaromatización del fenol **321** para generar la correspondiente 2,5-ciclohexadienona que a su vez evolucionó a través de una reacción de oxa-Michael intramolecular la cual dio lugar al compuesto **332** (ver **Esquema 5**). Tras diferentes transformaciones químicas la lactona-**328** fue sintetizada. La síntesis en cinco etapas se puede llevar a cabo de manera eficiente, realizando una sola purificación por columna cromatográfica obteniéndose así el compuesto-**328** con un rendimiento global del 17%.

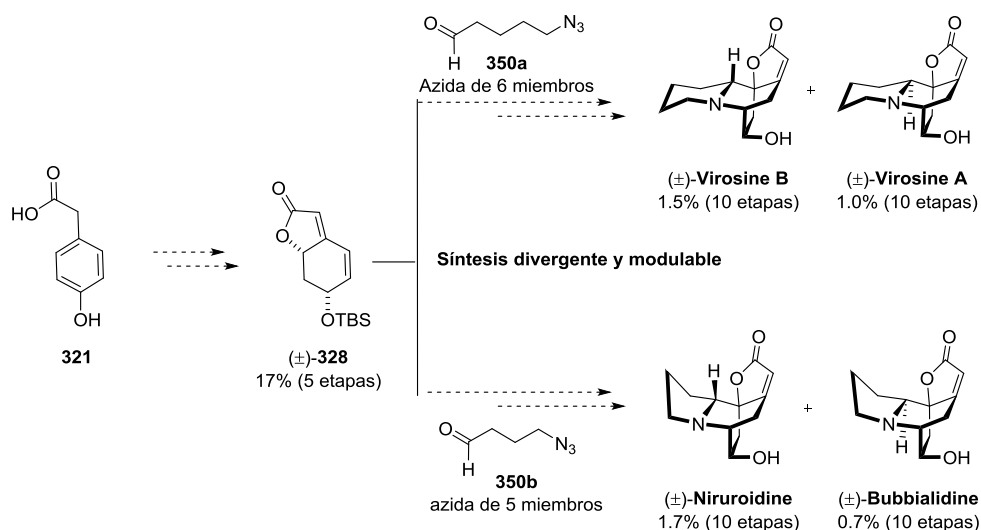


Esquema 5. Síntesis de **328**, empleado como intermediario clave en la síntesis total de los alcaloides.

Una vez obtenido este resultado, se sugirió una ruta sintética para la obtención de la lactona-**328** en una manera enantiopura (reacción de oxa-Michael en **Esquema 5**). Para ello, se evaluaron los diferentes ligandos tipo ferrocenil prolina en presencia de sales metálicas obteniéndose en todos los casos la lactona-**328** en su forma racémica. Asimismo, diferentes organocatalizadores fueron empleados en la misma reacción. El mejor resultado se obtuvo al emplear el ácido fosfórico *R*-TRIP (17% de ee para la lactona-**328**) como organocatalizador.

En vista de estos resultados, se propuso una síntesis alternativa, en la que la quiralidad se podría transmitir mediante la reacción de desimetrización para formar 1,4-dioxanos. El empleo de diaminas quirales mostró un buen enantiocontrol para la generación del dioxano, pero desafortunadamente no se pudo obtener el producto deseado.

En lo que respecta a la síntesis racémica de estos productos naturales, la lactona-**328** reaccionó con la correspondiente azida **350a-b** (de 6 o 5 miembros) permitiendo el acceso a los precursores de los anillos pirrolidina y piperidina de estos alcaloides. La posterior formación de la imina mediante una reacción Staudinger/aza-Wittig, la aminación reductiva de ésta y la reacción tipo aza-Michael generó los productos protegidos que incorporan un sistema de azabicyclo[2.2.2]octano. Una última etapa de desprotección dio lugar a los cuatro productos naturales (**Esquema 6**).



Esquema 6. Síntesis total divergente y modulable que permite acceder cuatro alcaloides de *Securinega*.

Los productos que se pueden clasificar como alcaloides de tipo neosecurinina, es decir, aquellos que incluyen en su estructura una unidad de piperidina, se obtuvieron con rendimientos globales alrededor del 1-2% y en una proporción diastereomérica de 55:45. Los datos físicos y de espectroscopia de RMN descritos en literatura ayudó a la identificación de los productos naturales **(±)-Virosina B** y **(±)-Virosina A**, respectivamente.

Asimismo, los productos naturales **(±)-Niruroidina** y **(±)-Bubbialidina** fueron obtenidos en una proporción diastereomérica de 75:25 y con rendimientos globales

Resumen de la Tesis Doctoral

similares. Estas moléculas se encuentran dentro de los alcaloides de tipo neonorsecurinina, ya que presentan una pirrolidina como anillo fusionado al azabíciclo [2.2.2]octano. Se realizaron estudios computacionales para justificar la relación diastereoimérica obtenida experimentalmente. Los cálculos DFT demostraron que la etapa limitante es la de aminación reductiva. La diferencia de energía libre entre los estados de transición es de 0.98 kcal/mol, que predice una proporción de 81:19 a favor del ataque por la cara *Si* (para dar como producto mayoritario la (±)-**Niruroidina**). Este valor está en concordancia con el valor obtenido experimentalmente de 75:25.

En conclusión se ha desarrollado una síntesis divergente y colectiva de alcaloides de *Securinega*, en 10 etapas de reacción con un rendimiento global de 0.7 a 1.7% en la que se pueden obtener los productos naturales (±)-**Virosina B**, (±)-**Virosina A**, (±)-**Niruroidina** y (±)-**Bubbialidina**.

Les alcaloïdes sont des molécules organiques constituant une famille importante de substances naturelles hétérocycliques azotées. Généralement biologiquement actives (activités antipaludéenne, anti-cancéreuse, analgésique, sédatrice...), ces molécules sont structurellement complexes, et présentent fréquemment de nombreux centres stéréogènes incorporés dans des motifs pipéridiniques, ou encore pyrrolidiniques. Ces singularités structurales, combinées à leurs diverses activités biologiques, font donc de ces composés des cibles de choix pour l'industrie pharmaceutique.

Un des principaux objectifs de la chimie de synthèse est la mise au point de méthodes permettant d'accéder de façon concise et efficace à des structures hydrocarbonées (naturelles) complexes. Au cours des dernières décennies, la catalyse organométallique, de grâce à la grande variété de complexes disponibles, s'est avérée être un outil puissant et polyvalent pour atteindre cet objectif. En particulier, les ligands du type ferrocényle ont montré une grande versatilité en tant que catalyseurs dans des réactions asymétriques.

Notre groupe de recherche a une expérience dans la synthèse et l'emploi de ligands ferrocényles, et deux de nos ligands, le **NH-D-EhuPhos-91a** et le **NMe-L-EhuPhos-93**, se sont révélés efficaces dans des réactions de cycloaddition [3+2] entre les α -iminoesters et les nitroalcènes, pour générer les pyrrolidines **exo-90** et **endo-92** avec d'excellents excès énantiomériques (voir **Schéma 1**). Ce travail a donc conduit à l'obtention de prolines non-naturelles densément substituées.

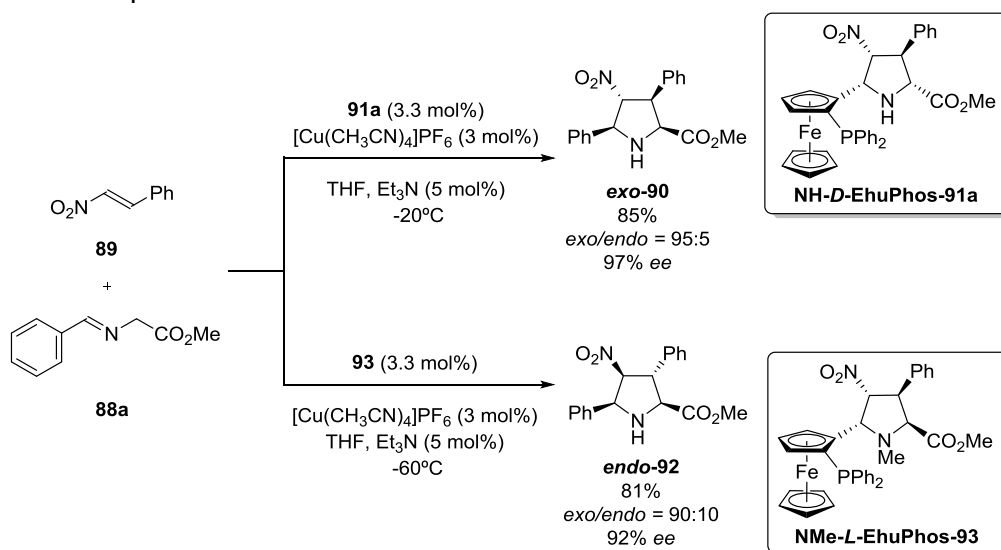


Schéma 1. Synthèse énantiosélective de cycloadduits **endo-92** et **exo-90** catalysée par les ligands de ferrocényle-proline **93** et **91a**.

Les cycloadditions sont probablement les transformations permettant l'accès à la complexité moléculaires le plus rapide. La grande efficacité observée de nos ligands ferrocényles nous a donc incité à évaluer leurs performances dans des réactions énantiosélective de cycloaddition [2+1] et dans de réactions de cycloaddition intra- et intermoléculaires [3+2].

Résumé de la thèse de doctorat

La cycloaddition énantiosélective [2+1] est la réaction la plus souvent décrite pour accéder à des cyclopropanes, motif structuraux très utiles en synthèse totale de produits naturels, mais aussi en tant que pharmacophore induisant fréquemment des propriétés biologiques intéressantes. La mise en réaction d'alcènes et de composés diazoïques catalysée par des métaux de transition en présence des ligands ferrocényles **NH-D-EhuPhos-91a** et **NMe-L-EhuPhos-93** a conduit à la synthèse exclusive de *trans*-cyclopropanes. Cependant, seuls des produits racémiques ont été obtenus.

D'autre part, l'intérêt de synthétiser des composés tricycliques contenant un cycle pyrrolidine attaché à un chromène nous a conduits à l'évaluation de nos ligands dans des réactions de cycloaddition énantiosélective intramoléculaire [3+2]. La fragment chromène[4,3-b]pyrrole est particulièrement intéressante en raison de ses propriétés biologiques. Par conséquent, la réaction intramoléculaire de l'imine **126** a été évaluée sous différentes conditions. Contrairement aux essais de cyclopropanation, un excès énantiomérique de 60% a été observé pour le produit **endo-127**, lorsque la réaction est catalysée par le ligand **NH-TB-D-EhuPhos-91b** en présence de AgClO_4 (**Schéma 2**). Notons que la liberté conformationnelle de l'imine **126** peut expliquer la formation du **dimère-128** dans le cadre de processus compétitifs impliquant une cycloaddition de type intramoléculaire ou intermoléculaire.

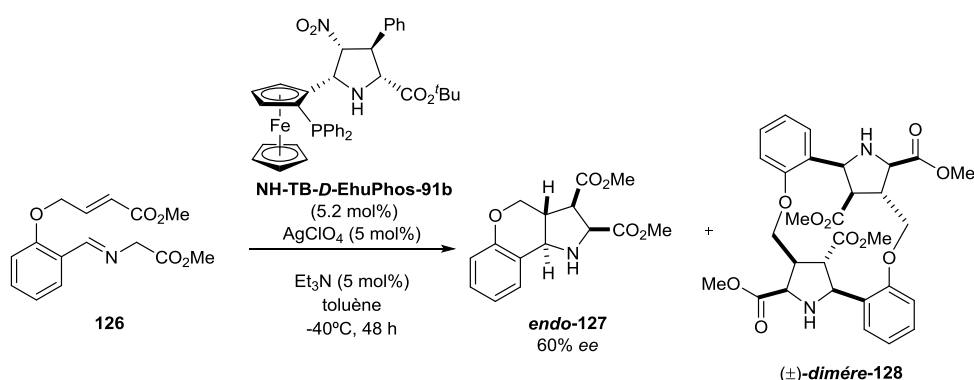


Schéma 2. Réaction de cycloaddition intramoléculaire [3 + 2] énantiosélective qui conduit aux produits tricycliques **endo-127** et **dimère-128**.

Compte tenu des résultats obtenus pour la version intramoléculaire, une nouvelle stratégie a été développée pour la synthèse asymétrique de composés tricycliques incorporant une structure de type chroménopyrrolidine. Ainsi, une réaction de cycloaddition intermoléculaire énantiosélective [3+2] entre le 3-nitro-2*H*-chromène et différents α -iminoesters a été réalisée en présence du ligand **NH-TB-D-EhuPhos-91b**. Cette réaction a donné lieu à la formation de chromène[3,4-*c*]pyrrolidines **130** et **130'** avec un énantiocontrol élevé (jusqu'à 97% ee). Notons que la configuration absolue de ces composés énantiomères a pu être déterminée par analyse de diffraction des rayons X des cristaux correspondants.

Puisque les composés synthétisés **130** et **130'** ont une certaine analogie structurale avec les chroménopyrazoles développées par l'équipe du Dr. Jagerovic, l'affinité de nos nouveaux chromène [3,4-*c*]pyrrolidines pour les récepteurs cannabinoïdes a été

testée. Malheureusement, les résultats obtenus n'ont pas montré d'interactions significatives avec ces récepteurs. Par la suite, nous avons envisagé d'augmenter la lipophilie de nos composés en leur incorporant une chaîne aliphatique afin d'améliorer leurs affinités avec ces récepteurs cannabinoïdes (voir **Schéma 3**). Ces composés sont actuellement testés au sein du laboratoire du Dr. Jagerovic pour évaluer leurs affinités aux récepteurs CB1 et CB2.

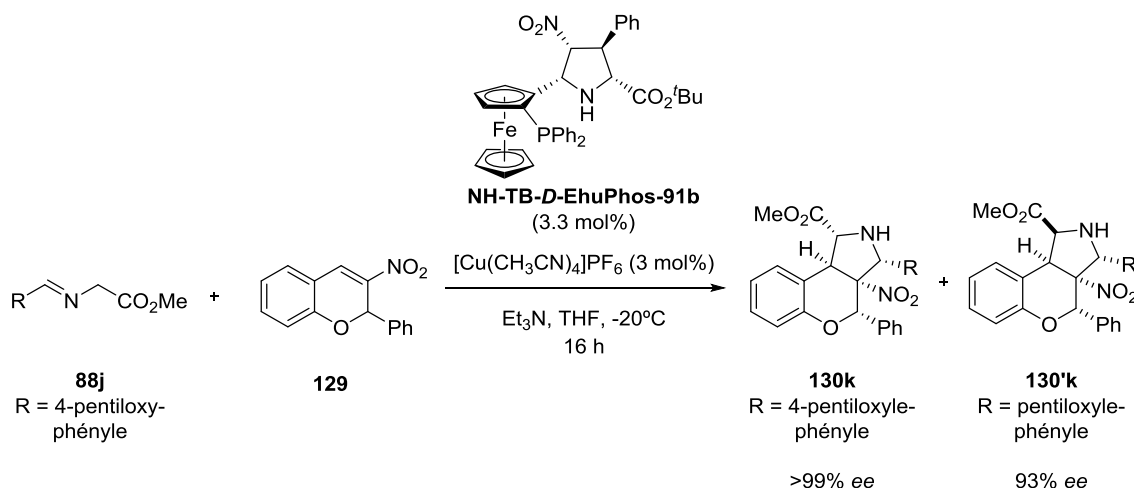


Schéma 3. Réaction de cycloaddition enantiosélective [3 + 2] pour la synthèse des produits **130k** et **130'k** portant une chaîne aliphatique.

La configuration absolue des cycloadduits **130** et **130'** a donné lieu à la nécessité d'effectuer à la fois une analyse computationnelle et une analyse expérimentale du mécanisme de cette réaction. Des études préliminaires indiquent que le processus est par étapes (stepwise). En plus de l'addition de Michael et de la réaction aza-Henry, l'inversion de la configuration du carbone asymétrique en α du groupe phényle du chromène pourrait se produire par un procédé d'isomérisation médié par le groupe nitronate de l'intermédiaire de Michael. L'étude DFT du mécanisme unimoléculaire d'isomérisation postulé à ce jour a démontré la non viabilité de ce procédé en raison des énergies d'activation élevées. Des calculs supplémentaires, y compris des corrections énergétiques associées à des énergies de dispersion non covalentes et à des effets de solvant, sont actuellement en cours.

L'objectif principal du troisième chapitre de cette thèse est la synthèse totale des alcaloïdes de *Securinega*. En général, les stratégies employées pour la synthèse de ces alcaloïdes sont basées sur l'utilisation de dérivés de pipéridine ou de pyrrolidine (cycle A) comme réactifs de départ, suivie de la formation du fragment buténolide (cycle CD) et d'une cyclisation intramoléculaire finale pour donner naissance à la formation de systèmes azabicyclo[3.2.1]octane (**Schéma 4**).

Résumé de la thèse de doctorat

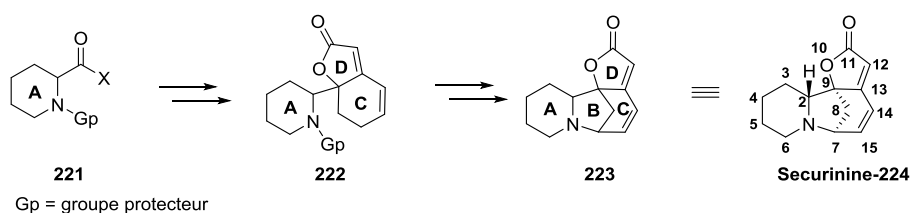


Schéma 4. Stratégie générale décrite pour la synthèse totale des alcaloïdes de la famille *Securinega*.

Notre objectif était une synthèse collective de ces produits naturels basée sur la formation d'une lactone intermédiaire bicyclique. Notons que des lactones similaires ont déjà été proposées en tant qu'intermédiaire dans certaines synthèses totales rapportées.

La stratégie suivie est basée sur la désaromatisation du phénol **321** pour générer la 2,5-cyclohexadiénone-**331** correspondante. Une réaction d'oxa-Michael intramoléculaire donne alors accès au composé **332** (voir **Schéma 5**) qui, après réduction sélective de la cétone au borohydrure de sodium et protection de l'alcool secondaire, permet d'isoler l'intermédiaire clé **328**. Cette synthèse est très efficace, peut être réalisée par un opérateur en 8h de travail de paillasse à l'échelle du multi-gramme, ne nécessite qu'une seule purification, et conduit à un rendement global de 17%.

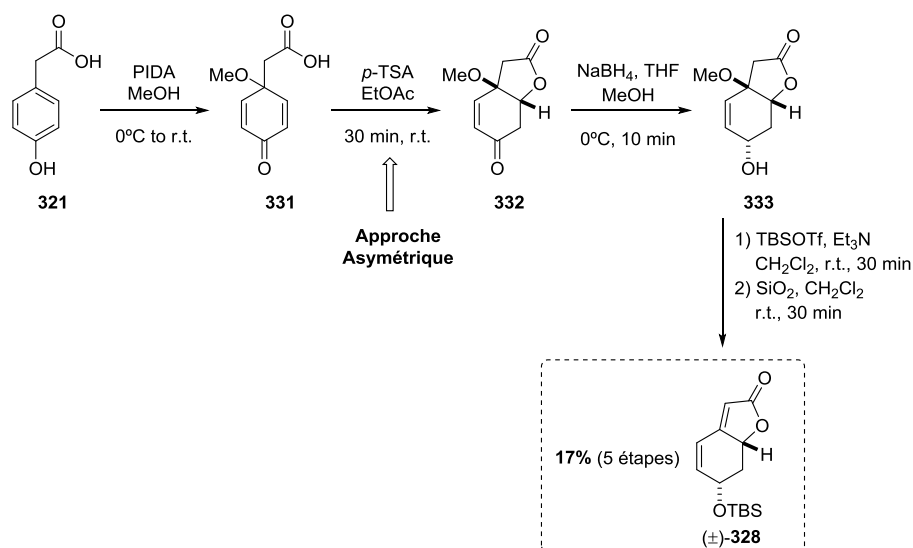


Schéma 5. Synthèse de **328**, intermédiaire clé dans la synthèse totale d'alcaloïdes *Securinega*.

Plusieurs tentatives de synthèse asymétrique de la lactone **328** ont été réalisées. La stratégie directe repose sur une désymétrisation de la 2,5-cyclohexadiénone méso par réaction d'oxa-Michael énantiosélective. Les ligands ferrocényles en combinaison avec des métaux de transition ont été évalués pour cette transformation. Malheureusement, toutes les tentatives ont conduit à un mélange racémique de lactone-**328**. De plus, l'emploi de différents types d'organocatalyseurs n'a permis aucune amélioration significative; meilleurs résultats ayant été obtenus par l'utilisation d'acide phosphorique chiral de type (*R*)-TRIP (17% ee).

Au vu de ces résultats, une autre approche asymétrique, par synthèse énantiosélective de 1,4-dioxanes par désymétrisation oxa-Michael, a montré un bon enantiocontrôle (jusqu'à 86% ee) en présence de diamines chirales. Malheureusement, les efforts pour générer l'intermédiaire lactone ont échoué en raison de l'impossibilité d'élimination fragment 1,4-dioxane.

Nonobstant notre incapacité à produire l'intermédiaire clé de façon énantiosélective, la synthèse racémique de quatre alcaloïdes *Securinega* a été entamée. Ainsi, la mise en réaction de l'énolate de la lactone **328** avec les aldéhydes **350a** et **350b** a permis d'accéder, aux cycles pyrrolidinique et pipéridiniques des Niruroidine, Bubbialidine, Virosines A et B. En effet, la formation de l'imine par réaction de Staudinger/aza-Wittig, l'amination réductrice et la réaction terminale de type aza-Michael ont généré les produits naturels protégés incorporant un système azabicyclo[2.2.2]octane. Une étape finale de déprotection permet alors d'isoler les produits naturels (**Schéma 6**).

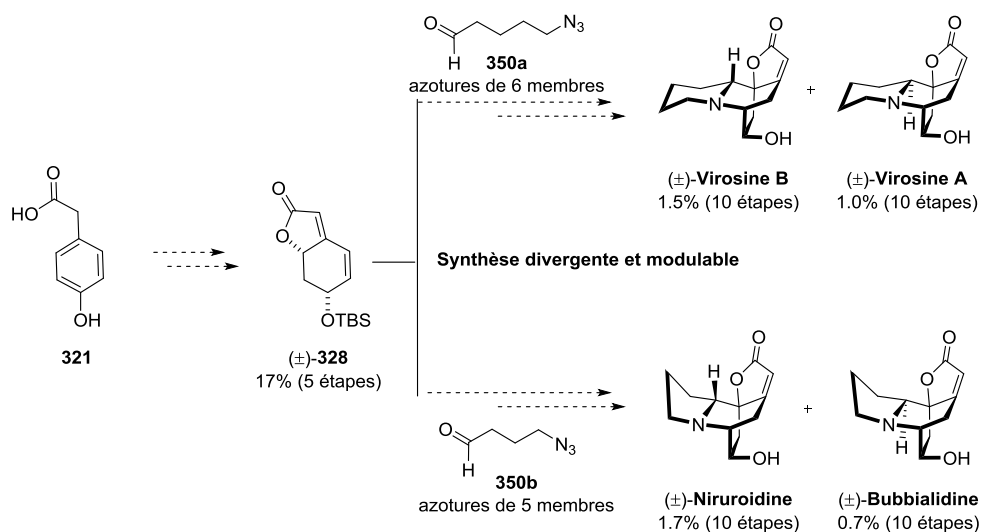


Schéma 6. Synthèse totale divergente et modulable donnant accès à quatre alcaloïdes *Securinega*.

Les produits classés comme alcaloïdes de type neosecurinine, ceux qui comprennent dans leur structure une unité pipéridine, ont été obtenus avec des rendements globaux d'environ 1-2% et dans un rapport diastéréoisomérique de 55:45.

La (±)-**Niruroidine** et la (±)-**Bubbialidine** ont été obtenus de façon similaire dans un rapport diastéréoisomérique de 75:25. Des études computationnelles ont été réalisées pour justifier le rapport diastéréoisomérique obtenu expérimentalement. En effet, l'étude des états de transition optimisés de l'amination réductrice pour chaque composé a montré une différence d'énergie relative libre de 0,98 kcal/mol. Cette différence énergétique relative libre se réfère à un rapport de 81:19 en faveur de l'attaque par rapport à la face *Si* (conduisant à (±)-**Niruroidine** comme produit majeur); une valeur proche du rapport 75:25 obtenu expérimentalement.

Résumé de la thèse de doctorat

En conclusion, une synthèse collective des alcaloïdes de *Securinaga* a été développée en 10 étapes avec un rendement global de 0.7 à 1.7% pour les quatre produits naturels (±)-**Virosine B**, (±)-**Virosine A**, (±)-**Niruroidine** et (±)-**Bubbialidine**.

Acronyms and Abbreviations

Ac	acetyl
AcOEt	ethyl Acetate
ACN	acetonitrile
B	Base
BINAP	(2,2'-bis(diphenylphosphino)-1,1'-binaphtyl)
BINOL	1,1'-bi-2-naphtol
BOX	(bis)-oxazoline
br	broad
^t Bu	<i>tert</i> -butyl
cat.	catalyst
CB1	cannabinoid receptor 1
CB2	cannabinoid receptor 2
CNS	central nervous system
COSY	correlation spectroscopy
Cbz	carbenziloxy
CSA	camphorsulfonic acid
Cp	cyclopentadienyl
d	doublet (NMR)
DCC	<i>N,N</i> -dicyclohexylcarbodiimide
DCE	dichloroethane
DCM	dichloromethane
dd	double doublet (NMR)
deg	degrees
DFT	density functional theory
DIPEA	<i>N,N</i> -diisopropylethylamine
DMF	<i>N,N</i> -dimethyl formamide
DMSO	dimethyl sulfoxide
d. r.	diastereoisomeric ratio
Δ^9 -THC	Δ^9 -tetrahydrocannabinol
E	electrophile
ee	enantiomeric excess
ECS	endocannabinoid system
EDA	ethyl diazoacetate

Acronyms and Abbreviations

EDG	electron-donating group
e.d.	excess diastereoisomeric
EI (ESI)	electrospray ionization
<i>ent</i>	enantiomer
equiv.	equivalents
Et	ethyl
EWG	electron-withdrawing group
Fc	ferrocenyl
FMO	frontier molecular orbital
FTIR	fourier transform infrared spectroscopy
g	gram (s)
GABA	γ -aminobutyric acid
GABA _A R	GABA receptor A
h	hour
HOMO	highest occupied molecular orbital
HPLC	high pressure /performance liquid chromatography
HMRS	high resolution mass spectrometry
HSQC	heteronuclear single quantum coherence
Hz	Hertz
INT	intermediate
<i>J</i>	coupling constant
kcal	kilocalories
Ln	ligand
LUMO	lowest unoccupied molecular orbital
m	multiplet (NMR)
<i>m</i> -CPBA	meta-chloroperoxybenzoic acid
Me	methyl
MEDA	methyl ethyl diazoacetate
MO	molecular orbital
mg	miligram
mmol	milimol
min	minute
mL	mililiter
MS	mass spectrum
MS	molecular sieves
n.d.	not determined

Acronyms and Abbreviations

NMR	nuclear magnet resonance
NOESY	nuclear overhauser spectroscopy
Nu	nucleophile
P	product
PG	protecting group
Ph	phenyl
ppm	parts per million
ⁱ Pr	<i>iso</i> -propyl
<i>p</i> -TSA	para-toluenesulfonic acid
Py	pyridine
R	arbitrary substituent
r.t.	room temperature
s	singlet (NMR)
t	time
T	temperature
t	triplet (NMR)
TBS	tert-butyldimethylsilyl
TS	transition state
TFA	trifluoroacetic acid
THF	tetrahydrofuran
TLC	thin layer chromatography
(<i>R</i>)-TRIP	3,3'-bis(2,4,6-triisopropylphenyl)-1,1'-binaphthyl-2,2'-diyl hydrogen phosphate

CHAPTER 1
INTRODUCTION

1.1 Chirality

Chirality is an inherent characteristic of matter; it is present when one object is non-superposable to its mirror image.¹ Molecular chirality refers to a molecule which incorporates a stereogenic element and suffers of an absence of reflection symmetry. Life itself depends on chirality, since most of the physiological processes emerge from precise molecular interactions, where a chiral receptor recognizes and discriminates between two enantiomers. This fact justifies the important role that chiral molecules play in different fields of science and technology.

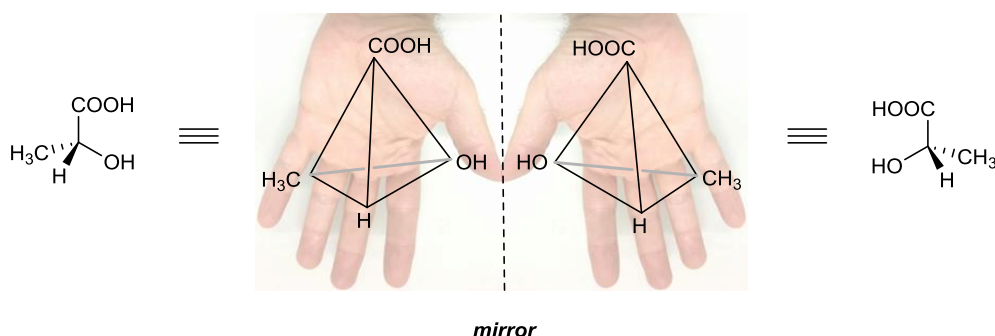


Figure 1.1. Enantiomers of lactic acid as mirror images.

Receptors in the organism interact with small molecules that have an specific absolute configuration. This fact is in concordance with the different pharmacological activity that each enantiomer shows. Therefore, it is not surprising that in the last 20 years organic chemistry has been focused on the development of enantiomerically pure compounds.²

A clear example that shows the importance of enantiopurity in pharmaceutical industry is Ethambutol, a drug described and used in the treatment of tuberculosis. Indeed, this drug was used since 1960's as a racemic mixture. Unfortunately, it was found that its L-enantiomer was responsible for visual disorders in patients while the D-enantiomer exhibited the desired therapeutic effects. In any case, it has been reported that the long-term use of the D-enantiomeric form can give rise to a real risk of severe visual issues, possibly due to its double isomerization to L-Ethambutol.³

¹ a) Avalos, M.; Babiano, R.; Cintas, P.; Jiménez, J. L.; Palacios, J. C. *Tetrahedron Asymmetry* **2000**, *11*, 2845-2874. b) Heilbronner, E.; Dunitz, J. *Reflections on Symmetry*, VHCA: Basel, **1993**. c) *The New Ambidextrous Universe*; Gardner, M. W. H. & Co.: New York, **1990**. d) Hoffmann, R. *The Same and Not the Same*; Columbia University Press: New York, **1995**. e) H. Brunner, *Rechts oder links in der Natur und anderswo*; Wiley-VCH: Weinheim, **1999**.

² Noyori, R. *Adv. Synth. Catal.* **2003**, *345*, 15-32.

³ Lim, S.-A. *Ann Acad. Med. Singapore* **2006**, *35*, 274-278.

CHAPTER 1

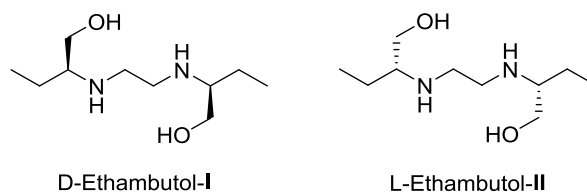


Figure 1.2. On the left enantiomeric form used as drug against tuberculosis and on the right its enantiomer involved in provoking blindness.

1.2 Strategies for the obtention of enantiomerically pure compounds (EPC)

The importance of enantiomerically pure compounds has given a boost to the research of new strategies for their synthesis. In this area, three main strategies have been developed as it is gathered in **Figure 1.3**.

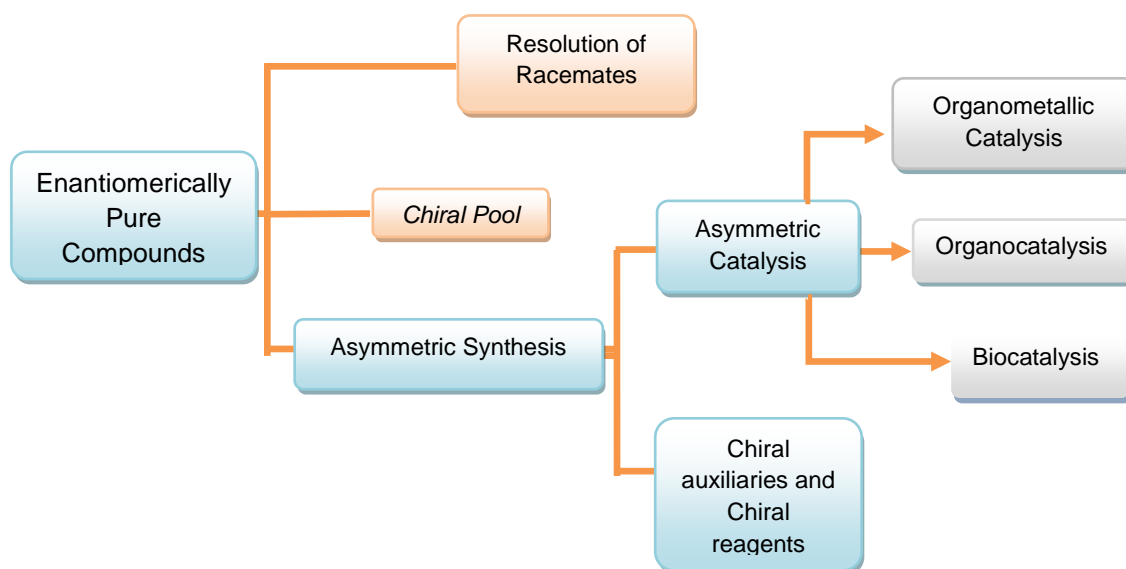


Figure 1.3. General strategies for the attainment of enantiopure compounds.

1.2.1 Resolution of racemates

Resolution of racemates was first discovered by Prof. Pasteur in 1848, when he was able to separate manually two types of crystals of tartaric acid salts.⁴ Most of the resolutions go through the conversion of a racemate into a diastereomeric salt, using an enantiomer of a chiral compound. The different physical and chemical properties of the diastereoisomers make them easily separable after conventional techniques (chromatography, crystallization...). Kinetic resolution is based on the different reaction rates of both enantiomers, where the one with higher reaction rate is chemically modified while the other remains intact and can thus be recovered. The main drawback

⁴ Pasteur, L. C. R. *Hebd. Séanc. Acad. Sci. Paris* **1848**, 26, 535-539.

of this method is that yields are limited to 50 %. This latter limitation can be resolved if there is a method to promote *in situ* racemization of the less reactive enantiomer into the most reactive one. If the required methodology is available, standard kinetic resolution allows converting a racemic mixture into a single enantiopure product. This strategy is called dynamic kinetic resolution (DKR).^{5,6}

1.2.2 Chiral Pool

In the chiral pool strategy enantiomerically pure compounds are produced by a sequence of chemical transformations starting from chiral compounds extracted from natural sources (amino acids, carbohydrates, hydroxy acids and terpenes).⁷ This strategy requires many synthetic steps when the abundance of natural sources is not enough for the demand of enantiomerically pure compounds. However, most of the biologically active products synthesized in industry are obtained this way.

1.2.3 Asymmetric synthesis

Asymmetric synthesis relies on the stereocontrolled conversion of a prochiral substrate into a chiral product with one or more stereogenic centers. Chiral compounds can transfer their chirality using chiral auxiliaries in stoichiometric amounts or employing catalysts in substoichiometric amounts.

1.2.3.1 Chiral auxiliaries and chiral reagents

According to this strategy, chiral auxiliaries are organic compounds which can be introduced into the substrates to generate new stereogenic centers via intramolecular asymmetric induction. At the end of the reaction the auxiliary is removed under conditions that will not cause the loss of the chirality. The possibility to recover the chiral auxiliary is important taking into account that they are used in stoichiometric amounts. Normally their preparation has to be easy and not expensive. Some chiral auxiliaries are very well known because they are efficient in many different reactions. Evans' oxazolidinones or Oppolzer's sultams are typical chiral auxiliaries.⁵

1.2.3.2 Asymmetric catalysis

Asymmetric catalysis is a process in which an enantiopure molecule named catalyst, employed in substoichiometric amount, induces chirality to a prochiral substrate during the reaction. In this strategy the catalyst activates the substrate in

⁵ Muñoz-Torrero, D.; Haro, D.; Valles, J. *Recent Advances in Pharmaceutical Sciences II*, Transworld research network, Kerala, **2012**.

⁶ Caddick, S.; Jenkins, K. *Chem. Soc. Rev.* **1996**, 25, 447-456.

⁷ Christmann, M.; Bräse, S. *Asymmetric Synthesis: More Methods and Applications*; First Edition. Wiley-VCH, Weinheim, **2012**.

CHAPTER 1

order to increase the reaction rate by lowering the activation energy. This methodology presents the advantage of producing one single enantiopure compounds even with the use of 1% of catalyst amounts. Thus, from a synthetic point of view, this kind of reactions has a high atomic economy and can give rise to products with a high enantiomeric excess.⁷

Relying on the nature of the catalyst, the asymmetric catalysis can be divided in three fields:

1. **Biocatalysis:** This type of catalysis is performed mainly by enzymes. These biomolecules are capable to catalyze many reactions in regio- and enantioselective fashion under soft conditions. The main drawback of this kind of asymmetric induction is its high specificity for the substrate and the need of an aqueous media, since most enzymes are not compatible with many organic substrates.⁸
2. **Organocatalysis:** It is a type of catalysis performed by purely organic molecules in total absence of metals in the active site. The use of organocatalysts in enantioselective reactions has received considerable attention in the last twenty years, and now its relevance is comparable to classical catalysis employing transition metals.⁹ Many organocatalysts are non-toxic, robust, and commercially available. Nowadays there is a huge number of organocatalysts capable of carrying out many different reactions, which demonstrates its great versatility, but they are limited because of the need to use, in most cases, more quantity of catalyst than in the traditional organometallic catalysis.¹⁰
3. **Organometallic catalysis:** This kind of catalysis employs well defined organometallic complexes as catalyst in order to accelerate different types of reactions. Moreover, it offers the possibility to modulate the ligand, changing the environment around the metal, can lead not only to the improvement of the reactivity, but also the diastereo- and enantioselectivity depending on the targeted reaction.² Compared to organocatalysis, smaller catalyst loadings are usually required and one sole complex can catalyze different types of reactions.

Therefore, Knowles¹¹, Noyori^{2,12} and Sharpless¹³ were awarded with the Nobel Prize of Chemistry due to their contributions in the field of asymmetric synthesis, more specifically in asymmetric catalytic hydrogenations and asymmetric catalytic oxidations, respectively.

⁸ Patel, R. N. *Coord. Chem. Rev.* **2008**, 252, 659-701.

⁹ Dalko, P. I.; Moisan, L. *Angew. Chem., Int. Ed.* **2004**, 43, 5138-5175.

¹⁰ Alemán, J.; Cabrera, S. *Chem. Soc. Rev.* **2013**, 42, 774-793.

¹¹ a) Knowles, W. S. *Adv. Synth. Catal.* **2003**, 345, 3-13. b) Knowles, W. S. *Angew. Chem., Int. Ed.* **2002**, 41, 1998-2007.

¹² Noyori, R. *Angew. Chem. Int. Ed.* **2002**, 41, 2008-2022.

¹³ Sharpless, K. B. *Angew. Chem. Int. Ed.* **2002**, 41, 2024-2032.

1.3 Chiral ligands in organometallic catalysis

In organometallic catalysis, the possible success of a certain ligand depends on its geometrical, steric and electronic properties. These properties can affect the reactivity of the reaction and the selectivity of the metallic center.

For example, chiral bidentate ligands tend to form more rigid organometallic intermediates that often enable excellent enantioinduction. On the other hand, a limited number of monodentate ligands¹⁴ have exhibited successful results in terms of diastereo- and enantioinduction.

1.3.1 Bidentate ligands possessing C_2 symmetry

In the last 50 years, a great variety of catalysts, which present C_2 symmetry, have been developed but just some of them, such as BINAP¹⁵, have been used in a wide range of reactions.¹⁶ For instance, BINAP in combination with metallic sources of Rh, Ir and Cu, is capable of catalyzing asymmetric hydrogenation reactions and generation of C-C bonds with excellent enantiomeric excesses. In addition to BINOL¹⁷, BINAP incorporates a C_2 stereogenic axis. This type of ligands presents coordination to the metallic centre through identical heteroatoms. In addition to these ligands, TADDOL¹⁸, MeDUPHOS¹⁹, Evans' bisoxazolines²⁰, and Salen²¹ type ligands are included in this group (**Fig. 1.4**).

¹⁴ a) Teichert, J. F.; Feringa, B. L. *Angew. Chem., Int. Ed.* **2010**, *49*, 2486-2528. b) Eberhardt, L.; Armspach, D.; Harrowfield, J.; Matt, D. *Chem. Soc. Rev.* **2008**, *37*, 839-864. c) Erre, G.; Enthaler, S.; Junge, K.; Gladiali, S.; Beller, M. *Coord. Chem. Rev.* **2008**, *252*, 471-491. d) Xie, J.-H.; Zhou, Q.-L. *Acc. Chem. Res.* **2008**, *41*, 581-593.

¹⁵ Berthod, M.; Mignani, G.; Woodward, G.; Lemaire, M. *Chem. Rev.* **2005**, *105*, 1801-1836.

¹⁶ a) Pfaltz, A. *Asymmetric Synthesis* **2007**, 131-135. b) Pfaltz, A.; Drury III, W. J. *Proc. Nat. Acad. Sci. USA* **2004**, *101*, 5723-5726. c) Yoon, T. P.; Jacobsen E. N. *Science* **2003**, *299*, 1691-1693.

¹⁷ Soriente, A.; de Rosa, M.; Villano, R.; Scettri, A. *Curr. Org. Chem.* **2004**, *8*, 993-1007.

¹⁸ Seebach, D.; Beck, A. K.; Heckel, A. *Angew. Chem., Int. Ed.* **2001**, *40*, 92-138.

¹⁹ Burk, M. J.; Stammers, T. A.; Straub, J. A. *Org. Lett.* **1999**, *1*, 387-390.

²⁰ a) McManus, H. A.; Guiry, P. J. *Chem. Rev.* **2004**, *104*, 4151-4202. b) Basak, R. *Synlett*, **2003**, 1223-1224.

²¹ a) Cozzi, P. *Chem. Soc. Rev.* **2004**, *33*, 410-421. b) Katsuki, T. *Chem. Soc. Rev.* **2004**, *33*, 437-444. c) Jacobsen, E. N. *Acc. Chem. Res.* **2000**, *33*, 421-431.

CHAPTER 1

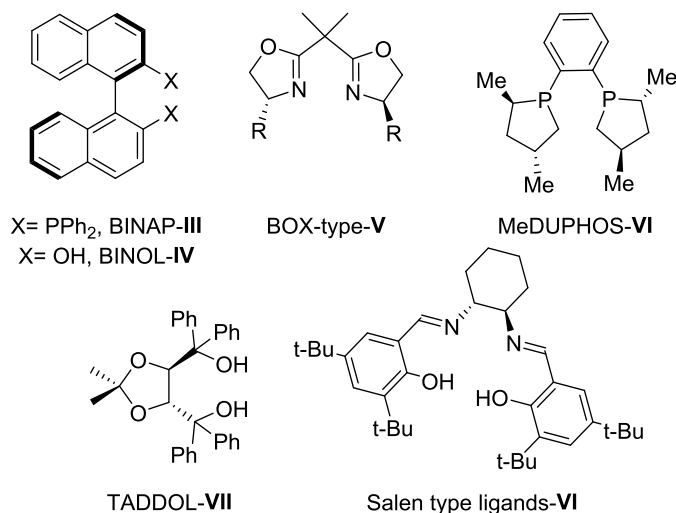


Figure 1.4. Main chiral ligands containing C_2 symmetry outlined due to their success in several asymmetric reactions.

1.3.2 Bidentate ligands without C_2 symmetry

These bidentate ligands are coordinated to the metallic center through two different heteroatoms, which causes a distinct electronic environment. For example, in systems with P, N coordination²², phosphine acts as a π -acceptor and nitrogen atom behaves as σ -donor. QUINAP²³ and phosphine-oxazolines²⁴ are the most representative examples of this group of ligands.

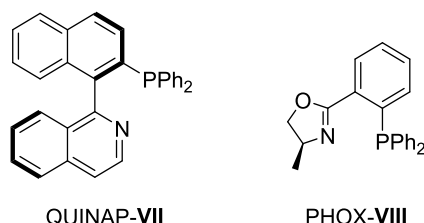


Figure 1.5. Chiral ligands containing different heteroatoms. QUINAP incorporates axial chirality and PHOX central chirality.

²² a) Kostas, I. P. *Curr. Org. Syn.* **2008**, 5, 227-249. b) Guiry, P. J.; Saunders, C. P. *Adv. Synth. Catal.* **2004**, 346, 497-537.

²³ Alcock, N. W.; Brown, J. M.; Hulmes, D. I. *Tetrahedron: Asymmetry* **1993**, 4, 743-756.

²⁴ a) Koch, G.; Pfaltz, A. *Tetrahedron: Asymmetry* **1996**, 7, 2213-2216. b) Pfaltz, A.; *Acta Chem. Scand.* **1996**, 50, 189-194. c) Langer, T.; Helmchen, G. *Tetrahedron Lett.* **1996**, 37, 1381-1384. d) Williams, J. M. J. *Synlett* **1996**, 705-710. e) Newman, L. M.; Williams, J. M. J.; McCague, R.; Potter, G. A. *Tetrahedron: Asymmetry* **1996**, 7, 1597-1598. f) Baldwin, I. C.; Williams, J. M. J. *Tetrahedron: Asymmetry* **1995**, 6, 1515-1518. g) Dawson, G. J.; Williams, J. M. J.; Coote, S. J. *Tetrahedron Lett.* **1995**, 36, 461-462.

1.3.3 Chiral ligands containing a ferrocene structure

Since ferrocene was discovered in 1951²⁵, the interest for this compound has grown in different areas of chemistry and materials science. With the emergence of asymmetric catalysis the so-called sandwich compounds have become of great importance.²⁶ For example, Xiliphos (bidentate *P,P*-ferrocenyl ligand) is employed in combination with iridium for an industrial asymmetric hydrogenation process, in which 10.000 tons/year of (*S*)-metolachlor herbicide precursor are produced.²⁷

The importance of ferrocene relies on the following inherent characteristics:²⁸

1. Rigidity: ferrocene presents two cyclopentadienyl rings coordinated to the iron atom as η^5 ligands. This provides the whole complex a unique environment with considerable structural rigidity.
2. Easy derivatization: the cyclopentadienyl rings carry a partial negative charge which makes the complex highly susceptible to electrophilic substitution by a great variety of donor groups.
3. Planar chirality (disubstituted derivatives): when two different functionalities are introduced in the Cp rings the ferrocene moiety exhibits planar chirality (**Fig. 6**)
4. Steric Bulkiness: This feature plays a relevant role in terms of stereo- and enantiocontrol. Ferrocene usually behaves as a bulky substituent.
5. Other stereo-electronic properties: the partial charge of the Cp rings mentioned before gives ferrocene a donor character. In addition the iron atom may interact, in some cases, with other metals used in the catalytic system.
6. Stability: ferrocene ligands are usually thermally stable and resistant to oxygen and moisture.
7. The starting materials required for the preparation of Ferrocenyl derivatives are cheap and readily available.

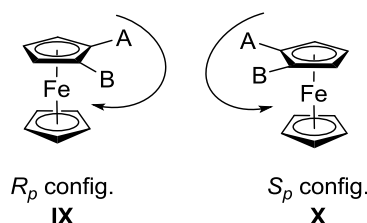


Figure 1.6. R_p and S_p assignment for chiral disubstituted ferrocenes.

²⁵ Kealy, T. J.; Pauson, P. L. *Nature*, **1951**, 168, 1039-1040.

²⁶ Gomez, R.; Adrio, J.; Carretero, J. C.; *Angew. Chem., Int. Ed.* **2006**, 45, 7674-7715.

²⁷ a) Blaser, H.-U. *Adv. Synth. Catal.* **2002**, 344, 17-31. b) Blaser, H.-U.; Brieden, W.; Pugin, B.; Spindler, F.; Studer, M.; Togni, A. *Top. Catal.* **2002**, 19, 3-16.

²⁸ Dai, L.-X.; You, S.-L.; Deng W.-P.; Hou, X.-L. *Acc. Chem. Res.*, **2003**, 36, 659-667.

CHAPTER 1

Ferrocene derivatives can be mono-, di-, tri-²⁹ or tetra-substituted in both Cp rings. The nature of the heteroatoms can also be varied, being *P,P* and *P,N* containing ligands the most frequent. *P,S* type ligands exist as well. For example Fesulphos type ligands are well-known in many chiral transformations.³⁰

In general, the most studied ligands have been the 1,2-substituted ones, which, incorporate planar chirality by themselves. The functionalization of this type of ligands has permitted to find derivatives which contain planar and central chirality by introduction of a new stereogenic center (**Fig. 1.7**).

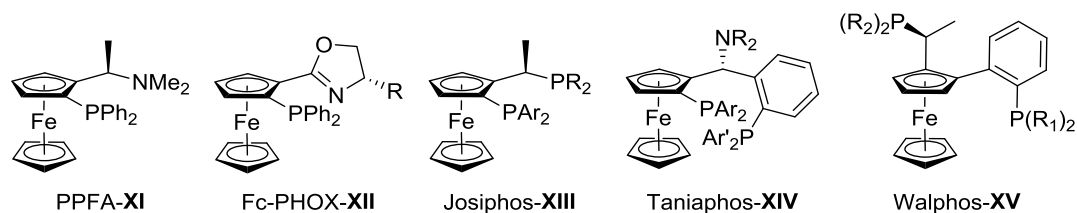
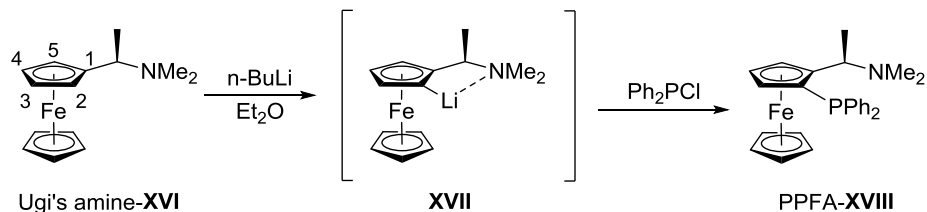


Figure 1.7. A brief example of 1,2-disubstituted ferrocene ligands **XI** to **XV**.

The most employed methodology for the synthesis of 1,2-disubstituted ferrocenes which incorporate planar chirality is the *ortho*-metalation of Ugi's amine **XVI** (**Scheme 1.1**). *Ortho*-lithiation proceeds with high diastereoselectivity in position 2 (not in 5). Final addition of the adequate electrophile affords the PPFA ligand.³¹



Scheme 1.1. Generation of disubstituted ferrocene by *ortho*-lithiation of Ugi's amine.

Ligands like Josiphos-**XIII**, Taniaphos-**XIV** and Walphos-**XV** (**Fig. 1.7**) can be synthesized by means of different reactions starting from Ugi's amine-**XVI**.^{32,33,34} As an

²⁹ Hierso, J.-C.; Ivanov, V. V.; Amardeil, R.; Richard, P.; Meunier, P., *Chem. Lett.* **2004**, 33, 1296–1297.

³⁰ a) García Mancheño, O.; Priego, J.; Cabrera, S.; Gómez Arrayás, R.; Llamas, T.; Carretero, J. C. *J. Org. Chem.* **2003**, 68, 3679–3686. b) Priego, J.; García Mancheño, O.; Cabrera, S.; Gómez Arrayás, R.; Llamas, T. Carretero, J. C. *Chem. Commun.* **2002**, 2512–2513.

³¹ Hayashi, T.; Mise, T.; Fukushima, M.; Kagotani, M.; Nagashima, N.; Hamada, Y.; Matsumoto, A.; Kawakami, S.; Konishi, M.; Yamamoto, K.; Kumada, M. *Bull. Chem. Soc. Jpn.* **1980**, 53, 1138–1151.

³² Togni, A.; Breutel, C.; Schnyder, A.; Spindler, F.; Landert, H.; Tijani, A. *J. Am. Chem. Soc.* **1994**, 116, 4062–4066.

³³ a) Ireland, T.; Tappe, K.; Grossheimann, G.; Knochel, P. *Chem. Eur. J.* **2002**, 8, 843–852. b) Spindler, F.; Malan, C.; Lotz, M.; Kesselgruber, M.; Pittelkow, U.; Rivas-Nass, A.; Briel, O.; Blaser, H.-U.; *Tetrahedron: Asymmetry*, **2004**, 15, 2299–2306.

³⁴ Sturm, T.; Weissensteiner, W.; Spindler, F. *Adv. Synth. Catal.* **2003**, 345, 160–164.

alternative to this amine, other chiral *ortho*-directing groups can be used, such as oxazolines³⁵, sulfoxides³⁶ and ketals³⁷.

Ferrocene ligands have been used as chiral assistants in a wide variety of metal catalyzed reactions such as reduction of alkenes, ketones and imines, 1,2-additions to carbonyl containing compounds and imines, conjugated additions and (4+2) and (3+2) cycloaddition reactions. They offer a wide range of possibilities just by simple modulation of the functional groups.²⁶ Therefore, sandwich compounds can be used in organometallic catalysis as efficient tools for the asymmetric synthesis of complex biological systems and molecules present in nature.

1.4 Nitrogen in natural products and drugs

Alkaloids are molecules present in nature containing nitrogenous heterocyclic rings. Within these compounds, amine moiety is present as the most common functional group, conferring to these molecules their basic character.

Nitrogen atoms of alkaloids contribute directly to the biological properties of these molecules: 1) the lone pair of the nitrogen acts as a proton acceptor; 2) hydrogen in primary or secondary amines acts as a proton donor. In many cases, an alkaloid scaffold is inserted into more complex molecules in order to enhance the biological activities.³⁸

1.4.1 Pyrrolidine and Piperidine scaffolds

Pyrrolidine and piperidine are cyclic secondary amines that belong to the family of saturated heterocycles. Remarkably, both are very important building blocks in Medicinal and Synthetic chemistry. In particular, pyrrolidine is a well known heterocycle in organocatalysis.³⁹

Pyrrolidine and piperidine moieties have been widely reported in the literature as drugs or drug precursors and alkaloids. Some of the most popular heterocycles are gathered in **Fig. 1.8**. Cocaine is a CNS stimulant and induces feeling of happiness with loss of reality. Morphine, on the other hand, is an opiate found in plants and animals, which is also a CNS agent used as ultimate pain killer.⁴⁰ Paroxetine, as other drugs from nortropane family, exhibits high potency and selectivity for serotonin transporters,

³⁵ a) Sammakia, T.; Latham, H. A. *J. Org. Chem.* **1996**, 61, 1629-1635. b) Richards, C. J.; Damalidis, Y.; Hibbs, D. E.; Hursthouse, M. B. *Synlett* **1995**, 74-76. c) Sammakia, T.; Latham, H. A. *J. Org. Chem.* **1995**, 60, 6002-6003. d) Sammakia, T.; Latham, H. A.; Schaad, D. R. *J. Org. Chem.* **1995**, 60, 10-11. e) Nishibayashi, Y.; Uemura, S. *Synlett* **1995**, 79-81.

³⁶ Riant, O.; Argouarch, G.; Guillaneux, D.; Samuel, O.; Kagan, H. B. *J. Org. Chem.* **1998**, 63, 3511-3514. b) Rebière, F.; Riant, O.; Ricard, L.; Kagan, H. B. *Angew. Chem., Int. Ed.* **1993**, 105, 644-646.

³⁷ Riant, O.; Samuel, O.; Flessner, T.; Taudien, S.; Kagan, H. B. *J. Org. Chem.* **1997**, 62, 6733-6745.

³⁸ Kittakoop, P.; Mahidol, C.; Ruchirawat, S., *Curr. Top. Med. Chem.* **2014**, 14, 239-52.

³⁹ Ahmed, A.; Molvi, K. I.; Nazim, S.; Baig, I.; Memon, T.; Rahil, M., *J. Chem. Pharm. Res.* **2012**, 4, 872-880.

⁴⁰ Hanessian, S., *Chem. Med. Chem.* **2006**, 1, 1301-1330.

CHAPTER 1

so it is used as antidepressant and against panic disorders.⁴¹ (–)-Epibatidine is an alkaloid that has shown analgesic properties and is an agonist of nicotine. On the other hand, Atropine is an anticholinergic drug, helpful in the treatment of loss of memory.⁴² (+)-Hygroline and Fagomine are several examples of alkaloids containing the five-membered and six-membered scaffolds, respectively.⁴³

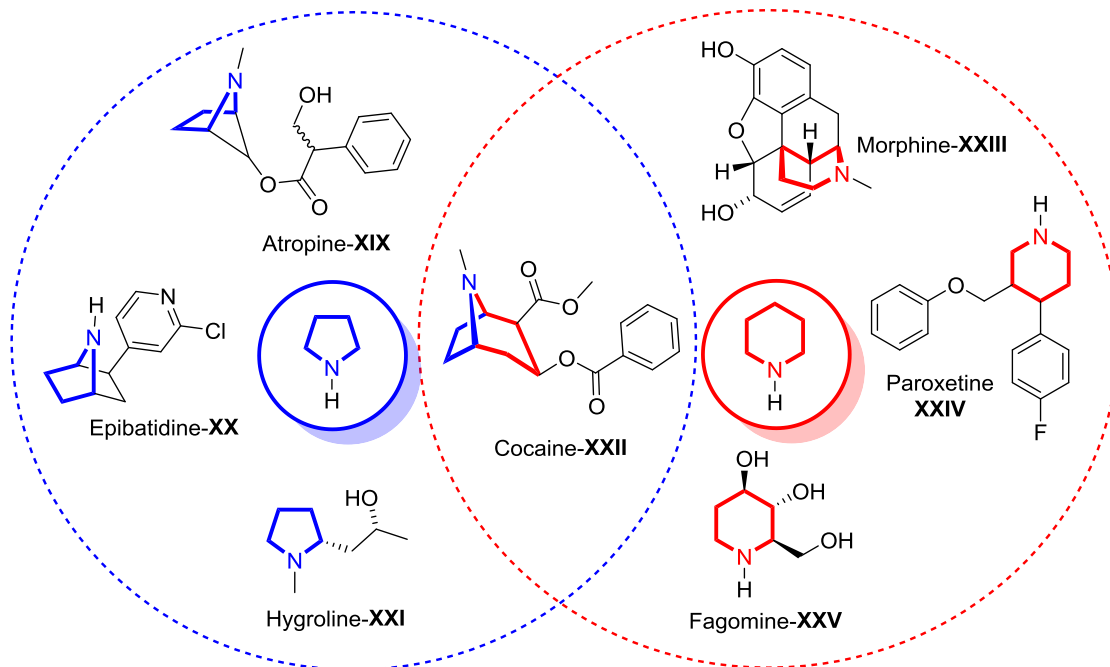


Figure 1.8. Some of the most common pyrrolidine and piperidine containing drugs and natural products.

Within the most popular drugs incorporating a piperidine ring, we can find Penfluridol⁴⁴ and Risperidone⁴⁵ as antipsychotics; Donepezil⁴⁶, which can be used in the treatment of neurodegenerative diseases such as Alzheimer; Trihexyphenidyl⁴⁵ a drug employed for the therapy against Parkinson disease, and (±)-Halofuginone⁴⁷, a compound that exhibited promising properties as antimalarial and anticancer agent.

Some pyrrolidine containing compounds which have shown certain activity are: Nicotine⁴⁸, which serves as defense of plants against fungi, insects and animals; Moxifloxacin⁴⁹, which is an antibiotic for respiratory tract infections (sinusitis,

⁴¹ Keverline-Frantz, K. I.; Boja, J. W.; Kuhar, M. J.; Abraham, P.; Burgess, J. P.; Lewin, A. H.; Carroll, F. I., *J. Med. Chem.* **1998**, *41*, 247–257.

⁴² Boccia, M. M.; Blake, M. G.; Acosta, G. B.; Baratti, C. M., *Neurosci. Lett.* **2003**, *345*, 97–100. b) Badio, B.; Daly, J. W., *Mol. Pharmacol.* **1994**, *45*, 563–569.

⁴³ *Reviews of synthesis of alkaloids containing piperidine or pyrrolidine*: a) Bhat, C.; Tilve, S. G., *RSC Adv.* **2014**, *4*, 5405. b) Felpin, F.-X.; Lebreton, J., *European J. Org. Chem.* **2003**, *2003*, 3693–3712. c) Mauger, A. B., *J. Nat. Prod.* **1996**, *59*, 1205–1211.

⁴⁴ Migdalof, B. H.; Grindel, J. M.; Heykants, J. J.; Janssen, P. A., *Drug Metab. Rev.* **1979**, *9*, 281–299.

⁴⁵ Ahmed, A.; Molvi, K. I.; Nazim, S.; Baig, I.; Memon, T.; Rahil, M., *J. Chem. Pharm. Res.* **2012**, *4*, 872–880.

⁴⁶ Misson, J.; Kendall, M. J., *J. Clin. Pharm. Ther.* **1997**, *22*, 251–255.

⁴⁷ McLaughlin, N. P.; Evans, P.; Pines, M., *Bioorganic Med. Chem.* **2014**, *22*, 1993–2004.

⁴⁸ Siegmund, B.; Leitner, E.; Pfannhauser, W., *J. Agric. Food Chem.* **1999**, *47*, 3113–3120.

⁴⁹ Nightingale, C. H., *Pharmacotherapy* **2000**, *20*, 245–256.

pneumonia, chronic bronchitis...); Ramipril⁴⁰ is used in the inhibition of angiotensin-converting enzyme (ACE); Lincomycin⁴⁰ is an antibiotic for certain gram-(+) infections. Finally, Avanafil³⁸ has been described for the treatment of erectile dysfunction.

The synthesis of several pyrrolidine derivatives has been performed by (3+2) cycloaddition reactions. One example is the asymmetric synthesis of pyrrolidines **XXVI** (**Fig 1.9**). These molecules, depending on the length of the alkyl chain in α to the nitrogen have two possible activities. If the chain is short ($n=0$) then the molecules inhibit the VLA-4/VCAM-1 interaction, which results in potent antimetastatic *in vivo* activity against melanoma.⁵⁰ When $n>0$ these molecules inhibit the LFA-1/ICAM-1 interaction, which plays a key role in psoriasis, rheumatoid arthritis as well as various types of cancer metastasis like melanoma, lymphoma and colon carcinoma (**Fig. 1.9**).⁵¹

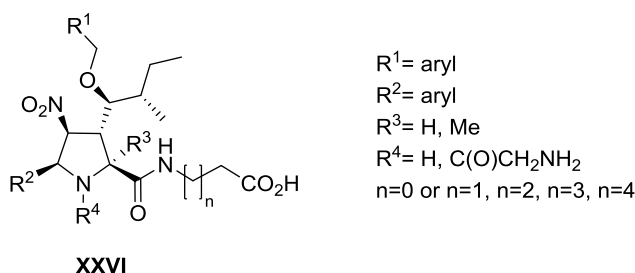


Figure 1.9. VLA-4/VCAM-1 inhibition or LFA-1/ICAM-1 inhibition agent depending on value of n .

Spirooxindole alkaloids are natural products exhibiting biological activity. Spirotryprostatin B arrests cell cycle at G2/M phase and non-natural spirooxindoles have shown inhibition of p53-MDM2 protein-protein interaction, which is critical for the cellular tumor suppression activity of protein p-53.⁵² In addition, it has been reported that this type of molecule increased mortality of zebrafish embryos.⁵³

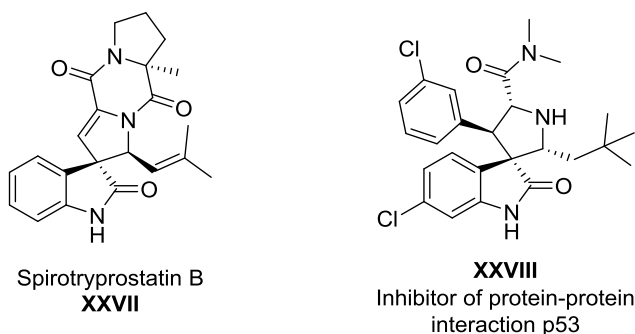


Figure 1.10. Natural and non-natural spirooxindoles.

⁵⁰ Zubia, A.; Mendoza, L.; Vivanco, S.; Aldaba, E.; Carrascal, T.; Lecea, B.; Arrieta, A.; Zimmerman, T.; Vidal-Vanaclocha, F.; Cossío, F. P., *Angew. Chem., Int. Ed.* **2005**, *44*, 2903–2907.

⁵¹ Zimmerman, T.; Zubia, A.; Vara, Y.; Martin, E.; Sirockin, F.; Mendoza, L.; Vidal-Vanaclocha, F.; Cossío, F. P.; Blanco, F. J., *J. Med. Chem* **2013**, *56*, 735–747.

⁵² *Review of biology oriented synthesis by cycloaddition reactions*: Narayan, R.; Potowski, M.; Jia, Z.-J.; Antonchick, A. P.; Waldmann, H., *Acc. Chem. Res.* **2014**, *47*, 1296–1310.

⁵³ Galvis, C. E. P.; Kouznetsov, V. V., *Org. Biomol. Chem.* **2013**, *11*, 7372.

CHAPTER 1

Pyrrolizidine and indolizidine alkaloids are also part of bicyclic compounds including pyrrolidine or piperidine frameworks. (–)-Pyrrolam A, a pyrrolizidine with carcinogenic and mutagenic nature, is an example of naturally occurring toxic compounds. The inherent biological properties that this family exhibits have promoted the total synthesis of (–)-Supinidine and (–)-Petasinecine. Swainsonine is a polyhydroxy substituted indolizidine which presents anticancer and anti-HIV activity and works as glycosidase enzyme inhibitor.^{43a,b}

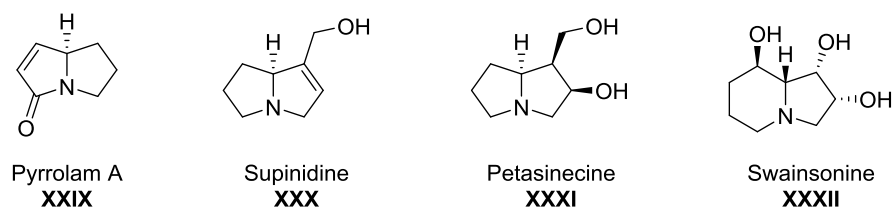
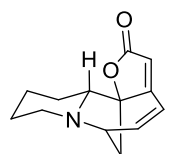


Figure 1.11. Pyrrolizidine and indolizidine natural occurring alkaloids.

1.4.2 *Securinega* alkaloids

Regarding to piperidine and pyrrolidine derivatives there is a group of bases which comprise an indolizidine (Securinine type) or pyrrolizidine (Norsecurinine type) heterocycle and a $\alpha,\beta,\gamma,\delta$ -unsaturated lactone motif which results in a highly rigid and complex skeleton. Compounds with this structure are called *Securinega* alkaloids, since they were first isolated from *Securinega Suffruticosa* plant. The first isolated compound in 1956 by Murav'eva *et al.*, named Securinine, is the most abundant in nature (**Fig. 1.12**).⁵⁴ Since then, more than 50 compounds of this family have been isolated and characterized.



Securinine-XXXIII

Figure 1.12. First isolated alkaloid from *Securinega* family.

Plants from the Euphorbiaceae family have been widely used in Chinese and Amazonian folk medicine, and are rich in such alkaloid-type natural products. More specifically, alkaloids extracted from their twigs, leaves and roots have shown a wide

⁵⁴ Murav'eva, V. I.; Ban'kovskii, A. I. *Dokl. Akad. Nauk SSSR*, **1956**, 110, 998-1000.

range of biological properties. The interest of this family has boosted different studies on its chemistry, synthesis and pharmaceutical properties.⁵⁵

1.4.2.1 *Securinega* alkaloids: structural classification

These compounds contain the previously described indolizidine and pyrrolizidine scaffold. During the last years 30 new compounds have been isolated and characterized.^{55a}

As a general rule, *Securinega* alkaloids are polycyclic compounds, usually tetracyclic, which contain a pyrrolidine or piperidine ring (A ring), which is fused with an azabicyclo octane system (B and C rings) and a butenolide moiety (D ring). Two skeleton types can be distinguished depending on the A ring size: norsecurinane skeleton (pyrrolidine) or securinane skeleton (piperidine) (**Fig. 1.13**)

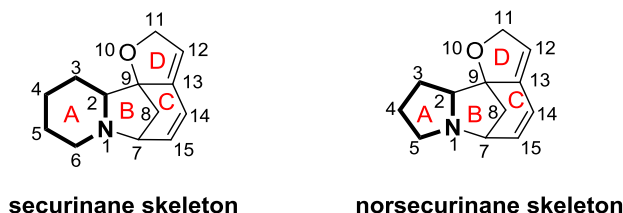


Figure 1.13. Classification depending on the size of the A ring of the alkaloid.

When the alkaloid comprises an azabicyclo[3.2.1]octane system (BC) and a piperidine ring (A), we are referring to Securinine. Some examples of this type of alkaloids are depicted in **Figure 1.14**.

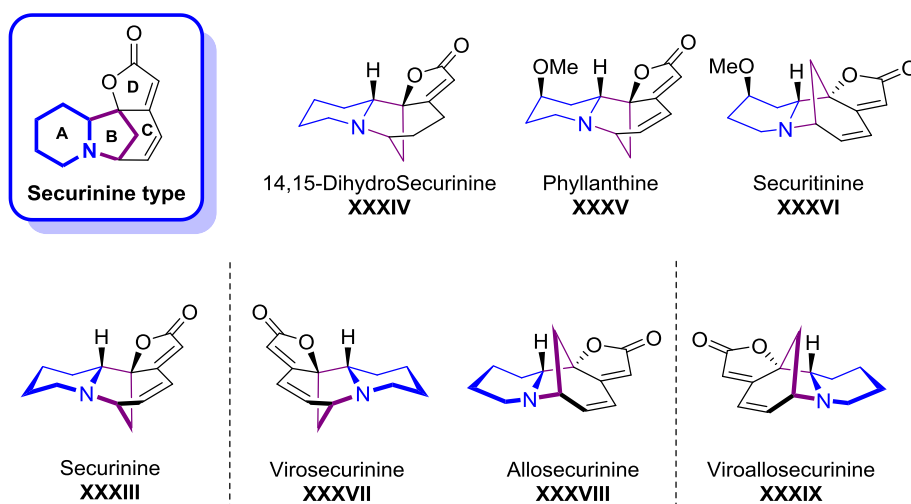


Figure 1.14. Securinine type alkaloid examples.

⁵⁵ Reviews: a) Chirkin, E.; Atkatiian, W. and Porée, F.-H. *The Alkaloids, Chapter 1: The Securinega Alkaloids*, Ed. Elsevier, Paris, **2015**. b) Weinreb, S. M., *Nat. Prod. Rep.* **2009**, 26, 758–775.

CHAPTER 1

On the contrary, when the alkaloids incorporate a pyrrolidine ring and an azabicyclo[3.2.1]octane system we make reference to norsecurinine type compounds (see **Fig.1.15**).

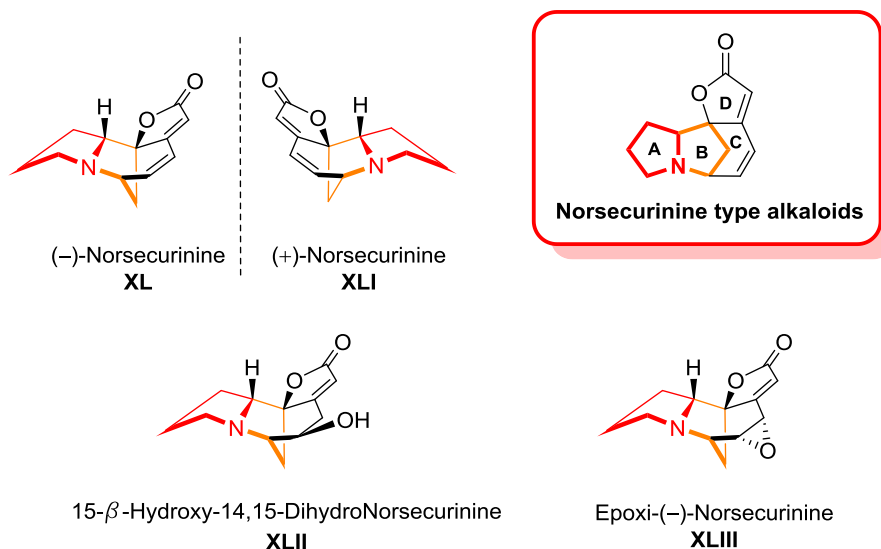


Figure 1.15. Some examples of Norsecurinine type alkaloid.

Additionally, if the molecule contains an azabicyclo[2.2.2]octane system (BC), and A is a pyrrolidine or piperidine scaffold, they are called neosecurinane (**Fig 1.16**) or neonorsecurinane (**Fig. 1.17**) type of alkaloids, respectively.

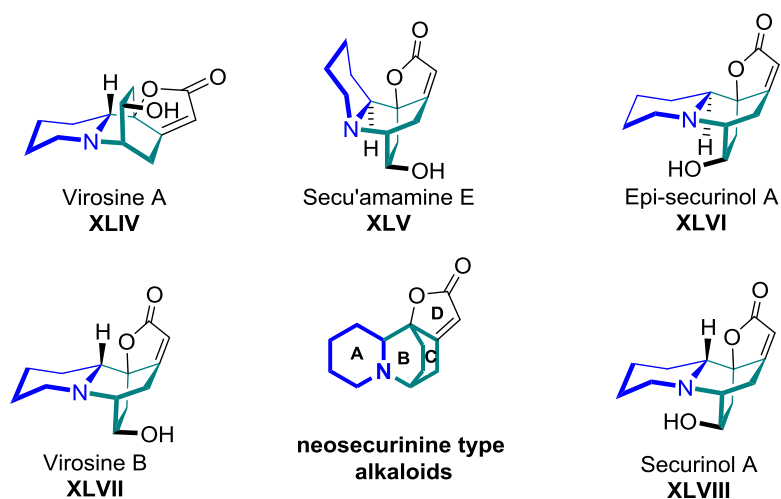


Figure 1.16. Neosecurinine type alkaloids, contain azabicyclo[2.2.2]octane system (BC) and a piperidine ring.

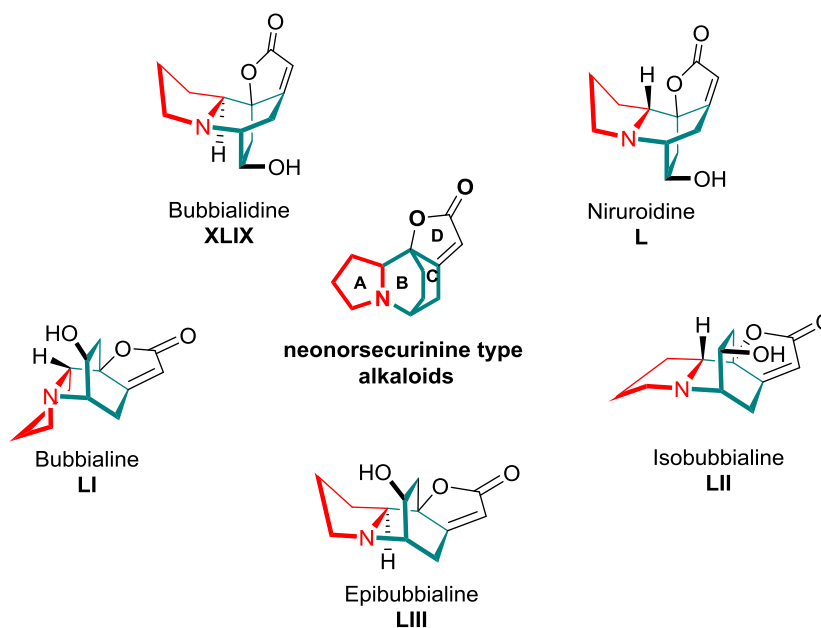


Figure 1.17. Neonorsecurinane type alkaloids, containing azabicyclo[2.2.2]octane (BC) system and pyrrolidine ring.

In addition, dimeric, trimeric and tetrameric compounds have been characterized too, termed according to the nature of the oligomeric group and generally containing a norsecurinane scaffold. Some other unique structures have been isolated and characterized containing a pentacyclic backbone featuring a 7-oxa-1-azabicyclo[3.2.1]octane ring system (Virosaine A and B, **Fig 1.17**).

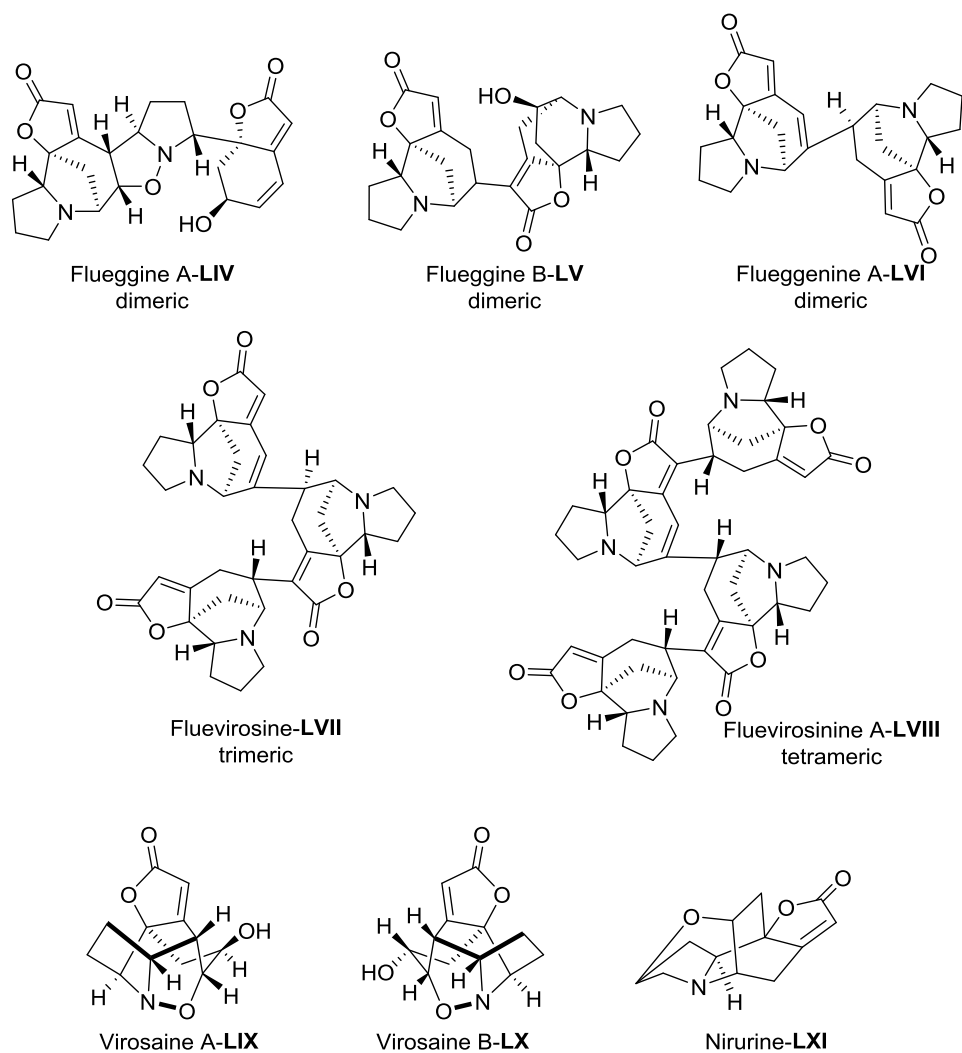


Figure 1.17. Miscellaneous alkaloids and oligomeric species.

1.4.2.2 Occurrence and biological activity of *Securinega* alkaloids

Securinega alkaloids are secondary metabolites possible to find in the plants of Euphorbiaceae family. Plants from *Securinega* (or *Flueggea*) and *Phyllanthus*⁵⁶ genus were the first ones to show the presence of these tetracyclic compounds. Later, these alkaloids were also isolated from *Margaritaria*, *Breynia* (Euphorbiaceae) and *Zygogynum pauciflorum* (Winteraceae).⁵⁷

Securinine was the first isolated alkaloid of the family. This compound was isolated from shrub of *Securinega suffruticosa*, *Margaritaria indica*, *Phyllanthus niruri*, *S. suffruticosa* var. *amamiensis*, *Phyllanthus discoides* and *Phyllanthus discoideus*.^{55a}

⁵⁶ a) Houghton, P. J.; Woldemariam, T. Z.; O'Shea, S.; Thyagarajan, S. P., *Phytochemistry* **1996**, 43, 715–717. b) Babady-Bila; Gedris, T. E.; Herz, W., *Phytochemistry* **1996**, 41, 1441–1443. c) Petchnaree, P.; Bunyapraphatsara, N.; Cordell, G. A.; Cowe, H. J.; Cox, P. J.; Howie, R. A.; Patt, S. L., *J. Chem. Soc. Perkin Trans. 1* **1986**, 1, 1551–1556.

⁵⁷ Ahond, A.; Guilhem, J.; Hamon, J.; Poupat, C.; Pusset, J.; Pusset, M.; Sevenet, T.; Potier, P., *J. Nat. Prod.* **1990**, 53, 875–881.

Securinine structure was determined in 1963 by chemical and spectroscopic studies and verified by X-ray crystallography in 1965 as a hydrobromide ammonium salt.⁵⁸ Free base crystals were obtained in 1995 and absolute configuration of this structure matched perfectly with its enantiomer Virosecurinine.⁵⁹ Finally, Thadani and coworkers were able to obtain suitable crystals for Securinine, and thus, absolute configuration was elucidated. In addition, X-ray diffraction studies confirmed the chair conformation of the piperidine ring and also the planar geometry of the butenolide moiety with respect to the double bond.⁶⁰ These compounds are known to be convulsive agents. In particular, Securinine is known to induce “strychnine like” seizures. For this reason, it was clinically used in Russia as CNS stimulating drug.⁵⁸

GABA_A receptor (GABA_AR) is a ligand-gated ion channel that admits chloride upon binding of the γ -aminobutyric acid (GABA) and can be modulated by several endogenous or therapeutically important agents.⁶¹ Therefore, in response to the binding of GABA, GABA_AR channels present an “open” conformation that permits the passing of chloride across the cell membranes, and thus, the neuronal excitability of the central nervous system is depressed.⁶² This way, anxiety, sleeping disorders, and convulsing disorders have been treated with different agonists that can enhance the action of GABA or increase the concentration of GABA at the receptor. On the other hand, antagonists that bind the GABA site of the receptor block the inhibitory action of GABA_AR. For example, Bicuculline is a competitive antagonist of these receptors and its action mimics epilepsy. Other antagonists that decline the signaling of GABA receptors can lead to hyperactive neurological disorders such as insomnia and anxiety.

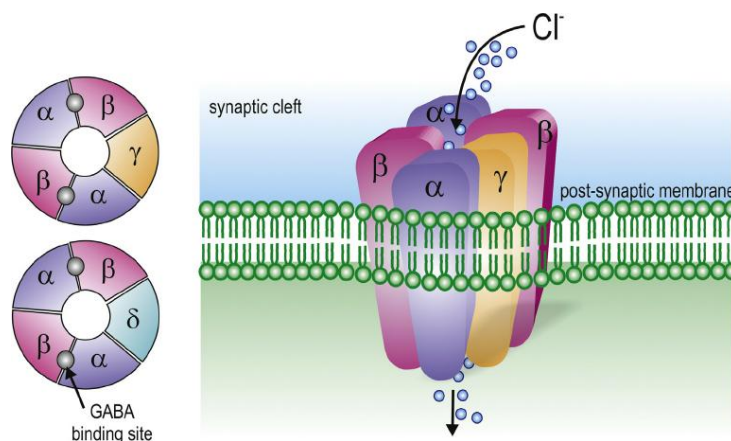


Figure 1.18. GABA_A receptor representation and transport of chloride through the cellular membrane.
Figure taken from review Brunton *et al.* ref 63.⁶³

⁵⁸ Honda, T.; Namiki, H.; Kaneda, K.; Mizutani, H., *Org. Lett.* **2004**, 6, 87–89.

⁵⁹ Luger, P.; Weber, M.; Dung, N. X.; Ky, P. T.; Long, P. K., *Acta Crystallogr. Sect. C.* **1995**, 51, 127–129.

⁶⁰ Dhudshia, B.; Cooper, B. F. T.; Macdonald, C. L. B.; Thadani, A. N., *Chem. Commun.* **2009**, 463–465.

⁶¹ Rabow, L. E.; Russek, S. J.; Farb, D. H., *Synapse* **1995**, 21, 189–274.

⁶² Miller, P. S.; Aricescu, A. R., *Nature* **2015**, 512, 270–275.

⁶³ Brunton, P. J.; Russell, J. A.; Hirst, J. J., *Prog. Neurobiol.* **2014**, 113, 106–136.

CHAPTER 1

Some studies carried out with Securinine and Dihydrosecurinine showed that both are selective antagonists of GABA_A receptors in mammalian CNS. They present affinity for GABA_A binding recognition in brain membranes of rats and specifically reduce the inhibitory effect of GABA_A on the firing of neurons of spinal cord of rats. Even they showed weaker effect than Bicuculline, Securinine salts are much more soluble in water and they are stable in a wider range of pH.^{64,65} Related to this antagonist behavior, Securinine has been used in clinical treatment for multiple sclerosis, amyotrophic lateral sclerosis (ALS) and poliomyelitis.⁶⁰

Table 1. Securinine induced activity against different cancer cell lines and antimicrobial activity.

Cancer cell line	IC ₅₀ ^{55a}	LD ₅₀ ^{55a}
HCT116 p53 – (human colon cancer)		17.5 μM
HCT116 p53 + (human colon cancer)		50 μM
SW480 (human colon cancer)	19.1 μM	
KB (human epidermoid carcinoma)	10.0 μM	
L1210 (murine lymphomia)	8.8 μM	
HL60 (human leukemia) (72 h)	18.9 μM	
Antimicrobial activity	IC ₅₀ ^{55a}	
<i>Plasmodium falciparum</i> (antiplasmodial)	24.7 μM	
MIC against <i>Enterococcus faecium</i>	4.6 mM	

Securinine has shown *in vivo* activity in mice against acute myeloid leukemia HL-60 cell line. In addition, *in vitro* studies for HL-60, THP-1 and OCI-AML3 cell lines were performed.⁶⁶ Moreover, it was reported to induce growth inhibition and apoptosis in human colon SW480 and apoptosis in human colon HCT-116 cell lines in micromolar range.^{55a} Recently, Ratovelomana-Vidal and coworkers have reported that introduction of acetylenic group bearing an aromatic chain in C-14 position (γ,δ-unsaturation) of Securinine leads to an increase of growth inhibition against HCT-116 cancer cell line (**Fig 1.19**). Furthermore, two of the compounds resulted to be highly cytotoxic in four different tumoral lines (HCT-116, colon; A-375, melanoma; HL-60 leukemia; and A549, lung).⁶⁷

⁶⁴ Beutler, J. A.; Karbon, E. W.; Brubaker, A. N.; Malik, R.; Curtis, D. R.; Enna, S. J., *Brain Res.* **1985**, 330, 135–140.

⁶⁵ a) Rognan, D.; Boulanger, T.; Hoffmann, R.; Vercauteren, D. P.; Andre, J.-M.; Durant, F.; Wermuth, C.-G., *J. Med. Chem.* **1992**, 35, 1969–1977. b) Galvez-Ruano, E.; Aprison, M. H.; Robertson, D. H.; Lipkowitz, K. B., *J. Neurosci. Res.* **1995**, 42, 666–673.

⁶⁶ Gupta, K.; Chakrabarti, A.; Rana, S.; Ramdeo, R.; Roth, B. L.; Agarwal, M. L.; Tse, W.; Agarwal, M. K.; Wald, D. N., *PLoS One* **2011**, 6, 1–10.

⁶⁷ Perez, M.; Ayad, T.; Maillos, P.; Poughon, V.; Fahy, J.; Ratovelomanana-Vidal, V., *ACS Med. Chem. Lett.* **2016**, 7, 403–407.

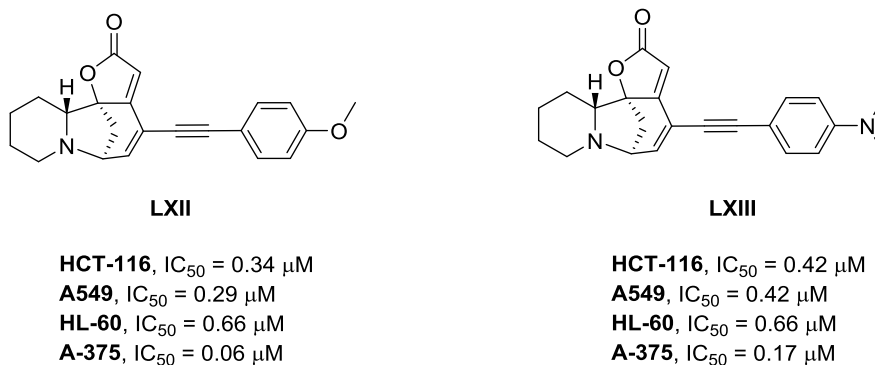


Figure 1.19. Efficient cytotoxic activity of securinine derivatives against several tumoral cell lines.

Furthermore, Securinine has been reported to inhibit ACE (angiotensin-converting enzyme) so it can be used in hypertension. Securinine and Virosecurinine have shown antibacterial activity against *Escherichia coli*, *Enterococcus faecium*, *Pseudomonas aeruginosa*, *Mycobacterium smegmatis* and *Staphylococcus aureus*.^{55a}

Securinega virosa plant was used in Asia for the treatment of pain, inflammation and cancer. From this plant, several alkaloids of the family were isolated, but special attention was paid to Virosecurinine and Viroallosecurinine. *In vitro* cytotoxic activity against P-388 lymphocytic leukemia cells induced by Virosecurinine and Viroallosecurinine was reported, exhibiting $ED_{50} = 2.9$ and $0.9 \mu g/mL$ respectively.^{68,69}

Flueggea virosa plant (Roxb. ex Willd.) has shown to contain a wide variety of alkaloids possessing interesting structural features. For example, alkaloids with a unique cage type compounds are present in the twigs of these plants. These compounds present an unprecedented 7-oxa-1-azabicyclo[3.2.1]octane scaffold and were named as Virosaine A and Virosaine B (see **Fig 1.17**). Furthermore, two additional compounds presenting an octacyclic skeleton were discovered.⁷⁰

Flueggine A presents an isoxazolidine scaffold, whereas Flueggine B, on the contrary, includes two indolizidine rings. Both are considered as dimeric species belonging to the oligomeric group of *Securinega* family (see **Fig 1.17**). Both compounds were tested on the inhibitory growth effect of three different human breast cancer cell lines: MCF-7, MDA-MB-231 and MCF-7/ADR. Flueggine B showed significant results in the inhibition on growth of MCF-7 ($IC_{50} = 135 \pm 5 nM$) and MDA-MB-231 ($IC_{50} = 147 \pm 3 nM$). In contrast, Flueggine A showed modest values for the same cell lines.⁷¹

⁶⁸ Arbain, D.; Birkbeck, A. A.; Byrne, L. T.; Sargent, M. V.; Skelton, B. W.; White, A. H., *J. Chem. Soc. PerkinTrans 1*, **1991**, 1863–1869.

⁶⁹ Tatematsu, H.; Mori, M.; Yang, T.-H.; Chang, J.-J.; Tung-Ying Lee, T.; Kuo-Hsiung, L., *J. Pharm. Sci.* **1991**, 80, 325–327.

⁷⁰ Zhao, B. X.; Wang, Y.; Zhang, D. M.; Huang, X. J.; Bai, L. L.; Yan, Y.; Chen, J. M.; Lu, T. B.; Wang, Y. T.; Zhang, Q. W.; et al., *Org. Lett.* **2012**, 14, 3096–3099.

⁷¹ a) Zhao, B. X.; Wang, Y.; Zhang, D. M.; Jiang, R. W.; Wang, G. C.; Shi, J. M.; Huang, X. J.; Chen, W. M.; Che, C. T.; Ye, W. C., *Org. Lett.* **2011**, 13, 3888–3891. b) Han, J.-C.; Li, C.-C., *Synlett* **2015**, 26, 1289–1304.

CHAPTER 1

1.4.2.3 Biosynthesis of *Securinega* alkaloids

Alkaloids from *Securinega* family have shown distinctive tetracyclic backbones comparing to other alkaloids obtained from natural sources. Due to the large abundance of Securinine the biosynthetic pathway of it has been principally studied. These studies mainly consisted in degradation and feeding experiments by administration of radiolabeled precursors.

Elucidation of the biosynthetic pathway was dependent on two features: the origin of the piperidine ring and the synthetic process leading to the CD rings (which include $\alpha,\beta,\gamma,\delta$ -unsaturated lactone). By extrapolation with other piperidine alkaloids it was proposed that A ring could derive from lysine. It was reported that lysine could be transformed into cadaverine and finally could lead to Δ -piperideine. Radioactive ^{14}C lysine and 1,5- ^{14}C cadaverine were incorporated into the plant, and it was observed that proportion of labeled carbons was equally distributed in the piperidine ring, confirming the origin of A ring.⁷²

Scheme 1.2 presents a plausible biosynthetic pathway for Securinine proposed by Parry. The origin of CD ring was elucidated by means of experiments with radioactive tyrosine and phenylalanine. As a result, it was established that CD ring is generated from tyrosine.⁷³ As lysine showed to be decarboxylated in order to give cadaverine, one of the hypotheses suggests that it could be possible to observe a second decarboxylation right after the reaction between C and A rings that affords compound **LXIX**. Mechanism of union between the C and A moieties remains still unknown nowadays. Compound **LXX** would possibly present a decarboxylation and a following oxidation, which would tend to be followed by an oxa-Michael reaction giving compound **LXXI**. This molecule already includes the fused CD ring structure. Aminoalcohol **LXXII** would undergo through a subsequent nucleophilic substitution which gives rise to Securinine-**XXXIII**.⁷⁴

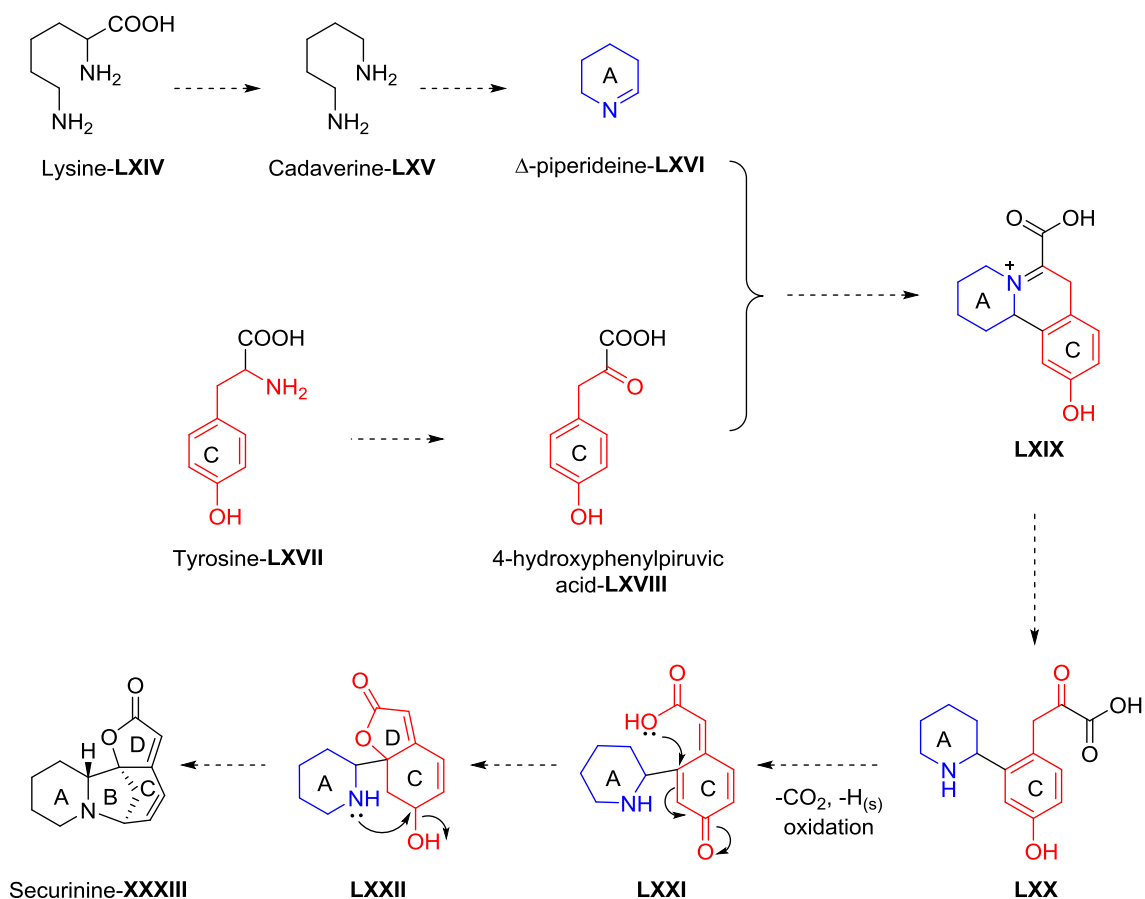
In 1984, bicyclic lactones (–)-Menisdaurilide-**LXXIV** and (–)-Aquilegiolide-**LXXV** were isolated from *Aquilegia atrata*, besides of their presence in plants of the genus *Securinega* and *Phyllanthus*. In literature, there is no biosynthetic route proposed for these lactones, but as they resemble to another natural product called rengyolone, their origin is presumed to be in shikimic acid. Due to the structural similarity of the CD rings, bicyclic lactones were suggested as intermediates in the biosynthesis of Securinine by Font and coworkers (**Scheme 1.3**).⁷⁵ Actually, the plausible biosynthetic route proposed by Font corresponds with previous labeling experiments. The main difference for the route of Font comparing to the one proposed by Parry is that the piperidine (A ring) would be directly coupled to bicyclic compound **LXXIII** which includes already CD fused rings. In line with Parry's proposal, corresponding aminoalcohol **LXXII** would react via a nucleophilic substitution to afford Securinine.⁷⁵

⁷² a) Sankawa, U.; Yamasaki, K.; Ebizuka, Y., *Tetrahedron Lett.* **1974**, 21, 1867–1868. b) Sankawa, U.; Ebizuka, Y.; Yamasaki, K., *Phytochemistry* **1977**, 16, 561–563. c) Golesbiewski, W. M.; Horwood, P.; Spenser, I. D., *Chem. Commun.* **1976**, 217–218.

⁷³ a) Parry, R. J., *Tetrahedron Lett.* **1974**, 4, 307–310. b) Parry, J., *Chem. Commun.* **1975**, 144–145.

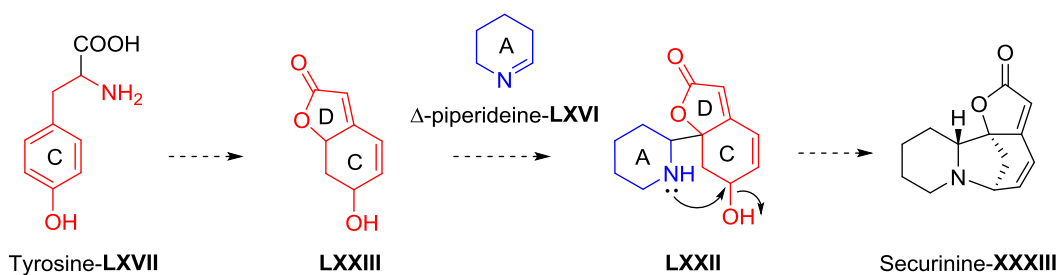
⁷⁴ Parry, R., *Bioorg. Chem.* **1978**, 7, 277–288.

⁷⁵ Bardají, G. G.; Cantó, M.; Alibés, R.; Bayón, P.; Busqué, F.; De March, P.; Figueredo, M.; Font, J., *J. Org. Chem.* **2008**, 73, 7657–7662.

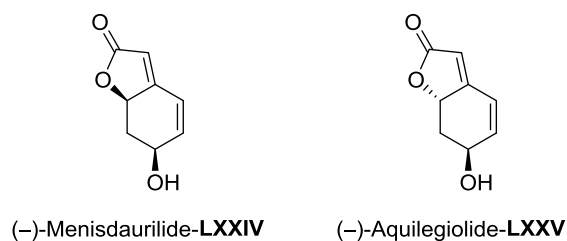


Scheme 1.2. Plausible biosynthesis of Securinine proposed by Parry and coworkers.

a)



b)



Scheme 1.3. a) Plausible biosynthesis of Securinine proposed by Font and coworkers. b) Bicyclic lactones (-)-Menisdaurilide-LXXIV and (-)-Aquilegolide-LXXV.

CHAPTER 1

1.5 Endocannabinoid system and cannabinoid ligands

Medicinal use of plant *Cannabis Sativa* has a millenarian history, starting from 2600 B.C. in the Chinese empire. Taking cannabis was recommended for rheuma, relief of cramps and menstrual pain. However, it was not until the end of nineteenth century when its great therapeutic potential was shown to the Western world.⁷⁶ Three major compounds of marijuana are Δ^9 -tetrahydrocannabinol (Δ^9 -THC), cannabinol (CBN) and cannabidiol (CBD) (**Fig 1.20**). Unlike Δ^9 -THC, the last two composes are non-psycotropic phytocannabinoids.⁷⁷ These active constituents of *Cannabis Sativa* have been widely used as drugs and medicines.⁷⁸

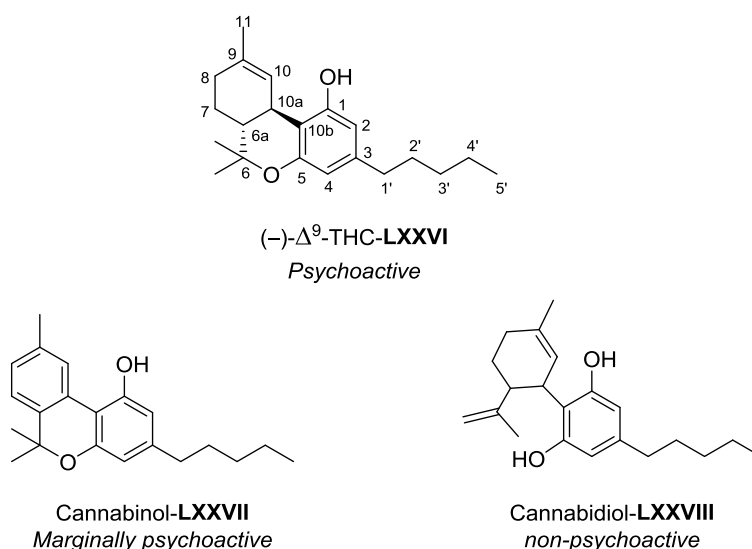


Figure 1.20. Classical cannabinoid ligands and components of *Cannabis Sativa*.

On the other hand, the endogenous cannabinoid system (ECS) includes cannabinoid receptors, endocannabinoids (such as 2-arachidonoyl glycerol, anandamide), and enzymes for the synthesis and inactivation (reuptake and degradation) of previous endocannabinoids. The name of the system was attributed to the fact that the first ligand to have effect on the receptors was the psychoactive compound of cannabis Δ^9 -THC. This system is implicated in a growing number of physiopathological conditions in the central nervous system (CNS) and peripheral system, as it is also involved in a broad range of functions. In addition, it has shown to be implicated in appetite, metabolic functions, food intake, neuroprotection, modulation of nociception, antitumor effects and immune and inflammatory responses. For these reasons, it is an attractive target for the development of new drugs which act as ligands

⁷⁶ Di Marzo, V.; Bifulco, M.; De Petrocellis, L., *Nat. Rev. Drug Discov.* **2004**, 3, 771–784.

⁷⁷ Cumella, J.; Hernández-Folgado, L.; Girón, R.; Sánchez, E.; Morales, P.; Hurst, D. P.; Gómez-Cañas, M.; Gómez-Ruiz, M.; Pinto, D. C. G. A.; Goya, P., *ChemMedChem* **2012**, 7, 452–463.

⁷⁸ Samson, M.-T.; Small-Howard, A.; Shimoda, L. M. N.; Koblan-Huberson, M.; Stokes, A. J.; Turner, H., *J. Immunol.* **2003**, 170, 4953–4962.

and interact with the corresponding receptors.⁷⁹ The importance of the mentioned interaction between the ECS and endocannabinoids or cannabinoid ligands relies on the cannabinoid receptors.

Cannabinoid receptors are G-protein coupled receptors (GPCR) which are integral membrane proteins characterized by seven hydrophobic transmembrane helices and connected by three intracellular and three extracellular loops.⁸⁰ Two types of cannabinoid receptors were identified. CB1 receptor was the first one to be cloned and is mainly expressed in the CNS, while CB2 receptors are preferentially found in peripheral immune cells and tissues. Determination of the latter receptors has been lagged due to their low abundance. CB1 and CB2 receptors have been found in a few tissues.

CB1 receptors mediate in the inhibition processes of release of several neurotransmitters, such as acetylcholine, noradrenaline, dopamine, γ -aminobutyric acid, glutamate, D-aspartate, etc. They possess one or more allosteric sites that can be targeted by different ligands that, in turn, can enhance or inhibit activation of the receptor by exogenous administration or endogenous release of direct agonist.⁸¹ CB2 receptors have been studied in a lesser extent. However, their targeting has become very important in order to avoid undesired CNS related adverse effects generated by the activation of CB1 receptors.

Several cannabinoid ligands that bind CB1 and CB2 receptors have been discovered and synthesized in the last 30 years. On one hand, non-selective cannabinoid ligand Nabilone (synthetic analogue of Δ^9 -THC, also known as Cesamet®) was the first licensed medicine to be used in the suppression of nausea and vomiting for patients treated from chemotherapy and chronic pain.⁸¹

Some molecules have shown significant selectivity toward CB1 or CB2 receptors. This fact is of great importance in order to induce different biological responses. For example, diarylpyrazole SR141716 showed remarkable selectivity toward CB1 receptor as an antagonist.⁸² Therefore, it was marketed for obesity treatment as Rimonabant (Acompliat®). Unfortunately, after its commercialization several cases of suicides and depression were reported and the sales of this medicine were halted. This is a notable example of the CNS side effects related to the binding of CB1 receptors.

⁷⁹ a) Salo, O. M. H.; Raitio, K. H.; Savinainen, J. R.; Nevalainen, T.; Lahtela-Kakkonen, M.; Laitinen, J. T.; Järvinen, T.; Poso, A., *J. Med. Chem.* **2005**, *48*, 7166–7171. b) Scrima, M.; Di Marino, S.; Grimaldi, M.; Mastrogiacomo, A.; Novellino, E.; Bifulco, M.; D'Ursi, A. M., *Biochemistry* **2010**, *49*, 10449–10457. c) Mackie, K., *J. Neuroendocrinol.* **2008**, *20*, 10–14.

⁸⁰ Montero, C.; Campillo, N. E.; Goya, P.; Pérez, J. A., *Eur. J. Med. Chem.* **2005**, *40*, 75–83.

⁸¹ Pertwee, R. G., *Br. J. Pharmacol.* **2009**, *156*, 397–411.

⁸² Rinaldi-Carmona, M.; Pialot, F.; Congy, C.; Redon, E.; Barth, F.; Bachy, A.; Brelière, J.-C.; Soubrié, P.; Le Fur, G., *Life Sci.* **1996**, *58*, 1239–1247.

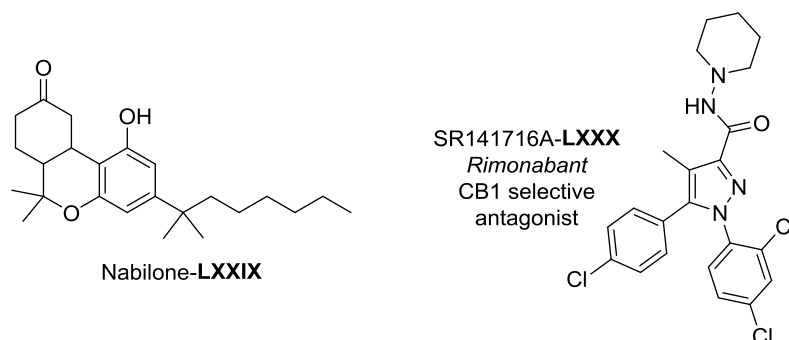


Figure 1.21. Structure of Nabilone, first licensed medicine, and Rimonabant, antiobesity agent.

More recently, Jagerovic *et al.* described the synthesis of chromenopyrazoles inspired by the structure of Cannabinol. These compounds demonstrated selectivity for CB1 receptor, probably due to its interaction with the pyrazole moiety. The effect of compound **XXVI** in peripheral CB1 receptors was confirmed by measuring its nociceptive response for orofacial pain in rat model.⁸³

Later, additional structural modifications of chromenopyrazole **LXXXI** were implemented, which gave rise to the synthesis of 36 different derivatives covering the structural diversity. Among these compounds chromenoisoxazole **PM226-LXXXII** showed great affinity for CB2 receptor as agonist. In addition, **PM226-LXXXII** has been tested in acute inflammatory phase of the TMEV model (Theiler's murine encephalomyelitis virus), its administration resulted in a significant reduction of the microglial activation.⁸⁴

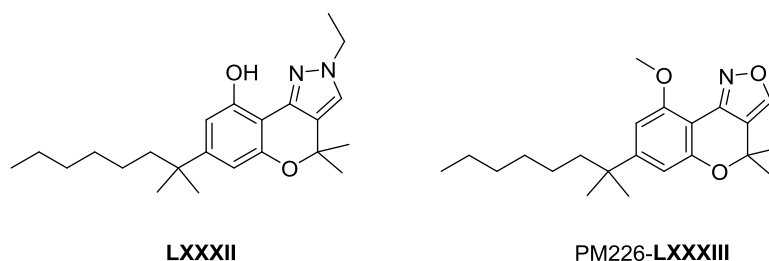


Figure 1.22. **XXVI** chromenopyrazole and chromenoisoxazole **PM226**, tested in acute inflammatory phase of TMEV model.

⁸³ Cumella, J.; Hernández-Folgado, L.; Girón, R.; Sánchez, E.; Morales, P.; Hurst, D. P.; Gómez-Cañas, M.; Gómez-Ruiz, M.; Pinto, D. C. G. A.; Goya, P.; Martín, M. I.; Fernández-Ruiz, J.; Silva, A. M. S.; Jagerovic, N., *ChemMedChem*, **2012**, 7, 452–463.

⁸⁴ Morales, P.; Gómez-Cañas, M.; Navarro, G.; Hurst, D. P.; Carrillo-Salinas, F. J.; Lagartera, L.; Pazos, R.; Goya, P.; Reggio, P. H.; Guaza, C.; Franco, R.; Fernández-Ruiz, J.; Jagerovic, N., *J. Med. Chem.* **2016**, 59, 6753–6771.

CHAPTER 2

Synthesis of Tricyclic Molecules by Ferrocenyl-Proline Catalyzed Enantioselective (2+1) and (3+2) Cycloaddition Reactions

2.1 Cycloaddition reactions

Cycloaddition reactions are pericyclic reactions in which two new σ -bonds are generated as the result of the addition of two π -systems. Diels-Alder and 1,3-dipolar reactions are the most characteristic type of cycloaddition reactions and represent a versatile route for the synthesis of cyclic compounds with a high degree of stereoselectivity.¹

In order to understand the stereochemistry of this type of reactions it is necessary to explain the possible addition modes for the two unsaturated systems. Therefore, it is considered as a *suprafacial* approach if molecular orbitals (MOs) of one conjugated system are added to the other on the same face (see **Fig. 2.1**). On the contrary, if addition of MOs occurs through opposite faces is termed as an *antarafacial* approach. *Antarafacial* overlap in cycloaddition reactions would need a long flexible conjugated system, and therefore, almost all pericyclic cycloaddition reactions occur through a *suprafacial* addition mode.^{1b}

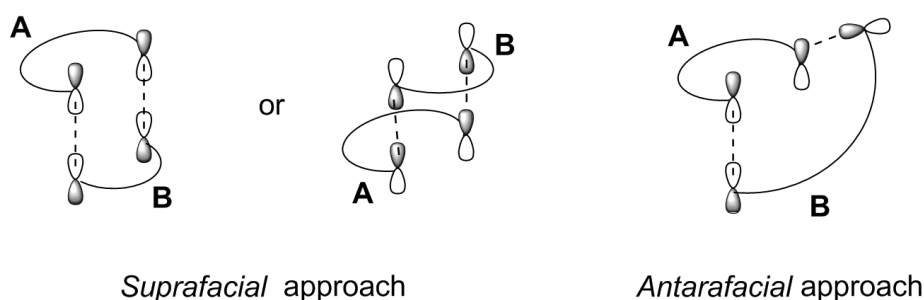


Figure 2.1. *Suprafacial* and *antarafacial* approach for cycloaddition reactions.

Other classification depends on the transition state of the cycloaddition. As it is depicted in **Figure 2.2** MOs can approach in a *suprafacial* mode but can undergo through two different transition states, *endo* or *exo*. Considering that a π -system bears a certain substituent (-R), an *endo* attack is referred to a transition state in which the substituent of a π -system is oriented toward the other π -system. On the contrary, it is considered an *exo* attack when the substituent is oriented away from the second π -system during the transition state of the reaction.^{1a}

¹ a) Fleming, I., *Pericyclic Reactions*, Oxford University Press, Oxford, **1999**. b) Kumar, S.; Kumar, V.; Singh, S. P., *Pericyclic Reactions: A Mechanistic and Problem-Solving Approach*, Elsevier Academic Press, London, **2015**.

CHAPTER 2

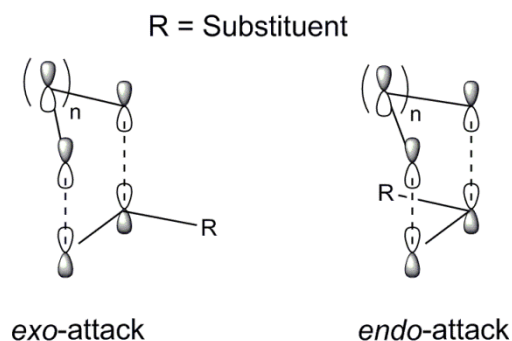


Figure 2.2. *Exo* and *endo* attack, respectively.

In addition to the possible approaches and transition states involved in cycloaddition reactions other parameters are of great importance to understand their possible stereochemistry and viability. Woodward and Hoffman's concept of *conservation of orbital symmetry* is one of the bases for the development of a method to predict the feasibility of cycloadditions reactions. Therefore, orbital symmetry correlation diagram method permits predicting thermally or photochemically allowed cycloadditions by identifying the symmetry properties of the MOs during the bond forming and breaking with respect the symmetry elements (C_2 and σ). Afterwards, correlation diagrams are drawn, and MOs are connected to their products, in this way predicting symmetry allowed or symmetry forbidden processes.

On the other hand, perturbation molecular orbital (PMO) method predicts the feasibility of a cycloaddition reaction by studying the *supra-* or *antarafacial* approach of the conjugated systems and the electrons involved ($4n+2$ or $4n$) in the reaction process as well as the aromaticity of the transition state.

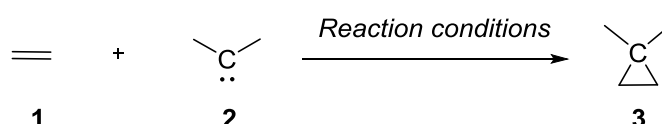
Additionally, in the frontier molecular orbital (FMO) method the viability of the cycloaddition depends on the symmetry properties of highest occupied molecular orbitals (HOMO) of one reactant and lowest unoccupied molecular orbital (LUMO) of the other. A favorable bonding is allowed if the lobes of the HOMO and LUMO orbitals participating present the same phases. Selection rules for cycloadditions by FMO method are shown in **Table 1**.^{1a}

Table 1. FMO method permits to predict required conditions for pericyclic cycloadditions to happen.

Number of e^-	Stereochemical mode of action	Reaction condition
$4n$	Supra-supra Antara-antara	$h\nu$
$4n$	Supra-antara Antara-supra	Thermal
$4n+2$	Supra-supra Antara-antara	Thermal
$4n+2$	Supra-antara Antara-supra	$h\nu$

2.1.1 (2+1) Cycloaddition Reactions

Cyclopropanes have emerged as interesting compounds because of their biological and pharmaceutical properties, as well as they are valuable building blocks. Their synthesis has been extensively studied through (2+1) cycloaddition reactions involving alkenes (2 pairs of electrons) and carbenes (sole electron pair). Transition metals are usually involved in the formation of the carbenoid species. Asymmetric synthesis of cyclopropanes usually requires the combination of these transition metals with a variety of chiral ligands.



Scheme 2.1. General (2+1) cycloaddition reaction of alkenes with carbenoids in order to give rise to cyclopropanes.

2.1.1.1 Importance of cyclopropanes in nature and chemistry

Cyclopropane ring is present in a large amount of natural products, insecticides and pharmaceutical drug candidates. Furthermore, cyclopropanes are versatile intermediates due to their reactivity, which makes them important building blocks in organic chemistry. Actually, activated cyclopropane rings are important synthons as they act as electrophiles. Multi-substituted cyclopropanes have shown several pharmaceutical applications such as, antibacterial, antifungal, antiviral, anticancer, antitumoral, and antimicobacterial properties, among others.² For example, Pyrethrums **4A** extracted from *Chrysanthemum cinerariaefolium* and *C. coccineum* plants have exhibited powerful activity as insecticide (**Fig. 2.3**).

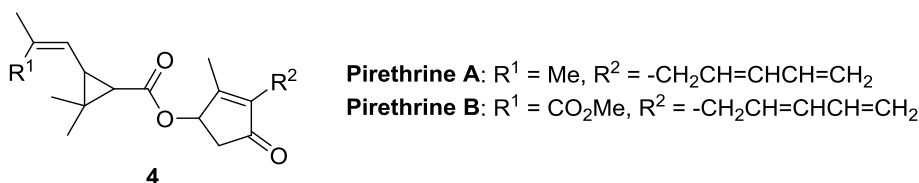


Figure 2.3. Pyrethrums examples Pyrethrine A and B.

Betulins and their derivatives bearing a cyclopropane moiety exhibited excellent cytotoxic activities against human melanoma Colo38 and Bro cell lines, as well as in human ovarian carcinoma CaOv cell line.³ Five new pestaloficiols A-E showed

² Ajay Kumar, K., *Int. J. Pharm. Pharm. Sci.* **2013**, 5, 454–459.

³ Symon, A. V.; Veselova, N. N.; Kaplun, A. P.; Vlasenkova, N. K.; Fedorova, G. A.; Liutik, A. I.; Gerasimova, G. K.; Shvrt, V.I. *Bioorg. Khim.* **2005**, 31, 320-325.

CHAPTER 2

inhibitory effects on HIV-1 replication in C8166 cells.⁴ In addition, phenyl cyclopropyl methanones were synthesized and evaluated for their activity against tuberculosis H37 Rv, showing *in vitro* MICs ranging from 25 to 3.125 $\mu\text{g/mL}$.⁵

Curacin A is a natural product which exhibited cytotoxic activity against L1210 leukemia cell line and CA46 for Burkitt lymphoma cell lines. Cilastatin and Ambruticin are also some of the natural occurring products containing the cyclopropane ring; Cilastatin inhibits the activity of β -lactam antibiotic *Imipenem*, and Ambruticin present oral activity against histoplasmosis and coccidiomycosis fungal infections (**Fig. 2.4**).⁶

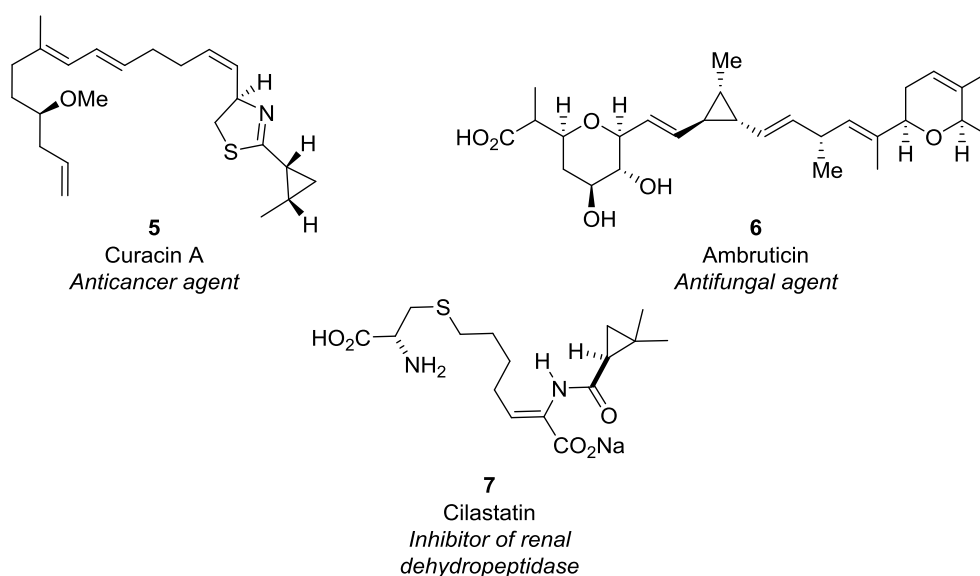


Figure 2.4. Naturally occurring examples of cyclopropane compounds.

2.1.1.2 Metal catalyzed cyclopropanation reactions between alkenes and diazocompounds

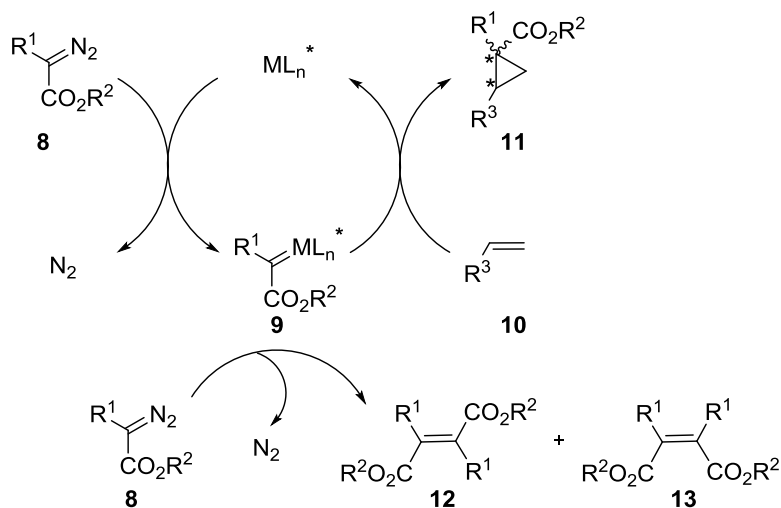
Among all the methods to prepare cyclopropanes, addition to an alkene of a carbene coming from a diazo compound has been widely studied in the last decades. At first, the formation of these compounds was accomplished either thermally or photochemically, but the use of transition-metal catalysts led to the control of the selectivity of the reaction. In a typical olefin cyclopropanation, olefin reacts with a diazo compound in the presence of a catalyst. Substitution on the olefins leads to two possible diastereoisomers, *cis* and *trans*. Each diastereoisomer can give rise in turn to two enantiomers. However, in most of the cases, the same catalyst that promotes the cyclopropanation reactions can yield non-desired side reactions.

⁴ Liu, L.; Tian, R.; Liu, S.; Chen, X.; Guo, L.; Che, Y., *Bioorganic Med. Chem.* **2008**, 16, 6021–6026.

⁵ Dwivedi, N.; Tewari, N.; Tiwari, V. K.; Chaturvedi, V.; Manju, Y. K.; Srivastava, A.; Giakwad, A.; Sinha, S.; Tripathi, R. P., *Bioorg Med Chem Lett.*, **2005**, 15, 4526–4530.

⁶ Donaldson, W. A., *Tetrahedron* **2001**, 57, 8589–8627.

CYCLOADDITION REACTIONS



Scheme 2.2. Catalytic cycle for the olefin cyclopropanation reaction with diazoacetate compounds in presence of transition metals, and homocoupling side reaction.

It is well known that the reaction occurs through a metalcarbene intermediate, which is formed between the catalyst precursor and the diazo compound. The homocoupling side reaction takes place very fast, so, in order to avoid side products and promote the formation of the three membered rings, slow addition of the diazo compound into the catalyst/olefin solution is employed.⁷ Since the development by Nozaki and Noyori in 1966 for the first enantioselective intermolecular cyclopropanation reaction using copper(II) salt and salicylaldehyde as ligand, this methodology has emerged as the most efficient and direct routes to obtain optically active cyclopropanes. Since then, a variety of chiral ligands have been developed.^{7,8}

Although good to excellent enantioselectivities are usually observed, diastereocontrol of the reaction has found to be more difficult to induce. The hypothesis was that the interaction between the metalcarbene and the olefin takes place far from the chiral induction area, and thus, is responsible for this lack of diastereocontrol.

However, in the last two decades some catalysts have been reported to be able to induce a good to excellent selectivity toward *cis* or *trans* adducts. Some other variables that can affect the final outcome are the substituents of the diazo compound, and the substituents of the alkene.⁷

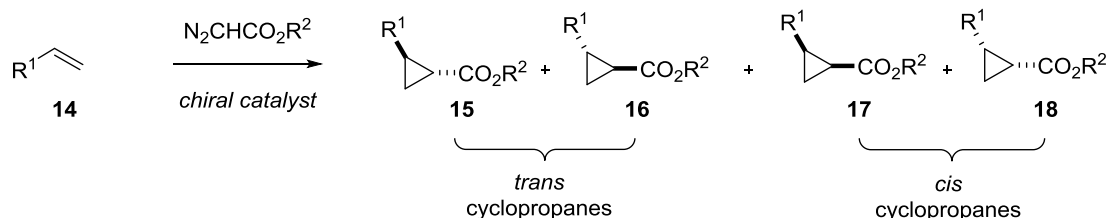
⁷ Caballero, A.; Prieto, A.; Díaz-Requejo, M. M.; Pérez, P. J., *Eur. J. Inorg. Chem.* **2009**, 1137–1144.

⁸ a) Doyle, M. P.; Protopopova, M. N., *Tetrahedron* **1998**, *54*, 7919–7946. b) Lebel, H.; Marcoux, J.-F.; Molinaro, C.; Charette, A. B., *Chem. Rev.* **2003**, *103*, 977–1050. c) Bartoli, G.; Bencivenni, G.; Dalpozzo, R., *Synthesis*, **2014**, *46*, 979–1029.

CHAPTER 2

2.1.1.3 Chiral ligands and transition metals in enantioselective cyclopropanation

Several transition metals have been studied in cyclopropanation reactions and each one has shown interesting properties depending on the chiral ligand. Cu, Rh, Ru, Co, Os, Fe, Pd, Pt and Ir have been reported to catalyze (2+1) cycloaddition reactions.



Scheme 2.3. Olefin cyclopropanation reaction with diazoacetate and formation of *cis/trans* cyclopropanes.

Regarding to the *trans* selectivity, copper ligands have shown the widest scope, while rhodium catalyst are very efficient but not as *trans* selective. Ruthenium catalysis also has exhibited good diastereoselectivity but in a narrower scope. Instead, cobalt catalysts have preferred *cis* selectivity but the structures of the ligands are more complex.^{8b}

Starting with copper catalyzed processes, ligands like salicylaldimines, semicorrins, bis(oxazolines) and bipyridines are efficient ligands in (2+1) cycloadditions (see Fig. 2.5). Since 1986, when Pfaltz⁹ discovered the high enantiocontrol induced by semicorrin ligand **19** for reaction with styrene, even more effective ligands have been developed. Many bis(oxazoline) and related bidentate ligands have been reported. Copper complex of bis(oxazoline) **20** discovered by Evans demonstrated excellent results in styrene reaction and with 1,1-disubstituted alkenes. Further reactions with cyclic silyl enol ethers, furans and vinyl fluorides were also described.^{8b,10} Masamune developed bis(oxazoline) ligand **21**, which was not efficient for cyclopropanation of styrene but turned out to be good enough for trisubstituted and unsymmetrically 1,2-disubstituted alkenes.¹¹ Some bipyridine derived ligands **22**¹², **23**¹³ and diamine **24**¹⁴ gave also good results.^{8b} Bisazaferrocene ligand **25** gave very high enantioselectivities with monosubstituted alkenes.¹⁵

⁹ Fritschi, H.; Leutenegger, U.; Pfaltz, A. *Angew.Chem., Int. Ed.* **1986**, 25, 1005-1006.

¹⁰ Evans, D. A.; Woerpel, K. A.; Hinman, M. M.; Faul, M. M. *J. Am. Chem. Soc.* **1991**, 113, 726-728.

¹¹ Lowenthal, R. E.; Masamune, S. *Tetrahedron Lett.* **1991**, 32, 7373-7376.

¹² Ito, K.; Katsuki, T. *Tetrahedron Lett.* **1993**, 34, 2661-2664.

¹³ Kwong, H.-L.; Lee, W.-S.; Ng, H.-F.; Chiu, W.-H.; Wong, W.-T. *J. Chem. Soc. Dalton Trans.* **1998**, 21, 1043-1046.

¹⁴ Kanemasa, S.; Hamura, S.; Harada, E.; Yamamoto, H. *Tetrahedron Lett.* **1994**, 35, 7985-7988.

¹⁵ Lo, M. M.-C.; Fu, G. C. *J. Am. Chem. Soc.* **1998**, 120, 10270-10271.

CYCLOADDITION REACTIONS

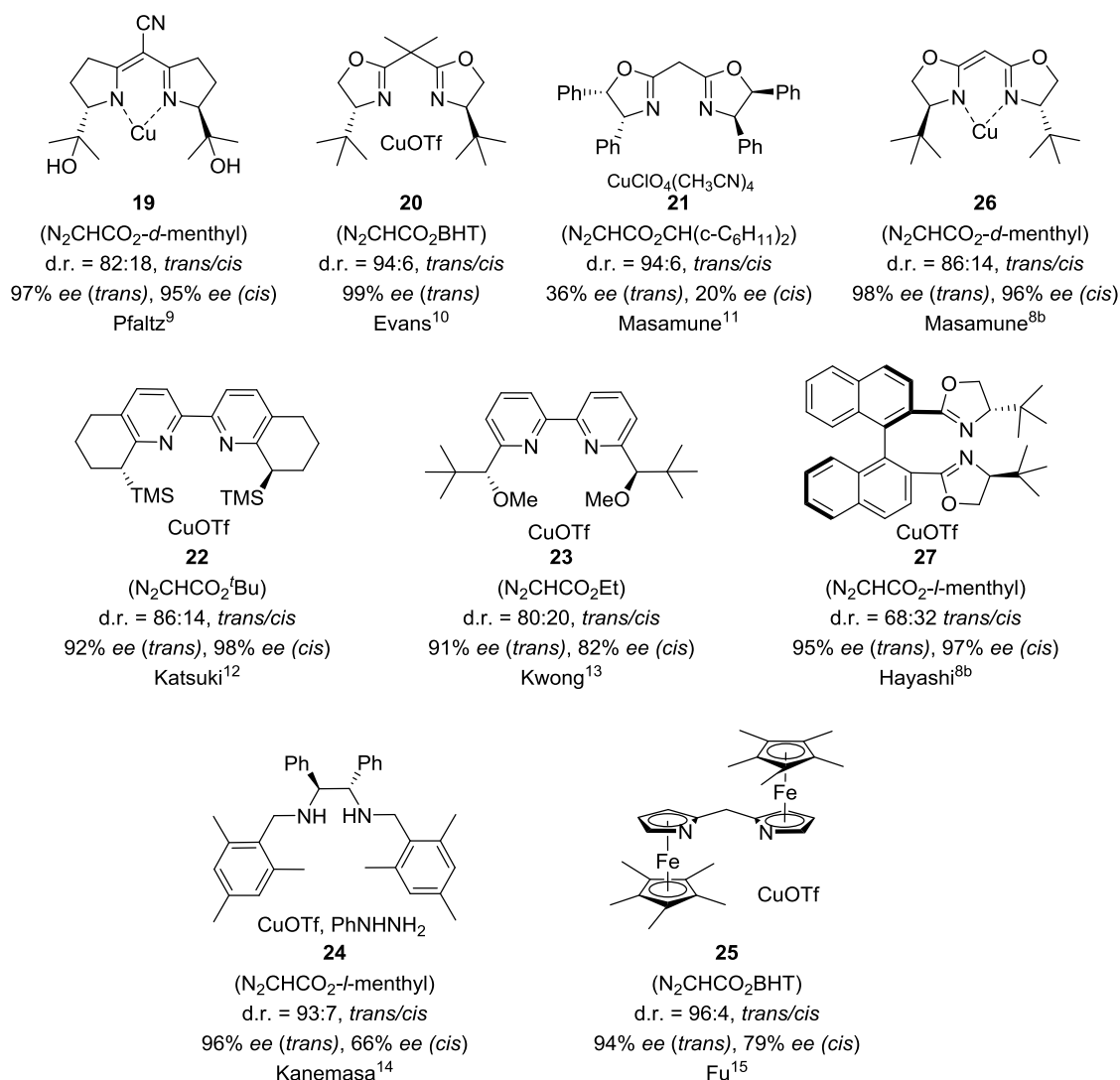


Figure 2.5. Successful ligands and complexes in copper catalyzed styrene cyclopropanation reaction.

In general, ruthenium carbenes are less reactive than copper and rhodium ones. Aryl alkenes are efficiently converted into the corresponding cyclopropanes but they are not that efficient for alkyl substituted alkenes. First cyclopropanation with a ruthenium Pybox complex **28** was reported by Nishiyama (**Fig. 2.6**). Excellent results were reported for *trans* cyclopropanes.¹⁶ Apart from Pybox systems, ruthenium porphyrin **29**¹⁷ and Schiff bases **30**^{18,19} produced excellent enantio- and diastereocontrol. On the other hand, Mezzetti and Katsuki reported some ruthenium based catalysts, like **31**, which showed good to excellent *cis* diastereoselectivity.²⁰

¹⁶ Nishiyama, H.; Itoh, Y.; Matsumoto, H.; Park, S.-B.; Itoh, K. *J. Am. Chem. Soc.* **1994**, 116, 2223-2224.

¹⁷ Lo, W.-C.; Che, C.-M.; Cheng, K.-F.; Mak, T. C. W. *J. Chem. Soc., Chem. Commun.* **1997**, 1205-1206.

¹⁸ Munslow, I. J.; Gillespie, K. M.; Deeth, R. J.; Scott, P. *J. Chem. Soc., Chem. Commun.* **2001**, 1638-1639.

¹⁹ Tang, W.; Hu, X.; Zhang, X. *Tetrahedron Lett.* **2002**, 43, 3075-3078.

²⁰ a) Stoop, R. M.; Bauer, C.; Setz, P.; Wörle, M.; Wong, T. Y. H.; Mezzetti, A. *Organometallics*, **1999**, 18, 5691-5700. b) Uchida, T.; Irie, R.; Katsuki, T. *Synlett*, **1999**, 1793-1795.

CHAPTER 2

Ruthenium Salen complexes **32** showed to be highly enantioselective in the cyclopropanation of 1,1-disubstituted alkenes when reacted with ethyl diazoacetate.²¹

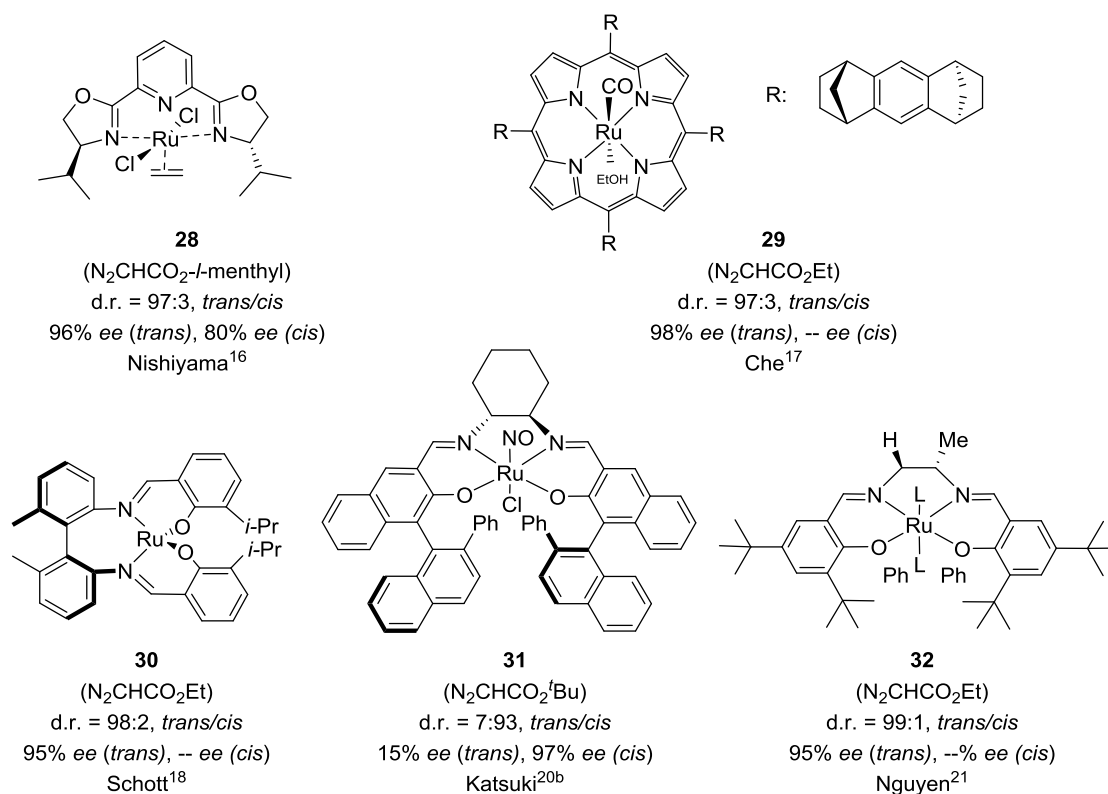


Figure 2.6. Ruthenium-complexes for olefin cyclopropanation reaction using Salen type ligands, Schiff bases and porphyrins.

Cyclopropanation of olefins catalyzed by cobalt complexes was the first enantioselective reaction reported, even though the ee values were low.²² Yamada developed an excellent complex **33** for the *trans* selective cyclopropanation of monosubstituted alkenes.²³ Katsuki published the synthesis of different ligands that exhibited *trans* or *cis* selectivity; *trans* selective Salen cobalt complex **34** catalyzed reaction of styrene showing excellent enantioselectivity.²⁴ *Cis* selective synthesis of enantiopure cyclopropanes employing monosubstituted alkenes catalyzed by cobalt and Salen ligand **35** demonstrated its efficiency. However, when disubstituted alkenes were used the enantiocontrol was excellent but the diastereoselectivity slightly decreased.²⁵

²¹ Miller, J. A.; Jin, W. C.; Nguyen, S. T. *Angew.Chem., Int. Ed.* **2002**, 41, 2953-2956.

²² Nozaki, H.; Moriuti, S.; Takaya, H.; Noyori, R. *Tetrahedron Letters*, **1966**, 5239-5244.

²³ Ikeno, T.; Sato, M.; Yamada, T. *Chem. Lett.* **1999**, 1345-1346.

²⁴ Fukuda, T.; Katsuki, T. *Synlett*, **1995**, 825-826.

²⁵ Ito, Y. N.; Katsuki, T. *Bull. Chem. Soc. Jpn.* **1999**, 72, 603-619.

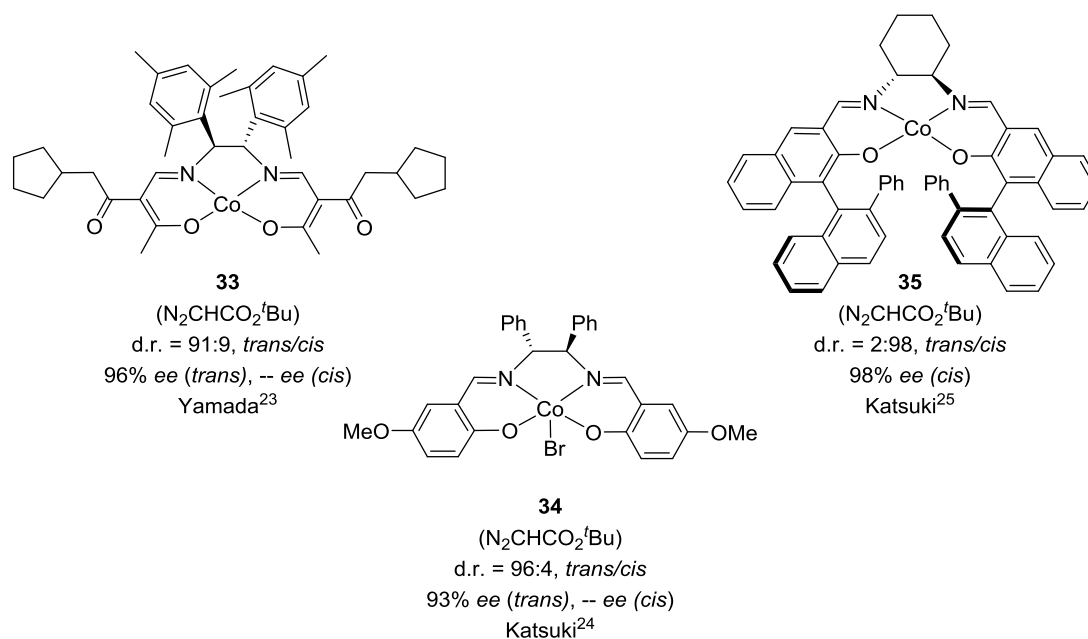


Figure 2.7. Cobalt-complexes **33–35** showed excellent results for the catalytic alkene cyclopropanation reaction.

Rhodium complexes have been extensively studied in intermolecular cyclopropanation reactions. This is the reason why literature reports a large number of rhodium-based chiral complexes. These ligands can be classified into two groups: dirhodium(II) carboxylates and dirhodium(II) carboxamidates. Rhodium complexes are very reactive, but different results were often observed in terms of diastereoselectivity. Even with the use of sterically hindered diazoesters they did not show similar results and tendencies with respect to other transition metals.^{8b}

However, complex **37a** (see **Fig. 2.8**) permitted to develop a chemoselective, enantioselective and *trans*-selective protocol for intermolecular cyclopropanation of alkenes and sterically hindered diazoesters. The scope of the reaction with different substituted cyclic and acyclic alkenes and benzofurans showed great diastereo- and enantioselective for the formation of corresponding cyclopropanes.²⁶ The same methodology with **36a–c** and derivatives, led to the reaction of vinyl diazomethanes in the presence of different alkenes to form highly diastereoselective and enantioselective cyclopropanes. Furthermore, it was successfully applied to the synthesis of the four stereoisomers of 2-phenylcyclopropanamino acid.²⁷

In addition, complex **37d**, has been successfully used for the proper activation of electron-deficient alkenes reacting with vinyl diazoacetates and aryl diazoacetates to obtain highly diastereocontrolled and enantiocontrolled (2+1) cycloadducts. In this case, cyclopropanes can be obtained from acrylates and acrylamides but unsaturated

²⁶ Deangelis, A.; Dmitrenko, O.; Yap, G. P. A.; Fox, J. M., *J. Am. Chem. Soc.* **2009**, 131, 7230–7231.

²⁷ Davies, H. M. L.; Bruzinski, P. R.; Lake, D. H.; Kong, N.; Fall, M. J., *J. Am. Chem. Soc.* **1996**, 118, 6897–6907.

CHAPTER 2

aldehydes led to the formation of epoxides.²⁸ Other applications of rhodium complexes are collected in different reviews.⁸

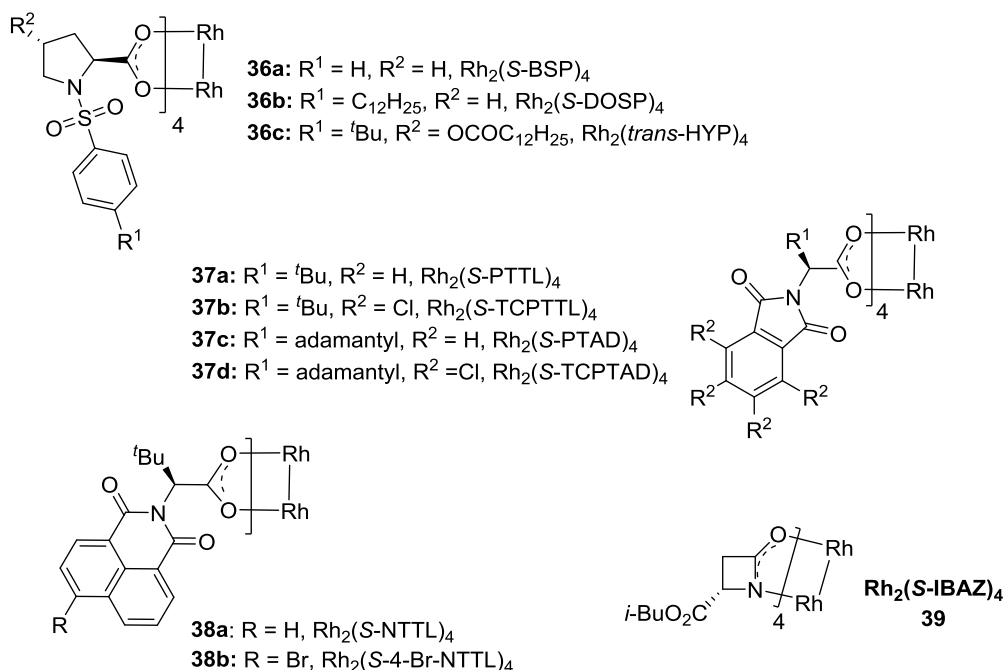


Figure 2.8. Some of the rhodium complex examples showing the extensive variety of catalysts.

Cobalt (II) porphyrins have emerged as efficient and potent catalysts in diastereo- and enantioselective cyclopropanations.²⁹ Efficient diastereoselective cyclopropanation of olefins with EDA and mediated by iridium (III) porphyrin complexes has been recently described too.³⁰ In addition, a highly *trans*-selective reaction using α -methylstyrene in the presence of iron porphyrin complex was performed with good enantioselectivities (97:3 *trans/cis*, ee_{trans} up to 87 %). This iron porphyrin catalyst showed outstanding TON and TOF values.³¹

Diastereocontrol of transition metal catalyzed cyclopropanations has proved to be a difficult task. The *trans*-favored enantioselective reaction has been more studied than the *cis*-selective one. Among the complexes formed with metals of group IX, cobalt and rhodium have been the most studied. Iridium in combination with Salen type ligands including an aryl ligand in apical position led to air-stable iridium (III) complex **40** (see **Fig. 2.9**). Moreover, when the reaction proceeded at -78°C totally *cis*-selective cyclopropanes were synthesized with 95 to 99% of *ee*. Interestingly, indene and

²⁸ Wang, H.; Guptil, D. M.; Varela-Alvarez, A.; Musaev, D. G.; Davies, H.M. *Chem. Sci.* **2013**, *4*, 2844-2850.

²⁹ Doyle, M. P. *Angew.Chem., Int. Ed.* **2009**, *48*, 850-852.

³⁰ Anding, B. J.; Ellern, A.; Woo, L. K. *Organometallics*, **2012**, *31*, 3628-3635.

³¹ Intrieri, D.; Le Gac, S.; Caselli, A.; Rose, E.; Boitrel, B.; Gallo, E. *Chem. Commun.* **2014**, *50*, 1811-1813.

CYCLOADDITION REACTIONS

benzofuran derived optically active cyclopropanes were highly *cis* selective.³²

Ferrocenyl ruthenium complex **41** was also highly *cis*-selective when $\text{Ru}(\text{DMSO})_4\text{Cl}_2$ was used as metallic source. They exhibited up to 99% of diastereo- and enantiomeric excess. In this publication the authors demonstrated that the metal/ligand ratio had a great impact on diastereocontrol.³³

Rhodium (I) NHC catalyst **42** showed impressive results in small catalytic loadings for the non-chiral highly *cis*-selective cyclopropanation of alkenes. The nature on the diazocompound and the alkene did not affect the diastereoselectivity of the reaction. Biologically interesting 2,5-dihydrofuran and benzofuran cyclopropane derivatives were also synthesized in good to excellent yields.³⁴

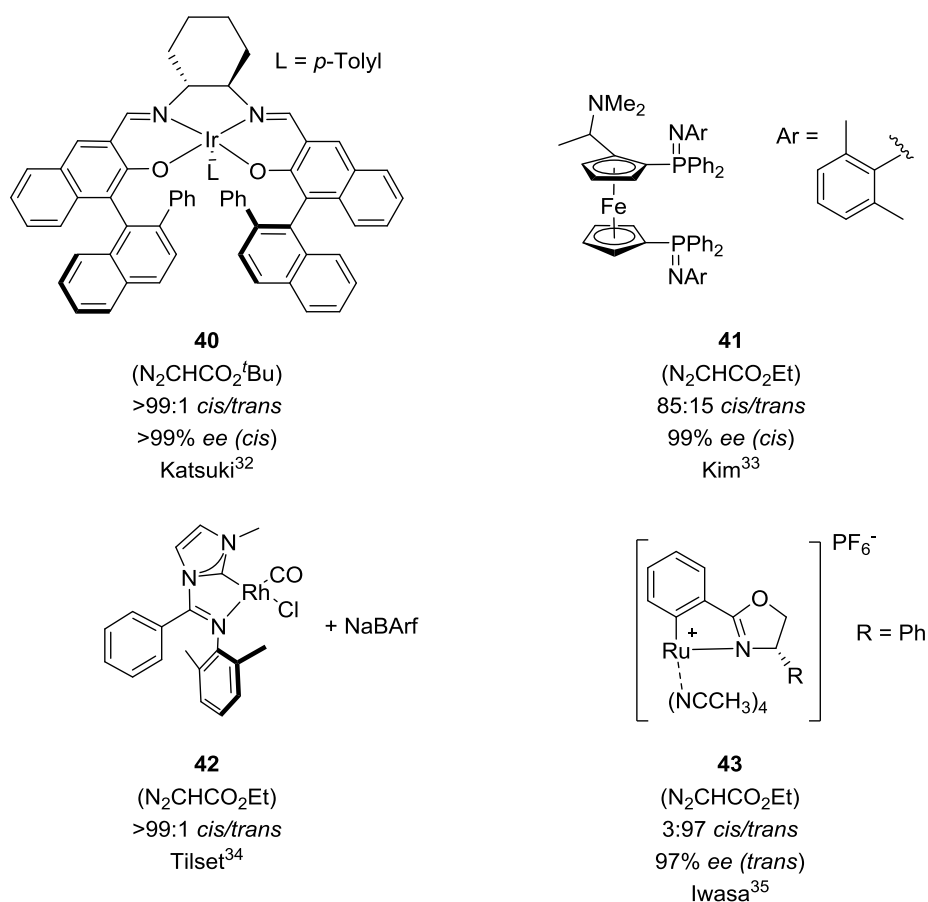


Figure 2.9. *Cis*-selective **40-42** complexes and Ru(II)-PheOX complex **43**.

Recently, Ru(II)-Pheox type complexes **43** were developed and resulted to be very efficient in asymmetric cyclopropanation of electron deficient olefins, including

³² a) Kanchiku, S.; Suematsu, H.; Matsumoto, K.; Uchida, T.; Katsuki, T. *Angew.Chem., Int. Ed.* **2007**, 46, 3889-3891. b) Suematsu, H.; Kanchiku, S.; Uchida, T.; Katsuki, T. *J. Am. Chem. Soc.* **2008**, 130, 10327-10337.

³³ Hoang, V. D. M.; Reddy, P. A. N.; Kim, T.-J. *Tetrahedron Lett.* **2007**, 48, 8014-8017.

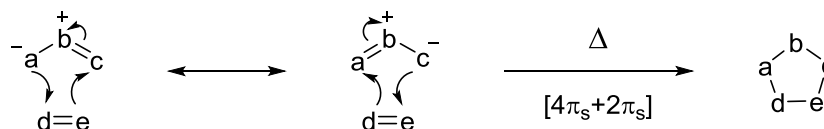
³⁴ Rosenber, M. L.; Vlasana, K.; Gupta, N. S.; Wragg, D.; Tilset, M. *J. Org. Chem.* **2011**, 76, 2465-2470.

CHAPTER 2

vinyl carbamates, allenes, and α,β -unsaturated carbonyl compounds. Cyclopropanation of styrene showed its tendency to produce *trans*-cyclopropanes with excellent enantioselectivity.³⁵

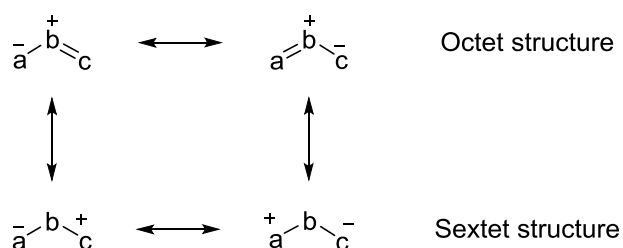
2.1.2 1,3-dipolar Cycloaddition Reactions

1,3-dipolar or (3+2) cycloaddition reaction is a very common and versatile route for the synthesis of five membered ring heterocyclic compounds.^{1b,36} Moreover, concerted (3+2) cycloadditions are reactions with a great potential in the formation of new chiral centers in organic molecules.³⁶ As this type of processes belong to the pericyclic reactions when they are concerted, they present an aromatic transition state of six π -electrons in which one of the components embeds four π -electrons along three atoms and it is named 1,3-dipole, and the other component is a two π -electrons containing element called dipolarophile.³⁷ Therefore, (3+2) cycloadditions are formal $[4\pi_s+2\pi_s]$ processes and are thermally allowed according to Woodward and Hoffman orbital symmetry rules.¹



Scheme 2.4. General thermal reaction between 1,3-dipoles and a dipolarophiles.

The 1,3-dipole component includes at least one central heteroatom of the total three atoms. Typically, they can be represented by four zwitterionic resonance structures for allyl type dipoles: the first two present an octet structure in which the positive charge is located on the central atom and the negative charge is distributed over the two terminal atoms; the other two are sextet structures in which two of the four π -electrons are localized in the central atom (**Scheme 2.5**).^{1b,38}



Scheme 2.5. Resonance hybrid structures of 1,3-dipoles.

³⁵ Chanthamath, S.; Iwasa, S., *Acc. Chem. Res.* **2016**, 49, 2080–2090.

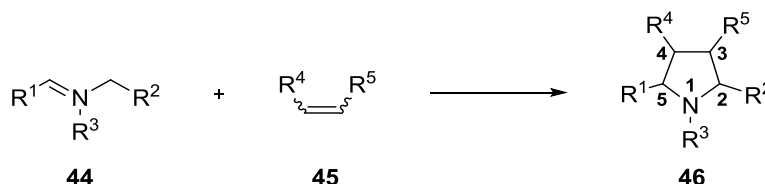
³⁶ Kobayashi, S.; Jørgensen, K. A.; Eds. *Cycloaddition Reactions in Organica Synthesis*, Wiley-VCH, Weinheim, **2001**.

³⁷ Carruthers, W. *Cycloaddition Reactions in Organic Synthesis*, ed. Pergamon Press, Oxford, **1990**.

³⁸ Huisgen, R. *J. Org. Chem.* **1976**, 41, 403-419.

2.1.2.1 Azomethine ylides in 1,3-dipolar cycloadditions

Azomethine ylides are planar dipoles that include a nitrogen atom in central position and two terminal sp^2 carbon atoms. Their cycloaddition reaction with alkenes provides the formation of pyrrolidine rings which can give access to the formation of four new stereogenic centers in one synthetic step.³⁹ Pyrrolidine rings are interesting scaffolds found in organocatalysis (Proline derivatives), pharmaceuticals and alkaloids (see Chapter 1).



Scheme 2.6. General (3+2) cycloaddition between imines (as precursors of azomethine ylides) and alkenes to yield pyrrolidines.

Because of their unstable nature, azomethine ylides are usually prepared *in situ* starting from their precursors. Different processes are developed to obtain this type of dipole, such as ring opening of aziridines, desilylation, prototropy/metallo-azomethine ylides of amino acids derived imines, decarboxylative condensation of amino acids, deprotonation of iminium and more.³⁹

General stereoselectivity of 1,3-dipoles has been mentioned depending upon the configuration of the dipolarophile. Stereochemistry related to the additional positions is determined by the dipole geometry. In the case of azomethine ylides we can find four types of dipoles. Stereochemistry in 2,5 positions of the pyrrolidine stems from of the geometry of the ylide, which can be W and U for *cis* disubstituted pyrrolidines or S-shaped for 2,5-*trans* disubstituted ones.⁴⁰

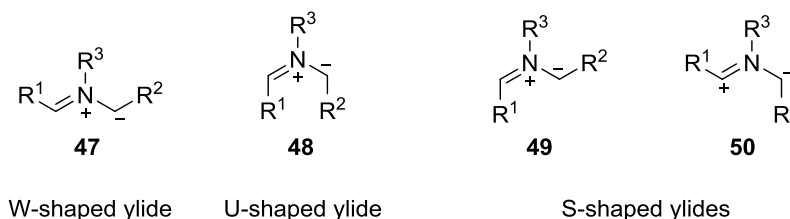


Figure 2.10. Azomethine ylide dipole geometries.

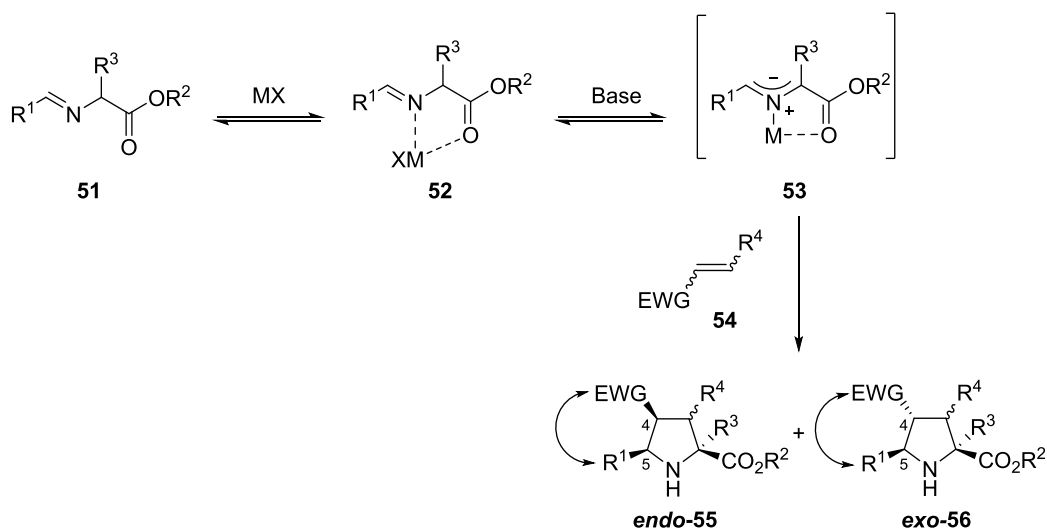
Ylides can be *NH*-ylides, *N*-substituted or *N*-metalated species. Generally, they can be classified as stabilized, metal-stabilized and non-stabilized azomethine ylides, depending on the presence of an electron-withdrawing group (EWG) in the terminal carbon of the dipole. Stabilization comes from a larger negative charge delocalization and consequent additional resonant forms due to the EWG.⁴⁰

³⁹ Husinec, S.; Savic, V., *Tetrahedron Asymmetry* **2005**, 16, 2047–2061.

⁴⁰ Pandey, G.; Banerjee, P.; Gadre, S. R., *Chem. Rev.* **2006**, 106, 4484–4517.

CHAPTER 2

The diastereoselectivity provided by *N*-metalated azomethine ylides depends on the EWG and the orientation of the substituents of the dipole. Thus, when the EWG and the substituent in position 5 are *cis* to each other, the cycloadducts obtained will be *endo* and if they are in *trans* the generation of cycloadducts *exo* will be achieved. As mentioned before, the approach of the dipole to the dipolarophile occurs suprafacially, which means that configuration of the initial dipolarophile will be retained.



Scheme 2.7. General reaction for azomethine ylide precursor and alkenes.

Experimental and computational studies on the stereochemistry of the reaction between *N*-metalated azomethine ylides and nitroalkenes permitted to find out the origin of the stereocontrol. The studies provided a model for the dependence of diastereoselectivity with the metallic source employed. For instance, lithium promoted formation of *endo* adducts, whereas silver salts in the presence of tertiary bases in general favor the preferential formation of *exo* compounds.⁴¹

Mechanistically, Huisgen⁴² and Firestone⁴³ proposed two different pathways for 1,3-dipolar cycloadditions. Huisgen proposed a *supra-supra* pericyclic mechanism in a concerted manner while Firestone was in favor of a stepwise mechanism involving a diradical intermediate. Afterwards, in collaboration with Houk,⁴⁴ Firestone accepted Huisgen's theory of concerted mechanism. Later it was found that 1,3-dipolar cycloaddition reactions can occur through a stepwise mechanism depending on the nature of the dipole and dipolarophile.⁴⁵

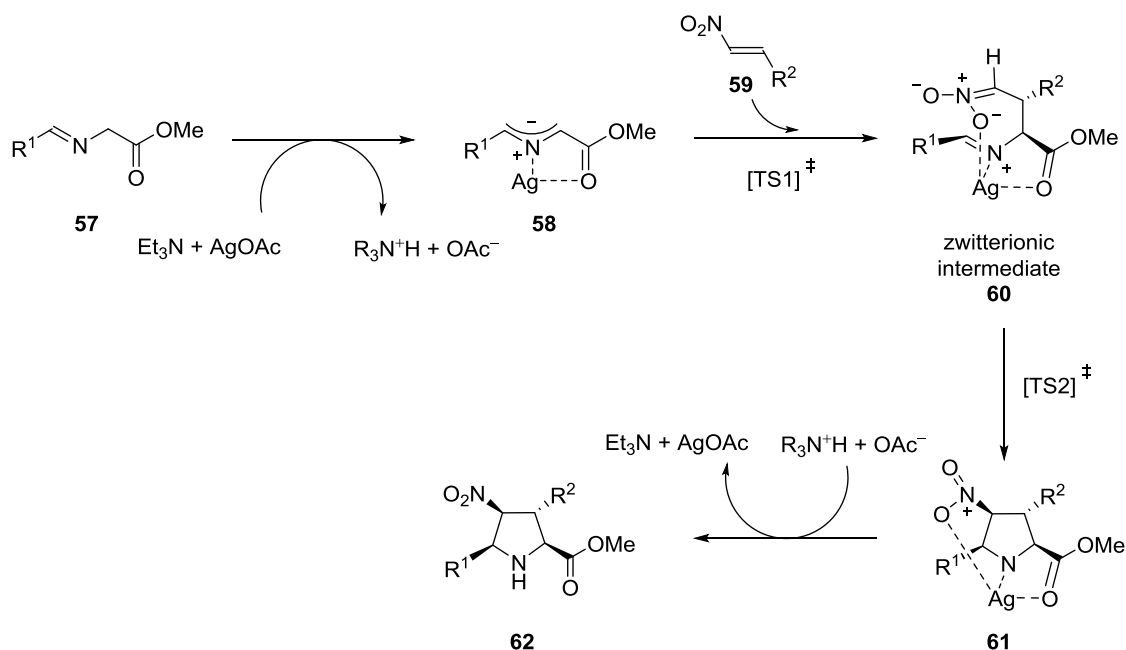
⁴¹ a) Ayerbe, M.; Arrieta, A.; Cossío, F. P.; Linden, A., *J. Org. Chem.* **1998**, 63, 1795–1805. b) Nyerges, M.; Rudas, M.; Tóth, G.; Herényi, B.; Kádas, I.; Töke, L., *Tetrahedron* **1995**, 51, 13321–13330.

⁴² Huisgen, R., *Angew. Chem. Int. Ed.* **1963**, 2, 633–645.

⁴³ a) Firestone, R. A.; *Tetrahedron* **1977**, 33, 3009–3039. b) Firestone, R. A., *J. Org. Chem.* **1972**, 37, 2181–2191.

⁴⁴ Houk, K. N.; Firestone, R. A.; Munchausen, L. L.; Mueller, P. H.; Arison, B. H.; García, L. A., *J. Am. Chem. Soc.* **1985**, 107, 7227–7228.

⁴⁵ a) Huisgen, R.; Mloston, G.; Lagnhals, E. *J. Org. Chem.* **1986**, 51, 4085–4087. b) Neumann, F.; Lambert, C.; Schleyer, P. V. R., *J. Am. Chem. Soc.* **1998**, 120, 3357–3370.



Scheme 2.8. *Endo*-selective stepwise mechanism proposed by Cossío for 1,3-dipolar cycloaddition between metal stabilized azomethine ylides and nitroalkenes.

Azomethine ylides are HOMO controlled dipoles and the incorporation of a EWG group to the dipolarophile shows an energy decrease in the LUMO-dipolarophile. Furthermore, Cossío and coworkers discovered that stabilization of the ylide by transition metals made the reaction with electron-deficient alkenes to go through a stepwise process instead of a concerted one.⁴⁶

The mechanism is described in **Scheme 2.8** employing silver acetate and triethylamine as base. The first reaction step is a conjugated Michael type nucleophilic attack of the α-carbon of the azomethine ylide, *in situ* generated from the corresponding α-iminoester, to the β-carbon of nitroalkene. In a second reaction step zwitterionic intermediate **60** cyclizes through an intramolecular aza-Henry reaction to afford final heterocycle **62**.

2.1.3 Asymmetric 1,3-dipolar cycloadditions of azomethine ylides

2.1.3.1 Diastereoselective reactions

In diastereoselective reactions chirality can be transferred by incorporating a chiral auxiliary into the azomethine ylide which is later eliminated in order to obtain the desired enantiopure product. First example of chiral induction between a chiral azomethine ylide and an achiral alkene was carried out by Padwa *et al.* in 1985.⁴⁷

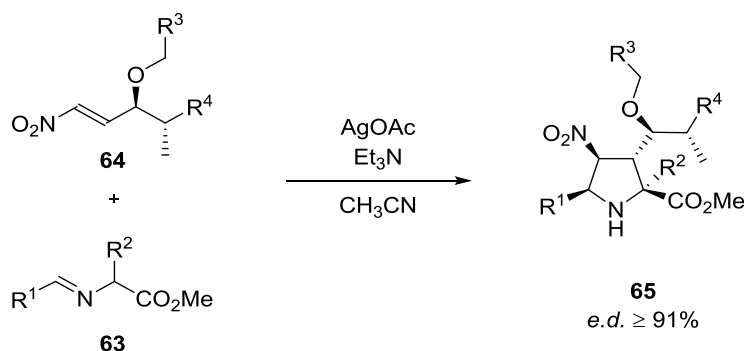
⁴⁶ a) Vivanco, S; Lecea, B.; Arrieta, A.; Prieto, P.; Morao, I.; Linden, A.; Cossío, F.P., *J. Am. Chem. Soc.* **2000**, 122, 6078-6092. b) de Cozár, A.; Cossío, F.P., *Phys. Chem. Phys.*, **2011**, 13, 10858-10868.

⁴⁷ Padwa, A; Chen, Y. Y.; Chiacchio, U.; Dent, W., *Tetrahedron* **1985**, 41, 3529-3535.

CHAPTER 2

Several examples were reported afterwards, some dipoles have been of great interest due to the excellent diastereoselectivities obtained.⁴⁸

Nájera used a strategy with chiral acrylates as dipolarophiles to synthesize inhibitors of hepatitis C virus RNA-dependent RNA polymerase. 1,3-dipolar cycloaddition was carried out using AgOAc and toluene as solvent affording selectively *endo* adducts.⁴⁹ Cossío *et al.* developed a diastereoselective synthesis of pyrrolidines using chiral nitroalkenes as dipolarophiles (**Scheme 2.10**). Total diastereocontrol of the reaction was observed. In addition, obtained cycloadducts were transformed in order to synthesize new inhibitors of VLA-4/VCAM-1 interaction and later for LFA-1/ICAM interaction. These compounds showed antimetastatic activity *in vivo* against colon cancer and melanoma.⁵⁰



Scheme 2.10. Diastereoselective 1,3-dipolar cycloaddition reaction with chiral nitroalkenes using AgOAc.⁵⁰

2.1.3.2 Enantioselective 1,3-dipolar cycloaddition reactions

Enantioselective 1,3-dipolar cycloaddition reactions have emerged as the most powerful process to synthesize optically active five-membered heterocycles. This approach has demonstrated several advantages, highlighting the use of chiral catalysts in substoichiometric amounts. In fact, azomethine ylides as dipoles that react with electron-deficient dipolarophiles catalyzed by chiral Lewis acids is the most convergent and versatile strategy for enantioselective synthesis of highly functionalized pyrrolidines. Metal-stabilization of azomethine ylides is the key for the required conformational restriction in order to discriminate between enantiotopic faces during reaction.^{39,51}

⁴⁸ a) Gothelf, K. V.; Jørgensen, K. A., *Chem. Rev.* **1998**, *98*, 863–909. b) Pandey, G.; Banerjee, P.; Gadre, S. R., *Chem. Rev.* **2006**, *106*, 4484–4517.

⁴⁹ Nájera, C.; Retamosa, M. de G.; Sansano, J. M.; De Cózar, A.; Cossío, F. P., *European J. Org. Chem.* **2007**, 5038–5049.

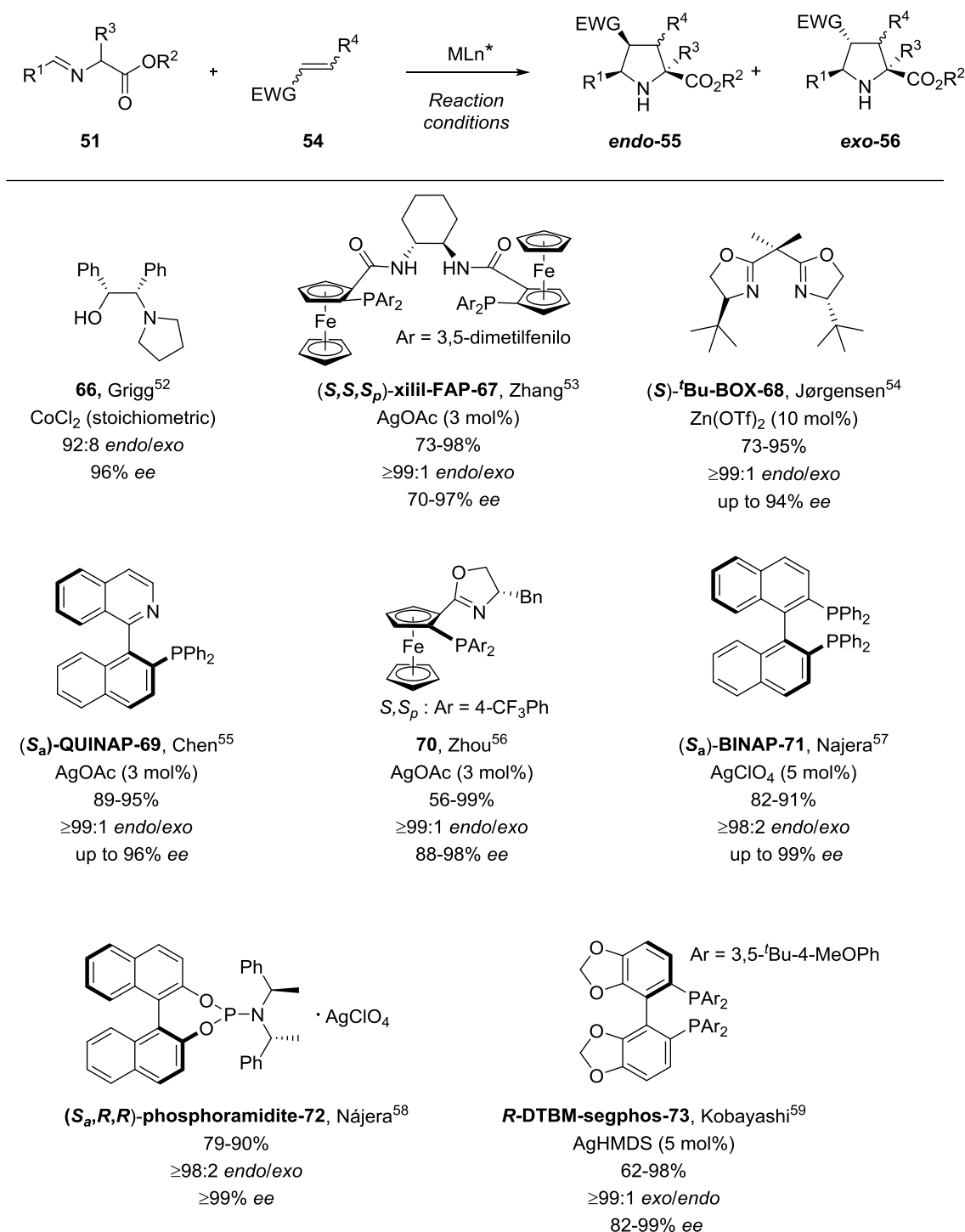
⁵⁰ a) Zubia, A.; Mendoza, L.; Vivanco, S.; Aldaba, E.; Carrascal, T.; Lecea, B.; Arrieta, A.; Zimmerman, T.; Vidal-Vanaclocha, F.; Cossío, F. P., *Angew. Chem., Int. Ed.* **2005**, *44*, 2903–2907. b) Zimmerman, T.; Zubia, A.; Vara, Y.; Martín, E.; Sirockin, F.; Mendoza, L.; Vidal-Vanaclocha, F.; Cossío, F. P.; Blanco, F. J., *J. Med. Chem.* **2013**, *56*, 735–747.

⁵¹ Nájera, C.; Sansano, J. M., *Angew. Chem., Int. Ed.* **2005**, *44*, 6272–6276.

CYCLOADDITION REACTIONS

- Intermolecular enantioselective 1,3-dipolar cycloaddition reactions

Many enantiopure ligands have been reported to promote catalytically intermolecular (3+2) cycloadditions between *N*-metalated azomethine ylides and π -deficient alkenes. Selected examples are depicted in **Scheme 2.11** and **Scheme 2.12**. They have been successfully employed in order to give rise to highly functionalized enantiopure pyrrolidines.



Scheme 2.11. Selected examples of pioneering ligands in enantioselective (3+2) cycloaddition reactions and ligands that showed excellent enantiocontrol in combination with silver salts.

CHAPTER 2

Grigg and coworkers developed the first enantioselective 1,3-dipolar reaction using naphthyl derived iminoesters and acrylate as dipolarophile but using a stoichiometric amount of ephedrine-derived ligand **66** with cobalt as metallic source (see **Scheme 2.11**).⁵² Later, Zhang and coworkers described the first catalytic enantioselective reaction between several dipolarophiles and a variety of azomethine ylide precursors using **xilil-FAP-67**.⁵³ Jørgensen found out that the use of $\text{Zn}(\text{OTf})_2$ as metallic source in combination with chiral **'Bu-bis(oxazoline)-68** catalyzed asymmetrically the reaction between aryl glycine derived iminoesters and various acrylates.⁵⁴

Silver catalyzed enantioselective (3+2) cycloadditions have been described as efficient, high yielding and fast reactions (see **Scheme 2.11**). Preferentially, they are able to afford *endo* cycloadducts, typically in a total diastereoselective and enantioselective fashion. Chen *et al.* employed ligand (**S_a**)-**QUINAP-69** for the enantioselective (3+2) cycloaddition reaction of tert-butyl acrylate with aryl α -iminoesters.⁵⁵ In addition, ferrocenyloxazoline ligand **70** reported by Zhou and coworkers exhibited excellent results for the formation of highly functionalized pyrrolidines.⁵⁶

Nájera described an enantioselective synthesis of cycloadducts using $\text{AgClO}_4/$ (**S_a**)-**BINAP-71** system in the reaction between aryl α -iminoesters and *N*-methyl maleimide.⁵⁷ The same group reported the use of monodentate (**S_a**,**R**,**R**)-**phosphoramidite-AgClO₄** complex **72** which was found to be efficient for a wide range of enantioselective 1,3-dipolar cycloaddition reactions.⁵⁸ Kobayashi published as well the efficient combination of ligand (**R**)-**DTBM-segphos-73** with AgHDMS in order to generate selectively **exo-56** derivatives.⁵⁹

Copper catalyzed 1,3-dipolar cycloaddition reactions tend to afford *exo*-cycloadducts (see **Scheme 2.12**). Zhang described the enantioselective synthesis of pyrrolidines by using **FOXAP** ligand **74** using as metallic source CuClO_4 , which showed excellent results for acrylates as dipolarophiles.⁶⁰ **Fesulphos-75** is a ferrocenyl ligand synthesized by Carretero *et al.*, which in combination with $[\text{Cu}(\text{CH}_3\text{CN})_4]\text{ClO}_4$ gave excellent results for the *endo*-adduct formation of phenylmaleimide derivatives. Later, this ligand showed a great versatility in cycloaddition reaction for different dipolarophiles.⁶¹ $\text{CuOAc/ClickFerrophos-76}$ catalyzed 1,3-dipolar cycloaddition was

⁵² Allway, P.; Grigg, R., *Tetrahedron Lett.* **1991**, 32, 5817–5820.

⁵³ Longmire, J. M.; Wang, B.; Zhang, X., *J. Am. Chem. Soc.* **2002**, 124, 13400–13401.

⁵⁴ Gothelf, A. S.; Gothelf, K. V.; Hazell, R. G.; Jørgensen, K. A., *Angew. Chemie. Int. Ed.* **2002**, 41, 4236–4238.

⁵⁵ Chen, C.; Li, X.; Schreiber, S. L., *J. Am. Chem. Soc.* **2003**, 125, 10174–10175.

⁵⁶ Zeng, W.; Zhou, Y. G., *Org. Lett.* **2005**, 7, 5055–5058.

⁵⁷ a) Nájera, C.; Retamosa, M. de G.; Sansano, J. M., *Org. Lett.* **2007**, 9, 4025–4028. b) Nájera, C.; Retamosa, M. de G.; Sansano, J. M.; Cózar, A. de; Cossío, F. P., *Tetrahedron Asymmetry* **2008**, 19, 2913–2923.

⁵⁸ a) Nájera, C.; Retamosa, M. de G.; Sansano, J. M., *Angew. Chem., Int. Ed.* **2008**, 47, 6055–6058. b) Nájera, C.; Retamosa, M. de G.; Martín-Rodríguez, M.; Sansano, J. M.; De Cózar, A.; Cossío, F. P., *European J. Org. Chem.* **2009**, 5622–5634.

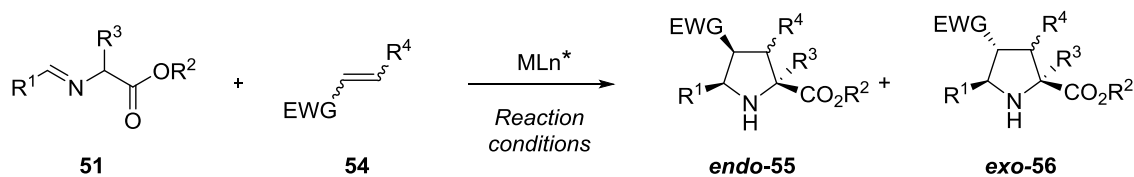
⁵⁹ Yamashita, Y.; Imaizumi, T.; Kobayashi, S., *Angew. Chem., Int. Ed.* **2011**, 50, 4893–4896.

⁶⁰ Gao, W.; Zhang, X.; Raghunath, M., *Org. Lett.* **2005**, 7, 4241–4244.

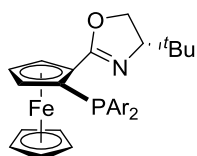
⁶¹ a) Cabrera, S.; Arrayás, R. G.; Carretero, J. C., *J. Am. Chem. Soc.* **2005**, 127, 16394–16395. b) Cabrera, S.; Arrayás, R. G.; Martín-Matute, B.; Cossío, F. P.; Carretero, J. C., *Tetrahedron* **2007**, 63,

CYCLOADDITION REACTIONS

found to be enantioselective for a large diversity of dipolarophiles and almost exclusively *exo*-adducts were obtained.⁶²



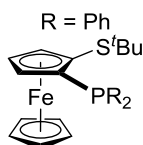
S,S_P : Ar = 3,5-Me₂-Ph



FOXAP-74, Gao⁶⁰

CuClO₄ (5 mol%)
61-87%

76:24 to 98:2 *exo/endo*
up to 98% *ee*

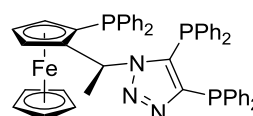


Fesulphos-75, Carretero⁶¹

[Cu(CH₃CN)₄]ClO₄ (5 mol%)

98:2 *endo/exo*

≥ 99% *ee*



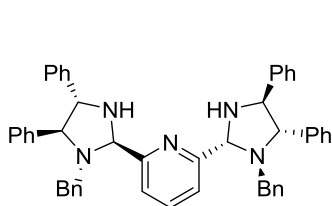
ClickFerrophos-76, Fukuzawa⁶²

CuOAc (10 mol%)

80-94%

≥99:1 *exo/endo*

93-99% *ee*



PyBidine-77, Arai^{63,64}

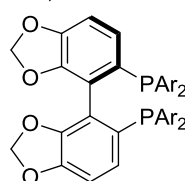
Cu(OTf)₂ (5 mol% or 10 mol%)

60-99%

95:5 to ≥99:1 *endo/exo*

87-99% *ee*

Ar = 3,5-*t*Bu-4-MeOPh



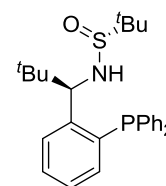
R-DTBM-segphos-78, Martin⁶⁵

Cu(OTf)₂ (10 mol%)

62-98%

50:50 to 99:1 *trans/cis*

90-97% *ee*



79, Zhang⁶⁶

[Cu(CH₃CN)₄]ClO₄ (5 mol%)

70-99%

95:5 *endo/exo*

80-98% *ee*

Scheme 2.12. Ligand examples that resulted efficient in combination with copper salts for the enantioselective (3+2) cycloaddition reactions.

Arai and coworkers reported the synthesis of **PyBidine-Cu(OTf)₂** complex **77** which was capable of catalyzing (3+2) cycloaddition reactions between azomethine ylides and substituted nitroalkenes with high *endo*-selectivity and excellent enantiomeric excesses (**Scheme 2.12**).⁶³ Therefore, the same complex was able to catalyze the diastereoselective *exo'*-adduct formation of tricyclic molecules by enantioselective (3+2) cycloaddition reaction between glycine derived iminoesters and

6587–6602.

⁶² Fukuzawa, S. I.; Oki, H., *Org. Lett.* **2008**, 10, 1747–1750.

⁶³ Arai, T.; Mishiro, A.; Yokoyama, N.; Suzuki, K.; Sato, H., *J. Am. Chem. Soc.* **2010**, 132, 5338–5339.

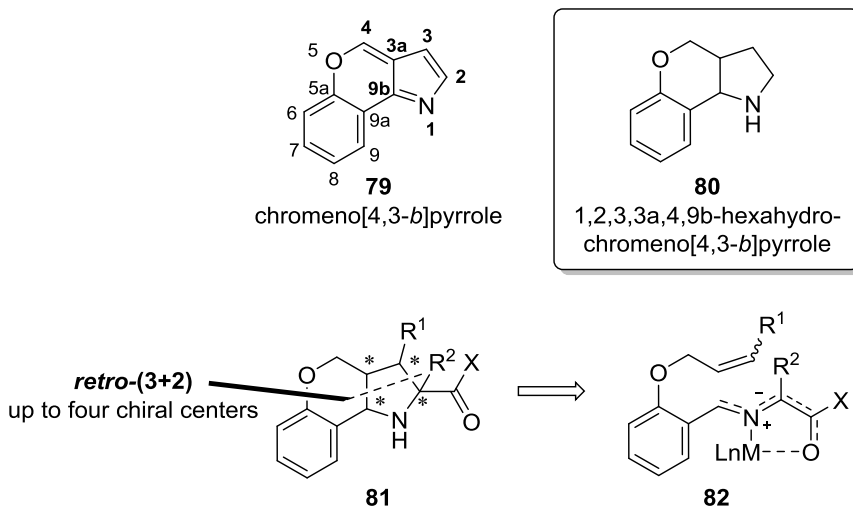
CHAPTER 2

3-nitroindoles.⁶⁴ Studies on the reactivity of fullerenes as dipolarophiles led to the efficient combination of Cu(OTf)₂ and ligand (**R**)-DTBM-segphos-**73** capable of catalyzing first *trans*-diastereoselective synthesis of enantiopure fulleropyrrolidines, compounds of great importance in biomedicine and material science.⁶⁵ Novel enantioselective (3+2) cycloaddition reaction catalyzed by copper and ligand **78** between azomethine ylides with β -trifluoromethyl β -disubstituted enones has been recently described, showing high efficiency, diastereo- and enantiocontrol.⁶⁶

- Intramolecular enantioselective 1,3-dipolar cycloaddition reactions

Enantioselective intramolecular (3+2) cycloaddition reactions have been studied in a lesser extent. The fact that both the dipole and the dipolarophile are tethered makes the reaction more favorable in terms of entropy and often only one regioisomer is energetically available.⁶⁷ In addition, another advantage of the intramolecular cycloaddition reaction is that it is effective for electron-rich dipolarophiles. Therefore, the intramolecular fashion presents high regio- and stereoselectivity and the ability to generate complex bicyclic or larger ring systems in few steps.

Among different tricyclic pyrrolidines that can be synthesized via intramolecular (3+2) cycloaddition reaction, scaffolds derived from chromeno[4,3-*b*]pyrrole (**Scheme 2.13**) constitute a particularly interesting target because of their biological properties.



Scheme 2.13. Retrosynthesis of hexahydrochromeno[4,3-*b*]pyrroles that can be obtained by intramolecular (3+2) cycloaddition reaction between alkenes and stabilized *N*-metalated azomethine ylides. **X** = -OR³, -NHR⁴; **M** = Ag, Cu.

⁶⁴ Awata, A.; Arai, T., *Angew.Chem., Int. Ed.* **2014**, 53, 10462–10465.

⁶⁵ Maroto, E. E.; Filippone, S.; Martín-Domenech, A.; Suarez, M.; Martín, N., *J. Am. Chem. Soc.* **2012**, 134, 12936–12938.

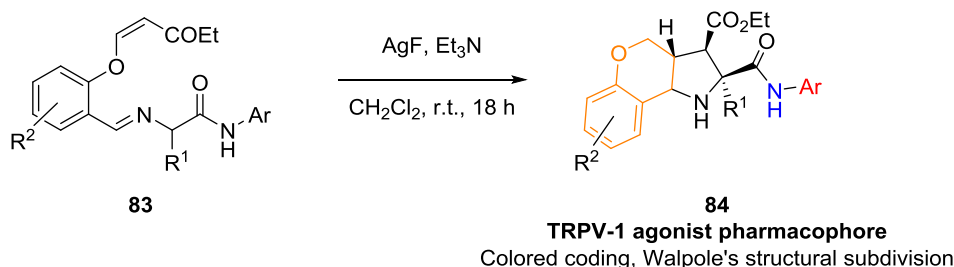
⁶⁶ Zhang, Z. M.; Xu, B.; Xu, S.; Wu, H. H.; Zhang, J., *Angew.Chem., Int. Ed.* **2016**, 55, 6324–6328.

⁶⁷ Coldham, I.; Hufton, R., *Chem. Rev.* **2005**, 105, 2765–2809.

CYCLOADDITION REACTIONS

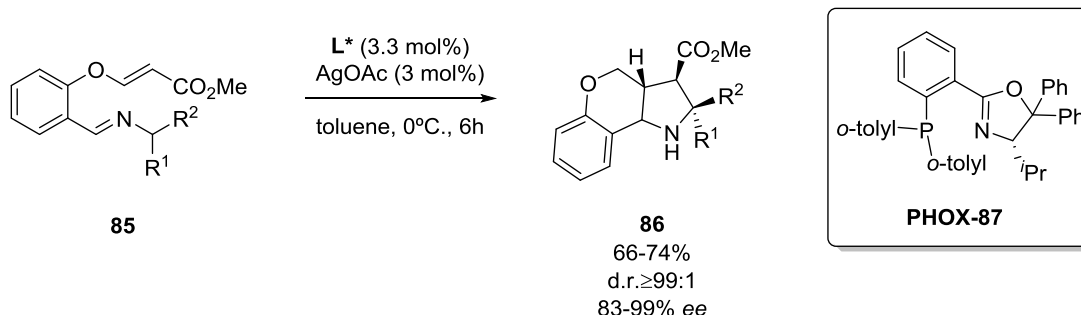
Different syntheses of racemic chromenopyrrolidines have been reported using this approach. Some of the molecules thus obtained exhibited interesting antitubercular activity with good MIC results.⁶⁸

Silver mediated intramolecular cycloaddition afforded racemic chromeno[4,3-b]pyrrolidines, which after appropriate transformations exhibited partial agonist activity on TRPV-1 cation channel, which has a relevant effect on chronic pain diseases.⁶⁹ The pharmacophore presents a colored coding for the structural subdivisions (see **Scheme 2.14**).



Scheme 2.14. Intramolecular non-enantioselective cycloaddition reaction to afford TRPV-1 partial agonists.⁶⁹

The first enantioselective intramolecular cycloaddition reaction of azomethine ylides was reported by Pfaltz in 2005.⁷⁰ These authors obtained excellent enantioselectivities by using Ag(I)/PHOX catalyst at low temperatures.



Scheme 2.15. First enantioselective intramolecular reaction catalyzed by AgOAc and **PHOX-87** ligand.⁷⁰

Since then, there has not been described any other asymmetric synthesis of these compounds using organometallic catalysis. However, it was reported the use of chiral phosphoric acid organocatalysts to obtain substituted tricycles similar to **86** with good to excellent enantioselectivities.⁷¹

⁶⁸ a) Virányi, A.; Mart, G.; Drancsó, A.; Blaskó, G.; Tóke, L.; Nyerges, M. *Tetrahedron*, **2006**, 62, 8720–8730. b) Tripathi, R. P.; Bisht, S. S.; Pandey, V. P.; Pandey, S. K.; Singh, S.; Sinha, S. K.; Chaturvedi, V., *Med. Chem. Res.* **2011**, 20, 1515–1522.

⁶⁹ Painter, T. O.; Kaszas, K.; Gross, J.; Douglas, J. T.; Day, V. W.; Iadarola, M. J.; Santini, C., *Bioorganic Med. Chem. Lett.* **2014**, 24, 963–968.

⁷⁰ Stohler, R.; Wahl, F.; Pfaltz, A., *Synthesis* **2005**, 1431–1436.

⁷¹ Li, N.; Song, J.; Tu, X.-F.; Liu, B.; Chen, X.-H.; Gong, L.-Z., *Org. Biomol. Chem.* **2010**, 8, 2016–2019.

CHAPTER 2

- Previous work developed with Ferrocenyl-Prolines

A new family of ferrocenyl-pyrrolidine ligands has been developed by Cossío and coworkers. These novel enantiopure ligands incorporate densely substituted unnatural prolines and 1,2-disubstituted ferrocenyl ligands. Compounds of this type permit the interplay between the four chiral centers of the pyrrolidine ring and the planar chirality of the ferrocenyl diphenylphosphine moiety.

These catalytic systems were employed in 1,3-dipolar cycloaddition reactions between glycine derived iminoesters **51** and nitrostyrene **89**. Although Ag(I) salts were tested, the best results were obtained when Cu(I) salts were employed.⁷²

When $[\text{Cu}(\text{CH}_3\text{CN})_4]\text{PF}_6$ was used along with ferrocenyl-proline ligand **91a**, which bears a -NH pyrrolidine, reaction between **88a** and nitroalkenes **89** resulted in the diastereoselective **exo-90** pyrrolidine formation with good yield and excellent enantiomeric excess of 97%. Instead, the same reaction catalyzed by *N*-Me substituted ligand **93** led to **endo-92** cycloadducts in 92% ee. These results were explained by DFT studies. The transition state **endo-TS1** (Scheme 2.16, a) showed that in the case of the reaction catalyzed by ligand **93**, Cu(I) interacted with phosphine moiety, and with the nitrogen and oxygen atoms of the azomethine ylide. No interaction of Cu(I) with the *N*-substituted nitrogen of ligand was observed, which offers a coordination vacancy that can be occupied by the oxygen of the nitro group of the dipolarophile. Hence, efficient blockage of the (2*Re*, 5*Si*) prochiral face resulted in the formation of cycloadducts **endo-92**.

In the case of ligand **91a**, as it can be observed in **exo-TS2** (Scheme 2.16, b), interaction of copper with azomethine ylide is similar to **TS1** but in this case the NH moiety of the pyrrolidine ring interacts with the Cu(I) center, thus, saturating its coordination sphere and promoting the formation of **exo-90**, in which the two electron-withdrawing groups (the phenyl and the nitro moieties) are away from each other.

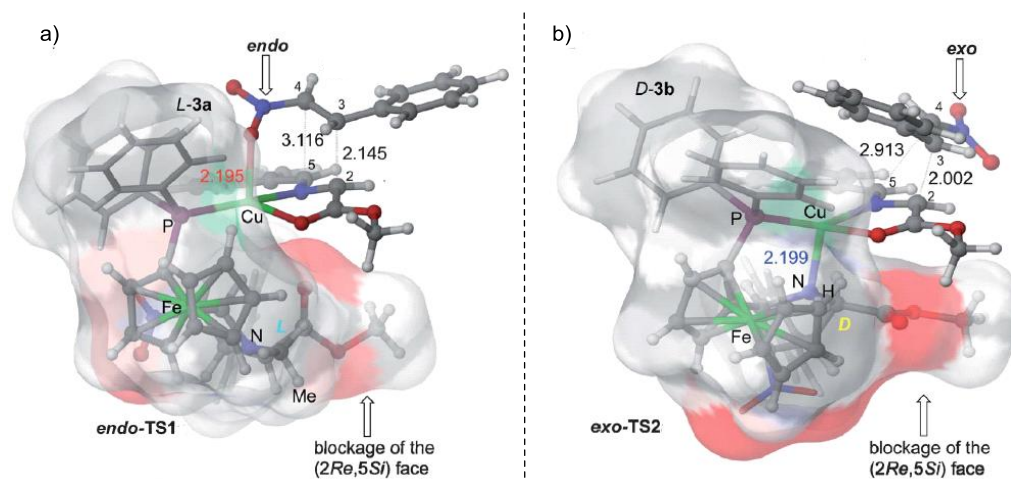
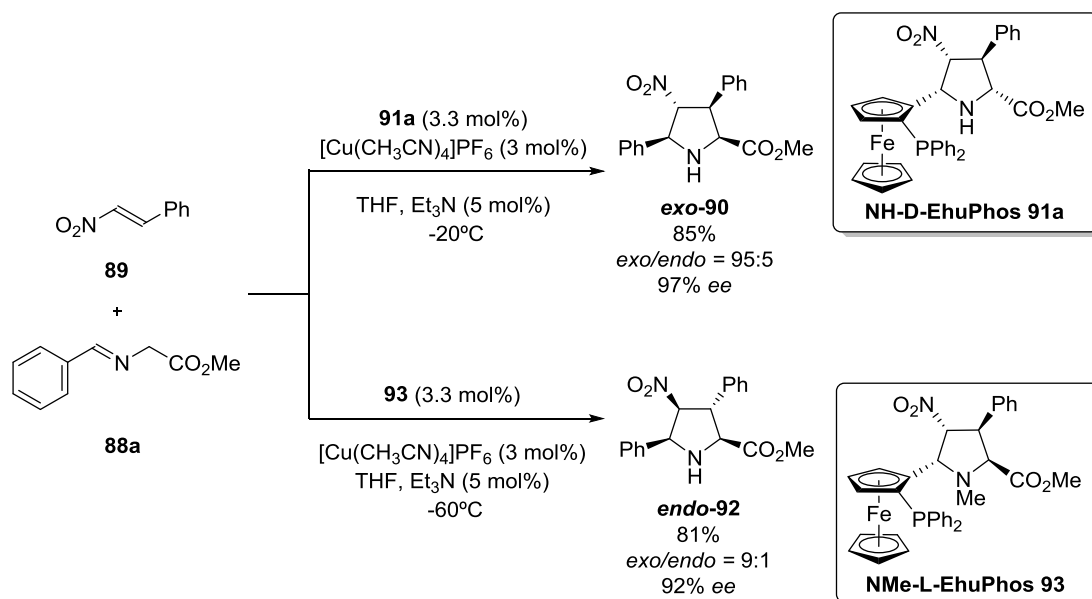
This preliminary work led to the formation of highly functionalized unnatural prolines which inspired the design of a totally new family of organocatalysts that have shown excellent results in enantioselective aldol and Michael reactions.⁷³ Some of the unnatural proline derivatives have been tested for their use as proteasome inhibitors and therapeutic agents in order to prevent or treat cancer, neurodegenerative diseases, autoimmune diseases or viral infections.⁷⁴

⁷² Conde, E.; Bello, D.; de Cózar, A.; Sánchez, M.; Vázquez, M. A.; Cossío, F. P., *Chem. Sci.* **2012**, 3, 1486-1491.

⁷³ a) Retamosa, M. de G.; de Cózar, A.; Sánchez, M.; Miranda, J. I.; Sansano, J. M.; Castelló, L. M.; Nájera, C.; Jiménez, A. I.; Sayago, F. J.; Cativiela, C., *Eur. J. Org. Chem.* **2015**, 2503-2516. b) Ruiz-Olalla, A.; Retamosa, M. D. G.; Cossío, F. P., *J. Org. Chem.* **2015**, 80, 5588-5599.

⁷⁴ Cossío Mora, F. P.; Retamosa Hernández, M. de G.; Larumbe Gárata, A.; Zubia Olascoaga, A.; Bello Iglesias, T.; Vara Salazar, Y. I.; Masdeu Margalef, M. del C.; Aldaba Arévalo, E., *Enantiopure Tetrasubstituted Pyrrolidines as Scaffolds for Proteasome Inhibitors and Medicinal Application Thereof*, **2015**, WO2015/124663.

CYCLOADDITION REACTIONS



Scheme 2.16. Ferrocenyl-proline ligand catalyzed enantioselective (3+2) cycloaddition reactions using copper as metallic source. Below computational studies of transition state for **endo-92** and **exo-90** adduct formation are represented. TS figures taken from publication of Cossio *et al.*, ref 72 (**L-3a** equals to ligand **93** and **D-3b** equals to **91a**).

Furthermore, the stepwise mechanism of this type of reactions demonstrated that bis(spiropyrrolidine) compounds can be obtained by consecutive frustrated and completed (3+2) cycloadditions. Some of these novel compounds showed interesting biological activities in micromolar range.⁷⁵

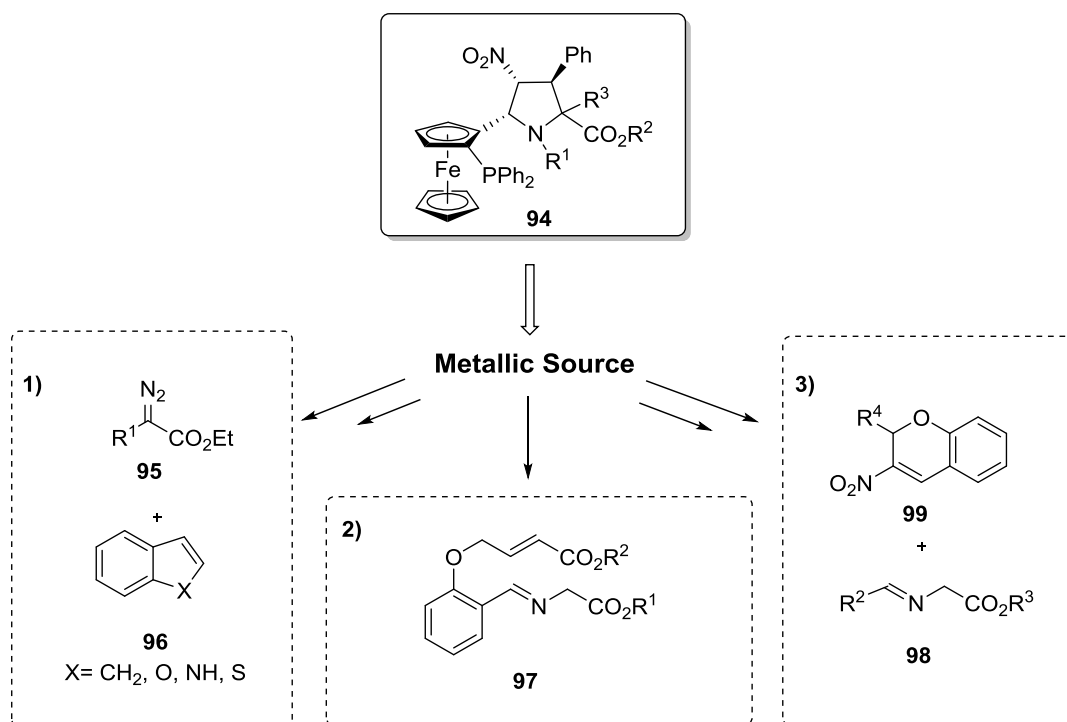
⁷⁵ Conde, E.; Rivilla, I.; Larumbe, A.; Cossio, F. P., *J. Org. Chem.* **2015**, *80*, 11755–11767.

CHAPTER 2

2.2 Objectives

On the basis of the results provided by the ferrocenyl-proline ligands previously reported by our research group, we proposed the synthesis of new ferrocenyl-proline ligand derivatives and their use in combination with a variety of metal sources in order to generate catalytic systems from enantioselective (2+1) and (3+2) cycloadditions. In particular, the main objectives of this Chapter is focused on the following reactions:

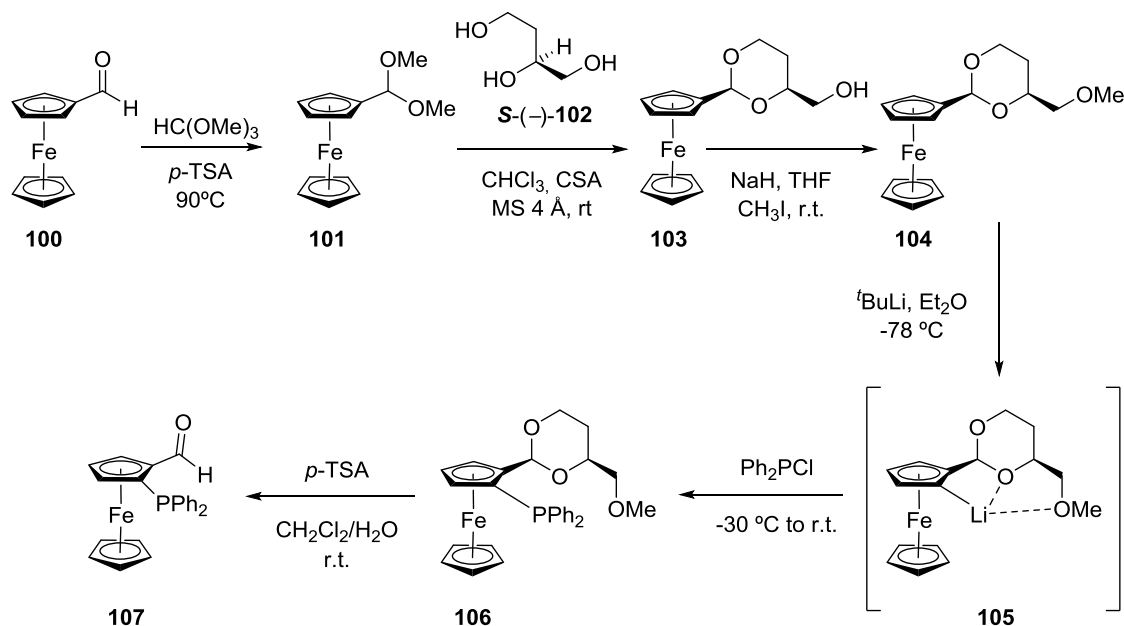
- 1) Enantioselective (2+1) cycloadditions between heterocyclic alkenes and diazo compounds in order to obtain substituted cyclopropanes.
- 2) Intramolecular enantioselective (3+2) cycloaddition reactions as a interesting approach in the synthesis of enantiopure tricyclic chromeno[4,3-*b*]pyrrolidine compounds.
- 3) Intermolecular enantioselective (3+2) cycloaddition reactions in the presence of new dipolarophiles like nitrochromenes, in order to provide an access to enantiopure tricyclic chromeno[3,4-*c*]pyrrolidines.



Scheme 2.17. Main reactions as objective to be catalyzed by ferrocenyl-proline ligands and different metallic salts.

2.3 Novel Ferrocenyl-proline ligand derivatives

First of all, diphenylphosphine ferrocenecarboxaldehyde **107** was synthesized following the methodology reported by Kagan *et al.*⁷⁶ Protection of ferrocene **100** followed by transacetalization reaction with chiral *S*-(-)-butanetriol **102** gave rise to dioxane **103**. Methylation, ortho-lithiation and introduction of the diphenylphosphine group resulted in compound **106**. Brønsted acid catalyzed deprotection led to the desired 1,2-disubstituted ferrocenyl carboxaldehyde **107**.

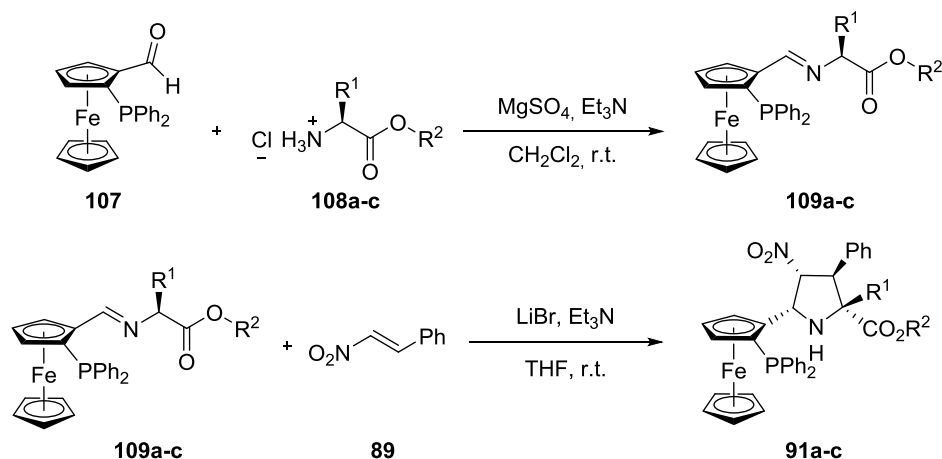


Scheme 2.18. Synthesis sequence reported by Kagan for ferrocenyl carboxaldehyde **107**, precursor of ferrocenyl-proline ligands.

The strategy for the synthesis of ferrocenyl-proline ligand **91a** relied on the condensation of glycine ester **108a** and aldehyde **107** to form imine **109a** (see **Scheme 2.19**). Subsequent (3+2) cycloaddition reaction between imine **109a** and (*E*)-nitrostyrene **89** yielded ligand **NH-D-EhuPhos-91a** in good yield and complete regio-, diastereo- and enantiocontrol.⁷² This procedure was extended to imines **109b-c**. Thus, (3+2) cycloaddition between these imines and dipolarophile **89** in the presence of LiBr and Et₃N yielded with excellent selectivity cycloadducts **NH-TB-D-EhuPhos-91b** and **NH-Bn-D-EhuPhos-91c**.

⁷⁶ Riant, O.; Samuel, O.; Flessner, T.; Taudien, S.; Kagan, H. B. *J. Org. Chem.* **1997**, 62, 6733-6745.

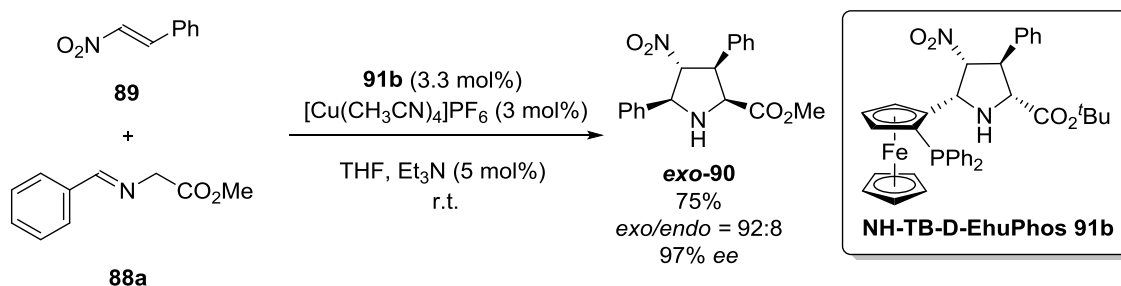
CHAPTER 2



NH-D-EhuPhos 91a: $\text{R}^1 = \text{H}, \text{R}^2 = \text{Me}$
NH-TB-D-EhuPhos 91b: $\text{R}^1 = \text{H}, \text{R}^2 = \text{tBu}$
NH-Bn-D-EhuPhos 91c: $\text{R}^1 = \text{Bn}, \text{R}^2 = \text{Me}$

Scheme 2.19. Transformation of ferrocenyl **107** into hybrid ferrocenyl-proline ligands **91a-c**.

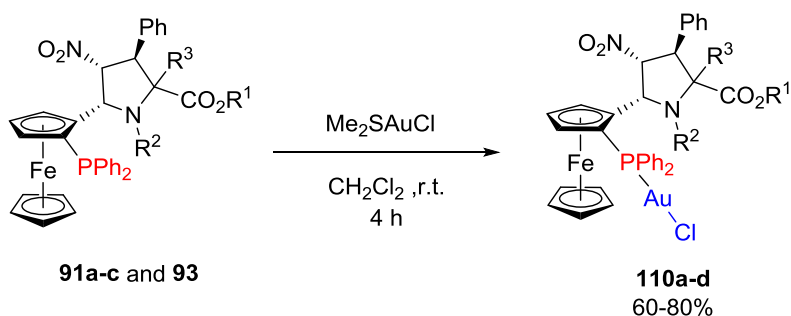
Interestingly, in model reaction between **88a** and **89**, ligand **91b** showed excellent enantiocontrol in presence of $[\text{Cu}(\text{CH}_3\text{CN})_4]\text{PF}_6$ at room temperature, whereas ligand **91a** showed similar result at lower reaction temperatures (**Scheme 2.20**). This fact could be related to the large steric hindrance applied by the tert-butyl group of the ester, thus probably blocking one enantiotopic face more efficiently. Hence, cycloadduct **exo-90** was obtained at room temperature in a 75% yield with a 97% of ee (**Scheme 2.20**).



Scheme 2.20. Enantioselective (3+2) cycloaddition reaction at room temperature catalyzed by ligand **NH-TB-D-EhuPhos-91b**.

Gold complexes **110a-d** were synthesized in order to study their efficiency in intermolecular 1,3-dipolar cycloaddition reactions. These compounds were synthesized under inert atmosphere by reacting with Me_2SAuCl yielding yellow solids with good yields (**Scheme 2.21**). Previous formation of active cationic species of gold(I) was required before their use in catalysis.

CYCLOADDITION REACTIONS



NH-D-EhuPhosAu110a: $R^1 = \text{Me}$, $R^2 = \text{H}$, $R^3 = \text{H}$

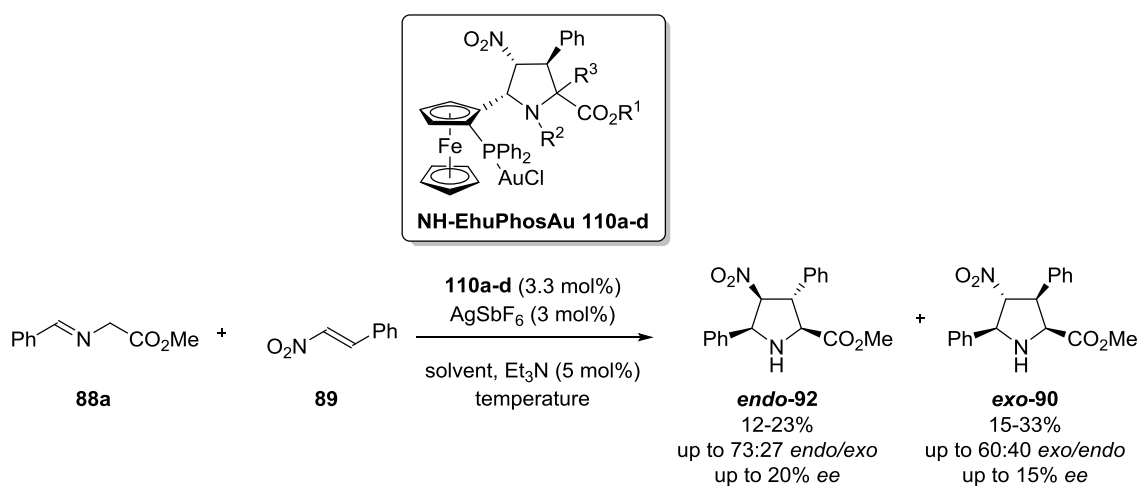
NMe-L-EhuPhosAu110b: $R^1 = \text{Me}$, $R^2 = \text{Me}$, $R^3 = \text{H}$

NH-TB-D-EhuPhosAu110c: $R^1 = \text{tBu}$, $R^2 = \text{H}$, $R^3 = \text{H}$

NH-Bn-D-EhuPhosAu110d: $R^1 = \text{Me}$, $R^2 = \text{H}$, $R^3 = \text{benzyl}$

Scheme 2.21. Synthesis of various Au(I) ferrocenyl-proline complexes.

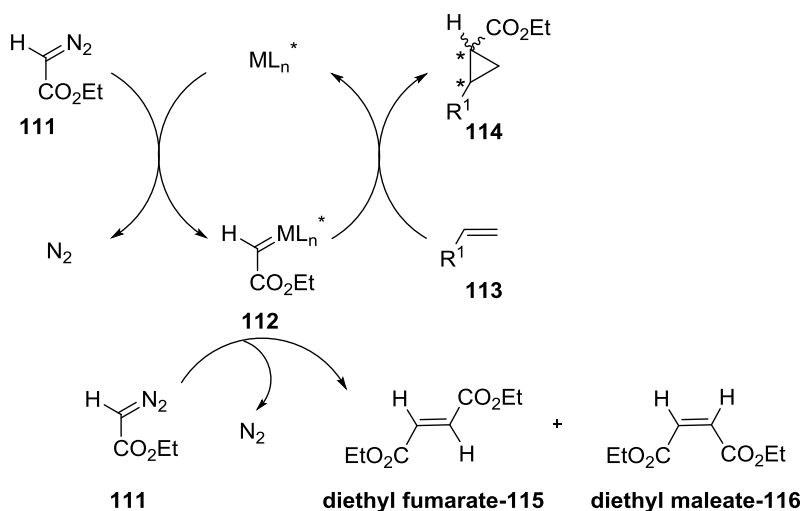
Catalytic (3+2) cycloaddition reaction was carried out by *in situ* activation of gold(I) complexes **110a-d** using AgSbF_6 . These complexes were capable of producing cycloadducts **endo-92** and **exo-90** in lower yields than obtained for copper catalyzed reactions. The temperature and the solvent effects were studied in order to achieve high enantiocontrol of the reaction. Unfortunately, none of the tested Au(I) complexes provided efficient enantiocontrol (up to 20% ee) in the (3+2) cycloaddition reaction between glycine iminoester **88a** and nitrostyrene **89** (**Scheme 2.22**).



Scheme 2.22. Gold(I) complexes **110a-d** catalyzed (3+2) cycloaddition between iminoester **88a** and dipolarophile **89**.

2.4 (2+1) cycloadditions reactions catalyzed by ferrocenyl-proline ligands and transition metals

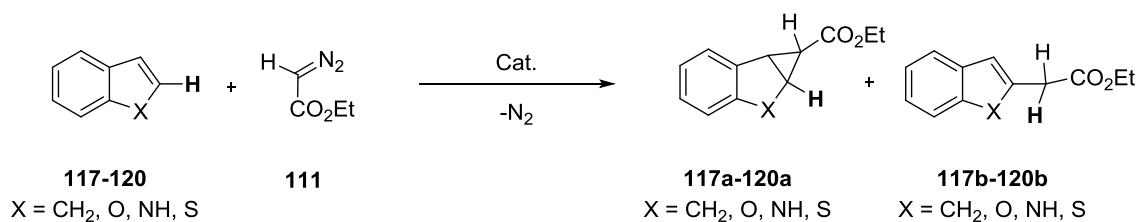
Ethyldiazoacetate (EDA), is the most common diazo compound due to its relative stability and easy manipulation. Cyclopropanes can be obtained in (2+1) cycloadditions between EDA and alkenes, by previous formation of metallocarbene specie **112**. At the same time, metallocarbene **112** can react with another molecule of EDA and lead to non-desirable homocoupling reactions showing the formation of diethyl fumarate and diethyl maleate (**Scheme 2.23**).



Scheme 2.23. Catalytic cycle for (2+1) cycloaddition between EDA and alkenes in presence of metallic complexes.

In order to evaluate the reactivity of EDA, different combinations of metallic sources and heterocyclic alkenes were investigated first. Indene, 2,3-benzofuran, indole and thianaphtene were selected as model substrates. The reactions were monitored by 1H NMR spectroscopy of the crude reaction mixtures. The reactions of indene and benzofuran in the presence of $[Cu(CH_3CN)_4]PF_6$ showed the disappearance of the starting material and formation of a new compounds, although diethyl fumarate and diethyl maleate were present in significant quantities. Ag(I) and Au(I) did not show similar reactivities with EDA. In some cases Ag(I) salts exhibited little reactivity, such as with indene, but there was no full conversion of the starting material into the final product. It is worth to note that reaction of EDA and heterocyclic alkenes in the absence of transition metals did not evolve at all.

CYCLOADDITION REACTIONS



Scheme 2.24. Possible (2+1) and C-H insertion reactions for alkene **117-120** and EDA.

Thus, $[\text{Cu}(\text{CH}_3\text{CN})_4]\text{PF}_6$ salt was selected to be used in combination with ferrocenyl-proline ligands on the efforts to afford cyclopropanes. 2,3-Benzofuran **117** ($\text{X} = \text{O}$) (**Table 2**, entries 1 and 2) afforded the corresponding cyclopropane, yielding solely the *trans* diastereoisomer. Similar results were obtained either when **91a** or **93** were used as ligands. Indene **118** ($\text{X} = \text{CH}_2$) showed the presence of a *trans/cis* mixture in a 75:25 ratio when ligand **91a** catalyzed the reaction (**Table 2**, entry 3). In these case, the chemical yields of adducts **117** and **118** were low and significant amounts of diethyl fumarate and maleate were observed. Although in these reactions both (2+1) cycloaddition and carbene insertion between C-H bonds can be expected (see **Scheme 2.24**), only homocoupling products and (2+1) cycloadducts were observed.

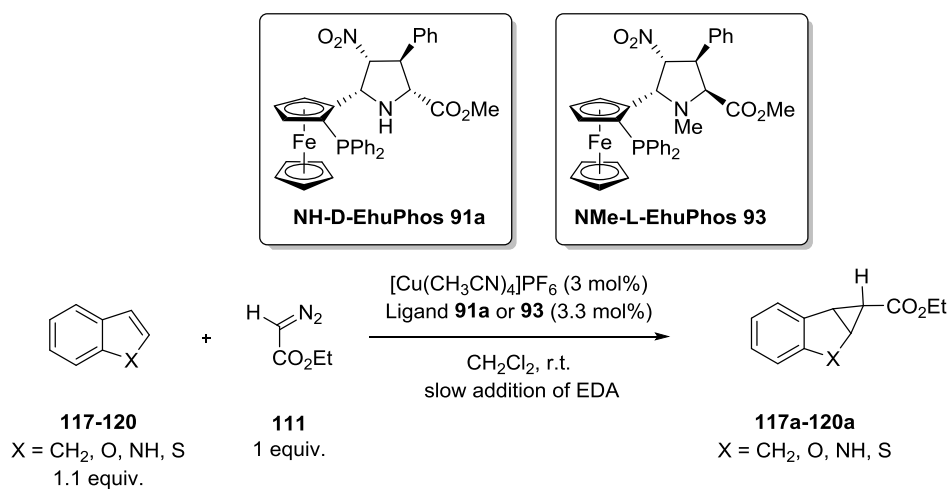
The use of ligand **93** resulted in the sole formation of *trans* isomer (**Table 2**, entry 4). Indole **119** ($\text{X} = \text{NH}$) (**Table 2**, entry 5) and tianaphtene **120** ($\text{X} = \text{S}$) (**Table 2**, entry 6) showed no conversion into the desired products in the presence of Cu(I) and ferrocenyl-proline ligands.

Unfortunately, none of the isolated cyclopropanes showed any enantiomeric excess induced by Cu(I)-ferrocenyl complexes during the reaction. Two hypotheses for the lack of enantiocontrol were considered: 1) The Cu(I) coordination sphere could be complete during the generation of metallocarbene. Therefore, the chiral ligand does not behave as bidentate ligand; 2) ferrocenyl-proline ligands do not provide a suitable environment for the enantioselective cyclopropanation of alkenes.

As a consequence, we envisioned the possibility of changing EDA by a more hindered diazo compounds in order to improve the enantiocontrol. Since methyl ethyldiazoacetate (MEDA) is known to exhibit less reactivity than EDA, lower formation of non-desirable byproducts from homocoupling reaction could be expected.

CHAPTER 2

Table 2. Different heterocyclic substrates in the reaction with EDA catalyzed by Cu(I) and ferrocenyl-proline ligands.

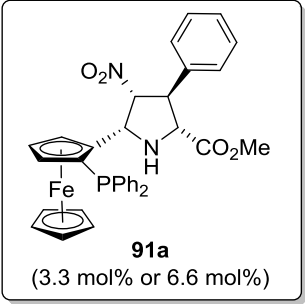


Entry	Alkene	Metal	Ligand	Product	d.r. ^a	Yield (%)		ee ^b
					<i>trans/cis</i>	<i>trans</i>	<i>cis</i>	
1	 117	Cu(CH ₃ CN) ₄ PF ₆	91a	 <i>trans</i> - 117a	100:0	10	-	Rac.
2	 117	Cu(CH ₃ CN) ₄ PF ₆	93	 <i>trans</i> - 117a	100:0	11	-	Rac.
3	 118	Cu(CH ₃ CN) ₄ PF ₆	91a	 118a (<i>trans/cis</i>)	75:25	24	3	Rac.
4	 118	Cu(CH ₃ CN) ₄ PF ₆	93	 <i>trans</i> - 118a	100:0	27	-	Rac.
5	 119	Cu(CH ₃ CN) ₄ PF ₆	93	n.r.	-	-	-	-
6	 120	Cu(CH ₃ CN) ₄ PF ₆	91a	n.r.	-	-	-	-

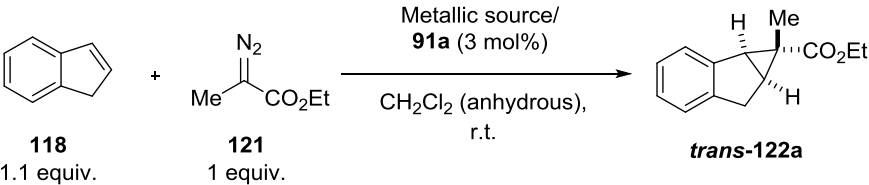
^aDiastereomeric ratio was determined by ¹H NMR spectroscopy. ^bEnantiomeric excess was determined by chiral Daicel OD-H column for HPLC, *n*-Hexane:PrOH 99:1, flow 1.0-0.5 ml/min, λ = 220, 254 nm. n.r. = no reaction.

CYCLOADDITION REACTIONS

Table 3. Screening of different transition metals in the reaction between indene and MEDA.



91a
(3.3 mol% or 6.6 mol%)



118 1.1 equiv. + **121** 1 equiv. $\xrightarrow[\text{CH}_2\text{Cl}_2 \text{ (anhydrous), r.t.}]{\text{Metallic source/ 91a (3 mol\%)}}$ **trans-122a**

Entry	Metal	Ligand	d.r. ^b	Yield (%)	
			<i>trans/cis</i>	<i>trans</i>	<i>cis</i>
1	Cu(CH ₃ CN) ₄ PF ₆	91a	100:0	30	-
2	Rh ₂ (OAc) ₄	91a	100:0	50	-
3 ^c	ZnCl ₂	91a	100:0	n.d.	-

^aBest conversion was for dirhodium tetraacetate with 100%, 2.1/1 equiv. of **91a**/dirhodium tetraacetate used. ^bDiastereoisomeric ratio was determined by ¹H NMR. ^cZnCl₂ catalyzed carbene transfer reaction showed a small conversion but the product was possible to identify by ¹H NMR. ^dByproducts from homocoupling reaction of MEDA were not present.

The results obtained for the reaction of indene **118** in presence of MEDA are collected in **Table 3**. Although Cu(I)/**91a** system catalyzed the reaction (**Table 3**, entry 1) affording **trans-122a** in a 30% yield, dirhodium tetraacetate (**Table 3**, entry 2) exhibited best yield for the synthesis of same compound. On the contrary, ZnCl₂ demonstrated low conversion into compound **122** observed by ¹H NMR of the crude reaction mixture. All attempts with further metallic sources failed to produce (2+1) cycloadduct: FeCl₂, AgOAc, Au(I) complex **110a** and Ru(PPh₃)₃Cl₂.

Therefore, Rh₂(OAc)₄/**91a** complex was the most efficient system to carry out (2+1) cycloaddition between indene **118** and MEDA. The use of other rhodium salts and different temperatures were studied, but no significant difference was observed in the yield either in the enantiocontrol of the reaction.

CHAPTER 2

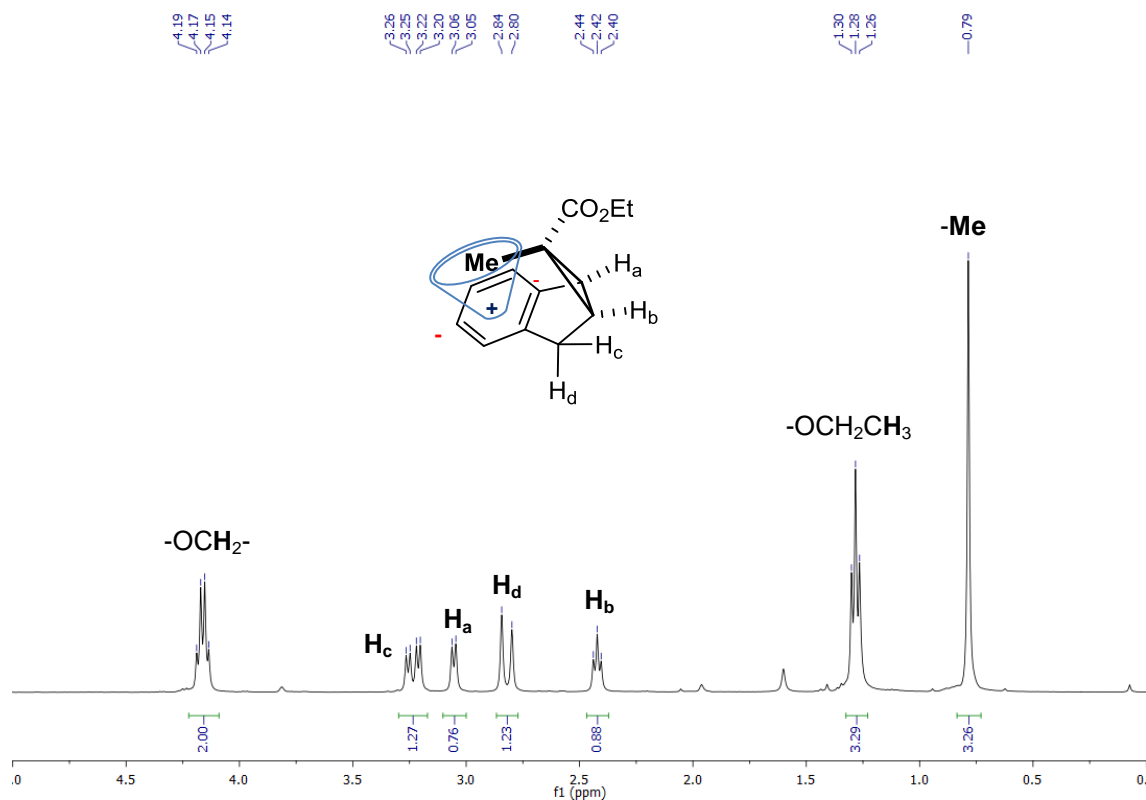


Figure 2.11. Extended ^1H NMR spectrum of compound ***trans*-122a**. It presents characteristic signal of methyl group at 0.79 ppm.

Spectroscopic data of ***trans*-122a** revealed its relative configuration. The methyl group of this compound was observed at 0.79 ppm, a higher field than the commonly observed one. This suggests that the methyl group is in the positive shielding cone of the phenyl group of the indene (see **Fig. 2.11**).

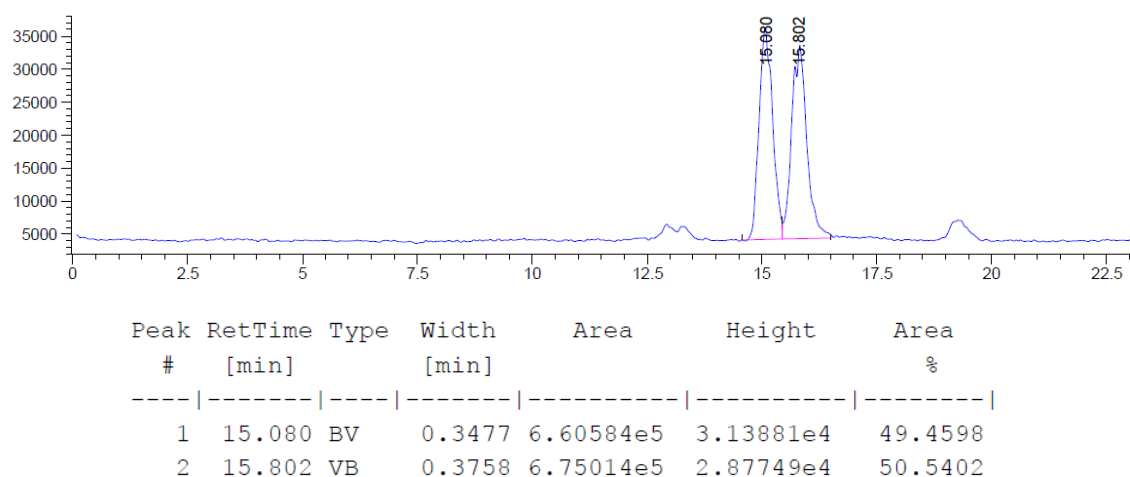


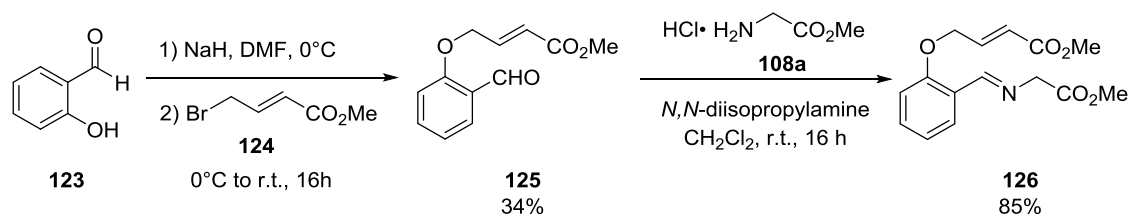
Figure 2.12. HPLC chromatogram of compound ***trans*-122a** using chiral IC column under the following conditions: *iso*-Propanol/*n*-hexane 1:99 flow = 0.5 mL/min, t_{r1} = 15.08 min, t_{r2} = 15.80 min, λ = 220 nm.

The determination of the enantiomeric excess was performed by HPLC coupled to a mass spectrometer in which the enantiomers were separated by the use of chiral column Daicel Chiralpak IC. Unfortunately, HPLC and mass analysis of compound **trans-122a** revealed the racemic nature of the molecule under all the reaction conditions described before. An example for the formation of racemic **trans-122a** by using $\text{Rh}_2(\text{OAc})_4$ in combination with ligand **91a** is gathered in **Figure 2.12**.

2.5 Ferrocenyl-proline ligand catalyzed intramolecular (3+2) cycloaddition reactions

2.5.1 Synthesis of the precursor 126

First of all, imine precursor **126** was synthesized starting from salicylaldehyde **123**. Williamson reaction of compound **123** and **124** afforded aldehyde **125** in a low yield. Aldehyde condensation with glycine methyl ester hydrochloride **108a** allowed the synthesis of imine **126** in good yield.



Scheme 2.25. Williamson reaction of compound **123** and condensation of aldehyde **125** into imine **126**.

Racemic synthesis of chromen[4,3-*b*]pyrrolidine **endo-127** was performed using AgOAc in stoichiometric amount and *N,N*-diisopropylamine as base in acetonitrile at room temperature.⁷⁷ This racemic compound was used as a reference in the studies on the enantioselective intramolecular (3+2) cycloaddition (*vide infra*).



Scheme 2.26. Racemic synthesis of **(±)-endo-127** adduct, formation of tricyclic [4,3-*b*] chromanopyrrolidine.

⁷⁷ Barr, D. A.; Grigg, R.; Gunaratne, H. Q. N.; Kemp, J.; McMeekin, P.; Shridharan, V., *Tetrahedron* **1988**, *44*, 557–570.

CHAPTER 2

2.5.2 Intramolecular enantioselective (3+2) cycloaddition reaction and proposed reaction mechanism

First attempts for the intramolecular (3+2) cycloaddition reaction using ferrocenyl-proline catalysts showed the formation of two products in 50:50 ratio. Physical and spectroscopic data for cycloadduct **endo-127** were identical to those reported in literature.⁷⁸

On the other hand, the second compound isolated was supposed to be an **exo**-cycloadduct due to the chemical shifts observed for the methyl group of the ester. Subsequently, it was possible to obtain a suitable crystal for this **exo**-cycloadduct, which was analyzed by X-ray diffraction. In addition, compound was obtained as a dimer, whose X-ray diffraction analysis can be observed in **Figure 2.13**. Structure observed was similar to the one reported by Pfaltz.⁷⁸

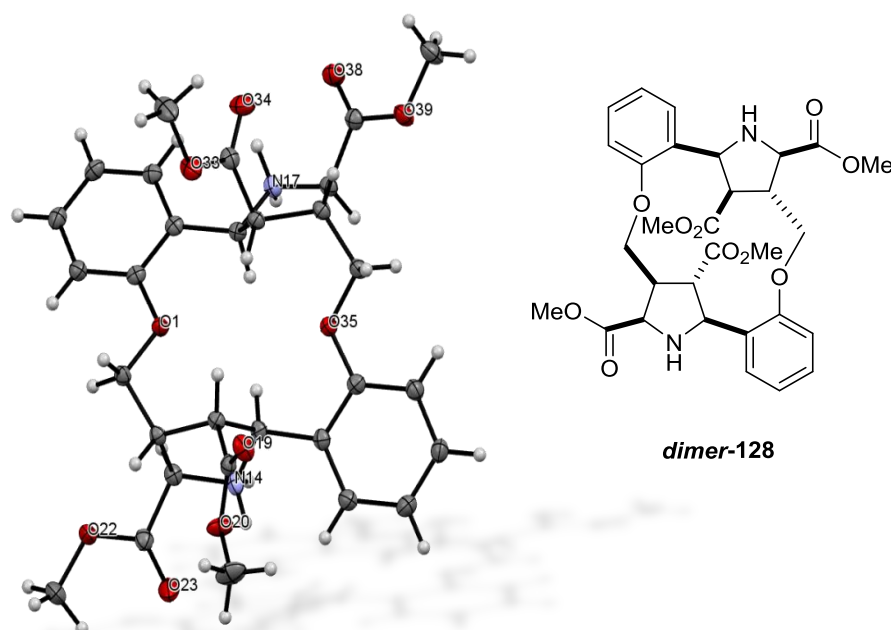


Figure 2.13. ORTEP diagram with thermal ellipsoids in a 50% probability for molecule **dimer-128**.

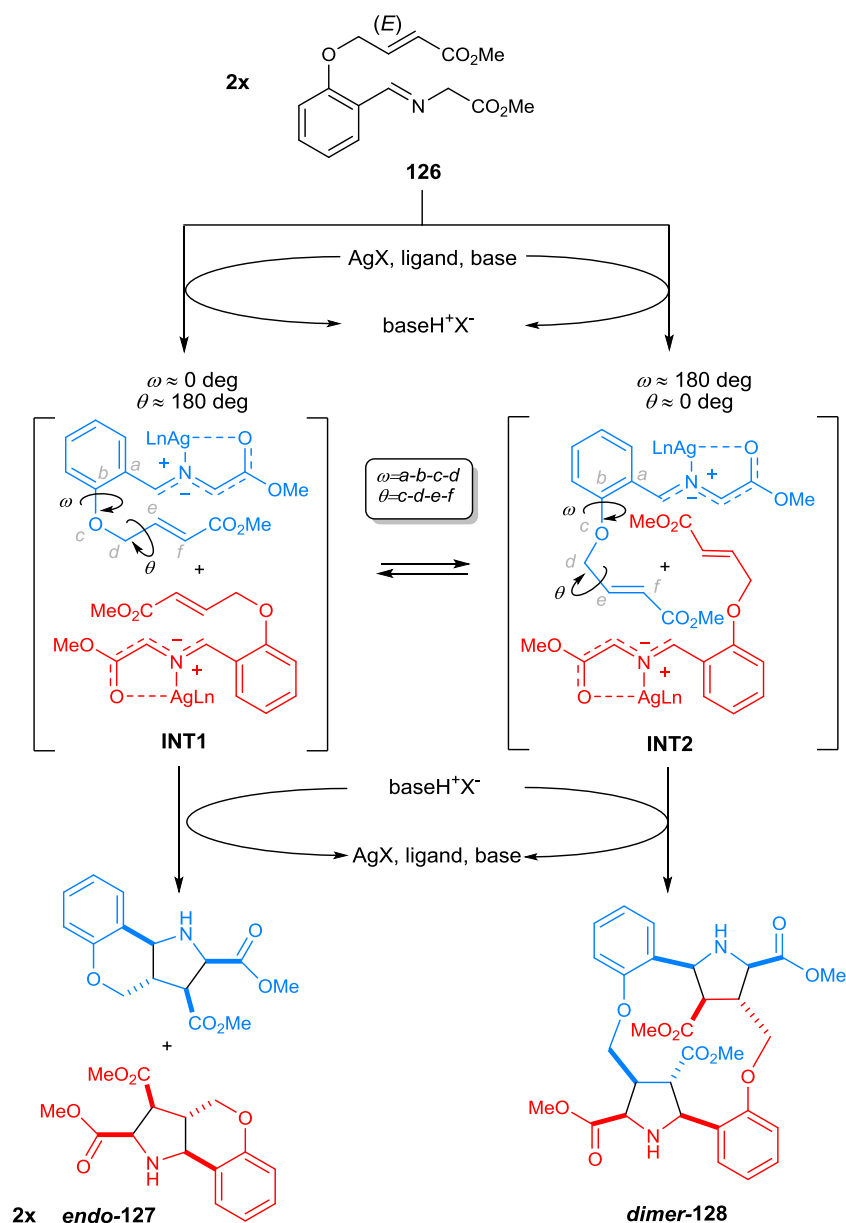
The formation of dimeric cycloadduct **dimer-128** can be rationalized taking into account the double character of imine **126** as source of *N*-metalated azomethine ylide and as a dipolarophile. This compound has a considerable conformational freedom around the Ph-O-CH₂ moiety. Thus, if we define the dihedral angles ω and θ as depicted in **Scheme 2.27** we can get the two different situations. When $\omega \approx 0$ deg and $\theta \approx 180$ deg, the intermediate azomethine ylide **INT1** (**Scheme 2.27**) adopts the *closed* conformation required for the intramolecular (3+2) cycloaddition (concerted and stepwise) and it can yield **endo-127**.

In contrast, when $\omega \approx 180$ deg and $\theta \approx 0$ deg, the *open* conformation of azomethine ylide **INT2** precludes the intramolecular (3+2) cycloaddition and favors an

⁷⁸ Stohler, R.; Wahl, F.; Pfaltz, A., *Synthesis* **2005**, 1431–1436.

CYCLOADDITION REACTIONS

intermolecular process through a crossed interaction between 1,3-dipole of one molecule of **INT2** and the dipolarophile moiety of the other component, as it is depicted in **Scheme 2.27**. As a consequence, in this second case the dimeric cycloadduct **dimer-128** will be obtained. The relative abundance of this latter compound suggests that the conformational freedom of **126** should result in similar proportion of azomethine ylides **INT1** and **INT2**. Probably only under high dilution conditions (in which low conversions and large reaction times would be observed) the formation of **dimer-128** could be avoided or, at least minimized.



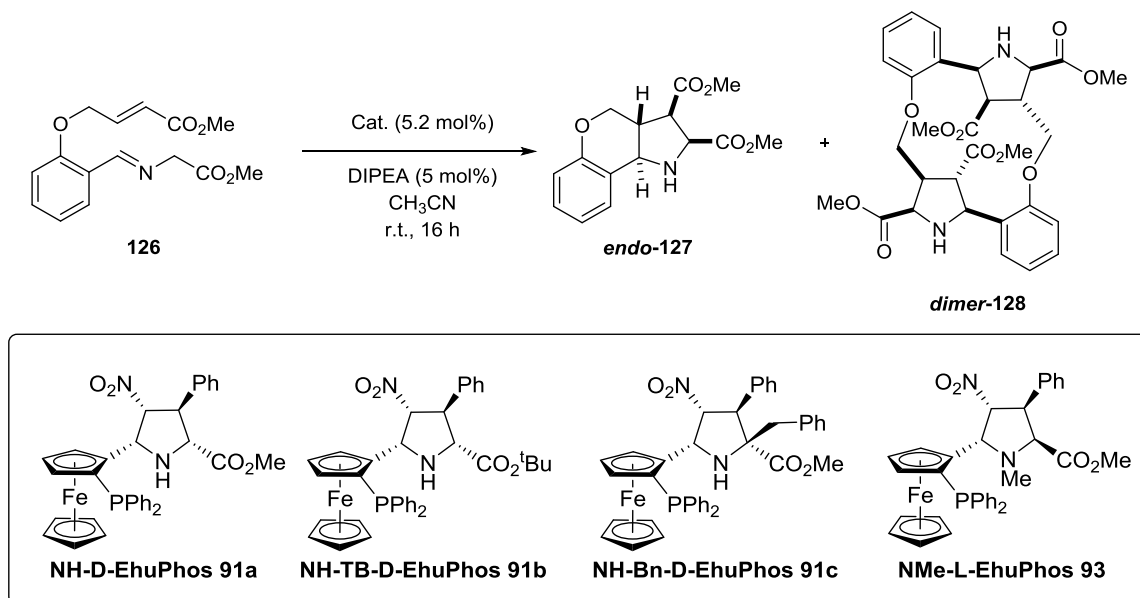
Scheme 2.27. Proposed inter- and intramolecular (3+2) cycloaddition mechanism of compound **126** to yield either **endo-127** and **dimer-128**.

CHAPTER 2

2.5.3 Optimization of enantioselective intramolecular reaction conditions

The results summarized in **Table 4** show at first the effect of metallic salts of group XI. Au(I), Cu(I) and Ag(I) salts (**Table 4**, entries 1-3) were tested in the intramolecular (3+2) cycloaddition reaction of **126** in the presence of DIPEA and acetonitrile at room temperature.

Table 4. Screening of metallic salts and ligands in the intramolecular cycloaddition reaction of **126**.



Entry	Ligand	Metallic salt	<i>endo</i> -127/ <i>dimer</i> -128	Yield ^a (%)		ee ^b (%)	
				<i>endo</i> -127	<i>dimer</i> -128	<i>endo</i> -127	<i>dimer</i> -128
1	110c^c	Au(I)/BARF	n.r.	n.r.	n.r.	n.d.	n.d.
2	91b	Cu(CH ₃ CN) ₄ PF ₆	n.r.	n.r.	n.r.	n.d.	n.d.
3	91b	AgClO ₄	50:50	33	40	30	Rac.
4	91a	AgClO ₄	50:50	8	15	25	Rac.
5	91c	AgClO ₄	50:50	16	30	Rac.	Rac.
6	93	AgClO ₄	50:50	23	40	Rac.	Rac.
7	91b	AgOAc	60:40	30	25	20	Rac.
8	91b	AgSbF ₆	55:45	27	36	15	Rac.
9	91b	AgOTf	50:50	17	37	9	Rac.
10	91b	AgPF ₆	50:50	18	38	15	Rac.

^aYield determined from isolated product after purification. ^b Enantiomeric excess was measured by HPLC: IB column; **endo**-127 cycloadducts: 95:5 Hex:ⁱPrOH, 1 mL/min, λ = 277 nm; **dimer**-128: 75:25 Hex:ⁱPrOH, 1 mL/min, λ = 233, 273 nm. ^cGold(I) complex **110c**'s structure is depicted in **Scheme 2.21**. n.d. = not determined. n.r. = no reaction.

CYCLOADDITION REACTIONS

Silver complexes showed the formation of two products whereas gold and copper complexes did not show the formation of desired product. Ligand **91b** and silver perchlorate catalyzed (3+2) intramolecular reaction led to the formation of adduct **endo-127** which showed 30 % of ee (**Table 4**, entry 3).

Different ferrocenyl ligands were tested in the intramolecular (3+2) cycloaddition reaction. Ligand **91a** or **91b** showed similar ee values for **endo-127**, although the enantiocontrol obtained with **91b** was slightly higher (**Table 4**, entries 3 and 4). In comparison, ligands **93** and **91c** (**Table 4**, entries 5 and 6) bearing *N*-methyl and α -benzyl groups respectively, destroyed the enantiomeric excess. Owing to the slight improvement induced by tert-butyl ester group of ligand **91b**, it was selected for further studies.

Considering the enantiomeric excess and diastereocontrol demonstrated by different silver (I) salts (**Table 4**, entries 3 and 7 to 10) AgClO₄ showed best enantiocontrol of the reaction (**Table 4**, entry 3). Although, the **endo/dimer** diastereocontrol obtained with AgOAc was slightly better favoring **endo-127** product formation slightly (**Table 4**, entry 7), improvement of the enantiomeric excess was prioritized for the optimization of the process. It is worth it to note that **dimer-128** was found to be racemic in all cases. Following the optimization process of the intramolecular reaction solvent effect was studied (**Table 5**, entries 1-5).

As it can be observed in **Table 5**, toluene and DCM exhibited better enantioselectivities comparing to the rest of solvents (**Table 5**, entries 2 and 4). Distinctively, THF exhibited better diastereocontrol but the enantiomeric excess was found to be the lowest (**Table 5**, entry 3).

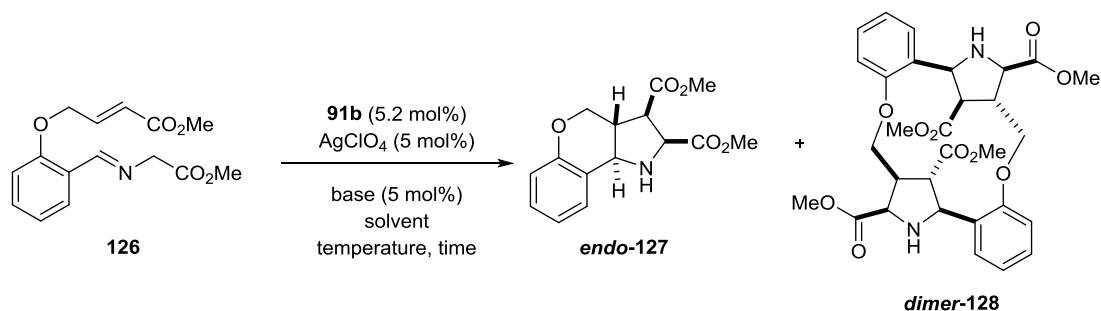
Screening at different temperatures was carried out in order to improve the ee value of **endo-127**. When reaction was carried out in toluene, at -80°C, reaction showed a conversion smaller than 5% after 60 h of reaction (**Table 5**, entry 7). On the other hand, when the reaction was carried out using toluene, at -40°C total conversion of the starting material was observed and best enantiomeric excess of 60% was achieved for **endo-127** (**Table 5**, entry 8). Interestingly, CH₂Cl₂ showed conversion of just 50 % after 48 h at -40°C, but **endo-127** adduct was isolated with 60% of ee (**Table 5**, entry 9).

At last, influence of the type of base was analyzed. AgOAc was employed instead of AgClO₄ observing no improvement of the enantiocontrol (AgOAc can act as source of coordinating metal and AcO⁻ can act as base) (**Table 5**, entry 9). Et₃N was also employed as base of the reaction observing similar results as when DIPEA was used (**Table 5**, entry 10).

Unfortunately, under the best reaction conditions, **endo-127** adduct was obtained with a maximum enantiomeric excess of 60% ee. We concluded that ferrocenyl-proline ligands were able to induce a moderate enantiomeric excess for the intramolecular (3+2) cycloaddition of imine **126**.

CHAPTER 2

Table 5. Solvent, base and temperature effect in enantiocontrol of intramolecular reaction.



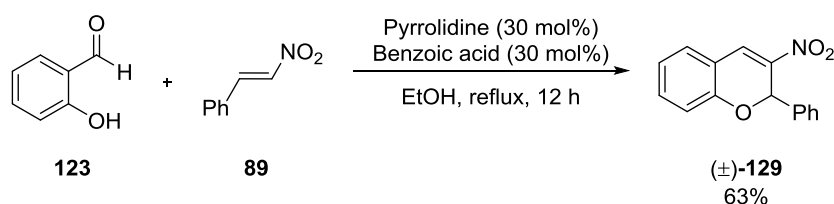
Entry	Solvent	Base (5 mol%)	T (°C)	Reaction Time (h)	<i>endo</i> -127/ <i>dimer</i> -128	Yield ^a (%)		ee ^b (%)	
						127	128	127	128
1	CH ₃ CN	DIPEA	r.t.	16	50:50	33	40	30	Rac.
2	Toluene	DIPEA	r.t.	16	60:40	47	50	40	Rac.
3	THF	DIPEA	r.t.	16	65:35	20	20	20	Rac.
4	CH ₂ Cl ₂	DIPEA	r.t.	16	60:40	35	63	50	Rac.
5 ^c	DMF	DIPEA	r.t.	16	50:50	n.d.	n.d.	n.d.	n.d.
6	Toluene	DIPEA	-80°C	60	-	-	-	-	-
7	Toluene	DIPEA	-40°C	48	n.d.	Conv. >99%		60	Rac.
8	CH ₂ Cl ₂	DIPEA	-40°C	84	n.d.	Conv. = 50%		60	Rac.
9 ^d	Toluene	AgOAc	-40°C	48	60:40	Conv. >99%		57	Rac.
10	Toluene	Et ₃ N	-40°C	48	60:40	Conv. >99%		60	Rac.

All reactions performed using 5 mol% of AgClO_4 and 5.2 mol% of **91b**. ^aYield determined from isolated products after purification and conversion determined by ¹H NMR spectroscopy. ^b Enantiomeric excess was measured by HPLC: IB column; **endo**-127: 95:5 Hex: ⁱPrOH, 1 mL/min, λ = 277 nm; **dimer**-128: 75:25 Hex: ⁱPrOH, 1 mL/min, λ = 233, 273 nm. ^cAlmost no conversion of the reaction. ^dAgOAc (5 mol%) was used as base and as metallic source. n.d. = not determined.

2.6 Intermolecular enantioselective (3+2) cycloadditions catalyzed by ferrocenyl-proline ligands and transition metals

2.6.1 Synthesis of 3-nitrochromene and optimization of reaction conditions

We prepared 2-aryl-3-nitrochromers by means of the procedure reported by Wang and coworkers. These authors have recently synthesized 2-aryl-3-nitro-2*H*-chromenes starting from readily available starting materials such as salicylaldehyde and nitrostyrene derivatives.⁷⁹ Pyrrolidine and benzoic acid are present in 30 mol% as catalyst/cocatalyst and the reaction is carried out under reflux of EtOH. Mechanistically, compound **129** is obtained after oxa-Michael addition of the phenyl moiety of **123**, followed by a Henry addition/elimination sequence.



Scheme 2.28. 2-phenyl-3-nitrochromene **129** synthesis.

To the best of our knowledge, enantioselective (3+2) cycloadditions of α -iminoesters with 3-nitrochromenes as dipolarophiles in enantioselective fashion has not been studied previously. Thus, following our interest in the synthesis of tricyclic molecules of biological interest via (3+2) cycloadditions, we decided to study the reaction between bicyclic dipolarophile **129** and *N*-metalated azomethine ylides derived from imines, taking into account the previous work developed with ferrocenyl-proline ligands.⁷²

Screening of ligands was performed at room temperature. The diastereomeric ratios, conversion into products and enantiomeric excesses of the crude reaction mixtures were compared in order to select the best ligand for this reaction (**Table 6**, entries 1 to 4). ¹H NMR analysis of the reaction mixtures showed two major products, which presented similar spectroscopic data, leading us to consider them as diastereoisomers **130a** and **130'a**. Further studies of elucidation of the structure of these compounds will be explained in the next section.

Ligand **91a** showed moderate diastereomeric ratio, good conversion and moderate enantiomeric excess for the reaction (**Table 6**, entry 1). Comparing ligand **91a** versus ligand **91b** (**Table 6**, entry 2), the latter demonstrated better results in terms of diastereo- and enantiocontrol and a slightly higher conversion.

⁷⁹ Wang, P.; Zhang, D.; Liu, X., *Arkivoc* **2014**, v, 408–419.

CHAPTER 2

Table 6. Optimization of model reaction involving iminoester **88a** and dipolarophile **129**.

<div style="display: flex; justify-content: space-around; align-items: center;"> <div style="text-align: center;"> <p>NH-D-EhuPhos-91a</p> </div> <div style="text-align: center;"> <p>NMe-L-EhuPhos-93</p> </div> <div style="text-align: center;"> <p>NH-TB-D-EhuPhos-91b</p> </div> <div style="text-align: center;"> <p>NH-TB-D-EhuPhosAu-110c</p> </div> </div>						
Entry	Ligand/Additive	Temperature (°C)	130a/ 130'a	Conversion (%) ^a	ee ^b (%)	
					130a	130'a
1	91a	r.t.	68:32	60	50 ^c	n.d.
2	91b	r.t.	80:20	75	65 ^c (45)	n.d.
3	93	r.t.	>99:1	65	33 ^c	n.d..
4 ^d	110c /BARF	r.t.	55:45	29	n.d.	n.d.
5	91b	40°C.	85:15	70	33	n.d.
6	91b	0°C.	60:40	n.d.	77	73
7	91b	-20°C.	52:48	84	89	67
8	91b	-40°C.	46:54	85	73	40

^aConversion determined by ¹H NMR spectroscopy. ^bEnantiomeric excess was measured by HPLC: IB column 95:5 Hex: iPrOH, 1 mL/min, λ = 233 nm. ^cEnantiomeric excess measured for the crude, in parenthesis after purification. ^dReaction with Au(I) was carried out for 76 h without further conversion (no presence of [Cu(CH₃CN)₄]PF₆). n.d. = not determined.

Although ligand **93** showed full diastereocontrol favoring formation of **130a** exclusively, poor enantiomeric excess was observed. Activation of gold (I) complex **110c** promoted the formation of **130a** and **130'a**, but even after 76 h of reaction conversion was did not evolved from 29%. In summary, ligand **91b** exhibited best results at room temperature, probably due to the steric hindrance exerted by the spinning of tert-butyl group of the ester.

The effect of the temperature on the enantio- and diastereocontrol was also studied. It was observed that when the reaction was carried out from high to lower temperatures the diastereocontrol decreased considerably while enantiocontrol rose up

(Table 6, entry 2 and entries 5 to 9). Hence, the optimal temperature selected for the model reaction was -20°C (Table 6, entry 7). At this temperature the reaction presented no diastereocontrol, although, both diastereoisomers were isolated with acceptable 89% and 67% enantiomeric excesses, respectively.

2.6.2 Relative and absolute configuration of diastereoisomers

In the model reaction two diastereoisomers were synthesized and under optimized reaction conditions both isomers were found to be present in equal amounts (see Table 6). Cycloadduct **130a** was first analyzed by ^1H NMR spectroscopy.

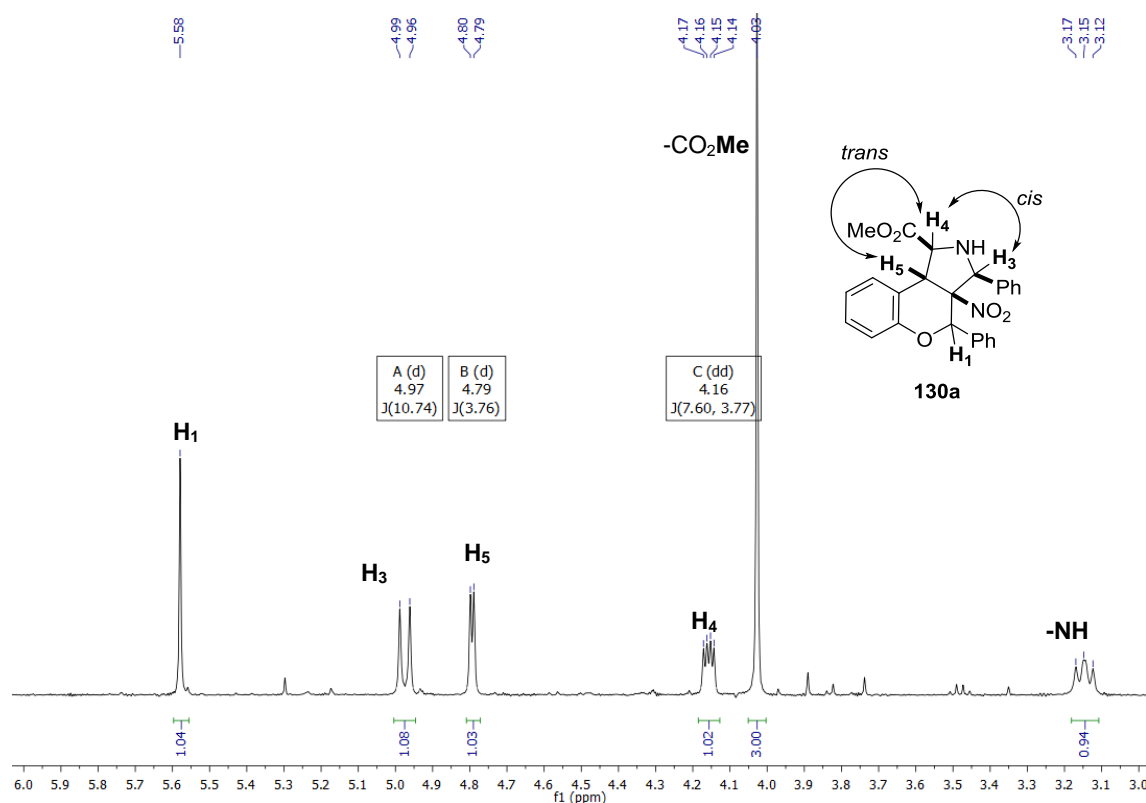


Figure 2.14. ^1H NMR spectrum for diastereoisomer **130a** and representative signals of pyrrolidine ring.

Signals corresponding to the pyrrolidine are shown in Figure 2.14. With exception of the singlet at 5.58 ppm which was unequivocally assigned to H_1 , all the signals of adduct **130a** were assigned by COSY and HSQC-correlation (see Annex I). Owing to the coupling constants and multiplicities observed for proton at 4.16 ppm we assumed it was the proton in α to the ester group, H_4 . Assignment of signals at 4.97 and 4.16 ppm, respectively, was made by comparing the respective coupling constants. It is well known that pyrrolidines in nearly envelope conformation present a $J\text{-cis} > J\text{-trans}$ in the flat part of the envelope. In view of that, proton at 4.97 ppm presents a large coupling constant of 10.74 Hz. Therefore, it can be concluded that proton H_4 and the one at 4.97 ppm are in *cis* disposition. On the other hand, coupling constant of 3.77 Hz was measured for the proton signal at 4.79 ppm, which was assumed to be compatible with a *trans* disposition with respect to H_4 . 2D-HSQC correlation

CHAPTER 2

experiments showed that proton at 4.79 ppm was adjacent to carbon at 46.2 ppm. This permitted us to assign this signal as **H**₅. Hence, relative configuration of the pyrrolidine ring in compound **130a** was assigned. Configuration of **H**₁ was not possible to determine from the analysis of the spectroscopic data.

We were able to obtain suitable crystals of enantiopure compound **130a** which were studied by X-ray diffraction. The absolute configuration of cycloadduct **130a** was assigned for all asymmetric carbons C1, C2, C3, C4, C5 as *S*, *R*, *R*, *R*, *S*, respectively. (see Annex III). The ORTEP diagram is shown in **Figure 2.15**.

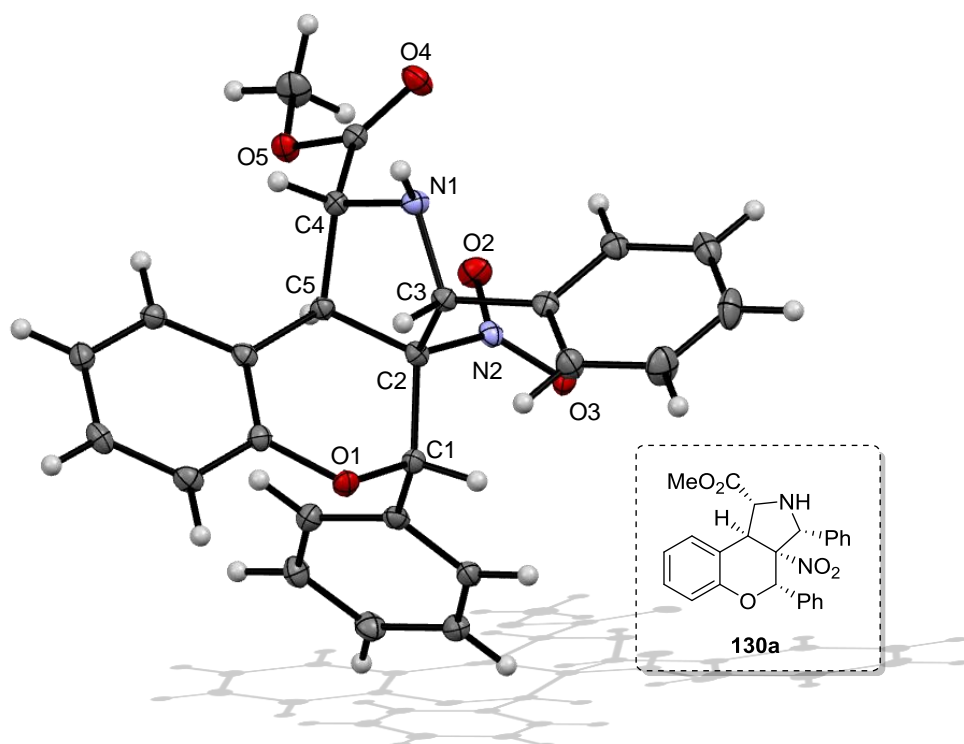
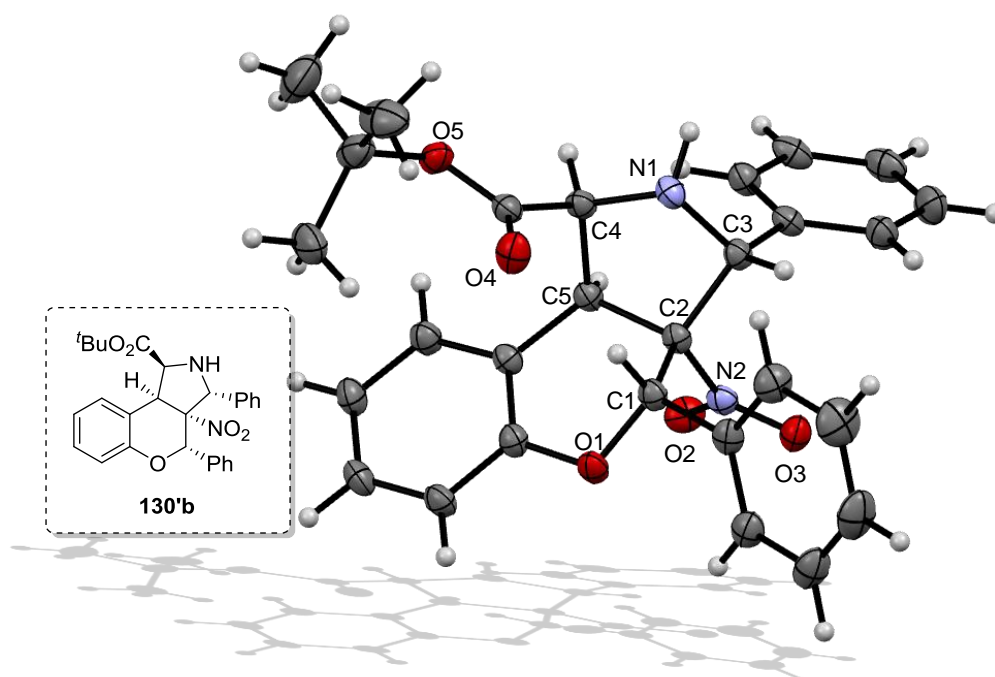
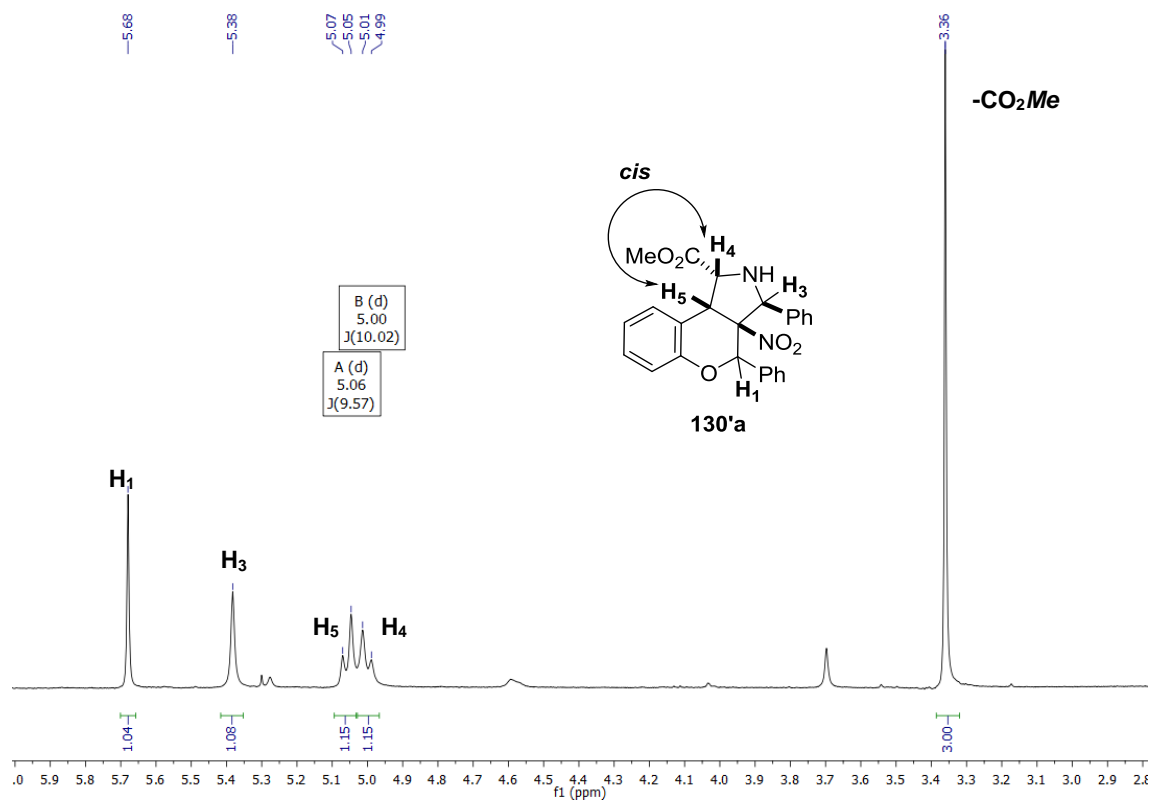


Figure 2.15. ORTEP diagram with thermal ellipsoids in a 50% probability for cycloadduct **130a**.

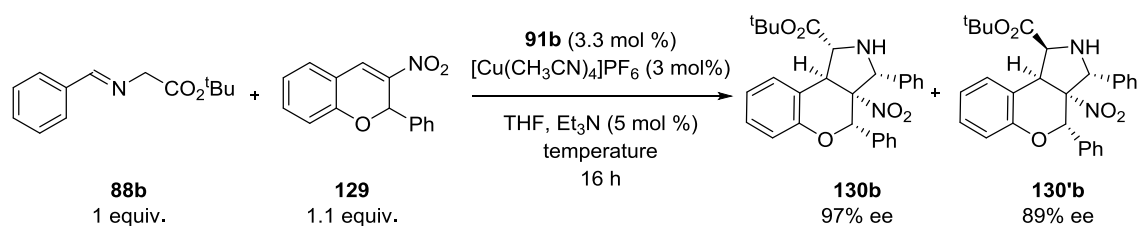
Additionally, the second diastereoisomer **130'a** was analyzed by ¹H NMR. In this case protons **H**₄ (5.00 ppm) and **H**₅ (5.06 ppm) were found to be in *cis* disposition to each other since their coupling constants are 9.57 and 10.02 Hz, respectively. Interestingly, the methoxy signal of the ester, which was placed at 4.03 ppm for **130a**, now is observed at 3.36 ppm. This effect is related to the inversion of configuration observed in the **H**₄ proton. In this case we were not able to obtain suitable crystals of **130'a** for their study by X-ray diffraction.

In view that we could not elucidate the structure for compound **130'a** we carried out the enantioselective (3+2) cycloaddition reaction between tert-butyl iminoester **88b** and dipolarophile **129**. Compounds **130b** and **130'b** were obtained with high enantiomeric excesses (see **Scheme 2.29**).

CYCLOADDITION REACTIONS



CHAPTER 2



Scheme 2.29. Synthesis of tert-butyl ester cycloadducts **130b** and **130'b** by (3+2) cycloaddition reaction.

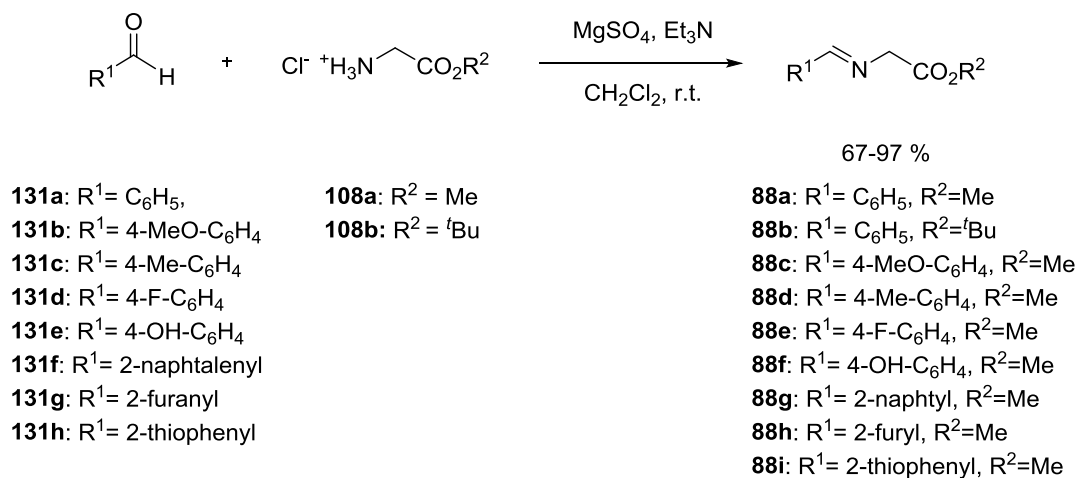
Suitable crystals were obtained for compound **130'b**, and thus, they were studied by X-ray diffraction analysis. Compound **130'b** showed the same configuration found for compound **130a** but with an inversion of configuration in the asymmetric carbon α to the ester group (compare C4 of **Fig 2.19** and **Fig 2.17**). Thus, **130'b** revealed absolute configuration for asymmetric carbons C1, C2, C3, C4 y C5 as S, R, R, S y S, respectively (see Annex III).

Regarding to the structure, tert-butyl ester group is placed in the positive shielding cone of the phenyl group of the chromene, similarly methyl group could be placed as well for compound **130'a**. This effect would justify the displacement of the –CO₂Me signal to higher field.

On the basis of these studies we concluded that the configuration of major enantiomers of cycloadducts **130a** and **130'a** is the one shown in **Table 6**.

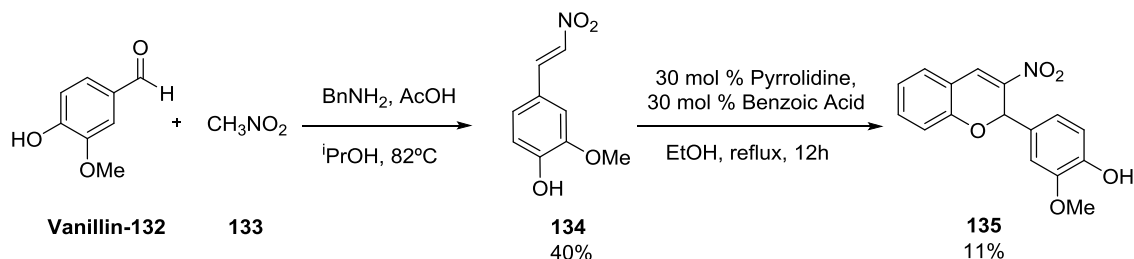
2.6.3 Synthesis of α -iminoesters **88a-i** and aryl chromene derivative **135**

In order to enlarge the scope of the reaction several substitution patterns were explored. For that, it was necessary to synthesize several α -iminoester derivatives, as well as different dipolarophiles.



Scheme 2.30. Synthesis of glycine derived α -iminoester compounds **88a-i**.

α -Iminoesters **88a-i** were synthesized starting from their corresponding aldehyde and glycine ester. In general aldehydes were totally converted into the respective imines with good to excellent yields. Vanillin-**132** reacted with **133** in presence of benzylamine and acetic acid to afford nitroalkene **134** in a moderate yield. Following the synthetic procedure described by Liu⁷⁹ chromene **135** was obtained in low yield.



Scheme 2.31. Synthesis of nitroalkene **134** and modulated dipolarophile **135**.

2.6.4 Scope of the reaction: chromeno[3,4-*c*]pyrrolidine derivatives

The scope of this reaction was analyzed under the previously optimized reaction conditions. The substitution pattern of the azomethine ylide was first analyzed. In addition, substitutions in the ester and on the 2-aryl group of the chromene were studied. All the results obtained are collected in **Table 7**.

As we have previously discussed in the elucidation of the stereochemistry of the reaction, installation of a tert-butyl group instead of a methyl ester showed a similar stereochemical outcome (**Table 7**, entry 1 and entry 2). However, the presence of a tert-butyl group slightly favors the formation of adduct **130b** compared to methylester cycloadduct formation. Moreover, enantiomeric excess for both diastereoisomers increased, obtaining for **130b** a 97% value of ee.

The effect of different electron-donating and electron-withdrawing groups placed in *para*-position of the aromatic ring was also analyzed. Methoxy is a strong activating group and when it was introduced in *para*-position showed higher reactivity in terms of conversion of the reaction (**Table 7**, entry 3). On the other hand, *para*-fluorophenyl as electron-withdrawing group presented lower reactivity with a maximum conversion of 47% (**Table 7**, entry 5). Reaction with *para*-nitrophenyl group was tried but small conversion was observed and isolation of products was not possible.

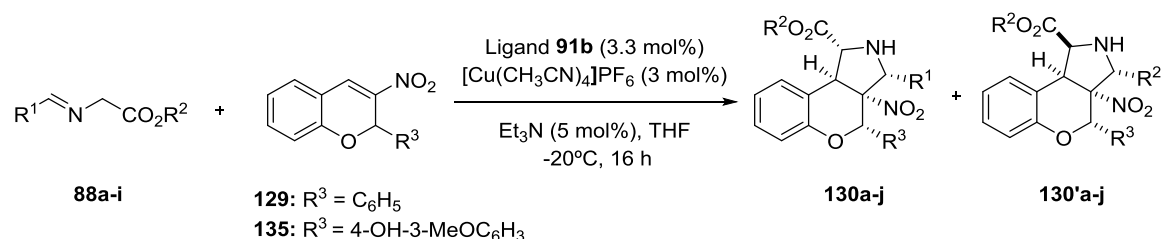
No diastereocontrol was observed either for *para*-fluorophenyl or other substitution patterns (**Table 7**, entries 3-10). The enantiomeric excesses observed for both strong electron-donating and electron-withdrawing groups were good to excellent (**Table 7**, entries 3-6). The compound bearing the most electron-donating *para*-methoxyphenyl moiety showed the highest enantiomeric excess (91% ee, **Table 7**, entry 3). Lower ee values were observed for cycloadducts **130e** and **130'e**, including *para*-fluorophenyl group to the substituted tricycles (83% ee, **Table 7**, entry 5).

Reactions with different aromatic frameworks were studied as well. 2-Naphtyl moiety behaved similar to phenyl containing compounds in terms of reactivity,

CHAPTER 2

diastereo- and enantiocontrol (**Table 7**, entry 7). 2-Furyl substituted compound, on the other hand, exhibited excellent enantiomeric excess for cycloadduct **130h** (**Table 7**, entry 8). However, introduction of 2-thiophenyl moiety in the tricyclic compound decreased considerably the enantiocontrol (**Table 7**, entry 9).

Table 7. Scope of the reaction with different substituents.



Entry	R^1	R^2	R^3	Conv. (%) ^a	d.r. ^a	Product	Yield ^b (%)		ee ^c (%)	
							130	130'	130	130'
1	Ph	Me	Ph	85	52:48	a	32	31	89	67
2	Ph	^t Bu	Ph	76	63:37	b	24	15	97	89
3	4-MeO-Ph	Me	Ph	90	48:52	c	22	16	91	72
4	4-Me-Ph	Me	Ph	74	48:52	d	27	24	89	77
5	4-F-Ph	Me	Ph	47	46:54	e	22	22	83	68
6	4-OH-Ph	Me	Ph	70	45:55	f	14	16	85	68
7	2-naphtyl	Me	Ph	66	51:49	g	27	32	84	58
8	2-furyl	Me	Ph	83	45:55	h	21	27	97	71.
9	2-thiophenyl	Me	Ph	71	50:50	i	21	26	63	64
10	Ph	Me	4-OH-3-MeO-Ph	49	45:55	j	15	18	90	44

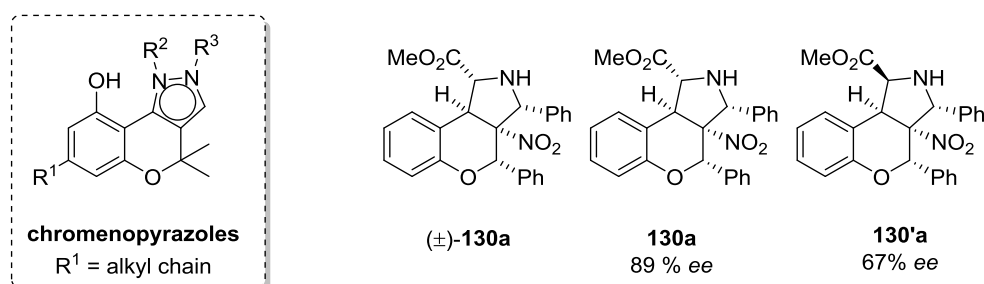
All reactions were performed starting from 0.34 to 0.29 mmol of corresponding imine. ^aConversion and diastereomeric ratio were determined by ^1H NMR of crude reaction. ^bYield was determined from isolated product after purification. ^c Enantiomeric excess was measured by HPLC with different chiral columns (see experimental part) in $\lambda = 233$ nm.

If chromene **135** was employed as dipolarophile, bearing a *para*-hydroxy-*meta*-methoxyphenyl ring on it, lower reactivity was observed (**Table 7**, entry 10). Enantiomeric excess for **130j** was excellent, but in contrast **130'j** isomer showed a dramatic decrease on the enantiomeric excess compared to model reaction using chromene **129** (**Table 7**, compare entry 1 with entry 10).

2.6.5 Cannabinoid receptor affinity of chromeno[3,4-*c*]pyrrolidines

In view of the similarity of our developed structures with chromenopyrazoles reported by Jagerovic that have shown interesting results in the binding of CB1 and CB2 receptors, our compounds were sent to analyze their affinity abilities.⁸⁰ Radioligand displacement studies were performed with molecule (\pm)-**130a** (racemic), **130a** (89% ee) and **130'a** (67% ee). The results obtained by Jagerovic and coworkers (Instituto de Química Médica, Madrid) are described in **Table 8**.

Table 8. Affinities measured for chromenopyrrolidines **130a** and **130'a**.



Entry	Compound	e.r.	% Affinity CB1 ^a	% Affinity CB2 ^a
1	(\pm)- 130a	50:50	57	55
2	130a	94.5:5.5	50	44
3	130'a	83.5:16.5	41	39

^aAverage of three experiments run three times in different dates. Compounds were tested at 40 μ M.

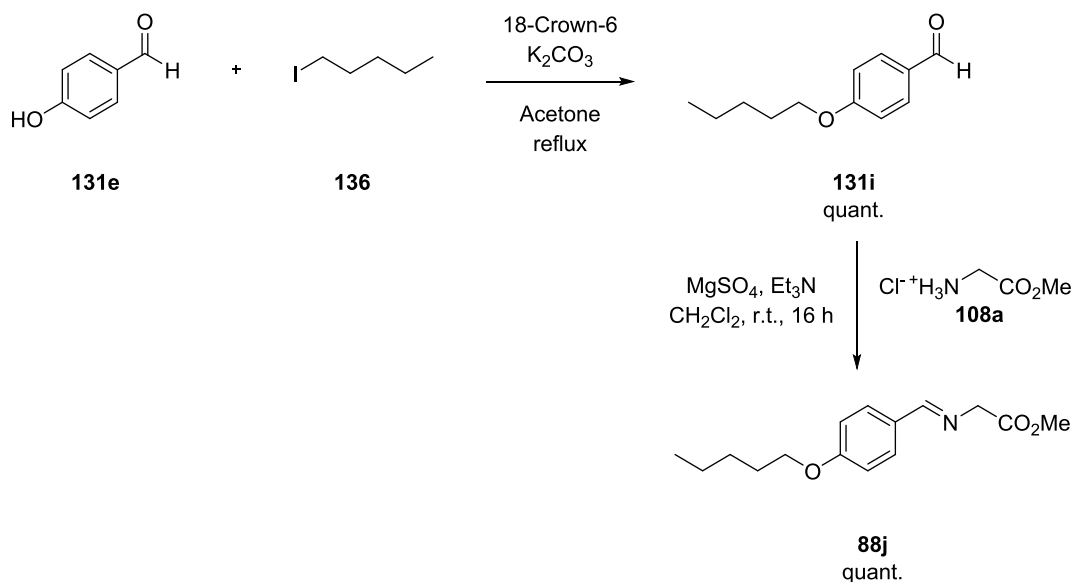
Compound (\pm)-**130a** showed best affinity toward both CB2 and CB1 receptors although it was a racemic mixture. Unfortunately, compounds that displace radioligand must show a percentage superior to 70% in order to measure the affinity in increasing concentrations of the compound. Thus, it was considered that compounds do not bind to CB1 and CB2 receptors or they bind them with an affinity constant (K_i) that requires concentrations higher than 40 μ M.

We considered that it would be possible to improve the affinity of our cycloadducts for both receptors by increasing their lipophilicity. Therefore, we decided to introduce a *para*-pentyloxy group at the phenyl moiety.

⁸⁰ a) Cumella, J.; Hernández-Folgado, L.; Girón, R.; Sánchez, E.; Morales, P.; Hurst, D. P.; Gómez-Cañas, M.; Gómez-Ruiz, M.; Pinto, D. C. G. A.; Goya, P.; Martín, M. I.; Fernández-Ruiz, J.; Silva, A. M. S.; Jagerovic, N., *ChemMedChem*, **2012**, 7, 452–463. b) Morales, P.; Gómez-Cañas, M.; Navarro, G.; Hurst, D. P.; Carrillo-Salinas, F. J.; Lagartera, L.; Pazos, R.; Goya, P.; Reggio, P. H.; Guaza, C.; Franco, R.; Fernández-Ruiz, J.; Jagerovic, N., *J. Med. Chem.* **2016**, 59, 6753–6771.

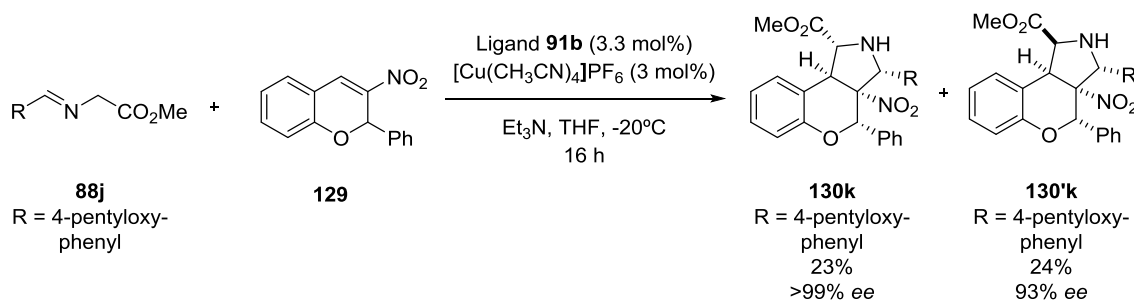
CHAPTER 2

In a first step corresponding aldehyde **131i** was synthesized quantitatively by Williamson reaction using *n*-pentyl iodide **136** in the presence of K₂CO₃ and 18-Crown-6 ether. Then, aldehyde **131i** reacted with glycine methyl ester hydrochloride **108a** to afford azomethine ylide precursor **88j** in quantitative yield



Scheme 2.32. Williamson reaction that permitted introduction of alkyl chain that led to the formation of aldehyde **131i** and its following condensation with glycine ester hydrochloride **108a** to provide azomethine ylide precursor **88j**.

Finally, [Cu(CH₃CN)₄]PF₆/ligand **91b** catalyzed (3+2) cycloaddition afforded compounds **130k** and **130'k** with no diastereocontrol. Both diastereoisomers exhibited the best enantiomeric excesses obtained to date for this type of chromane derivatives. It seems that the presence of the alkoxy chain results in an improved enantiocontrol.



Scheme 2.33. Synthesis of compounds **130k** and **130'k** that bear an alkoxy chain by (3+2) cycloaddition reaction.

Diastereoisomers **130k** and **130'k** were sent to test their affinity toward CB1 and CB2 receptors. The results obtained with these molecules are currently being analyzed by Dr. Jagerovic's group.

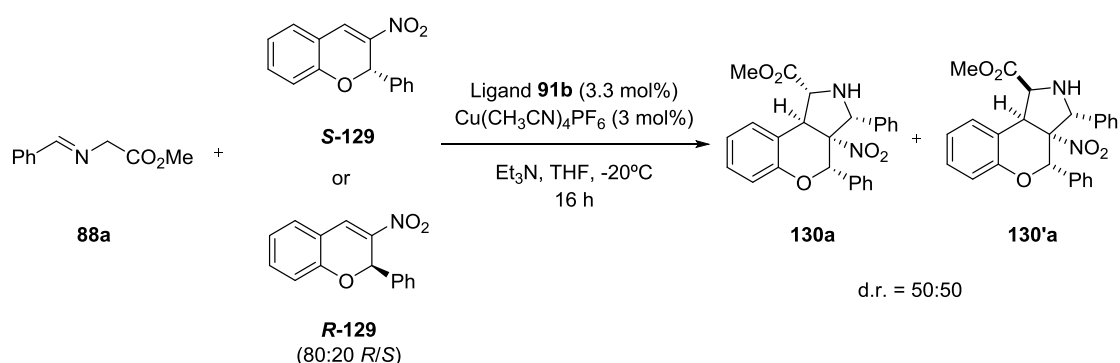
2.6.6 Preliminary experimental and computational studies on the configuration of chromene stereogenic center for **130** and **130'** cycloadducts

The enantioselective (3+2) cycloaddition reaction of azomethine ylides with 3-nitro-2-phenyl-2*H*-chromene afforded the formation of two cycloadducts **130** and **130'**. These compounds only differ in the absolute configuration of a chiral center. For this reason, further considerations about the mechanism insights were carried out.

3-nitro-2-phenyl-2*H*-chromene was employed as a racemic mixture in the reaction with different α -iminoesters. This nitro compound presents an asymmetric carbon not involved in the cycloaddition reaction. Because of this, it could be expected that in the generation of compounds **130** and **130'** this carbon would present both *R* and *S* configurations. Instead, X-ray structures of the isolated products showed exclusively *S* configuration in this carbon (see **Figures 2.17** and **2.15**, carbon C1, ORTEP diagram). In order to shed light on the mechanism of this reaction some experimental and computational studies were performed.

We analyzed the behavior of enantiomerically pure chromene in order to observe a possible improvement on the selectivity of the (3+2) cycloaddition reaction. For that, racemic mixtures of chromene were purified by semipreparative HPLC. *S*-enantiomer was successfully isolated and its configuration was confirmed by X-ray diffraction analysis of the crystal (see Annex III). Unfortunately, all attempts to obtain *R*-enantiomer pure were not successful. Instead, an enantio-enriched mixture of it was obtained (20:80 *S/R*).

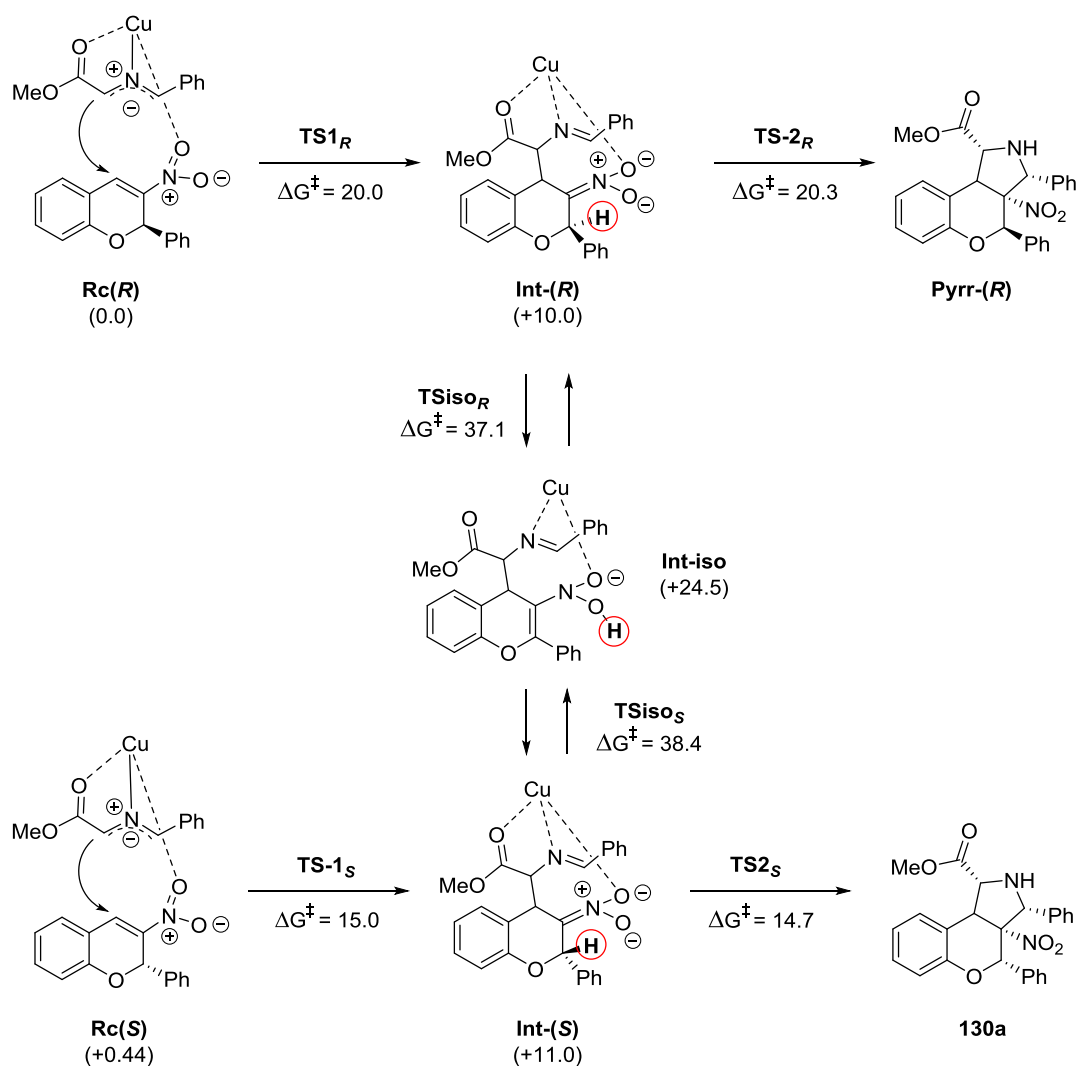
Subsequently, *S*-**129** or *R*-enantio-enriched mixture of **129**, respectively, were employed as dipolarophiles under the previously optimized (3+2) cycloaddition conditions. The results obtained were similar to those observed with the racemic mixture. Therefore, no preferential formation of one of the cycloadducts was observed. As a consequence, a plausible mechanism for the reaction must involve the isomerization of the asymmetric carbon (C1) of the chromene reagent.



Scheme 2.34. (3+2) cycloaddition reaction with **S-129** or enantio-enriched **R-129**, afforded both diastereoisomers equally.

We performed DFT calculations on the azomethine ylide and 3-nitro-2-phenyl-2*H*-chromene reaction mechanism in order to identify any possible isomerization process on carbon C1 during the (3+2) cycloaddition reaction.

CHAPTER 2



Scheme 2.35. Proposed formation of cycloadducts and possible unimolecular isomerization pathway. Free activation and free relative energies of each process are in kcal/mol and calculated at B3LYP/ 6-31G(d) &LANDL2DZ level of theory.

Initially we considered a simplified model system that does not involve the ferrocenyl-proline ligand and focuses only on the W-shaped azomethine ylide. Within the proposed mechanism of *N*-metalated (3+2) cycloaddition reaction (see **Scheme 2.8**), the process would start with the coordination of copper(I) with azomethine ylide and nitro group of the dipolarophile. Since the dipolarophile is a racemic mixture we need to consider two pseudo-diastereomeric reactive complexes **Rc(R)** and **Rc(S)**, one for each enantiomer (**Scheme 2.36**).

At this point, each reactive complex **Rc(R)** or **Rc(S)** reacts through a Michael addition yielding zwitterionic intermediates **Int-(R)** and **Int-(S)**. These intermediates could react via aza-Henry intramolecular cyclization giving rise to compounds **130a** and **Pyrr-(R)**, respectively.

Besides, zwitterionic intermediates *R* and *S* bear a nitronate group that can give rise to the enoether intermediate **Int-iso**, in which the chiral information of electrophiles (*R*)- or (*S*)-**129** is lost. Therefore, unimolecular isomerization of phenylchromene

CYCLOADDITION REACTIONS

intermediates was envisaged prior to the second step of the stepwise (3+2) reaction, normally the intramolecular aza-Henry cyclization.

The whole reaction profile for the model system is depicted in **Scheme 2.36**. In all the process free activation energies and free relative energies are given in kcal/mol (fully optimized structures of all TS are depicted in **Fig. 2.18** and **Fig. 2.19**). As far as the energetic profile of our proposed mechanism is concerned, the free activation energy associated with the initial Michael step of **Rc(S)** is 5.0 kcal/mol less energetic than its *R* counterpart. This can be attributed to the steric hindrance of the phenyl group of (R)-**129** in **TS1_R**, to be compared with the distal position of this group in less energetic **TS1_S** saddle point (**Figure 2.18**).

Once the corresponding intermediates are formed, the activation barrier associated with the second aza-Henry step is also lower for the *S*-chromene derivative. In this case, this barrier is slightly lower than the one associated with the first Michael step. Therefore, as soon as **Int-(S)** is formed it would be prompted to go through cyclization and give rise to **130a**.

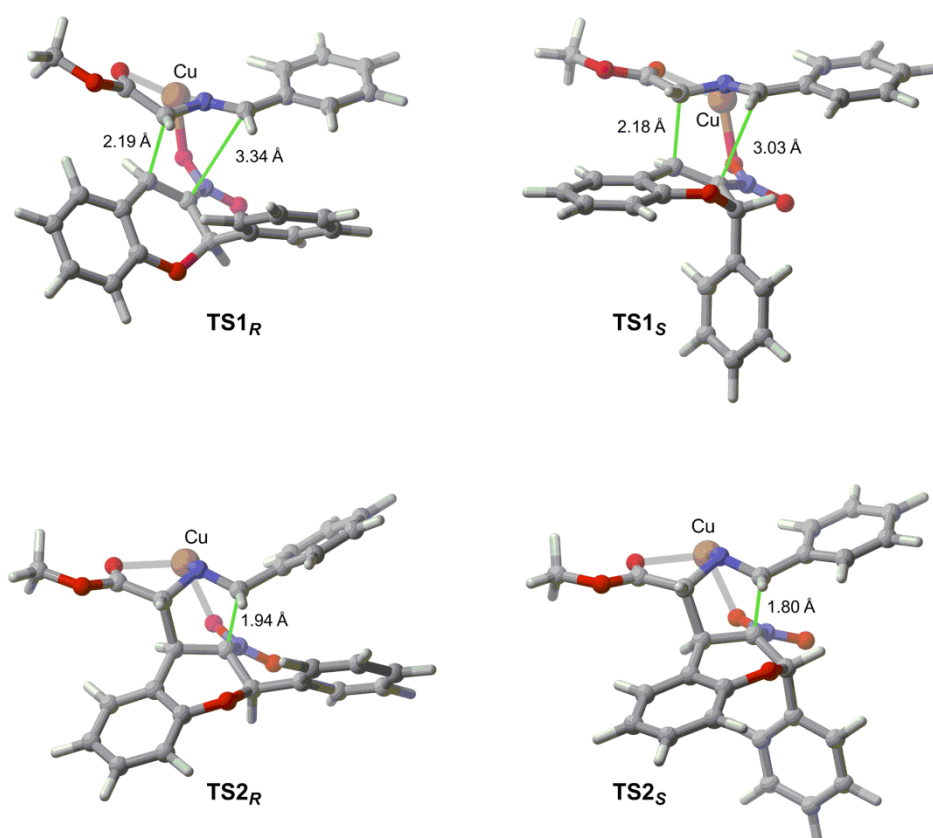


Figure 2.18. Fully optimized transition states associated with the Michael and aza-Henry steps depicted in **Scheme 2.35** obtained at B3LYP/ 6-31G(d) & LANDL2DZ level of theory.

CHAPTER 2

On the other hand, the free activation energy for cyclization step of **Int R** is slightly higher than the one of the first step. In this case, **Int R** could isomerize to **Int-(S)** before the aza-Henry step.

In view of these results, we analyzed the isomerization process that could connect both zwitterionic intermediates. We initially postulated an intramolecular process in which **Int-(R)** could be transformed into **Int-(S)** through intermediate **Int-iso** bearing a planar C=C double bond and no asymmetric carbons. The chief geometric features of saddle points **TSiso_R** and **TSiso_S** that connect intermediates **Int-(R)** and **Int-(S)** are gathered in **Figure 2.19**. Our results showed that the activation energies associated with the proton shifts for both intermediates are quite high (**Scheme 2.36**, **TSiso_R** and **TSiso_S**).

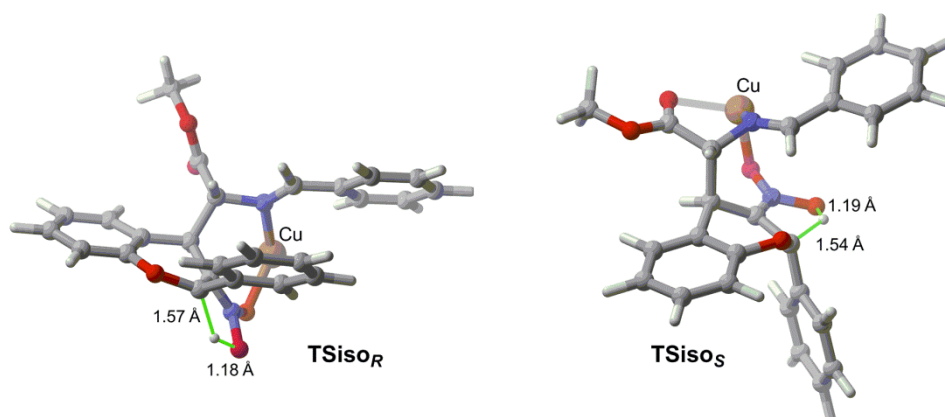


Figure 2.19. Fully optimized transition states associated with the proposed isomerization unimolecular process obtained at B3LYP/ 6-31G(d) &LANDL2DZ level of theory.

Since these calculations involve a model simplified system, completion of the coordination sphere of the Cu(I) center could affect the energy balance of the process. In addition, neither energy correction associated with non-covalent dispersion energies nor solvent effects (that could stabilize these polar species) were considered. Additional calculations including these factors are being conducted in our group.

2.7 Conclusions

- Ferrocenyl-proline/[Cu(CH₃CN)₄]PF₆ catalyzed (2+1) cycloaddition reactions of heterocyclic alkenes with ethyl diazoacetate afforded racemic cyclopropanes in low yield.
- Ligand **91a** in combination with dirhodium tetraacetate was able to yield new tricyclic compound **trans-122a** in a 50% yield, but with no enantiomeric excess.
- AgClO₄ and **91b** ligand catalyzed intramolecular (3+2) cycloaddition reaction afforded a maximum of 60% ee value for tricyclic chromeno [4,3-*b*] pyrrolidine **endo-127**, whereas **dimer-128** was racemic in all the cases.
- The presence of **dimer-128** is rationalized by the conformational freedom of Ph-O-CH₂ moiety in imine **126**. This fact, conferred a plausible mechanistic explanation in which inter- and intramolecular processes compete to yield **dimer-128** and cycloadduct **endo-127**, respectively.
- Ligand **91b** was employed along with [Cu(CH₃CN)₄]PF₆ in order to catalyze new intermolecular (3+2) cycloaddition reactions between glycine derived iminoesters **88a-j** and chromenes **129** and **135** with no diastereocontrol but in good to excellent enantiomeric excesses. Different substitution patterns were analyzed in the aromatic position of the azomethine ylide, ester group of the azomethine ylide and substitution in the aromatic ring of dipolarophile. The absolute configuration of compounds **130a** and **130'a** was established by X-ray diffraction.
- Compounds (±)-**130a** and **130a** (racemic and enantiopure) and **130'a** (enantiopure) were tested in a preliminary affinity test as possible cannabinoid ligands. Racemic compound (±)-**130a** exhibited best percentage of radioligand displacement but still not enough for a considerable binding to CB1 and CB2 receptors. Compounds **130k** and **130'k** demonstrated an excellent enantiomeric excess by introducing a pentyloxy chain as substituent in *para* position to the phenyl of the azomethine ylide (>99% and 93% ee, respectively). Binding analysis toward cannabinoid receptors for these two compounds are currently ongoing.
- Preliminary computational and experimental studies indicate that the cycloaddition reaction occurs through a stepwise process. Aside from the conjugate Michael-like step and the intramolecular aza-Henry cyclization, inversion of the configuration of the chiral carbon present in the chromene moiety can occur through an isomerization and equilibration mechanism via the nitronate moiety of the Michael intermediate. Unfortunately, free activation energies associated with the isomerization process are elevated for unimolecular process. Additional calculations including energy corrections associated to non-covalent dispersion energies and solvent effects are being conducted.

CHAPTER 2

2.8 Experimental part

2.8.1 General remarks

All reactions were carried out under a nitrogen or argon atmosphere with dry solvents under anhydrous conditions, unless otherwise noted. All the glassware has been previously dried in an oven at 90°C. Room temperature is related to around 20-25°C. Reactions at 0°C were carried out using an ice bath; reactions from -78°C to -10°C were carried out using a cryostat with acetone.

Diethyl ether (Et₂O), tetrahydrofuran (THF) and toluene were obtained by passing commercially available dry, oxygen-free formulations through activated alumina columns from a SPS (solvent purification system) machine. If necessary, tetrahydrofuran (THF) was distilled over sodium and benzophenone and used directly. Ethyl acetate (EtOAc), diethyl ether (Et₂O), dichloromethane (DCM) and *n*-hexane were purchased at the highest commercial quality and used without further purification, unless otherwise stated. Reagents were purchased at the highest commercial quality and used without further purification, unless otherwise stated. Yields refer to chromatographically and spectroscopically (¹H NMR) homogeneous materials, unless otherwise noted. Reactions were monitored by thin-layer chromatography (TLC) carried out on 0.25 mm E. Merck silica gel plates (60F-254). Ethanolic solution of phosphomolybdic acid, aqueous cerium molybdate and aqueous potassium permanganate were used as developing agents. E. Merck silica gel (60, particle size 40-63 μm) was used for column chromatography.

NMR spectra were recorded on Bruker Avance Ultrashield spectrometer of 400 MHz and 500 MHz, and were calibrated using residual undeuterated solvent as an internal reference.

Infrared spectra were recorded between 4000 and 400 cm⁻¹ on an Alpha Bruker FT-IR spectrometer with a single reflection ATR module.

High-Resolution Mass Spectra (HRMS). SGIker services (Central Service of Alava, and Central Service of Bizkaia, University of the Basque Country) performed the mass analysis on a LC/QTOF, Agilent mass spectrometer using electrospray ionization sources and a Water Chromatography model, UPLC-DAD-QTOF of Waters, using electrospray ionization (ESI), respectively.

Analytical High Performance Resolution Chromatography (HPLC)

experiments were performed using Daicel Chiralpack IA, IB, IC, OD-H and OJ-H columns (250 x 4.6 mm I.D) which contain a chiral stationary phase. The equipment was the following: Waters chromatograph 2487 with a dual wavelength UV detector using as eluent mixtures of iso-propanol and *n*-hexane.

Optical rotation coefficient, $[\alpha]_D^T$, was measured at 589 nm (sodium line) in a digital polarimeter JASCO P-2000. T is referred to the temperature of measurement.

X-ray diffraction analysis. Intensity data were collected on an Agilent Technologies Super-Nova diffractometer, which was equipped with monochromated Cu $\kappa\alpha$ radiation ($\lambda = 1.54184 \text{ \AA}$) and Atlas CCD detector (SGIker service, Service of Bizkaia). Measurement was carried out at 100.00 K with the help of an Oxford Cryostream 700 PLUS temperature device. Data frames were processed (unit cell determination, analytical absorption correction with face indexing, intensity data integration and correction for Lorentz and polarization effects) using the CrysAlis software package.⁸¹ The structure was solved using Superflip⁸² and refined by full-matrix least-squares with SHELXL-97⁸³. Final geometrical calculations were carried out with Mercury⁸⁴ and PLATON⁸⁵ as integrated in WinGX⁸⁶.

Elemental analysis of samples was measured using a Euro EA Elemental Analyzer (CHNS) from EuroVector, by SGIker service (Central Service of Bizkaia, University of the Basque Country).

Computational methods. All the calculations reported in **Chapter 2** were performed by Density Functional Theory (DFT),⁸⁷ using the hybrid three-parameter functional denoted as B3LYP.⁸⁸ The standard 6-31G(d) basis set⁸⁹ as implemented in

⁸¹ CrysAlisPro, Agilent Technologies, Version 1.171.37.31 (release 14-01-2014 CrysAlis171.NET)(compiled Jan 14 2014, 18:38:05).

⁸² Palatinus L., Chapuis G., *J. Appl. Cryst.* **2007**, *40*, 786.

⁸³ Sheldrick, G. M., *Acta Cryst.* **2008**, A64, 112; Sheldrick, G. M., *Acta Cryst.* **2015**, C71, 3.

⁸⁴ Macrae, C. F., *J. Appl. Cryst.* **2008**, *41*, 466.

⁸⁵ A. L. Spek (**2010**) PLATON, A Multipurpose Crystallographic Tool, Utrecht University, Utrecht, The Netherlands; A. L. Spek, *J. Appl. Cryst.* **2003**, *36*, 7.

⁸⁶ Farrugia, L. J., *J. Appl. Cryst.* **1999**, *32*, 837.

⁸⁷ Parr, R. G.; Yang, W. *Density-Functional Theory of Atoms and Molecules*, Oxford, New York **1989**.

⁸⁸ (a) Lee, C.; Yang, W.; Parr, R. G. *Phys. Rev. B* **1988**, *37*, 785–789. (b) Becke, A. D. *J. Chem. Phys.* **1993**, *98*, 1372–1377. (c) Becke, A. D. *J. Chem. Phys.* **1993**, *98*, 5648–5652.

⁸⁹ Hehre, W. J.; Radom, L.; Schleyer, P. v. R.; Pople, J. A. *Ab initio Molecular Orbital Theory*, Wiley, New York, **1986**; pp. 76-87 and references cited therein.

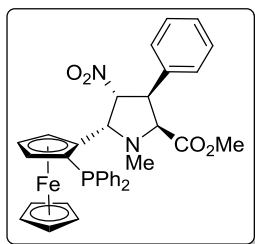
CHAPTER 2

the Gaussian09⁹⁰ was used to describe hydrogen, carbon, nitrogen and oxygen atoms. Copper atom was described by the Hay-Wadt effective core potential (ECP)⁹¹ including double- ξ valence and LanL2DZ basis set.⁹² All stationary points were characterized by harmonic analysis. Reactants, intermediates and cycloadducts have positive definite Hessian matrices. Transition structures show only one negative eigenvalue in their diagonalized force constant matrices, and their associated eigenvector were confirmed to correspond to the motion along the reaction coordinate. Thermal corrections to Gibbs free energies (TCGE) at 298 K were computed at the same level and were not scaled.

2.8.2 Ferrocenyl-Proline ligand synthesis:

2.8.2.1 Procedure for synthesis of NMe-L-EhuPhos-93

(2*S*,3*S*,4*R*,5*S*)-Methyl-5-((*S*_p)-2-(diphenylphosphino)ferrocenyl)-1-methyl-4-nitro-3-phenylpyrrolidine-2-carboxylate. (**93**)⁹³



In a flask a mixture of ((*S*_p)-2-(diphenylphosphino)ferrocenecarboxaldehyde **107** (0.46 g, 1.15 mmol), sarcosine methyl ester hydrochloride (0.21 g, 1.50 mmol), Et₃N (0.21 mL, 1.50 mmol), *trans*- β -nitrostyrene **89** (0.22 g, 1.50 mmol) and MgSO₄ were placed and dissolved in toluene. Mixture was stirred at reflux of toluene until full conversion. Reaction was monitored by TLC (thin layer chromatography) and reaction showed completion in 5-6 hours. After that, mixture was filtered through a pad of Celite and evaporated under reduced pressure. Purification by flash column chromatography in a mixture of eluent EtOAc/*n*-hexane = 20:80 afforded 378 mg of ligand **93** as a yellow solid in a 52% yield. ¹H NMR (500 MHz, CDCl₃) δ (ppm) = 7.75 – 7.68 (m, 2H), 7.43 – 7.34 (m, 5H), 7.26 – 7.19 (m, 6H), 7.08 – 7.04 (m, 2H), 5.42 (t, *J* = 7.7 Hz, 1H), 5.20 (dd, *J* = 8.0, 5.0 Hz, 1H), 4.48 (t, *J* = 2.4 Hz, 1H), 4.46 (d, *J* = 1.1 Hz, 1H), 4.40 (t, *J* = 7.8 Hz, 1H), 4.35 (d, *J* = 8.4 Hz, 1H), 4.33 – 4.29 (m, 1H), 3.84 (s, 5H), 3.33 (s, 3H), 2.92 (s, 3H).

⁹⁰ Frisch, M. J. et al. Gaussian 09, Revision B.01; Gaussian, Inc., Wallingford CT, **2009**.

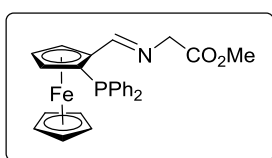
⁹¹ Hay, P. J.; Wadt, W. R. *J. Chem. Phys.* **1985**, *82*, 299-303.

⁹² McIver, J. W.; Komornicki, A. K. *J. Am. Chem. Soc.* **1972**, *94*, 2625-2633.

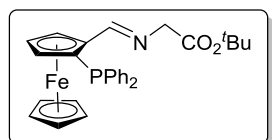
⁹³ Conde, E.; Bello, D.; de Cozar, A.; Sanchez, M.; Vazquez, M. A.; Cossio, F. P., *Chem. Sci.* **2012**, *3*, 1486–1491.

2.8.2.2 General procedure for synthesis of ferrocene ligands **91a-c**

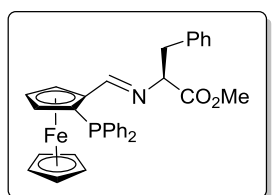
Synthesis of ligands **91a-c** was performed in two steps. In the first one, corresponding amine hydrochloride **108a-c** (1 equiv.) was dissolved in DCM, in presence of MgSO_4 and Et_3N (1.1 equiv.). After stirring at room temperature for 1 hour, ((S_p)-2-(diphenylphosphino)) ferrocenecarboxaldehyde **107** (1 equiv.) was added and reaction was stirred for 16 to 24 hours at room temperature. Then, reaction mixture was filtered in order to remove MgSO_4 and the mixture was washed with H_2O (2 x 20 mL) and extracted three times with 20 mL of DCM. Collected organic layers were dried over Na_2SO_4 and solvent was evaporated under reduced pressure. Corresponding imine was obtained as oil, and it was used without further purification.

((S_p)-2-(Diphenylphosphino)-[(2-methoxy-2oxoethyl)iminomethyl]ferrocene (**109a**)⁹³

0.30 g of ((S_p)-2-(diphenylphosphino))ferrocenecarboxaldehyde **107** (0.75 mmol) were placed and 0.32 g of imine **109a** were obtained as an orange oil, yield = 92%. ³¹P NMR (202 MHz, CDCl_3) δ (ppm) = -22.26 (s). ¹H NMR (500 MHz, CDCl_3) δ (ppm) = 8.48 (d, J = 2.9 Hz, 1H), 7.55 (d, J = 7.6 Hz, 2H), 7.41 (d, J = 5.6 Hz, 4H), 7.27 – 7.21 (m, 3H), 7.15 (d, J = 7.6 Hz, 2H), 5.20 (s, 1H), 4.56 (d, J = 2.7 Hz, 1H), 4.32 (d, J = 15.8 Hz, 1H), 4.15 (s, 4H), 3.91 (s, 1H), 3.73 (s, 3H).

((S_p)-2-(Diphenylphosphino)-[(2-tertutoxy-2oxoethyl)iminomethyl]ferrocene (**109b**)

0.20 g of S_p -2-(diphenylphosphino)) ferrocenecarboxaldehyde **107** (0.50 mmol) were used and 0.23 g of imine **109b** as a yellow solid obtained, yield = 90 %. ¹H NMR (500 MHz, CDCl_3) δ (ppm) = 8.45 (d, J = 2.9 Hz, 2H), 7.59 – 7.53 (m, 4H), 7.45 – 7.37 (m, 4H), 7.24 (dt, J = 4.1, 1.5 Hz, 3H), 7.16 – 7.10 (m, 3H), 5.22 (dt, J = 2.9, 1.5 Hz, 1H), 4.55 (t, J = 2.6 Hz, 1H), 4.22 (s, 1H), 4.18 (d, J = 1.4 Hz, 1H), 4.14 (s, 5H), 4.03 (d, J = 1.0 Hz, 1H), 3.90 (dt, J = 2.4, 1.2 Hz, 1H), 1.47 (s, 9H).

((S_p)-2-(Diphenylphosphino)-[methyl-(S,E)-2-(ethylideneamino)-phenylpropanoate] ferrocene (**109c**)

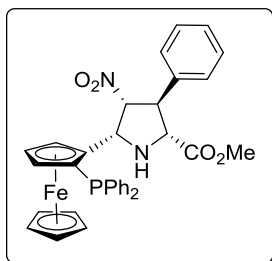
Imine **109c** was obtained as a yellow solid, always in a quantitative yield. ¹H NMR (500 MHz, CDCl_3) δ (ppm) = 8.26 (d, J = 2.8 Hz, 1H), 7.54 – 7.47 (m, 2H), 7.38 (d, J = 6.5 Hz, 3H), 7.33 – 7.28 (m, 2H), 7.25 – 7.18 (m, 6H), 7.12 (m, J = 2H), 5.05

CHAPTER 2

(s, 1H), 4.47 (t, $J = 2.7$ Hz, 1H), 4.12 (dd, $J = 9.8, 4.5$ Hz, 1H), 3.84 (d, $J = 4.9$ Hz, 5H), 3.56 (s, 3H), 3.31 (dd, $J = 13.8, 4.5$ Hz, 1H), 3.15 (dd, $J = 13.8, 9.7$ Hz, 1H).

In a second step, corresponding imine **109a-c** (1 equiv.) was dissolved in anhydrous THF and subsequently LiBr (1.5 equiv.) and *trans*- β -nitrostyrene **89** (1.2 equiv.) were added. Finally addition of Et₃N (1 equiv.) afforded the formation of corresponding azomethine ylide and the cycloaddition process. This process was fully carried out under argon atmosphere. Reaction was monitored by thin layer chromatography (TLC) using as eluent a mixture of EtOAc/*n*-hexane depending on the nature of the substituent. After completion, THF was removed under reduced pressure. Afterwards, crude of the reaction was dissolved in 20 mL of DCM and washed with aqueous saturated NH₄Cl (2 x 20 mL) and NaCl aq. sat. (2 x 20 mL). Collected organic layers were dried over Na₂SO₄ anhydrous and solvent was evaporated. Purification by flash column chromatography using different eluent mixtures of EtOAc/*n*-hexane afforded the correct formation of ligands **91a-c** as yellow solids.

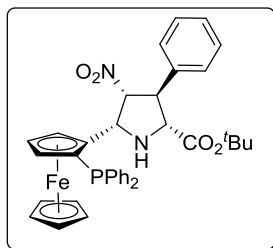
(2*R*,3*S*,4*R*,5*S*)-Methyl-5-((*Sp*)-2-(diphenylphosphino)ferrocenyl)-4-nitro-3-phenylpyrrolidine-2-carboxylate (**NH-D-EhuPhos-91a**)⁹³



Starting from 0.29 g of imine **109a** (0.63 mmol) 0.26 g of **91a** as yellow solid obtained in a overall yield of 78% (2 steps). Chromatography was carried out in an eluent mixture of EtOAc/*n*-hexane EtOAc/*n*-hexane = 20:80. Spectroscopic data was in concordance with literature. ¹H NMR (500 MHz, CDCl₃) δ (ppm) = 7.60 – 7.57 (m, 2H), 7.42 – 7.37 (m, 3H), 7.35 – 7.18 (m, 8H), 7.08 – 7.03 (m, 2H), 4.94 (dt, $J = 11.4, 5.6$ Hz, 1H), 4.50 – 4.47 (m, 1H), 4.35 (t, $J = 2.6$ Hz, 1H), 4.22 (dd, $J = 5.4, 1.2$ Hz, 1H), 4.17 (s, 5H), 4.03 – 3.98 (m, 2H), 3.88 – 3.85 (m, 1H), 3.84 (s, 3H), 3.27 (dd, $J = 10.8, 8.1$ Hz, 1H).

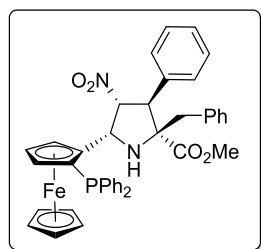
CYCLOADDITION REACTIONS

(2R,3S,4R,5S)-tert-butyl-5-((Sp)-2-(diphenylphosphino)ferrocenyl)-4-nitro-3-phenylpyrrolidine-2-carboxylate (NH-TB-D-EhuPhos-91b)



Starting from 0.31 g of corresponding imine **109b** (0.61 mmol), 0.11 g of ligand **91b** were obtained as yellow solid in yield of 27%. Overall yield = 49% (2 steps). Chromatography was carried out in an eluent mixture of EtOAc/*n*-hexane EtOAc/*n*-hexane = 11:89. **¹H NMR** (500 MHz, CDCl₃) δ (ppm) = 7.58 (s, 2H), 7.40 (s, 3H), 7.35 – 7.17 (m, 9H), 7.05 (d, J = 7.2 Hz, 2H), 4.99 – 4.89 (m, 1H), 4.48 (s, 1H), 4.35 (s, 1H), 4.21 (t, J = 6.9 Hz, 1H), 4.17 (s, 4H), 3.94 (d, J = 4.5 Hz, 1H), 3.91 (m, 1H), 3.83 (s, 1H), 3.26 (d, J = 9.4 Hz, 1H), 1.52 (s, 9H). **³¹P NMR** (202 MHz, CDCl₃) δ (ppm) = -23.13 (s). **¹³C NMR** (126 MHz, CDCl₃) δ (ppm) = 171.5, 140.1, 138.7, 138.6, 136.7 (2x), 135.0, 134.9, 133.6, 133.4, 129.5, 129.2, 128.8, 128.5 (2x), 128.4, 127.7, 127.4, 95.7, 86.7, 86.5, 82.5, 72.2, 70.6, 70.3, 69.0, 66.8, 64.4, 64.3, 56.7, 28.3. **FT-IR** (cm⁻¹): 3316, 1730, 1541, 1367, 815, 742, 697. $[\alpha]_D^{25}$ = -67 (c 1.00, CHCl₃). **HRMS (ESI/Q-TOF) m/z**: C₃₇H₃₈FeN₂O₄P [M + H]⁺, calculated: 661.1762, found: 661.1964. **Elemental anal.** calculated for C₃₇H₃₇FeN₂O₄P: C, 67.3; H, 7.3; N, 2.9; O, 9.7. Found: C, 67.7; H, 5.7; N, 4.6; O, 9.8.

(2R,3S,4R,5S)-2-Benzyl-((Sp)-2-(diphenylphosphino)ferrocenyl)-4-nitro-3-phenylpyrrolidine-2-carboxylate (NH-Bn-D-EhuPhos-91c)



(1.33 mmol) of ligand **91c** were obtained as a yellow solid in a 75% yield. Overall yield = 87% (2 steps). Chromatography was carried out in an eluent mixture of EtOAc/*n*-hexane = 20:80. **¹H NMR** (500 MHz, CDCl₃) δ = 7.70 – 7.58 (m, 2H), 7.48 – 7.36 (m, 5H), 7.36 – 7.12 (m, 11H), 7.06 (d, J = 7.0 Hz, 2H), 5.23 (s, 1H), 4.55 (dt, J = 22.6, 11.3 Hz, 1H), 4.44 (d, J = 1.1 Hz, 1H), 4.30 (dd, J = 24.7, 7.3 Hz, 2H), 4.22 – 4.08 (m, 4H), 3.85 (s, 1H), 3.79 (s, 3H), 3.42 (s, 1H), 2.51 (d, J = 13.5 Hz, 1H), 2.37 (d, J = 13.5 Hz, 1H). **³¹P NMR** (202 MHz, CDCl₃) δ = -23.30 (s). **¹³C NMR** (126 MHz, CDCl₃) δ = 174.4, 138.6, 138.5, 137.2, 136.5, 136.4, 136.3, 135.0, 134.8, 133.3, 133.2, 130.0, 129.4, 128.8, 128.7, 128.4 (2x), 128.3, 127.8, 127.7, 126.7, 96.5, 86.9, 86.7, 73.7, 72.1, 72.0, 71.0, 70.3, 70.2, 66.4 (2x), 62.4, 62.3, 59.2, 53.4, 52.6, 42.5. **FT-IR** (cm⁻¹): 3324, 1736, 1547, 1371, 819, 743, 697. $[\alpha]_D^{25}$ = +11 (c 1.00, CHCl₃). **HRMS (ESI/Q-TOF) m/z**: C₄₁H₃₉FeN₂O₄P [M + H]⁺, calculated

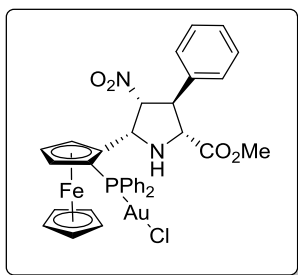
CHAPTER 2

709.1965, found 709.1935. **Elemental anal.** calculated for $C_{41}H_{38}FeN_2O_4P$: C, 69.5; H, 5.3; N, 4.0; O, 9.0. Found: C, 68.8; H, 5.7; N, 4.5; O, 10.9.

2.8.2.3 General procedure for the synthesis of Gold(I) complexes **110a-d**

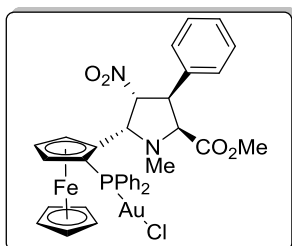
To a solution of the corresponding ferronyl-proline **91a-c** and **93** (1 equiv.) in DCM (0.05 M) $(CH_3)_2SAuCl$ (1 equiv.) was added and mixture was stirred for 4 hours at room temperature under nitrogen atmosphere. After this time, mixture was filtered through Celite and corresponding yellow solution was evaporated to remove solvents and afforded yellow solids **110a-d**.

(2R,3S,4R,5S)-Methyl-5-((*Sp*)-2-(chloro-diphenylphosphino-gold(I))ferrocenyl)-4-nitro-3-phenylpyrrolidine-2-carboxylate (**NH-D-EhuPhosAuCl-110a**)



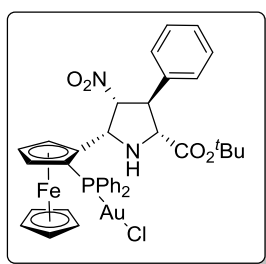
Ligand **91a** (0.13 mmol) reacted with $(CH_3)_2SAuCl$ (0.13 mmol) and stable complex **110a** was obtained in a 60% yield (0.04 mmol). 1H NMR (500 MHz, $CDCl_3$) δ = 7.76 (dd, J = 13.4, 7.2 Hz, 2H), 7.56 (d, J = 6.0 Hz, 1H), 7.51 (t, J = 6.2 Hz, 2H), 7.48 – 7.41 (m, 3H), 7.40 – 7.36 (m, 1H), 7.35 – 7.28 (m, 3H), 7.28 – 7.21 (m, 4H), 5.82 (s, 1H), 4.71 (s, 1H), 4.48 (s, 1H), 4.41 (s, 4H), 4.13 (d, J = 4.8 Hz, 1H), 4.02 (d, J = 12.4 Hz, 1H), 3.90 (s, 1H), 3.82 (s, 4H), 3.24 (t, J = 8.9 Hz, 1H). ^{31}P NMR (202 MHz, $CDCl_3$) δ = 23.78 (s). ^{13}C NMR (126 MHz, $CDCl_3$) δ = 172.5, 138.9, 134.5, 134.4, 134.0, 133.8, 132.2 (2x), 132.0, 131.9, 130.0, 129.6, 129.1 (2x), 129.0 (2x), 128.6, 128.0, 127.6, 95.7, 85.1, 85.0, 73.9 (2x), 71.6, 71.3, 71.2, 69.6 (2x), 69.4, 68.8, 67.1, 63.3, 63.2, 56.1, 52.6. **FT-IR** (cm^{-1}): 3323, 1742, 1541, 1364, 801, 744, 692. $[\alpha]_D^{25}$ = -10 (c 1.00, $CHCl_3$). **HRMS (ESI/Q-TOF) m/z**: $C_{34}H_{31}AuFeN_2O_4P$ $[M]^+$, calculated: 815.1036, found: 815.1026. **Elemental anal.** calculated for $C_{34}H_{31}AuClFeN_2O_4P$: C, 48.0; H, 3.7; N, 3.3; O, 7.5. Found: C, 47.6; H, 3.7; N, 3.4; O, 7.0.

(2*S*,3*S*,4*R*,5*S*)-Methyl-5-((*Sp*)-2-(chloro-diphenylphosphino-gold(*I*))ferrocenyl)-1-methyl-4-nitro-3-phenylpyrrolidine-2-carboxylate (**NMe-L-EhuPhosAuCl-110b**)



Ligand **93** (0.32 mmol) reacted with $(\text{CH}_3)_2\text{SAuCl}$ (0.32 mmol) and stable complex **110b** was obtained in a 81% yield (0.26 mmol). **^1H NMR** (500 MHz, CDCl_3) δ = 7.96 (dd, J = 13.3, 7.0 Hz, 2H), 7.84 – 7.76 (m, 2H), 7.60 – 7.50 (m, 3H), 7.47 (d, J = 2.5 Hz, 3H), 7.24 – 7.16 (m, 3H), 6.97 – 6.90 (m, 2H), 5.76 (d, J = 7.8 Hz, 1H), 5.04 (dt, J = 7.2, 4.7 Hz, 1H), 4.66 (s, 1H), 4.61 (s, 1H), 4.35 (t, J = 6.2 Hz, 2H), 4.26 (s, 1H), 4.18 (s, 4H), 3.53 (s, 3H), 3.01 (s, 3H). **^{31}P NMR** (202 MHz, CDCl_3) δ = 24.80 (s). **^{13}C NMR** (126 MHz, CDCl_3) δ = 170.6, 134.7, 134.6, 134.0, 133.8, 133.7, 131.7, 131.6, 130.4, 129.9, 129.8, 129.3, 128.7, 128.6 (2x), 128.5, 128.3, 127.6, 127.4, 92.8, 89.5, 89.4, 73.0 (2x), 72.0, 71.4, 70.7 (2x), 66.9, 66.4, 63.1 (2x), 51.6, 48.9, 37.4. **FT-IR** (cm^{-1}): 3310, 1727, 1553, 1375, 827, 749, 690. $[\alpha]_D^{25}$ = -44 (c 1.00, CHCl_3). **HRMS (ESI/Q-TOF) m/z** : $\text{C}_{35}\text{H}_{33}\text{AuFeN}_2\text{O}_4\text{P}$ $[\text{M}]^+$, calculated: 829.1193, found: 829.1183. **Elemental anal.** calculated for $\text{C}_{35}\text{H}_{33}\text{AuClFeN}_2\text{O}_4\text{P}$: C, 48.6; H, 3.8; N, 3.2; O, 7.4. found: C, 48.8; H, 3.9; N, 3.4; O, 7.8.

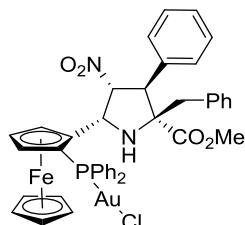
(2*R*,3*S*,4*R*,5*S*)-*tert*butyl-5-((*Sp*)-2-(chloro-diphenylphosphino-gold(*I*))ferrocenyl)-4-nitro-3-phenylpyrrolidine-2-carboxylate (**NH-TB-D-EhuPhosAuCl-110c**)



Ligand **91b** (0.15 mmol) reacted with $(\text{CH}_3)_2\text{SAuCl}$ (0.15 mmol) and stable complex **110c** was achieved as a yellow solid in 79% yield (0.12 mmol). **^1H NMR** (500 MHz, CDCl_3) δ = 7.69 (dd, J = 13.3, 7.2 Hz, 2H), 7.53 – 7.47 (m, 1H), 7.47 – 7.33 (m, 7H), 7.31 (d, J = 5.9 Hz, 1H), 7.24 (d, J = 6.3 Hz, 3H), 7.16 (d, J = 7.2 Hz, 2H), 5.73 (d, J = 3.5 Hz, 1H), 4.63 (s, 1H), 4.39 (d, J = 18.3 Hz, 1H), 4.34 (s, 4H), 3.93 (d, J = 5.1 Hz, 1H), 3.86 (d, J = 3.8 Hz, 1H), 3.81 (s, 1H), 3.77 (d, J = 4.0 Hz, 1H), 3.16 (s, 1H), 1.41 (s, 9H). **^{31}P NMR** (202 MHz, CDCl_3) δ = 23.75 (s). **^{13}C NMR** (126 MHz, CDCl_3) δ = 171.2, 139.3, 134.5, 134.4, 133.9, 133.8, 132.1, 131.9, 130.0, 129.4, 129.1, 129.0 (2x), 128.9, 128.1, 127.8, 127.6, 95.7, 85.2, 85.1, 82.2, 73.8 (2x), 71.6, 71.3, 71.2 (2x), 69.5, 69.4, 68.7, 67.9, 63.4, 63.3, 56.8, 30.9, 28.0, 27.2. **FT-IR** (cm^{-1}): 3313, 1727, 1544, 1366, 827, 729, 692. $[\alpha]_D^{25}$ = -8 (c 1.00, CHCl_3). **HRMS (ESI/Q-TOF) m/z** : $\text{C}_{37}\text{H}_{37}\text{AuFeN}_2\text{O}_4\text{P}$ $[\text{M}]^+$, calculated: 857.1506, found: 857.1503. **Elemental anal.** calculated for $\text{C}_{37}\text{H}_{37}\text{AuClFeN}_2\text{O}_4\text{P}$: C, 49.8; H, 4.2; N, 3.1; O, 7.2. Found: C, 48.5; H, 4.1; N, 3.2; O, 7.0.

CHAPTER 2

(2*R*,3*S*,4*R*,5*S*)-methyl-2-benzyl-5-((*Sp*)-2-(chloro-diphenylphosphigold(*I*))ferrocenyl)-4-nitro-3-phenylpyrrolidine-2-carboxylate (**NH-Bn-D-EhuPhosAuCl-110d**)



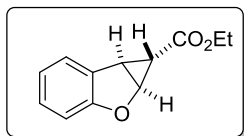
Ligand **91c** (0.14 mmol) reacted with (CH₃)₂SAuCl (0.14 mmol) and stable complex **110d** was achieved as a yellow solid in 90% yield (0.12 mmol). ¹H NMR (500 MHz, CDCl₃) δ = 7.76 (dd, *J* = 13.5, 7.1 Hz, 2H), 7.53 (m, 5H), 7.40 – 7.27 (m, 6H), 7.26 – 7.20 (m, 2H), 7.18 – 7.14 (m, 4H), 7.12 – 7.04 (m, 1H), 6.14 (s, 1H), 4.64 (s, 1H), 4.40 (s, 1H), 4.38 (s, 1H), 4.28 (s, 1H), 4.25 (s, 4H), 3.86 (s, 1H), 3.77 (s, 3H), 3.24 (s, 1H), 2.67 (d, *J* = 13.6 Hz, 1H), 2.36 (d, *J* = 13.6 Hz, 1H). ³¹P NMR (202 MHz, CDCl₃) δ = 23.55 (s). ¹³C NMR (126 MHz, CDCl₃) δ = 174.8, 137.2, 135.9, 134.9, 134.7, 134.0, 133.8, 132.4, 132.3, 132.2 (2x), 130.5, 130.2, 130.0, 129.3, 129.2 (2x), 129.1, 129.0, 128.5, 128.0 (2x), 126.8, 96.7, 86.3, 86.2, 74.1, 74.0, 73.3, 71.6, 71.5, 71.0 (2x), 69.8, 69.7, 69.0, 68.5, 62.0 (2x), 59.3, 52.6, 42.3. FT-IR (cm⁻¹): 3311, 1735, 1546, 1363, 824, 745, 696. [α]_D²⁵ = -2 (c 1.00, CHCl₃). HRMS (ESI/Q-TOF) *m/z*: C₄₁H₃₇AuFeN₂O₄P [M]⁺, calculado: 905.1506, encontrado: 905.1473. Elemental anal. calculated for C₄₁H₃₇AuClFeN₂O₄P: C, 52.3; H, 4.0; N, 3.0; O, 6.8. found: C, 53.4; H, 4.4; N, 3.5; O, 8.2.

2.8.3 Metal catalyzed cyclopropanation reactions:

2.8.3.1 General procedure for the synthesis of cyclopropanes *trans*-117a and *trans*-118a

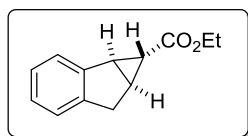
Ligand **NH-D-EhuPhos 91a** or **NMe-L-EhuPhos 93** (3.3 mol %) and [Cu(CH₃CN)PF₆] (3 mol %) were stirred for 30 minutes in DCM (anhydrous) at room temperature to afford the formation of the complex. After this time, corresponding substrate **117** or **118** (1.1 equiv.) was added to the reaction mixture and then stirred for additional 30 minutes. Ethyl diazoacetate **111** (1 equiv.) diluted in 10 mL of DCM (anhydrous) was added by a syringe pump at a rate of 1 mL/min to the reaction mixture and all was stirred for 16 hours at room temperature. Afterwards, the mixture was reduced to dryness and conversion and diastereoselectivity were determined by ¹H NMR spectroscopy. Products were purified by flash column chromatography (AcOEt/*n*-hexane = 8:92).

*Ethyl (1S,1aS,6bR)-1a,6b-dihydro-1H-cyclopropa[b]benzofuran-1-carboxylate (trans-117a)*⁹⁴



71 μL of 2,3-benzofuran-**117** (0.65 mmol) as starting material afforded the synthesis of 15 mg of **trans-117a** as colorless oil in 12% yield. $^1\text{H NMR}$ (400 MHz, CDCl_3) δ (ppm) = 7.40 (d, J = 7.5 Hz, 1H), 7.16 (t, J = 7.9 Hz, 1H), 6.99 – 6.85 (m, 2H), 5.07 (d, J = 5.5 Hz, 1H), 4.17 (q, J = 7.1 Hz, 2H), 3.33 – 3.22 (m, 1H), 1.33 – 1.22 (m, 4H).

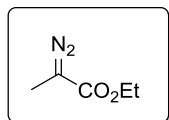
*Ethyl (1R,1aR,6aS)-1,1a,6,6a-tetrahydrocyclopropa[a]indene-1-carboxylate (trans-118a)*⁹⁵



74 μL of indene-**118** (0.63 mmol) as starting material afforded the formation of 34 mg of colorless oil **trans-118a** in 27 % yield. $^1\text{H NMR}$ (400 MHz, CDCl_3) δ = (ppm) 7.34 (d, J = 5.6 Hz, 1H), 7.17 – 7.10 (m, 3H), 4.15 (q, J = 7.2 Hz, 2H), 3.28 (dd, J = 17.6, 6.3 Hz, 1H), 3.05 (d, J = 17.5 Hz, 2H), 2.95 (d, J = 6.7 Hz, 1H), 2.44 (s, 1H), 1.27 (t, J = 7.1 Hz, 3H).

2.8.3.2 General procedure for synthesis of Ethyl α -diazo methyl acetate

*Ethyl α -diazo methyl acetate (121)*⁹⁶



NaH (0.67 g, 27.74 mmol) was dissolved in dry Et_2O (10.0 mL) and ethyl-2-methyl acetoacetate (2.00 g, 13.87 mmol) was added dissolved in 5.0 mL of Et_2O . Following, the mixture was cooled down to 0°C using a water-ice bath. Then, TsN_3 (3.28 g, 16.64 mmol) dissolved in Et_2O was added dropwise for 5 min. Reaction was stirred for 16 hours at room temperature and subsequently was filtered for the removal of remaining NaH. Reaction mixture was washed with 4 x 20 mL H_2O and extracted four times with 20 mL Et_2O . Collected organic layers were dried over Na_2SO_4 and evaporated to dryness. 1.42 g of yellow oil was obtained in 40% yield. $^1\text{H NMR}$ (400 MHz, CDCl_3) δ (ppm) = 4.19 (q, J = 7.1 Hz, 2H), 1.93 (s, 3H), 1.24 (t, J = 7.1 Hz, 3H).

⁹⁴ Matlin, S. A.; Chan, L.; Catherwood, B., *J. Chem. Soc. PerkinTrans* **1990**, 1, 89–96.

⁹⁵ Jiang, G.; Fu, X.; Li, Q.; Yu, Z., *Org. Lett.* **2012**, 14, 692–695.

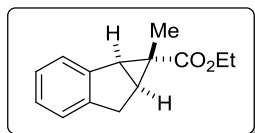
⁹⁶ Bachmann, S.; Fielenbach, D.; Jørgensen, K. A., *Org. Biomol. Chem.* **2004**, 2, 3044–3049.

CHAPTER 2

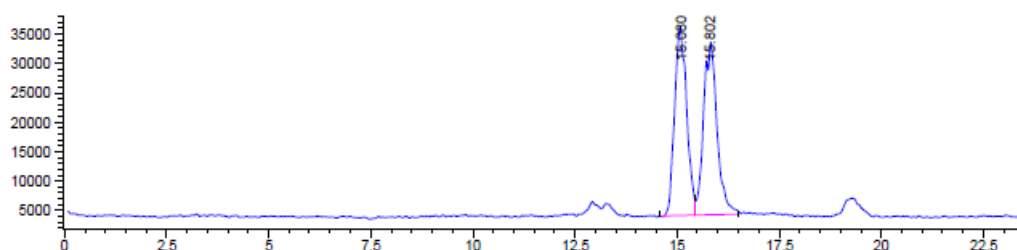
2.8.3.3 General procedure for synthesis of cyclopropanes derived from MEDA

Corresponding **ligand 91a** or **93** (6.2 mol %) and **Rh₂(OAc)₄** (3 mol %) were stirred for 30 minutes in a solution of DCM (anhydrous) at room temperature to afford the formation of the complex. After this time, indene **117** (1 equiv.) was added to the mixture and stirred for additional 30 min. at room temperature. The corresponding ethyl α -diazo methyl acetate **121** (1.1 equiv.) was added to the reaction mixture and stirred for 48 h at room temperature. Following, the mixture was concentrated to *vacuo* and conversion and diastereoselectivity were determined by ¹H NMR spectroscopy. Product was purified by flash column chromatography using a mixture of eluents EtOAc/*n*-hexane in 5:95 ratio.

Ethyl-(1R,1aS,6aS)-1-methyl-1,1a,6,6a-tetrahydrocyclopropa[a]indene-1-carboxylate
(**trans-122a**)



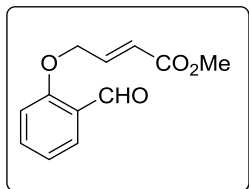
23 μ L of indene **117** (0.19 mmol) were used and 21 mg of colorless oil **trans-122a** was obtained. Yield = 50 %. *R_f*: 0.34 (EtOAc/*n*-hexane = 5:95). ¹H NMR (400 MHz, CDCl₃) δ (ppm) = 7.29 (d, *J* = 8.7 Hz, 1H), 7.14 (s, 3H), 4.17 (q, *J* = 7.1 Hz, 2H), 3.23 (dd, *J* = 18.0, 7.0 Hz, 1H), 3.06 (d, *J* = 6.9 Hz, 1H), 2.82 (d, *J* = 18.0 Hz, 1H), 2.43 (t, *J* = 6.9 Hz, 1H), 1.28 (t, *J* = 7.1 Hz, 3H), 0.79 (s, 3H). ¹³C NMR (101 MHz, CDCl₃) δ (ppm) = 175.2, 144.9, 141.4, 126.6, 126.4, 125.3, 124.1, 60.9, 38.9, 32.2, 30.6, 14.4, 7.8. FT-IR (cm⁻¹): 2978, 2933, 2909, 1711, 1585, 1542, 1476, 1380, 763, 738, 717. HRMS (ESI/Q-TOF) *m/z*: C₁₄H₁₇O₂ [M + H]⁺, calculated: 217.1229, found: 217.1224. HPLC/Mass: RACEMIC, Daicel Chiralpak IC column, *iso*-Propanol/*n*-hexane 1:99 flow = 0.5 mL/min, *tr*₁ = 15.08 min, *tr*₂ = 15.81 min, 220 nm.



Peak #	RetTime [min]	Type	Width [min]	Area	Height	Area %
1	15.080	BV	0.3477	6.60584e5	3.13881e4	49.4598
2	15.802	VB	0.3758	6.75014e5	2.87749e4	50.5402

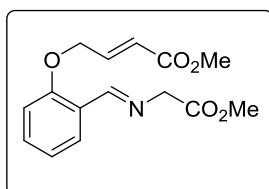
2.8.4 Ferrocenyl-proline ligands catalyzed intramolecular (3+2) cycloaddition reactions

*Methyl (E)-4-(2-formylphenoxy)but-2-enoate (125)*⁹⁷



To a solution of NaH (0.88 g, 36.84 mmol) in DMF (50 mL), salicylaldehyde **123** (2.62 g, 24.57 mmol) was added dropwise at 0°C. The mixture was stirred for 1 hour at room temperature. After that, methyl-4-bromobut-2-enoate **124** (3.18 mL, 27.03 mmol) was added dropwise to the mixture at 0°C. Once addition was finished the reaction was stirred at room temperature for 16 hours. 50 mL H₂O of were added to the mixture in order to quench the reaction and product was extracted with 40 mL of Et₂O. Further combination of organic layers were then washed with brine and dried over Na₂SO₄. After removal of the solvent the product precipitated in Et₂O and 1.84 g of yellowish solid **117** was obtained. Yield = 34%. ¹H NMR (400 MHz, CDCl₃) δ (ppm) = 10.54 (s, 1H), 7.86 (d, *J* = 7.7 Hz, 1H), 7.54 (t, *J* = 8.0 Hz, 1H), 7.17 – 7.04 (m, 2H), 6.94 (d, *J* = 8.4 Hz, 1H), 6.22 (d, *J* = 15.8 Hz, 1H), 4.89 – 4.79 (m, 3H), 3.77 (s, 4H).

*Methyl (E)-4-(2-((E)-((2-methoxy-2-oxoethyl)imino)methyl)phenoxy)but-2-enoate(126)*⁹⁷



Glycine methyl ester hydrochloride **108a** (0.12 g, 0.99 mmol) was dissolved in DCM (10 mL) in presence of molecular sieves 4Å and *N,N*-diisopropylamine (0.21 mL, 0.99 mmol). Mixture was stirred for 1 hour at room temperature. Subsequently, compound **117** (0.20 g, 0.91 mmol) was added to the mixture and stirred overnight. Molecular sieves were removed and mixture was washed with H₂O (3 x 10 mL) and extracted with 20 mL of DCM two times. Then, solvent was removed under reduced pressure and 0.22 g of white solid was obtained corresponding to **126**. Yield = 85%. ¹H NMR (400 MHz, CDCl₃) δ (ppm) = 8.65 (s, 1H), 7.92 (d, *J* = 7.6 Hz, 1H), 7.26 (t, *J* = 7.5 Hz, 1H), 6.98 (dt, *J* = 16.1, 4.3 Hz, 1H), 6.89 (t, *J* = 7.6 Hz, 1H), 6.74 (d, *J* = 8.3 Hz, 1H), 6.07 (d, *J* = 15.9 Hz, 1H), 4.63 (s, 2H), 4.33 (s, 2H), 3.66 (s, 3H), 3.65 (s, 3H).

⁹⁷ Stohler, R.; Wahl, F.; Pfaltz, A., *Synthesis*, **2005**, 1431–1436.

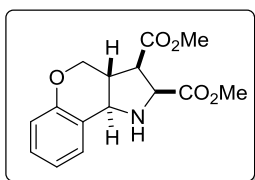
CHAPTER 2

2.8.4.1 General procedure for the synthesis of cycloadduct *endo*-127 and *dimer*-128

Racemic *endo*-127: To a solution of imine **127** (0.20 g, 0.69 mmol) and AgOAc (0.17 g, 1.03 mmol) in 10 mL of acetonitrile *N,N*-diisopropylamine (0.16 mL, 0.76 mmol) was added and mixture was stirred for 16 hours. After completion of reaction followed by TLC and ^1H NMR spectroscopy, mixture was filtered through a pad of Celite and then solvent was removed under reduced pressure. Ratio of formed regioisomers was determined by ^1H NMR spectroscopy and products were separated by column chromatography.

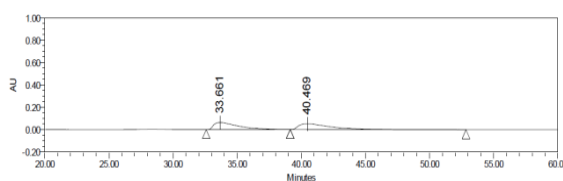
Chiral *endo*-127: Ferrocenyl-proline ligands **91a-c** or **93** (5.2 mol%) and metallic salts (5 mol%) were dissolved in 5 mL of corresponding solvent and stirred for 30 minutes until complex was formed. Then, imine **126** (1 equiv.) was placed in a round bottom flask at described temperature for each case. Complex was added and mixture was stirred for 10 minutes. Subsequently, base (5 mol%) was added to the mixture and reaction was carried out in described temperature until completion, which was monitored by ^1H NMR spectroscopy. Crude reaction was filtered through a pad of Celite and then solvent was removed under reduced pressure. Residue was purified by column chromatography to afford *endo*-127 and compound *dimer*-128.

*Dimethyl-1,2,3,3a,4,9b-hexahydrochromeno[4,3-*b*]pyrrole-2,3-dicarboxylate*
(*endo*-127)⁹⁷

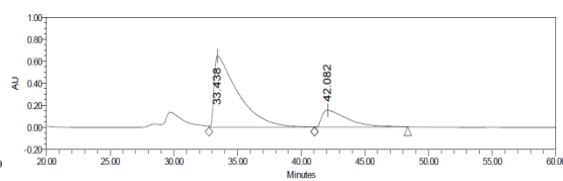


129 mg of imine **126** (0.44 mmol) were employed and 61 mg of product *endo*-127 were obtained corresponding to 47% yield. Chromatography was carried out in an eluent mixture of EtOAc/*n*-hexane = 50:50. ^1H NMR (400 MHz, CDCl_3) δ (ppm) = 7.22 (d, J = 7.6 Hz, 1H), 7.11 (t, J = 7.8 Hz, 1H), 6.84 (t, J = 7.5 Hz, 1H), 6.77 (d, J = 8.3 Hz, 1H), 4.51 (dd, J = 10.2, 4.3 Hz, 1H), 4.34 (d, J = 10.0 Hz, 1H), 4.14 (d, J = 7.2 Hz, 1H), 4.09 (d, J = 10.9 Hz, 1H), 3.72 (d, J = 11.3 Hz, 1H), 3.67 (s, 3H), 3.64 (s, 3H), 3.02 (t, J = 10.9 Hz, 1H). 60 % ee obtained under best reaction conditions. **HPLC:** Daicel Chiralpak IB column, *iso*-Propanol/*n*-hexane 5:95, flow = 1.0 mL/min, λ = 277 nm, $t_{\text{r major}}$ = 34.2 min, $t_{\text{r min}}$ = 42.5 min.

CYCLOADDITION REACTIONS

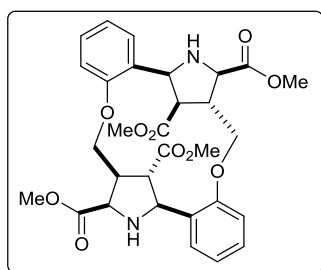


	Retention Time (min)	% Area
1	33.661	49.57
2	40.469	50.43



	Retention Time (min)	% Area
1	33.438	80.00
2	42.082	20.00

Dimerization Product (**dimer-128**)⁹⁷



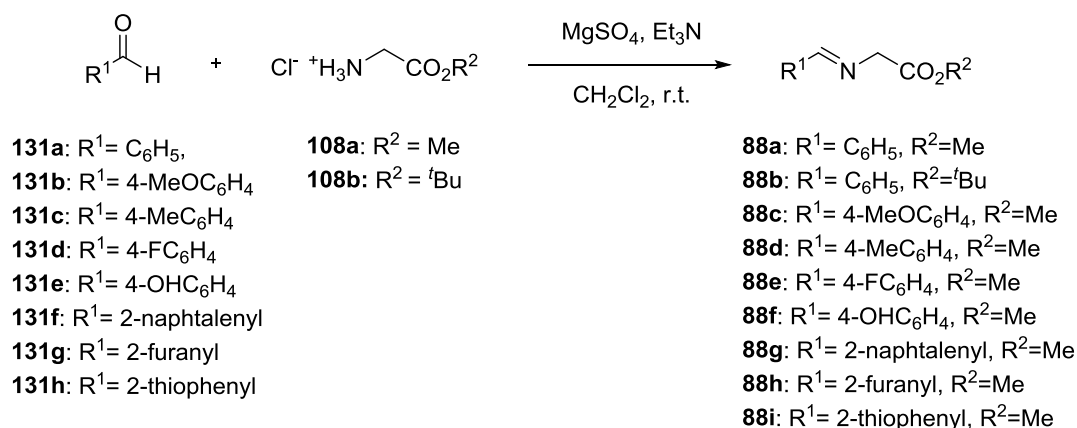
29 mg of dimer obtained starting from 129 mg of imine **126**. Yield = 12 %. Chromatography was carried out in an eluent mixture of EtOAc/*n*-hexane = 100:0. ¹H NMR (400 MHz, CDCl₃) δ (ppm) = 7.20 (t, *J* = 7.9 Hz, 1H), 7.15 (d, *J* = 7.6 Hz, 1H), 6.90 (t, *J* = 7.5 Hz, 1H), 6.84 (d, *J* = 8.2 Hz, 1H), 5.03 (d, *J* = 6.4 Hz, 1H), 4.40 (d, *J* = 9.3 Hz, 1H), 4.08 (dd, *J* = 9.5, 3.8 Hz, 1H), 3.88 (d, *J* = 7.3 Hz, 1H), 3.79 (s, 3H), 3.57 – 3.51 (m, 1H), 3.11 (s, 3H), 2.98 (d, *J* = 7.4 Hz, 2H). **HPLC**: Daicel Chiralpak IB column, *iso*-Propanol/*n*-hexane 25:75, flow = 1.0 mL/min, 233 and 273 nm. , *tr*₁ = 16.8 min, *tr*₂ = 45.4 min. All cases showed racemic nature of the product.

2.8.5 Intermolecular enantioselective (3+2) cycloadditions catalyzed by Ferrocenyl-proline ligands and transition metals

2.8.5.1 General procedure for the synthesis of α-iminoesters

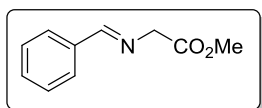
Glycine methyl or tert-butyl ester hydrochloride (**108a** or **108b**, 1.20 equiv.) was dissolved in anhydrous DCM (0.50 M) in presence of MgSO₄ as drying agent. Then, Et₃N (1.20 equiv.) was added and mixture was stirred for 1 hour at room temperature. Corresponding aldehyde (**131a-h**, 1 equiv.) was added to the reaction media and reaction was stirred at room temperature for 16 to 20 hours. After this time, MgSO₄ was filtered off, and then organic layer was washed with H₂O (3 x 10 mL) and with brine (1 x 10 mL), and compound was finally extracted two times 20mL of DCM. Collected organic layers were dried over Na₂SO₄ and solvent was removed under reduced pressure to afford α-iminoesters **88a-i** and they were used without further purification in next reaction step.

CHAPTER 2



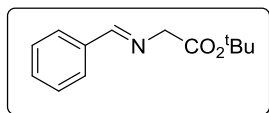
Scheme 2.37. Synthesis of different α-iminoesters **88a-i**.

Methyl (*E*)-2-(benzylideneamino)acetate (**88a**)⁹⁸



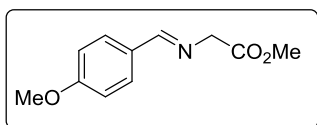
Yellow oil. Yield = 89 %. ¹H NMR (400 MHz, CDCl₃) δ (ppm) = 8.25 (s, 1H), 7.81 – 7.70 (m, 2H), 7.43 – 7.33 (m, 3H), 4.38 (s, 2H), 3.73 (s, 3H).

Tert-Butyl (*E*)-2-(benzylideneamino)acetate (**88b**)⁹⁹



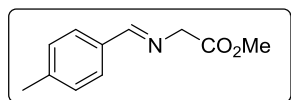
Yellow oil. Yield = 85 %. ¹H NMR (400 MHz, CDCl₃) δ (ppm) = 8.27 (s, 1H), 7.78 (dd, *J* = 7.7, 1.6 Hz, 2H), 7.45 – 7.38 (m, 3H), 4.31 (s, 2H), 1.50 (s, 9H).

Methyl (*E*)-2-((4-methoxybenzylidene)amino)acetate (**88c**)⁹⁸



White solid. Yield = 69 %. ¹H NMR (400 MHz, CDCl₃) δ (ppm) = 8.22 (s, 1H), 7.72 (dd, *J* = 8.8 Hz, 2H), 6.93 (d, *J* = 8.8 Hz, 2H), 4.38 (s, 2H), 3.84 (s, 3H), 3.77 (s, 3H).

Methyl (*E*)-2-((4-methoxybenzylidene)amino)acetate (**88d**)¹⁰⁰



White solid. Yield = 97 %. ¹H NMR (400 MHz, CDCl₃) δ (ppm) = 8.26 (s, 1H), 7.67 (d, *J* = 8.0 Hz, 2H), 7.23 (d, *J* = 7.8 Hz, 3H), 4.40 (s, 2H), 3.78 (s, 2H), 2.39 (s, 3H)

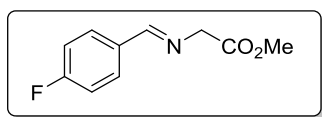
⁹⁸ Lopez-Perez, A.; Segler, M.; Adrio, J.; Carretero, J. C., *J. Org. Chem.* **2011**, 76, 1945–1948.

⁹⁹ Saito, S.; Tsubogo, T.; Kobayashi, S., *J. Am. Chem. Soc.* **2007**, 129, 5364–5365.

¹⁰⁰ Cabrera, S.; Carretero, J. C., *J. Am. Chem. Soc.* **2005**, 130, 17250–17251.

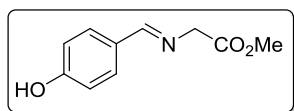
CYCLOADDITION REACTIONS

Methyl (E)-2-((4-fluorobenzylidene)amino)acetate (**88e**)¹⁰⁰



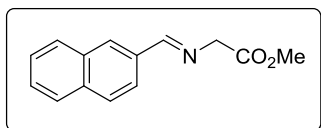
Yellow oil. Yield = 81 %. ¹H NMR (400 MHz, CDCl₃) δ (ppm) = 8.26 (s, 1H), 7.78 (dd, *J* = 8.7, 5.5 Hz, 2H), 7.11 (t, *J* = 8.6 Hz, 1H), 4.40 (s, 1H), 3.78 (s, 2H).

Methyl (E)-2-((4-hydroxybenzylidene)amino)acetate (**88f**)¹⁰¹



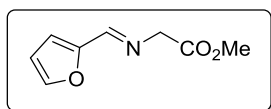
Orange solid. Yield = 60 %. ¹H NMR (400 MHz, CDCl₃) δ (ppm) = 8.09 (s, 1H), 7.49 (d, *J* = 8.1 Hz, 2H), 6.70 (d, *J* = 8.2 Hz, 3H), 6.28 (s, 1H, broad), 4.30 (s, 2H), 3.64 (s, 3H).

Methyl (E)-2-((naphthalen-2-ylmethylene)amino)acetate (**88g**)¹⁰²



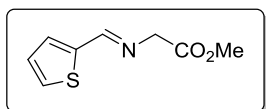
White solid. Yield = 86 %. ¹H NMR (400 MHz, CDCl₃) δ (ppm) = 8.45 (s, 1H), 8.09 (s, 1H), 8.03 (d, *J* = 7.8, 1H), 7.95 – 7.79 (m, 3H), 7.58 – 7.45 (m, 2H), 4.48 (s, 2H), 3.80 (s, 3H).

Methyl (E)-2-((furan-2-ylmethylene)amino)acetate (**88h**)¹⁰²



Brown oil. Yield = 83 %. ¹H NMR (400 MHz, CDCl₃) δ (ppm) = 8.11 (s, 1H), 7.55 (s, 1H), 6.85 (d, *J* = 3.0 Hz, 1H), 6.51 (s, 1H), 4.39 (s, 2H), 3.78 (s, 3H).

Methyl (E)-2-((thiophen-2-ylmethylene)amino)acetate (**88i**)¹⁰²



Yellow solid. Yield = 92%. ¹H NMR (400 MHz, CDCl₃) δ (ppm) = 8.30 (s, 1H), 7.36 (d, *J* = 5.1 Hz, 1H), 7.28 (d, *J* = 3.7 Hz, 1H), 6.99 (t, *J* = 4.4 Hz, 1H), 4.29 (s, 2H), 3.67 (s, 3H).

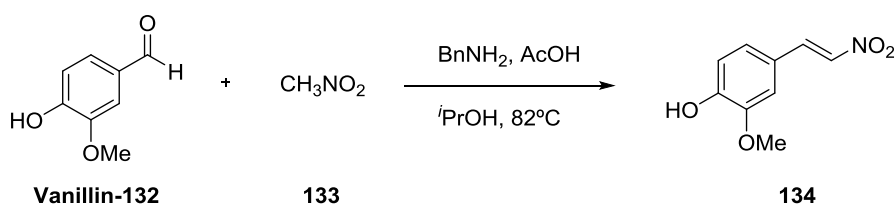
¹⁰¹ Arrieta, A.; Otaegui, D.; Zubia, A.; Cossio, F. P.; Diaz-Ortiz, A.; de la Hoz, A.; Herrero, M. A.; Prieto, P.; Foces-Foces, C.; Pizarro, J. L., *J. Org. Chem.* **2007**, 72, 4313–4322.

¹⁰² Lopez-Perez, A.; Segler, M.; Adrio, J.; Carretero, J. C., *J. Org. Chem.* **2011**, 76, 1945–1948.

CHAPTER 2

2.8.5.2 Synthesis of (*E*)-2-methoxy-4-(2-nitrovinyl)phenol-**134**¹⁰³

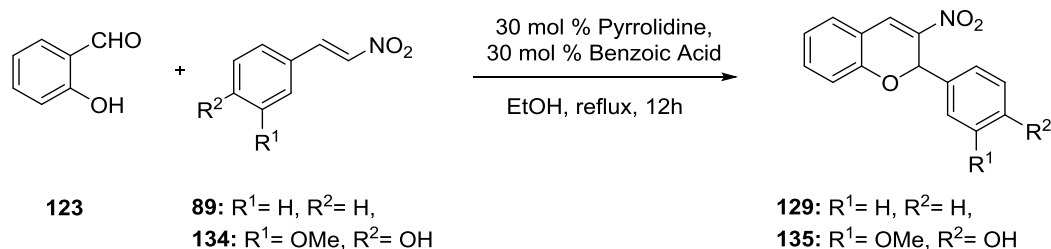
Vanillin **132** (1.00 g, 6.57 mmol) and nitromethane (**133**, 0.80 mL, 13 mmol) were dissolved in 66 mL of *i*PrOH (0.10 M) in the presence of BnNH₂ (0.09 g, 0.90 mmol) and AcOH (91 μ L, 0.90 mmol). Mixture was stirred at reflux of *i*PrOH for 16 hours. Solvent was evaporated under reduced pressure and product obtained was purified by flash column chromatography (EtOAc/*n*-hexane = 20:80 to 50:50). 509 mg of yellow solid **134** was obtained in 40 % yield. ¹H NMR (400 MHz, CDCl₃) δ (ppm) = 7.95 (d, *J* = 13.5 Hz, 1H), 7.51 (d, *J* = 13.5 Hz, 1H), 7.14 (d, *J* = 8.2 Hz, 1H), 7.02 – 6.94 (m, 2H), 6.05 (s, 1H), 3.96 (s, 3H).



Scheme 2.38. Synthesis of nitroalkene **134** bearing hydroxy and methoxy functional groups.

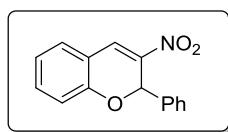
2.8.5.3 Synthesis of 3-nitro-2H-chromene derivatives **129** and **135**

Salicylaldehyde **123** (1.1 equiv.) and corresponding nitroalkene **89** or **134** (1 equiv.) were placed in a flask and dissolved in 25 mL of ethanol. Then, benzoic acid (0.3 equiv.) was added as additive and final addition of pyrrolidine (0.3 equiv.) was performed dropwise. Reaction mixture was refluxed for 12 hours upon completion of reaction observed by ¹H NMR spectroscopy. After reaction was cooled down to room temperature, solvent was removed under reduced pressure. Crude of corresponding chromene was purified by flash column chromatography in silica gel (EtOAc/*n*-hexane = 1:50) to obtain a yellow solid in all cases (**129** and **135**).



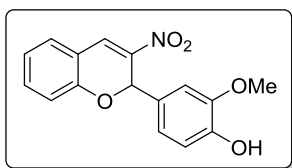
Scheme 2.39. Synthesis of chromene derivatives **129** and **135** by oxa-Michael aza-Henry addition/elimination reactions.

¹⁰³ Kiyokawa, K.; Nagata, T.; Hayakawa, J.; Minakata, S., *Chem. Eur. J.* **2015**, 21, 1280–1285.

*3-nitro-2-phenyl-2H-chromene (129)*¹⁰⁴

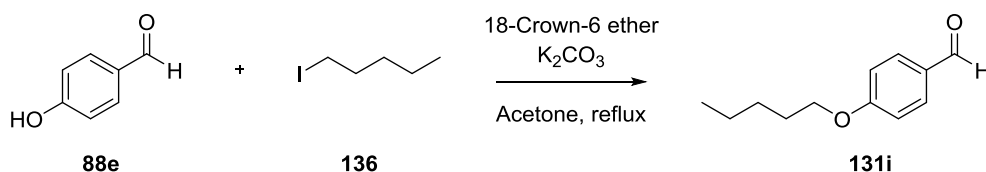
6.65 (s, 1H).

129 was obtained as a yellow solid. Yield = 63 %. ¹H NMR (400 MHz, CDCl₃) δ (ppm) = 8.09 (s, 1H), 7.49 – 7.42 (m, 2H), 7.35 (d, *J* = 7.9 Hz, 5H), 7.02 (t, *J* = 7.5 Hz, 1H), 6.91 (d, *J* = 8.2 Hz, 1H),

2-methoxy-4-(3-nitro-2H-chromen-2-yl)phenol (135)

1H), 6.87 – 6.78 (m, 3H), 6.50 (s, 1H), 5.64 (s, 1H), 3.85 (s, 3H).

Starting from 794 mg of nitroalkenes **170**, 135 mg were isolated for chromene **135** as yellow oil. Yield = 11%. ¹H NMR (400 MHz, CDCl₃) δ (ppm) = 8.05 (s, 1H), 7.33 (d, *J* = 7.4 Hz, 2H), 7.00 (td, *J* = 7.5, 1.1 Hz, 1H), 6.90 (d, *J* = 1.8 Hz, 1H), 6.87 – 6.78 (m, 3H), 6.50 (s, 1H), 5.64 (s, 1H), 3.85 (s, 3H).

2.8.5.4 Procedure for the synthesis of 4-(pentiloxy)benzaldehyde 131i¹⁰⁵

Scheme 2.40. Synthesis of aldehyde **131i** by Williamson reaction.

Under argon atmosphere, 4-hydroxybenzaldehyde **88e** (0.50 g, 4.09 mmol) was placed with K₂CO₃ (0.65 g, 4.70 mmol), 18-crown-6 ether (0.05 g, 0.20 mmol) and dry acetone (16.4 mL, 0.25 M) in a flask. Then, *n*-pentyl iodide **136** (0.59 mL, 4.50 mmol) was added and temperature was elevated to reflux of acetone. The reaction was monitored by TLC (EtOAc/*n*-hexane = 25:75) and stopped after 18 h. After removal of solvent, crude was redissolved in DCM and solution was washed four times with 10 mL of H₂O and then extracted three times with 20 mL of DCM. Organic layers were dried over Na₂SO₄, evaporated under pressure and crude was used in next step without further purification obtaining 0.79 g of compound **131i** as yellow oil in quantitative yield. ¹H NMR (400 MHz, CDCl₃) δ (ppm) = 9.88 (s, 1H), 7.96 – 7.71 (m, 2H), 7.07 – 6.89 (m,

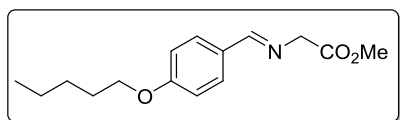
¹⁰⁴ Wang, P.; Zhang, D.; Liu, X., *Arkivoc* **2014**, v, 408–419.

¹⁰⁵ a) Hawker, C. J.; Fréchet, J. M. J., *J. Am. Chem. Soc.* **1990**, 112, 7638–7647. b) Aldaba, E., *Nuevas Aplicaciones de Las Cicloadiciones [3+2] En La Preparación de Compuestos de Interés En Biomedicina Y En Ciencia de Los Materiales*, Donostia, **2006**.

CHAPTER 2

2H), 4.04 (t, $J = 6.5$ Hz, 2H), 1.81 (dt, $J = 8.1, 6.5$ Hz, 2H), 1.55 – 1.34 (m, 4H), 0.94 (t, $J = 7.0$ Hz, 3H).

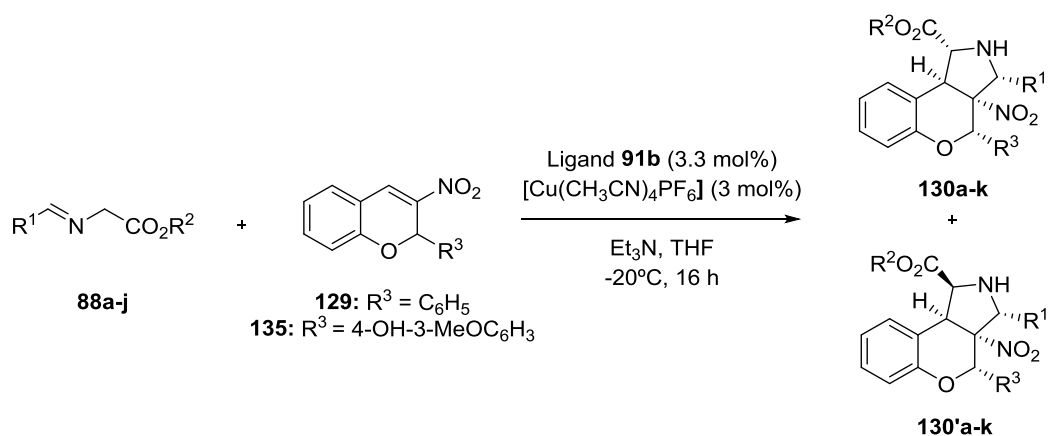
*Methyl (E)-2-((4-pentyloxy)benzylidene)amino)acetate (88j)*¹⁰⁵



General procedure for the synthesis of iminoesters was followed (**Scheme 2.37**). Yellow oil obtained in quantitative yield. ¹H NMR (400 MHz, CDCl₃) δ (ppm) = 8.21 (s, 1H), 7.70 (d, $J = 8.7$ Hz, 2H), 6.92 (d, $J = 8.7$ Hz, 2H), 4.38 (s, 2H), 3.99 (t, $J = 6.6$ Hz, 3H), 3.77 (s, 3H), 1.86 – 1.72 (m, 3H), 1.51 – 1.31 (m, 6H), 0.93 (t, $J = 7.1$ Hz, 4H).

2.8.5.5 Enantioselective synthesis of tricyclic chromane derivatives **130** and **130'**

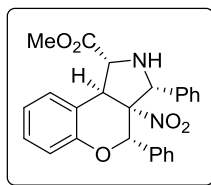
Ferrocenyl-proline ligand **91b** (3.3 mol%) and [Cu(CH₃CN)₄PF₆] (3 mol%) were dissolved in 2 mL of dry THF. The mixture was stirred for 15 minutes at room temperature to afford the formation of copper complex and then it was cooled to -20°C. After that, corresponding imine **88a-j** (1 equiv.) and dipolarophile **129** or **135** (1.1 equiv.) were dissolved in 2 mL of dry THF and precooled at -20°C, and subsequently this mixture was added to the complex. Finally, catalytic amount of Et₃N (5 mol%) was added. After stirring 16 hours at -20 °C, the mixture was filtered through a pad of Celite and the filtrate was evaporated under reduced pressure. Crude of the reaction was analyzed by ¹H NMR spectroscopy in order to determine the diastereomeric ratio. Purification by flash column chromatography in silica gel (EtOAc/*n*-hexane) afforded the corresponding products **130a-k** and **130'a-k**.



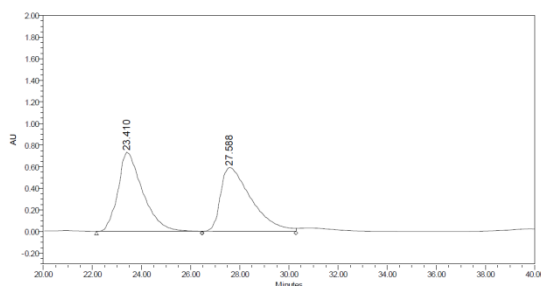
Scheme 2.41. Enantioselective ferrocenyl-proline and copper catalyzed (3+2) cycloaddition reaction to afford tricyclic compounds **130a-k** and **130'a-k**.

CYCLOADDITION REACTIONS

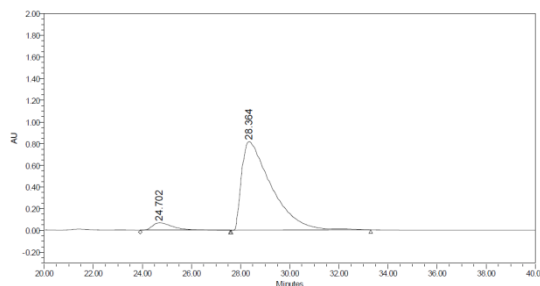
Methyl (1*R*, 3*R*, 3*aR*, 4*S*, 9*bS*)-3*a*-nitro-3,4-diphenyl-benzopyrano[3,4-*c*]-pyrrolidine-1-carboxylate (**130a**)



47 mg of a white solid obtained (starting from 60 mg, 0.340 mmol of corresponding imine **88a**), yield = 32 %. EtOAc/*n*-hexane 17:83, *R_f*: 0.48 (2x). ¹H NMR (400 MHz, CDCl₃) δ (ppm) = 7.55 (d, *J* = 7.6 Hz, 1H), 7.44 (dd, *J* = 5.0, 1.9 Hz, 3H), 7.38 (dd, *J* = 6.9, 3.1 Hz, 2H), 7.21 – 7.13 (m, 6H), 7.07 (t, *J* = 7.4 Hz, 1H), 6.82 (d, *J* = 8.1 Hz, 1H), 5.58 (s, 1H), 4.97 (d, *J* = 10.7 Hz, 1H), 4.79 (d, *J* = 3.8 Hz, 1H), 4.16 (dd, *J* = 7.6, 3.8 Hz, 1H), 4.03 (s, 3H), 3.18 – 3.12 (m, 1H). ¹³C NMR (101 MHz, CDCl₃) δ (ppm) = 172.6, 150.1, 135.2, 134.0, 129.8, 129.2, 129.1, 128.9, 128.6, 128.4, 127.1, 125.2, 123.4, 118.5, 96.8, 75.7, 70.6, 68.8, 53.2, 46.2. FT-IR (neat) = 3329, 3062, 3032, 2952, 1742, 1540, 1488, 1454, 1359, 1211, 799, 755 cm⁻¹. HRMS (ESI/Q-TOF) *m/z*: C₂₅H₂₃N₂O₅ [M + H]⁺, calculated: 431.1607, found: 431.1614. Elemental anal. calculated for C₂₅H₂₂N₂O₅: C, 69.8; H, 5.1; N, 6.5. Found: C, 69.0; H, 5.2; N, 6.6. [α]_D²³ = +58.1 (c 2.35, CH₂Cl₂), 89 % ee. HPLC: Daicel Chiralpak IB column, *iso*-Propanol/*n*-hexane 5:95, flow = 1.0 mL/min, *tr*_{min} = 24.7 min (1*S*, 3*S*, 3*aS*, 4*R*, 9*bR*), *tr*_{major} = 28.4 min (1*R*, 3*R*, 3*aR*, 4*S*, 9*bS*), 230 nm.

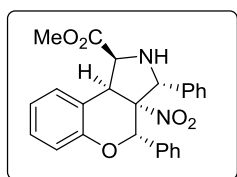


	RT	Area	% Area	Height
1	23.410	50739344	50.01	729923
2	27.588	50715869	49.99	588183



	RT	Area	% Area	Height
1	24.702	3998901	5.51	68679
2	28.364	68549909	94.49	816604

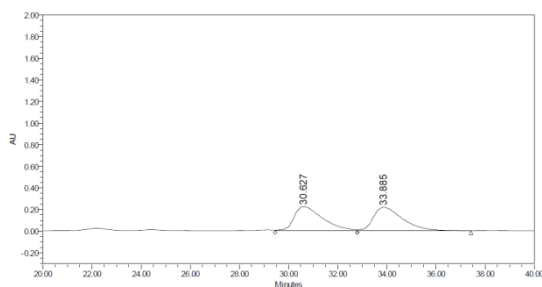
Methyl (1*S*, 3*R*, 3*aR*, 4*S*, 9*bS*)-3*a*-nitro-3,4-diphenyl-benzopyrano[3,4-*c*]-pyrrolidine-1-carboxylate (**130'a**)



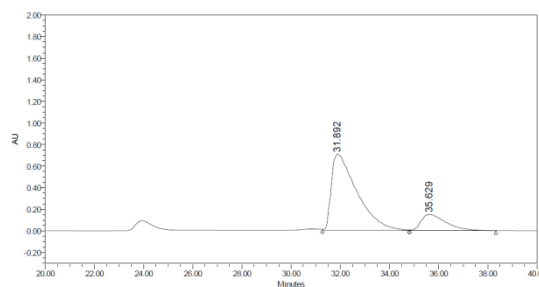
45 mg of a white solid obtained (starting from 60 mg, 0.340 mmol of corresponding imine **88a**), yield = 31 %. EtOAc/*n*-hexane 17:83 *R_f*: 0.33 (2x). ¹H NMR (400 MHz, CDCl₃) δ (ppm) = 7.36 – 7.32 (m, 2H), 7.32 – 7.26 (m, 5H), 7.26 – 7.23 (m, 1H), 7.12 (td, *J* = 7.7, 1.6 Hz, 1H), 6.97 (td, *J* = 7.6, 1.2 Hz, 1H), 6.83 (dd, *J* = 8.2, 1.2 Hz, 1H), 5.70 (s, 1H), 5.40 (s, 1H), 5.07 (d, *J* = 9.7 Hz, 1H), 5.01 (d, *J* = 9.8 Hz, 1H), 3.37 (s, 3H). ¹³C

CHAPTER 2

NMR (101 MHz, CDCl₃) δ (ppm) = 173.4, 152.7, 136.8, 134.9, 129.8, 129.2, 129.1, 129.0, 128.8, 128.5, 128.3, 127.5, 122.1, 120.7, 118.3, 98.0, 77.6, 68.7, 64.5, 51.9, 45.3. **FT-IR** (neat) = 3341, 3062, 3032, 2950, 1736, 1586, 1541, 1488, 1454, 1352, 1230, 756, 698 cm⁻¹. $[\alpha]_D^{23} = +8.58$ (c 1.35, CH₂Cl₂), 67 % ee. **HPLC**: Daicel Chiralpak IB column, *iso*-Propanol/*n*-hexane 5:95, flow = 1.0 mL/min, $t_{r\text{major}} = 31.9$ min (1*R*, 3*S*, 3*aS*, 4*R*, 9*bR*), $t_{r\text{min}} = 35.6$ min (1*S*, 3*R*, 3*aR*, 4*S*, 9*bS*), 230 nm.

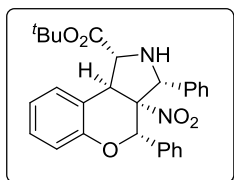


	RT	Area	% Area	Height
1	30.627	17989287	50.14	222973
2	33.885	17888423	49.86	216790



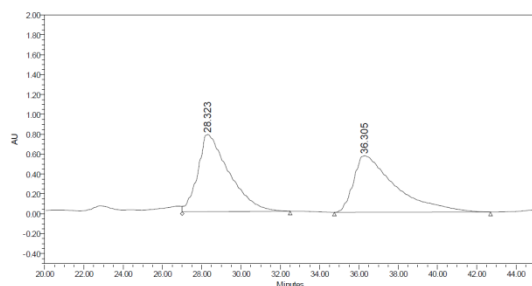
	RT	Area	% Area	Height
1	31.892	50972136	83.18	705932
2	35.629	10309309	16.82	148643

Tert-butyl (1*R*, 3*R*, 3*aR*, 4*S*, 9*bS*)-3*a*-nitro-3,4-diphenyl-benzopyrano[3,4-*c*]-pyrrolidine-1-carboxylate (**130b**)

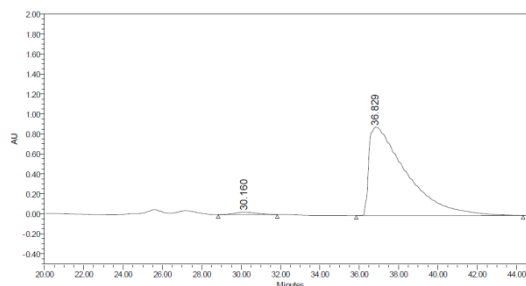


31 mg of a white solid obtained (starting from 60 mg, 0.274 mmol of corresponding imine **88b**), yield = 24 %. EtOAc/*n*-hexane 11:89, *R_f*: 0.29. ¹H NMR (400 MHz, CDCl₃) δ (ppm) = 7.56 (dt, *J* = 7.7, 1.2 Hz, 1H), 7.43 (dd, *J* = 5.0, 1.9 Hz, 3H), 7.26 (s, 0H), 7.22 – 7.12 (m, 6H), 7.07 (td, *J* = 7.5, 1.3 Hz, 1H), 6.82 (dd, *J* = 8.1, 1.2 Hz, 1H), 5.56 (s, 1H), 4.96 (s, 1H), 4.69 (d, *J* = 3.7 Hz, 1H), 4.05 (d, *J* = 3.8 Hz, 1H), 1.69 (s, 9H). ¹³C NMR (101 MHz, CDCl₃) δ (ppm) = 171.2, 150.2, 135.3, 134.1, 129.7, 129.2, 129.0, 129.0, 128.9, 128.6, 128.4, 127.0, 125.4, 123.3, 118.4, 97.0, 83.2, 75.8, 70.9, 69.7, 46.7, 28.3. **FT-IR** (neat) = 3359, 3063, 3034, 2976, 2931, 1729, 1585, 1540, 1488, 1454, 1368, 1249, 1232, 1152, 753, 697 cm⁻¹. **HRMS (ESI/Q-TOF) m/z**: C₂₈H₂₉N₂O₅ [M + H]⁺, calculated: 473.2076, found: 473.2076. **Elemental anal.** calculated for C₂₈H₂₈N₂O₅: C, 71.2; H, 6.0; N, 6.0. Found: C, 70.3; H, 5.8; N, 6.1. $[\alpha]_D^{23} = +11.2$ (c 1.00, CH₂Cl₂), 97 % ee. **HPLC**: Daicel Chiralpak IB column, *iso*-Propanol/*n*-hexane 1:99, flow = 0.7 mL/min, $t_{r\text{min}} = 30.1$ min (1*S*, 3*S*, 3*aS*, 4*R*, 9*bR*), $t_{r\text{major}} = 36.8$ min (1*R*, 3*R*, 3*aR*, 4*S*, 9*bS*), 230 nm.

CYCLOADDITION REACTIONS

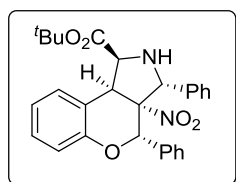


	RT	Area	% Area	Height
1	28.323	85552959	50.46	775569
2	36.305	84002348	49.54	567402

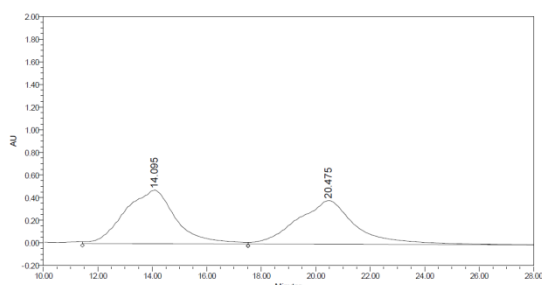


	RT	Area	% Area	Height
1	30.160	1888508	1.59	24304
2	36.829	116727965	98.41	885000

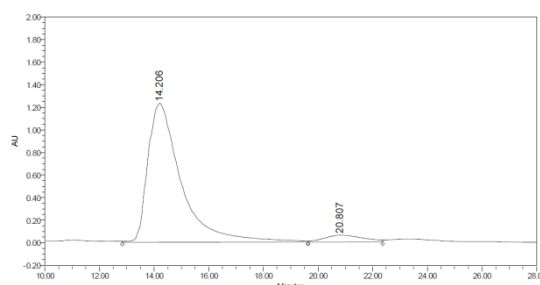
Tert-butyl (1S, 3R, 3aR, 4S, 9bS)-3a-nitro-3,4-diphenyl-benzopyrano[3,4-c]-pyrrolidine-1-carboxylate (130'b)



28 mg of a white solid obtained (starting from 60 mg, 0.274 mmol of corresponding imine **88b**), yield = 15 %. EtOAc/*n*-hexane 11:89, R_f : 0.25. $^1\text{H NMR}$ (400 MHz, CDCl_3) δ (ppm) = $^1\text{H NMR}$ (400 MHz, CDCl_3) δ = 7.44 (dd, J = 6.8, 3.2 Hz, 2H), 7.38 (dd, J = 6.4, 4.2 Hz, 4H), 7.24 (dd, J = 6.7, 3.4 Hz, 3H), 7.18 – 7.12 (m, 3H), 7.01 (t, J = 7.5 Hz, 1H), 6.87 (d, J = 8.4 Hz, 1H), 5.58 (s, 1H), 5.26 (s, 1H), 4.98 (d, J = 10.2 Hz, 1H), 4.82 (d, J = 10.1 Hz, 1H), 2.91 (s, 1H), 1.12 (s, 9H). $^{13}\text{C NMR}$ (101 MHz, CDCl_3) δ (ppm) = 172.6, 154.0, 138.3, 135.1, 131.4, 129.2, 128.7, 128.6, 128.6, 128.2, 127.8, 122.0, 119.6, 117.7, 97.2, 82.7, 78.5, 67.1, 64.4, 45.4, 27.6. **FT-IR** (neat) = 3343, 3063, 3033, 2976, 2932, 1716, 1586, 1542, 1489, 1455, 1367, 1232, 1152, 755, 699 cm^{-1} . $[\alpha]_D^{23}$ = +31.9 (c 0.90, CH_2Cl_2), 89 % ee. **HPLC**: Daicel Chiralpak IA column, *iso*-Propanol/*n*-hexane 10:90, flow = 1.0 mL/min, tr_{min} = (1*R*, 3*S*, 3a*S*, 4*R*, 9b*R*), tr_{major} (1*S*, 3*R*, 3a*R*, 4*S*, 9b*S*), 230 nm.



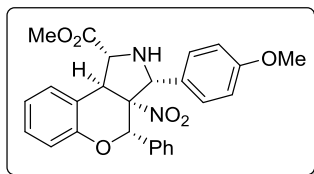
	RT	Area	% Area	Height
1	14.095	61994110	51.70	473015
2	20.475	57916329	48.30	386784



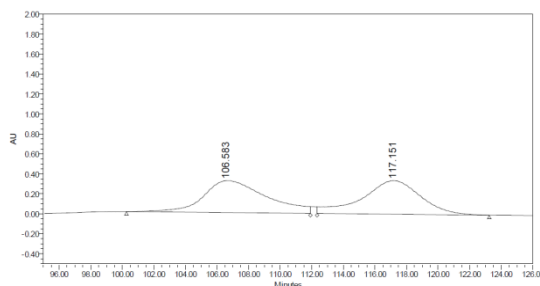
	RT	Area	% Area	Height
1	14.206	104455075	94.69	1231790
2	20.807	5862905	5.31	60156

CHAPTER 2

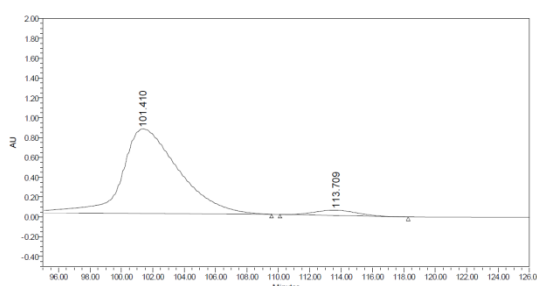
Methyl (1R, 3R, 3aR, 4S, 9bS)-3-(4-methoxyphenyl)-3a-nitro-4-phenyl-benzopyrano[3,4-c]-pyrrolidine-1-carboxylate (130c)



30 mg of a white solid obtained (starting from 60 mg, 0.290 mmol of corresponding imine **88c**), yield = 22 %. EtOAc/*n*-hexane 25:75 to 33:67, *R_f*: 0.17 (20:80). ¹H NMR (400 MHz, CDCl₃) δ (ppm) = 7.55 (d, *J* = 7.7 Hz, 1H), 7.30 (d, *J* = 8.3 Hz, 2H), 7.17 (t, *J* = 7.0 Hz, 6H), 7.06 (t, *J* = 7.5 Hz, 1H), 6.95 (d, *J* = 8.4 Hz, 2H), 6.81 (d, *J* = 8.1 Hz, 1H), 5.54 (s, 1H), 4.93 (d, *J* = 10.0 Hz, 1H), 4.77 (d, *J* = 3.7 Hz, 1H), 4.13 (t, *J* = 5.1 Hz, 1H), 4.02 (s, 3H), 3.83 (s, 3H), 3.07 (d, *J* = 9.6 Hz, 1H). ¹³C NMR (101 MHz, CDCl₃) δ (ppm) = 172.6, 160.7, 150.0, 135.3, 130.4, 129.0, 128.9, 128.6, 128.4, 128.2, 125.8, 125.3, 123.3, 118.4, 114.5, 113.6, 96.7, 75.7, 70.4, 68.6, 55.4, 53.2, 46.2. FT-IR (neat) = 3322, 3007, 2959, 1745, 1585, 1535, 1361, 1340, 1310, 1281, 1247, 758, 697 cm⁻¹. HRMS (ESI/Q-TOF) *m/z*: C₂₆H₂₅N₂O₆ [M + H]⁺, calculated: 461.1713, found: 461.1718. Elemental anal. calculated for C₂₆H₂₄N₂O₆: C, 67.8; H, 5.2; N, 6.1. Found: C, 67.2; H, 5.3; N, 6.6. [α]_D²² = +18.5 (c 1.70, CH₂Cl₂), 91 % ee. HPLC: Daicel Chiralpak IC column, *iso*-Propanol/*n*-hexane 5:95, flow = 0.7 mL/min, *tr*_{major} = 101.4 min (1*S*, 3*S*, 3a*S*, 4*R*, 9b*R*), *tr*_{min} = 113.7 min (1*R*, 3*R*, 3a*R*, 4*S*, 9b*S*), 230 nm.

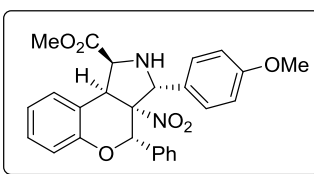


	RT	Area	% Area	Height
1	106.583	88415168	50.53	319313
2	117.151	86576235	49.47	336355



	RT	Area	% Area	Height
1	101.410	216797313	95.56	853251
2	113.709	10080819	4.44	54000

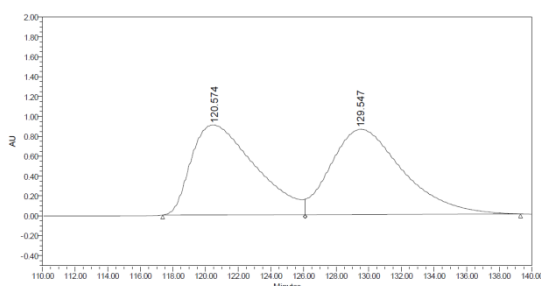
Methyl (1S, 3R, 3aR, 4S, 9bS)-3-(4-methoxyphenyl)-3a-nitro-4-phenyl-benzopyrano[3,4-c]-pyrrolidine-1-carboxylate (130'c)



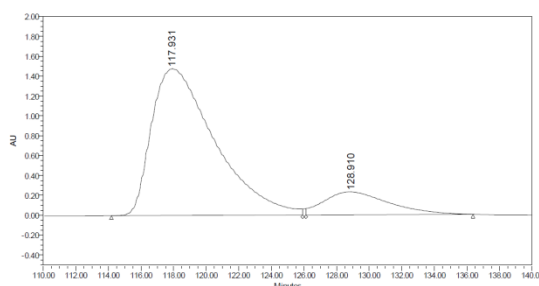
22 mg of a white solid obtained (starting from 60 mg, 0.290 mmol of corresponding imine **88c**), yield = 16 %. EtOAc/*n*-hexane 25:75 to 33:67. *R_f*: 0.33 (33:67). ¹H NMR (400 MHz, CDCl₃) δ (ppm) = 7.29 – 7.19 (m, 8H), 7.10 (ddd, *J* = 8.5,

CYCLOADDITION REACTIONS

7.4, 1.7 Hz, 1H), 6.95 (td, $J = 7.5, 1.2$ Hz, 1H), 6.88 – 6.83 (m, 2H), 6.80 (dd, $J = 8.2, 1.2$ Hz, 1H), 5.64 (s, 1H), 5.36 (s, 1H), 5.04 (d, $J = 9.6$ Hz, 1H), 4.98 (d, $J = 10.0$ Hz, 1H), 3.78 (s, 3H), 3.35 (s, 3H). ^{13}C NMR (101 MHz, CDCl_3) δ (ppm) = 173.5, 160.3, 152.6, 135.0, 129.8, 129.0, 128.6, 128.5, 128.3, 122.1, 121.0, 118.3, 114.2, 98.0, 77.6, 68.6, 64.4, 55.4, 51.8, 45.3. FT-IR (neat) = 3342, 3060, 3031, 3009, 2951, 2838, 1736, 1610, 1585, 1542, 1511, 1488, 1455, 1437, 1357, 1249, 1232, 1021, 1028, 758, 698 cm^{-1} . $[\alpha]_D^{24} = -9.78$ (c 1.24, CH_2Cl_2), 72 % ee. HPLC: Daicel Chiralpak IC column, *iso*-Propanol/*n*-hexane 3:97, flow = 0.7 mL/min, $\text{tr}_{\text{major}} = 117.9$ min (1*R*, 3*S*, 3*aS*, 4*R*, 9*bR*), $\text{tr}_{\text{min}} = 128.9$ min (1*S*, 3*R*, 3*aR*, 4*S*, 9*bS*), 230 nm.

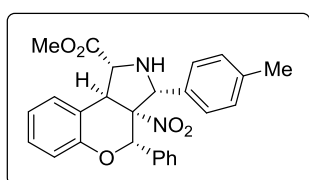


	RT	Area	% Area	Height
1	120.574	246402144	48.29	905566
2	129.547	263855203	51.71	858796



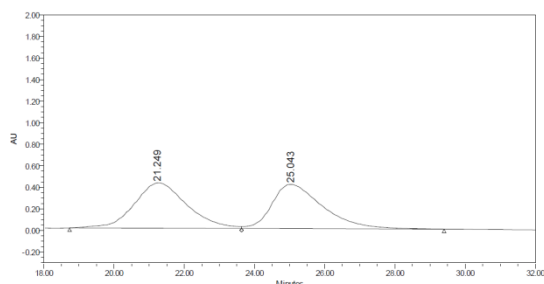
	RT	Area	% Area	Height
1	117.931	398810440	86.19	1477675
2	128.910	63919359	13.81	230805

*Methyl (1*R*, 3*R*, 3*aR*, 4*S*, 9*bS*)-3-(4-methylphenyl)-3*a*-nitro-4-phenyl-benzopyrano[3,4-*c*]pyrrolidine-1-carboxylate (130d)*

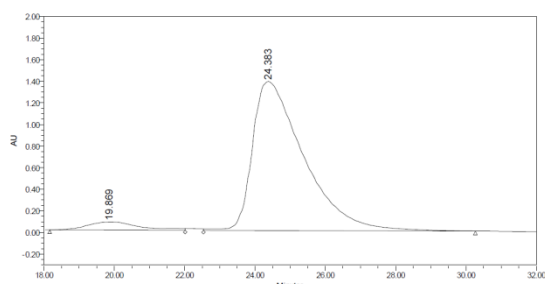


38 mg of a white solid obtained (starting from 60 mg, 0.314 mmol of corresponding imine **88d**), yield = 27 %. EtOAc/*n*-hexane 20:80, R_f : 0.35. ^1H NMR (400 MHz, CDCl_3) δ (ppm) = 7.53 (d, $J = 7.6$ Hz, 1H), 7.23 (t, $J = 7.0$ Hz, 4H), 7.14 (dq, $J = 13.4, 8.6, 6.6$ Hz, 6H), 7.04 (t, $J = 7.3$ Hz, 1H), 6.79 (d, $J = 8.1$ Hz, 1H), 5.54 (s, 1H), 4.92 (d, $J = 9.0$ Hz, 1H), 4.75 (d, $J = 3.8$ Hz, 1H), 4.12 (s, 1H), 4.00 (s, 3H), 3.11 (s, 1H), 2.35 (s, 3H). ^{13}C NMR (101 MHz, CDCl_3) δ (ppm) = 172.6, 150.0, 139.7, 135.3, 130.8, 129.9, 129.0, 129.0, 128.9, 128.6, 128.4, 126.8, 125.3, 123.4, 118.5, 96.8, 75.7, 70.6, 68.8, 53.2, 46.3, 21.4. FT-IR (neat) = 3466, 3028, 2970, 1739, 1609, 1585, 1540, 1488, 1453, 1436, 1365, 757, 697 cm^{-1} . HRMS (ESI/Q-TOF) m/z : $\text{C}_{26}\text{H}_{25}\text{N}_2\text{O}_5$ [$\text{M} + \text{H}$] $^+$, calculated: 445.1763, found: 445.1764. Elemental anal. calculated for $\text{C}_{26}\text{H}_{24}\text{N}_2\text{O}_5$: C, 70.3; H, 5.4; N, 6.3. Found: C, 68.8; H, 5.2; N, 6.3. $[\alpha]_D^{22} = +42.45$ (c 1.64, CH_2Cl_2), 89 % ee. HPLC: Daicel Chiralpak OD-H column, *iso*-Propanol/*n*-hexane 10:90, flow = 1.0 mL/min, $\text{tr}_{\text{min}} = 19.9$ min (1*S*, 3*S*, 3*aS*, 4*R*, 9*bR*), $\text{tr}_{\text{major}} = 24.3$ min (1*R*, 3*R*, 3*aR*, 4*S*, 9*bS*), 230 nm.

CHAPTER 2

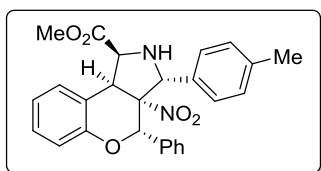


	RT	Area	% Area	Height
1	21.249	43897189	51.53	421507
2	25.043	41286756	48.47	411276

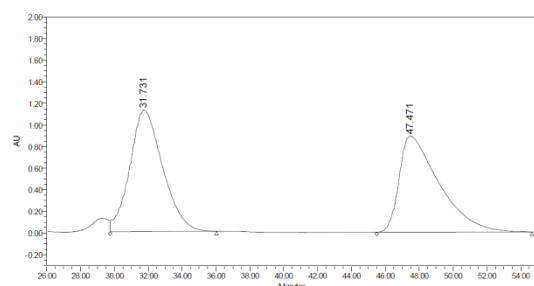


	RT	Area	% Area	Height
1	19.869	7805167	5.28	75840
2	24.383	139939756	94.72	1380445

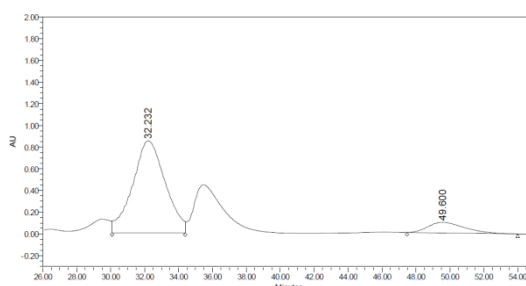
Methyl (1S, 3R, 3aR, 4S, 9bS)-3-(4-methylphenyl)-3a-nitro-4-phenyl-benzopyrano[3,4-c]-pyrrolidine-1-carboxylate (130'd)



34 mg of a white solid obtained (starting from 60 mg, 0.314 mmol of corresponding imine **80d**), yield = 24 %. EtOAc/*n*-hexane 20:80, *R_f*: 0.26. ¹H NMR (400 MHz, CDCl₃) δ (ppm) = 7.27 (s, 6H), 7.14 (dq, *J* = 15.6, 7.8 Hz, 4H), 6.96 (t, *J* = 7.7 Hz, 1H), 6.81 (d, *J* = 8.2 Hz, 1H), 5.68 (s, 1H), 5.35 (s, 1H), 5.05 (d, *J* = 9.8 Hz, 1H), 4.99 (d, *J* = 9.7 Hz, 1H), 3.35 (s, 3H), 2.77 (s, 1H), 2.32 (s, 3H). ¹³C NMR (101 MHz, CDCl₃) δ (ppm) = 173.6, 152.8, 139.2, 135.1, 133.8, 129.9, 129.7, 129.2, 128.6, 128.5, 127.4, 122.2, 118.4, 98.1, 77.7, 68.9, 64.7, 52.0, 45.5, 21.5. FT-IR (neat) = 3348, 3062, 3030, 2970, 2948, 1737, 1586, 1542, 1488, 1455, 1435, 1364, 758, 699 cm⁻¹. [α]_D²² = +0.37° (c 1.05, CH₂Cl₂), 77 % ee. HPLC: Daicel Chiralpak OD-H column, *iso*-Propanol/*n*-hexane 5:95, flow = 1.0 mL/min, tr_{min} = (1*R*, 3*S*, 3a*S*, 4*R*, 9b*R*), tr_{major} (1*S*, 3*R*, 3a*R*, 4*S*, 9b*S*), 230 nm.



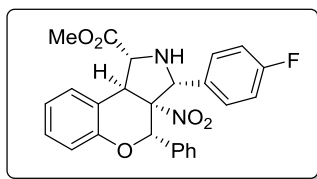
	RT	Area	% Area	Height
1	31.731	151840480	51.04	1125488
2	47.471	145669298	48.96	889061



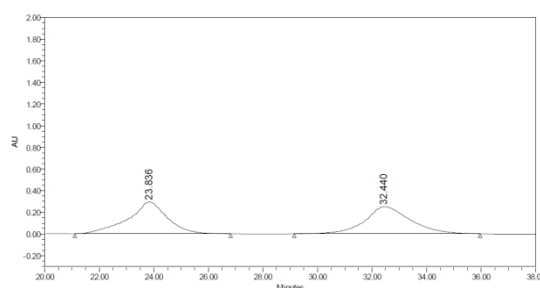
	RT	Area	% Area	Height
1	32.232	113117060	88.57	848313
2	49.600	14602226	11.43	97651

CYCLOADDITION REACTIONS

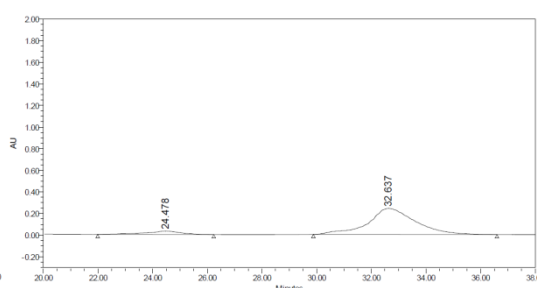
Methyl (1R, 3R, 3aR, 4S, 9bS)-3-(4-fluorophenyl)-3a-nitro-4-phenyl-benzopyrano[3,4-c]-pyrrolidine-1-carboxylate (130e)



31 mg of a white solid obtained (starting from 60 mg, 0.310 mmol of corresponding imine **88e**), yield = 22 %. EtOAc/*n*-hexane 17:83, *R_f*: 0.31 (2x 17:83). ¹H NMR (400 MHz, CDCl₃) δ (ppm) = 7.55 (d, *J* = 7.6 Hz, 1H), 7.38 (dd, *J* = 8.6, 5.3 Hz, 3H), 7.23 – 7.11 (m, 9H), 7.11 – 7.04 (m, 1H), 6.82 (d, *J* = 8.1 Hz, 1H), 5.53 (s, 1H), 4.97 (d, *J* = 9.0 Hz, 2H), 4.80 (d, *J* = 3.8 Hz, 1H), 4.14 (s, 1H), 4.02 (s, 4H), 3.03 (s, 1H). ¹⁹F NMR (376 MHz, CDCl₃) δ (ppm) = -111.6. ¹³C NMR (101 MHz, CDCl₃) δ (ppm) = 172.5, 164.8, 162.4, 150.0, 135.0, 130.0, 129.1, 128.9, 128.8, 128.8, 128.7, 128.4, 125.0, 123.4, 118.5, 116.3, 116.1, 96.6, 75.7, 69.7, 68.4, 53.2, 45.8. FT-IR (neat) = 3345, 3079, 2954, 1739, 1606, 1586, 1540, 1509, 1488, 1453, 1435, 1358, 1224, 757, 697 cm⁻¹. HRMS (ESI/Q-TOF) *m/z*: C₂₅H₂₂FN₂O₅ [M + H]⁺, calculated: 449.1513, found: 449.1500. Elemental anal. calculated for C₂₅H₂₁FN₂O₅: C, 67.0; H, 4.7; N, 6.2. Found: C, 67.6; H, 5.1; N, 6.5. [α]_D²³ = +1.15 (c 0.90, CH₂Cl₂), 83 % ee. HPLC: Daicel Chiralpak IB column, *iso*-Propanol/*n*-hexane 5:95, flow = 1.0 mL/min, *tr*_{min} = 24.5 min (1*S*, 3*S*, 3a*S*, 4*R*, 9b*R*), *tr*_{major} = 32.6 min (1*R*, 3*R*, 3a*R*, 4*S*, 9b*S*), 230 nm.

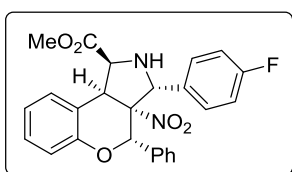


	RT	Area	% Area	Height
1	23.836	29451432	50.28	295376
2	32.440	29119207	49.72	251047



	RT	Area	% Area	Height
1	24.478	2694136	8.58	31031
2	32.637	28698154	91.42	240492

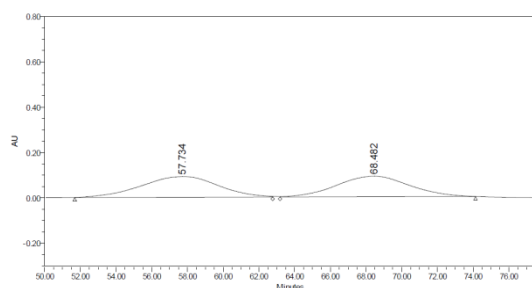
Methyl (1S, 3R, 3aR, 4S, 9bS)-3-(4-fluorophenyl)-3a-nitro-4-phenyl-benzopyrano[3,4-c]-pyrrolidine-1-carboxylate (130'e)



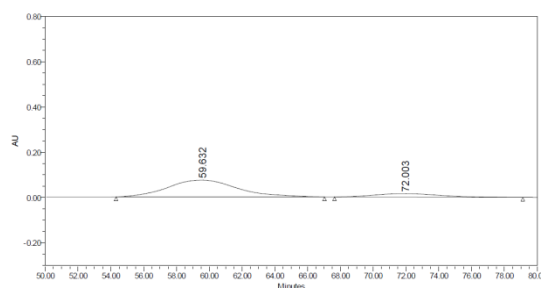
30 mg of a white solid obtained (starting from 60 mg, 0.310 mmol of corresponding imine **88e**), yield = 22 %. EtOAc/*n*-hexane 17:83, *R_f*: 0.15 (2x 17:83). ¹H NMR (400 MHz, CDCl₃)

CHAPTER 2

δ (ppm) = 7.30 – 7.22 (m, 8H), 7.14 – 7.09 (m, 1H), 7.04 – 6.94 (m, 3H), 6.81 (dd, J = 8.2, 1.2 Hz, 1H), 5.60 (s, 1H), 5.40 (s, 1H), 5.05 (d, J = 9.6 Hz, 1H), 4.97 (d, J = 9.6 Hz, 1H), 3.37 (s, 3H). **^{19}F NMR** (376 MHz, CDCl_3) δ (ppm) = -100.0. **^{13}C NMR** (101 MHz, CDCl_3) δ (ppm) = 173.6, 164.5, 162.0, 152.7, 134.7, 132.7, 129.9, 129.3, 129.2, 129.2, 129.1, 129.0, 128.5, 128.4, 128.4, 122.2, 120.6, 118.3, 115.9, 115.7, 97.9, 77.7, 67.9, 64.2, 51.9, 45.2. **FT-IR** (neat) = 3344, 3065, 3034, 2951, 1733, 1605, 1586, 1541, 1508, 1488, 1454, 1435, 1358, 1214, 758, 729, 697. $[\alpha]_D^{23}$ = -2.13 (c 0.41, CH_2Cl_2), 68 % ee. **HPLC**: Daicel Chiralpak OD-H column, *iso*-Propanol/*n*-hexane 3:97, flow = 1.0 mL/min, tr_{major} = 59.6 min (1*S*, 3*S*, 3*aS*, 4*R*, 9*bR*), tr_{min} = 72.0 min (1*R*, 3*R*, 3*aR*, 4*S*, 9*bS*), 230 nm.

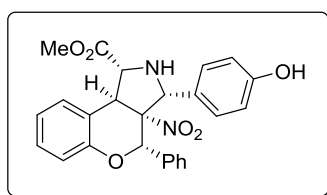


	RT	Area	% Area	Height
1	57.734	27385879	51.51	91304
2	68.482	25780432	48.49	91038



	RT	Area	% Area	Height
1	59.632	22077990	84.12	74234
2	72.003	4168699	15.88	15333

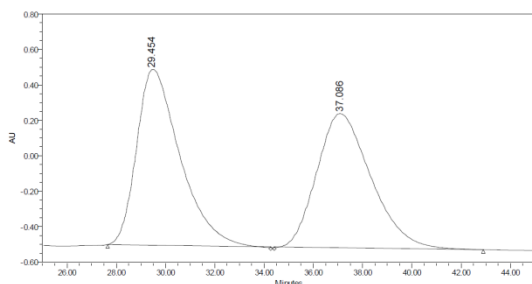
Methyl (1*R*, 3*R*, 3*aR*, 4*S*, 9*bS*)-3-(4-hydroxyphenyl)-3*a*-nitro-4-phenyl-benzopyrano[3,4-*c*]-pyrrolidine-1-carboxylate (**130f**)



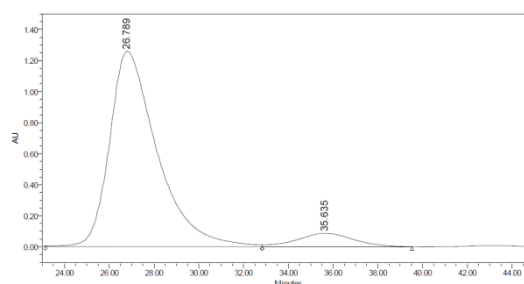
20 mg of a white solid obtained (starting from 60 mg, 0.310 mmol of corresponding imine **88f**), yield = 14 %. EtOAc/*n*-hexane 20:80, R_f : 0.33 (33:66). **^1H NMR** (400 MHz, CDCl_3) δ (ppm) = ^1H 7.60 – 7.49 (m, 1H), 7.22 – 7.11 (m, 8H), 7.07 (td, J = 7.5, 1.2 Hz, 1H), 6.88 – 6.75 (m, 3H), 5.53 (s, 1H), 5.00 – 4.83 (m, 1H), 4.77 (d, J = 3.0 Hz, 1H), 4.14 (s, 1H), 4.03 (s, 3H). **^{13}C NMR** (101 MHz, CDCl_3) δ (ppm) = 172.6, 157.2, 150.0, 135.2, 129.1, 129.0, 128.9, 128.6, 128.5, 128.4, 128.4, 125.4, 125.1, 123.4, 118.5, 116.2, 115.2, 96.6, 75.6, 70.3, 68.5, 53.3, 46.1. **FT-IR** (neat) = 3359, 3346, 3065, 3015, 2950, 1727, 1613, 1585, 1541, 1515, 1488, 1451, 1364, 763, 697 cm^{-1} . **HRMS (ESI/Q-TOF) m/z** : $\text{C}_{25}\text{H}_{23}\text{N}_2\text{O}_6$ [$\text{M} + \text{H}$] $^+$, calculated: 447,1556, found: 447.1563. **Elemental anal.** calculated for $\text{C}_{25}\text{H}_{22}\text{N}_2\text{O}_6$: C, 67.3; H, 5.0; N, 6.3. Found: C, 67.5; H, 5.3; N, 6.0. $[\alpha]_D^{23}$ = 24.80 (c 1.09, CH_2Cl_2), 85 % ee. **HPLC**: Daicel

CYCLOADDITION REACTIONS

Chiralpak OD-H column, *iso*-Propanol/*n*-hexane 10:90, flow = 1.0 mL/min, $t_{r\text{major}} = 26.8$ min (1*S*, 3*S*, 3*aS*, 4*R*, 9*bR*), $t_{r\text{min}} = 35.6$ min (1*R*, 3*R*, 3*aR*, 4*S*, 9*bS*), 230 nm.

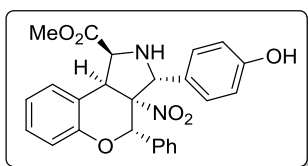


	RT	Area	% Area	Height
1	29.454	121371953	51.21	991431
2	37.086	115616725	48.79	757284

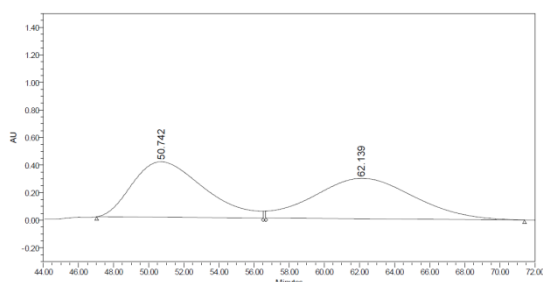


	RT	Area	% Area	Height
1	26.789	186450892	92.47	1259213
2	35.635	15182594	7.53	86793

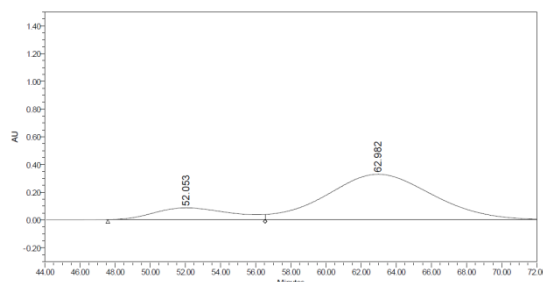
*Methyl (1*S*, 3*R*, 3*aR*, 4*S*, 9*bS*)-3-(4-hydroxyphenyl)-3*a*-nitro-4-phenyl-benzopyrano[3,4-*c*]-pyrrolidine-1-carboxylate (130'f)*



22 mg of a white solid obtained (starting from 60 mg, 0.310 mmol of corresponding imine **88f**), yield = 16 %. EtOAc/*n*-hexane 20:80, R_f 0.19 (33:66). $^1\text{H NMR}$ (400 MHz, CDCl_3) δ (ppm) = 7.28 – 7.20 (m, 6H), 7.11 (t, $J = 7.9$ Hz, 3H), 6.98 – 6.92 (m, 1H), 6.79 (d, $J = 8.1$ Hz, 1H), 6.73 (d, $J = 8.1$ Hz, 2H), 5.64 (s, 1H), 5.33 (s, 1H), 5.04 (d, $J = 9.5$ Hz, 1H), 4.97 (d, $J = 9.8$ Hz, 1H), 3.33 (s, 3H). $^{13}\text{C NMR}$ (101 MHz, CDCl_3) δ (ppm) = 173.5, 156.6, 152.6, 134.9, 129.8, 129.0, 128.8, 128.5, 128.4, 128.3, 122.1, 120.9, 118.3, 115.8, 98.0, 77.5, 68.6, 64.4, 51.9, 45.3. FT-IR (neat) = 3570-3223 (broad), 3349, 3032, 2950, 1730, 1613, 1587, 1539, 1515, 1488, 1454, 1210, 758, 733, 698 cm^{-1} . $[\alpha]_D^{22} = +1.11$ (c 1.06 CH_2Cl_2), 68 % ee. HPLC: Daicel Chiralpak OD-H column, *iso*-Propanol/*n*-hexane 10:90, flow = 1.0 mL/min, $t_{r\text{min}} = 52.0$ min (1*S*, 3*S*, 3*aS*, 4*R*, 9*bR*), $t_{r\text{major}} = 63.0$ min (1*R*, 3*R*, 3*aR*, 4*S*, 9*bS*), 230 nm.



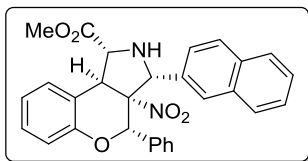
	RT	Area	% Area	Height
1	50.742	113974969	49.47	402621
2	62.139	116412902	50.53	294043



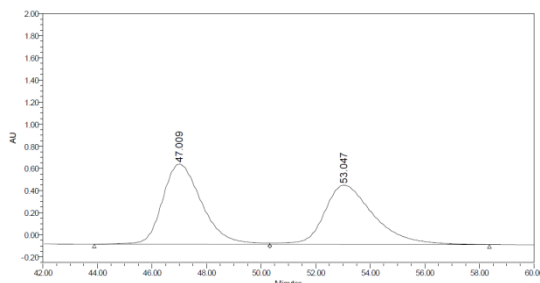
	RT	Area	% Area	Height
1	52.053	25629015	15.81	84654
2	62.982	136452417	84.19	326769

CHAPTER 2

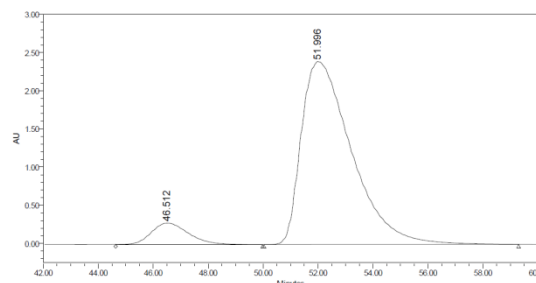
Methyl (1*R*, 3*R*, 3*aR*, 4*S*, 9*bS*)-3-(2-naphtyl)-3*a*-nitro-4-phenyl-benzopyrano[3,4-*c*]-pyrrolidine-1-carboxylate (**130g**)



34 mg of a white solid obtained (starting from 60 mg, 0.260 mmol of corresponding imine **88g**), yield = 27 %. EtOAc/*n*-hexane 20:80, *R_f*: 0.37. ¹H NMR (400 MHz, CDCl₃) δ (ppm) = 7.99 – 7.82 (m, 4H), 7.62 – 7.43 (m, 4H), 7.24 – 7.13 (m, 5H), 7.10 (td, *J* = 7.4, 1.3 Hz, 1H), 6.87 (dd, *J* = 8.1, 1.2 Hz, 1H), 5.66 (s, 1H), 5.23 – 5.09 (m, 1H), 4.85 (d, *J* = 3.4 Hz, 1H), 4.21 (s, 1H), 4.05 (s, 3H), 3.24 (s, 1H). ¹³C NMR (101 MHz, CDCl₃) δ (ppm) = 172.6, 150.1, 135.2, 134.1, 133.4, 131.4, 129.1, 129.1, 129.0, 129.0, 128.6, 128.4, 128.4, 127.9, 127.1, 126.8, 126.7, 125.2, 123.9, 123.4, 118.5, 96.7, 75.8, 70.7, 68.7, 53.2, 46.1. FT-IR (neat) = 3346, 3033, 2951, 1739, 1586, 1541, 1488, 1454, 1435, 1357, 756, 697 cm⁻¹. HRMS (ESI/Q-TOF) *m/z*: C₂₉H₂₅N₂O₅ [*M* + *H*]⁺, calculated: 481.1763, found: 481.1763. Elemental anal. calculated for C₂₉H₂₄N₂O₅: C, 72.5; H, 5.0; N, 5.8. Found: C, 72.8; H, 4.9; N, 6.0. [α]_D²³ = +31.78 (*c* 0.95, CH₂Cl₂), 84 % ee. HPLC: Daicel Chiralpak IC column, *iso*-Propanol/*n*-hexane 5:95, flow = 1.0 mL/min, *tr*_{min} = 46.5 min (1*S*, 3*S*, 3*aS*, 4*R*, 9*bR*), *tr*_{major} = 52.0 min (1*R*, 3*R*, 3*aR*, 4*S*, 9*bS*), 230 nm.

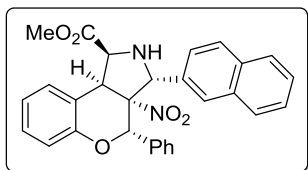


	RT	Area	% Area	Height
1	47.009	72238053	51.79	724146
2	53.047	67237142	48.21	535360



	RT	Area	% Area	Height
1	46.512	26524168	8.01	282078
2	51.996	304766818	91.99	2396749

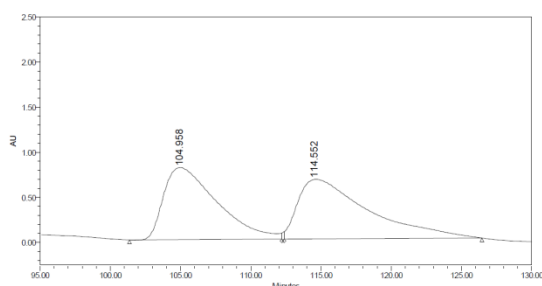
Methyl (1*S*, 3*R*, 3*aR*, 4*S*, 9*bS*)-3-(2-naphtyl)-3*a*-nitro-4-phenyl-benzopyrano[3,4-*c*]-pyrrolidine-1-carboxylate (**130'g**)



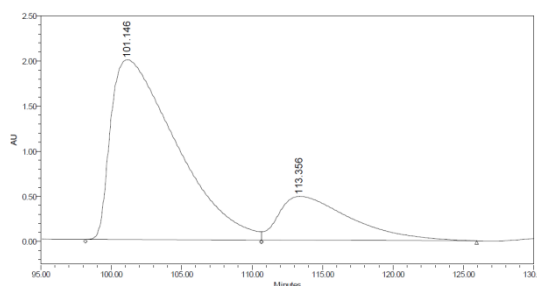
40 mg of a white solid obtained (starting from 60 mg, 0.260 mmol of corresponding imine **88g**), yield = 32 %. EtOAc/*n*-hexane 20:80, *R_f*: 0.35. ¹H NMR (400 MHz, CDCl₃) δ (ppm) = 7.89 – 7.73 (m, 4H), 7.53 – 7.46 (m, 2H), 7.40 – 7.24 (m, 7H), 7.13 (ddd, *J* = 8.7, 7.5, 1.7 Hz, 1H), 6.98 (td, *J* = 7.5, 1.3 Hz, 1H), 6.85 (dd, *J* =

CYCLOADDITION REACTIONS

8.2, 1.2 Hz, 1H), 5.75 (s, 1H), 5.57 (s, 1H), 5.13 (d, $J = 9.6$ Hz, 1H), 5.08 (d, $J = 9.5$ Hz, 1H), 3.39 (s, 3H), 2.88 (s, 1H). ^{13}C NMR (101 MHz, CDCl_3) δ (ppm) = 173.5, 152.7, 134.9, 134.3, 133.7, 133.2, 129.9, 129.1, 129.0, 128.9, 128.6, 128.4, 128.3, 127.8, 127.3, 126.6, 126.5, 124.7, 122.1, 120.7, 118.3, 98.0, 77.7, 68.8, 64.5, 51.9, 45.4. **FT-IR** (neat) = 3341, 2949, 1732, 1541, 1488, 1434, 1355, 861, 804, 754, 699 cm^{-1} . $[\alpha]_D^{22} = -13.87$ (c 0.60, CH_2Cl_2), 58 % ee. **HPLC**: Daicel Chiralpak OD-H column, *iso*-Propanol/*n*-hexane 5:95, flow = 0.7 mL/min, $\text{tr}_{\text{major}} = 101.1$ min (1*R*, 3*S*, 3*aS*, 4*R*, 9*bR*), $\text{tr}_{\text{min}} = 113.3$ min (1*S*, 3*R*, 3*aR*, 4*S*, 9*bS*), 230 nm.

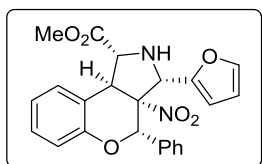


	RT	Area	% Area	Height
1	104.958	211283209	47.86	798314
2	114.552	230133316	52.14	660832



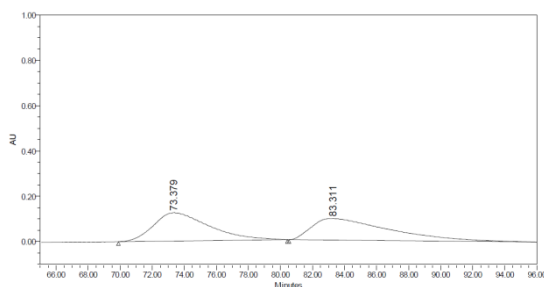
	RT	Area	% Area	Height
1	101.146	645240179	78.97	1992265
2	113.356	171796693	21.03	485345

*Methyl (1*R*, 3*R*, 3*aR*, 4*S*, 9*bS*)-3-(2-furyl)-3*a*-nitro-4-phenyl-benzopyrano[3,4-*c*]pyrrolidine-1-carboxylate (130h)*

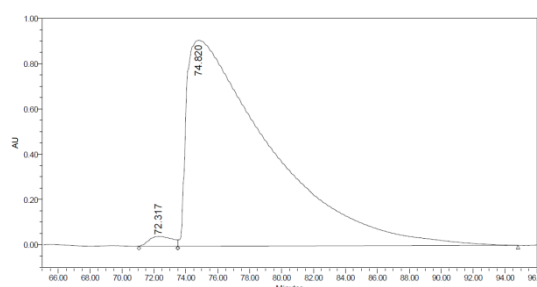


32 mg of a white solid obtained (starting from 60 mg, 0.359 mmol of corresponding imine **88h**), yield = 21%. EtOAc/*n*-hexane 20:80, R_f 0.24. ^1H NMR (400 MHz, CDCl_3) δ (ppm) = 7.63 (d, $J = 7.7$ Hz, 1H), 7.33 (d, $J = 22.0$ Hz, 7H), 7.18 (t, $J = 7.7$ Hz, 1H), 7.08 (t, $J = 7.5$ Hz, 1H), 6.88 (d, $J = 8.1$ Hz, 1H), 6.35 (s, 2H), 5.67 (s, 1H), 4.87 (s, 1H), 4.82 (d, $J = 4.7$ Hz, 1H), 4.12 (d, $J = 4.6$ Hz, 1H), 3.94 (s, 3H), 3.15 (s, 1H). ^{13}C NMR (101 MHz, CDCl_3) δ (ppm) = 172.9, 151.7, 149.2, 143.3, 143.2, 134.9, 129.3, 129.3, 128.8, 128.6, 128.1, 124.1, 123.2, 118.0, 110.8, 109.3, 95.3, 77.2, 68.1, 62.7, 53.3, 45.0. **FT-IR** (neat) = 3346, 3321, 2970, 2951, 1738, 1586, 1543, 1436, 1364, 756, 699 cm^{-1} . **HRMS (ESI/Q-TOF) m/z** : $\text{C}_{23}\text{H}_{21}\text{N}_2\text{O}_6$ $[\text{M} + \text{H}]^+$, calculated: 420.1400, found: 420.1406. **Elemental anal.** calculated for $\text{C}_{23}\text{H}_{20}\text{N}_2\text{O}_6$: C, 65.7; H, 4.8; N, 6.7. Found: C, 63.5; H, 6.73; N, 5.43. $[\alpha]_D^{22} = +6.11$ (c 1.53, CH_2Cl_2), 97% ee. **HPLC**: Daicel Chiralpak IB column, *iso*-Propanol/*n*-hexane 1:99, flow = 0.7 mL/min, $\text{tr}_{\text{min}} = 72.3$ min (1*S*, 3*S*, 3*aS*, 4*R*, 9*bR*), $\text{tr}_{\text{major}} = 74.8$ min (1*R*, 3*R*, 3*aR*, 4*S*, 9*bS*), 230 nm.

CHAPTER 2

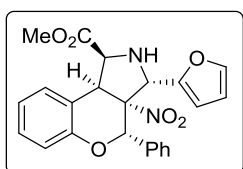


	RT	Area	% Area	Height
1	73.379	30103703	48.28	125713
2	83.311	32243343	51.72	96105

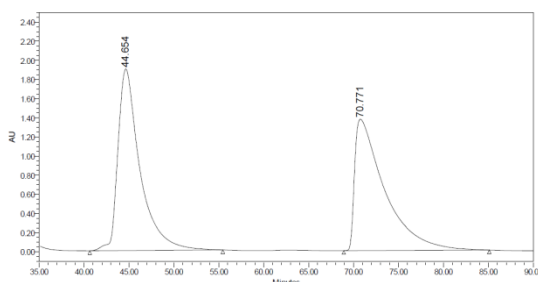


	RT	Area	% Area	Height
1	72.317	4426882	1.32	43363
2	74.820	329966497	98.68	910214

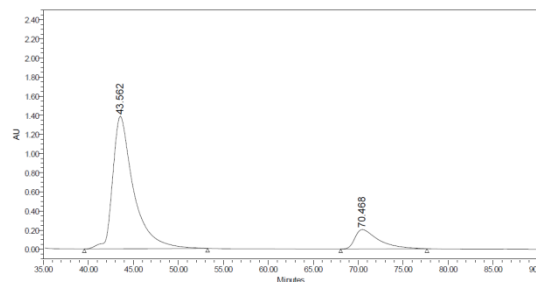
Methyl (1S, 3R, 3aR, 4S, 9bS)-3-(2-furyl)-3a-nitro-4-phenyl-benzopyrano[3,4-c]-pyrrolidine-1-carboxylate (130'h).



41 mg of a white solid obtained (starting from 60 mg, 0.359 mmol of corresponding imine **88h**), yield = 27 %. EtOAc/*n*-hexane 20:80, *R_f*: 0.16. ¹H NMR (400 MHz, CDCl₃) δ (ppm) = 7.39 (s, 6H), 7.25 (d, *J* = 6.8 Hz, 2H), 7.16 (t, *J* = 7.9 Hz, 1H), 6.98 (t, *J* = 7.5 Hz, 1H), 6.89 (d, *J* = 8.1 Hz, 1H), 6.29 (s, 1H), 6.21 (d, *J* = 3.3 Hz, 1H), 5.89 (s, 1H), 5.04 (s, 1H), 5.00 (d, *J* = 10.9 Hz, 1H), 4.95 (d, *J* = 10.9 Hz, 1H), 3.36 (s, 3H), 2.79 (s, 1H). ¹³C NMR (101 MHz, CDCl₃) δ (ppm) = 172.7, 153.6, 151.1, 143.0, 134.7, 130.1, 129.5, 128.8, 128.5, 128.0, 121.7, 117.6, 110.8, 109.5, 94.9, 77.7, 64.0, 61.2, 52.0, 44.3. FT-IR (neat) = 3467, 3346, 3311, 2970, 2950, 1739, 1542, 1455, 1435, 1365, 756, 670 cm⁻¹. [α]_D²² = +12.8 (*c* 2.05, CH₂Cl₂), 71 % ee. HPLC: Daicel Chiralpak IA column, *iso*-Propanol/*n*-hexane 5:95, flow = 1 mL/min, *tr*_{min} = 43.6 min (1*R*, 3*S*, 3*aS*, 4*R*, 9*bR*), *tr*_{major} = 70.5 min (1*S*, 3*R*, 3*aR*, 4*S*, 9*bS*), 230 and 273 nm.



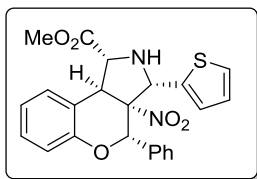
	RT	Area	% Area	Height
1	44.654	323798834	50.50	1897198
2	70.771	317430360	49.50	1371682



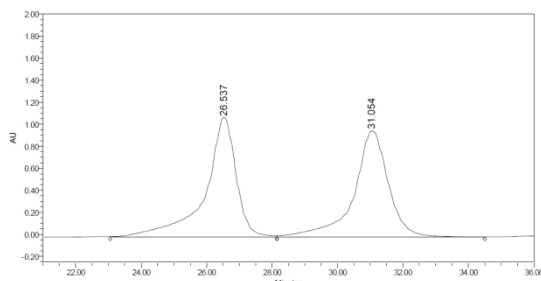
	RT	Area	% Area	Height
1	43.562	222901942	85.81	1383899
2	70.468	36870541	14.19	201742

CYCLOADDITION REACTIONS

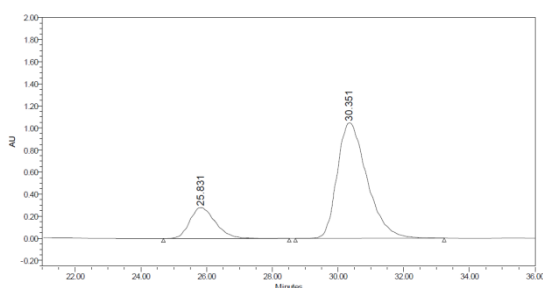
Methyl (1R, 3R, 3aR, 4S, 9bS)-3a-nitro-4-phenyl-3-(2-thiophenyl)-benzopyrano[3,4-c]-pyrrolidine-1-carboxylate (130i)



30 mg of a white solid obtained (starting from 60 mg, 0.328 mmol of corresponding imine **88i**), yield = 21 %. EtOAc/*n*-hexane 17:83, *R_f*: 0.31. ¹H NMR (400 MHz, CDCl₃) δ (ppm) = 7.56 (d, *J* = 7.6 Hz, 1H), 7.34 (d, *J* = 5.1 Hz, 1H), 7.21 (d, *J* = 3.4 Hz, 4H), 7.14 (d, *J* = 5.0 Hz, 2H), 7.07 (d, *J* = 6.1 Hz, 2H), 6.83 (d, *J* = 8.1 Hz, 1H), 5.70 (s, 1H), 5.21 (s, 1H), 4.82 (d, *J* = 4.3 Hz, 1H), 4.13 (d, *J* = 4.3 Hz, 1H), 4.00 (s, 3H). ¹³C NMR (101 MHz, CDCl₃) δ (ppm) = 172.4, 150.5, 137.1, 135.1, 129.1, 129.1, 129.0, 128.6, 128.4, 127.6, 126.2, 125.9, 124.8, 123.4, 118.4, 96.4, 76.3, 68.4, 66.1, 53.2, 45.7. FT-IR (neat) = 3350, 3065, 3032, 2951, 1737, 1586, 1542, 1488, 1453, 1435, 1356, 758, 698 cm⁻¹. HRMS (ESI/Q-TOF) *m/z*: C₂₃H₂₁N₂O₅S [M + H]⁺, calculated: 437.1171, found: 437.1177. Elemental anal. calculated for C₂₃H₂₀N₂O₅S: C, 72.5; H, 5.0; N, 5.8. Found: C, 72.8; H, 4.9; N, 6.0. [α]_D²¹ = +99.28 (*c* 1.72, CH₂Cl₂), 63 % ee. HPLC: Daicel Chiralpak IC column, *iso*-Propanol/*n*-hexane 10:90, flow = 1.0 mL/min, tr_{min} = 25.8 min (1*S*, 3*S*, 3a*S*, 4*R*, 9b*R*), tr_{major} = 30.3 min (1*R*, 3*R*, 3a*R*, 4*S*, 9b*S*), 230 nm.

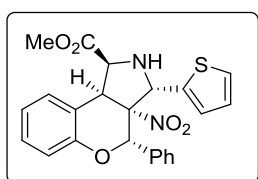


	RT	Area	% Area	Height
1	26.537	71539027	50.32	1083336
2	31.054	70634681	49.68	963043



	RT	Area	% Area	Height
1	25.831	15180178	18.72	280188
2	30.351	65900306	81.28	1045555

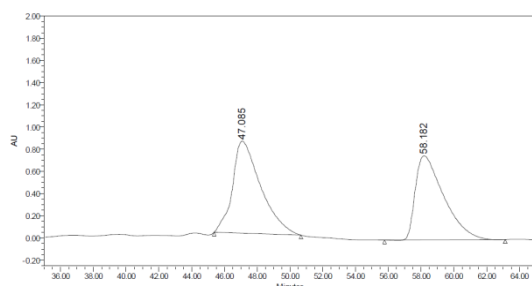
Methyl (1S, 3R, 3aR, 4S, 9bS)-3a-nitro-4-phenyl-3-(2-thiophenyl)-benzopyrano[3,4-c]-pyrrolidine-1-carboxylate (130'i)



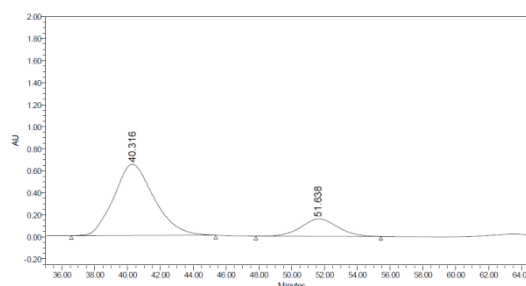
38 mg of a white solid obtained (starting from 60 mg, 0.328 mmol of corresponding imine **88i**), yield = 26 %. EtOAc/*n*-hexane 17:83, *R_f*: 0.38 (20:80). ¹H NMR (400 MHz, CDCl₃) δ (ppm) = 7.37 (s, 5H), 7.25 (d, *J* = 5.4 Hz, 3H), 7.14 (t, *J* = 7.8 Hz,

CHAPTER 2

¹H), 7.01 – 6.91 (m, 2H), 6.87 (t, *J* = 6.8 Hz, 2H), 5.80 (s, 1H), 5.47 (s, 1H), 4.99 (d, *J* = 10.6 Hz, 1H), 4.95 (d, *J* = 10.2 Hz, 1H), 3.37 (s, 3H), 2.90 (s, 1H). ¹³C NMR (101 MHz, CDCl₃) δ (ppm) = 173.1, 153.4, 140.6, 134.8, 130.2, 129.3, 128.9, 128.4, 128.3, 127.4, 126.8, 125.9, 121.9, 119.5, 117.9, 96.6, 77.9, 63.7, 63.6, 52.0, 44.2. FT-IR (neat) = 3017, 2970, 2948, 1738, 1586, 1543, 1487, 1450, 1435, 1365, 756, 701 cm⁻¹. [α]_D²² = +11.92 (*c* 1.23, CH₂Cl₂), 64 % ee. HPLC: Daicel Chiralpak OD-H column, *iso*-Propanol/*n*-hexane 5:95, flow = 1.0 mL/min, *tr*_{major} = 40.3 min (1*R*, 3*S*, 3*aS*, 4*R*, 9*bR*), *tr*_{min} = 51.6 min (1*S*, 3*R*, 3*aR*, 4*S*, 9*bS*), 230 nm.

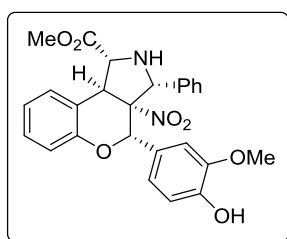


	RT	Area	% Area	Height
1	47.085	99634604	52.21	828601
2	58.182	91196308	47.79	757072



	RT	Area	% Area	Height
1	40.316	109786834	81.77	646213
2	51.638	24471559	18.23	158672

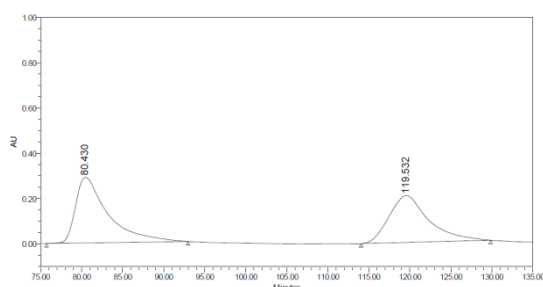
*Methyl (1*R*, 3*R*, 3*aR*, 4*S*, 9*bS*)-4-(4-hydroxy-3-methoxyphenyl)-3*a*-nitro-3-phenyl-benzopyrano[3,4-*c*]-pyrrolidine-1-carboxylate (130j)*



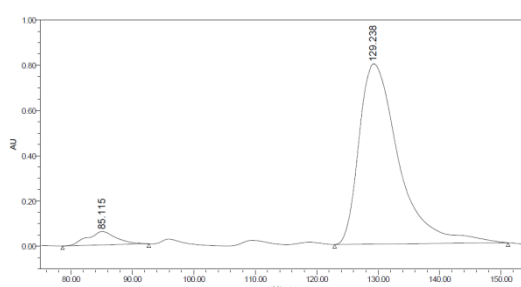
24 mg of a white solid obtained (starting from 60 mg, 0.340 mmol of corresponding imine **88a**), yield = 15 %. EtOAc/*n*-hexane 33:66, *R*_f: 0.26. ¹H NMR (400 MHz, CDCl₃) δ (ppm) = 7.55 (d, *J* = 7.6 Hz, 1H), 7.46 – 7.42 (m, 4H), 7.40 – 7.36 (m, 3H), 7.17 (t, *J* = 7.7 Hz, 1H), 7.07 (t, *J* = 7.4 Hz, 1H), 6.84 (d, *J* = 8.1 Hz, 1H), 6.69 (d, *J* = 2.1 Hz, 1H), 6.64 (d, *J* = 8.3 Hz, 1H), 6.58 (dd, *J* = 8.3, 2.1 Hz, 1H), 5.57 (s, 1H), 5.49 (s, 1H), 4.95 (s, 1H), 4.75 (d, *J* = 3.8 Hz, 1H), 4.14 (s, 1H), 4.02 (s, 3H), 3.72 (s, 3H), 3.11 (s, 1H). ¹³C NMR (101 MHz, CDCl₃) δ (ppm) = 172.6, 150.2, 146.5, 146.3, 134.2, 129.7, 129.1, 129.1, 128.9, 127.1, 125.3, 123.4, 121.0, 118.5, 114.2, 111.9, 97.1, 75.7, 70.5, 68.6, 56.0, 53.2, 46.1. FT-IR (neat) = 3446, 3333, 3006, 2953, 1734, 1584, 1538, 1486, 1455, 1434, 1368, 763, 750, 696, 655 cm⁻¹. HRMS (ESI/Q-TOF) *m/z*: C₂₆H₂₅N₂O₇ [*M* + *H*]⁺, calculated: 477.1662, found: 477.1665. Elemental anal. calculated for C₂₆H₂₄N₂O₇: C, 65.5; H, 5.0; N, 5.9. Found: C, 64.0; H, 4.9; N, 5.9. [α]_D²² = +37 (*c* 1.20, CH₂Cl₂), 90 % ee. HPLC: Daicel Chiralpak IA column,

CYCLOADDITION REACTIONS

iso-Propanol/*n*-hexane 5:9, flow = 1 mL/min, $t_{r_{min}}$ = 85.1 min (1*R*, 3*S*, 3*aS*, 4*R*, 9*bR*), $t_{r_{major}}$ = 129.2 min (1*S*, 3*R*, 3*aR*, 4*S*, 9*bS*), 230 and 273 nm.

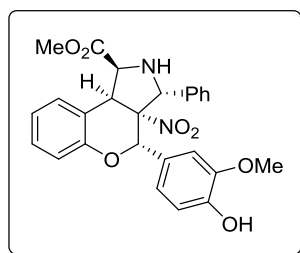


	RT	Area	% Area	Height
1	80.430	79808930	53.52	290013
2	119.532	69307565	46.48	207457



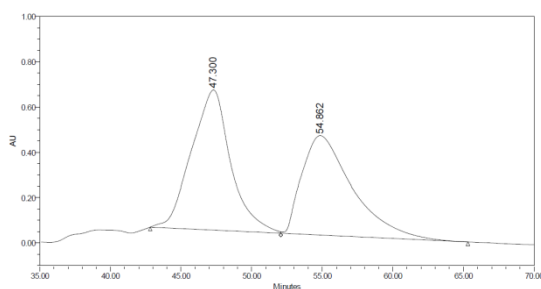
	RT	Area	% Area	Height
1	85.115	19245673	5.10	59419
2	129.238	358316552	94.90	797804

*Methyl (1*S*, 3*R*, 3*aR*, 4*S*, 9*bS*)-4-(4-hydroxy-3-methoxyphenyl)-3*a*-nitro-3-phenyl-benzopyrano[3,4-*c*]-pyrrolidine-1-carboxylate (130'j)*

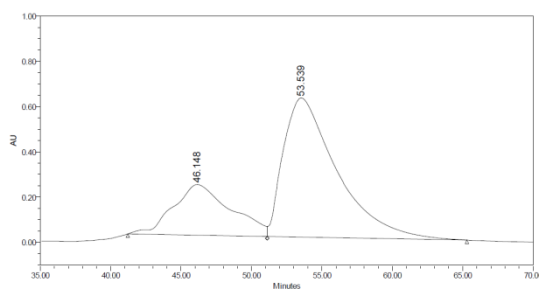


30 mg of a white solid obtained (starting from 60 mg, 0.340 mmol of corresponding imine **88a**), yield = 18 %. EtOAc/*n*-hexane 33:66, R_f : 0.22. $^1\text{H NMR}$ (400 MHz, CDCl_3) δ (ppm) = 7.55 (d, J = 7.6 Hz, 1H), 7.43 (s, 4H), 7.38 (s, 3H), 7.17 (t, J = 7.6 Hz, 1H), 7.08 (t, J = 7.4 Hz, 1H), 6.84 (d, J = 8.1 Hz, 1H), 6.69 (s, 1H), 6.64 (d, J = 8.2 Hz, 1H), 6.58 (d, J = 8.4 Hz, 1H), 5.54 (s, 1H), 5.48 (s, 1H), 4.95 (d, J = 10.7 Hz, 1H), 4.75 (d, J = 3.6 Hz, 1H), 4.15 (s, 1H), 4.02 (s, 3H), 3.73 (s, 3H), 3.10 (s, 1H). $^{13}\text{C NMR}$ (101 MHz, CDCl_3) δ (ppm) = 173.5, 152.8, 146.5, 146.4, 137.0, 129.8, 129.2, 129.0, 128.8, 127.6, 126.7, 122.1, 121.7, 120.8, 118.4, 113.8, 111.3, 98.1, 77.7, 68.7, 64.4, 56.1, 51.9, 45.3. **FT-IR** (neat) = 3446, 3333, 3006, 2953, 1738, 1604, 1586, 1541, 1489, 1455, 1435, 1366, 1354, 757, 700 cm^{-1} . $[\alpha]_D^{22}$ = +4.95 (c 0.80, CH_2Cl_2), 44 % ee. **HPLC**: Daicel Chiralpak IA column, *iso*-Propanol/*n*-hexane 10:90, flow = 1 mL/min, $t_{r_{min}}$ = 46.1 min (1*R*, 3*S*, 3*aS*, 4*R*, 9*bR*), $t_{r_{major}}$ = 53.5 min (1*S*, 3*R*, 3*aR*, 4*S*, 9*bS*), 230 and 273 nm.

CHAPTER 2

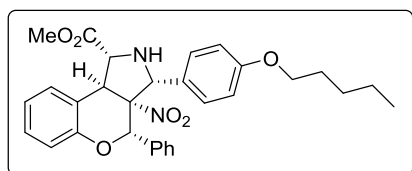


	RT	Area	% Area	Height
1	47.300	119554293	52.27	619008
2	54.862	109160943	47.73	439288



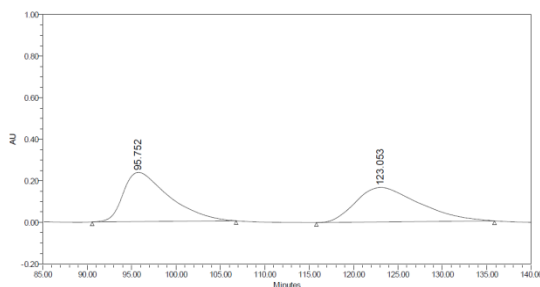
	RT	Area	% Area	Height
1	46.148	63606201	28.12	223760
2	53.539	162612623	71.88	614935

Methyl (1R, 3R, 3aR, 4S, 9bS)-3-(4-pentiloxypheyl)-3a-nitro-4-phenyl-benzopyrano[3,4-c]-pyrrolidine-1-carboxylate (130k)

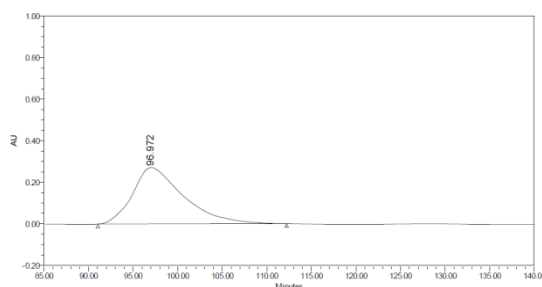


29 mg of a white solid obtained (starting from 60 mg, 0.240 mmol of corresponding imine **88j**), yield = 23 %. EtOAc/*n*-hexane 17:83, *R_f*: 0.25. ¹H NMR (400 MHz, CDCl₃) δ (ppm) = 7.58 – 7.54 (m, 1H), 7.28 (d, *J* = 8.5 Hz, 2H), 7.21 – 7.13 (m, 5H), 7.06 (td, *J* = 7.5, 1.2 Hz, 1H), 6.94 (d, *J* = 8.6 Hz, 2H), 6.81 (dd, *J* = 8.1, 1.3 Hz, 1H), 5.54 (s, 1H), 4.93 (d, *J* = 10.4 Hz, 1H), 4.77 (d, *J* = 3.5 Hz, 1H), 4.13 (s, 1H), 4.02 (s, 3H), 3.97 (t, *J* = 6.5 Hz, 2H), 1.85 – 1.76 (m, 2H), 1.50 – 1.35 (m, 4H), 0.94 (t, *J* = 7.0 Hz, 3H). ¹³C NMR (101 MHz, CDCl₃) δ (ppm) = 172.6, 160.3, 150.0, 135.3, 129.0, 128.9, 128.6, 128.4, 128.1, 125.5, 125.3, 123.3, 118.4, 115.0, 96.7, 75.7, 70.5, 68.7, 68.1, 53.2, 46.2, 29.1, 28.3, 22.6, 14.1. FT-IR (neat) = 3344, 3064, 3034, 2953, 2931, 2870, 1736, 1610, 1585, 1540, 1512, 1488, 1454, 1359, 1238, 820, 756, 696 cm⁻¹. HRMS (ESI/Q-TOF) *m/z*: C₃₀H₃₃N₂O₆ [M + H]⁺, calculated: 517.2332, found: 517.2334. Elemental anal. calculated for C₃₀H₃₂N₂O₆: C, 69.7; H, 6.2; N, 5.4. Found: C, 69.6; H, 6.4; N, 6.0. [α]_D²³ = +86.34 (*c* 0.94, CH₂Cl₂), >99 % ee. HPLC: Daicel Chiralpak OD-H column, *iso*-Propanol/*n*-hexane 2:98, flow = 0.7 mL/min, *tr*_{major} = 97.0 min (1*S*, 3*S*, 3*aS*, 4*R*, 9*bR*), *tr*_{min} = 128.9 min (1*R*, 3*R*, 3*aR*, 4*S*, 9*bS*), 230 nm.

CYCLOADDITION REACTIONS

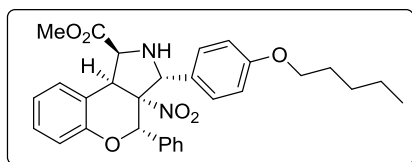


	RT	Area	% Area	Height
1	95.752	84711826	50.59	237178
2	123.053	82735059	49.41	166518

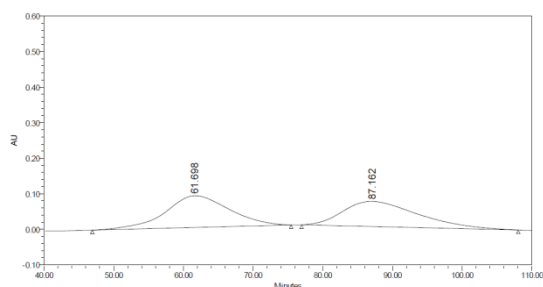


	RT	Area	% Area	Height
1	96.972	107661429	100.00	271429

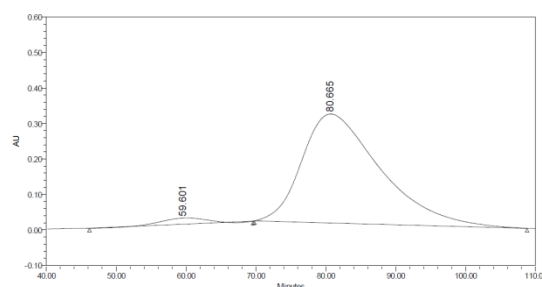
Methyl (1S, 3R, 3aR, 4S, 9bS)-3-(4-pentiloxypheyl)-3a-nitro-4-phenyl-benzopyrano[3,4-c]-pyrrolidine-1-carboxylate (130'k)



30 mg of a white solid obtained (starting from 60 mg, 0.240 mmol of corresponding imine **88j**), yield = 24 %. EtOAc/*n*-hexane 17:83, R_f : 0.18 (20:80). $^1\text{H NMR}$ (400 MHz, CDCl_3) δ (ppm) = 7.31 (s, 6H), 7.25 (d, J = 8.6 Hz, 2H), 7.17 – 7.12 (m, 1H), 7.00 (td, J = 7.5, 1.2 Hz, 1H), 6.91 – 6.87 (m, 2H), 6.85 (dd, J = 8.1, 1.2 Hz, 1H), 5.70 (s, 1H), 5.39 (s, 1H), 5.09 (d, J = 9.7 Hz, 1H), 5.03 (d, J = 9.8 Hz, 1H), 3.97 (t, J = 6.6 Hz, 2H), 3.39 (s, 3H), 1.81 (p, J = 6.7 Hz, 2H), 1.45 (ddd, J = 18.8, 9.0, 2.9 Hz, 4H), 0.97 (t, J = 7.0 Hz, 3H). $^{13}\text{C NMR}$ (101 MHz, CDCl_3) δ (ppm) = 173.4, 159.9, 152.6, 135.0, 129.8, 129.0, 128.6, 128.5, 128.3, 122.0, 121.0, 118.3, 114.7, 97.9, 77.5, 68.6, 68.1, 64.4, 51.8, 45.2, 29.1, 28.3, 22.5, 14.1. **FT-IR** (neat) = 3346, 2952, 2933, 1733, 1611, 1542, 1455, 1372, 757, 698 cm^{-1} . $[\alpha]_D^{23}$ = -4.36 (c 1.20, CH_2Cl_2), 93 % ee. **HPLC**: Daicel Chiralpak OJ-H column, *iso*-Propanol/*n*-hexane 15:85, flow = 1.0 mL/min, $t_{\text{r min}}$ = 59.6 min (1*S*, 3*S*, 3a*S*, 4*R*, 9b*R*), $t_{\text{r major}}$ = 80.7 min (1*R*, 3*R*, 3a*R*, 4*S*, 9b*S*), 230 nm.



	RT	Area	% Area	Height
1	61.698	56872013	51.72	89293
2	87.162	53099193	48.28	70746



	RT	Area	% Area	Height
1	59.601	8046848	3.25	17215
2	80.665	239602567	96.75	307172

CHAPTER 3

Total Synthesis of *Securinega* Alkaloids

Modern asymmetric catalysis consists principally of three basic pillars: biocatalysis, metal catalysis and organocatalysis. In Chapter 1 we described the main advantages and drawbacks of the three types of catalysis and we focused on ligands employed mainly in organometallic catalysis.

The asymmetric approach proposed for the synthesis of *Securinega* alkaloids requires a deeper explanation of the concept of organocatalysis and the possible activation modes.

3.1. Organocatalysis

This type of catalysis, using small organic molecules and where a metal is not part of the active center, has emerged strongly in the field of asymmetric synthesis as a useful tool in the construction of complex chiral structures.¹

List classified organocatalysts by their Lewis or Brønsted nature but nowadays is preferably to classify organocatalysts by their mechanistic pathway or activation mode. This classification is based on the interactions between the substrate and the organocatalyst. On one hand, these interactions can be non-covalent showing weak interactions such as hydrogen bonds or ionic pairs. On the other hand, some organocatalysts present strong interactions with the substrate, and therefore, the formation and cleavage of covalent bonds.

3.1.1 Covalent activation

Covalent activation involves the formation of new reversible covalent bonds between the catalyst and substrate to create an active substrate, followed by the chemical reaction *per se*, and lastly, the cleavage of the covalent bond to afford the product and release the catalyst. Organocatalysts employed in this type of activations are Lewis bases.

Aminocatalysis relies on the activation of a carbonyl compound (aldehyde or ketone) using a primary or secondary amine.² This activation can occur through two different manners: via enamine or iminium ion. Catalytic version of aminocatalysis has shown to generate reversible and transitory reactive species. Among others, proline based catalysts have emerged during the last decade due to the excellent results presented in different reactions with carbonyl compounds.³

¹ List, B., *Chem. Rev.* **2007**, 107, 10–12.

² Nielsen, M.; Worgull, D.; Zweifel, T.; Gschwend, B.; Bertelsen, S.; Jørgensen, K. A., *Chem. Commun.* **2011**, 47, 632–649.

³ List, B., *Acc. Chem. Res.* **2004**, 37, 548–557.

CHAPTER 3

3.1.1.1 Enamine catalysis

Enamine catalysis can be performed by primary or secondary chiral amines in presence of non-saturated carbonyls.^{3,4} Reversibility of the process allows this type of activation to create a catalytic cycle (**Fig. 3.1**). *L*-proline has recently emerged as important organocatalyst, showing excellent results in enantioselective reactions such as aldol-type reactions and Michael reactions with different ketones and aldehydes.

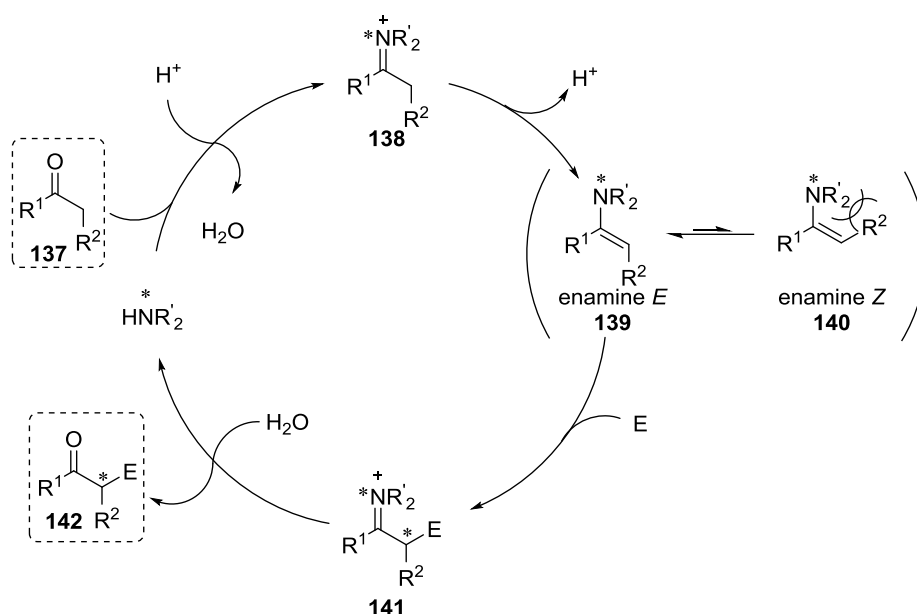


Figure 3.1. Catalytic cycle for the catalysis via enamine. Arrows are drawn in one direction for clarity, but all steps are reversible.

One of the most important aspects to reach high asymmetric induction is the conformation and configuration of the enamine during the transition state. The transition state of the *E* configuration is generally more stable than the *Z* one. In addition, *E*-enamine can present two possible conformations, *syn* and *anti*. The *anti*-enamine which presents the double bond oriented in the opposite direction of the bulky group in α position to the pyrrolidine nitrogen is more stable (**Fig. 3.2**).

⁴ Kano, T.; Maruoka, K., *Chem. Commun.* **2008**, 5465–5473.

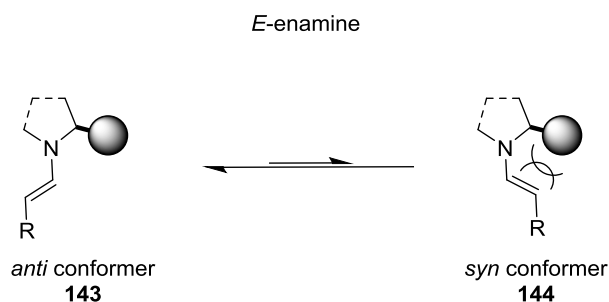


Figure 3.2. *anti* and *syn* conformers for *E*-enamine configuration.

Assuming that during the transition state of the reaction enamine participates mainly through the *anti-E* form, two different models can be distinguished related to the approximation of the electrophile (**Fig 3.3**). Generally, products obtained from the two different models present opposite configuration. Catalysts that contain a hydrogen donor group (as acids, sulfonamides...) in α to the nitrogen of the pyrrolidine they induce the attack from the *Re* face and simultaneously enamine activates the electrophile (**Fig 3.3**, 1). On the other hand, other organocatalysts determine the stereocontrol due to the steric blockage made by the bulky group in carbon α to the nitrogen. Consequently, attack occurs from *Si* face, controlled mainly by steric reasons (**Fig 3.3**, 2).⁵

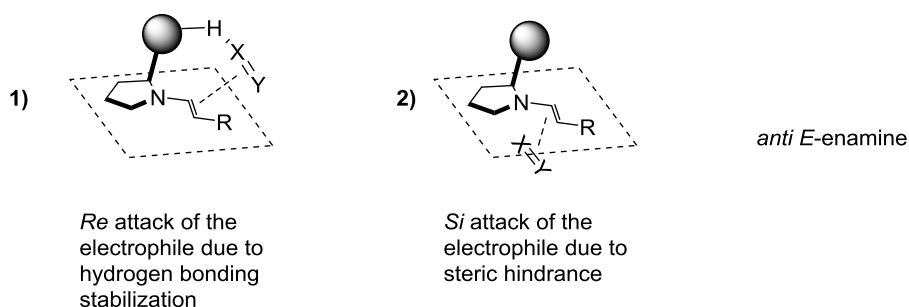


Figure 3.3. *Re* and *Si* attack of the electrophile depending on the organocatalyst type.

3.1.1.2 Catalysis via iminium ion

Iminium ion catalysis is based on the generation of a more electrophilic iminium intermediate formed when an amine reacts with α,β -unsaturated aldehydes or ketones.⁶ In this type of catalysis the presence of an acid as cocatalyst is typically required to afford the reversibility of the process.

⁵ Diner, P.; Kjærsgaard, A.; Lie, M. A.; Jørgensen, K. A., *Chem. Eur. J.* **2008**, *14*, 122–127.

⁶ a) Erkkilä, A.; Majander, I.; Pihko, P. M., *Chem. Rev.* **2007**, *107*, 5416–5470. b) Ahrendt, K. A.; Borths, C. J.; Macmillan, D. W. C., *J. Am. Chem. Soc.* **2000**, *122*, 4243–4244.

CHAPTER 3

Activation via iminium ion has demonstrated similarities with the activation of carbonyl compounds by Brønsted acid or bases. In both cases, the HOMO-LUMO energy gap is decreased, and this directs the reaction under orbital frontier control. As in the case of enamine catalysis, all steps are reversible.

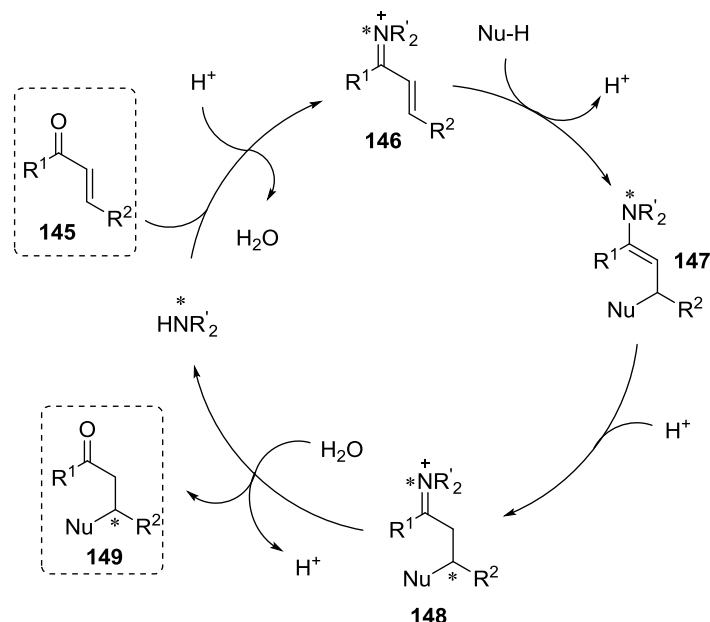


Figure 3.4. Catalytic cycle for activation via iminium ion. Arrows are drawn in one direction for clarity, but all steps are reversible.

In iminium ion catalysis, as well as for enamine catalysis, the conformation and configuration is a determinant factor in order to obtain a good stereocontrol. In this type of activation the *s-trans*-(*E*) conformer is the most stable.

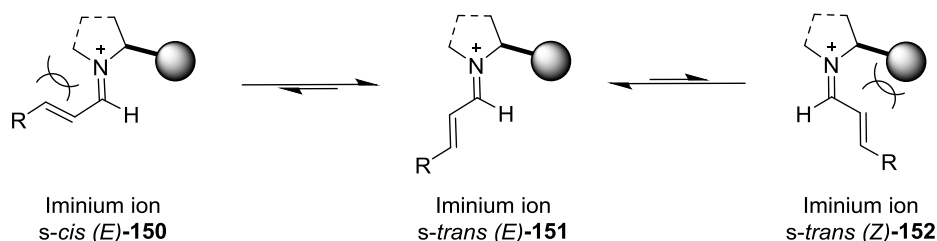


Figure 3.5. *anti* and *syn* conformers for *E*-enamine configuration.

3.1.2 Non-Covalent activation

Non-covalent activation in organocatalysis presents weak interactions between the catalyst and the substrate. Acid/base interactions are possible due to hydrogen bonds between the substrate and Brønsted acids such as, thioureas, phosphoric acids and guanidines.⁷

⁷ Akiyama, T.; Itoh, J.; Fuchibe, K., *Adv. Synth. Catal.* **2006**, 348, 999–1010.

3.1.2.1 Thiourea catalysts

Urea and thiourea compounds have been widely used for a long time for molecular recognition because of their strong hydrogen bonding nature. For the last two decades these compounds have emerged as excellent acid catalysts in asymmetric reactions. Jacobsen reported the first use of chiral urea derivatives in catalysis of different reactions with high enantiomeric excess.⁸

Takemoto and coworkers designed a bifunctional thiourea catalyst incorporating a tertiary amine on a chiral scaffold. The advantage of these thioureas is that they can activate both the electrophile and nucleophile (see **Fig. 3.6**). This type of catalysts showed excellent results for Michael additions, being afterwards efficiently used in a large variety of reaction types.

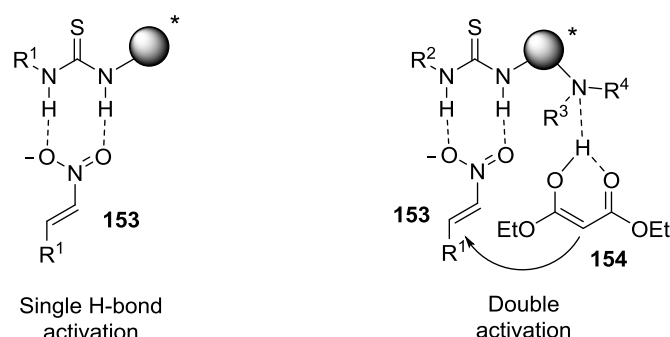


Figure 3.6. Monofunctional and bifunctional non-covalent activation of thiourea compounds.

3.1.2.2 Phosphoric acid catalysts

BINOL-derived chiral phosphoric acids, which include axial chirality, have emerged in the last years as highly efficient in a variety of organic reactions in an enantioselective manner. In this type of activation, hydrogen-bonding or ion pairing interactions are key factors in the control of the stereochemical outcome.

Computational studies suggested that this type of organocatalysts have two main sites which show hydrogen-bonding interactions between the substrate and the catalyst and are crucial for the achievement of high enantiomeric excess. These sites interact with both the electrophile and nucleophile, and thus, prompting the bifunctional nature of the catalyst. 3,3' substituents of the phosphoric acids play a key role in the elevated enantioselectivities induced.⁹

⁸ a) Okino, T.; Hoashi, Y.; Takemoto, Y., *J. Am. Chem. Soc.* **2003**, *125*, 12672–12673. b) Okino, T.; Yasutaka, H.; Furukawa, T.; Xu, X.; Takemoto, Y., *J. Am. Chem. Soc.* **2005**, *127*, 119–125.

⁹ a) Akiyama, T., *Chem. Rev.* **2007**, *107*, 5744–5758. b) Kanomata, K.; Toda, Y.; Shibata, Y.; Yamanaka, M.; Tsuzuki, S.; Gridnev, I. D.; Terada, M., *Chem. Sci.* **2014**, *5*, 3515–3523.

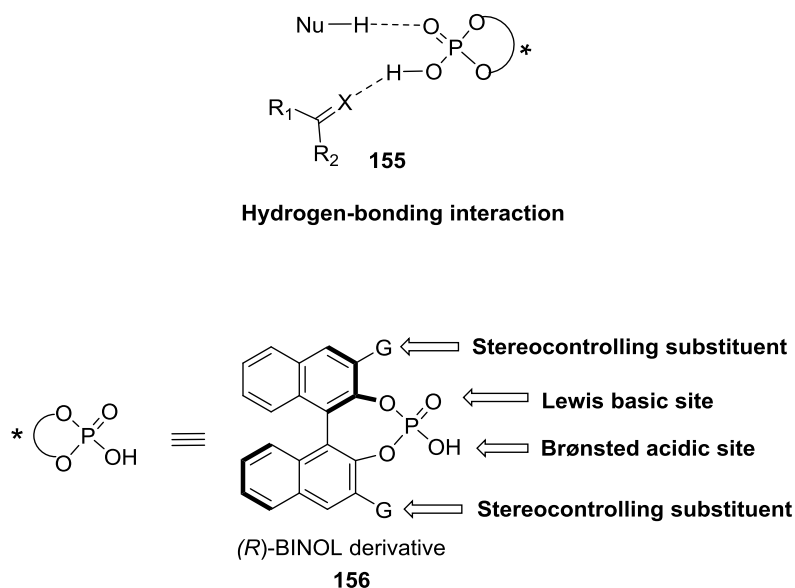


Figure 3.7. Representation of the bifunctional nature of chiral phosphoric acids by activation of the nucleophile and the electrophile.

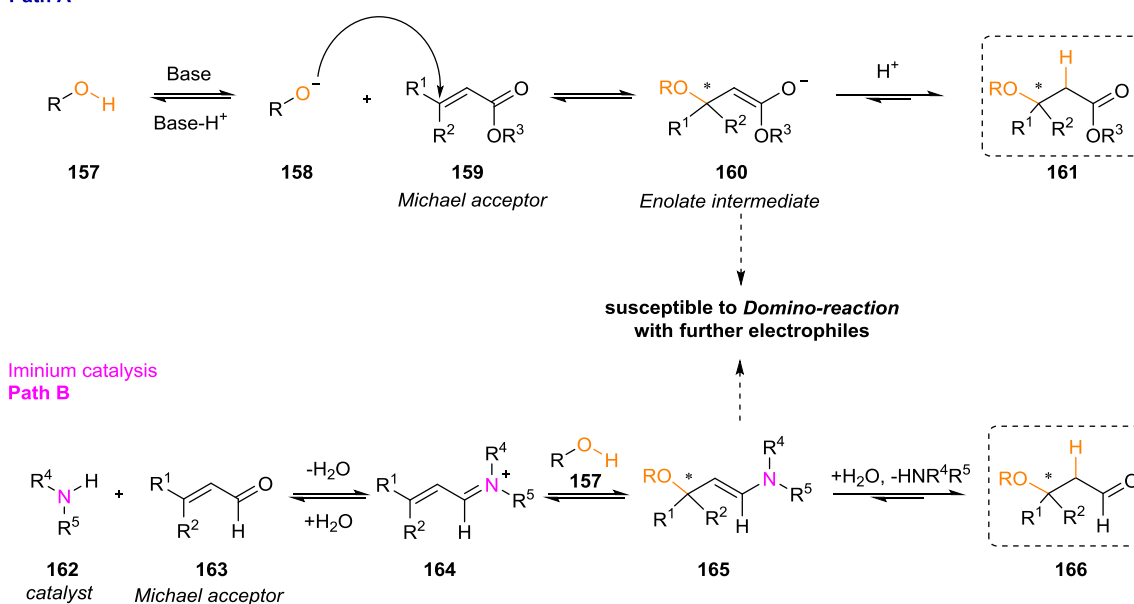
3.1.2 Enantioselective oxa-Michael reactions

Complex oxygenated molecules usually present a unique structure and broad range of biological activities. In view of that, C-O bond formation has inspired many attempts toward the chemical synthesis of mentioned compounds.¹⁰ Similar to C-C bond construction strategies, oxygen nucleophiles have been employed in additions to conjugate acceptors as one of the most efficient methodologies for C-O bond formation (**Scheme 3.1**). For example, when alcohols are employed as nucleophiles, reaction is called oxa-Michael addition. Actually, it was not until recently that hetero-Michael type additions have received significant attention from the synthetic community.¹¹

¹⁰ Hu, J.; Bian, M.; Ding, H., *Tetrahedron Lett.* **2016**, 57, 5519–5539.

¹¹ a) Nising, C. F.; Bräse, S., *Chem. Soc. Rev.* **2008**, 37, 1218–1228. b) Nising, C. F.; Bräse, S., *Chem. Soc. Rev.* **2012**, 41, 988–999.

Base Induced
Path A



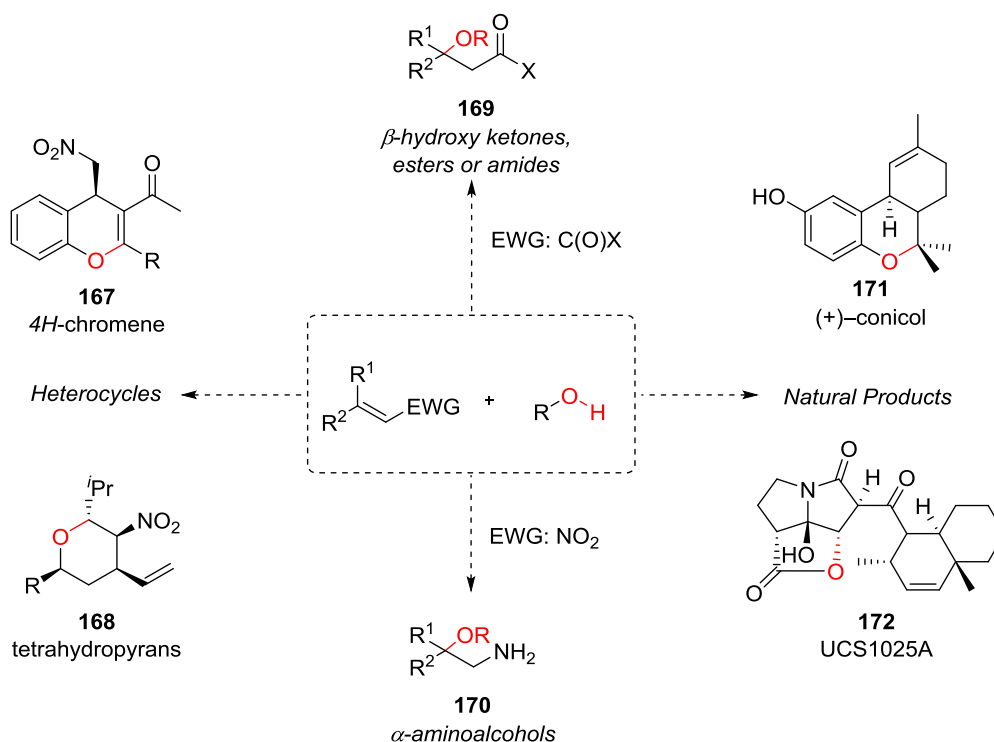
Scheme 3.1. Common oxa-Michael reaction pathways, base induced and iminium catalyzed.

Loydl discovered in 1878 the first oxa-Michael reaction, long before first Michael addition, in order to achieve the synthesis of malic acid. C-O bond reactions were not as interesting as conventional Michael or aldol reactions because they presented reversibility in the alcohol addition step, relatively poor nucleophilicity toward acceptor and sometimes lack of stereocontrol¹¹

During the last decades a significant enhancement on the reactivity and stereoselectivity of these reactions was reported. In fact, the enolates generated in oxa-Michael reactions are valuable intermediates that can react with other electrophiles to give rise to further *domino reactions* (**Scheme 3.1**). Several examples of oxa-Michael/organocascade reactions have been reported, usually giving an efficient access to oxygen containing heterocycles and natural products (**Scheme 3.2**).^{10,11,12} Moreover, β -hydroxyketones and α -aminoalcohols are found in a variety of natural products and are considered important synthetic intermediates. Organocatalysis have been widely employed for the development of efficient enantioselective oxa-Michael reactions.¹⁰

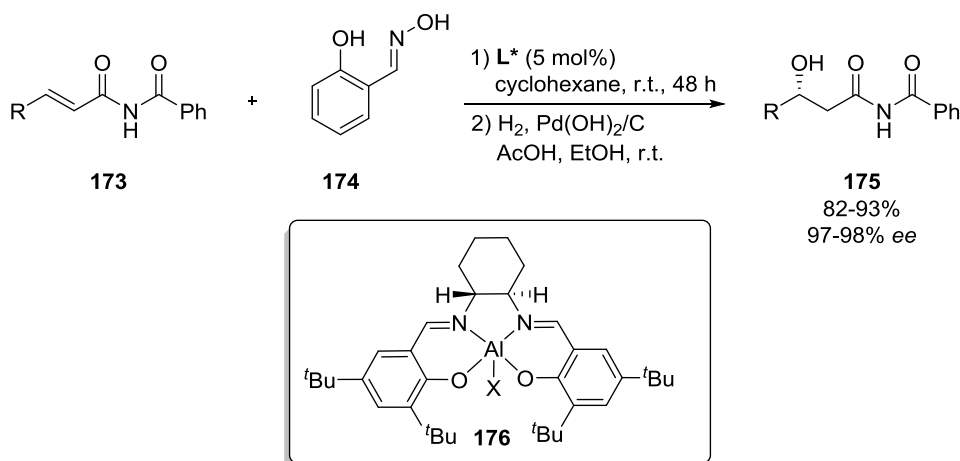
¹² a) Grondal, C.; Jeanty, M.; Enders, D., *Nat. Chem.* **2010**, 2, 167–178. b) Heravi, M. M.; Hajiabbasi, P., *Mol. Divers.* **2014**, 18, 411–439.

CHAPTER 3



Scheme 3.2. Wide scope of the oxa-Michael reaction.

Jacobsen and coworkers developed the first catalytic oxa-Michael reaction to obtain β -hydroxy carboxylic acid derivatives by addition of salicylaldoxime to α,β -unsaturated imides. Salen-Al complexes were employed as catalysts for a high enantioinduction in the conjugate addition (**Scheme 3.3**).¹³

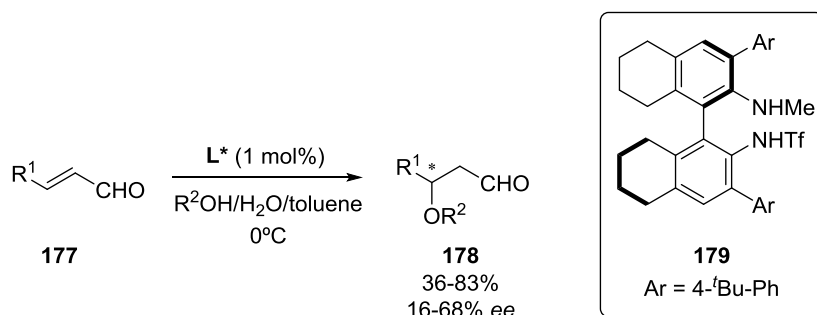


Scheme 3.3. Enantioselective oxa-Michael reaction catalyzed by Salen-Al **176**.¹³

Conjugated reaction between alcohols and α,β -unsaturated aldehydes remained a challenge due to the competitive acetal formation. β -hydroxy and β -alkoxy

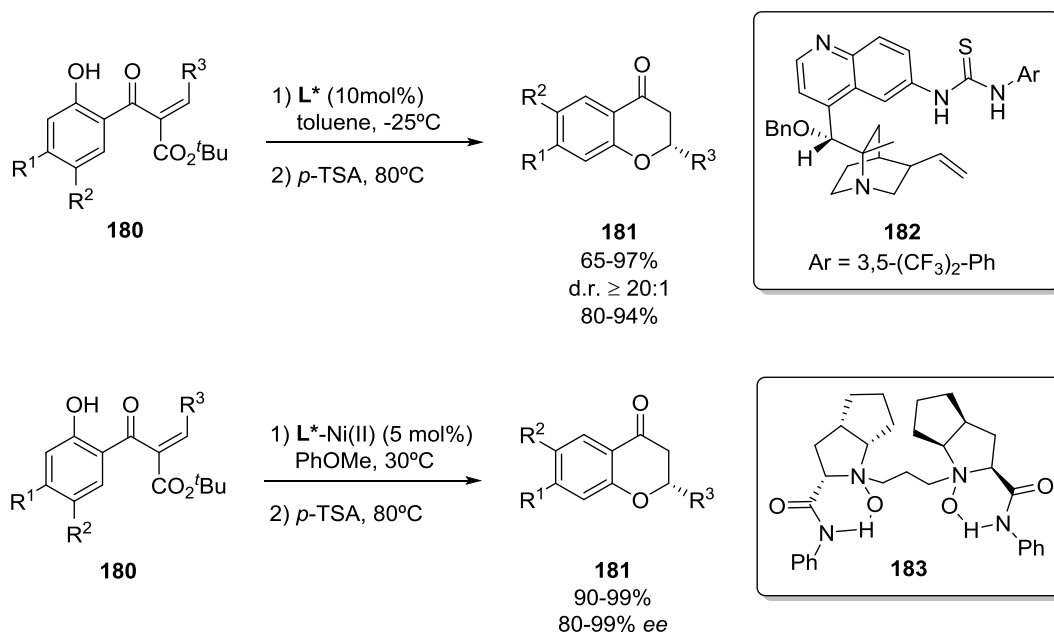
¹³ Vanderwal, C. D.; Jacobsen, E. N., *J. Am. Chem. Soc.* **2004**, 126, 14724–14725.

carbonyl compounds generated in this type of reactions are valuable building blocks and structural motifs. Biphenyl diamine **179** catalyzed oxa-Michael reactions gave rise to β -substituted aldehydes with moderate yields and moderate enantiomeric excess (**Scheme 3.4**).¹⁴



Scheme 3.4. Enantioselective oxa-Michael addition of alcohols to α,β -unsaturated aldehydes.¹⁴

Scheidt reported the use of a bifunctional quinine derived thiourea catalyst **182** which activates a β -ketoester alkylidene and promotes an intramolecular oxa-Michael addition of a phenol. In this way, enantioselective cyclization and decarboxylation afforded valuable flavanones and chromanones which are abundant features in natural products and they exhibit a wide array of biological activities.¹⁵ Similarly, ligand **183** in combination with Ni(II) catalyzed oxa-Michael reaction afforded a promising approach toward flavanones showing a broad substrate scope and excellent enantiocontrol.¹⁶



Scheme 3.5. Enantioselective intramolecular oxa-Michael addition with thiourea **182** and nickel(II)-**183**.^{15,16}

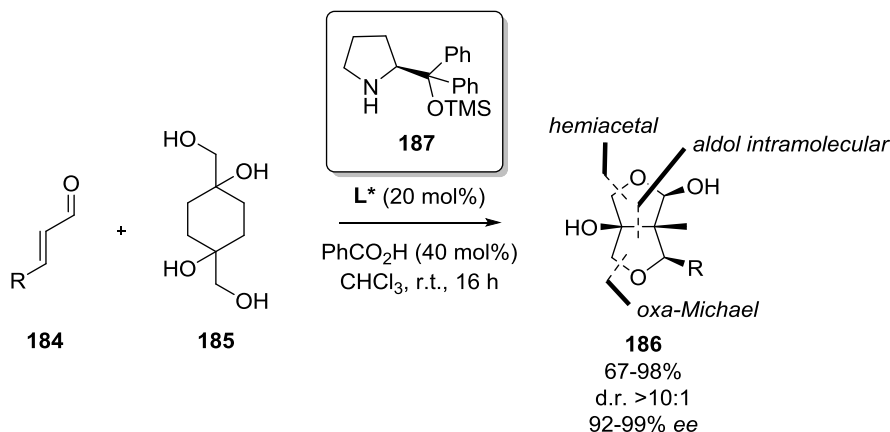
¹⁴ Kano, T.; Tanaka, Y.; Maruoka, K., *Tetrahedron* **2007**, 63, 8658–8664.

¹⁵ Biddle, M. M.; Lin, M.; Scheidt, K. A., *J. Am. Chem. Soc.* **2007**, 129, 3830–3831.

¹⁶ Wang, L.; Liu, X.; Dong, Z.; Fu, X.; Feng, X., *Angew. Chem., Int. Ed.* **2008**, 47, 8670–8673.

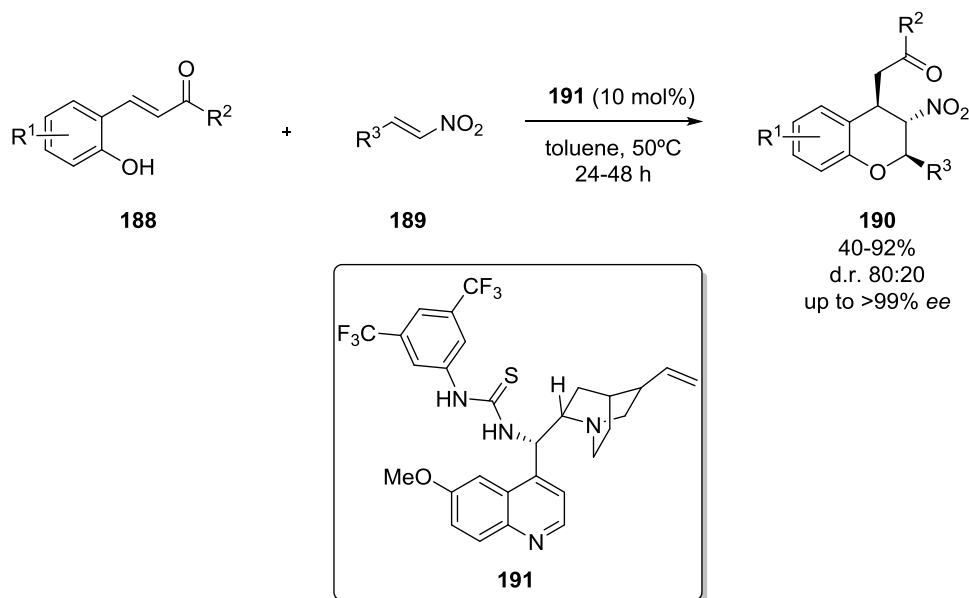
CHAPTER 3

Vicario published a domino oxa-Michael/aldol/hemiacetalization process employing prolinol organocatalyst **187** in order to obtain hexahydrofuro[3,4-*c*]furanes with excellent diastereo- and enantiocontrol (see **Scheme 3.6**). In the reaction, one C-C bond and two C-O bond are formed, and manipulation of functional groups allowed the production of a wide range of different chiral building blocks.¹⁷



Scheme 3.6. Enantioselective domino oxa-Michael/aldol/hemiacetalization catalyzed by prolinol **187**.¹⁷

Recently, description of the synthesis of polysubstituted chroman derivatives was described by a intermolecular cascade oxa-Michael/Michael reaction between *o*-hydroxy-substituted α,β -unsaturated ketones and *trans*-nitroalkenes using chiral bifunctional thiourea organocatalyst **191** with excellent enantioinduction¹⁸ (**Scheme 3.7**).

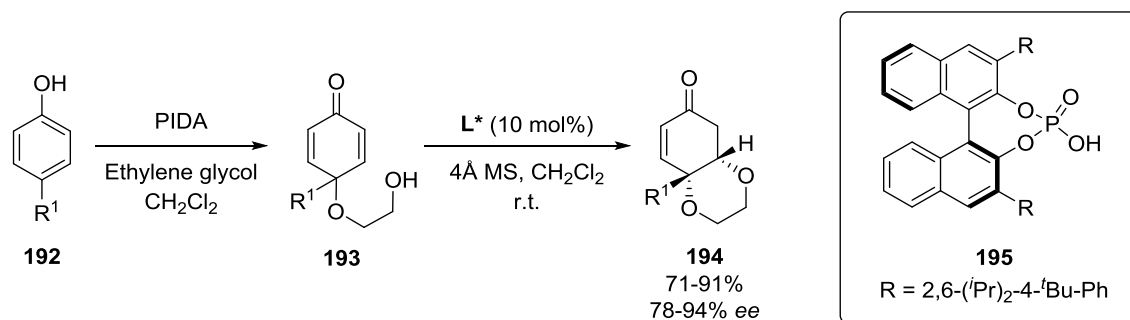


Scheme 3.7. Synthesis of chroman derivatives with excellent enantioinduction in tandem oxa-Michael/Michael reaction catalyzed by bifunctional thiourea **191**.¹⁸

¹⁷ Reyes, E.; Talavera, G.; Vicario, J. L.; Badia, D.; Carrillo, L., *Angew. Chem., Int. Ed.* **2009**, *48*, 5701–5704.

¹⁸ Saha, P.; Biswas, A.; Molleti, N.; Singh, V. K., *J. Org. Chem.* **2015**, *80*, 11115–11122.

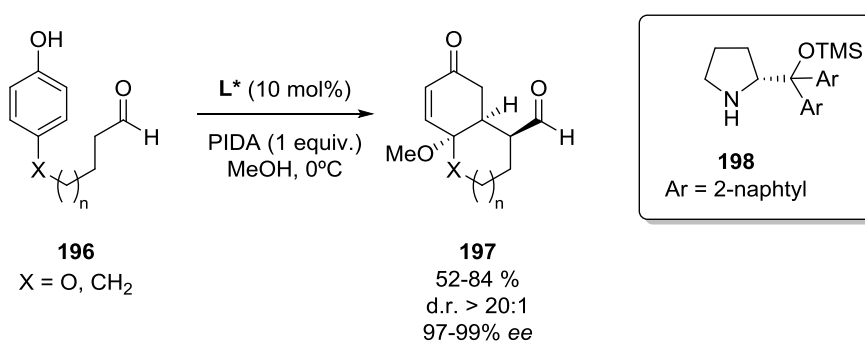
Interestingly, enantioselective desymmetrization of 2,5-cyclohexadienones was carried out after phenol dearomatization reaction. Chiral Brønsted acid catalyzed intramolecular oxa-Michael reaction afforded desymmetrized compounds **194** with excellent enantiomeric excess¹⁹ (**Scheme 3.16**).



Scheme 3.8. First reported oxa-Michael desymmetrization catalyzed by phosphoric acid **195**.¹⁹

3.1.3 Enantioselective desymmetrization reactions

A desymmetrization, for definition, is the modification of a prochiral molecule that results in the loss of one or more symmetry elements (mirror plane, center of inversion...), while one or more new stereocenters are set.²⁰ Non-enzymatic desymmetrization has proven to be a powerful and versatile synthetic tool for the synthesis of chiral building blocks in order to obtain asymmetrically complex structural features.²¹ Gaunt was the first author to report a one-pot organocatalytic oxidative dearomatization strategy.²² *para*-Substituted phenol compounds were exposed under oxidative dearomatization conditions to directly undergo through an amine-catalyzed intramolecular Michael desymmetrization (**Scheme 3.9**). In this way, three new stereogenic centers were introduced giving rise to a broad range of bicyclic compounds in one synthetic step.



Scheme 3.9. One pot oxidative dearomatization/intramolecular Michael desymmetrization catalyzed by prolinol **198**.²²

¹⁹ Gu, Q.; Rong, Z. Q.; Zheng, C.; You, S. L., *J. Am. Chem. Soc.* **2010**, 132, 4056–4057.

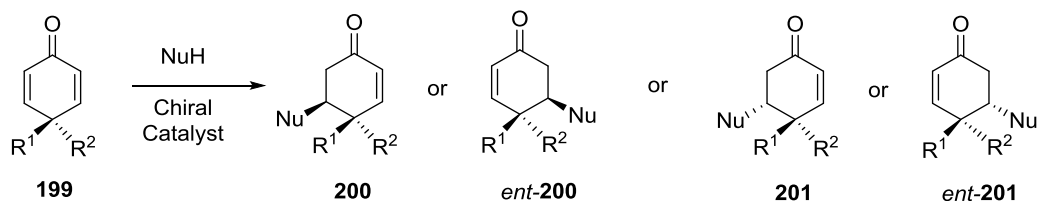
²⁰ Review: Kalstabakken, K. A.; Harned, A. M., *Tetrahedron* **2014**, 70, 9571–9585.

²¹ a) Spivey, A. C.; Andrews, B. I., *Angew. Chem., Int. Ed.* **2001**, 40, 3131–3134. b) Ramachary, D. B.; Barbas, C. F., *Org. Lett.* **2005**, 7, 1577–1580.

²² Vo, N. T.; Pace, R. D. M.; O'Hara, F.; Gaunt, M. J., *J. Am. Chem. Soc.* **2008**, 130, 404–405.

CHAPTER 3

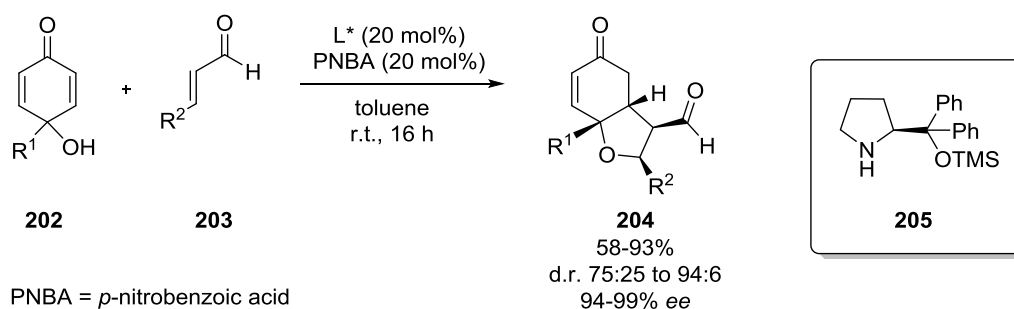
Phenol oxidative dearomatization using hypervalent iodine reagents often affords 2,5-cyclohexadienone intermediates that can react in a following Michael or hetero-Michael addition to offer chiral complex architectures in presence of organocatalysts. 2,5-cyclohexadienones can lead to four possible stereochemical outcomes (**Scheme 3.10**) due to two factors: 1) the selective approach of the face and 2) the preferential reaction on one of the two present alkenes.²⁰



Scheme 3.10. Possible four stereochemical outcomes of desymmetrization reactions of 2,5-cyclohexadienones.

Gaunt's work lead the way for further dearomatization/desymmetrization reaction strategies. Some of the advantages of dearomatization followed by desymmetrization reactions are: the use of cheap aromatic compounds as starting materials, the formation of more than two stereogenic centers in a sole step, and the installation of chiral quaternary carbon centers with high enantioselectivity.²³

Dearomatization reaction followed by intermolecular oxa-Michael/Michael tandem reactions afforded efficient and rapid formation of bicyclic frameworks containing hindered ethers. Prolinol derived catalyst **205** showed good to excellent diastereoselectivities and high enantioselectivities.²⁴



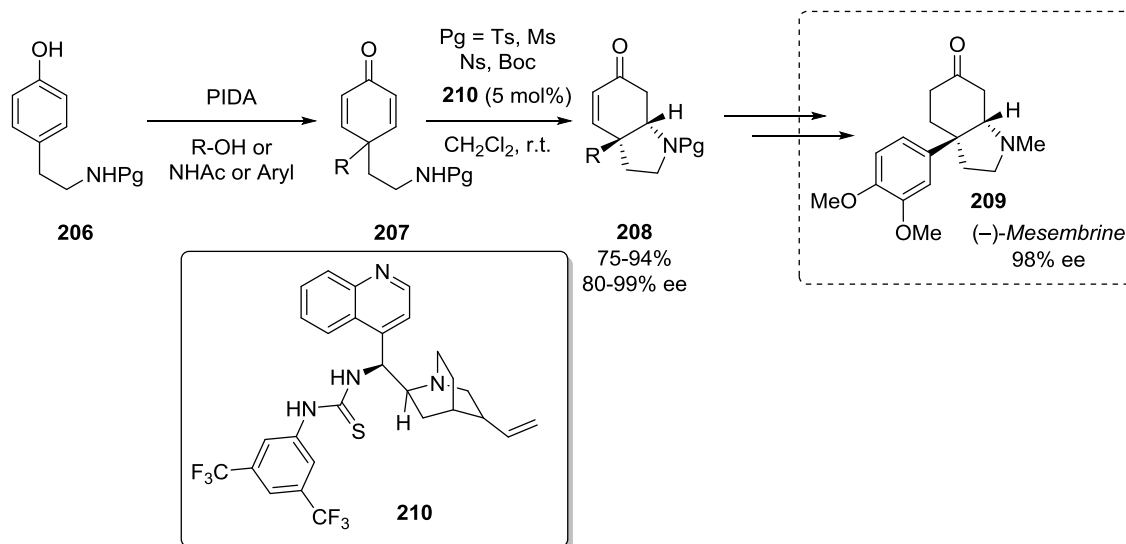
Scheme 3.11. Prolinol derived catalyzed reaction to afford substituted enantiopure ether compounds **204**.²⁴

As it has been mentioned before (**Scheme 3.8**), You and coworkers developed the first dearomatization/oxa-Michael desymmetrization of compound **193**. This

²³ Gu, Q.; You, S. L., *Org. Lett.* **2011**, 13, 5192–5195.

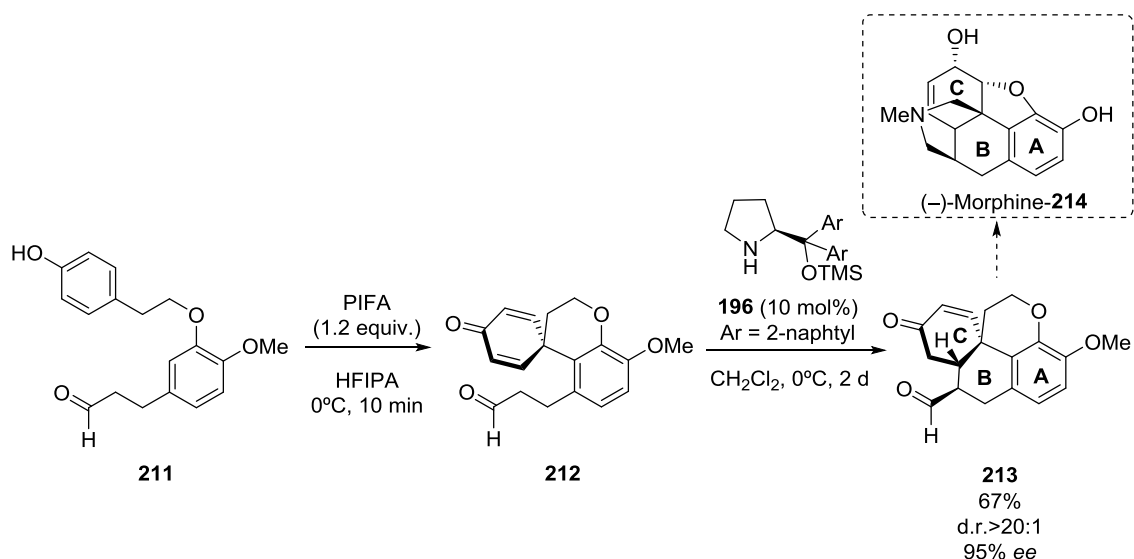
²⁴ Corbett, M. T.; Johnson, J. S., *Chem. Sci.* **2013**, 4, 2828–2832.

methodology gave rise to the total synthesis of Cleroindicin C, D and F.¹⁹ In addition, same group reported the enantioselective dearomatization/Michael addition of cyclohexadienones bearing active methylenes being catalyzed by cinchonine-derived ureas.²³ Similarly, cinchonine-derived thiourea catalyst **210** presented excellent results for the first dearomatization/intramolecular aza-Michael reaction.²⁵ Utility of this methodology was proved by the total synthesis of (–)-Mesembrine (**Scheme 3.12**).



Scheme 3.12. First reported aza-Michael desymmetrization for the total synthesis of (–)-Mesembrine.^{23,25}

Recently, Gaunt and coworkers performed a catalytic enantioselective dearomatization (CED) protocol followed by an intramolecular Michael addition which permitted an efficient strategy for the synthesis of (–)-Morphine core (**Scheme 3.13**).²⁶



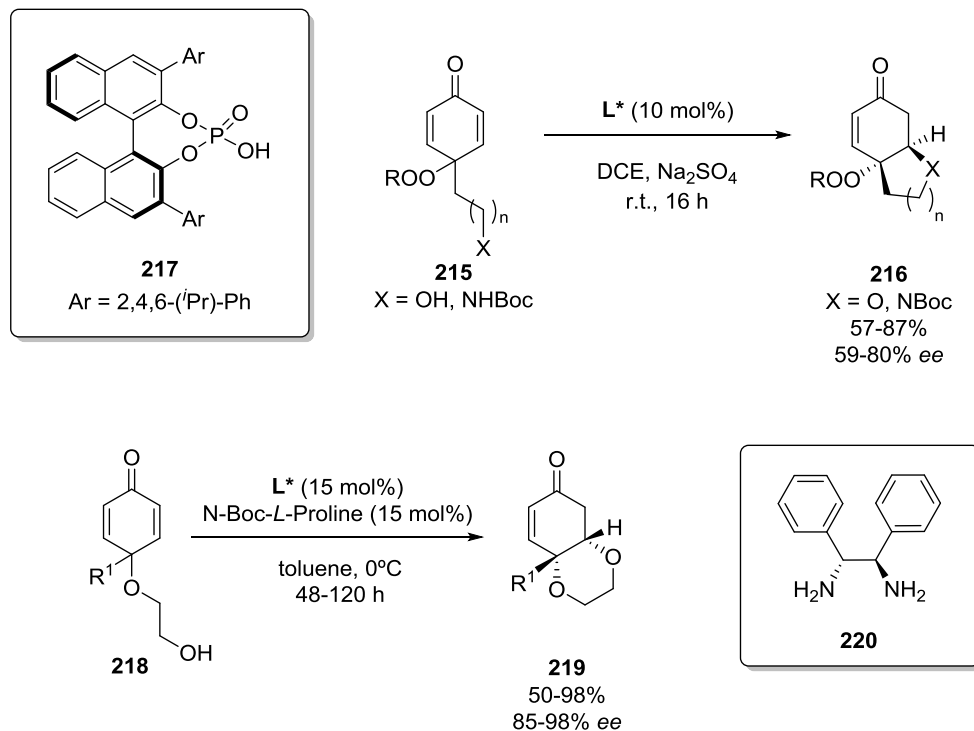
Scheme 3.13. CED strategy to obtain tetracycle **213** in enantioselective manner, core of morphine.²⁶

²⁵ Gu, Q.; You, S.-L., *Chem. Sci.* **2011**, 2, 1519–1522.

²⁶ Williamson, A. E.; Ngouansavanh, T.; Pace, R. D. M.; Allen, A. E.; Cuthbertson, J. D.; Gaunt, M. J., *Synlett* **2016**, 27, 116–120.

CHAPTER 3

Phenol oxidation reaction was reported by Doyle employing dirhodium caprolactone with *tert*-butyl hydroperoxide. This strategy gave rise to interesting peroxi-2,5-cyclohexadienones which, in presence of chiral phosphoric acid **217**, were transformed by oxa-Michael and aza-Michael reactions into bicyclic peroxi-compounds with good enantioselectivities.²⁷



Scheme 3.14. Peroxi-compounds **216** obtained by desymmetrization catalyzed by phosphoric acid **217**, and chiral diamine **220** catalyzed oxa-Michael desymmetrization to afford 1,4-dioxanes.^{27,28}

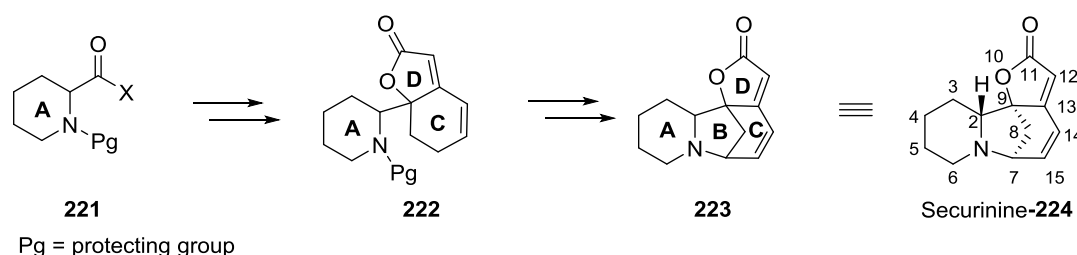
Chiral diamine catalysts **220** in combination with N-Boc-*L*-proline were also reported to catalyze efficiently oxa-Michael reactions through iminium ion activation. 1,4-dioxanes obtained from the desymmetrization reaction were compounds with multiple chiral centers and high enantiomeric excesses.²⁸

²⁷ Ratnikov, M. O.; Farkas, L. E.; Doyle, M. P., *J. Org. Chem.* **2012**, *77*, 10294–10303.

²⁸ Wu, W.; Li, X.; Huang, H.; Yuan, X.; Lu, J.; Zhu, K.; Ye, J., *Angew. Chem., Int. Ed.* **2013**, *52*, 1743–1747.

3.2 Precedents in the total synthesis of *Securinega* alkaloids

As it has been described in **Chapter 1**, *Securinega* alkaloids possess a unique tetracyclic skeleton and exhibit interesting bioactivities. Thereby, a significant number of publications describing innovative approaches targeting such alkaloids are reported to date. Most of the strategies toward the achievement of the main natural product of the family, Securinine, started with the formation of piperidine ring **A**, followed by the subsequent formation of **CD** rings. Final intramolecular cyclization allowed the formation of ring **B** and, thus, Securinine synthesis (**Scheme 3.15**).²⁹



Scheme 3.15. General strategy for the total synthesis of *Securinega* alkaloids.

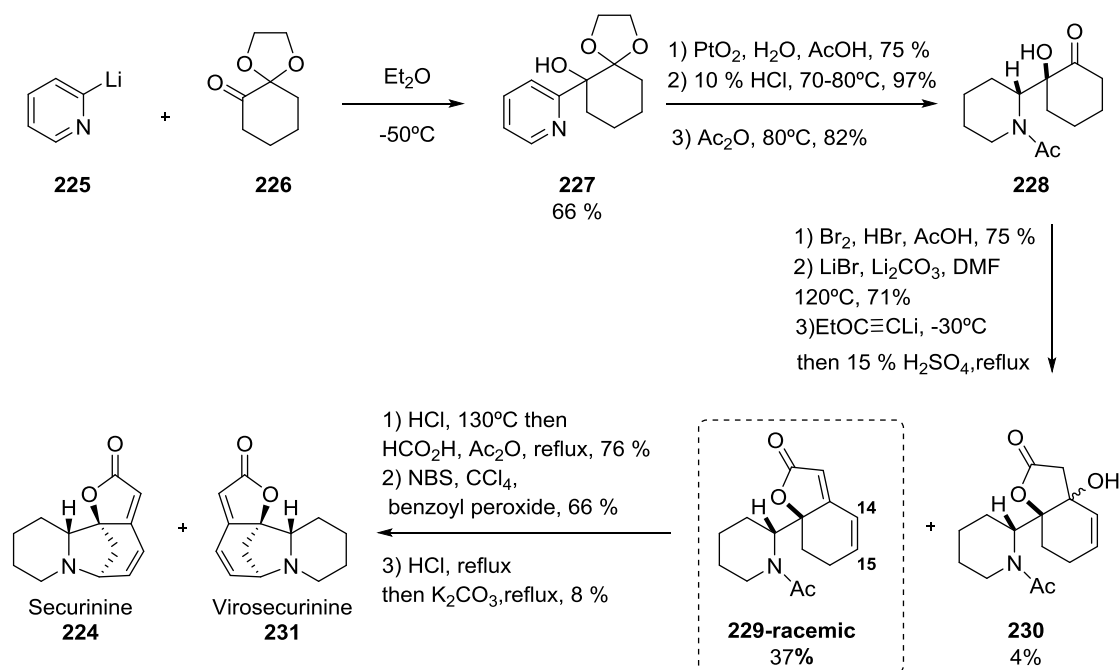
Horii was the first to develop a racemic approach toward Securinine. With no tools for a chiral approach, first synthesis yielded an equimolecular mixture of enantiomers Securinine and Virosecurinine. Enantiomers were separated by recrystallization of camphorsulfonate derivatives. Strategy relied on the initial pyridine **A** ring to form **CD** rings and final cyclization to afford **B** ring as it is represented in **Scheme 3.24**.³⁰

Therefore, synthesis started with pyridyllithium **225** reacting with ketone **226** which gave rise to pyridyl alcohol **227**. Compound **227** was transformed into ketoalcohol **228** by pyridine ring hydrogenation, ketal hydrolysis and *N*-acetylation. Later bromination of **228** was able to afford formation of the double bond in C14-C15 position. Then, following incorporation of lithium ethoxyacetylene followed by treatment with sulfuric acid led to the mixture of butenolide formation **229** and β -hydroxylactone **230**. Acetal of **229** was hydrolyzed and introduction of a formyl group took place. The following bromination and acid hydrolysis led to the synthesis of the racemic mixtures of Securinine/Virosecurinine.

²⁹ Chirkin, E.; Atkalian, W.; Porée, F.-H., *The Securinega Alkaloids*, Elsevier Ltd, **2015**.

³⁰ Horii, Z.; Hanaoka, M.; Yamawaki, Y.; Tamura, Y.; Saito, S.; Shigematsu, N.; Kotera, K.; Yoshikawa, H.; Sata, Y.; Nakai, H.; Sugimoto, N., *Tetrahedron* **1967**, 23, 1165–1174.

CHAPTER 3



Scheme 3.16. First racemic synthesis of Securinine developed by Horii.³⁰

40 years later, Honda, was also able to synthesize racemic compound **229** using an alternative Diels Alder approach.³¹ However, he finally developed the first stereoselective synthesis of Securinine by an original approach toward **CD** ring via tandem ring closing metathesis (RCM).³² Moreover, depending on the chelation to the amine **232** or not (when amine is protected) during the 1,2-addition of the acetylenic moiety on to the carbonyl, synthesis of Securinine or Viroallosecurinine³³ was possible. Stereochemistry in C2 position was set by the enantiopure thioester **232** which was obtained from *R*-pipecolinic acid.

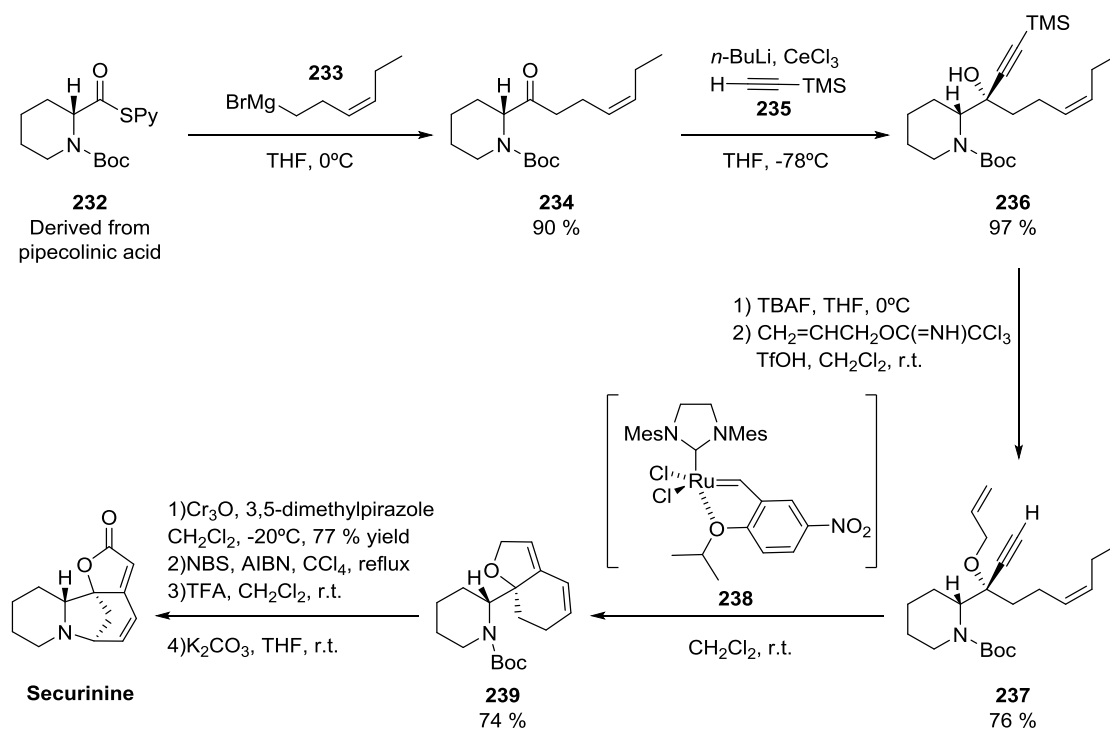
Therefore, thioester **232** was treated with hexenylmagnesium bromide **233** in order to afford ketone **234** in a good yield. Then, diastereoselective alkynylation with lithium trimethylsilyl acetylide **235** in presence of CeCl_3 afforded the tertiary alcohol **236** in a 97 % yield, in this way setting stereochemistry in C9 position. Subsequent deprotection of the alcohol and *O*-allylation gave compound **237**, which was used in the RCM in presence of highly active Ru-catalyst **238** to afford compound **239**. This way stereoselective formation of **A-CD** rings was achieved in a relatively short sequence.

Diene **239** was oxidized by CrO_3 , followed by bromination and removal of protecting group with TFA, and a final cyclization employing potassium carbonate afforded Securinine with 17% of overall yield.

³¹ Honda, T.; Namiki, H.; Kudoh, M.; Watanabe, N.; Nagase, H.; Mizutani, H., *Tetrahedron Lett.* **2000**, 41, 5927–5930.

³² Honda, T.; Namiki, H.; Kaneda, K.; Mizutani, H., *Org. Lett.* **2004**, 6, 87–89.

³³ Honda, T.; Namiki, H.; Watanabe, M.; Mizutani, H., *Tetrahedron Lett.* **2004**, 45, 5211–5213.

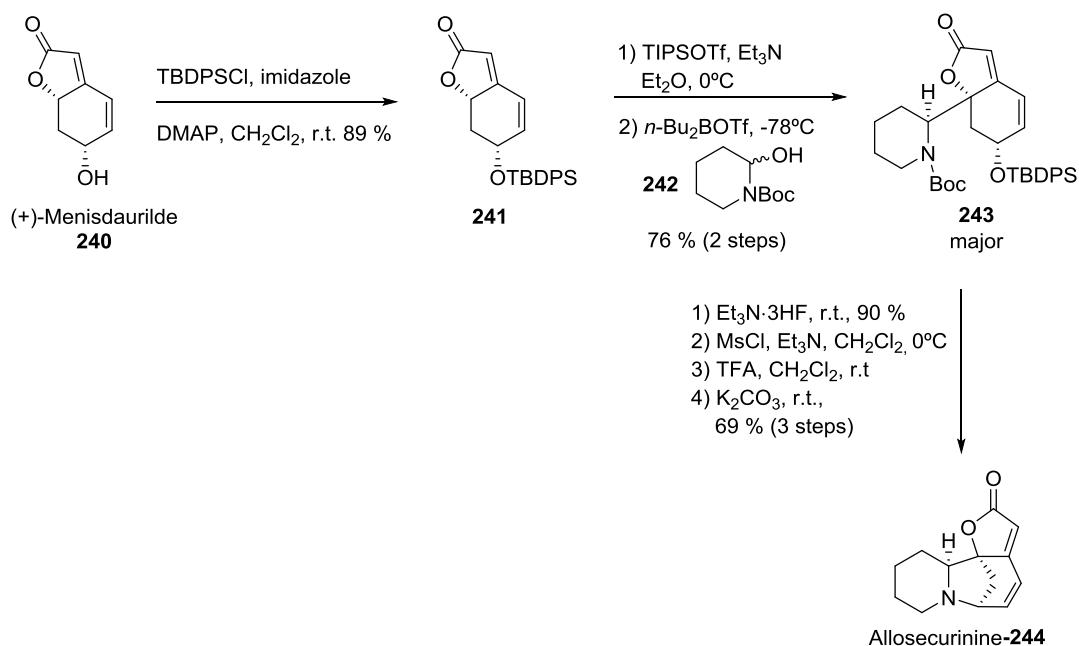


Scheme 3.17. Honda's total synthesis of Securinine using as key step tandem RCM.³²

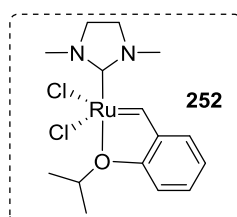
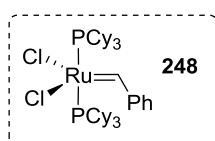
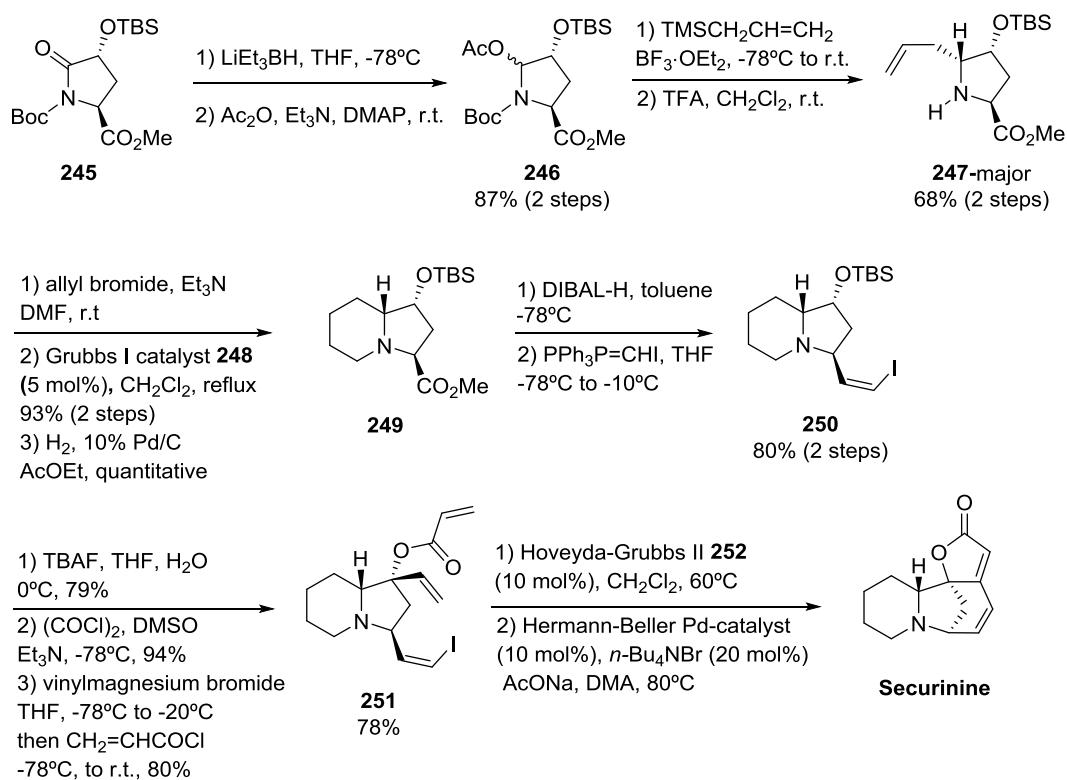
Securinine's epimer Allosecurinine was synthesized by Busqué and coworkers. They started from unnatural (+)-Menisdaurilide employing a vinylogous Mannich reaction as key step.³⁴ (+)-Menisdaurilide (see **Scheme 3.18**) was first protected with *tert*-butyldiphenylsilyl ether affording compound **241**. *In situ* generated piperidinium ion **242** and compound **241** reacted under a vinylogous Mannich reaction. Two of the four possible diastereoisomers were generated in a 4:1 ratio, being diastereoisomer **243** the major one. Deprotection and mesylation of the alcohol, followed by the removal of carbamate using TFA, pave the way for a last cyclization step in presence of K_2CO_3 . Allosecurinine-**244** was obtained in overall yield of 42% through seven synthetic steps.

³⁴ Bardají, G. G.; Cantó, M.; Alibés, R.; Bayón, P.; Busqué, F.; De March, P.; Figueredo, M.; Font, J., *J. Org. Chem.* **2008**, 73, 7657–7662.

CHAPTER 3



Scheme 3.18. Busqué reported total synthesis of Allosecurinine-**244** starting from non-natural (+)-Menisdaurilide.³⁴

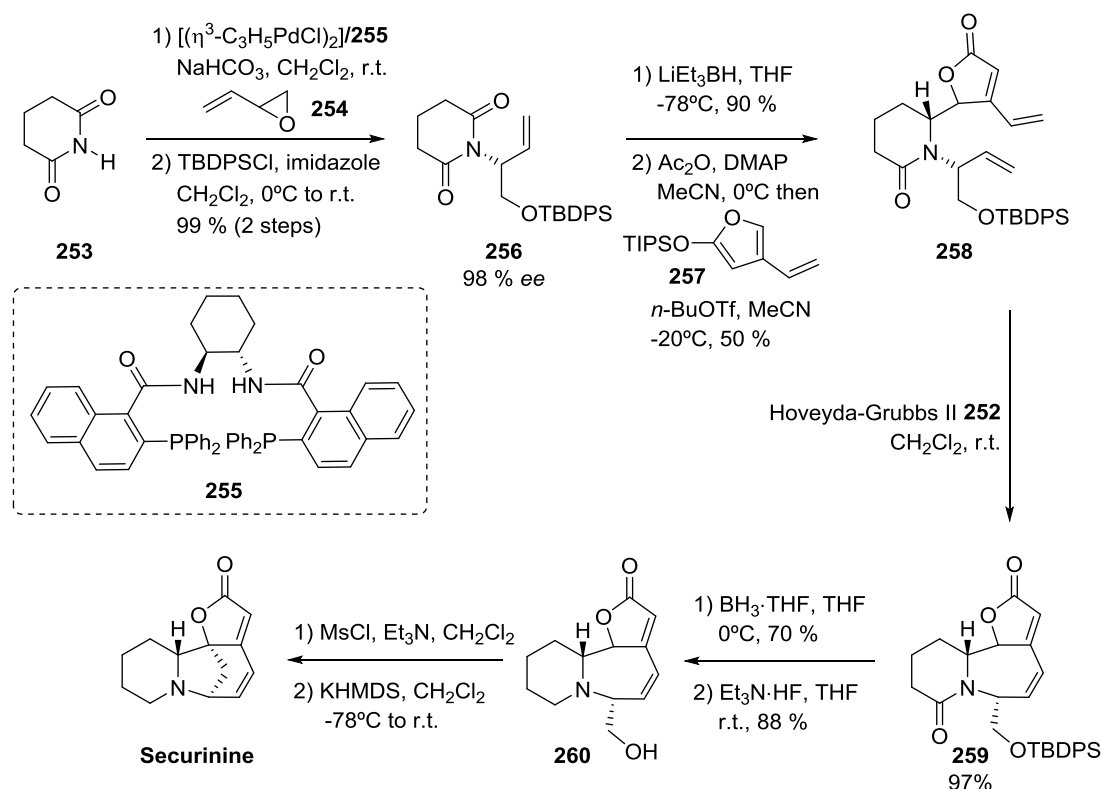


Scheme 3.19. Thadani's total synthesis of Securinine by two RCM and a Pd-catalyzed Heck reaction.³⁵

Thadani developed an original strategy for the synthesis of Securinine (**Scheme 3.19**).³⁵ Starting reagent was part of the **B** ring of Securinine, and then piperidine **A** ring was synthesized. Butenolide **D** ring and the **C** ring were formed during the sequence. Palladium catalyzed Heck reaction and two ring closing metathesis are key steps in the synthesis of the natural product.

Compound **245** was synthesized in four steps from *trans*-4-hydroxy-*L*-proline in 96% yield. Compound **245** was then reduced by LiEt_3BH and directly converted into acetate **246**. Treatment of **246** with allyl trimethylsilane in presence of $\text{BF}_3 \cdot \text{OEt}_2$ and removal of the carbamate protecting group led to major diastereoisomer **247** in 4:1 diastereomeric ratio. After separation of diastereoisomers, *N*-allylation of major compound **247**, followed by RCM and reduction of the obtained alkene by hydrogenation gave rise to substituted indolizidine **249**. Reduction of the ester gave rise to an aldehyde that reacted in a Wittig reaction permitting the access to the corresponding *Z*-iodoalkene **250**.

Deprotection of the alcohol allowed the formation of the corresponding ketone, and addition of vinylmagnesium bromide generated an alkoxy intermediate that was trapped by acryloyl chloride to form triene **251**. Hoveyda-Grubbs II catalyzed RCM was followed by an intramolecular Heck reaction catalyzed by Herman-Beller palladium catalyst. Total synthesis of Securinine was performed in 18 steps with an overall yield of 16%.



Scheme 3.20. Pd-catalyzed enantioselective allylation and following Bayon's total synthesis toward Securinine.³⁶

³⁵ Dhudshia, B.; Cooper, B. F. T.; Macdonald, C. L. B.; Thadani, A. N., *Chem. Commun.* **2009**, 463–465.

CHAPTER 3

Bayon developed an alternative total synthesis of Securinine based on the palladium catalyzed enantioselective allylation of glutarimide **253**.³⁶ It is important to note that depending on the size of the imide ring, 5 membered (–)-Norsecurinine or 6 membered Securinine could be synthesized. Bayon's synthetic sequence started with **A** glutarimide ring followed by the coupling of **AD** moieties through vinylogous Mannich reaction. Further RCM generated the **BC** ring which, in a later intramolecular nucleophilic substitution, afforded the bridged natural product (**Scheme 3.20**).

Chiral diphosphine ligand **255** in combination with palladium salt catalyzed the enantioselective allylation between glutarimide **253** and epoxide **254** leading to the formation of compound **256** in a 98% of enantiomeric excess after protection of the alcohol. The reduction of ketone gave an aminal that directly reacted in a vinylogous Mannich reaction with silyloxyfuran **257**, and gave rise to triene **258**. RCM using Hoveyda-Grubbs catalyst II afforded tricyclic compound **259** in almost quantitative yield and with the direct insertion of the distinctive C14-C15 double bond to the structure. Then, after the elimination of ketone group in C6 position, silyl protected alcohol was deprotected and mesylated. The formation of potassium enolate using KHMDS induced the intramolecular nucleophilic substitution in order to yield Securinine in ten reaction steps with an overall yield of 20%. On the other hand, (–)-Norsecurinine was obtained in nine steps with 14% of overall yield.

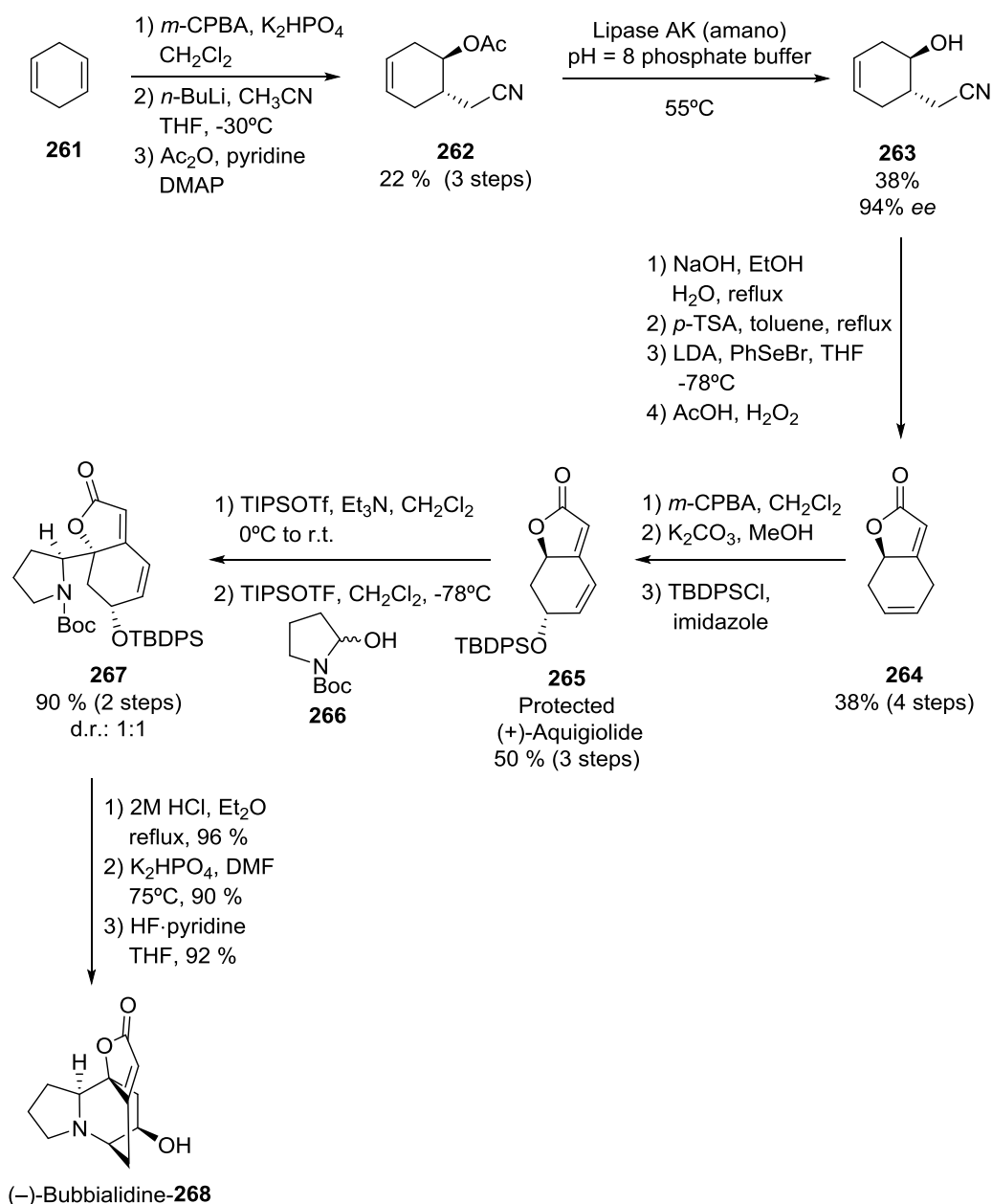
Recently, Gademan published an efficient total synthesis of (–)-Bubbialidine, an alkaloid that present an azabicyclo[2.2.2]octane system.³⁷ They described the synthesis of (–)-Bubbialidine in 16 synthetic steps with a 1% of overall yield (**Scheme 3.21**). Strategy followed started from **C** ring and continued with the formation of **D**, **A**, **B** rings.

This synthesis is very interesting due to the versatility provided by protected (+)-Aquilegolide intermediate. In addition, this intermediate is a stereoisomer of (+)-Menisdaurilide, bicycle employed in the total synthesis reported by Busqué.³⁴ Starting from a simple 1,4-cyclohexadiene **261**, the subsequent epoxidation, ring opening and acetylation reactions afforded racemic compound **262**. Enzymatic kinetic resolution using a lipase gave rise to compound **263** in a 94 % ee and 38% yield. After hydrolysis of the nitrile moiety, followed by acid catalyzed lactonization, the compound was exposed to selenation and oxidative elimination conditions to afford **CD** moiety **264**. The protection of alcohol with TBDPS and the vinylogous Mannich reaction between *in situ* generated aminol **266** and lactone **265** afforded a mixture of diastereoisomers in a 1:1 ratio, **267**. After separation of diastereoisomers, the correspondent one was converted into its chlorhydrate salt by removal of the Boc group.

The salt was treated under high temperature and in presence of K₂HPO₄ promoted intramolecular aza-Michael addition to obtain protected natural product. Interestingly at this stage they were able to diverge in the synthesis in order to obtain two possible natural products: 1) deprotection of alcohol led to desired (–)-Bubbialidine; 2) further four step sequence afforded Virosaine A, in 19 steps.

³⁶ González-Gálvez, D.; García-García, E.; Alibés, R.; Bayón, P.; De March, P.; Figueredo, M.; Font, J., *J. Org. Chem.* **2009**, *74*, 6199–6211.

³⁷ Miyatake-Onozabal, H.; Bannwart, L. M.; Gademann, K., *Chem. Commun.* **2013**, *49*, 1921–1923.

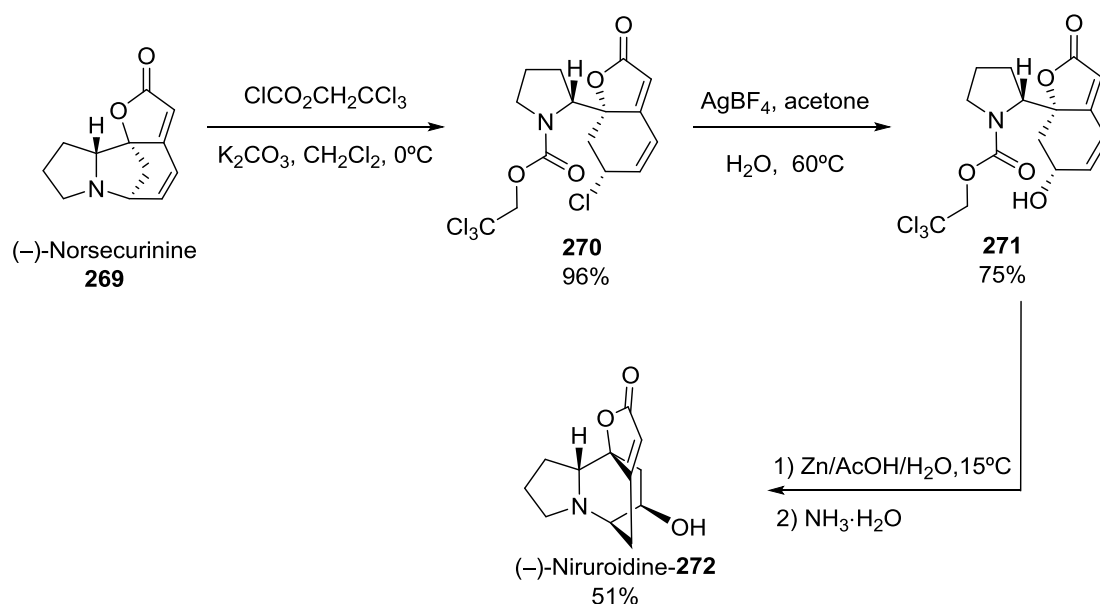


Scheme 3.21. Total synthesis of (-)-Bubbialidine reported by Gademan and coworkers.³⁷

Jiang reported more recently the total synthesis of (-)-Norsecurinine, (-)-Niruroidine and dimeric alkaloid (-)-Flueggine A.³⁸ (-)-Norsecurinine was obtained in 9 steps with an overall yield of 12%. Interestingly, synthesis of (-)-Niruroidine was obtained for the first time in four chemical steps from (-)-Norsecurinine with 37% of overall yield (**Scheme 3.22**).

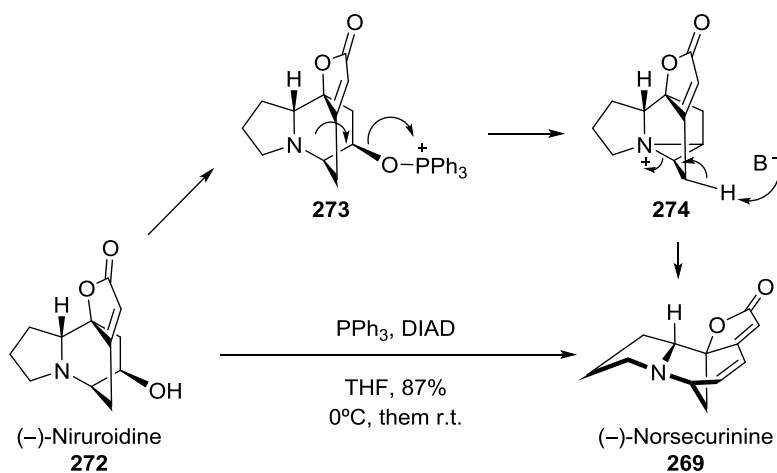
³⁸ Ma, N.; Yao, Y.; Zhao, B.-X.; Wang, Y.; Ye, W.-C.; Jiang, S., *Chem. Commun.* **2014**, 50, 9284–9287.

CHAPTER 3



Scheme 3.22. Transformation of (-)-Norsecurinine into (-)-Niruroidine.³⁸

Moreover, it was considered that the three natural products were biosynthetically related due to their presence in plants of the same genus. Thus, (-)-they were able to obtain (-)-Norsecurinine from (-)-Niruroidine, supporting the fact that this process could occur in nature (**Scheme 3.23**)



Scheme 3.23. Transformation (-)-Niruroidine of into (-)-Norsecurinine and possible mechanism of rearrangement by PPh_3 .³⁸

Li reported a collective and concise total synthesis of some *Securinega* alkaloids by tandem RCM reactions. In this way, total synthesis of (-)-Flueggine A, (+)-Virosaine B, C7'-epi-Flueggine A and Bubbialine was achieved.³⁹

³⁹ Han, J.-C.; Li, C.-C., *Synlett* **2015**, 26, 1289–1304.

3.3 Hypervalent iodine reagents and enantioselective oxidative dearomatization reactions

Hypervalent iodine reagents have found broad application in organic chemistry and are nowadays frequently used in synthesis. For example, we have previously described their importance in oxidative dearomatization reactions that can later undergo enantioselective desymmetrization reactions (section 3.1.3 of this Chapter).

Wilgerodt was the first to prepare dichloriodobenzene in 1886, first organic hypervalent iodine compound. Since then, these reagents have emerged as important oxidants in organic synthesis, often able to replace metallic oxidants due to their reactivity, and with the advantage of low toxicity. In particular, during last decades, hypervalent iodine reagents have demonstrated to promote different types of reactions such as ligand exchange, oxidative addition, reductive elimination and ligand coupling reactions, typically performed by transition metals.⁴⁰

Organoiodine compounds present a linear three-center-four-electron (3c-4e) bond (L-I-L) which is formed by the overlap of the 5p-orbital on iodine atom with the orbitals on the two ligands. The particular reactivity and structure for polyvalent iodine compounds is explained by the presence of the described weak and highly polarized hypervalent bond.⁴¹

Hipervalent iodine compounds can be classified into two groups:^{41,42}

- 1) **Iodine (III) compounds or λ^3 -iodanes:** RIX_2 compounds present 10 electrons placed in the iodine atom, and they exhibit a sp^3d^1 hybridization featuring a trigonal/bipyramidal geometry as demonstrated in structure **278** (see **Fig. 3.8**). As depicted in **Figure 3.8** for PIDA, PIFA and Koser's reagent, the oxygenated ligands are typically positioned in the apical positions, while the remaining lone pairs sit in the equatorial position along with the aromatic ring. These compounds thus are T-shaped structures and their I-X bond is longer than an average covalent bond for other organoiodine molecules.

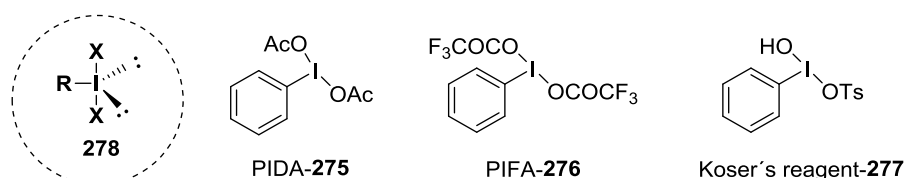


Figure 3.8. PIDA and PIFA, representative examples of λ^3 -iodanes.

⁴⁰ a) Willgerodt, J. *Prakt. Chem.* **1886**, 33, 154-160. b) Zhdankin, V. V.; *Hypervalent Iodine Chemistry: Preparation, Structure and Synthetic Applications of Polyvalent Iodine Compounds*, Wiley, Chichester, **2014**.

⁴¹ Yoshimura, A.; Zhdankin, V. V., *Chem. Rev.* **2016**, 116, 3328–3435.

⁴² Parra, A.; Reboredo, S., *Chem. Eur. J.* **2013**, 19, 17244-17260.

CHAPTER 3

- 2) **Iodine (V) compounds or λ^5 -iodanes:** RIX_4 compounds exhibit sp^3d^2 hybridization featuring a square pyramidal geometry as demonstrated in structure **281**. As gathered in **Figure 3.9**, Dess-Martin periodinane and IBX reagents present their oxygenated ligands in basal position, while the lone pair and the aromatic ring are placed in apical positions.

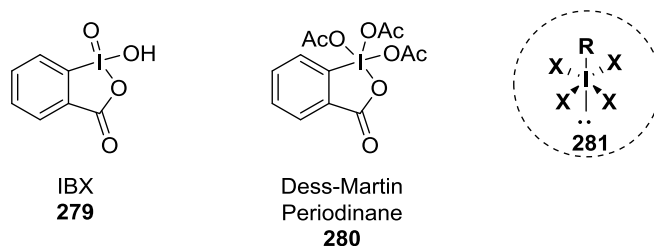


Figure 3.9. Most common examples of λ^5 -iodanes.

Hypervalent iodine reagents are useful in a wide range of reactions; such as, oxidations of sulfide to sulfoxides, dearomatization reactions, arylation reactions, α -functionalization of ketones, functionalization of alkenes and dehydrogenation of alcohols into carbonyl compounds.

3.3.1 Chiral Hypervalent iodine reagents

Imamoto and coworkers were the first to prepare chiral hypervalent iodine reagent, back in 1986, which showed moderate enantiomeric excess for the oxidation of sulfides to sulfoxides (**Fig. 3.10, 282**).^{43,44} On the other hand, Wirth *et al.* were the first to introduce the chirality in the aromatic backbone of a hypervalent iodine reagent (**Fig. 3.10, 283**), which showed effectiveness in different oxidation reactions.⁴⁵ Ochiai⁴⁶ and Kita⁴⁷, independently, reported the first achiral catalytic oxidation employing aryl iodides as organocatalyst and *m*-CPBA as stoichiometric oxidant. Later, Wirth was capable of developing the first catalytic asymmetric version.⁴⁸

⁴³ Imamoto, T.; Koto, H., *Chem. Lett.* **1986**, 967-968.

⁴⁴ Berthiol, F., *Synthesis* **2015**, 47, 587-603

⁴⁵ Wirth, T.; Hirt, U. H., *Tetrahedron: Asymmetry* **1997**, 8, 23-26.

⁴⁶ Ochiai, M.; Takeuchi, Y.; Katayama, T.; Sueda, T.; Miyamoto, K., *J. Am. Chem. Soc.* **2005**, 127, 12244-12245.

⁴⁷ Dohi, T.; Maruyama, A.; Yoshimura, M.; Morimoto, K.; Tohma, H.; Kita, Y., *Angew. Chem., Int. Ed.* **2005**, 44, 6193-6196.

⁴⁸ Richardson, R. D.; Page, T. K.; Altermann, S.; Paradine, S. M.; French, A. N.; Wirth, T., *Synlett* **2007**, 538-542.

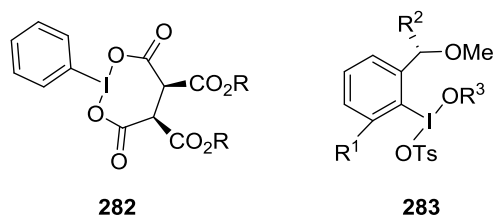


Figure 3.10. First chiral hypervalent iodine ligands **282** and **283**.

Since then, a broad variety of hypervalent iodine reagents have been synthesized as it is gathered in **Figure 3.11**. These ligands promote efficiently different asymmetric reactions such as, dearomatization reactions, oxidation of alkenes or oxidation of sulfides to sulfoxides.

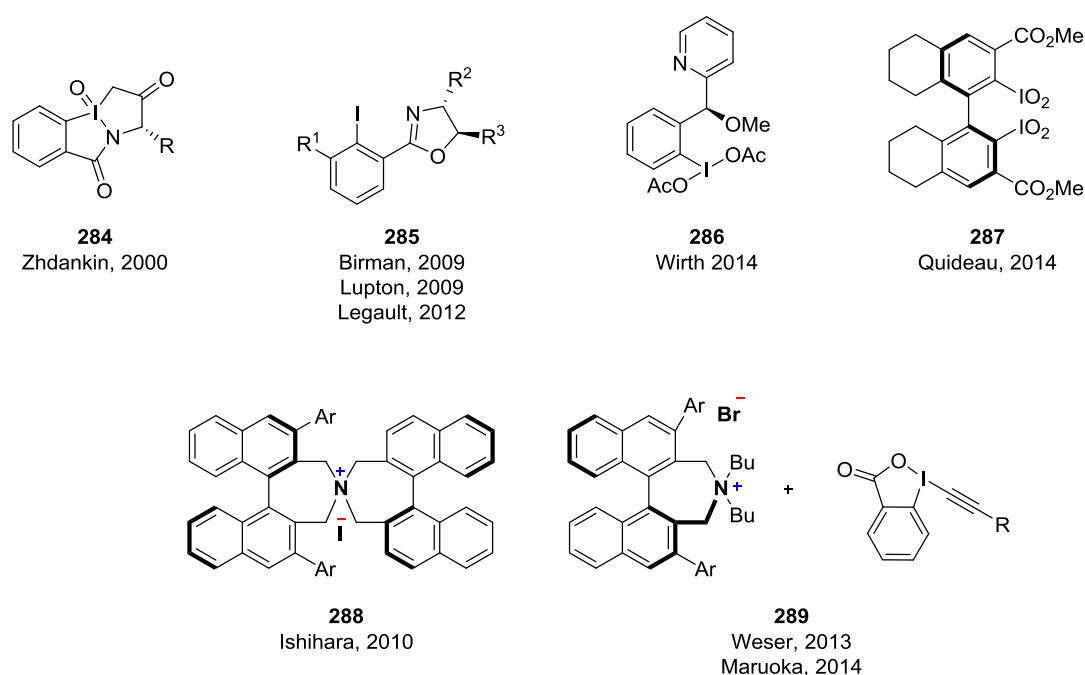


Figure 3.11. Chiral hypervalent iodine reagents developed in the last two decades.

3.3.2 Dearomatization reactions

Among the different reactions mediated by hypervalent iodine reagents, oxidative dearomatization reactions of phenols and naphthols are of special interest. Since the first works of Siegel and Antony⁴⁹ on iodoarene diacetates, dearomatization reactions have been widely employed as key organic reactions for natural product synthesis.⁵⁰ Amongst the hypervalent iodine reagents commercially available, PIDA ((diacetoxyiodo)benzene) and PIFA [bis(trifluoroacetoxy)iodo]benzene are probably the most common reagents used in phenolic oxidative dearomatization reactions. In the

⁴⁹ Siegel, A.; Antony, F., *Monatsh. Chem.* **1955**, 86, 292-300.

⁵⁰ a) Pouységu, L.; Deffieux, D.; Quideau, S., *Tetrahedron* **2010**, 66, 2235–2261. b) Pouységu, L.; Sylla, T.; Garnier, T.; Rojas, L. B.; Charris, J.; Deffieux, D.; Quideau, S., *Tetrahedron* **2010**, 66, 5908–5917.

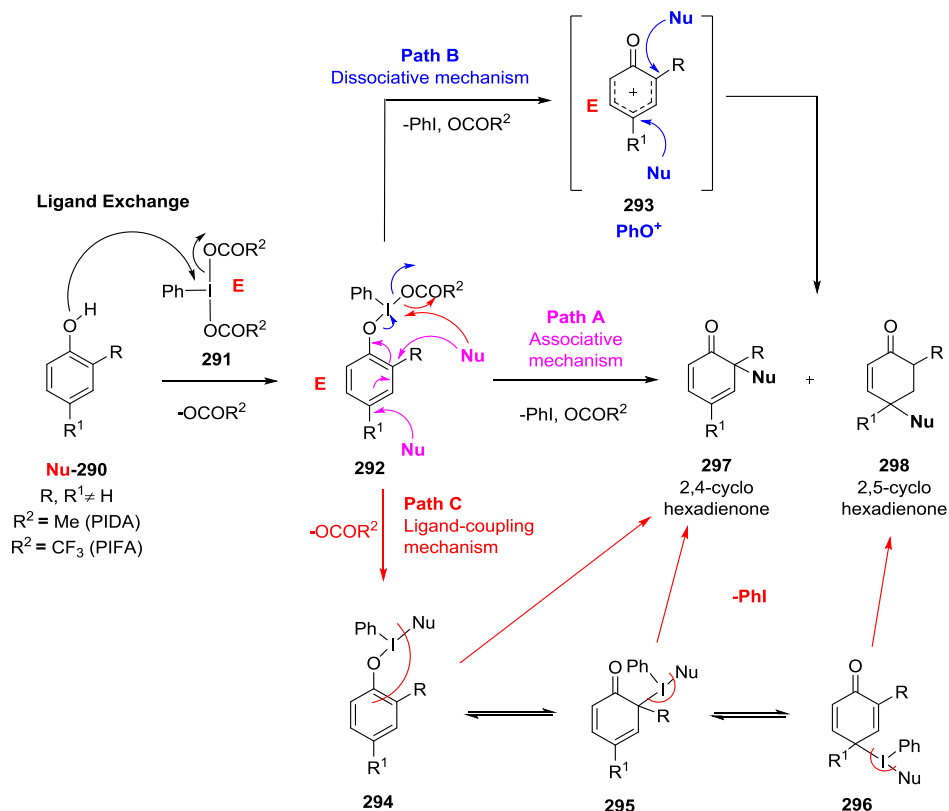
CHAPTER 3

particular case of λ^3 -iodanes, nucleophiles can be introduced into the *ortho*- or *para*-positions of the aromatic ring giving rise to the corresponding 2,4-cyclohexadienones or 2,5-cyclohexadienones.⁵¹

Mechanistic insights of this transformation remain uncertain but three main mechanisms are postulated (**Scheme 3.24**). All proposed mechanisms start with a ligand exchange step of one carboxylate ligand being substituted by the phenol, owing to the electrophilic nature of the iodine (III) atom. Once the phenoxy group is bounded to the iodine (III) center, the development of the reaction depends on the nucleofugality of the λ^3 -phenyliodanyl group. The reduction of two of the electrons of the iodine (III) center and the elimination of the iodine (I) compound formed is the driving force of the reaction.^{50a,52}

First mechanism, named as **path A** in **Scheme 3.24**, postulates an associative bimolecular mechanism in which the attack of the nucleophiles and the withdrawal of the λ^3 -phenyliodanyl group take place at the same time, in a concerted manner. This path does not imply the possible formation of phenoxenium ion intermediate.

Alternatively, a dissociative mechanism (**Scheme 3.24, path B**) goes through a phenoxonium ion intermediate **293** due to the great nucleofugality nature of the λ^3 phenyliodane. Subsequently, the nucleophile would attack the *ortho* or *para* position and lead to the corresponding product.



Scheme 3.24. Postulated mechanistic behavior of λ^3 -iodanes through **Path A, B or C**.

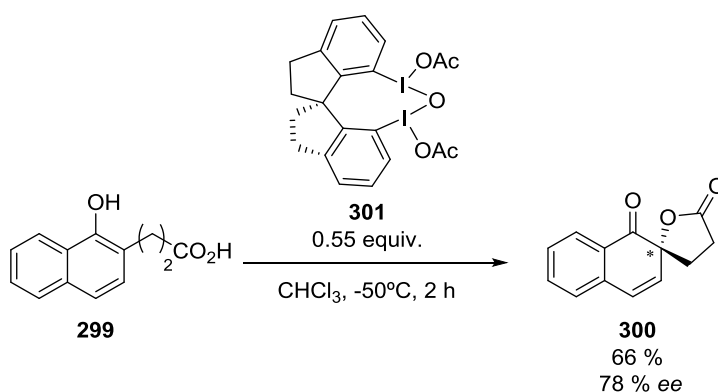
⁵¹ Harned, A. M., *Tetrahedron Letters*, **2014**, 55, 4681-4689.

⁵² Wu, W.-T.; Zhang, L.; You, S.-L., *Chem. Soc. Rev.*, **2016**, 45, 1570-1580.

The third mechanistic pathway (**Scheme 3.24, path C**) involves a second ligand exchange of the λ^3 -phenyliodane with an incoming nucleophile, and subsequently, leads to the reductive elimination of the respective iodobenzene (PhI) with the simultaneous formation of a bond between the two other ligands (phenoxy unit and nucleophile). This mechanism is similar to the transition metal mediated coupling reactions.

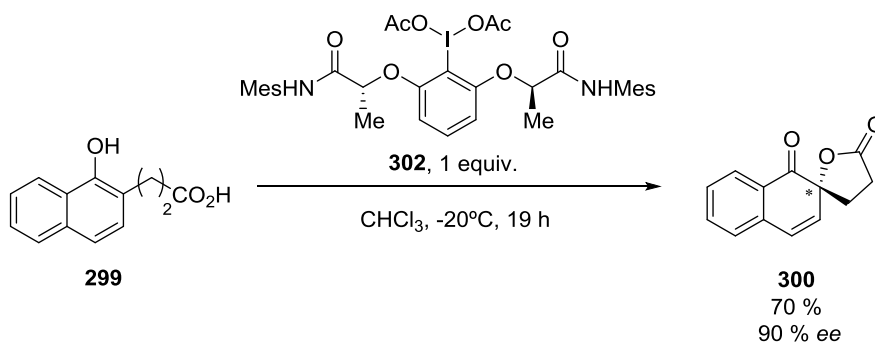
3.3.2.1 Stoichiometric enantioselective reactions

Kita developed a strategy for the enantioselective phenolic dearomatization in order to obtain chiral *ortho*-spirolactone **300** using chiral organohypervalent iodine **301** (**Scheme 3.25**). Reaction between *ortho*-carboxy substituted naphthol **299** and chiral reagent **301** afforded the spirolactone with high enantiocontrol.⁵³



Scheme 3.25. First asymmetric spirolactonization by organohypervalent iodines developed by Kita.⁵³

Ishihara and coworkers published an even more efficient asymmetric spirolactonization of naphthols by the use of a novel C_2 -symmetric hypervalent iodine (III) reagent **302** bearing two lactate derivatives (**Scheme 3.26**).⁵⁴



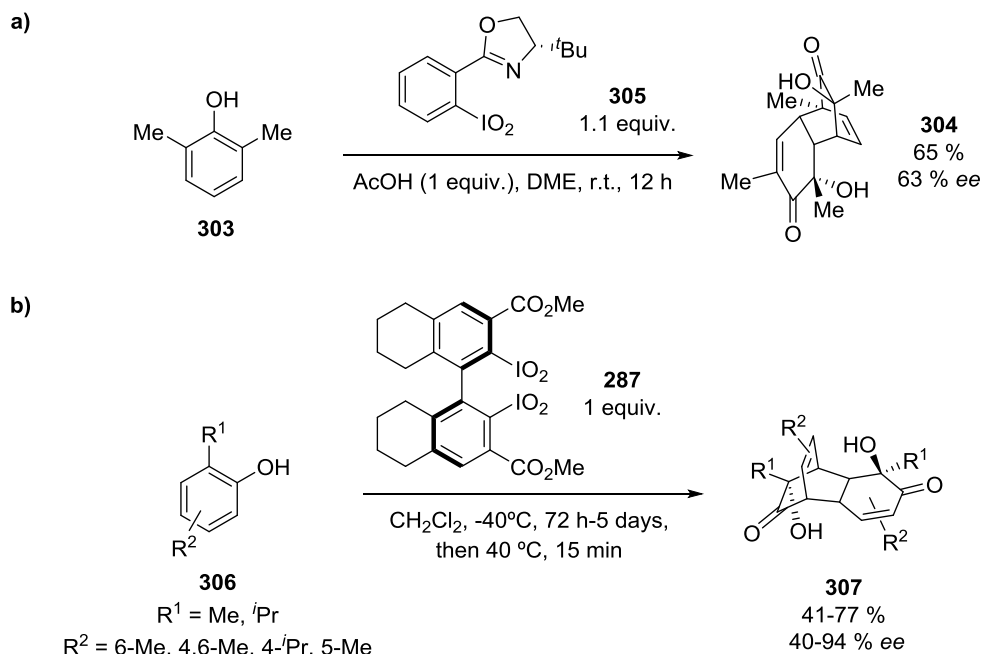
Scheme 3.26. Asymmetric spirolactonization mediated by C_2 -symmetry hypervalent iodine (III) **302**.⁵⁴

⁵³ Dohi, T.; Maruyama, A.; Takenaga, N.; Senami, K.; Minamitsuji, Y.; Fujioka, H.; Caemmerer, S. B.; Kita, Y.A., *Angew. Chem., Int. Ed.* **2008**, *47*, 3787–3790.

⁵⁴ a) Uyanik, M.; Yasui, T.; Ishihara, K., *Angew. Chem., Int. Ed.* **2010**, *49*, 2175–2177. b) Uyanik, M.; Yasui, T.; Ishihara, K., *Tetrahedron* **2010**, *66*, 5841–5851.

CHAPTER 3

Pseudocyclic iodylarenes bearing a chiral oxazoline scaffold, promoted the formation of *ortho*-quinol dimers in moderate enantiomeric excess using *ortho*-alkylphenols as substrates. Reaction with 2,6-dimethylphenol **303** afforded corresponding dimer **304** in a 63 % ee (**Scheme 3.27.a**).⁵⁵



Scheme 3.27. Asymmetric hydroxylative phenol dearomatizations by chiral oxazolines and biphenyl hypervalent iodines.^{55,56}

Quideau and coworkers have published the synthesis of binaphthyl and biphenyl containing C_2 -symmetric iodine (V) reagents like **287**. Reactions with different substituted phenols resulted in an asymmetric phenol dearomatization which led to the corresponding *ortho*-quinol derivatives after a [4+2] Diels-Alder reaction observing for the obtained products enantioselectivities up to 94 % ee (**Scheme 3.27.b**).⁵⁶

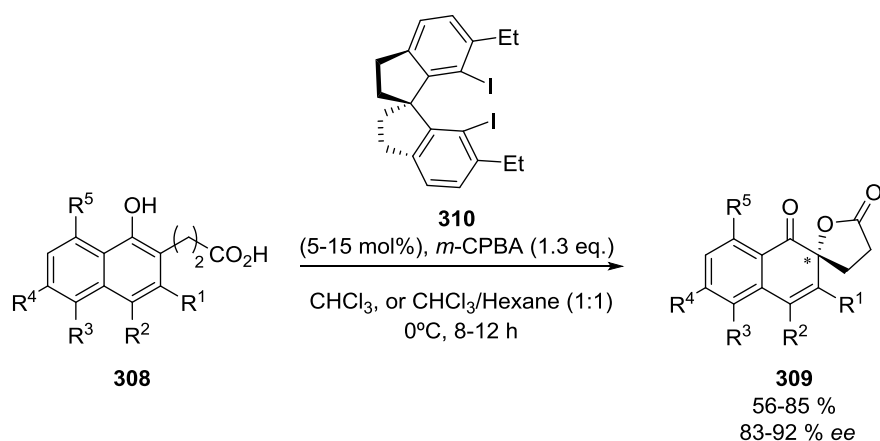
3.3.2.1 Catalytic enantioselective reactions

Many catalytic reactions have been developed since Wirth discovered first catalytic α -tosyloxylation in 2007.⁴⁸ Kita reported the spirobiindane backbone first used in a substoichiometric amount of 0.55 equiv (**Scheme 3.25**). Subsequently, they were capable of modifying the chiral iodine by introducing a substituent in *ortho* position of the spirobiindane, which was used as precatalyst giving rise to products with high enantiocontrol (**Scheme 3.28**).⁵⁷

⁵⁵ Boppisetti, J. K.; Birman, V. B., *Org. Lett.* **2009**, 11, 1221-1123.

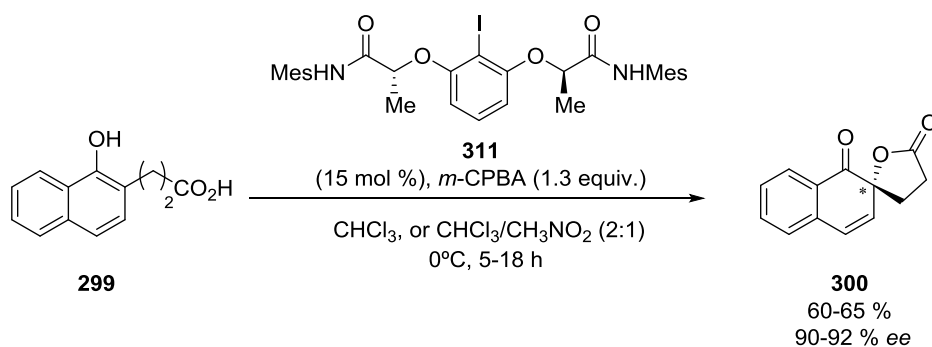
⁵⁶ Bosset, C.; Coffinier, R.; Peixoto, P. A.; El Assal, M.; Miqueu, K.; Sotiropoulos, J.-M.; Pouysegue, L.; Quideau, S., *Angew. Chem., Int. Ed.* **2014**, 53, 9860-9864.

⁵⁷ Dohi, T.; Takenaga, N.; Nakae, T.; Toyoda, Y.; Yamasaki, M.; Shiro, M.; Fujioka, H.; Maruyama, A.; Kita, Y., *J. Am. Chem. Soc.* **2013**, 135, 4558-4566.



Scheme 3.28. Successful catalytic enantioselective spirolactonization developed by Kita.⁵⁷

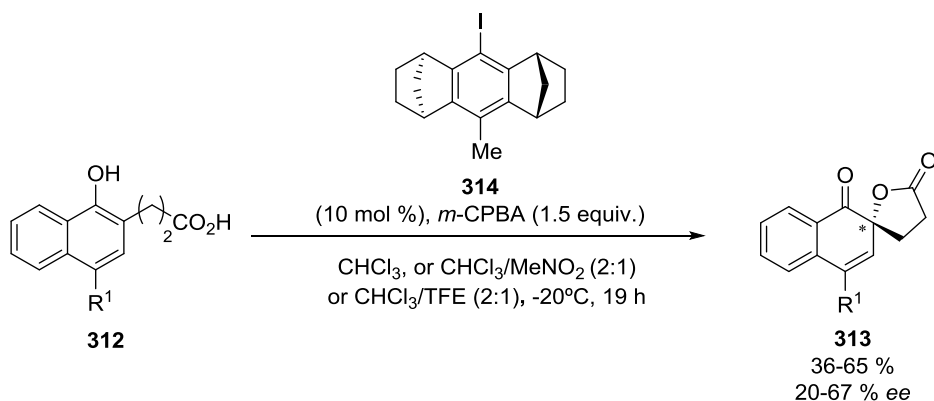
Ishihara's group reported similar catalytic enantioselective spirolactonization using a flexible C_2 -symmetric leading to product with up to 92% ee (**Scheme 3.29**). They suggested that the intramolecular hydrogen bonds are crucial for this improvement in the enantioselectivity.⁵⁴



Scheme 3.29. Catalytic enantioselective spirolactonization using C_2 -symmetric iodoarene.⁵⁴

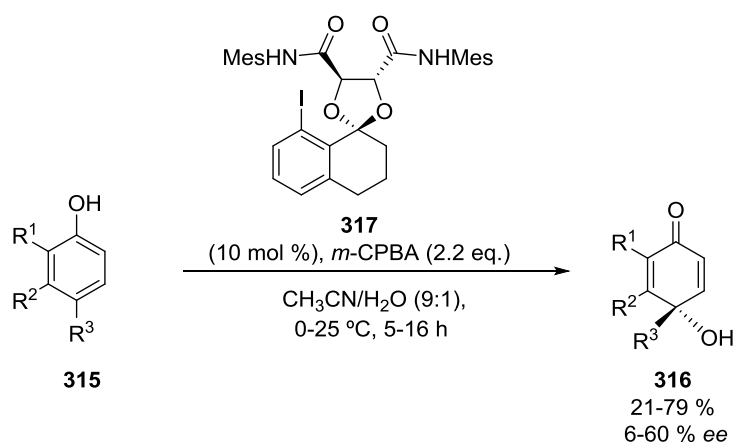
Ibrahim reported the use of a unique C_2 -symmetric iodoarene precatalyst able to efficient catalyzed spirolactonization reactions of naphthols bearing substituents in *para*- position to the hydroxyl group (**Scheme 3.30**).⁵⁸

⁵⁸ Murray, S. J.; Ibrahim, H., *Chem. Commun.* **2015**, 51, 2376-2379.



Scheme 3.30. Anthracene derivative **314** as C_2 -symmetric chiral precatalyst used in spirolactonization reactions.⁵⁸

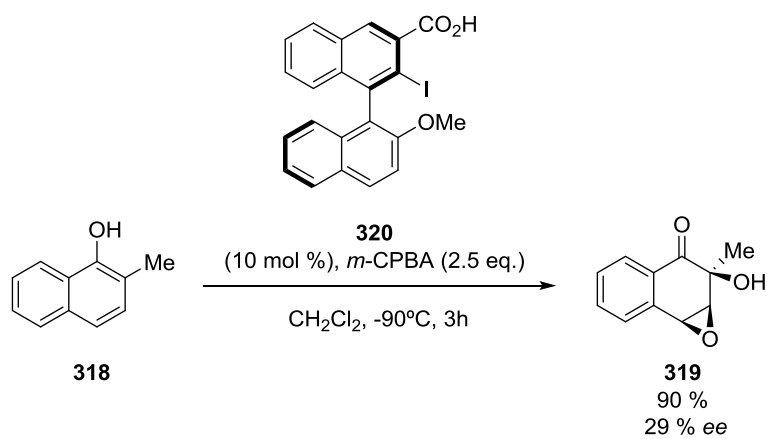
Harned reported the synthesis of new chiral iodoarene that was used as precatalyst for intermolecular oxidative dearomatization of phenol derivatives inducing moderate levels of enantiocontrol (**Scheme 3.31**). The same catalyst was also able to provide moderate enantiomeric excess for the intramolecular spirolactonization of phenols.⁵⁹ Intermolecular hydroxylative dearomatization of phenols catalyzed by chiral binaphthyl iodoarene **320** was described by Quideau *et al.* (**Scheme 3.32**). This methodology gave rise to dearomatized epoxide **319** with 29% ee.⁶⁰



Scheme 3.31. Harned's precatalyst showed a moderate asymmetric oxidative dearomatization of phenols.⁵⁹

⁵⁹ Volp, K. A.; Harned, A. M., *Chem. Commun.* **2013**, 49, 3001-3003.

⁶⁰ Quideau, S.; Lyvinec, G.; Marguerit, M.; Bathany, K.; Ozanne-Beaudenon, A.; Buffeteau, T.; Cavagnat, D.; Chenede, A., *Angew. Chem., Int. Ed.* **2009**, 48, 4605-4609.

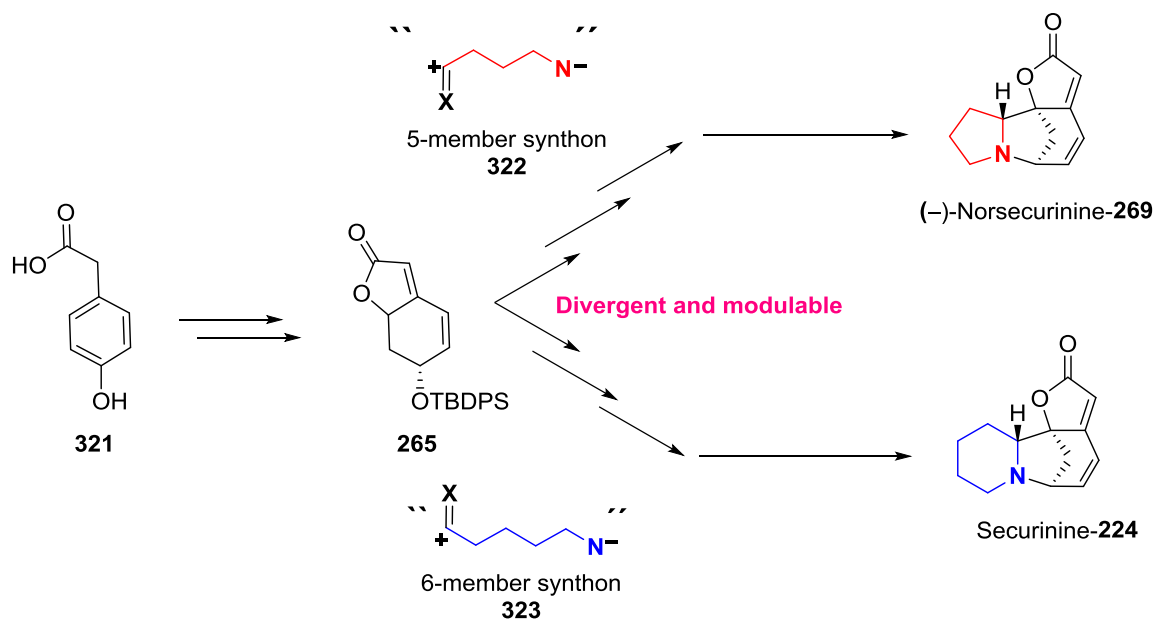


Scheme 3.32. Quideau's strategy for the asymmetric oxidative dearomatization of phenols and subsequent epoxidation.⁶⁰

CHAPTER 3

3.4 Objectives

Our main goal is to develop a versatile, collective synthesis of *Securinega* alkaloids inspired by the total synthesis of (–)-Bubbialidine reported by Gademan³⁷ (lactone **265** as a key intermediate). Intermediate **265** could thus be combined with either a 5 member or 6 member synthon in order to provide an expeditive and divergent access to both families of Norsescurinine- and Securinine-type natural products.



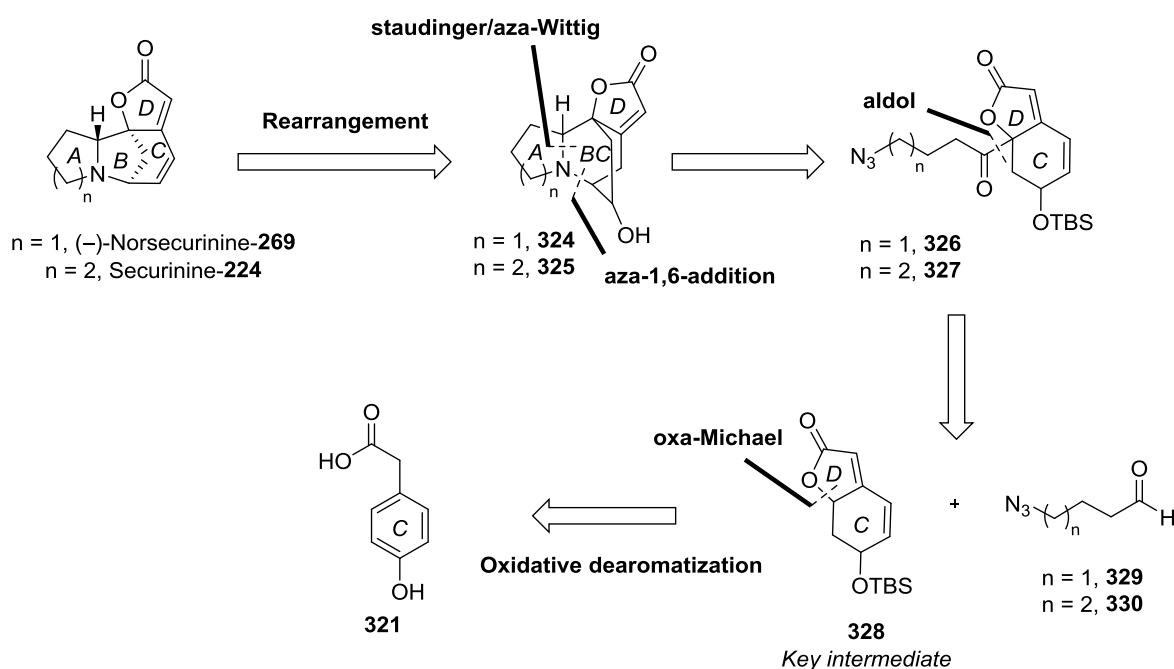
Scheme 3.33. Proposed divergent and modifiable strategy that gives access to natural compounds of *Securinega* family.

At the same time, lactone **265** could be synthesized through a phenol dearomatization-based strategy starting from simple and cheap phenol acetic acid **321**. Asymmetric synthesis of alkaloids could be developed by a catalytic enantioselective dearomatization/desymmetrization strategy using, for example, chiral ferrocenyl derivatives or organocatalysts.

A second objective is the synthesis of hypervalent iodine derivatives of ferrocene. Therefore, after the synthesis of chiral ferrocenyl iodanes their efficacy as chiral hypervalent reagents will be analyzed in model reactions, such as, phenol oxidative dearomatization and naphthol spirocyclization reactions.

3.5 Retrosynthetic analysis of *Securinega* natural products

Inspired by the synthesis sequence (C-D-A-B) developed by Busqué³⁴ and Gademan³⁷, we envisioned a synthetic roadmap toward *Securinega* natural products designed on the basis of retrosynthetic analysis shown in **Scheme 3.34**.



Scheme 3.34. Retrosynthetic analysis of Securinine-224 and (-)-Norsecurinine-269.

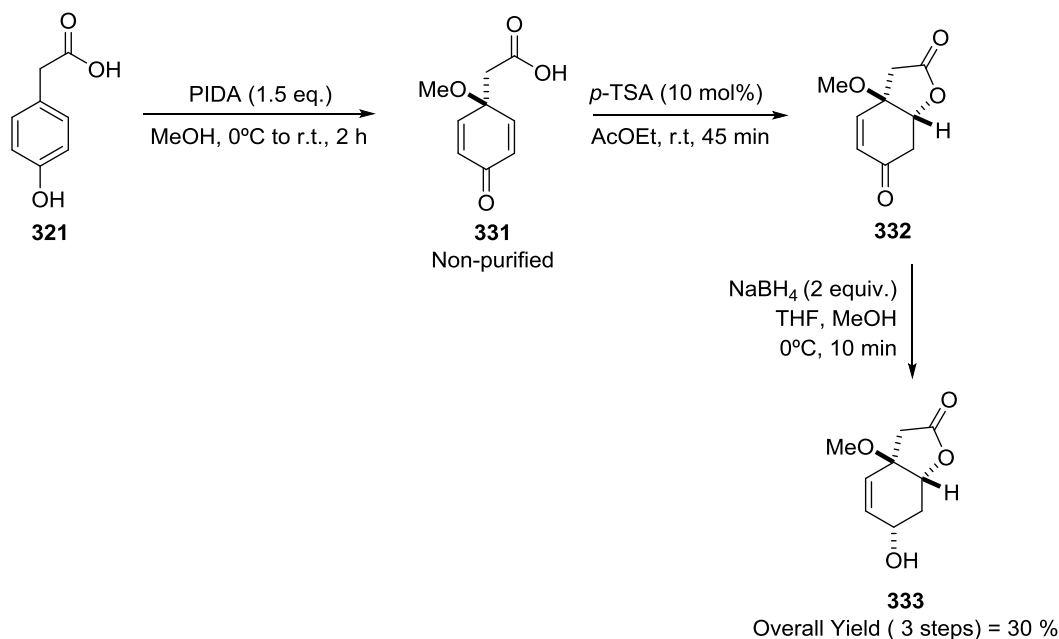
Rearrangement of azabicyclo[3.2.1]octane system of natural products **269** and **224** led to their azabicyclo[2.2.2]octane congeners **324** and **325** as potential precursors. Disconnection of the carbon-nitrogen bonds revealed azidoketones **326** and **327** as potential advanced intermediates for cascade reactions consisting of Staudinger/aza-Wittig reactions followed by an aza-Michael type addition. Azidoketones were further disconnected at the carbon-carbon bond adjacent to the carbonyl group furnishing azidoaldehydes **329** and **330**, and bicyclic lactone **328** as potential precursors for aldol reaction. Finally lactone **328** was traced back to phenol acetic acid **321** as building block by disconnection of carbon-oxygen bond that could be formed by dearomatization and oxa-Michael reaction.

Proposed bicyclic lactone **321** is similar to the intermediate **265** that Gademan³⁷ reported for the total synthesis of (-)-Bubbialidine, just as the one reported by Busqué³⁴ in view of the total synthesis of Allonorsecurinine. Moreover, a expedite access, allowing a short multigram synthesis of this compound is planned using the venerable phenol oxidative dearomatization followed by desymmetrization of 2,5-cyclohexadienone.

3.6 Total Synthesis of *Securinega* Alkaloids3.6.1 Racemic synthesis of lactone intermediate **328**

The access toward lactone **328** starts with the oxidative dearomatization of phenol **321**. The use of 1.5 equivalents of λ^3 -iodane in methanol as solvent at room temperature furnished 2,5-cyclohexadienone **331** in a near quantitative conversion based on the ^1H NMR. Both PIDA and PIFA were evaluated for their capacity to promote such dearomatization. In order to avoid the formation of many byproducts, their addition was made at 0°C and reaction was stirred for 10 minutes. After this time the reaction was monitored at room temperature until completion.

PIDA was able to generate a cleaner compound but with lower yields than PIFA. This might be due to the release of trifluoroacetic acid from PIFA during the reaction, which can directly promote oxa-Michael reaction. This could be an advantage, but our interest relies on a synthesis of compound **331** without further cyclization toward bicyclic structure **332**. For all this reasons, PIDA was chosen as oxidizing agent, which afforded compound **331** in a 25% yield when purified (see **Scheme 3.35**). This low yield is mainly explained by the sensitivity of compound **331** on silica gel. Compound **331** was thus engaged crude in the following oxa-michael reaction in view of a high yielding racemic access to lactone **332**.



Scheme 3.35. Dearomatization, oxa-Michael reaction and reduction of ketone afforded lactone **333**.

The oxa-Michael reaction was then promoted by the use of a Brönsted acid, the *p*-toluenesulfonic acid in EtOAc. A full conversion to desired lactone derivative **332** was again observed on the crude ^1H NMR after 1h of reaction at room temperature. However, the attempts to purify lactone **332** through silica gel unambiguously showed

the reversibility of this transformation. For this reason, crude of the compound was again used in the next step, without further purification.

Crude of compound **332** was thus placed in anhydrous THF, and then cooled down to 0°C before the addition of 2 equivalents of NaBH₄ and MeOH. A fully diastereoselective reduction of ketone **332** to alcohol **333** was observed after 15 minutes of reaction. At this stage, lactone **333** was purified obtaining 30% yield from phenol **321** (average of 67% step)

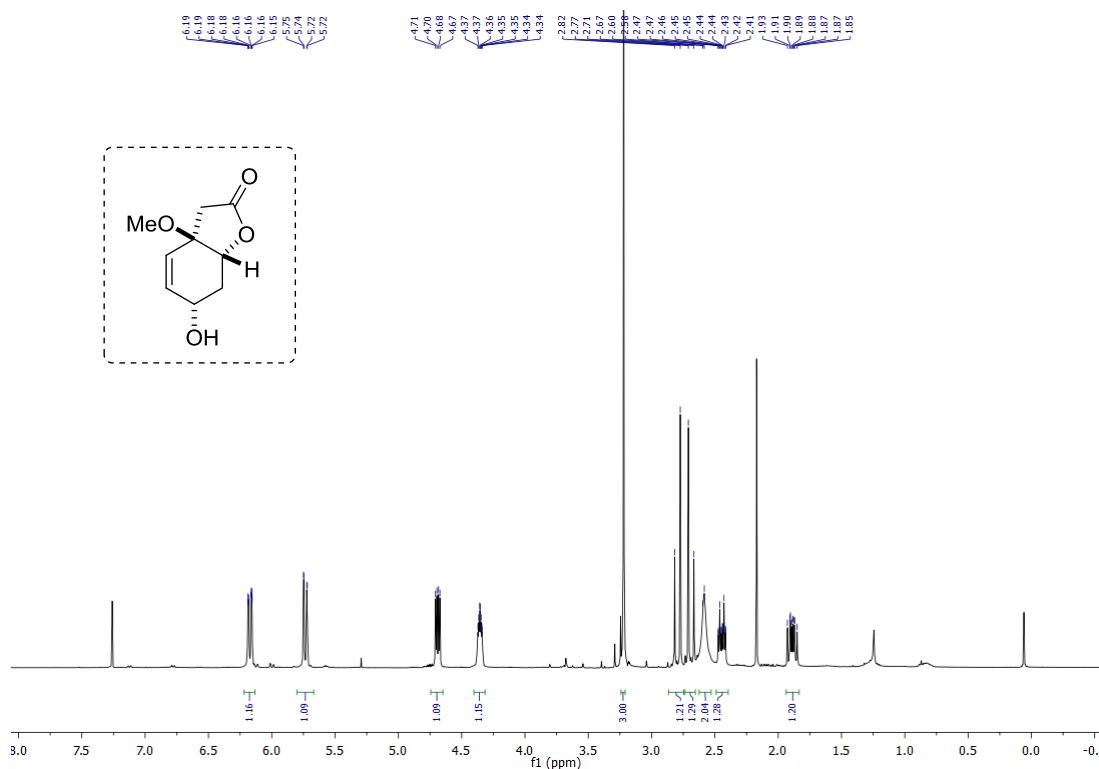


Figure 3.12. ¹H NMR spectrum of lactone **333**.

Stereochemistry of molecule **333** was assigned by NOESY 1D experiments irradiating the signals at 4.71 (H_c), 4.38 (H_d) and 3.25 ppm (-OMe) in CDCl₃ as deuterated solvent. Just with the irradiation of the H_c proton (**Fig. 3.13**) we can deduce that the protons H_d, H_c, H_f, H_e and -OMe are showing a NOE effect. This fact suggests that hydroxyl group must exhibit a *trans* relation with the methoxy group. The strong diastereoselectivity observed is thus due to the so-called umbrella effect of the bridgehead -OMe moiety, thus inducing an approach of the hydride from the convex face. Stereochemistry of compound **333** is the one depicted in **Scheme 3.35**.

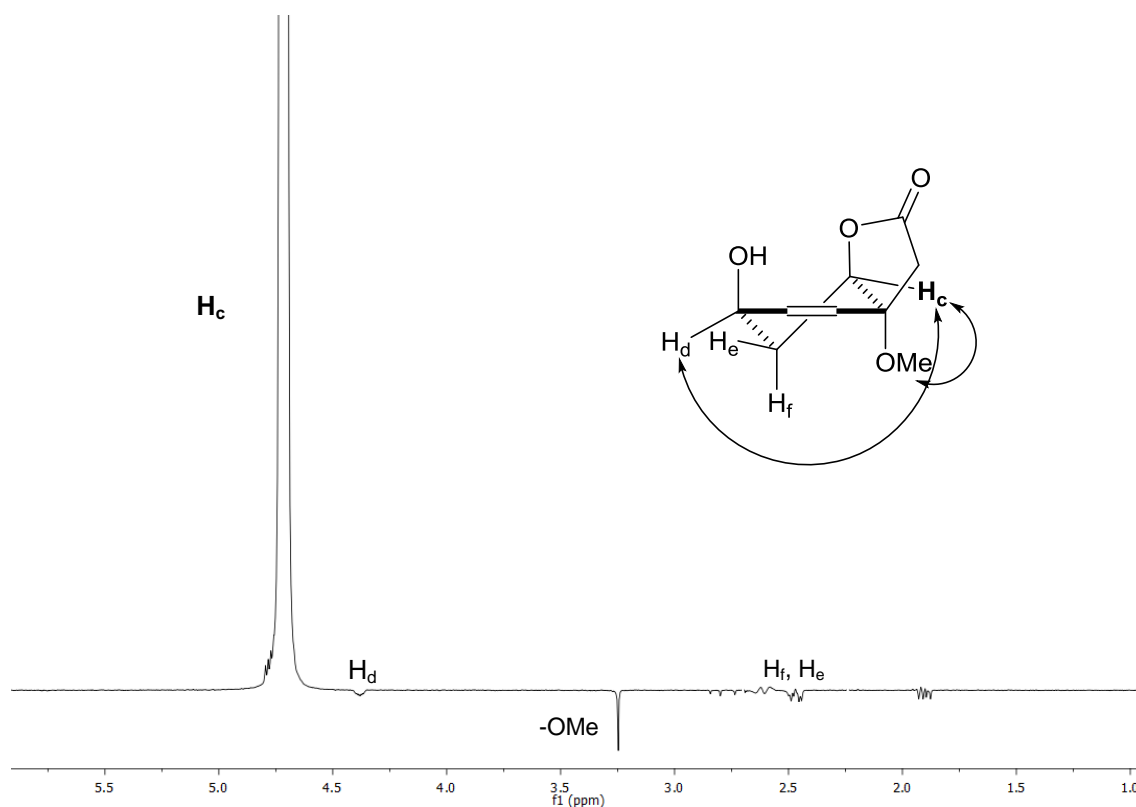
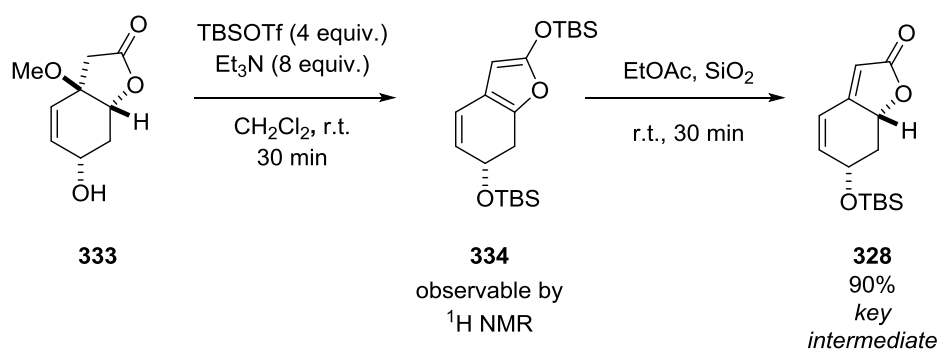


Figure 3.13. NOESY 1D experiment after irradiation of signal at 4.17 ppm (H_c).

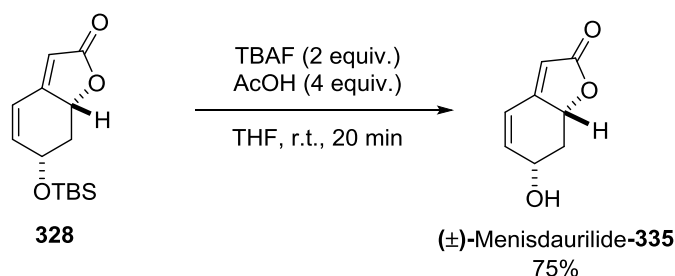
Alcohol of lactone **333** was then protected with TBSOTf in presence of Et_3N using DCM as solvent. The formation of silyl enol ether **334** was observed under basic work up conditions (saturated bicarbonate solution). Silyl enol ether **334** was after dissolved in EtOAc and protonated selectively by the presence of SiO_2 (silica gel). This last step gave rise to lactone **328**, key intermediate of the total synthesis.



Scheme 3.36. Protection of alcohol **333** into lactone **328**, passing through silyl enol ether **334**.

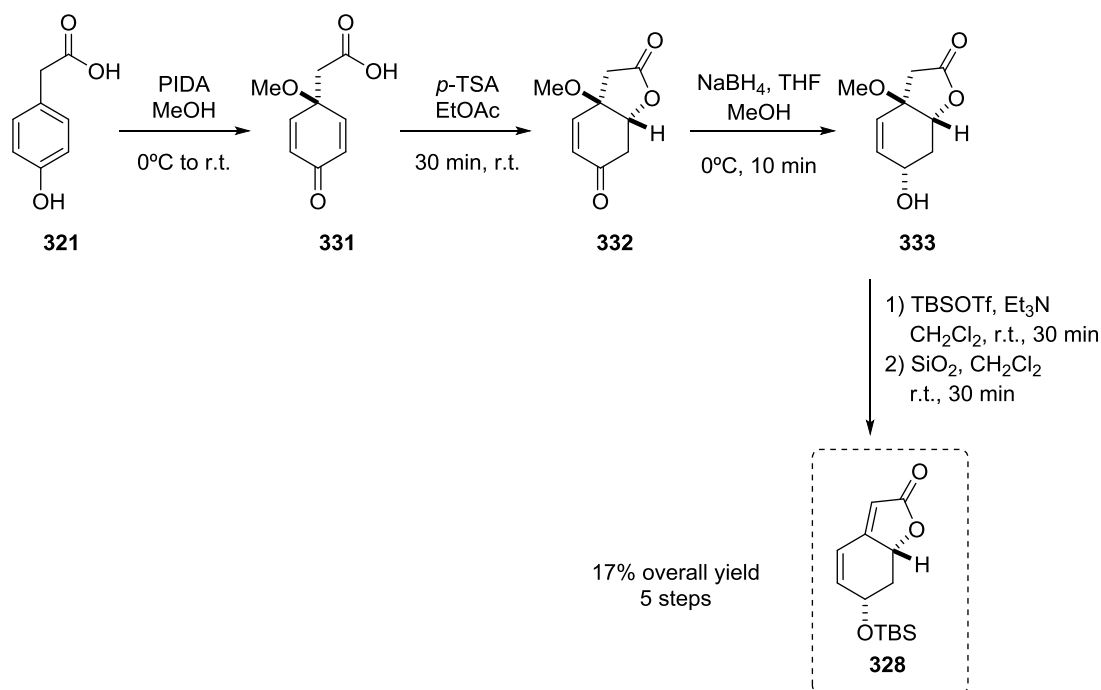
In order to determine the stereochemistry of lactone **328**, a simple deprotection of the alcohol could lead to the formation of known natural products. In this case, the deprotection of the lactone intermediate using TBAF in presence of AcOH afforded (\pm)-Menisdaurilide-**335** in a 75% yield. As a consequence, the stereochemistry of lactone

328 was set, being as depicted in **Scheme 3.36**. Spectroscopic data of synthesized (\pm)-Menisdaurilide-**335** was in concordance with literature.⁶¹



Scheme 3.37. Desilylation of lactone **328** using TBAF to afford (\pm)-Menisdaurilide-**335**.

It is important to highlight that the five step sequence is scalable, and can be achieved with a single final purification. Indeed, carrying out the whole five step sequence on crudes from phenol **321** yielded lactone **328** with 17% overall yield (70% per step on average). This sequence is thus competitive with literature precedents in terms of overall yield towards intermediate **328**. Moreover, it is of paramount importance to highlight that these five steps can be performed in one work-day. This turns our approach also highly competitive in terms of time-efficiency; a parameter too often neglected in the field of total synthesis.



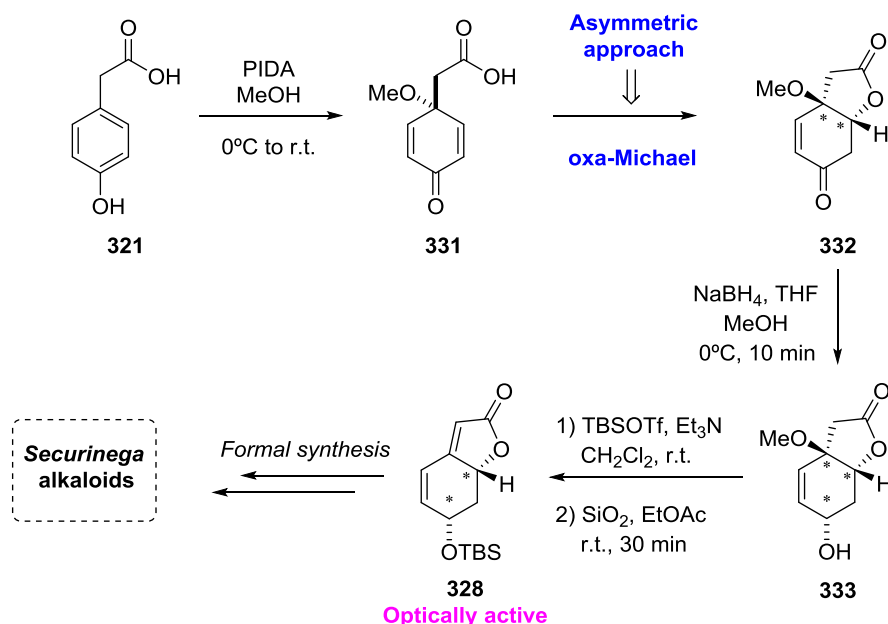
Scheme 3.38. Efficient synthetic sequence to afford racemic lactone **328**.

⁶¹ a) Takahashi, K.; Matsuzawa, S.; Takani, M., *Chem. Pharm. Bull.* **1978**, 26, 1677-1681. b) Yogo, M; Ishiguro, S.; Murata, H.; Furukawa, H., *Chem. Pharm. Bull.* **1990**, 38, 225-226.

CHAPTER 3

3.6.2 Asymmetric direct approach through oxa-Michael desymmetrization

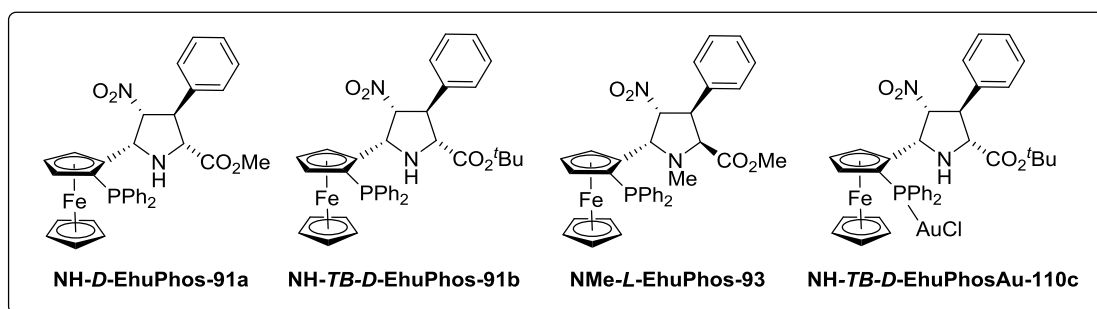
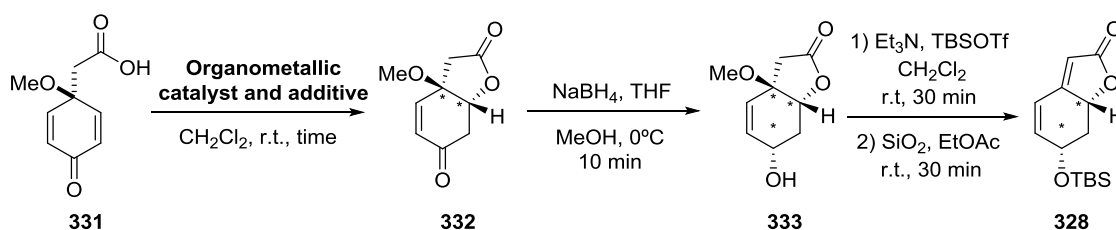
Following the same synthetic pathway, asymmetric oxa-Michael desymmetrization of 2,5-cyclohexadienone **331** could lead to the enantiopure formation of lactone intermediate **328**.



Scheme 3.39. Possible synthetic route toward the synthesis of lactone **328**. Oxa-Michael desymmetrization can be carried out in an enantioselective fashion.

First of all, some differences need to be highlighted between the racemic and asymmetric version. Initially, compound **331** was purified prior to its use in the asymmetric approach in order to avoid the presence of any possible cyclized lactone **332**. Secondly, compound **332** showed to be unstable in presence of silica gel and compound **333** exhibited degradation products if it was injected in HPLC and passed through a chiral column. Hence, enantiomeric excesses of the transformation were always measured by injecting compound **328** in HPLC.

Our first asymmetric approach toward oxa-Michael reaction was to test the ferrocenyl-proline ligands employed in cycloaddition reactions in the previous Chapter. The use of the ligand in combination with different metallic salts was considered being the results collected in **Table 1**. Results obtained for oxa-Michael desymmetrization starting from quinone **331** showed long reaction times for reactions that were not fully converted into lactone **332**. Furthermore, the overall yields were between 19-31% obtaining intermediate **328** with no enantiocontrol at all. In summary, metallic catalysis using ferrocenyl-proline ligands or ferrocenyl gold complexes did not provide any asymmetric approach toward lactone **328**.

Table 1. Results for the asymmetric synthesis of key intermediate **328** catalyzed by ferrocenyl compounds and metallic salts

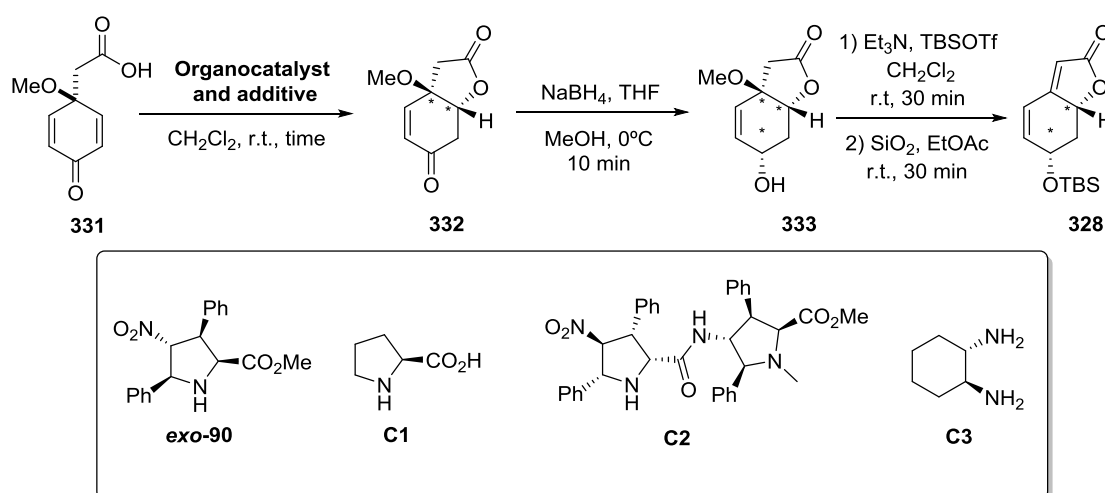
Entry	Metallic salt	Ligand or precatalyst	Additive	Reaction time ^a	Conversion ^b (%)	ee ^c (%)	Yield ^d (%)
1	$\text{Cu}(\text{CH}_3\text{CN})_4\text{PF}_6$	91b	-	4d	77	4	31
2	$\text{Cu}(\text{CH}_3\text{CN})_4\text{PF}_6$	93	-	5d	82	0	19
3	$\text{Cu}(\text{OTf})_2$	91b	-	4d	67	0	25
4	AgBF_4	91b	-	7d	73	4	25
5	Au(I) complex	110c	AgBF_4	3d	74	4	10
6	Au(I) complex	110c	$\text{Cu}(\text{OTf})_2$	5d	64	0	19
7	$\text{Pd}(\text{OAc})_2$	91b	-	3d	>95	6	19

All reactions were carried out using 3 mol% of metallic salt and 3.3 mol% of ligand. ^aReaction time for oxa-Michael desymmetrization. ^bConversion determined by ^1H NMR spectroscopy for oxa-Michael reaction. ^cEnantiomeric excess was measured by injection in HPLC, chiral column AS-H in 85/15 *n*-hexane/isopropanol, 0.7 mL/min, $\lambda = 254$ nm, $t_{\text{r}1}=9.6$ min, $t_{\text{r}2}=11.1$ min. ^dOverall yield calculated for purified compound **328** after four synthetic steps.

In view of these results we envisioned the enantioselective approach by using organocatalysts in order to generate lactone **328**. In that sense, proline-derived catalysts have been widely used in efficient enantioselective oxa-Michael reactions and desymmetrization reactions with 2,5-cyclohexadienones. Combination of this type of catalysts and α,β -unsaturated carbonyl compounds lead us to iminium ion catalysis. Indeed, the use of proline derivatives as catalysts could activate the carbonyl of the dienone, accelerate the oxa-Michael reaction and promote a diastereofacial impediment.

CHAPTER 3

Table 2. Results obtained by using proline based organocatalysts and diamine **C3**.



Entry	Organocatalyst	Additive/Solvent	Reaction time ^a	Conversion ^b (%)	ee ^c (%)	Yield ^d (%)
1	exo-90	CH ₂ Cl ₂	40 h	75	4	38
2	C1	CH ₃ CN	16 h	51	0	8
3	C2	CH ₂ Cl ₂	23 h	74	0	25
4	C3	CH ₂ Cl ₂	16 h	78	2	17
5	C3	TFA/CH ₂ Cl ₂	4d	50	0	10
6	C3	B.A./CH ₂ Cl ₂	20 h	80	4	11

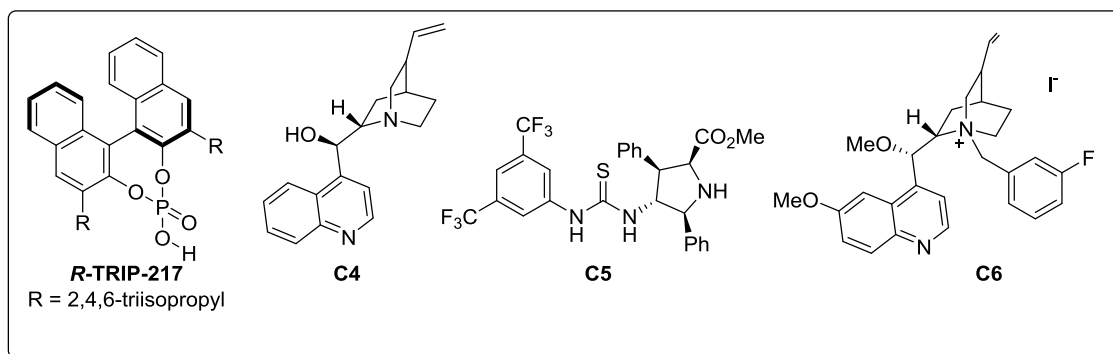
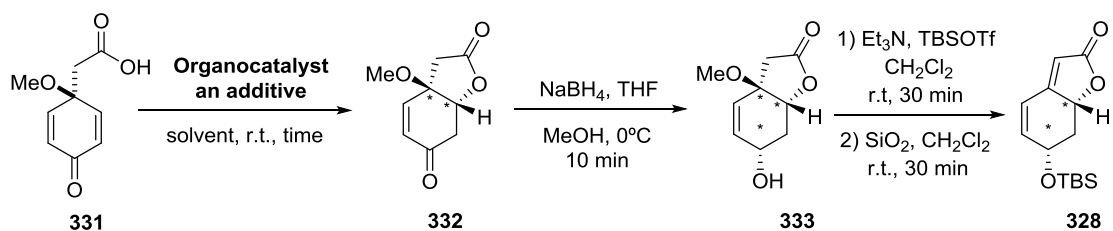
All catalysts were employed in a 10 mol% catalytic loadings. When additives were employed, loading of 20 mol% was used. ^aReaction time for oxa-Michael desymmetrization. ^bConversion determined by ¹H NMR spectroscopy for oxa-Michael reaction. ^cEnantiomeric excess was measured by injection in HPLC, chiral column AS-H in 85/15 *n*-hexane/isopropanol, 0.7 mL/min, λ = 254 nm, *t*_{r1}=9.6 min, *t*_{r2}=11.1 min. ^dOverall yield calculated for purified compound **328** after four synthetic steps. B.A. = benzoic acid.

The three proline based organocatalysts employed in the oxa-Michael desymmetrization gave rise to racemic lactone **328** in all the cases (Table 2, entries 1-3). Remarkably, catalyst **C2** showed good reactivity in shorter reactions times than the other two catalysts.

On the other hand, cyclic chiral diamine **C3** considered also as a covalent organocatalyst was used in different reaction conditions. Once more, desymmetrization in presence of catalyst **C3** in DCM led to similar reactivity and enantiomeric excesses as for the proline derivatives (Table 2, entry 5). Then, we envisioned the combination of organocatalyst **C3** with additives such as, TFA or benzoic acid in the oxa-Michael reaction. Although the iminium catalysis is generally favored in the presence of acid cocatalysts, in this case did not improve either the reactivity or the enantioinduction. (Table 2, entries 6 and 7). Moreover, the use of TFA as additive presented a lower conversion (50% after 4 days) for the oxa-Michael step (Table 2, entry 6).

This last result suggests that the basicity of the reaction media is necessary for the full conversion of the reaction. Thus, this could mean that the organocatalysts are acting as bases more than generating the iminium ion. In any case, it could also be possible that even the iminium ion is properly formed these catalysts do not induce an efficient blockage of one of the enantiotopic faces, and thus, all products obtained are racemic.

Table 3. Results obtained for the asymmetric synthesis using ligands **C4**- **C6** and **217**.



Entry	Organocatalyst	Additive/Solvent	Reaction time ^a	Conversion ^b (%)	ee ^c (%)	Yield ^d (%)
1	217	CH ₂ Cl ₂	23 h	85	16	5
2	217	Toluene	41 h	83	0	18
3	217	MeOH	4d	50	0	18
4	217	EtOAc	7d	60	0	26
5	C4	CH ₂ Cl ₂	16 h	72	0	25
6	C5	CH ₂ Cl ₂	19 h	70	0	40
7	C6	CH ₂ Cl ₂	16 h	90	0	36

All catalyst were employed in a 10 mol% catalytic load. ^aReaction time for oxa-Michael desymmetrization. ^bConversion determined by ¹H NMR spectroscopy for oxa-Michael reaction. ^cEnantiomeric excess was measured by injection in HPLC, chiral column AS-H in 85/15 *n*-hexane/isopropanol, 0.7 mL/min, λ = 254 nm, tr₁ = 9.6 min, tr₂ = 11.1 min. ^dOverall yield calculated for purified compound **328** after four synthetic steps.

CHAPTER 3

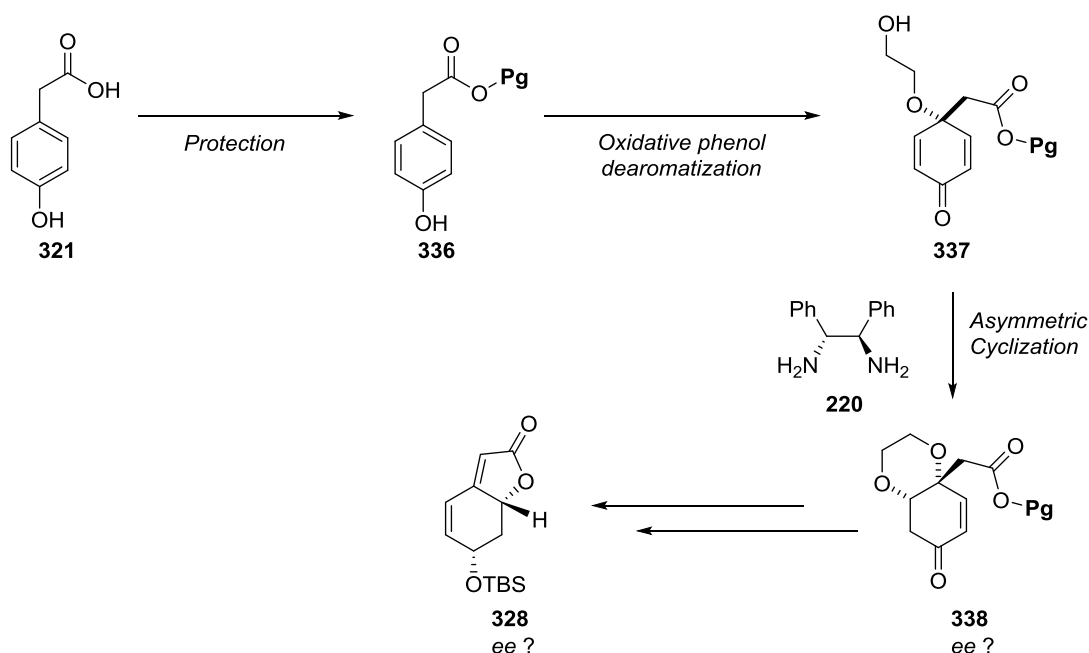
In view of the results obtained with organocatalysts that bind the substrate in a covalent way, we decided to focus on the non-covalent organocatalysts. This type of catalysts generally presents weak interactions with the substrate such as, hydrogen bonds or ionic pair interactions. In this field, the use of chiral phosphoric acids (strong Brønsted acids) in enantioselective desymmetrization of alcohols has been previously reported. On the contrary, it is important to note that there are no references in literature related to the oxa-Michael desymmetrization of carboxylic acids in an enantioselective fashion. In view of this background, we envisioned the use of chiral phosphoric acid **R-TRIP-217** as organocatalyst that could possibly lead to the desired improvement of the enantiomeric excess.

Therefore, the results obtained from the employment of **R-TRIP-217** in our asymmetric approach are gathered in **Table 3**. When the reaction with this chiral phosphoric acid was carried out in DCM we observed the best enantiomeric excess value obtained to date for the lactone **328** (**Table 3**, entry 1, 16% ee). Then, we studied the influence of the solvent in the enantiocontrol of the reaction. When toluene was selected as solvent we noticed a similar conversion toward the product but with the total loss of the enantiomeric excess (**Table 3**, entry 2). The switch to more polar solvents such as, EtOAc and MeOH, led to the formation of lactone intermediate in long reaction times as a racemic mixture (**Table 3**, entry 3-4). As it has been mentioned before, literature does not describe any asymmetric oxa-Michael desymmetrization with carboxylic acids. The hybridization of carbon in carboxylic acid is sp^2 , and the carbon adjacent to alcohols that undergo efficient oxa-Michael desymmetrization are sp^3 hybridized. Hence, it is possible that the lack of enantiocontrol observed can be related to the not optimal approximation of the orbitals during the oxa-Michael step.

In the light of this, other type of non-covalent organocatalysts were tried. Cinchonidine **C4** (Brønsted base) catalyzed efficiently the oxa-Michel reaction, but once again, giving rise to a racemic compound (**Table 3**, entry 5). Pyrrolidine derived thiourea **C5** (Brønsted acid) and the chiral ammonium salt **C7** (presents ionic pair interaction), as well as cinchonidine, afforded racemic mixtures of the lactone **328** (**Table 3**, entry 6-7).

3.6.3 Asymmetric alternative strategy in oxa-Michael desymmetrization

In view of the unfortunate results obtained with the direct approach toward the oxa-Michael reaction, another strategy was proposed for the achievement of enantiopure lactone **328**. As it has been reported by Ye²⁸ and coworkers, desymmetrization of 2,5-cyclohexadienones to obtain 1,4-dioxane compounds works in a highly enantioselective way using chiral primary diamines.

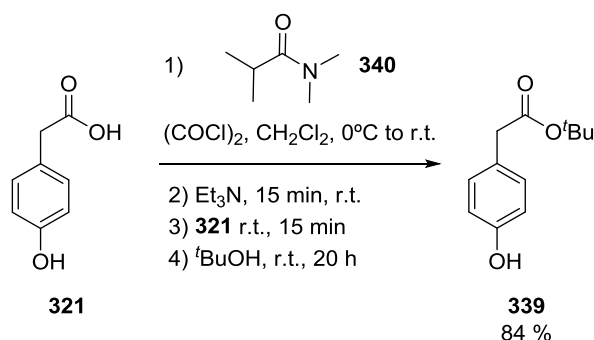


Scheme 3.40. Novel synthetic strategy toward the generation of enantiopure intermediate **328**.

In this strategy, our goal was to introduce an ethylene glycol moiety instead of methoxy group coming from methanol, and protect the acid moiety (**Scheme 3.40**). The use of chiral diamines could then afford a first desymmetrization in which excellent enantiocontrol will be accomplished. Then a second oxa-Michael addition by removal of protecting group of the acid would generate a tricyclic compound, that after elimination of 1,4-dioxane could led to lactone intermediate **328**.

First of all, protection of the carboxylic acid was studied. Protection by transforming the acid into a *tert*-butyl ester was best candidate for this strategy because it can be deprotected in the presence of Brønsted acids but is stable under other reaction conditions. Several coupling agents were studied in order to find a mild methodology for the protection of the carboxylic acid. After several tests for the generation of the *tert*-butyl ester derivative of **321**, the most efficient methodology was found to be the use of Ghosez's reagent (**Scheme 3.41**). Indeed, unlike coupling reaction using DCC, less byproducts were observed. Due its high cost, and to its instability over time, *in situ* formation of the active species was studied by our group. This study has led to a 4 steps/one pot procedure yielding 84% of compound **339** (unpublished results, Dr. Peixoto). This is to the best of our knowledge the most efficient synthetic procedure to form *tert*-butyl ester in basic conditions.

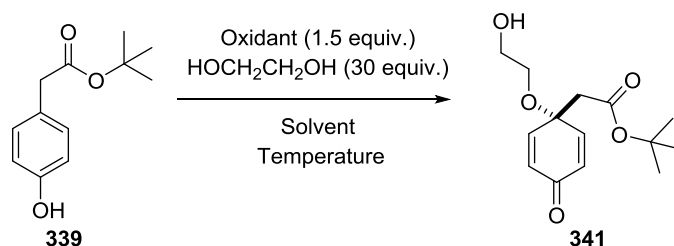
CHAPTER 3



Scheme 3.41. Synthesis of the *tert*-butyl ester **339** by *in situ* formation of Ghosez reagent.

Secondly, we evaluated the conditions for the oxidative dearomatization of compound **339** in which ethylene glycol could be introduced. For that, PIDA was first chosen to carry out a preliminary test using DCM as solvent of choice (**Table 4**, entry 1).

Table 4. Optimization of the oxidative phenol dearomatization of ester **339** toward compound **341**..

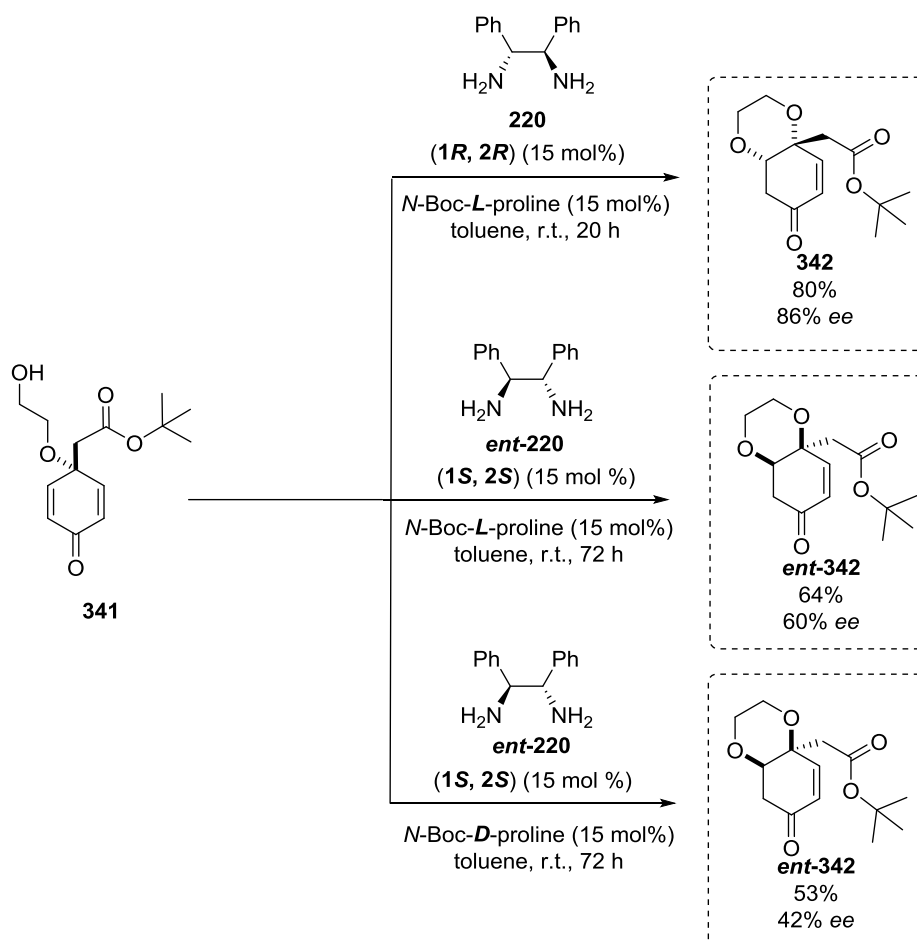


Entry	Solvent	Oxidant	T ($^\circ\text{C}$)	Yield (%)
1	CH_2Cl_2	PIDA	0°C to r.t.	9
2	CH_2Cl_2	PIFA	0°C	Cyclized Product
3	-	PIDA	0°C to r.t.	11
4	CH_2Cl_2	PIDA	r.t.	18
5	CH_3CN	PIDA	r.t.	31

All reactions were carried out in concentration of 0.25 M. Reaction was monitored by TLC.

In order to improve the yield of the reaction we evaluated other λ^3 -iodanes such as PIFA (**Table 4**, entry 2). Due to the fact that PIFA is more reactive than PIDA, reaction was carried at 0°C for 2 hours. Unfortunately, before the reaction was finished, it was possible to observe the formation of lactone due to the cyclization favored by TFA released during the reaction. Another test carried out was the use of pure ethylene

glycol in absence of solvent (**Table 4**, entry 3) in which there was no significant improvement of the yield. When the addition of PIDA was tried directly at room temperature a slight increase in the yield was observable (**Table 4**, entry 4). Finally the change of solvent to ACN made the reaction mixture more soluble, and thus, improved the yield of the reaction to 31% at room temperature (**Table 4**, entry 5).



Scheme 3.42. Enantioselective oxa-Michael desymmetrization by using chiral diamines **220** and **ent-220**.

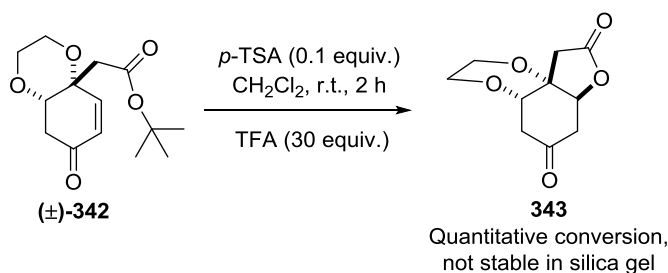
At this point, desymmetrization catalyzed by chiral diamines was applied to substrate **341**. As it is depicted in **Scheme 3.42**, enantioselective oxa-Michael reaction in presence of diamines **210** and **ent-210** led to the formation of two different enantiomers **342** and **ent-342**, respectively. Diamine **210** catalyzed desymmetrization of compound **341** led to the corresponding 1,4-dioxane **342** in 86% of enantiomeric excess. On the other hand, if chiral diamine **ent-220** was used for desymmetrization of molecule **341**, **ent-342** was obtained with moderate enantiocontrol (**Scheme 3.42**, reaction 2).

CHAPTER 3

The employment of *N*-Boc-*D*-Proline (**Scheme 3.42**, reaction 3) led to the formation of **ent-342** but with a slight decrease on the enantiomeric excess of the compound comparing to the use of *L*-Proline additive.

These results were really encouraging in order to develop the asymmetric total synthesis of *Securinega* alkaloids. Crystals of enantioenriched compound **342** were obtained several times, but unfortunately they were not suitable for their analysis by X-ray diffraction. Due to that, absolute configuration of each enantiomer remains unknown, and enantiomers are represented in their relative configurations.

Although the asymmetric desymmetrization was successful by using chiral diamines, the optimization of the rest of the process was developed with racemic compounds. Thus, compound (\pm)-**342** was deprotected (removal of *tert*-butyl moiety) and exposed to subsequent oxa-Michael cyclization in presence of *p*-TSA. The crude mixture of the reaction demonstrated the formation of clean compound **343**, which was used without further purification in order to avoid the reversibility of the transformation.



Scheme 3.43. Deprotection of *tert*-butyl ester and direct cyclization to compound **343**.

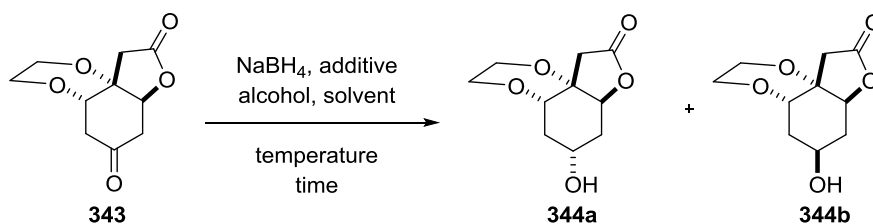
Inspired by the racemic synthesis of intermediate **328**, the reduction of ketone **343** was studied. The same reaction conditions for the reduction were first applied to ketone **343**, observing the formation of two alcohols in a 78:22 diastereomeric ratio (**Table 5**, entry 1). Further attempts were carried out in order to improve the diastereocontrol, and thus, the yield of the reaction.

When the reaction was run in THF with a subsequent addition of methanol at -40°C alcohols **344** were not afforded (**Table 5**, entry 2). On the contrary, when MeOH was used in absence of THF, compounds **344a** and **344b** were obtained in a similar diastereomeric ratio as entry 1 (**Table 5**, entry 3). Additionally, reaction was tried using isopropanol, a more hindered alcohol than methanol, just to observe the effect in the diastereocontrol, in which a 80:20 ratio was obtained for compounds **344a** and **344b** (**Table 5**, entry 4). Furthermore, we envisioned the use of $\text{CeCl}_3 \cdot 7 \text{H}_2\text{O}$ in order to increase the diastereocontrol, but reaction did not go to completion at -78°C (**Table 5**, entry 5). The presence of $\text{CeCl}_3 \cdot 7 \text{H}_2\text{O}$ in the reaction at -40°C using MeOH as solvent did not provide the desired products, and in THF at 0°C did not improve the diastereocontrol of the reduction process (**Table 5**, entries 6-7).

Finally the use of 5 equiv. of NaBH_4 in THF/MeOH 4:1 ratio, starting at the temperature of -40°C and stirring for 2 hours until 0°C was achieved, showed full

conversion and best diastereomeric relation of 86:14 (**Table 5**, entry 8). If reaction was carried out at -78°C , similar diastereomeric excess as in entry 8 was observed but the crude mixture presented some byproducts (**Table 5**, entry 9). Assignment of the relative configuration for major compound **344a** was determined by the spectroscopic analysis of compound **345**.

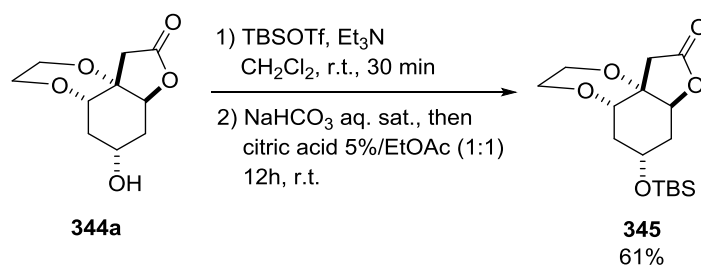
Table 5. Optimization of ketone reduction of compound **343**.



Entry	Solvent	NaBH ₄ equiv.	Additive	Alcohol	Temperature, time	d.r. ^a
1	THF	2	-	MeOH	0°C, 10 min	78:22
2 ^b	THF	2	-	MeOH	-40°C, 20 min	-
3	MeOH	2	-	-	-40°C, 20 min	76:24
4	THF	2	-	<i>i</i> PrOH	0°C, 10 min	80:20
5 ^c	MeOH	0.5	CeCl ₃ ·7H ₂ O (1 equiv.)	-	-78°C, 40 min	-
6 ^d	MeOH	1	CeCl ₃ ·7H ₂ O (2 equiv.)	-	-40°C, 20 min	-
7	THF	2	CeCl ₃ ·7H ₂ O (2 equiv.)	MeOH	0°C, 10 min	72:28
8	THF	5	-	MeOH	-40°C to 0°C, 2 h 0°C to r.t. 15 min	86:14
9 ^e	THF	5	-	MeOH	-78°C, 3 h r.t. 15 min	85:15

^ad.r. = diastereomeric ratio, measured by ¹H NMR in CDCl₃. ^bStarting material recovered, no trace of reduction product. ^cReaction was not complete so starting material does not let to estimate the diastereomeric ratio. ^dStarting material and several byproducts observed. ^eReaction showed byproduct formation in the crude but no more starting material.

The major alcohol **344a** obtained after the reduction of ketone was protected with TBSOTf, as our previous experience in the synthesis of lactone **328** suggested the possible formation of corresponding silyl enol ether. Treatment of the crude with saturated solution of NaHCO₃, and subsequent stirring of the crude mixture in EtOAc/citric acid 5% (1:1) for 12 hours gave rise to product **345** as a major product in a 61% yield.



Scheme 3.44. Secondary alcohol silylation of compound **344a**.

Relative configuration of compound **345** was established by bidimensional NOESY experiment. Methylene protons belonging to the 1,4-dioxane moiety showed a chemical correlation in space with the protons of the tert-butyl fragment of the TBS group, thus concluding that the lactone ring is placed in *trans* to the OTBS and 1,4-dioxane. Therefore, configuration of major alcohol was set, the one depicted in **Table 5** for **344a**.

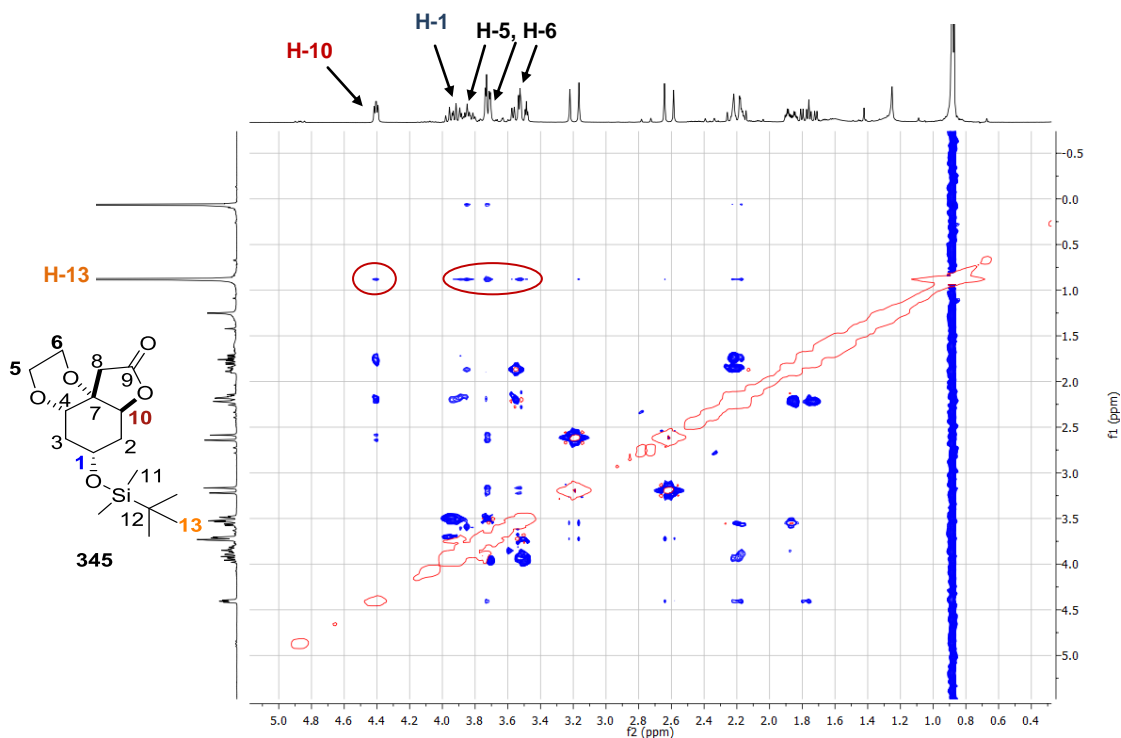
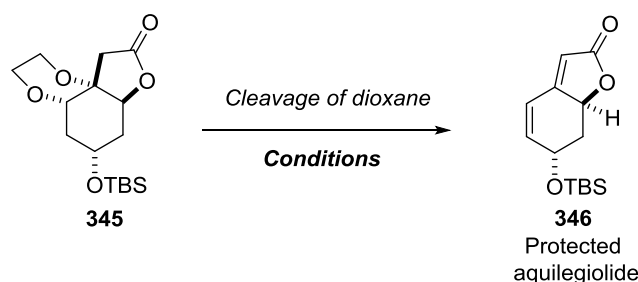


Figure 3.14. 2D NOESY experiment of compound **345**.

Our efforts were focused on the cleavage of 1,4-dioxane of tricyclic compound **345**. In **Table 6** are herein described the different reagents tried for the removal by elimination of the dioxane moiety with the purpose to achieve lactone intermediate **328**. Instead, the stereochemistry set for compound **345** suggested that after cleavage, protected Aquilegiolide **346** could be obtained.

Table 6. Reaction conditions for the removal of 1,4-dioxane moiety of compound **345**.

Entry	Solvent	Reagents	T (°C)	Observed
1	Acetone	1) Iodine 2) <i>p</i> -TSA and TFA	r.t. to reflux	Degradation
2	THF	PIDA, 2,6-lutidine	r.t.	345
3	THF	<i>t</i> BuO [−] K ⁺	0°C	Degradation
4	Toluene	Iodine, PPh ₃	r.t. to 100°C	345
5	Acetone	Cu(OTf) ₂	0°C, 30 min then r.t. 2 h	344a
6	CH ₂ Cl ₂	BBr ₃	0°C and r.t.	??

All reactions were carried out in concentration of 0.25 M. Reaction was monitored by TLC.

Usual cleavage of 1,3-dioxanes was tried first by using iodine/acetone first, then addition of *p*-TSA and finally addition of TFA at r.t. and reflux. Compound suffered degradation under reflux and presence of TFA, while it remained intact under other conditions (**Table 6**, entry 1). Activation of oxygen atoms by using hypervalent iodine reagents like PIDA did not showed any conversion (**Table 6**, entry 2). Strong basic conditions by using potassium *tert*-butoxide just led to the degradation of compound **345**, (**Table 6**, entry 3).

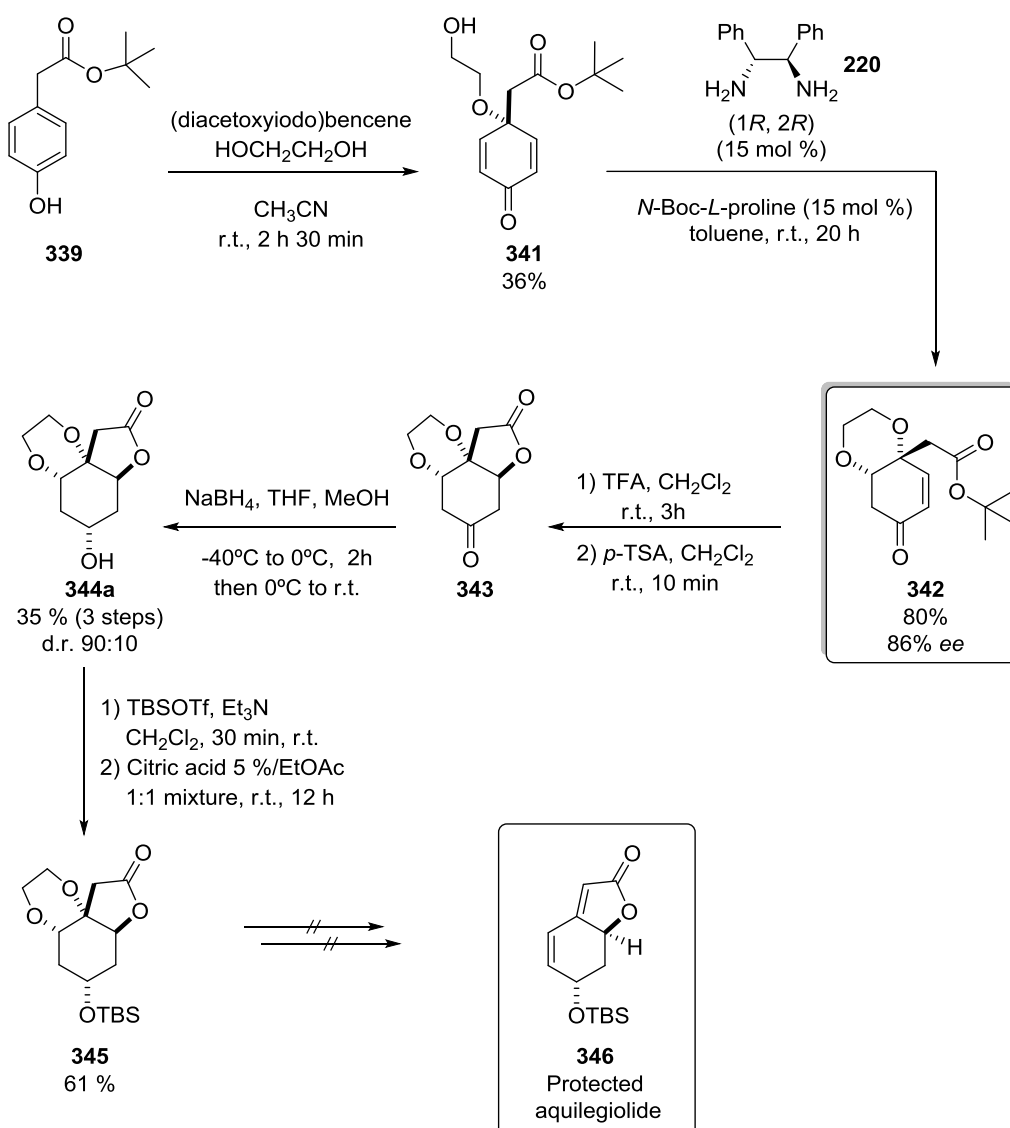
PPh₃ and iodine in combination were not able to activate enough the oxygens of dioxane and starting material was recovered (**Table 6**, entry 4). Lewis acid activation led to the sole deprotection of the secondary alcohol it was obtained as **344a** (**Table 6**, entry 5). Similar cleavage of ethers in presence of lactones was reported.⁶² The methodology using BBr₃ was applied to compound **345** and led to the formation of new compound observable by ¹H NMR spectroscopy. Unfortunately, due to small amount of product isolated efforts to purify it and characterize by NMR spectroscopy were not enough and low mass spectroscopy did not provide conclusive results.

To conclude, the removal of 1,4-dioxane moiety of compound **345** was found to be impossible. Due to the lack of alternatives in literature associated with the difficulties encountered with the removal of this dioxane moiety, this asymmetric version was finally abandoned. We thus turned our attention to the completion of the stereoselective (but racemic) total synthesis of neosecurinane and neonorsecurinane-related natural

⁶² Corey, E. J.; Weinshenker, N. M.; Schaaf, T. K.; Huber, W., *J. Amer. Chem. Soc.*, **1969**, 91, 5675-5677.

CHAPTER 3

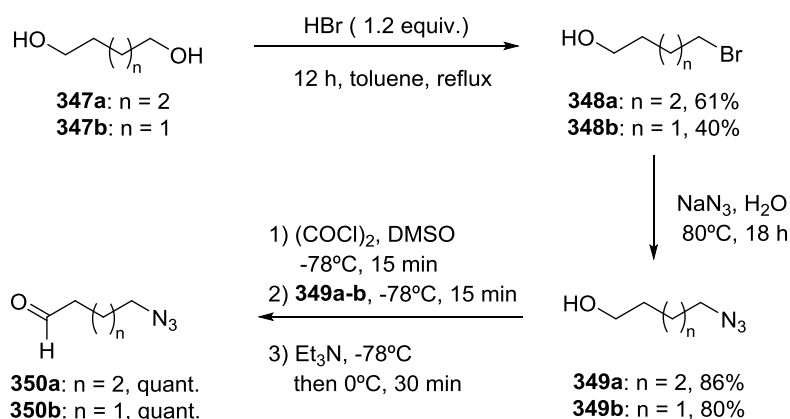
products. The synthetic effort developed for the alternative asymmetric strategy is depicted in **Scheme 3.45**.



Scheme 3.45. Synthetic efforts for the alternative asymmetric synthesis of intermediate **346**.

3.6.4 Development of Aldol reaction and Swern oxidation

Inspired by Gademan' and Busqué's approaches, with lactone **328** in hand, we have then planned to construct the **A** cycle thanks to the reactivity of the enol(ate) deriving from β -deprotonation of the butenolide moiety. However, instead of performing a Mannich-type condensation on a cyclic amine, we herein decided to couple an azidoaldehyde through a classical aldol reaction. Such aldol-type mediated linkage would thus turn the synthetic sequence more divergent, and could possibly lead to a collective access to the members of this natural product family. The synthesis of corresponding azido-aldehydes is described in **Scheme 3.46**.



Scheme 3.46. Synthesis of aldehydes **350a-b** bearing an azide functional group.

The synthesis of the aldehydic synthons **350a** and **350b** starts from the monobromination of the respective diol **347a** or **347b**.⁶³ Brominated compounds **348a-b** were then dissolved in H_2O and a nucleophilic substitution using sodium azide yielded azides **349a-b** in good yields.⁶⁴ It is important to note that both bromination and azide formation steps provided a sole product with no need of purification. With azides **349a-b** in hand, a final oxidation of alcohols into aldehydes was carried out in Swern conditions to form the corresponding aldehydes **350a-b** in a quantitative yield.

These aldehydes were then used in the following step for the **A** ring connection. In the following aldol reaction between azidoaldehydes **350a-b** and lactone **328**, LiHMDS stood out as the reagent for the formation of the lithium enolate. Then, we studied the optimization of the aldol process conditions being reported in **Table 7**. For all the cases, we obtained a crude mixture containing four aldol products. Since the four aldol diastereoisomers are later transformed into two easily separable diastereoisomers by Swern oxidation, we did not isolate each of the products in this step. In addition, the yields reported in **Table 7** are related to the mixture of the four diastereoisomers.

When the reaction was carried out in the presence of 1.5 equivalents of LiHMDS and the posterior addition of 3 equivalents of azidoaldehyde **350a** (for the generation of six membered ring) at -78°C we observed the formation of the aldol products as well as a large amount of a new aldehyde containing product. Our hypothesis is that this new aldehyde could result from the homoaldol polymerization reaction of azidoaldehyde **350a**, owing to the presence of LiHMDS in excess (**Table 7**, entry 1).

In order to avoid the formation of the azidoaldehyde derived polymer, we used lower equivalents of LiHMDS and aldehyde **350a**. As a consequence, we observed the

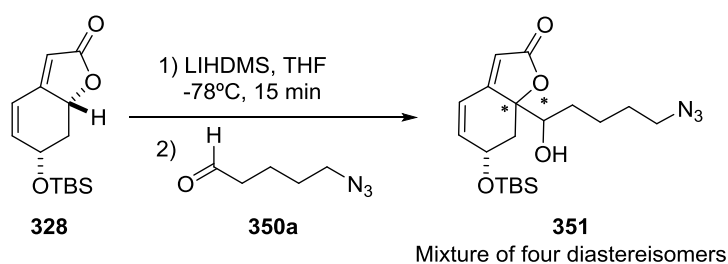
⁶³ Nickel, S.; Serwa, R. A.; Kaschani, F.; Ninck, S.; Zweerink, S.; Tate, E. W.; Kaiser, M., *Chem. Eur. J.* **2015**, 21, 10721–10728.

⁶⁴ Moreno, P.; Quéléver, G.; Peng, L., *Tetrahedron Lett.* **2015**, 56, 4043–4046.

CHAPTER 3

formation of the same products described before, but in this case with a slight improvement of the yield (**Table 7**, entry 2). Moreover, adjusting the equivalents of LiHMDS to 1.5 and adding 1.1 equivalents of azidoaldehyde **350a** at -50°C , right after the formation of the enolate, gave rise to mixture of compounds **351** in a 54% yield (**Table 7**, entry 3). Finally, performing the addition of compound **350a** at -78°C and warming up the reaction to -50°C led to best yield observed for the formation of the mixture of aldol products **351** (**Table 7**, entry 4).

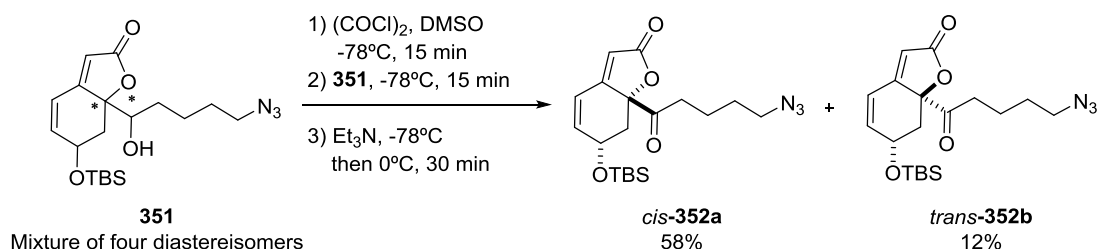
Table 7. Optimization for aldol reaction with LiHMDS.



Entry	LiHMDS equiv.	Aldehyde equiv.	T ($^{\circ}\text{C}$) ^a	Yield (%) ^b
1	1.5	3.0	-78°C to -50°C	24
2	1.1	1.1	-78°C to -50°C	37
3	1.5	1.1	-50°C	54
4	1.5	1.1	-78°C to -50°C	59

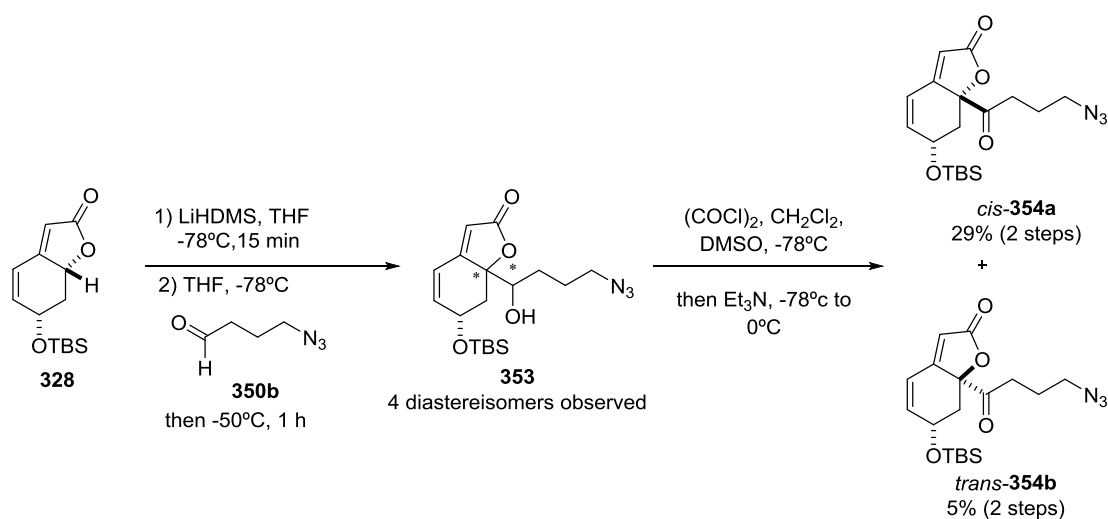
All reactions were carried out using distilled THF in 0.05M concentration and quenched with NH_4Cl at described temperature. ^aTemperature of addition of aldehyde and after addition.
^bIsolated yield respective to the four diastereoisomers after purification.

All the diastereoisomers formed during this aldol reaction were recovered and exposed to Swern oxidation conditions. The reaction led to azidoketones **352a** and **352b** which derived from a *cis* or *trans* bicyclic junction. The diastereomeric ratio observed for the *cis/trans* ketones was 80:20, respectively. Relative configuration of compounds **352a** and **352b** was confirmed by the configuration observed for the final natural products derived from each one.



Scheme 3.47. Synthesis of *cis*-**352a** and *trans*-**352b** from oxidation of aldol mixture **351**.

Similarly, five-membered aldehyde **350b** carried out aldol reaction under optimized reaction conditions. The following Swern oxidation gave rise to compounds **354a** and **354b** as five-membered chain analogues of **352a-b**.



Scheme 3.48. Synthesis of *cis*-**354a** and *trans*-**354b** obtained through classical aldol and subsequent Swern oxidation.

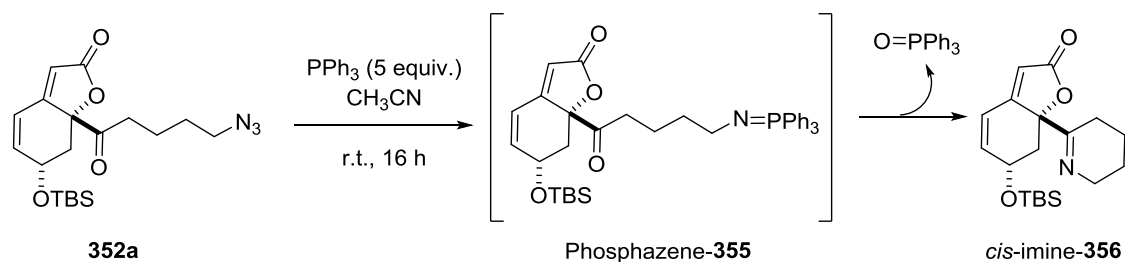
3.6.5 Synthesis of neosecurinine-type natural products

For the synthesis of natural products featuring a 6-membered ring **A** cycle, compound **352a** was first used, as it was obtained as the major product in the Swern oxidation. At this point we envisioned the formation of piperidine ring of the final natural products. For that, Staudinger reaction of azide **352a** could allow the formation of a phosphazene intermediate, which would after undergo through an aza-Wittig reaction in presence of the ketone group (**Scheme 3.49**).⁶⁵ This way, we would be able to obtain a cyclic imine formation just in presence of PPh_3 .

This reaction requires of an optimization in order to enhance the reactivity. After several attempts, in which acetonitrile was distilled carefully in order to avoid presence of water, we found out that degassing the solvent was of major importance. Hence, acetonitrile was degassed for 10 minutes before its use and this way, compound was fully converted into *cis*-imine-**356** within 5 hours. There was no influence on the use of solvent directly from a commercially dried or freshly distilled one. As all the efforts to isolate the imine were in vain, crude of the product was further used without purification.

⁶⁵ Example of combination of Staudinger/aza-Wittig strategy: Pavlova, A. S.; Ivanova, O. A.; Chagarovskiy, A. O.; Stebunov, N. S.; Orlov, N. V.; Shumsky, A. N.; Budynina, E. M.; Rybakov, V. B.; Trushkov, I. V., *Chem. Eur. J.* **2016**, 22, 17967–17971.

CHAPTER 3



Scheme 3.49. Suggested reaction by Staudinger/aza-Wittig combination for azide **352a**.

Crude mixture of compound **356** was then engaged into the following reductive amination. Imine **356** was dissolved in a 1:1 (v/v) mixture of AcOH/THF, and the reaction was monitored by ^1H NMR. Interestingly, prior to the addition of NaBH_3CN , we were able to observe the formation of a new compound that presents the absence of unsaturated proton signal, and thus, suggested an intramolecular cyclization process (compare **Fig. 3.15, A and B**). At this stage we proposed the formation of an enamine intermediate **357** (due to the relative acidity of protons in α position, susceptible to be abstracted with a base) that could directly cyclize through an aza-1,6-addition (see **Scheme 3.50**). This enamine will be favored in the equilibrium with its iminium congener prior to the addition of NaBH_3CN . Further computational studies could shed light on the mechanism of this reaction. Once the imine-**356** signals fully disappeared, NaBH_3CN was added to the mixture and two new products were observable after 30 minutes of reaction (**Scheme 3.50**).

Protected compounds **358a** and **358b** were obtained in a 55:45 diastereomeric ratio. These compounds were susceptible to basic or acidic work up, as it could be observed by ^1H NMR. Depending on this, we observed the formation of different products but after deprotection the different products were capable to yield the same natural products. This could be related to the nature of the amine functionality present in the skeleton of compounds **358a** and **358b** (possible quaternary amine under acidic conditions and tertiary under basic conditions). For all these reasons, compounds **358a** and **358b** were not characterized. Furthermore, in order to avoid the acidity or basicity of the work up, compounds were treated with brine and H_2O , extracted with EtOAc and evaporated to dryness.

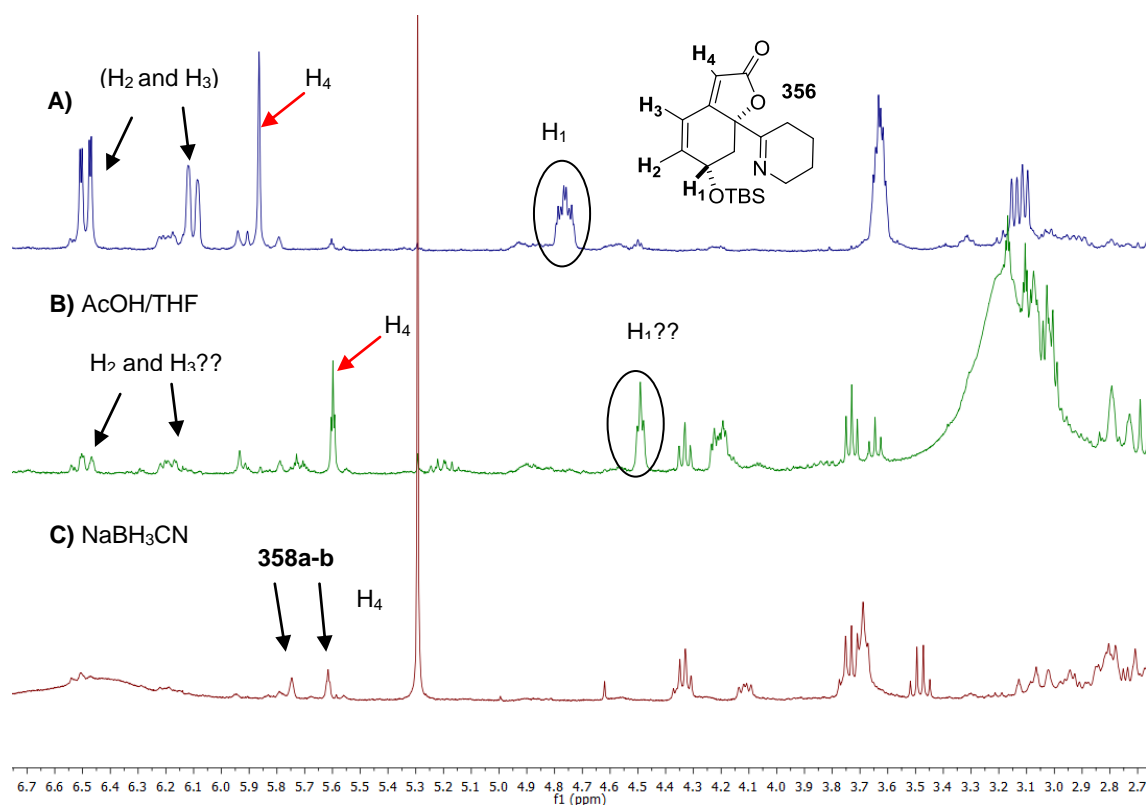
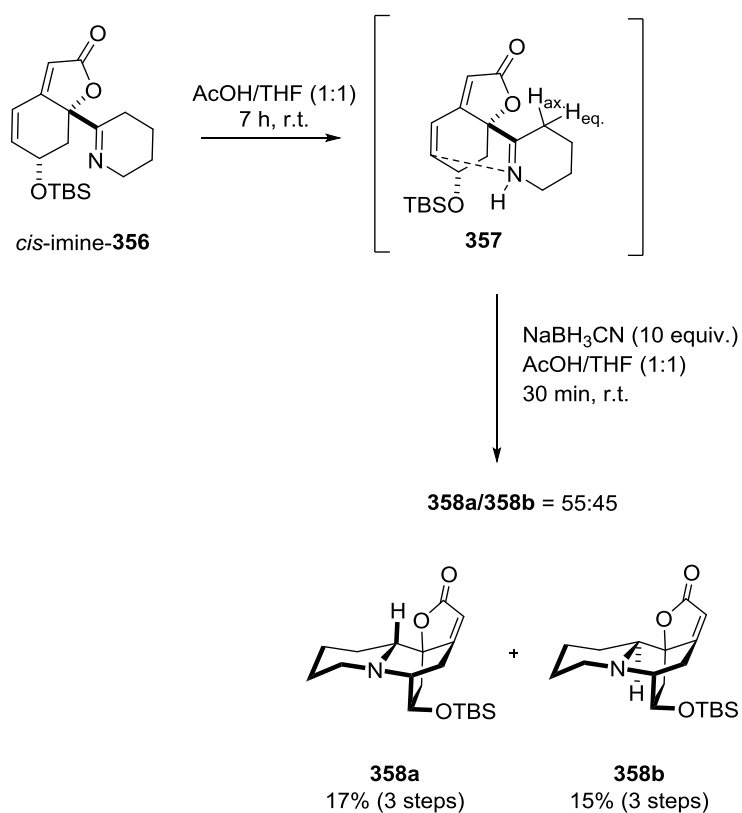


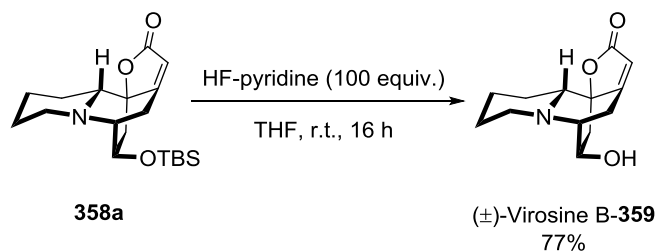
Figure 3.15. Spectra: **1**) compound **356**, **2**) in presence of AcOH/THF 1:1, **3**) after addition of NaBH₃CN, compounds **358a** and **358b** are formed.



Scheme 3.50. Synthesis of protected neosecurinine type compounds by reductive amination and proposed intermediates during the reaction. We suggested this mechanism without further computational or experimental data to confirm it.

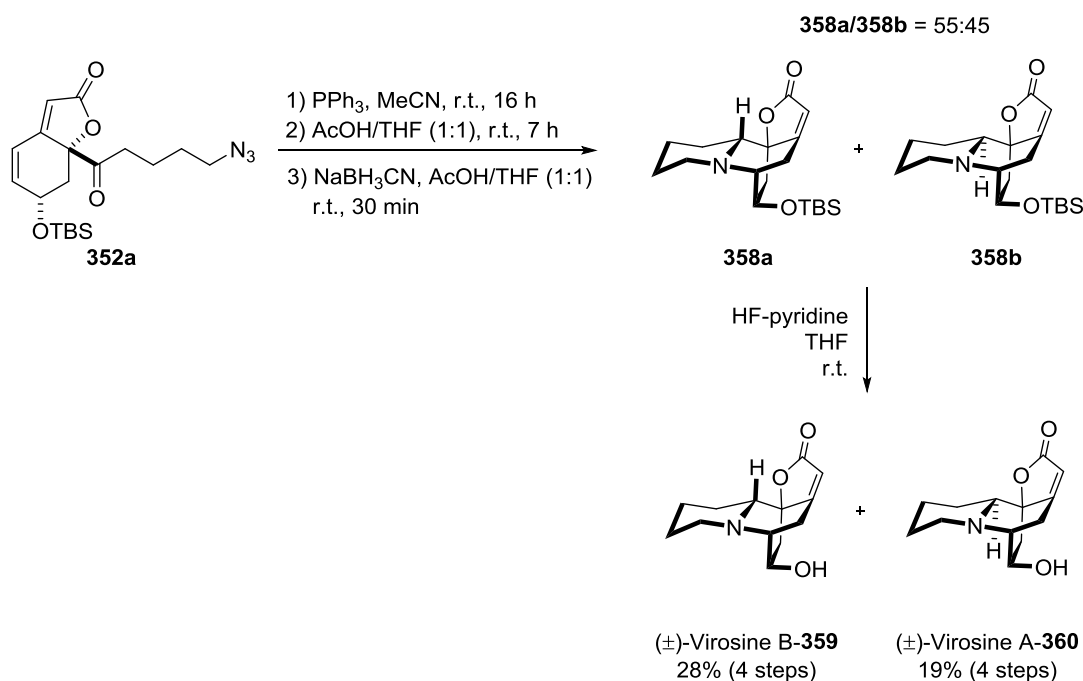
CHAPTER 3

Deprotection using TBAF/AcOH in THF was tested but, in all cases, the formation of several byproducts was observed within the formation of desired product. Only the use of HF-pyridine in THF showed full deprotection of compound **358a** and formation of natural product (\pm)-**Virosine B** (**Scheme 3.51**).³⁷ Methodology could also be applied to the synthesis of **Virosine A** by removal of TBS group from tetracyclic compound **358b**. Spectroscopic data and mass analysis for these natural products were in correspondence with the ones reported in literature⁶⁶ (see Experimental part **3.9.2.5**, **Table 8** and **Table 9**, **Virosine A** and **Virosine B**, respectively).



Scheme 3.51. HF-pyridine mediated deprotection of compound **359a** to afford naturally occurring (\pm)-**Virosine B**.

After studying the whole process, its optimization led to a cascade synthesis starting from azide **352a**, followed by the imine formation, which through a reductive amination and further deprotection led to both natural products by a single purification step. This process is summarized in **Scheme 3.52** for each of the racemic natural products.



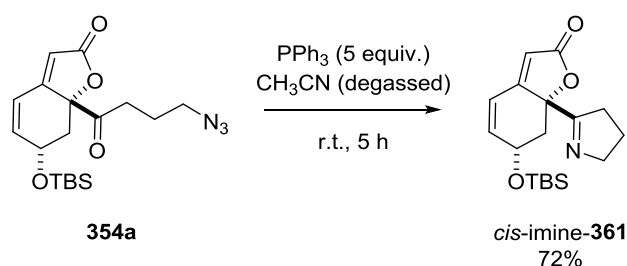
Scheme 3.52. Four step process for the synthesis of neosecurinine type natural products **Virosine B** and **Virosine A**.

⁶⁶ Wang, G.-C.; Wang, Y.; Li, Q.; Liang, J.-P.; Zhang, X.-Q.; Yao, X.-S.; Ye, W.-C., *Helv. Chim. Acta* **2008**, *91*, 1124–1129.

3.6.6 Synthesis of neonorsecurinine-type natural products

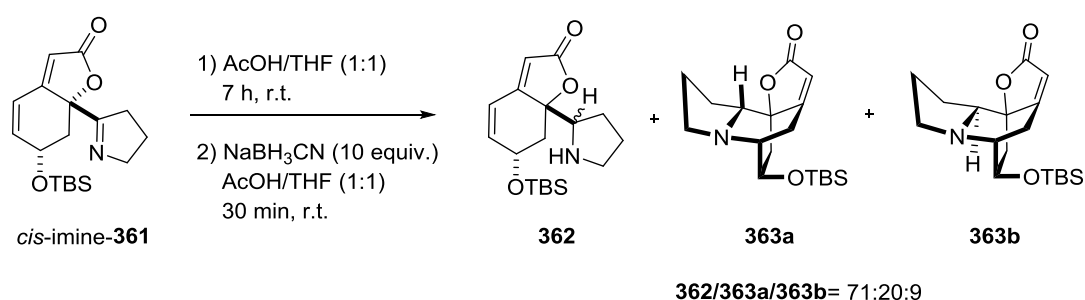
Synthesis of neonorsecurinine-type alkaloids was carried out in similar manner as the previous synthesis of 6-membered ring natural products. Even so, some particularities were observed during the process.

At this time, the Staudinger/aza-Wittig reaction conditions applied to azidoketone **352a** were employed with azide **354a**, which led to the formation of *cis*-imine-**362** as a stable compound. Thereby, it seems that the formation of pyrrolidine derived imine is more stable than the piperidine one.



Scheme 3.53. Staudinger/aza-Wittig reaction of azide **354a** and formation of stable imine **361**.

In contrast to the results observed for the 6-membered ring, if imine **361** was dissolved in a mixture of AcOH/THF no evolution of the product was observed by ^1H NMR. Moreover, addition of NaBH_3CN to the mixture led to the formation of three products observed by ^1H NMR spectroscopy (**Fig. 3.16**): 71% of amine **362**, diastereoisomer **363a** in a 20% and 9% of diastereoisomer **363b**. Thus, we were not able to observe a full conversion toward compounds **363a-b** but amine **362** was mainly isolated.



Scheme 3.54. Reductive amination of imine **361** and presence of three different products in the crude of the reaction.

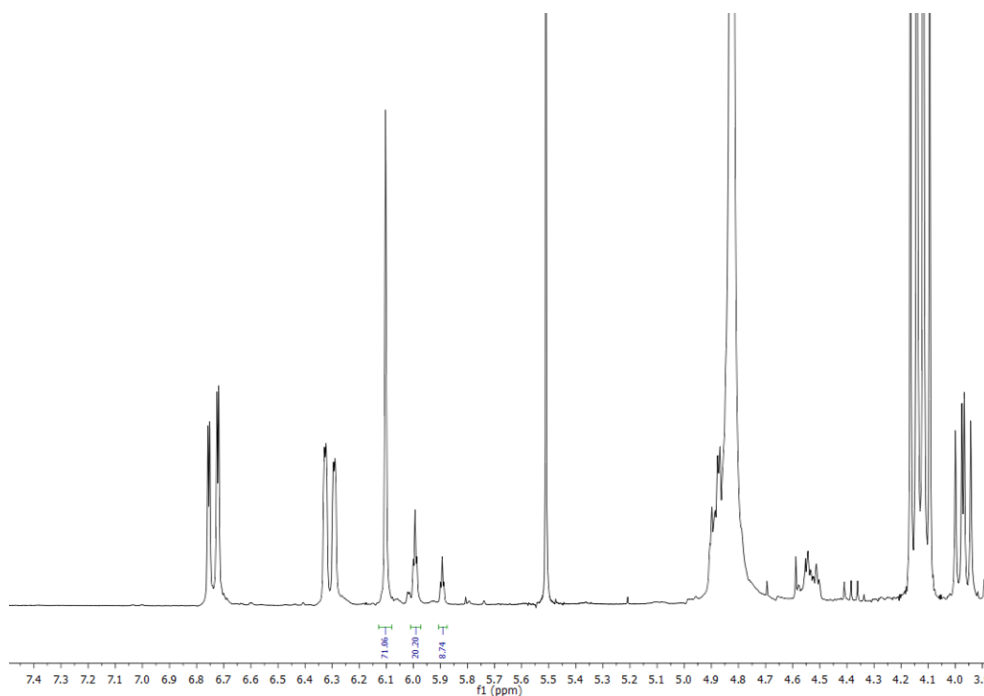


Figure 3.16. Spectrum of crude for the reductive amination explained in **Scheme 3.54**. Integration of signals showed is related to the proton in α to the carbonyl group.

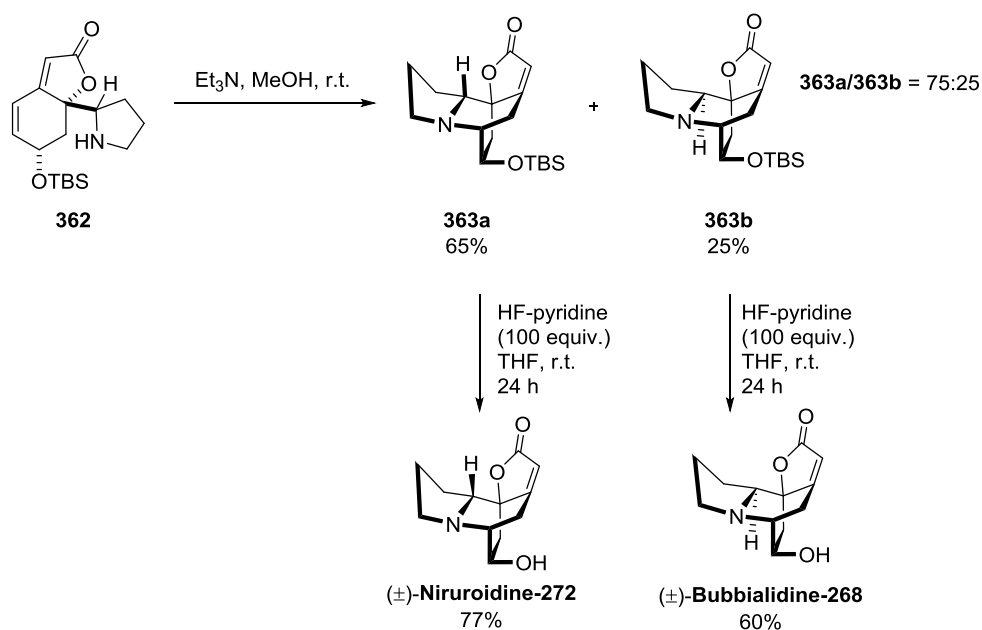
In view of these results, crude mixture of **363a/363b** was dissolved in THF/MeOH mixture 4:1 and tried to cyclize under basic conditions, and for that, aqueous saturated solution of K_2CO_3 was used as base in order to force the cyclization. Compounds **363a** and **363b** were obtained in a ratio of 72:28, but also formation of lactone intermediate **328** was observed, due to a possible retro-Mannich reaction induced by the base and the presence of water.

In view of the presence of byproducts, cyclization of amine **362** was carried out in MeOH and in the presence of 30 equiv. of Et_3N (optimized by M. Kevin Antien). Strategy provided full conversion into diastereoisomers **363a** and **363b** in a 75:25 diastereomeric ratio. After separation by chromatography, compounds were deprotected separately employing HF-pyridine (**Scheme 3.55**). Thus, similarly to neosecurinine-type alkaloids, neonorsecurinine alkaloids (\pm)-**Niruroidine-272** and (\pm)-**Bubbialidine-268** were obtained. Pleasingly, spectroscopic data were in agreement with the ones reported in literature for (–)-**Niruroidine**⁶⁷ and (–)-**Bubbialidine**⁶⁸ (see experimental part, section 3.9.2.6, **Table 10** for **Niruroidine** and **Table 11** for **Bubbialidine**).

⁶⁷ a) Gedris, T. E.; Herz, W.; Florida, T., *Phytochemistry* **1996**, *41*, 1441–1443. b) Ma, N.; Yao, Y.; Zhao, B.-X.; Wang, Y.; Ye, W.-C.; Jiang, S., *Chem. Commun.* **2014**, *50*, 9284–9287.

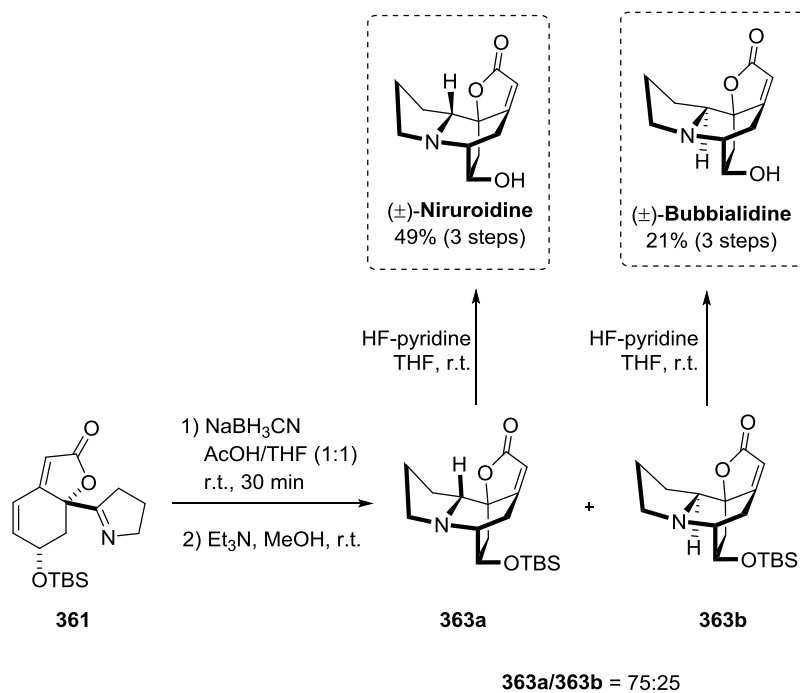
⁶⁸ a) Ahond, A.; Guilhem, J.; Hamon, J.; Poupat, C.; Pusset, J.; Pusset, M.; Sevenet, T.; Potier, P., *J. Nat. Prod.* **1990**, *53*, 875–881. b) Miyatake-Ondozabal, H.; Bannwart, L. M.; Gademann, K., *Chem. Commun.* **2013**, *49*, 1921–3.

SECURINEGA ALKALOIDS



Scheme 3.55. Et_3N mediated addition of amine to lactone and further deprotection of diastereoisomers **363a** and **363b** to afford neonorsecurinine type *Securinega* alkaloids.

Further attempts led to the optimized sequence of reductive amination, cyclization and deprotection as an improved access to *Securinega* alkaloids (**Scheme 3.56**). The optimized reaction sequence yielded **(±)-Niruroidine** and **(±)-Bubbialidine** in a 49% and 21%, respectively.



Scheme 3.56. Synthesis of natural products starting from imine **361**, in three synthetic steps.

CHAPTER 3

Interestingly, in view of the diastereisomeric proportion obtained after the whole process, which favored the formation of (\pm)-**Niruroidine**, we envisioned a computational study in order to understand the mechanism. It is important to note that the 6 membered ring derivatives do not follow the same mechanism due to the differences observed in the relative stability of the intermediates and the diastereomeric ratios of the final products. There is no precedent on the computational study of the stereoselective in the reductive amination reaction of cyclic imines in presence of NaBH_3CN .

The insights of the mechanism for the reductive amination step and the aza-1,6-addition were studied by DFT calculations. The reductive amination reaction was found to be the step that controls the diastereoselectivity of the process. As it can be observed in **Fig. 3.17**, **Rc-364** presents stabilization due to a hydrogen bonding interaction between the oxygen of the lactone and the hydrogen of N-H.

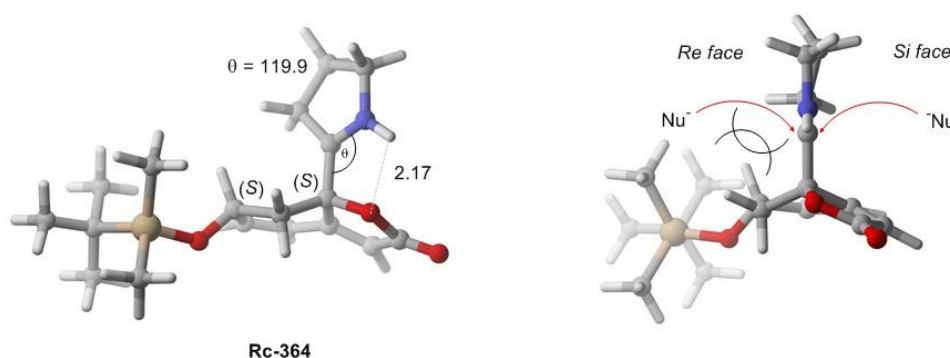


Fig.3.17. On the left, Reactive complex **364**, optimized structure presenting a hydrogen bonding interaction. On the right, possible hydride attacks. Structures obtained at MO6-2X(PCM)/6-311+G(d,p)//B3LYP/6-311G(d) level of theory. Distances are given in Å and angles in deg.

Subsequently, we considered the addition of sodium cyanoborohydride to **Rc-364**. *A priori* there are two possible hydride attacks on the iminium carbon of **Rc-364**, *Re* attack or *Si* attack, depicted in **Figure 3.17**. In this case, the cyanoborohydride could present different interactions with the target molecule, and thus, four possible approaches were considered. These four attacks were analyzed by DFT, and the most stable ones are the represented in **Fig. 3.18**. For both of the cases, there is a N-H bond interaction between the nitrogen of the cyanoborohydride and the proton of the iminium ion. The representation of the transition state for the *Re* attack of the hydride can be found in **Fig 3.18a**. In this case, the hydride attack would set the *S* configuration of the new stereogenic center. The following aza-1,6-addition and deprotection would give rise to (\pm)-Bubbialidine. On the other hand, *Si* attack of the hydride would lead to the formation of a new stereocenter with *R* configuration. After the following 1,6-addition and removal of TBS group, this approach would afford (\pm)-**Niruroidine** as the final product.

The difference of the free energy for these transition states is 0.98 kcal/mol and predicts a ratio of 81:19 in favor of the attack carried out from the *Si* face (leading to

(\pm)-**Niruroidine** as the major product). This value is in agreement with the experimentally obtained 75:25 ratio.

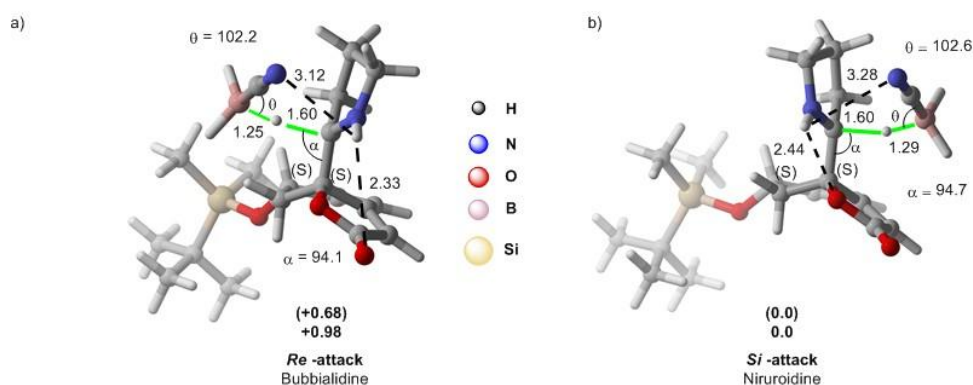
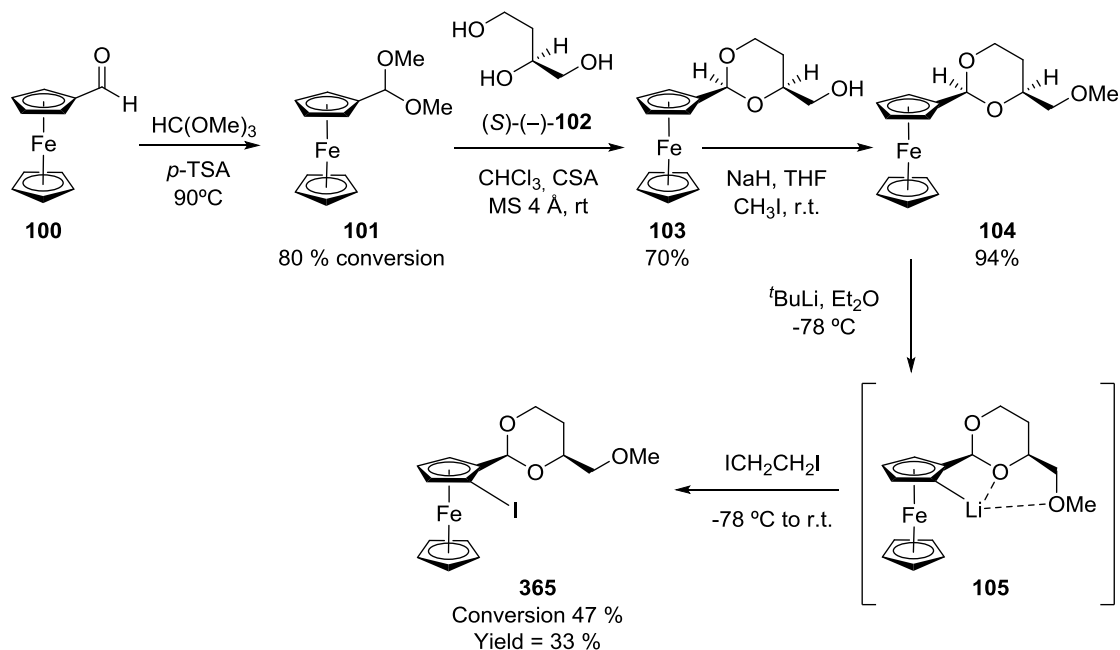


Figure 3.18. Fully optimized transition states associated with the *Re* and *Si* hydride attack and obtained at MO6-2X(PCM)/6-311+G(d,p)//B3LYP/6-311G(d) level of theory. The difference of free activation energies and free relative energies are given in kcal/mol. Distances are given in Å and angles in *deg*.

3.7 Synthesis of Ferrocenyl Iodanes

Our second objective is the synthesis of new ferrocenyl hypervalent iodine reagents, which incorporate planar chirality by themselves.

Synthesis of compound **365** was developed employing the strategy developed by Kagan and coworkers⁶⁹ (**Scheme 3.58**). Commercial ferrocenecarboxaldehyde **100** was converted by several transformations into compound **104**. At this stage, dioxane **104** was treated with *tert*-butyl lithium through a diastereoselective *ortho*-lithiation, controlled by chelation of lithium atom with the chiral 1,3 dioxane. Lithium was able to activate selectively one of the two *ortho* positions of the cyclopentadienyl ring. Finally, quenching with 1,2-diiodoethane afforded compound **365**. Maximum yield for this reaction was around 30-40 % while starting material was always recovered.



Scheme 3.58. Synthesis of iodine containing ferrocenyl compound reported by Kagan.⁶⁹

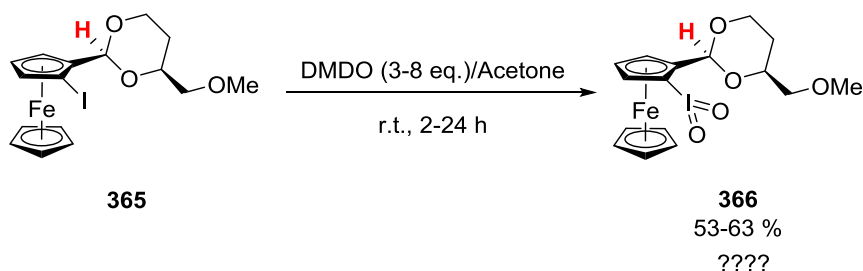
Mass analysis, and ^1H and ^{13}C NMR spectroscopy confirmed the nature of compound **365**. Furthermore, all of these results were in concordance with literature.^{69,70}

With this iodoferrocene synthesized, we turned our attention to the oxidation of the iodine atom according to Quideau's described literature procedure.⁵⁶ They reported the use of DMDO in order to oxidize iodine into λ^3 and λ^5 -iodanes employed in enantioselective phenol dearomatization reactions.

⁶⁹ Riant, O.; Samuel, O.; Flessner, T.; Taudien, S.; Kagan, H. B., *J. Org. Chem.* **1997**, 62, 6733–6745.

⁷⁰ Dayaker, G.; Sreeshailam, A.; Ramana, V.; Chevallier, F.; Roisnel, T.; Komagawa, S.; Takita, R.; Uchiyama, M.; Krishna, P. R.; Mongin, F., *Tetrahedron*, **2014**, 70, 2102-2117.

With this methodology in hand, we treated iodine **365** with 3,3-dimethyldioxirane also known as DMDO (**Scheme 3.59**). The reaction was monitored by taking aliquots from the reaction mixtures after two hours of continuous stirring at room temperature. After a reduction to dryness of the aliquots taken, a brownish solid was obtained and was found to be insoluble in most of the usual deuterated solvents (i.e. CDCl_3 , acetonitrile- d^3 , Methanol- d^4 , $(\text{CD}_3)_2\text{CO}$, TFE- d^3 , 9:1 mixture of $(\text{CD}_3)_2\text{CO}/\text{D}_2\text{O}$, mixture of TFA- d^4/CDCl_3). Finally, small amount of the solid was partially dissolved in $\text{DMSO}-d^6$ and analyzed by ^1H NMR spectroscopy.



Scheme 3.59. Possible λ^5 product **367** expected from oxidation with DMDO of iodoferrocenyl **365**.

It is important to note that signal of carbon ipso for compound **365** (C1-ipso in **Fig. 3.19**) to the iodine atom is known to present a characteristic shift to lower field when iodine is oxidized to λ^3 and λ^5 -iodanes. Similarly, C2 and C3 carbons could present a shift in their signals when iodine is transformed in iodane.

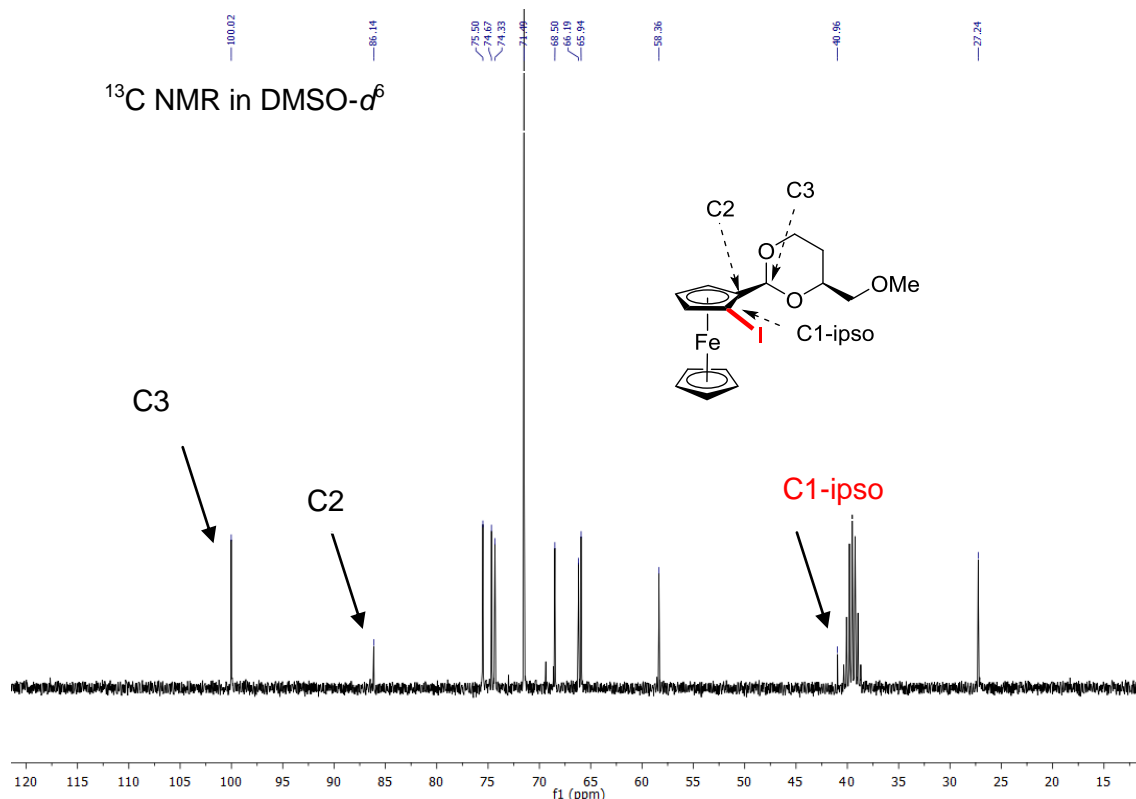


Figure 3.19. ^{13}C spectrum for compound **366** and signal for the carbon-ipso to iodine.

CHAPTER 3

Formation of a new product was observed by ^1H NMR. Indeed, a clear disappearance of the signal corresponding to the acetal proton present in ferrocene **365** (5.37 ppm) coincided with the consecutive formation of a new signal at 5.64 ppm. Interestingly, when the compound was kept dissolved in $\text{DMSO}-d^6$ the new compound was back transformed in iodine **365** through the time.

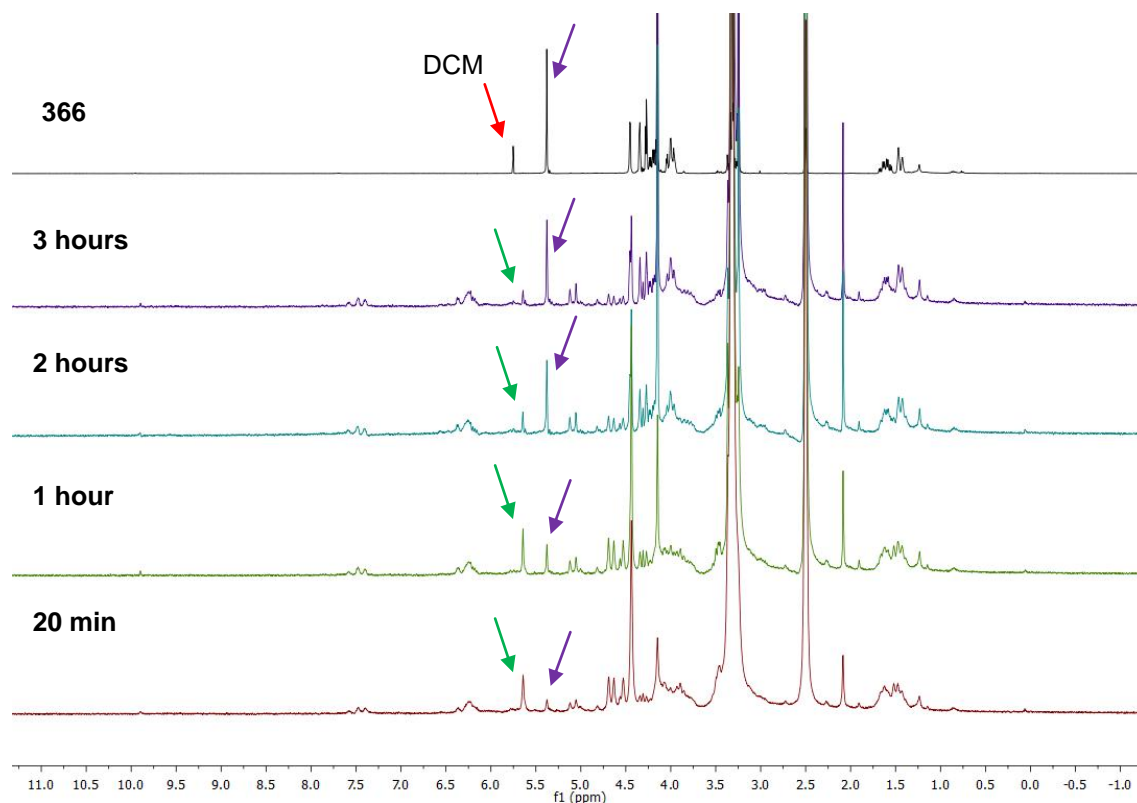


Figure 3.20. ^1H NMR spectra of possible iodane **366** showing the evolution through time in $\text{DMSO}-d^6$.

As it can be observed in **Figure 3.20**, when the reaction was stirred for 20 minutes almost the new acetal signal is observed as the major compound (see **Fig 3.20**, **20 min**, green arrow.). After one hour dissolved in DMSO compounds **365** and **366** showed equilibrated proportion of their signals. In addition, after more than three hours exclusively acetal signal of compound **365** was present (**Fig 3.20**, **3 hours**, purple arrow).

These results demonstrated the instability of iodane **366** in DMSO. Indeed, the later could be oxidized by compound **366** as well as it gets reduced to afford the respective iodine **365**. The insoluble nature of compound **366** limited its characterization by conventional techniques.

The analysis of carbon spectrum of compound **366** could provide an answer to its possible iodane nature. The comparison between the C1-ipso carbon of iodine **365** and the one of compound **366** could help with that. This specific position often presents a shift due to the transformation of iodine compounds into λ^3 and λ^5 -iodanes.

Unfortunately for us, C1-ipso is a quaternary carbon which needs a longer acquisition times to be observable due to its relaxation time. Just as in the case of ^1H NMR, we observed the reversibility of compound **366** through the time when the carbon spectra was acquired dissolved in $\text{DMSO}-d^6$. This could have been resolved if a large amount of **366** compound was dissolved in the NMR tube in order to acquire carbon spectrum in shorter time, but unfortunately, this was limited by the poor solubility of the compound.

Despite the fact that ipso quaternary carbon of iodane **366** was not possible to observe, cyclopentadienyl and acetal carbons (depicted in purple and orange, respectively, **Fig. 3.21**) presented a considerable shift in their carbon signals. This shift did not confirm the nature of iodine, and for this reason we continued searching for other techniques.

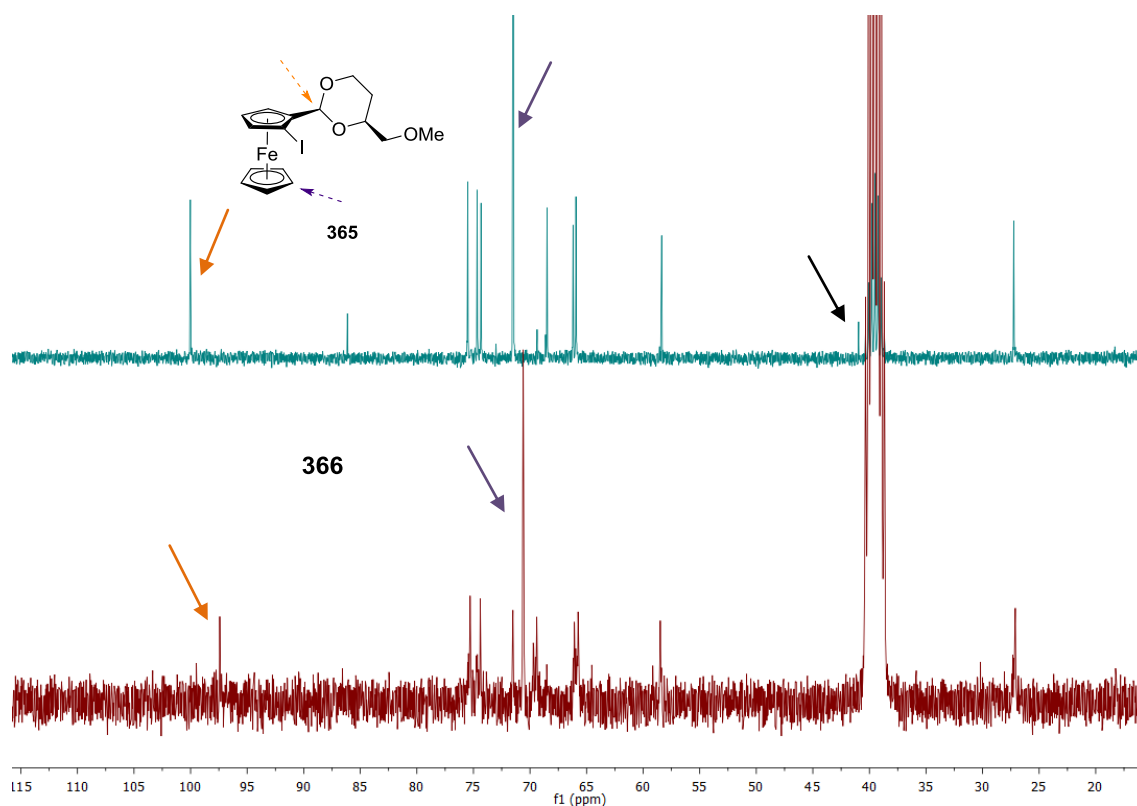


Figure 3.21. ^{13}C spectra for compounds **365** and **366** in deuterated DMSO.

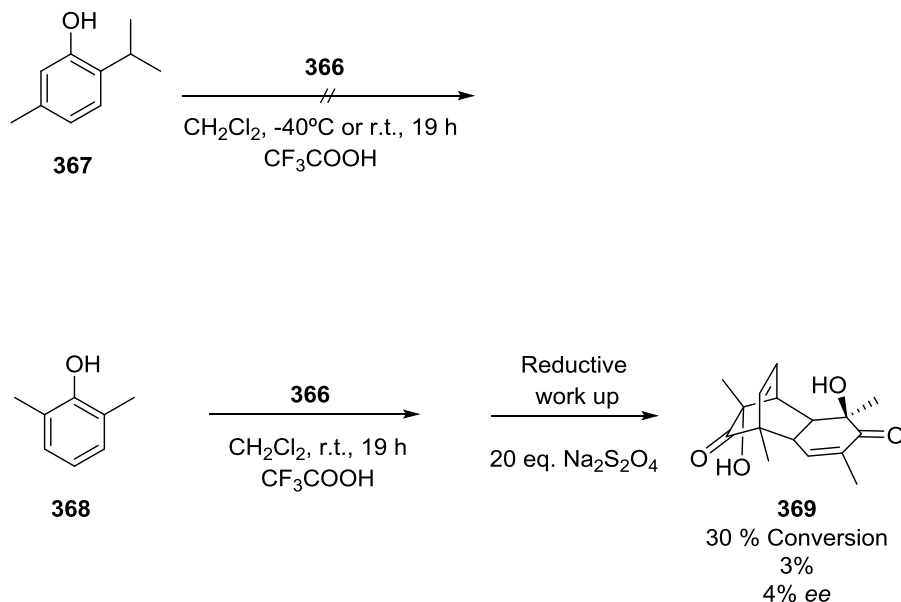
Infrared spectroscopy analysis of iodine **365** and compound **366** was performed and compared with the literature. Zhdankin *et al.*⁷¹ reported that the infrared vibration of the $\text{I}=\text{O}$ bond for a λ^5 -iodane can be observed around 749 cm^{-1} , and we were able to observe a broad signal at 767 cm^{-1} .

Although there was no certain confirmation of the nature of iodane **366**, compound was evaluated in the asymmetric dearomatization of simple thymol **367**

⁷¹ Yusubov, M. S.; Svitich, D. Y.; Yoshimura, A; Nemykin, V. N.; Zhdankin, V. V.; *Chem. Commun.*, **2013**, 49, 11269-11271

CHAPTER 3

(**Scheme 3.60**) in presence of TFA. In this reaction the substrate and iodine **365** were recovered. However, when the less hindered 2,6-dimethylphenol **368** was employed, a [4+2] dimer **369** was obtained in a 3 % yield. Unfortunately, evaluation of the optical purity of **317** revealed its complete racemic nature.

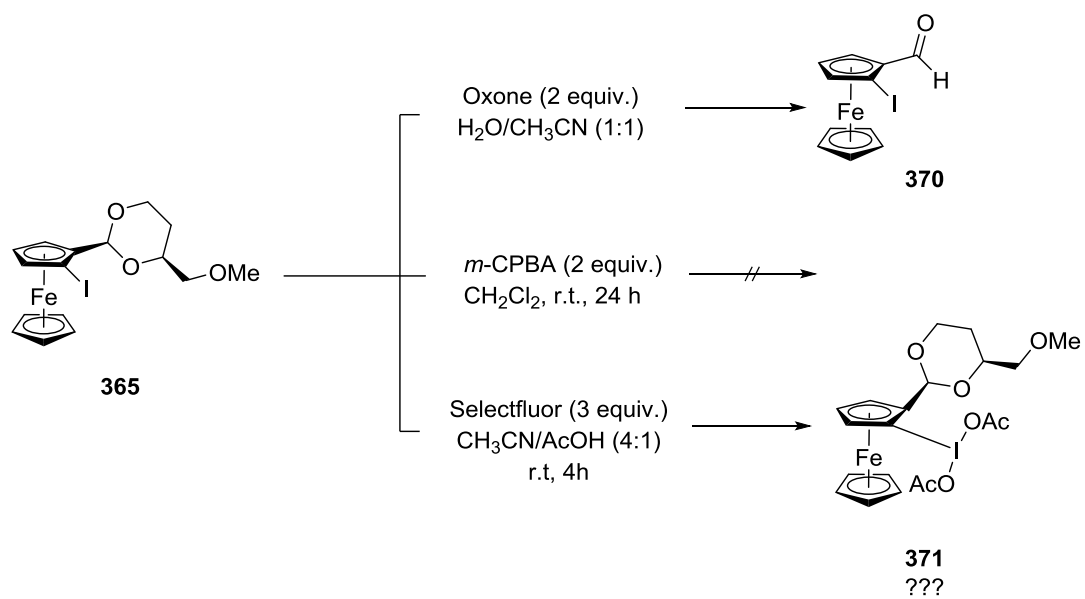


Scheme 3.60. Asymmetric dearomatization attempts of compound **367** with thymol and 2,6-dimethylphenol.

As compound **366** turned to be not efficient in asymmetric dearomatization reactions, iodine compound **365** was treated with other oxidizing agents (**Scheme 3.61**). Oxone was first chosen as oxidant using a mixture of ACN and H_2O . Unfortunately, a complete deprotection of 1,3-dioxane afforded aldehyde **370**. On the contrary, if *m*-CPBA was employed using DCM as solvent for the reaction of compound **365** and stirred for 8 hours at room temperature, starting material was fully recovered (**Scheme 3.61**). Some oxidation tests were tried with iodocarboxaldehyde ferrocene **370**, but no further oxidation was observed.

Finally, the use of Selectfluor in presence of a mixture (4:1) of ACN and AcOH could lead to the formation of the λ^3 derivatives of ferrocenyl compound **365**. Presence of some new products was observed by ^1H NMR. Unfortunately, the signals observed were broad similar to the ones observed for compound **366**. It could be possible that oxidation of the iron atom is taking place before the oxidation of iodine, as the potential for Fe^{2+} to Fe^{3+} is lower. Formation of Fe^{3+} could lead to a paramagnetic state of the molecule, which in is known to exhibit broader signals in ^1H NMR.

In conclusion, we were not able to oxidize the iodine atom placed in the ferrocenyl moiety or at least confirm the nature of this oxidation. Furthermore, these compounds were not able to induce any chirality on the typical hypervalent iodine reagent mediated reactions.



Scheme 3.61. Use of different oxidant to oxidize iodine **366** into λ^3 and λ^5 -iodanes

3.8 Conclusions

- A successful racemic synthetic route toward lactone **328** was developed in five steps, within 24 h, without purification of intermediates and in an overall yield of 17%.
- Asymmetric oxa-Michael desymmetrization employing organometallic catalysis and organocatalysis did not provide good results for intermediate lactone **328**. On the other hand, alternative asymmetric approach of lactone **328** catalyzed by chiral diamines through a desymmetrization process to yield dioxanes gave rise to a good enantiocontrol. Unfortunately, elimination of 1,4-dioxane moiety prevented the access to enantiopure lactone intermediate.
- Total synthesis of neosecurinine- and neonorsecurinine-type compounds (±)-**Virosine B**, (±)-**Virosine A**, (±)-**Niruroidine** and (±)-**Bubbialidine** was accomplished in 10 synthetic steps, with an overall yield for each compound of 1-2%. Lactone **328** resulted in a valuable key intermediate, which in combination with different azidoaldehydes **350a-b** permitted the divergent access toward neosecurinine and neonorsecurinine type alkaloids at the same time.
- Piperidine and pyrrolidine ring compounds demonstrated different mechanistic behavior during reductive amination and cyclization steps. Due to that, the study of the mechanism by DFT calculations confirmed the diastereoselectivity exhibited by neonorsecurinine derivatives. Unfortunately, no conclusive results were obtained for neosecurinine derivatives but further analysis are currently ongoing.
- The synthesis of ferrocenyl-iodanes was tried in order to catalyze asymmetric dearomatization reactions. Characterization of the possible hypervalent iodine ferrocene **366** was not conclusive due to its possible paramagnetic character (Fe^{2+} to Fe^{3+}) and low solubility in organic solvents. Unfortunately, compound **366** was not able to show either good reactivity or chiral induction in oxidative dearomatization reactions.

3.9 Experimental part

3.9.1 General remarks

All reactions were carried out under a nitrogen or argon atmosphere with dry solvents under anhydrous conditions, unless otherwise noted. All the glassware has been previously dried in an oven at 90°C. Room temperature is related to around 20-25°C. Reactions at 0°C were carried out using an ice bath; reactions from -78°C to -10°C were carried out with dry ice in acetone.

Dichloromethane (DCM) and toluene were obtained by passing commercially available dry, oxygen-free formulations through activated alumina columns from a SPS (solvent purification system) machine. Dry methanol (MeOH), dry acetonitrile (ACN) and Et₃N were obtained by distillation over calcium hydride. Tetrahydrofuran (THF), was freshly distilled over sodium and benzophenone prior to its use. Ethyl acetate (EtOAc), diethyl ether (Et₂O), dichloromethane (DCM), cyclohexane, *n*-hexane and petroleum ether (PET) were purchased at the highest commercial quality and used without further purification, unless otherwise stated. Reagents were purchased at the highest commercial quality and used without further purification, unless otherwise stated. Yields refer to chromatographically and spectroscopically (¹H NMR) homogeneous materials, unless otherwise noted. Reactions were monitored by thin-layer chromatography (TLC) carried out on 0.25 mm E. Merck silica gel plates (60F-254). Ethanolic solution of phosphomolybdic acid, aqueous cerium molybdate and aqueous potassium permanganate were used as developing agents. E. Merck silica gel (60, particle size 40-63 µm) was used for column chromatography.

NMR spectra were recorded on Bruker DPX-300 and Bruker Avance III 400 MHz instrument, and were calibrated using residual undeuterated solvent as an internal reference. The following abbreviations were used to explain the multiplicities: s = singlet, d = doublet, t = triplet, q = quartet, m = multiplet.

Infrared spectra were recorded between 4000 and 400 cm⁻¹ on a Bruker IFS55 (OPUS/IR 3.0.2) FT-IR spectrometer.

High-Resolution Mass Spectra (HRMS) were provided by the Centre d'Etude Structurale et d'Analyse des molécules Organiques (CESAMO, Université de Bordeaux, France) and performed on a Accutof JEOL mass spectrometer using ESI and EI ionization sources.

CHAPTER 3

Analytical High Performance Resolution Chromatography (HPLC)

experiments were performed using Daicel Chiralpack IA, AS-H, OD-H and OJ-H columns (250 x 4.6 mm I.D) which contain a chiral stationary phase. Equipment was the following: a Thermo system equipped with P1500 pumps and a UV 6000LP diode array detector.

Optical rotation coefficient, $[\alpha]_D^T$, was measured at 589 nm (sodium line) in a digital polarimeter JASCO P-2000. T is referred to the temperature of measurement.

Computational methods. All the calculations reported in **Chapter 3** were performed by Density Functional Theory (DFT),⁷² using the hybrid three-parameter functional denoted as B3LYP.⁷³ The standard 6-311 G(d) basis set⁷⁴ as implemented in the Gaussian09⁷⁵ was used to describe all the atoms. All stationary points were characterized by harmonic analysis. Reactants, intermediates and cycloadducts have positive definite Hessian matrices. Transition structures show only one negative eigenvalue in their diagonalized force constant matrices, and their associated eigenvector were confirmed to correspond to the motion along the reaction coordinate. Thermal corrections to Gibbs free energies (TCGE) at 298 K were computed at the same level and were not scaled. The final energies were obtained by performing single point M06-2X⁷⁶ calculations with the 6-31+G(d,p) basis set at the optimized B3LYP geometries. The solvent effects were included by means of the Polarization Continuum Model (PCM)⁷⁷ with the relative permittivity ($\epsilon=7.426$) and parameters corresponding to tetrahydrofuran.

⁷² Parr, R. G.; Yang, W. *Density-Functional Theory of Atoms and Molecules*, Oxford, New York **1989**.

⁷³ (a) Lee, C.; Yang, W.; Parr, R. G. *Phys. Rev. B* **1988**, 37, 785–789. (b) Becke, A. D. *J. Chem. Phys.* **1993**, 98, 1372–1377. (c) Becke, A. D. *J. Chem. Phys.* **1993**, 98, 5648–5652.

⁷⁴ Hehre, W. J.; Radom, L.; Schleyer, P. v. R.; Pople, J. A. *Ab initio Molecular Orbital Theory*, Wiley, New York, **1986**; pp. 76-87 and references cited therein.

⁷⁵ Frisch, M. J. et al. Gaussian 09, Revision B.01; Gaussian, Inc., Wallingford CT, **2009**.

⁷⁶ Zhao, Y.; Truhlar, D. G. *Theor. Chem. Acc.* **2008**, 120, 215-241.

⁷⁷ a) Cossi, M.; Rega, N.; Scalmani, G.; Barone, V.; *J. Comput. Chem.* **2003**, 24, 669–681; b) Tomasi, J.; Mennucci, B.; Cammi, R., *Chem. Rev.* **2005**, 105, 2999–3094.

3.9.2 Total Synthesis of *Securinega* Alkaloids

3.9.2.1 General procedure for racemic synthesis of key intermediate **328**

4-hydroxyphenylacetic acid **321** (5.00 g, 32.89 mmol) was dissolved in MeOH (165 mL, 0.20 M) and stirred at room temperature for 10 minutes. Subsequently, reaction mixture was cooled to 0°C and stirred for 5 minutes more. Then, (diacetoxyiodo)benzene (16.40 g, 49.33 mmol) was added as a solid directly in to the mixture. After additional 10 minutes of stirring at 0°C the reaction was led to stir at room temperature for 2 hours and followed by TLC (66:17:17 EtOAc/DCM/Acetone) and ¹H NMR spectroscopy. Once reaction was finished the reaction was quenched with Na₂S₂O₃ (1.11 mL, 4.43 M solution) and added 60 mL of DCM and 50 mL of HCl 1M. Then compound was extracted three times with 20 mL of DCM, dried over Na₂SO₄ and evaporated to dryness. Crude of compound **331** (see **Scheme 3.62**) was used in next step without further purification.

Compound **331** was dissolved in 165 mL of EtOAc (0.20 M) and then *p*-toluenesulfonic acid monohydrate (1.88 g, 9.87 mmol) was added at room temperature. Reaction was followed by ¹H NMR due to the instability of the new product in silica gel. After 1 h, more than 95 % conversion of the starting material was observed and the mixture was just evaporated to dryness. ¹H NMR of crude showed the desired product and iodobenzene remaining from the first step. Crude of lactone **332** (see **Scheme 3.62**) was used as obtained for next step.

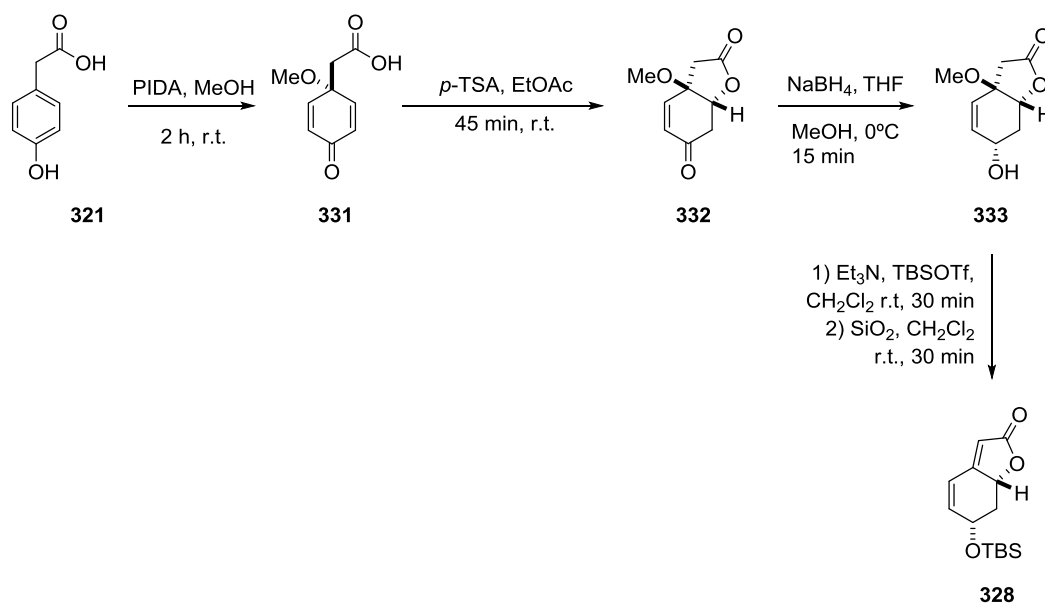
332 was then dissolved in THF (165 mL, 0.20 M) at room temperature, and subsequently the mixture was cooled down to 0°C. To the stirred solution NaBH₄ (2.49 g, 65.80 mmol) was added and stirred at low temperature for 5 minutes before adding MeOH (16.0 mL) dropwise until bubbling is observed, vigorous stirring is necessary to avoid formation of foam. Reaction was monitored by TLC (DCM/EtOAc 50:50) and product is observable after staining with KMnO₄. After 15 minutes reaction was finished, then 200 mL of EtOAc and 66 mL of HCl 0.1 N were added at 0°C. After extraction of the organic layer with 3 times 40 mL of EtOAc, organic layer was washed with brine. After that the organic layer was dried over Na₂SO₄ and evaporated to dryness under high vacuum. Crude **333** (**Scheme 3.62**) was confirmed by ¹H NMR spectroscopy and product was obtained in a total diastereoselective manner.

Crude of **333** (2.74 g, 14.88 mmol) was dissolved in anhydrous CH₂Cl₂ (75 mL, 0.20 M) and then distilled Et₃N (12.4 mL, 89.28 mmol) was added at room temperature

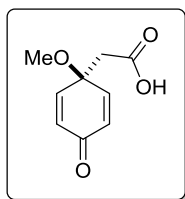
CHAPTER 3

and subsequently TBSOTf (10.4 mL, 44.64 mmol) Monitoring of the reaction was performed by TLC in 1 to 1 DCM/EtOAc to observe the disappearance of the starting material (stained in KMnO_4) and then 20/80 of EtOAc/cyclohexane mixture containing 1% of Et_3N . After 30 minutes of stirring at room temperature reaction is finished and quenched with 40 mL of NaHCO_3 aq. (sat.), then extracted 3 times with 40 mL of CH_2Cl_2 . After drying over Na_2SO_4 and evaporation to dryness ^1H NMR was performed for the silyl enol ether **334**.

334 was dissolved in anhydrous EtOAc (75 mL, 0.20 M) and 10 g of SiO_2 were added. Stirring was kept for 30 minutes when it was observed by TLC (EtOAc/Cyclohexane 20:80 containing 1% of Et_3N) total conversion to desired product. After evaporation to dryness the solid deposit was placed in a column to purify by flash column chromatography in silica gel eluting with a mixture 10:90 to 20:80 of EtOAc/Cyclohexane. 1.22 g of product **328** (Scheme 3.62) was obtained as a white solid in a 17 % global yield.



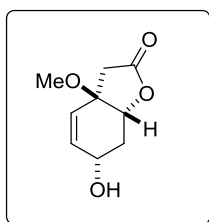
Scheme 3.62. Five step racemic synthesis of intermediate **328**.

2-(1-methoxy-4-oxocyclohexa-2,5-dien-1-yl)acetic acid (331)

Compound obtained as a white powder. R_f : 0.19 (EtOAc/DCM 25:75).

$^1\text{H NMR}$ (300 MHz, CDCl_3) δ (ppm) = 6.97 – 6.86 (m, 2H), 6.43 (d, J = 10.3 Hz, 2H), 3.27 (s, 3H), 2.75 (s, 2H). $^{13}\text{C NMR}$ (75 MHz, CDCl_3) δ (ppm) = 184.9, 173.2, 148.6, 132.0, 72.8, 53.3, 44.4. **FT-IR (DCM)**:

3414-3231 (br), 2939, 2833, 1715, 1672, 1518, 1464, 1398, 862. **HRMS (ESI/Q-TOF)**: $[\text{M} + \text{H}]^+$ calculated for $\text{C}_9\text{H}_{11}\text{O}_4$: 183.0657, found: 183.0666.

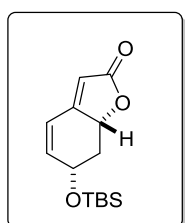
(3aS,6R,7aS)-6-hydroxy-3a-methoxy-3a,6,7,7a-tetrahydrobenzofuran-2(3H)-one (333)

Compound obtained as colorless oil. R_f : 0.40 (EtOAc/DCM 50:50).

$^1\text{H NMR}$ (300 MHz, CDCl_3) δ (ppm) = 6.17 (dd, J = 10.3, 3.7 Hz, 1H), 5.74 (dd, J = 10.3, 1.9 Hz, 1H), 4.69 (dd, J = 9.5, 4.4 Hz, 1H), 4.36 (ddt, J = 7.4, 4.8, 1.9 Hz, 1H), 3.22 (s, 3H), 3.15 (s, 1H), 2.75 (q, J = 17.6 Hz, 2H), 2.50 – 2.36 (m, 1H), 1.90 (ddd, J = 13.4, 9.5, 7.6 Hz,

1H). $^{13}\text{C NMR}$ (75 MHz, CDCl_3) δ (ppm) = 174.2, 136.3, 126.3, 78.8, 78.2, 63.9, 51.6, 41.5, 36.1. **FT-IR (DCM)**: 3433 (br), 2926, 2852, 1767, 1453, 1359, 1169, 1058, 996.

HRMS (ESI/Q-TOF): $[\text{M} + \text{H}]^+$ calculated for $\text{C}_9\text{H}_{13}\text{O}_4$: 185.0813, found: 185.0818.

(6R,7aS)-6-((tert-butyldimethylsilyl)oxy)-7,7a-dihydrobenzofuran-2(6H)-one (328)

Compound obtained as a white solid. R_f : 0.32 (EtOAc/Cyclohexane 20:80). $^1\text{H NMR}$ (300 MHz, CDCl_3) δ (ppm) = 6.52 (dd, J = 9.9, 2.4 Hz, 1H), 6.20 (dt, J = 10.0, 1.6 Hz, 1H), 5.81 – 5.76 (m, 1H), 4.84 (ddd, J = 13.4, 4.9, 1.8 Hz, 1H), 4.67 – 4.50 (m, 1H), 2.78 (dd, J = 6.2, 5.1 Hz, 1H), 1.71 (ddd, J = 13.4, 11.3, 10.0 Hz, 1H), 0.91 (s, 9H), 0.13 (d, J =

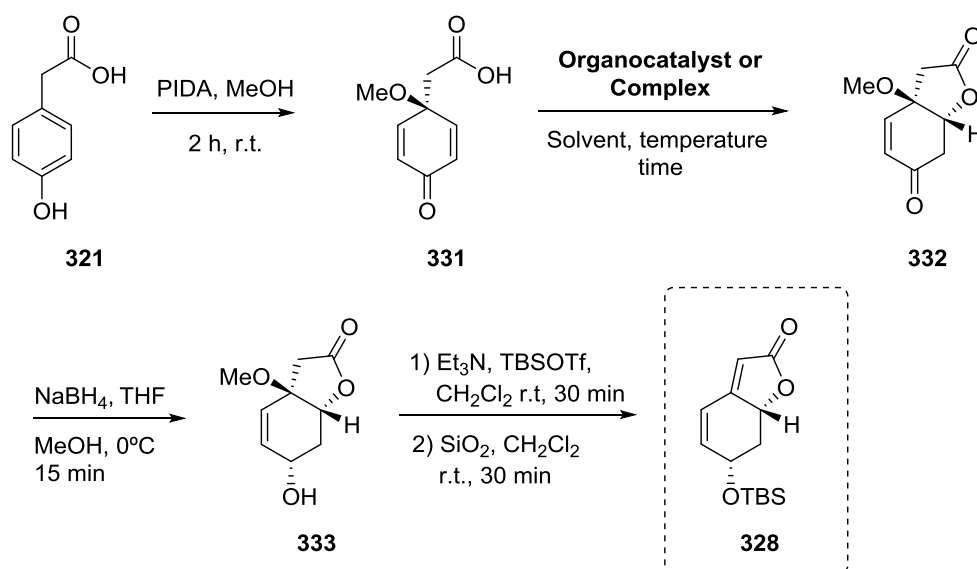
3.5 Hz, 6H). $^{13}\text{C NMR}$ (75 MHz, CDCl_3) δ (ppm) = 173.4, 163.1, 144.8, 119.4, 111.3, 78.2, 67.5, 40.6, 25.8, 18.2, -4.4, -4.7. **FT-IR (DCM)**: 3095, 2954, 2930, 2857, 1740, 1640, 1252, 1151, 1022, 878, 840, 725. **HRMS (ESI/Q-TOF)**: $[\text{M} + \text{H}]^+$ calculated for $\text{C}_{14}\text{H}_{23}\text{O}_3\text{Si}$: 267.1416, found: 267.1422.

3.9.2.2 Asymmetric direct approach through oxa-Michael desymmetrization

4-hydroxybenzoic acid **321** (0.50 g, 3.29 mmol) was dissolved in MeOH (16 mL, 0.20 M) and stirred at room temperature for 5 minutes. Subsequently, reaction mixture was cooled to 0°C and stirred for 5 additional minutes. Then, PIDA (1.56 g, 4.93 mL)

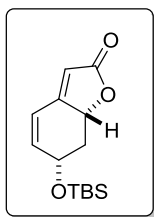
CHAPTER 3

was added as a solid directly in to the mixture (**Scheme 3.63**, step 1). After additional 10 minutes of stirring at 0°C the reaction was increased to room temperature and followed by TLC (66:17:17 EtOAc/DCM/Acetone). 1 hour and 30 minutes of reaction at room temperature was quenched with Na₂S₂O₃ (1.11 mL, 4.04 M) and added 60 mL of DCM and 50 mL of HCl 1M. Compound was extracted 3 times with 20 mL of DCM; organic layer was dried over Na₂SO₄ and evaporated to dryness. Purification by flash column chromatography in silica gel with EtOAc/DCM 20:80 EtOAc to 50:50 EtOAc/DCM afforded 125 mg of compound **331**, yield 21%.



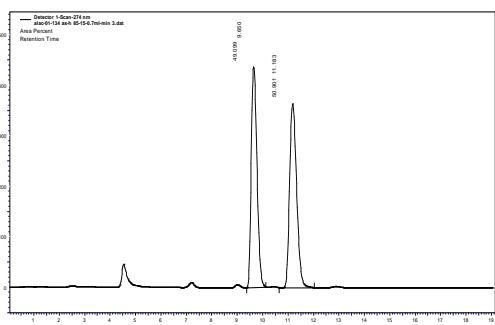
Scheme 3.63. Asymmetric direct approach toward intermediate **328**.

Corresponding catalyst (5 mol % of metallic salt + 5.5 mol % of ligand, or 10 mol % of organocatalyst) and additives (20 mol %) were placed in a round bottom flask with a magnetic stirrer and dissolved in corresponding solvent (0.10 M) (**Scheme 3.63**, step 2). Then compound **331** (1 equiv.) dissolved in the corresponding solvent was added to the mixture at certain reaction temperature. Reaction was monitored by ¹H NMR spectroscopy in CDCl₃ until full conversion to desired cyclic lactone **332** was observed. Once reaction was finished, the mixture was reduced to dryness and dried under high vacuum without further purification. Compound **328** was synthesized as reported for racemic procedure (**Scheme 3.62** and **3.63**). Enantiomeric excess of compound **328** was determined by HPLC.

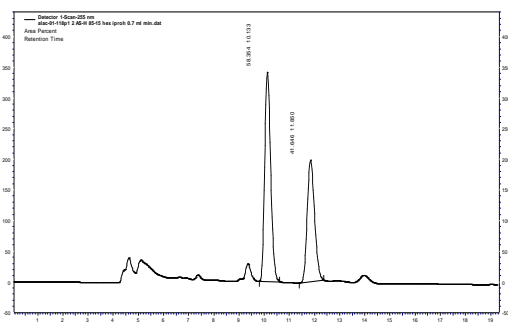
(6*R*,7*aS*)-6-((*tert*-butyldimethylsilyl)oxy)-7,7*a*-dihydrobenzofuran-2(6*H*)-one (328)

R_f: 0.32 (EtOAc/Cyclohexane 20:80). **¹H NMR** (300 MHz, CDCl₃) δ (ppm) = 6.52 (dd, *J* = 9.9, 2.4 Hz, 1H), 6.20 (dt, *J* = 10.0, 1.6 Hz, 1H), 5.81 – 5.76 (m, 1H), 4.84 (ddd, *J* = 13.4, 4.9, 1.8 Hz, 1H), 4.67 – 4.50 (m, 1H), 2.78 (dd, *J* = 6.2, 5.1 Hz, 1H), 1.71 (ddd, *J* = 13.4, 11.3, 10.0 Hz, 1H), 0.91 (s, 9H), 0.13 (d, *J* = 3.5 Hz, 6H). 17 % ee. **HPLC**: Daicel Chiralpak AS-H column, *iso*-Propanol/*n*-hexane 15:85, flow = 1.0 mL/min, *tr*_{major} = 10.3 min (6*R*, 7*aS*), *tr*_{major} = 11.8 min (6*S*, 7*aR*), 255 nm.

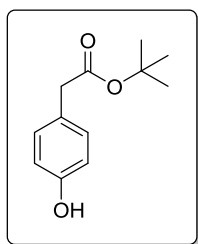
Best result: Use of ***R*-TRIP-217**, 10 mol %, in DCM as solvent and room temperature.



	RT	% Area
1	9.6 min	49.10
2	11.1 min	50.90



	RT	% Area
1	10.3 min	58.35
2	11.8 min	41.65

3.9.2.3 Asymmetric alternative strategy in oxa-Michael desymmetrization**(4-Hydroxyphenyl)acetic acid *tert*-butyl ester (339)**^{78,79}

N,N-dimethyl isobutyramide **340** (1 mL, 7.75 mmol) was dissolved in 32 mL of CH₂Cl₂ and cooled to 0°C in order to add oxalyl chloride (0.72 mL, 8.52 mmol). After stirring at room temperature for 30 minutes, Et₃N (1.3 mL, 9.3 mmol) was added. After 15 minutes, 4-hydroxybenzoic acid (591 mg, 3.88 mmol) was added and stirred at room temperature for another 20 minutes. Finally, *tert*-butanol (8 mL, excess) were added and the resulting mixture was stirred overnight. Reaction was monitored by TLC (EtOAc/PET 30:70). HCl 1M and EtOAc were used to extract the organic layer (3 x 30 mL). Then, drying over Na₂SO₄ and reduction to dryness afforded the crude. Purification by flash column chromatography in silica gel with EtOAc/PET

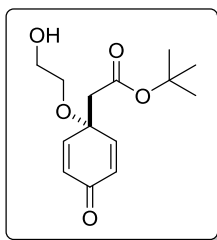
⁷⁸ Hama, T.; Liu, X.; Culkin, D. A; Hartwig, J. F., *J. Am. Chem. Soc.* **2003**, 125, 11176–7.

⁷⁹ Bhawal, B. M.; Khanapure, S. P.; Biehl, E. R., *Synthesis*, **1991**, 2, 112–114.

CHAPTER 3

30:70, isolated 675 mg of white powder in 84 % yield. **¹H NMR** (300 MHz, CDCl₃) δ (ppm) = 7.12 – 7.06 (m, 2H), 6.72 (d, J = 8.6 Hz, 2H), 5.57 (s, 1H), 3.45 (s, 2H), 1.44 (s, 9H). **¹³C NMR** (75 MHz, CDCl₃) δ (ppm) = 172.1, 154.9, 130.5, 126.5, 115.6, 81.2, 41.9, 28.2. **FT-IR** (DCM): 3314, 3010, 2982, 2935, 1698, 1518, 1447, 1370, 1272, 1134, 810, 767, 750. Title compound was in concordance with reported literature.

Synthesis of 4-(4,4-dimethyl-2-oxopentyl)-4-(2-hydroxyethoxy)cyclohexa-2,5-dien-1-one (341)



Compound **339** (480 mg, 2.30 mmol) was dissolved in 9.20 mL of anhydrous acetonitrile and the anhydrous ethylene glycol was added (3.89 mL, 69.00 mmol). After stirring 5 minutes at room temperature, PIDA (1.15 g, 3.45 mmol) was added as a solid and observed the change of color to purple and then to yellow. Monitoring by TLC (DCM/Et₂O 25:75) showed that reaction was over after 2 hours and 30 minutes. Reaction was quenched with Na₂S₂O₃ (5 equiv., 4.43 M, 3.90 mL) and H₂O and NaHCO₃ aq. (sat.) were added. Subsequently, EtOAc and NaHCO₃ aq. (sat.) were added in a 1 to 1 ratio v/v. Organic layer was washed 3 times with 20 mL of NaHCO₃ aq. (sat.) and dried over Na₂SO₄. After evaporation crude was obtained and was purified by flash column chromatography in silica gel in a gradient from 100 % DCM to 10:90 and 25:75 Et₂O/DCM, R_f : 0.18 (EtOAc/Cyclohexane 20:80). 180 mg of a yellow oil were obtained, Yield = 36 %. **¹H NMR** (300 MHz, CDCl₃) δ : (ppm) = 6.98 (d, J = 10.3 Hz, 2H), 6.39 (d, J = 10.3 Hz, 2H), 3.72 (t, J = 4.2 Hz, 2H), 3.48 (dd, J = 5.2, 4.0 Hz, 2H), 2.69 (s, 2H), 1.45 (s, 9H). **¹³C NMR** (75 MHz, CDCl₃) δ (ppm) = 184.9, 167.6, 149.0, 131.2, 81.8, 72.8, 66.3, 61.9, 45.7, 28.0. **FT-IR** (DCM): 3700 (br), 2978, 2934, 2873, 1728, 1672, 1631, 1457, 1393, 1369, 1151, 1091, 1064. **HRMS (ESI/Q-TOF)**: [M + Na]⁺ calculated for C₁₄H₂₀NaO₅ 291.1201, found 291.1208.

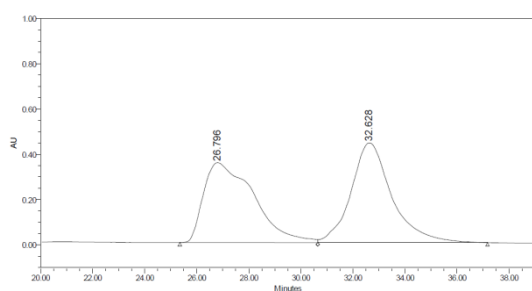
-Racemic synthesis of compound (±)-342

Compound **341** (8 mg, 0.03 mmol) was dissolved in 0.3 mL of anhydrous DCM and then *p*-toluenesulfonic acid (0.56 mg, 0.003 mmol) was added. While stirring at room temperature for 30 minutes reaction was monitored by TLC (Et₂O/DCM 20:80). Evaporation afforded the crude product and then purification by flash column chromatography in silica gel with a gradient from 100 % DCM to EtOAc/Cyclohexane 20:80 gave the cyclized product, 2.6 mg in a 32 % yield. Injection of racemic compound

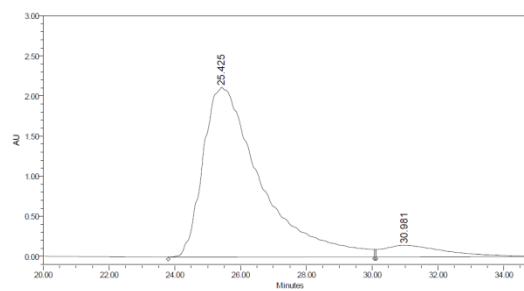
in HPLC Daicel chiralpack IA column with a mixture of eluents of iso-Propanol/*n*-hexane 25:75 in 0.7 mL/min at 220-250 nm showed one enantiomer at $tr_1 = 7.90$ min and at $tr_2 = 8.77$ minutes.

-Asymmetric synthesis of compound **342** and *ent*-**342**⁸⁰

Path 1: Compound **341** (50 mg, 0.19 mmol) was dissolved in 0.7 mL (0.25 M) of anhydrous toluene, **1*R*,2*R***-phenylethylenediamine **220** (6.00 mg, 0.03 mmol) and ***N*-Boc-*L*-proline** (6.00 mg, 0.03 mmol) were added and reaction was stirred at room temperature for 20 h while reaction conversion was monitored by ¹H NMR spectroscopy. Once full conversion was observed solvent was removed by evaporation. Purification by flash column chromatography in silica gel using 100 % DCM to EtOAc/Cyclohexane 20:80 afforded cyclized product **342**, 39 mg in a 80 % yield. $[\alpha]_D^{23} = +21.73$ (c 0.40, DCM). Injection of compound in HPLC Daicel chiralpack IA column with a mixture of eluents of iso-Propanol/*n*-hexane 5:95 in 0.7 mL/min at 210 nm showed 86 % of ee. $tr_{major} = 25.4$ min, $tr_{minor} = 30.9$ min.



	RT	Area	% Area	Height
1	26.796	47263396	49.69	352474
2	32.628	47845112	50.31	440643



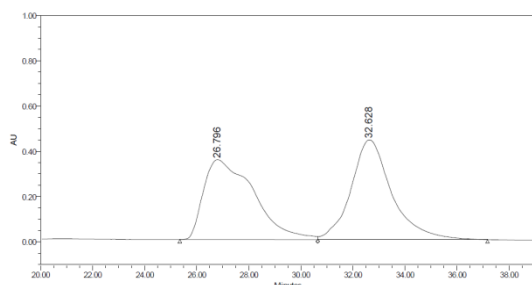
	RT	Area	% Area	Height
1	25.425	257900611	93.15	2117080
2	30.981	18970957	6.85	142786

Path 2: Compound **341** (50 mg, 0.19 mmol) was dissolved in 0.86 mL (0.25 M) of anhydrous toluene, **1*S*,2*S***-phenylethylenediamine *ent*-**220** (6.00 mg, 0.03 mmol) and ***N*-Boc-*L*-proline** (6.00 mg, 0.03 mmol) were added and reaction was stirred at room temperature for 72 h while reaction conversion was monitored by ¹H NMR spectroscopy. Once full conversion was observed solvents was removed by evaporation. Purification by flash column chromatography in silica gel using 100 % CH₂Cl₂ to EtOAc/Cyclohexane 20:80 gave cyclized product *ent*-**342**, **32** mg in a 64 %

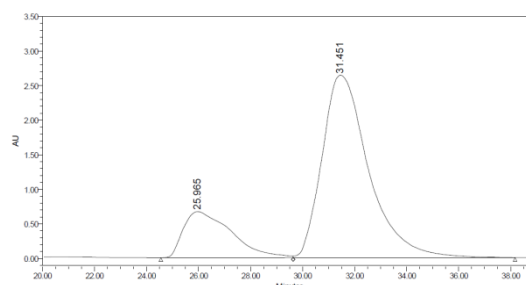
⁸⁰ Wu, W.; Li, X.; Huang, H.; Yuan, X.; Lu, J.; Zhu, K.; Ye, J., *Angew. Chem., Int. Ed.* **2013**, 52, 1743–1747.

CHAPTER 3

yield. Injection of compound in HPLC Daicel chiralpack IA column with a mixture of eluents of iso-Propanol/*n*-hexane 5:95 in 0.7 mL/min at 210 nm showed 60 % of ee for the opposite enantiomer observed when 1*R*,2*R*-phenylethylenediamine was used. $t_{r_{\text{minor}}} = 25.9 \text{ min}$, $t_{r_{\text{major}}} = 31.4 \text{ min}$.

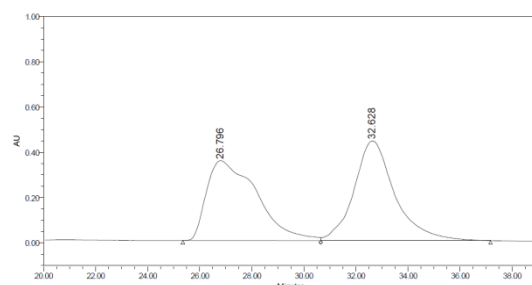


	RT	Area	% Area	Height
1	26.796	47263396	49.69	352474
2	32.628	47845112	50.31	440643

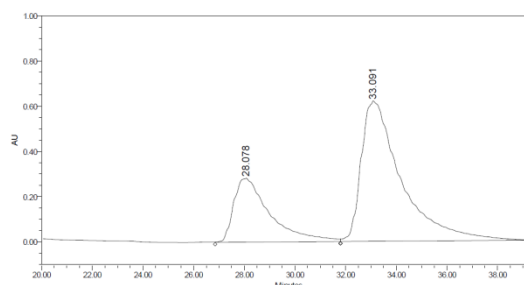


	RT	Area	% Area	Height
1	25.965	85309575	20.66	666775
2	31.451	327701906	79.34	2638655

Experiment 3: Compound **341** (57 mg, 0.19 mmol) was dissolved in 0.86 mL (0.25 M) of anhydrous toluene, **1*S*,2*S***-phenylethylenediamine **ent-220** (6.81 mg, 0.03 mmol) and **N-Boc-D-proline** (6.89 mg, 0.03 mmol) were added and reaction was stirred at room temperature for 72 h while reaction conversion was monitored by ^1H NMR spectroscopy. Once full conversion was observed solvents was removed by evaporation. Purification by flash column chromatography in silica gel using EtOAc/Cyclohexane 20:80 gave the cyclized product **ent-342**, 30 mg in a 53 % yield. $[\alpha]_D^{23} = -9.43$ (c 0.93, DCM). 42 % of ee. Injection of compound in HPLC Daicel chiralpack IA column with a mixture of eluents of iso-Propanol/*n*-hexane 5:95 in 0.7 mL/min at 210-254 nm showed $t_{r_{\text{minor}}} = 28.1 \text{ min}$, $t_{r_{\text{major}}} = 33.1 \text{ min}$.

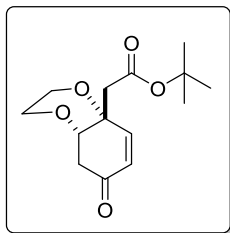


	RT	Area	% Area	Height
1	26.796	47263396	49.69	352474
2	32.628	47845112	50.31	440643



	RT	Area	% Area	Height
1	28.078	27973491	29.01	282810
2	33.091	68446516	70.99	621447

(4*aS*,8*aR*)-8*a*-(4,4-dimethyl-2-oxopentyl)-2,3,4*a*,8*a*-tetrahydrobenzo[*b*][1,4]dioxin-6(5*H*)-one (**342**)



Colorless oil, R_f : 0.62 (DCM/Et₂O 75:25). $^1\text{H NMR}$ (300 MHz, CDCl₃) δ (ppm) = 6.86 (dd, J = 10.5, 2.8 Hz, 1H), 6.14 (dd, J = 10.5, 1.0 Hz, 1H), 4.14 (q, J = 3.0 Hz, 1H), 3.83 (ddd, J = 12.2, 9.4, 5.3 Hz, 1H), 3.74 – 3.65 (m, 3H), 2.70 – 2.62 (m, 2H), 2.59 (d, J = 6.9 Hz, 2H), 1.46 (s, 9H). $^{13}\text{C NMR}$ (75 MHz, CDCl₃) δ (ppm) = 195.5, 168.1, 150.8, 131.2, 81.7, 76.5, 72.6, 66.3, 63.0, 44.6, 41.7, 28.2. **FT-IR** (DCM): 2970, 2917, 2866, 1729, 1685, 1455, 1367, 1152, 1112. **HRMS (ESI/Q-TOF)**: $[\text{M} + \text{Na}]^+$ calculated for C₁₄H₂₀NaO₅ 291.1203, found 291.1205. Crystals obtained several times, not suitable for their analysis by X-ray diffraction. No absolute configuration of each enantiomer.

Synthesis of tricyclic compound **344a**

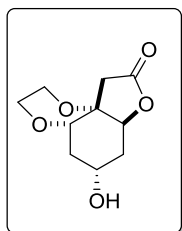
Racemic compound **342** (29 mg, 0.11 mmol) was dissolved in anhydrous DCM (0.10 M, 1.10 mL) and in the presence of *p*-toluenesulfonic acid (2.12 mg, 0.01 mmol) trifluoroacetic acid (252 μL , 3.30 mmol) was added. Monitoring of the reaction by TLC (KMnO₄ staining) (Et₂O/DCM 25:75) presented almost full conversion after 2 hours of stirring, and then aliquot of reaction mixture was analyzed by $^1\text{H NMR}$ spectroscopy which showed 88 % of conversion to compound **343**. Due to the possible low stability of the compound in silica gel the reaction mixture was reduced to dryness and dried under high vacuum obtaining 23 mg of crude and used in next step without further purification. R_f (Et₂O/DCM 25:75): 0.52.

Different collected fractions of compound **343** (91.0 mg, 0.43 mmol) were dissolved in anhydrous THF (4.29 mL) and then cooled to -40°C. After that, NaBH₄ (80.0 mg, 2.15 mmol) was added and reaction mixture was stirred for 5 minutes. Subsequently, MeOH (0.80 mL) was added dropwise and stirred for 2 hours letting the temperature increase to 0°C while was monitored by TLC (DCM/EtOAc 50:50). Reaction was finished in this time but two products (major and minor) were observable by TLC (KMnO₄ staining), then 20 mL of HCl 0.50 M were added and mixture was diluted with 20 mL of DCM. Compound was extracted several times with 10 mL of DCM. Organic layer was dried with Na₂SO₄ and evaporated to dryness. $^1\text{H NMR}$ spectrum in CDCl₃ showed a mixture of diastereoisomers in 86:14 ratio. Purification by

CHAPTER 3

flash column chromatography in silica gel (DCM/EtOAc 50:50) gave major compound **344a** as colorless oil, 22 mg obtained in 35 % yield.

(4a*S*,7a*S*,10a*S*)-9-hydroxyhexahydro-9*H*-[1,4]dioxino[2,3-*d*]benzofuran-6(5*H*)-one
(**344a**)

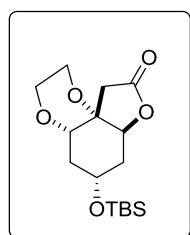


R_f: 0.24 (DCM/EtOAc 50:50), if runned TLC 2 times, 0.52. **¹H NMR** (300 MHz, CDCl₃) δ (ppm) = 5.01 (dd, *J* = 8.8, 6.4 Hz, 1H), 4.05 (s, 1H), 3.99 – 3.95 (m, 1H), 3.94 – 3.83 (m, 2H), 3.74 – 3.60 (m, 2H), 3.28 (s, 1H), 2.72 (d, *J* = 17.1 Hz, 1H), 2.61 – 2.49 (m, 1H), 2.45 (dd, *J* = 17.1, 0.8 Hz, 1H), 2.25 (dtd, *J* = 14.8, 4.6, 2.2 Hz, 1H), 1.88 (dt, *J* = 14.9, 3.7 Hz, 1H), 1.58 (ddd, *J* = 14.3, 8.8, 3.2 Hz, 1H). **¹³C NMR** (75 MHz, CDCl₃) δ (ppm) = 173.9, 76.4, 74.4, 65.8, 65.3, 61.7, 38.7, 37.9, 33.6. Quaternary carbon missed (maybe under CDCl₃ signals). **FT-IR** (DCM): 3603-3152 (br), 2928, 2872, 1779, 1106, 1070, 1012, 913. **HRMS (EI/Q-TOF)**: [*M*]⁺ calculated for C₁₀H₁₄O₅ 214.0841, found 214.0845.

Protection of secondary alcohol **344a**

Compound **344a** (22 mg, 0.10 mmol) was dissolved in anhydrous DCM (0.10 M, 1.0 mL) and then Et₃N (111 μL, 0.80 mmol) was added. Subsequently, TBSOTf (94 μL, 0.40 mmol) was added and stirred for 30 minutes at room temperature. Conversion of the reaction was monitored by TLC (DCM/EtOAc 50:50, KMnO₄ staining). At this point reaction was quenched with saturated solution of NaHCO₃, dissolved in mixture 1 to 1 of ethyl acetate and citric acid 5 % and stirred at room temperature for 12 h and then, product was extracted with EtOAc and finally organic layers were washed once with 10 mL of a saturated solution of NaHCO₃. Organic layer was dried with Na₂SO₄ and evaporated to dryness. Crude ¹H NMR showed mainly product **345**. Purification by flash column chromatography in silica gel (Et₂O/PET 25:75) afforded 8 mg of compound **331** as colorless oil in 61 % yield.

(4a*R*,7a*R*,9*S*)-9-((*tert*-butyldimethylsilyl)oxy)hexahydro-9*H*-[1,4]dioxino[2,3-*d*]benzofuran-6(5*H*)-one (**345**)



R_f: 0.31 (Et₂O/ PET 25:75). **¹H NMR** (300 MHz, CDCl₃) δ (ppm) = 4.41 (dd, *J* = 4.2, 2.7 Hz, 1H), 4.01 – 3.79 (m, 2H), 3.77 – 3.67 (m, 2H), 3.59 – 3.46 (m, 2H), 3.19 (d, *J* = 16.7 Hz, 1H), 2.61 (dd, *J* = 16.7, 0.8 Hz, 1H), 2.27 – 2.13 (m, 2H), 1.87 (dtd, *J* = 12.2, 4.1, 2.1

Hz, 1H), 1.76 (m, 1H), 0.88 (s, 9H), 0.06 (d, $J = 1.4$ Hz, 6H). ^{13}C NMR (75 MHz, CDCl_3) δ (ppm) = 173.1, 81.9, 75.1, 71.5, 65.3, 64.1, 60.0, 39.7, 34.9, 34.0, 25.9, 18.2, -4.6, -4.6. **FT-IR** (DCM): 2956, 2906, 2856, 1791, 1259, 1208, 1087, 836, 777. **LMS (ESI)**: 328.9 u $[\text{M} + \text{H}]^+$, 351 u $[\text{M} + \text{Na}]^+$, 679 u (100%) $[2\text{M} + \text{Na}]^+$.

3.9.2.4 Development of Aldol reaction and Swern oxidation

-General procedure for the synthesis of azidoaldehyde compounds (350a, 350b)

1,4-butanediol or 1,5-pentanediol (1 equiv.) was dissolved in toluene (0.30 M) and then an aqueous solution of HBr (1.20 equiv.) was added. Reaction was refluxed for 12 h and reaction was followed by thin layer chromatography (50:50 EtOAc/Cyclohexane). Mixture was diluted with EtOAc and then organic layer was washed twice with NaOH 1 M, followed by brine and H_2O . Organic layer was dried over Na_2SO_4 and solvents were removed under reduced pressure. Obtained compounds **348a-b** were used without further purification in next step.⁸¹

Corresponding compound **348a-b** (1 equiv.) was dissolved in H_2O (1 equiv.) and then NaN_3 (2 equiv.) was added. This mixture was heated for 18 h at 80°C and the reaction was monitored by ^1H NMR spectroscopy. Once reaction was complete it was diluted and extracted several times with EtOAc and the organic layer then dried over Na_2SO_4 . Final removal of solvents afforded the crude of reaction for compounds **349a-b** which was used without further purification.⁸²

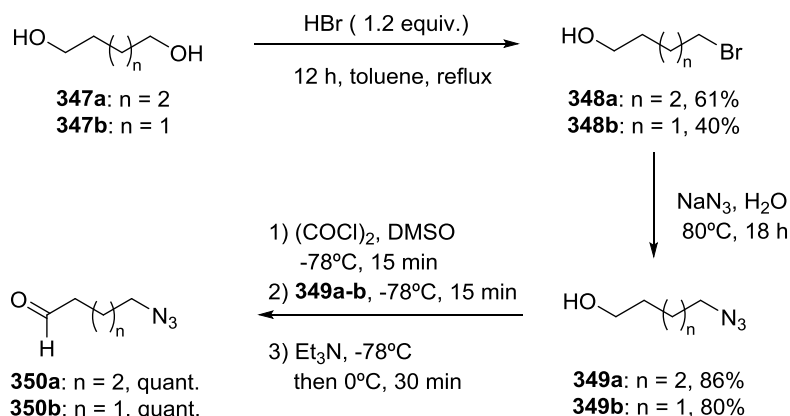
Last step was always performed just before the use of the azidoaldehyde in aldol reaction due to its instability. Oxalyl chloride (2 equiv.) was added to a precooled flask of DCM (0.20 M) at -78°C , and then DMSO (4 equiv.) was added dropwise. Reaction was stirred at the same temperature for 15 minutes and then corresponding compound **349a-b** (1 equiv.) was added dropwise in DCM at -78°C . After additional 30 minutes of stirring at -78°C , Et_3N (8 equiv.) was added and stirred for 5 minutes. Immediately, mixture was warmed up to 0°C and stirred for 30 minutes. Reaction was monitored by thin layer chromatography (30:70 EtOAc/Cyclohexane) and when reaction was finished it was quenched by adding saturated aqueous NaHCO_3 at 0°C . Then organic layer was extracted several times with DCM and dried over Na_2SO_4 . Evaporation of solvent was cautiously performed above 100 mbar due to the volatile character of the compounds.

⁸¹ Nickel, S.; Serwa, R. A.; Kaschani, F.; Ninck, S.; Zweerink, S.; Tate, E. W.; Kaiser, M., *Chem. Eur. J.* **2015**, 21, 10721–10728.

⁸² Moreno, P.; Quéléver, G.; Peng, L., *Tetrahedron Lett.* **2015**, 56, 4043–4046.

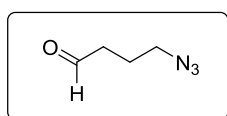
CHAPTER 3

Purification by flash column chromatography in silica gel using 40:60 Et₂O/PET afforded desired compound (**350a** or **350b**) typically in quantitative yields.



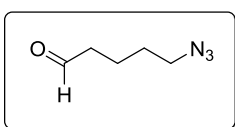
Scheme 3.64. Synthesis of azidoaldehydes **350a** and **350b**.

4-azidobutanal (**350a**)⁸³



Yellowish oil was obtained in overall yield of 85%. R_f : 0.40 (EtOAc/Cyclohexane 30:70). $^1\text{H NMR}$ (300 MHz, CDCl_3) δ (ppm) = 9.80 (d, $J = 1.2$ Hz, 1H), 3.35 (t, $J = 6.6$ Hz, 2H), 2.57 (td, $J = 7.0$, 1.1 Hz, 2H), 1.91 (pd, $J = 6.9$, 1.1 Hz, 2H). $^{13}\text{C NMR}$ (75 MHz, CDCl_3) δ (ppm) = 200.9, 50.4, 40.5, 21.3. Spectroscopic data in concordance with reported in literature.

5-azidopentanal (**350b**)⁸⁴



Yellowish oil was obtained in overall yield of 81%. R_f : 0.62 (EtOAc/Cyclohexane 30:70). $^1\text{H NMR}$ (300 MHz, CDCl_3) δ (ppm) = 9.78 (t, $J = 1.5$ Hz, 1H), 3.31 (t, $J = 6.5$ Hz, 2H), 2.49 (td, $J = 7.0$, 1.5 Hz, 2H), 1.78 – 1.58 (m, 4H). $^{13}\text{C NMR}$ (75 MHz, CDCl_3) δ (ppm) = 201.8, 51.2, 43.4, 28.4, and 19.4. Spectroscopic data in concordance with reported in literature.

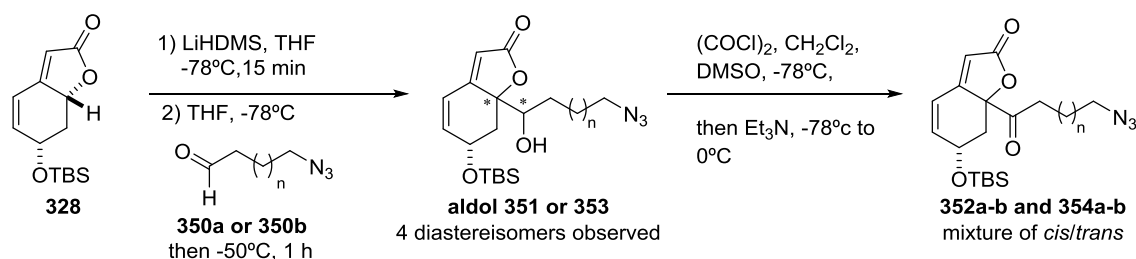
Diastereoselective aldol reaction and following swern oxidation

TBS-protected compound (**328**, 1 equiv.) was dissolved in freshly distilled THF (0.05 M) and cooled in a round bottom flask to -78°C . After 10 minutes LiHMDS (1.50 equiv.) was added and stirred for 30 minutes at same temperature while the mixture

⁸³ Bates, R. W.; Dewey, M. R., *Org. Lett.* **2009**, 11, 3706–3708

⁸⁴ John, J.; Thomas, J.; Parekh, N.; Dehaen, W., *European J. Org. Chem.* **2015**, 2015, 4922–4930.

turns orange. Corresponding aldehyde (**350a** or **350b**, 1.10 equiv.) then was added and reaction was warmed up to -50°C . Conversion was monitored by thin layer chromatography (20:80 EtOAc/Cyclohexane and 40:60 EtOAc/Cyclohexane). Reaction was quenched using aqueous saturated solution of NH_4Cl at -50°C and compound was extracted with EtOAc. Drying over Na_2SO_4 and evaporation to dryness afforded the crude of the reaction. Purification was made by flash column chromatography in silica gel using a ternary mixture (5:20:75 DCM/ Et_2O /Cyclohexane) and finally 100 % Et_2O to obtain the mixture of corresponding aldol compounds **351** or **353** as a mixture of diastereoisomers.



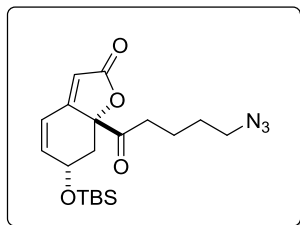
Scheme 3.65. Aldol reaction and swern oxidation.

To a round bottom flask containing DCM (0.10 M), oxalyl chloride (2 equiv.) was added at -78°C . After that DMSO (4 equiv.) was added dropwise keeping the temperature and stirring for 15 minutes. Then, mixture of aldol diastereoisomers **351** or **353** (1 equiv.) was added dissolved in DCM and stirred at low temperature for 30 additional minutes. Finally Et_3N (8 equiv.) was added and then led to stir at 0°C for another 30 minutes. Conversion of the reaction was monitored by thin layer chromatography (20:80 to 40:60 EtOAc/Cyclohexane) and aqueous saturated NaHCO_3 was added in order to quench the reaction. Extraction using DCM and then drying organic layer with Na_2SO_4 afforded after evaporation a crude mixture of **352a/352b** (*neosecurinine*) or **354a/354b** (*neonorsecurinine*) adducts in 80:20 ratio. Purification by flash column chromatography in silica gel using EtOAc/Cyclohexane mixture (10:90 then 20:80 respectively) afforded (*cis*) and (*trans*) adducts separately.

CHAPTER 3

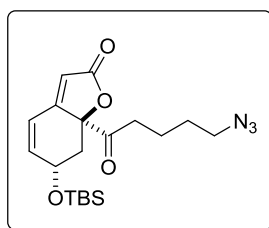
-Securinine precursors:

(6*R*,7*aS*)-7*a*-(5-azidobutanoyl)-6-((*tert*-butyldimethylsilyl)oxy)-7,7*a*-dihydrobenzofuran-2(6*H*)-one (**352a**)



(300 mg, 1.12 mmol of **328**) obtained 135 mg of colorless oil was afforded with a yield of 31 % (2 steps). R_f : 0.39 (EtOAc/Cyclohexane 20:80). $^1\text{H NMR}$ (300 MHz, CDCl_3) δ (ppm) = 6.48 (dd, J = 10.0, 2.2, 1H), 6.19 (dd, J = 9.8, 1.9 Hz, 1H), 5.93 (t, J = 0.7 Hz, 1H), 4.97 – 4.84 (m, 1H), 3.24 (t, J = 6.4 Hz, 2H), 2.99 – 2.84 (m, 1H), 2.60 (ddd, J = 18.5, 7.4, 6.3 Hz, 1H), 2.33 (dt, J = 18.6, 6.7 Hz, 1H), 1.77 (dd, J = 12.3, 8.8 Hz, 1H), 1.68 – 1.44 (m, 5H), 0.90 (s, 9H), 0.13 (d, J = 2.2 Hz, 6H). $^{13}\text{C NMR}$ (75 MHz, CDCl_3) δ (ppm) = 204.3, 172.2, 161.7, 144.8, 118.5, 112.6, 90.3, 66.4, 51.2, 41.0, 34.8, 28.2, 25.8, 20.7, 18.2, -4.6, -4.7. **FT-IR** (DCM): 2931, 2857, 2097, 1768, 1725, 1639, 1470, 1088, 1021. **HRMS (ESI/Q-TOF)**: $[\text{M} + \text{Na}]^+$ calculated for $\text{C}_{19}\text{H}_{29}\text{N}_3\text{NaO}_4\text{Si}$: 414.1819, found: 414.1808.

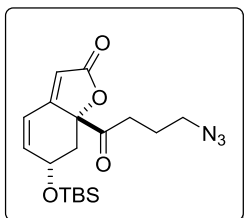
(6*R*,7*aR*)-7*a*-(5-azidobutanoyl)-6-((*tert*-butyldimethylsilyl)oxy)-7,7*a*-dihydrobenzofuran-2(6*H*)-one (**352b**)



(300 mg, 1.12 mmol of **328**) obtained 35 mg of product obtained in 8 % yield (2 steps). R_f : 0.27 (EtOAc/Cyclohexane 20:80). $^1\text{H NMR}$ (300 MHz, CDCl_3) δ (ppm) = 6.68 (d, J = 9.8 Hz, 1H), 6.12 (dd, J = 9.5, 4.8 Hz, 1H), 5.86 – 5.79 (m, 1H), 4.58 (td, J = 4.7, 1.8 Hz, 1H), 3.30 – 3.23 (m, 2H), 2.93 – 2.60 (m, 3H), 2.08 (dd, J = 13.5, 4.6 Hz, 1H), 1.71 – 1.51 (m, 4H), 0.87 (s, 9H), 0.11 (s, 2H), 0.07 (d, J = 3.5 Hz, 4H). $^{13}\text{C NMR}$ (75 MHz, CDCl_3) δ (ppm) = 201.3, 171.4, 163.0, 137.3, 121.7, 113.2, 87.8, 64.9, 51.3, 39.6, 37.4, 28.3, 25.8, 20.5, 18.3, 1.2, -4.6, -4.7. **FT-IR** (DCM): 2951, 2929, 2857, 2097, 1767, 1728, 1644, 1470, 1289, 1091, 1020, 778, 733. **HRMS (ESI/Q-TOF)**: $[\text{M} + \text{Na}]^+$ calculated for $\text{C}_{19}\text{H}_{29}\text{N}_3\text{NaO}_4\text{Si}$: 414.1819, found: 414.1827.

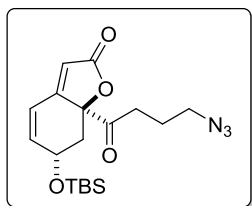
-Norsecurinine precursors:

(6*R*,7*aS*)-7*a*-(4-azidobutanoyl)-6-((*tert*-butyldimethylsilyl)oxy)-7,7*a*-dihydrobenzofuran-2(6*H*)-one (**354a**)



(400 mg, 1.50 mmol of **328**) obtained 167 mg of a yellowish oil in a 29 % yield (2 steps). *R*_f 0.35 (EtOAc/Cyclohexane 20:80). ¹H NMR (300 MHz, CDCl₃) δ (ppm) = 6.49 (dd, *J* = 10.0, 2.2 Hz, 1H), 6.19 (ddd, *J* = 10.1, 2.6, 0.9 Hz, 1H), 5.95 (t, *J* = 0.7 Hz, 1H), 4.98 – 4.81 (m, 1H), 3.25 (td, *J* = 6.6, 1.7 Hz, 2H), 2.91 (ddt, *J* = 12.3, 6.3, 0.9 Hz, 1H), 2.66 (dt, *J* = 18.7, 6.9 Hz, 1H), 2.41 (dt, *J* = 18.6, 7.0 Hz, 1H), 1.86 – 1.73 (m, 3H), 0.89 (s, 9H), 0.13 (d, *J* = 2.3 Hz, 6H). ¹³C NMR (75 MHz, CDCl₃) δ (ppm) = 204.0, 172.2, 161.6, 144.7, 118.5, 112.7, 90.2, 66.4, 50.4, 41.0, 32.4, 25.8, 25.8, 22.8, 18.2, -4.6, -4.7. FT-IR (DCM): 2955, 2931, 2099, 1773, 1725, 1639, 1464, 1385, 854, 728. HRMS (ESI/Q-TOF): [M + H]⁺ calculated for C₁₈H₂₈N₃O₄Si: 378.1845, found: 378.1845.

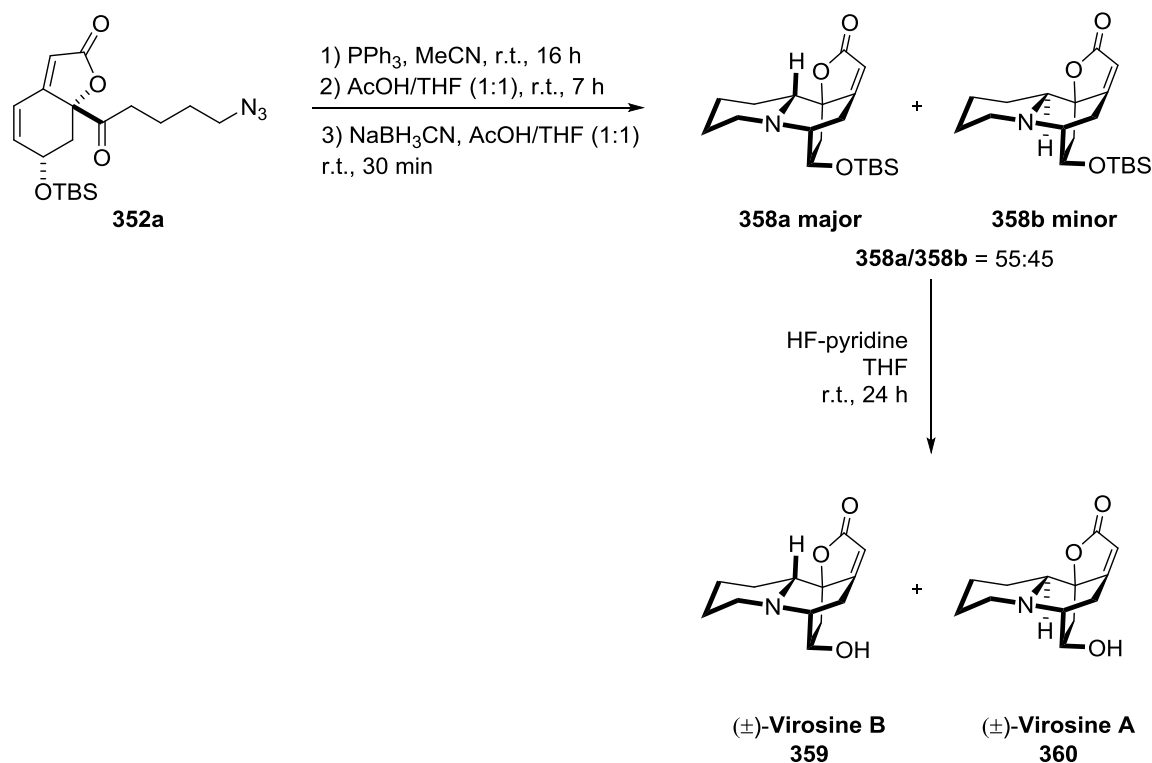
(6*R*,7*aR*)-7*a*-(4-azidobutanoyl)-6-((*tert*-butyldimethylsilyl)oxy)-7,7*a*-dihydrobenzofuran-2(6*H*)-one (**354b**)



(400 mg, 1.50 mmol of **328**) obtained 29 mg of yellowish oil in a yield of 5 % (2 steps). *R*_f 0.28 (EtOAc/Cyclohexane 20:80). ¹H NMR (300 MHz, CDCl₃) δ (ppm) = 6.71 – 6.64 (m, 1H), 6.12 (ddd, *J* = 9.9, 5.0, 1.1 Hz, 1H), 5.83 (s, 1H), 4.58 (td, *J* = 4.7, 1.8 Hz, 1H), 3.28 (td, *J* = 6.7, 4.6 Hz, 2H), 2.98 – 2.64 (m, 4H), 2.08 (dd, *J* = 13.5, 4.6 Hz, 1H), 1.83 (qd, *J* = 8.8, 7.9, 6.8 Hz, 3H), 0.86 (s, 9H), 0.08 (d, *J* = 8.9 Hz, 6H). ¹³C NMR (75 MHz, CDCl₃) δ (ppm) = 201.0, 171.3, 162.7, 137.3, 121.7, 113.2, 87.7, 64.8, 50.8, 39.5, 35.1, 25.8, 25.7, 22.9, 18.3, -4.6, -4.7. FT-IR (DCM): 2954, 2930, 2099, 1769, 1727, 1644, 1470, 1388, 856, 779, 712. HRMS (ESI/Q-TOF): [M + H]⁺ calculated for C₁₈H₂₈N₃O₄Si: 378.1845, found: 378.1849.

CHAPTER 3

3.9.2.5 Procedure for the synthesis of Securinega alkaloids of neosecurinine type

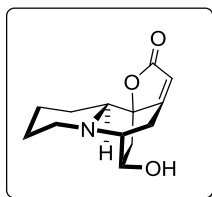


Scheme 3.66. Procedure for the racemic synthesis of **Virosine B** and **Virosine A** starting from **352a**.

(±)-Virosine A and (±)-Virosine B: To a stirred solution of azide precursor **352a** (0.18 g, 0.45 mmol) in argon-degassed ACN (9 mL) was added PPh_3 (0.59 g, 2.23 mmol) at room temperature. The mixture was stirred overnight at room temperature, and all volatiles were removed *in vacuo*. The resulting oil was dissolved in a THF/AcOH 1:1 mixture (9 mL), and was stirred 7 hours at room temperature. NaBH_3CN (0.281 g, 4.47 mmol) was then added, and the reaction mixture was stirred another 30 minutes at room temperature, before water (10 mL) and brine (5 mL) were added to quench the reaction. Organic compound was extracted with EtOAc (6 x 10 mL) from the aqueous solution. The combined organic layers were dried over Na_2SO_4 , and concentrated *in vacuo*. Filtration through a short pad of silica gel, eluting with $\text{Et}_2\text{O}/\text{DCM}/\text{Petroleum ether}$ (8:2:90 to 32:8:60), afforded the protected natural products as a mixture of diastereomers **358a** and **358b** (55:45 ratio). The resulting oil was dissolved in THF (9 mL) and transferred to a Teflon reactor, before hydrogen fluoride (70% in pyridine, 1.16 mL, 44.7 mmol) was added at room temperature. The reaction mixture was stirred 24 hours at room temperature, before an aqueous solution of K_2CO_3 (8.1 M, 5.52 mL, 44.7 mmol) was added to quench the reaction. The resulting mixture

was further diluted with a saturated aqueous solution of NaHCO_3 (6 mL), water (3 mL), and EtOAc (15 mL). The organic layer was separated and the aqueous layer was extracted with EtOAc (6 x 15 mL). The combined organic extracts were dried over Na_2SO_4 , and concentrated under reduced pressure. Purification by column chromatography on silica gel, eluting with $\text{Et}_2\text{O}/\text{DCM}$ (0:100 to 50:50), afforded (\pm)-**Virosine A** and (\pm)-**Virosine B**.

(\pm)-**Virosine A** (**360**)^{85,86}



20 mg of colorless oil were obtained (from azide **352a**, 175 mg, 0.45 mmol, yield = 19 %). R_f : 0.27 ($\text{Et}_2\text{O}/\text{DCM}$ 40:60). $^1\text{H NMR}$ (300 MHz, CDCl_3) δ (ppm) = 5.70 (t, J = 1.7 Hz, 1H), 4.42 – 4.33 (m, 1H), 2.98 (d, J = 18.2 Hz, 1H), 2.94 – 2.75 (m, 3H), 2.75 – 2.62 (m, 2H), 1.81 (d, J = 13.5 Hz, 2H, –OH), 1.63 – 1.51 (m, 2H), 1.46 (dd, J = 12.4, 4.8 Hz, 1H), 1.52 – 1.34 (m, 1H), 1.38 – 1.17 (m, 1H), 0.86 (ddd, J = 23.3, 12.1, 4.0 Hz, 1H). $^{13}\text{C NMR}$ (75 MHz, CDCl_3) δ (ppm) = 174.3, 174.2, 111.6, 84.6, 65.3, 65.0, 59.0, 52.8, 40.9, 29.5, 26.7, 25.7, 24.0. **FT-IR (neat)**: 3450, 2924, 2853, 1750, 1736, 1637, 1260, 1149 cm^{-1} . **HRMS (ESI/Q-TOF)**: $[\text{M} - \text{H}]^-$ calculated for $\text{C}_{13}\text{H}_{16}\text{NO}_3$ 234.1135, found 234.1137. Physical and spectroscopic data from (\pm)-**Virosine A** are identical to those reported in the literature.

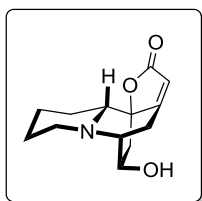
⁸⁵ Wang, G.-C.; Wang, Y.; Li, Q.; Liang, J.-P.; Zhang, X.-Q.; Yao, X.-S.; Ye, W.-C., *Helv. Chim. Acta* **2008**, *91*, 1124–1129.

⁸⁶ Bélanger, G.; Dupuis, M.; Larouche-Gauthier, R., *J. Org. Chem.* **2012**, *77*, 3215–3221.

CHAPTER 3

Table 8. Comparison of spectroscopic data for naturally occurring **Virosine A** and experimentally obtained one.

¹ H NMR This work (300 MHz, CDCl ₃) (ppm)	¹ H NMR Isolated Product (400 MHz, CDCl ₃) (ppm) ⁸⁵	¹³ C NMR This work (75 MHz, CDCl ₃) (ppm)	¹³ C NMR Isolated Product (50 MHz, CDCl ₃) (ppm) ⁸⁵
5.70 (t, <i>J</i> = 1.7 Hz, 1H)	5.65 (s, 1H)	174.3	174.7
4.42 – 4.33 (m, 2H)	4.35 – 4.29 (m, 1H)	174.2	174.3
2.98 (d, <i>J</i> = 18.2 Hz, 1H)	2.96 (br, d, <i>J</i> = 18.5 Hz, 1H)	111.6	111.2
2.94 – 2.75 (m, 3H)	2.95 – 2.89 (m, 1H)	84.6	84.6
	2.90 – 2.85 (m, 1H)	65.3	65.1
	2.78 – 2.72 (m, 1H)	65.0	64.6
2.75 – 2.62 (m, 2H)	2.72 – 2.66 (m, 1H)	59.0	58.8
	2.70 – 2.64 (m, 1H)	52.8	52.5
-	2.65 (dd, <i>J</i> = 12.2, 9.5 Hz, 1H)	40.9	40.6
1.81 (brd, <i>J</i> = 13.5 Hz, 2H, –OH)	1.78 (br, d, <i>J</i> = 12.6 Hz, 1H)	29.5	29.3
1.63 – 1.51 (m, 2H) and 1.52 – 1.34 (m, 1H)	1.54 – 1.46 (m, 3H)	26.7	26.4
1.46 (dd, <i>J</i> = 12.4, 4.8 Hz, 1H)	1.43 (dd, <i>J</i> = 12.3, 4.9 Hz, 1H)	25.7	25.5
1.38 – 1.17 (m, 1H)	1.32 – 1.24 (m, 1H)	24.0	23.8
0.86 (ddd, <i>J</i> = 23.3, 12.1, 4.0 Hz, 1H)	0.88 – 0.80 (m, 1H)		

(±)-Virosine B (**359**)⁸⁵

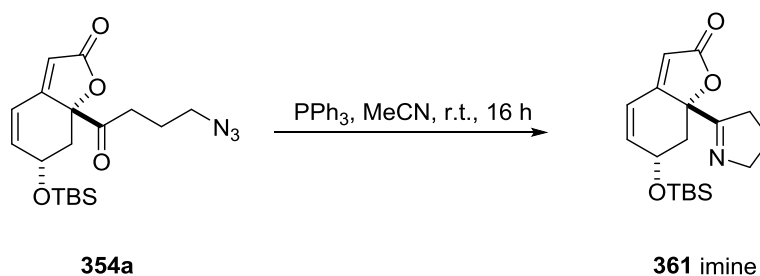
30 mg of crystalline solid were obtained (from azide **352a**, 175 mg, 0.45 mmol, yield = 29 %). *R_f*: 0.35 (Et₂O/DCM 40:60). ¹H NMR (300 MHz, CDCl₃) δ (ppm) = 5.60 (t, *J* = 1.8 Hz, 1H), 4.21 (dd, *J* = 8.4, 5.1 Hz, 1H), 3.11 (dt, *J* = 19.3, 2.0 Hz, 1H), 2.97 – 2.85 (m, 1H), 2.84 – 2.77 (m, 2H), 2.75 (brd, *J* = 8.9 Hz, 1H), 2.71 – 2.59 (m, 1H), 2.21 (brd, *J* = 10.2 Hz, 2H, –OH), 1.91 – 1.78 (m, 1H), 1.68 – 1.48 (m, 3H), 1.44 – 1.23 (m, 2H), 1.19 (d, *J* = 13.2 Hz, 1H). ¹³C NMR (75 MHz, CDCl₃) δ (ppm) = 176.9, 174.6, 108.8, 85.2, 66.7, 63.2, 57.6, 52.6, 36.4, 26.8, 25.9, 24.7, 23.1. FTIR (neat): 3450, 2937, 2853, 2786, 1749, 1733, 1652, 1152, 1050 cm⁻¹. HRMS (ESI/Q-TOF): [M + H]⁺ calculated for C₁₃H₁₉NO₃ 236.1280, found 236.1278. Physical and spectroscopic data from *(±)*-Virosine B are identical to those reported in the literature.

CHAPTER 3

Table 9. Comparison of spectroscopic data for naturally occurring **Virosine B** and experimentally obtained one.

¹ H NMR This work (300 MHz, CDCl ₃) (ppm)	¹ H NMR Isolated Product (400 MHz, CDCl ₃) (ppm) ⁸⁵	¹³ C NMR This work (75 MHz, CDCl ₃) (ppm)	¹³ C NMR Isolated Product (50 MHz, CDCl ₃) (ppm) ⁸⁵
5.60 (t, <i>J</i> = 1.8 Hz, 1H)	5.63 (s, 1H)	176.9	176.1
4.21 (dd, <i>J</i> = 8.4, 5.1 Hz, 1H)	4.23 (dd, <i>J</i> = 8.5, 5.1 Hz 1H)	174.6	174.1
3.11 (dt, <i>J</i> = 19.3, 2.0 Hz, 1H)	3.11 (td, <i>J</i> = 19.3, 2.1 Hz, 1H)	108.8	108.8
2.97 – 2.85 (m, 1H)	2.95 – 2.91 (m, 1H)	85.2	84.8
2.84 – 2.77 (m, 2H)	2.84 – 2.78 (m, 2H)	66.7	66.7
2.75 (d, <i>J</i> = 8.9 Hz, 1H)	2.76 (dd, <i>J</i> = 13.1, 8.6 Hz, 1H)	63.2	63.2
2.71 – 2.59 (m, 1H)	2.72 – 2.64 (m, 1H)	57.6	57.5
2.21 (br, d, <i>J</i> = 10.2 Hz, 2H, –OH)	2.24 (br, d, <i>J</i> = 10.4 Hz, 1H)	52.6	52.5
1.91 – 1.78 (m, 1H)	1.85 (td, <i>J</i> = 9.7, 3.1 Hz, 1H)	36.4	36.5
1.68 – 1.48 (m, 3H)	1.62 – 1.56 (m, 3H)	26.8	26.7
1.44 – 1.23 (m, 2H)	1.46 – 1.39 (m, 1H)	25.9	25.7
	1.36 – 1.28 (m, 1H)	24.7	24.6
1.19 (d, <i>J</i> = 13.2 Hz, 1H)	1.20 (br, d, <i>J</i> = 13.1 Hz, 1H)	23.1	22.9

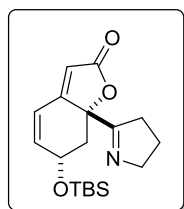
3.9.2.6 Synthesis of neonorsecurinine-type natural products



Scheme 3.67. Staudinger aza-Wittig reaction afforded 5 membered stable imine **361**-*cis*.

Compound **354a** (0.14 g, 0.37 mmol) was dissolved in previously degassed ACN (0.05 M, 7.40 mL). Subsequently PPh_3 (0.48 g, 1.84 mmol) was added and mixture was stirred at room temperature. Reaction was monitored by ^1H NMR in CDCl_3 observing full conversion into desired imine after 5 h. Then mixture was evaporated to dryness in order to obtain the crude imine. Compound was purified by flash column chromatography in silica gel, using a mixture 30:70 of $\text{Et}_2\text{O}/\text{PET}$. 90 mg of a white powder were obtained, corresponding to the desired product **361**, yield = 72 %.

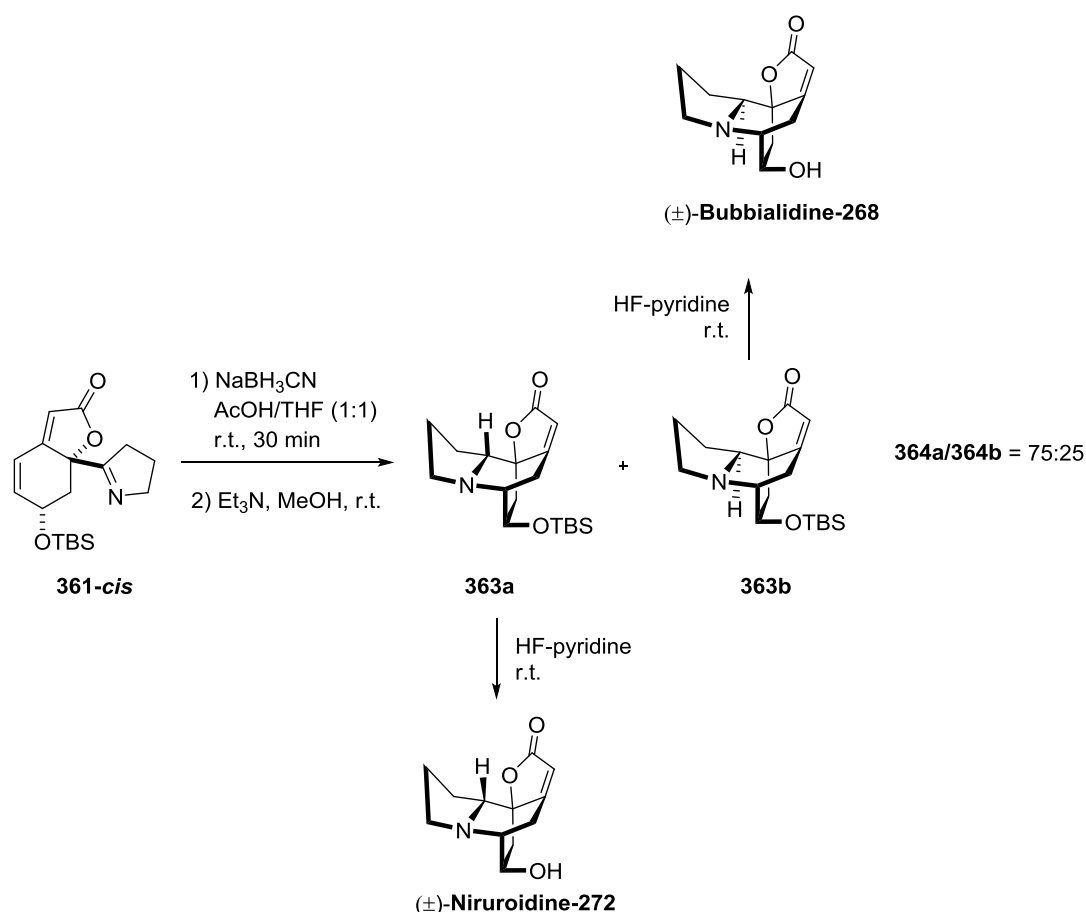
(6*R*,7*aS*)-6-((*tert*-butyldimethylsilyl)oxy)-7*a*-(3,4-dihydro-2*H*-pyrrol-5-yl)-7,7*a*-dihydrobenzofuran-2(6*H*)-one (**cis**-**361**)



R_f: 0.34 ($\text{Et}_2\text{O}/\text{PET}$ 30:70). **^1H NMR** (300 MHz, CDCl_3) δ (ppm) = 6.51 (dd, J = 10.0, 2.3 Hz, 1H), 6.13 (dd, J = 10.0, 2.4 Hz, 1H), 4.80 (m, 1H), 3.92 – 3.81 (m, 2H), 3.15 – 3.02 (m, 1H), 2.63 – 2.48 (m, 1H), 2.42 – 2.28 (m, 1H), 1.93 – 1.79 (m, 3H), 0.89 (s, 9H), 0.11 (s, 6H). **^{13}C**

NMR (75 MHz, CDCl_3) δ (ppm) =: 173.4, 172.2, 164.2, 144.0, 119.2,

112.2, 85.7, 67.1, 61.7, 41.9, 32.9, 25.9, 22.4, 18.2, -4.4, -4.6. **FT-IR** (DCM): 2955, 2931, 1767, 1642, 1471, 874, 864, 838, 779. **HRMS (ESI/Q-TOF)**: $[\text{M} + \text{H}]^+$ calculated for $\text{C}_{18}\text{H}_{28}\text{NO}_3\text{Si}$: 334.1834, found: 334.1832.



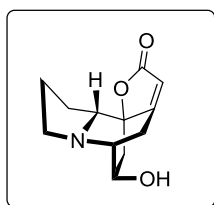
Scheme 3.68. Procedure for the racemic synthesis of Niruroidine and Bubbialidine starting from **361-*cis***.

(±)-Niruroidine and (±)-Bubbialidine: To a stirred solution of imine precursor **361** (52 mg, 0.16 mmol, *cis*) in THF (1.50 mL) and AcOH (1.50 mL) was added NaBH_3CN (98 mg, 1.56 mmol) at room temperature. The reaction mixture was stirred 30 minutes at room temperature, before water (5 mL) and brine (10 mL) were added to quench the reaction. The aqueous solution was then extracted with EtOAc (8 x 10 mL). The combined organic extracts were dried over Na_2SO_4 , and concentrated *in vacuo*. In order to obtain cyclized products, crude was dissolved in MeOH (3.12 mL) and Et_3N (0.65 mL, 4.68 mmol) was added. After 30 minutes at r.t. reaction was evaporated to dryness. Purification by column chromatography on silica gel, eluting with EtOAc/DCM (20:80 to 50:50), afforded both TBS-protected natural products as colorless oils in a 75:25 ratio. **363b** (minor, 14 mg): $R_f = 0.53$ (EtOAc/DCM 50:50); **363a** (major, 36 mg): $R_f = 0.44$ (EtOAc/DCM 50:50). ^1H and ^{13}C NMR data was not conclusive for either diastereomers **363a** and **363b**, which were not characterized.

Each separated fractions (**363b** or **363a**) were dissolved in THF (0.05 M) and transferred to a Teflon reactor, before hydrogen fluoride (70% in pyridine, 100 equiv.)

was added at room temperature. The reaction mixtures were stirred 24 hours at room temperature, before an aqueous solution of K_2CO_3 (8.10 M, 100 equiv.) was added to quench the reaction. The resulting solution was further diluted with a saturated aqueous solution of $NaHCO_3$ (3 mL), water (1 mL), and EtOAc (5 mL). The organic layer was separated and the aqueous layer was extracted with EtOAc (6 x 5 mL). The combined organic extracts were dried over Na_2SO_4 , and concentrated to dryness. Purification by column chromatography on silica gel, eluting with EtOAc followed by MeOH/DCM (10:90), afforded (\pm)-**Niruroidine** and (\pm)-**Bubbialidine**.

(\pm)-**Niruroidine** (**272**)^{87,88}



17 mg of colorless oil were obtained from major diastereoisomer **364a** (from imine **362**, 52 mg, 0.156 mmol, yield = 49 %). R_f : 0.25 (MeOH/DCM 10/90). 1H NMR (300 MHz, $CDCl_3$) δ (ppm) = 5.71 (t, J = 2.0 Hz, 1H), 4.46 – 4.37 (m, 1H), 3.25 (dt, J = 19.1, 2.0 Hz, 1H), 3.13 – 3.03 (m, 2H), 2.98 (t, J = 6.7 Hz, 1H), 2.94 – 2.83 (m, 2H), 2.78 (dd, J = 13.8, 9.8 Hz, 1H), 2.30 (s, 1H, –OH), 2.00 – 1.83 (m, 2H), 1.83 – 1.69 (m, 2H), 1.33 (ddd, J = 13.8, 3.2, 1.4 Hz, 1H). ^{13}C NMR (75 MHz, $CDCl_3$) δ (ppm) = 175.5, 174.1, 110.4, 84.5, 62.2, 61.7, 55.9, 51.4, 34.3, 27.5, 27.4, 25.8. FT-IR (neat): 3450, 2956, 2924, 2853, 1747, 1733, 1652, 1152, 1050 cm^{-1} . HRMS (ESI/Q-TOF) m/z : $[M - H]^+$ calculated for $C_{12}H_{14}NO_3$ 220.0974, found 220.0984. Physical and spectroscopic data from (\pm)-**Niruroidine** are identical to those reported in the literature.

⁸⁷ Gedris, T. E.; Herz, W.; Florida, T., *Phytochemistry* **1996**, 41, 1441–1443.

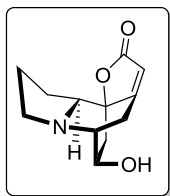
⁸⁸ Ma, N.; Yao, Y.; Zhao, B.-X.; Wang, Y.; Ye, W.-C.; Jiang, S., *Chem. Commun.* **2014**, 50, 9284–9287.

CHAPTER 3

Table 10. Comparison of spectroscopic data for naturally occurring Niruroidine and experimentally obtained one.

¹ H NMR This work (300 MHz, CDCl ₃) (ppm)	¹ H NMR Isolated Product (500 MHz, CDCl ₃) (ppm) ⁸⁷	¹³ C NMR This work (75 MHz, CDCl ₃) (ppm)	¹³ C NMR Isolated Product (50.3 MHz, CDCl ₃) (ppm) ⁸⁷
5.71 (t, <i>J</i> = 2.0 Hz, 1H)	5.74 (t, <i>J</i> = 12.0 Hz, 1H)	175.5	174.8
4.46 – 4.37 (m, 1H)	4.45 (br, ddd, <i>J</i> = 9.5, 3.0, 1.5 Hz, 1H)	174.1	173.9
3.25 (dt, <i>J</i> = 19.1, 2.0 Hz, 1H)	3.26 (ddd, <i>J</i> = 19.5, 2.0, 2.0 Hz, 1H)	110.4	110.8
3.13 – 3.03 (m, 2H)	3.15 (m, <i>J</i> = 3.0, 2.0 Hz 1H)	84.5	83.9
	3.12 (m, 1H)	62.2	62.1
2.98 (t, <i>J</i> = 6.7 Hz, 1H)	3.02 (ddd, <i>J</i> = 7.0, 1.5 Hz 1H)	61.7	61.5
2.94 – 2.83 (m, 2H)	2.91 (m, <i>J</i> = 19.5, 12.0, 1.5 Hz, 1H)	55.9	55.7
	2.89 (m, 1H)	51.4	51.0
2.78 (dd, <i>J</i> = 13.8, 9.8 Hz, 1H)	2.81 (dd, <i>J</i> = 14.0, 9.5 Hz, 1H)	34.3	34.0
2.30 (brs, 1H, –OH)			
2.00 – 1.83 (m, 2H)	1.97 (m, <i>J</i> = 7.0 Hz, 1H)	27.5	27.0
	1.91 (m, 1H)	27.4	26.9
1.83 – 1.69 (m, 2H)	1.79 (m, <i>J</i> = 7.0 Hz, 2H)	25.8	25.4
1.33 (ddd, <i>J</i> = 13.8, 3.2, 1.4 Hz, 1H)	1.36 (ddd, <i>J</i> = 14.0, 3.0, 1.5 Hz, 1H)		

(±)-*Bubbialidine* (**268**)^{89,90}



7 mg of colorless oil were obtained from minor diastereoisomer **364b** (from imine **362**, 52 mg, 0.156 mmol, yield = 21 %). *R_f*: 0.25 (MeOH/DCM 10:90). **¹H NMR** (300 MHz, CDCl₃) δ (ppm) = 5.78 (t, *J* = 2.0 Hz, 1H), 4.45 (dt, *J* = 9.5, 3.4 Hz, 1H), 3.51 (dd, *J* = 9.2, 6.1 Hz, 1H), 3.12 – 3.08 (m, 1H), 3.07 – 3.02 (m, 1H), 3.01 – 2.97 (m, 2H), 2.93 (s, 1H, –OH), 2.76 – 2.68 (m, 1H), 2.67 (dd, *J* = 12.9, 9.5 Hz, 1H), 1.86 – 1.65 (m, 3H), 1.51 (dd, *J* = 12.9, 3.1 Hz, 1H), 1.15 – 0.98 (m, 1H). **¹³C NMR** (75 MHz, CDCl₃) δ 173.5, 171.2, 112.9, 84.1, 67.5, 63.0, 55.6, 50.9, 40.5, 27.0, 25.2, 21.8. **FT-IR (neat)**: 3400, 2956, 2924, 2854, 1754, 1737, 1650, 1461, 1255, 1082, 921, 849 cm⁻¹. **HRMS (ESI/Q-TOF) m/z**: [M – H]⁺ calculated for C₁₂H₁₄NO₃ 220.0974, found 220.0971. Physical and spectroscopic data from (±)-**Bubbialidine** are identical to those reported in the literature.

⁸⁹ Ahond, A.; Guilhem, J.; Hamon, J.; Poupat, C.; Pusset, J.; Pusset, M.; Sevenet, T.; Potier, P., *J. Nat. Prod.* **1990**, 53, 875–881.

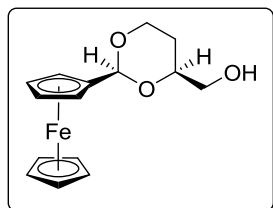
⁹⁰ Miyatake-Ondoababal, H.; Bannwart, L. M.; Gademann, K., *Chem. Commun.* **2013**, 49, 1921–1923.

CHAPTER 3

Table 11. Comparison of spectroscopic data for naturally occurring **Bubbialidine** and experimentally obtained one.

¹ H NMR This work (300 MHz, CDCl ₃) (ppm)	¹ H NMR Isolated Product (400 MHz, CDCl ₃) (ppm) ⁸⁹	¹³ C NMR This work (75 MHz, CDCl ₃) (ppm)	¹³ C NMR Isolated Product (50 MHz, CDCl ₃) (ppm) ⁸⁹
5.78 (t, <i>J</i> = 2.0 Hz, 1H)	5.77 (t, <i>J</i> = 2.0 Hz, 1H)	173.5	173.3
4.45 (dt, <i>J</i> = 9.5, 3.4 Hz, 1H)	4.47 (dt, <i>J</i> = 10.0, 3.0 Hz, 1H)	171.2	170.9
3.51 (dd, <i>J</i> = 9.2, 6.1 Hz, 1H)	3.54 (dd, <i>J</i> = 9.0, 6.0 Hz, 1H)	112.9	113.0
3.12 – 3.08 (m, 1H)	3.13 (sp, <i>J</i> = 8.0 Hz, 1H)	84.1	83.9
3.07 – 3.02 (m, 1H)	3.06 (m, 1H)	67.5	67.2
3.01 – 2.97 (m, 2H)	2.99 (m, 1H)	63.0	63.1
2.93 (brs, 1H, –OH)			
2.76 – 2.68 (m, 1H)	2.70 (dt, <i>J</i> = 10.0, 6.0 Hz, 1H)	55.6	55.8
2.67 (dd, <i>J</i> = 12.9, 9.5 Hz, 1H)	2.65 (dd, <i>J</i> = 13.0, 9.0 Hz, 1H)	50.9	51.0
1.86 – 1.65 (m, 3H)	1.78 (m, 2H)	40.5	40.5
1.51 (dd, <i>J</i> = 12.9, 3.1 Hz, 1H)	1.50 (dd, <i>J</i> = 13.0, 3.0 Hz, 1H)	27.0	27.0
1.15 – 0.98 (m, 1H)	1.06 (m, 1H)	25.2	25.1
		21.8	21.8

3.9.3 Synthesis of Ferrocenyl Iodanes and their applications

(2S,4S)-4-(Hydroxymethyl)-2-ferrocenyl-1,3-dioxane (**103**)

According to the procedure describe by Kagan⁹¹ commercially available ferrocenecarboxaldehyde **100** (3.00 g, 14.02 mmol) was dissolved in trimethyl orthoformate (18.00 mL) and then *p*-toluenesulfonic acid (130 mg, 0.68 mmol) was added to the reaction mixture. Then reaction was heated for 16 h at 80°C.

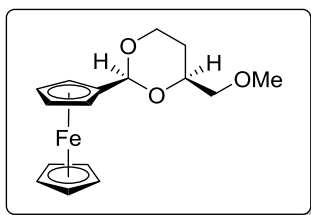
Once reaction is finished, K₂CO₃ anhydrous was added to the cold mixture and then diluted with diethyl ether. Then the product was filtered through a pad of CELITE and evaporated to dryness to afford a mixture 90:10 of desired product and starting material.

Then 1,2,4-butanetriol (1.04 g, 9.81 mmol) was previously washed 3 times by using as co-solvent toluene (10 mL) and dried under high vacuum for 6 hours. After, 1*S*-(+)-10-camphorsulfonic acid (114 mg, 0.491 mmol) was added to the flask and everything was dissolved in 20 mL of CHCl₃. Subsequently, in another flask the protected aldehyde (2.55 g, 9.81 mmol) was dissolved in CHCl₃ and was added dropwise at room temperature to the butanetriol. Reaction was followed by thin layer chromatography (30:70 EtOAc/cyclohexane), and was finished after 20 hours. Again addition of anhydrous K₂CO₃ and filtration through a pad of CELITE led to a filtrate which was evaporated to obtain the crude. Purification by flash column chromatography in silica gel in gradient of 10:90 to 30:70 EtOAc in cyclohexane afforded 2.06 g of dioxane. Yellow oil was obtained in a 54 % yield was obtained. ¹H NMR (300 MHz, CDCl₃) δ (ppm) = 5.41 (s, 1H), 4.34 (d, *J* = 2.0 Hz, 2H), 4.24 (ddd, *J* = 11.4, 5.2, 1.4 Hz, 1H), 4.17 (s, 5H), 4.14 (t, *J* = 1.9 Hz, 2H), 3.99 – 3.85 (m, 2H), 3.66 (ddd, *J* = 9.7, 7.0, 4.2 Hz, 2H), 2.04 (dd, *J* = 7.8, 5.3 Hz, 1H), 1.86 (tdd, *J* = 12.6, 11.5, 5.2 Hz, 1H), 1.41 (dtd, *J* = 13.2, 2.6, 1.4 Hz, 1H). ¹³C NMR (75 MHz, CDCl₃) δ (ppm) = 100.3, 85.9, 69.0, 68.2, 66.8, 66.6, 65.9 27.0.

⁹¹ Riant, O.; Samuel, O.; Flessner, T.; Taudien, S.; Kagan, H. B., *J. Org. Chem.* **1997**, 62, 6733–6745.

CHAPTER 3

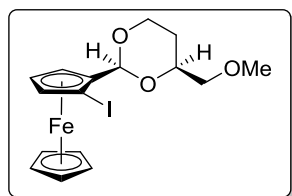
(2*S*,4*S*)-4-(Methoxymethyl)-2-ferrocenyl-1,3-dioxane (**104**)⁹¹



1,3-dioxane **103** (2.06 g, 6.82 mmol) was dissolved in THF (30 mL) under argon atmosphere. Reaction mixture was cooled to 0°C and NaH (0.49 g, 20.46 mmol) was added as a solid. After 10 minutes of stirring at 0°C, iodomethane (0.85 mL, 13.64 mmol) was added dropwise. Then reaction was led to stir at room temperature for 15 minutes. Monitored by TLC (30:70 EtOAc in cyclohexane), when reaction was finished reaction was quenched with 5 mL of MeOH and 5 mL of H₂O, then washed 2 times with H₂O and 2 times with brine. After drying over Na₂SO₄ and evaporating to dryness product was purified by flash column chromatography in silica gel with 20:80 EtOAc in cyclohexane. 2.02 g of a yellow oil were obtained with a yield of 94%.

¹H NMR (300 MHz, CDCl₃) δ (ppm) = 5.37 (s, 1H), 4.38 – 4.33 (m, 1H), 4.27 – 4.19 (m, 2H), 4.17 (s, 5H), 4.11 (t, *J* = 1.9 Hz, 2H), 4.00 (dddd, *J* = 11.1, 6.0, 4.6, 2.5 Hz, 1H), 3.90 (ddd, *J* = 12.4, 11.4, 2.6 Hz, 1H), 3.54 (dd, *J* = 10.4, 6.0 Hz, 1H), 3.43 (s, 3H), 3.42 – 3.33 (m, 1H), 1.78 (dddd, *J* = 13.2, 12.3, 11.4, 5.1 Hz, 1H), 1.49 (dtd, *J* = 13.2, 2.6, 1.4 Hz, 1H). ¹³C NMR (75 MHz, CDCl₃) δ (ppm) = 100.2, 86.1, 76.2, 75.7, 69.0, 68.0, 67.9, 66.8, 66.7, 59.5, 28.1. One signal is missing.

(2*S*,4*S*,*S_p*)-4-(Methoxymethyl)-2-(α-iodoferrocenyl)-1,3-dioxane (**365**)⁹¹



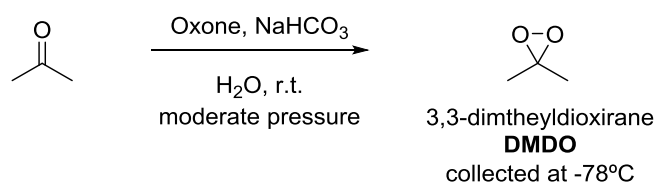
Methoxy dioxane **104** (1.51 g, 4.76 mmol) was dissolved in THF (20 mL, distilled) under argon atmosphere. Reaction mixture was cooled to -78°C and stirred 10 minutes. Then tertbutyl lithium solution (6.08 mL, 5.71 mmol) was added dropwise and led to reach room temperature. After 1 hour of stirring, mixture was cooled to -78°C again and 1,2-diiodoethane (1.74 g, 6.19 mmol) was added dropwise previously dissolved in THF. Then reaction was led to stirred for 10 minutes and then 4 hours at room. Reaction was monitored by TLC (ternary mixture 13:37:50 Et₂O/CH₂Cl₂/cyclohexane) and it was quenched with 8 mL of Na₂S₂O₃, 8 mL of H₂O, 8 mL of NaHCO₃ aq. (sat.) when starting material was consumed. Compound was extracted 3 times using 20 mL of EtOAc. Organic layer was dried over Na₂SO₄ and evaporated to dryness. Product was purified by flash column chromatography in silica gel eluting with a mixture 13:37:50 Et₂O/CH₂Cl₂/cyclohexane. 763 mg of orange oil were obtained, yield of 37%. ¹H NMR (300 MHz, CDCl₃) δ (ppm) = 5.40 (s, 1H, H-

acetal), 4.44 (dd, $J = 2.7, 1.4$ Hz, 1H), 4.40 (dd, $J = 2.5, 1.4$ Hz, 1H), 4.31 (ddd, $J = 11.3, 5.1, 1.4$ Hz, 1H), 4.20 (t, $J = 2.6$ Hz, 1H), 4.17 (s, 5H, H-Cp), 4.09 – 3.94 (m, 2H), 3.51 (dd, $J = 10.3, 5.6$ Hz, 1H), 3.40 (d, $J = 5.0$ Hz, 1H), 3.38 (s, 3H), 1.82 (dddd, $J = 13.3, 12.4, 11.4, 5.2$ Hz, 1H), 1.52 (dtd, $J = 13.3, 2.6, 1.4$ Hz, 1H). **^{13}C NMR** (75 MHz, CDCl_3) δ (ppm) = 101.0, 86.1 (C-quaternary, Cp), 76.3, 75.4, 74.9, 71.8, 68.7, 67.1, 66.3, 59.4, 41.5 (C-ipso), 28.1. **FT-IR** (KBr): 3097, 2922, 2852, 1478, 1376, 1106, 821. **LMS (ESI/Q-TOF)**: $[\text{M} + \text{H}]^+ = 442.9$ u.

Deuterated DMSO: **^1H NMR** (300 MHz, $\text{DMSO}-d_6$) δ (ppm) = 5.39 (s, 1H, H-acetal), 4.47 (dd, $J = 2.4, 1.4$ Hz, 1H), 4.36 (dd, $J = 2.7, 1.4$ Hz, 1H), 4.28 (t, $J = 2.5$ Hz, 1H), 4.22 (ddd, $J = 11.4, 5.2, 1.3$ Hz, 1H), 4.16 (s, 5H, Cp), 4.01 (ddd, $J = 11.8, 10.0, 2.8$ Hz, 2H), 3.39 – 3.28 (m, 2H), 3.26 (s, 3H), 1.63 (qd, $J = 12.2, 5.1$ Hz, 1H), 1.51 – 1.41 (m, 1H). **^{13}C NMR** (75 MHz, $\text{DMSO}-d_6$) δ (ppm) = 100.0, 86.1 (C-quaternary, Cp), 75.5, 74.7, 74.3, 71.5, 68.5, 66.2, 65.9, 58.4, 41.0 (C-ipso), 27.2.

Preparation and titration of 3,3-dimethyldioxirane (DMDO)⁹²

To a stirred solution of sodium bicarbonate (NaHCO_3 , 58 g, 0.69 mol, 0.27 equiv.) in water (254 mL) was added acetone (192 mL, 2.59 mol, 1.0 equiv.). The resulting mixture was cooled down to 0 °C, and Oxone® (120 g, 0.195 mol, 0.15 mol KHSO_5) was added every two minutes in successive portions to avoid too much foaming. The ice bath was then removed, and the resulting solution was distilled under reduced pressure (ca. 20-30 mmHg) for 1 hour, the distillate being collected at -78 °C, until no more distillation was observed. The distillate was stored at -18 °C on 4 Å molecular sieves, and could be kept between 10 and 15 days at this temperature.



Scheme 3.69. Synthesis of DMDO.

⁹² Bosset, C.; Coffinier, R.; Peixoto, P. A.; El Assal, M.; Miqueu, K.; Sotiropoulos, J. M.; Pouységu, L.; Quideau, S., *Angew. Chem., Int. Ed* **2014**, 53, 9860–9864.

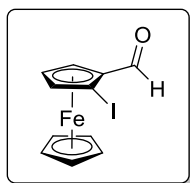
CHAPTER 3

Titration of the DMDO solution in acetone was performed by adding 1 mL of this freshly prepared solution (DMDO postulated at 0.2 M in acetone) to methyl *para*-tolyl sulfide (27 μ L) in a 4 mL vial. The resulting solution was stirred at room temperature for 1 hour, and the solvent was removed by nitrogen bubbling because of the low boiling point of the starting material (Eb₁ 52-54°C). Relative integration of the ¹H NMR methyl signals resonating at 2.71 and 2.46 ppm, for methyl *p*-tolyl sulfoxide and sulfide, respectively, gave the conversion rate of the reaction, and concentration values ranging between 50 and 70 mM were usually obtained for our solution of DMDO in acetone.

Compound (366)

Compound **365** (49 mg, 0.11 mmol) was dissolved directly in a predistilled solution of DMDO in acetone (5.97 mL, 0.44 mmol) at room temperature and stirred for 2 to 24 hours. Reaction was monitored by ¹H NMR spectroscopy in DMSO-*d*₆ due to the low solubility of the mixture in other organic deuterated solvents. Mixture was evaporated to dryness to afford 33 mg of brownish solid that could correspond to **352** in a maximum yield of 63%. ¹H NMR (300 MHz, DMSO-*d*₆) δ (ppm) = 5.64, 4.69, 4.63, 4.57, 4.53, 4.44, 4.15, 1.62, 1.52, 1.48, 1.43. Possible paramagnetic character, not possible to measure coupling constants. ¹³C NMR (75 MHz, DMSO-*d*₆) δ (ppm) = 99.5, 97.4, 75.3, 74.4, 71.5, 70.6, 69.4, 66.1, 65.7, 58.5, 27.1. Quaternary carbons are not observable because of oxidation of DMSO-*d*₆ in tube and reduction of iodosyl to iodine. Because of that it is really difficult to confirm the oxidation of iodine atom, it is not observable the shift of C-ipso which could be around 90 ppm. FT-IR (KBr): 3403 (br), 2929, 1636, 1100, 998, 779 (I=O maybe). Very broad signals were observed.

(*S*)- α -Iodoferrocenecarboxaldehyde (**370**)⁹¹



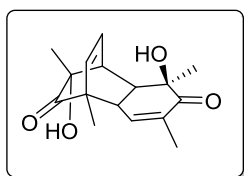
Compound **365** (144 mg, 0.32 mmol) was dissolved in anhydrous CH₂Cl₂ (5 mL) and H₂O (2 mL). Then, *p*-toluenesulfonic acid (88 mg, 0.46 mmol) was added to the reaction mixture and was heated to 50°C for 16 hours until the monitoring by TLC (5:95 EtOAc in cyclohexane) showed just desired product. Subsequently mixture was washed 3 times with 10 mL of H₂O and extracted with 20 mL of EtOAc. After drying over MgSO₄ the filtrate was evaporated and dried under high vacuum. Crude brown oil showed no need to purify and 111 mg were obtained quantitative yield. ¹H NMR (300 MHz, DMSO-*d*₆)

δ (ppm) = 9.95 (s, 1H), 5.01 – 4.92 (m, 1H), 4.84 (dt, J = 9.6, 2.6 Hz, 2H), 4.31 (s, 5H). ^{13}C NMR (75 MHz, DMSO- d_6) δ (ppm) = 193.6, 79.6, 76.6, 74.0, 72.2, 67.9, 41.0 (C-ipso).

3.9.3.1 Asymmetric hydroxylative phenol dearomatization procedure⁹²

Compound **365** (188 mg, 0.39 mmol) was dissolved in anhydrous CH_2Cl_2 , then 2,6-dimethylphenol was added at room temperature as a solid. After 30 minutes of stirring TFA was added (25 μL , 0.33 mmol) and mixture turned more soluble and dark yellow. Monitoring by TLC in 20:80 EtOAc in cyclohexane showed no evolution after 19 hours. After a reductive work up using 10 eq. of $\text{Na}_2\text{S}_2\text{O}_4$ and a ratio 1 to 1 in volume with NaHCO_3 aq. (sat) and stirred with EtOAc 1 hour, the mixtures was extracted and washed with brine. Drying with Na_2SO_4 and evaporation to dryness gave the crude mixture which showed 30% conversion to Diels-Alder product. Final purification by preparative TLC with 35:65 EtOAc in cyclohexane, afforded 2.5 mg of product, 3 % of yield.

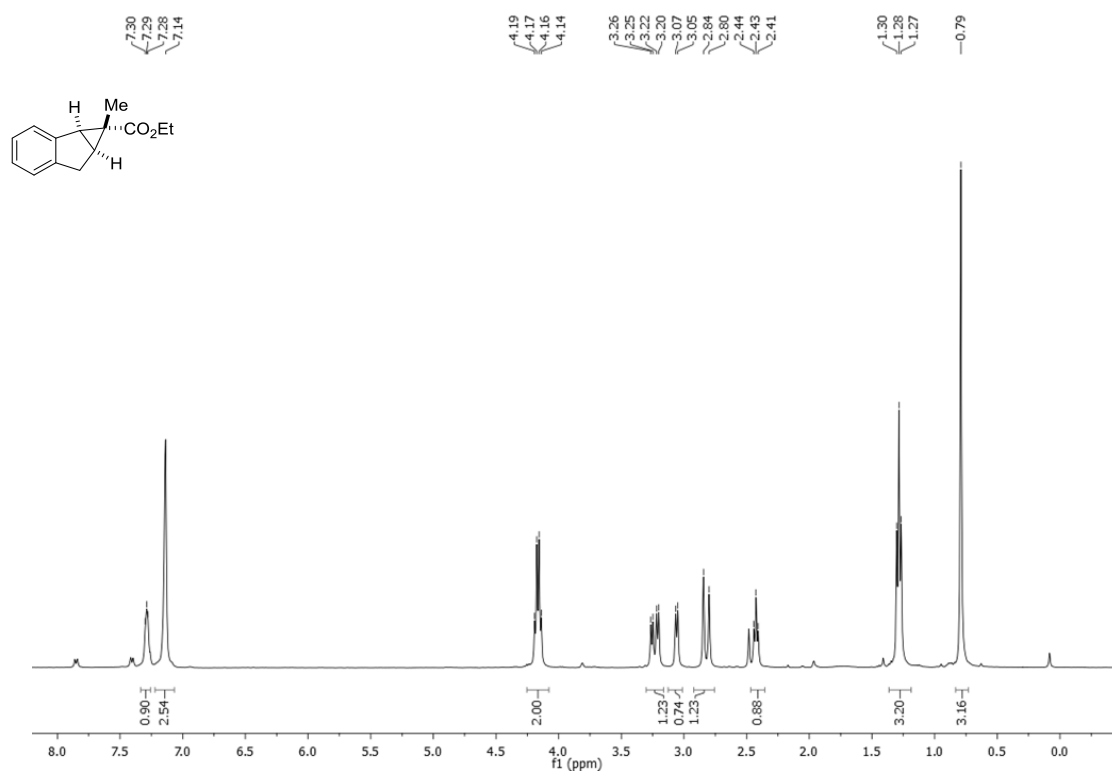
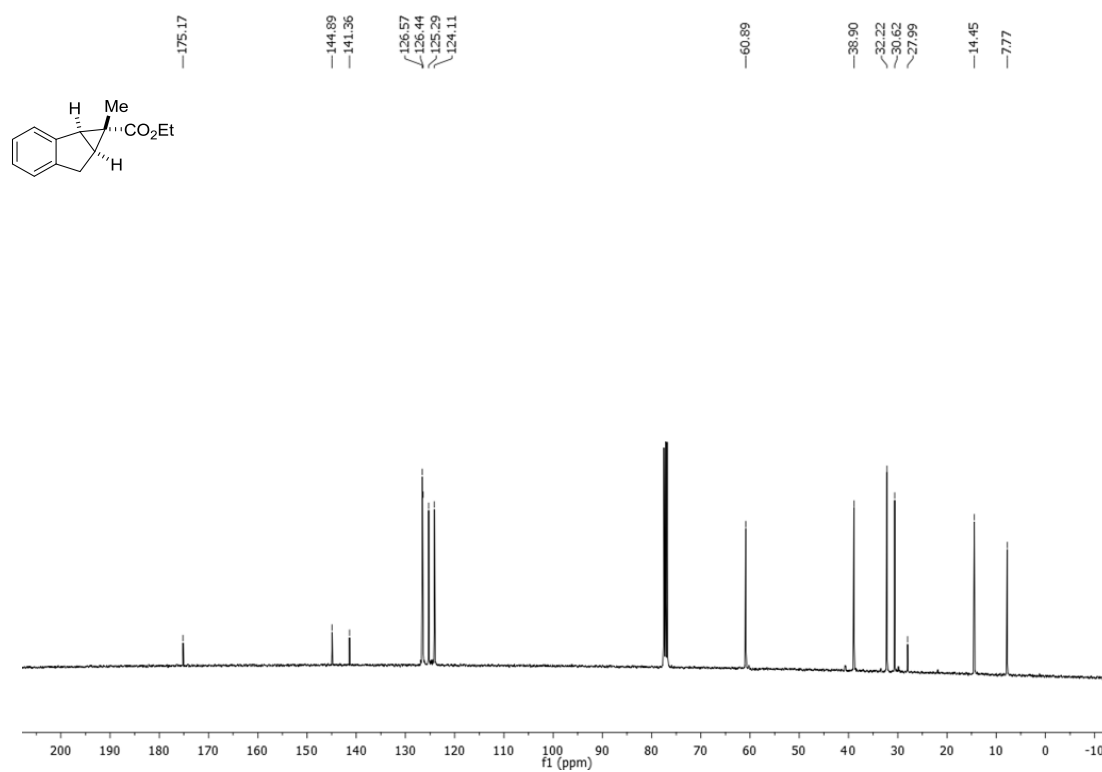
(1*R*,4*R*,8*R*,8*aS*,10*R*)-8,10-dihydroxy-4,6,8,10-tetramethyl-4,4*a*,8,8*a*-tetrahydro-1,4-ethanonaphthalene-7,9(1*H*)-dione (**369**)⁹²



Product was obtained as a white amorphous powder, and found by TLC with R_f of 0.20 (30:70 EtOAc/cyclohexane). 3% ee. HPLC conditions using chiral AS-H column: *n*-hexane/*i*-PrOH (90:10), 1.0 mL/min, UV detection at 254 nm; tr_1 = 12.8 min and tr_2 = 26.7

min. ^1H NMR (300 MHz, CDCl_3) δ (ppm) = 6.33 – 6.17 (m, 2H), 5.51 (ddd, J = 8.2, 1.7, 0.8 Hz, 1H), 4.00 (s, 1H), 3.39 (dt, J = 6.9, 1.9 Hz, 1H), 3.25 (dd, J = 8.4, 2.1 Hz, 1H), 2.87 (dd, J = 7.3, 4.8 Hz, 1H), 2.29 (s, 1H), 1.85 (t, J = 1.5 Hz, 3H), 1.34 (s, 3H), 1.32 (s, 3H), 1.24 (s, 3H).

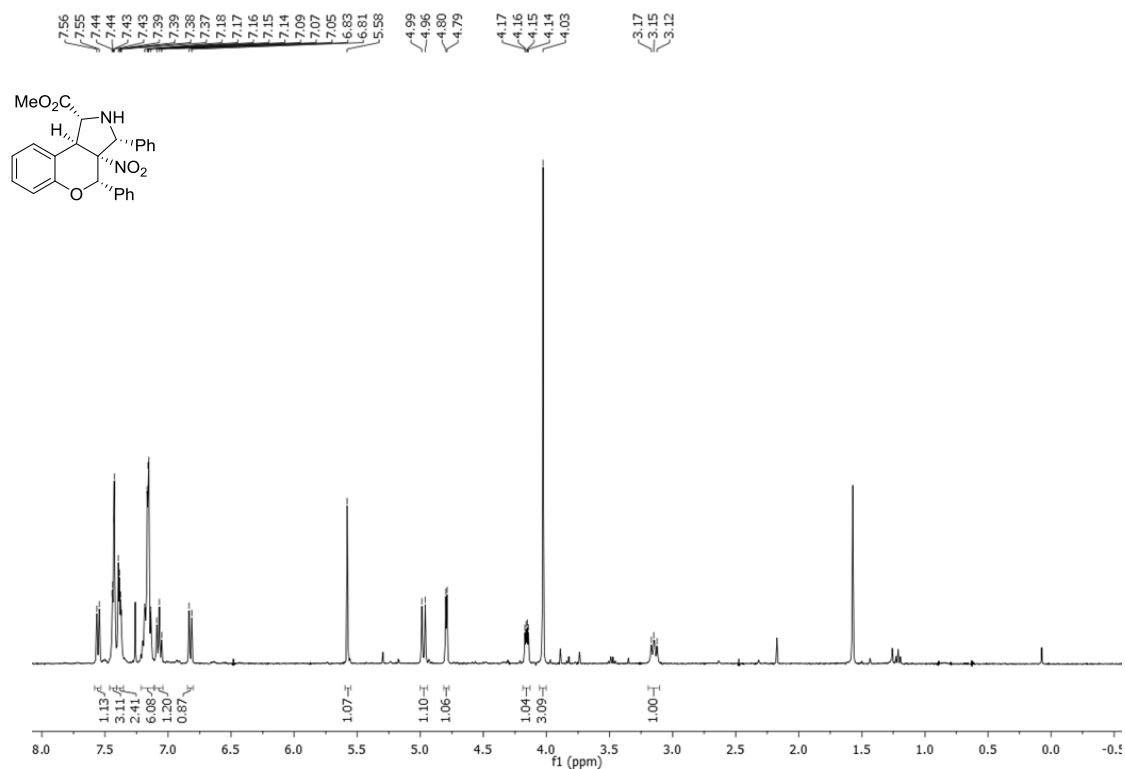
ANNEXES

ANNEX I. ^1H , ^{13}C spectra of Chapter 2Compound *trans*-122 ^1H -NMR (CDCl_3) 400 MHz ^{13}C NMR (CDCl_3) 101 MHz

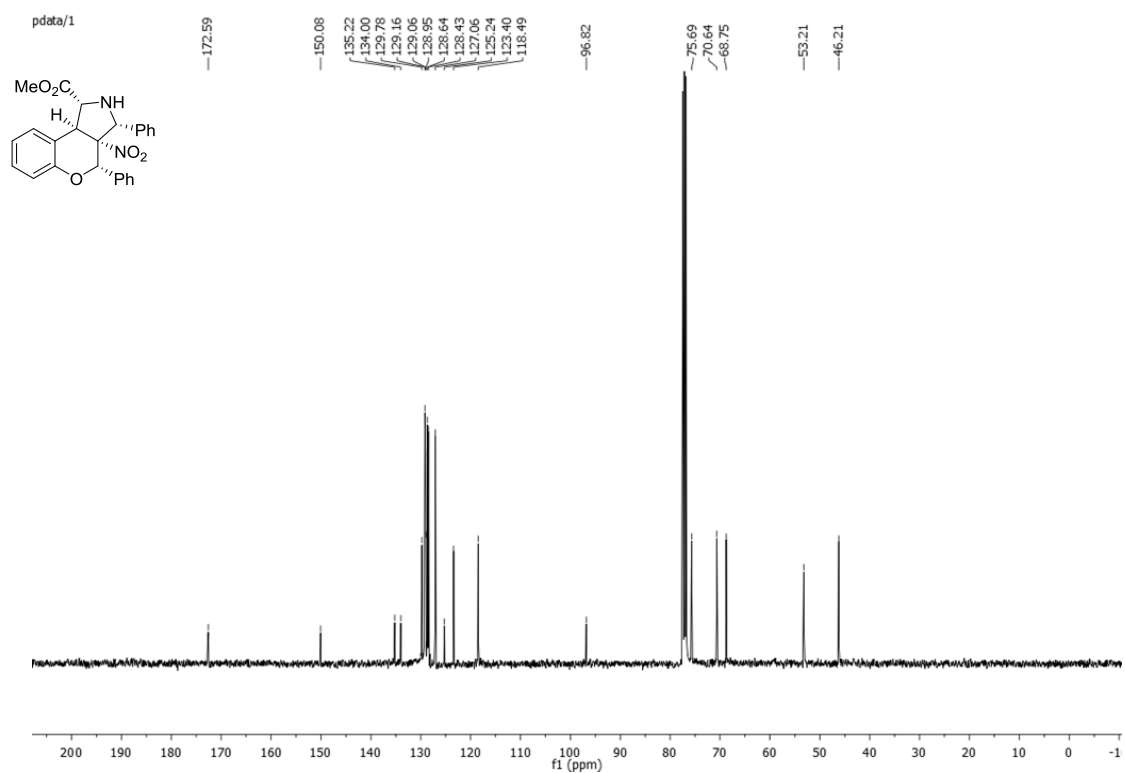
ANNEX I

Compound 130a

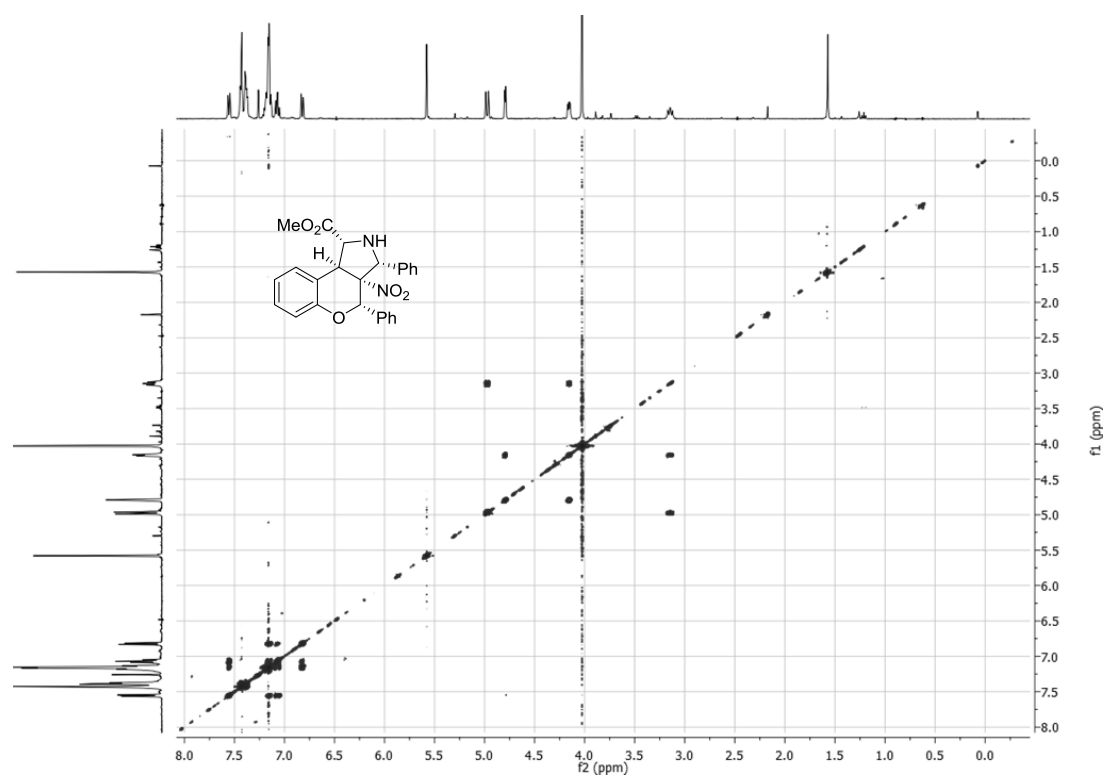
$^1\text{H-NMR}$ (CDCl_3) 400 MHz



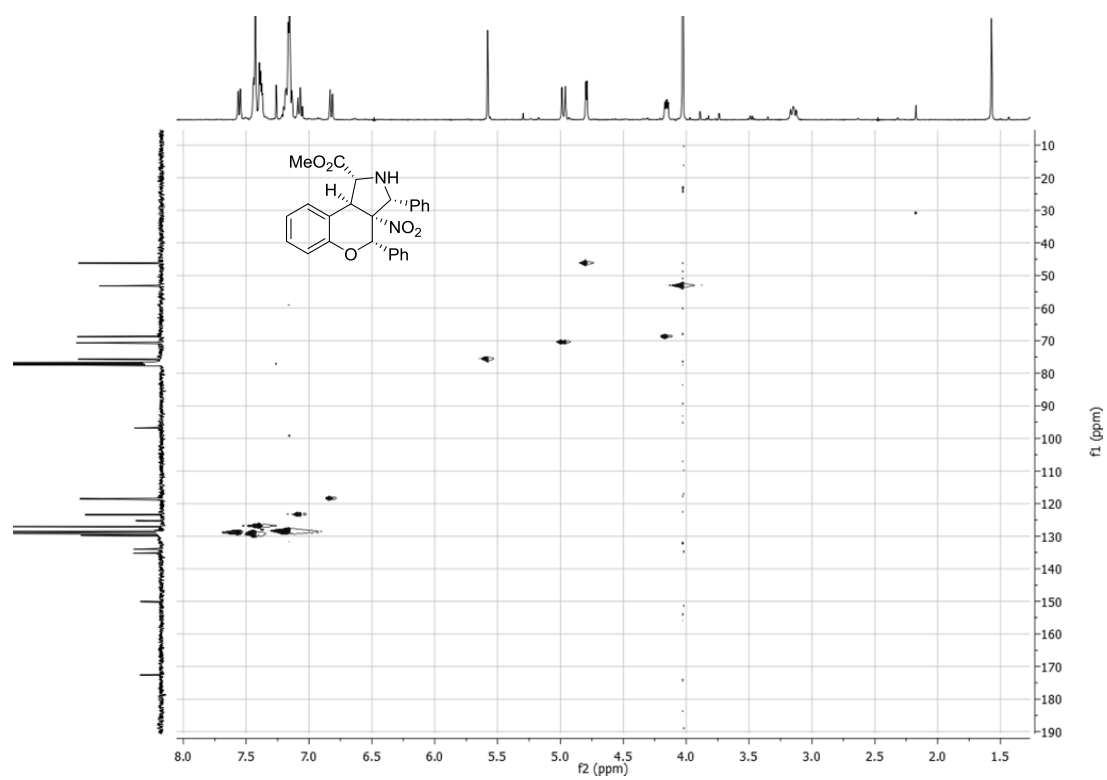
$^{13}\text{C NMR}$ (CDCl_3) 101 MHz



COSY 2D



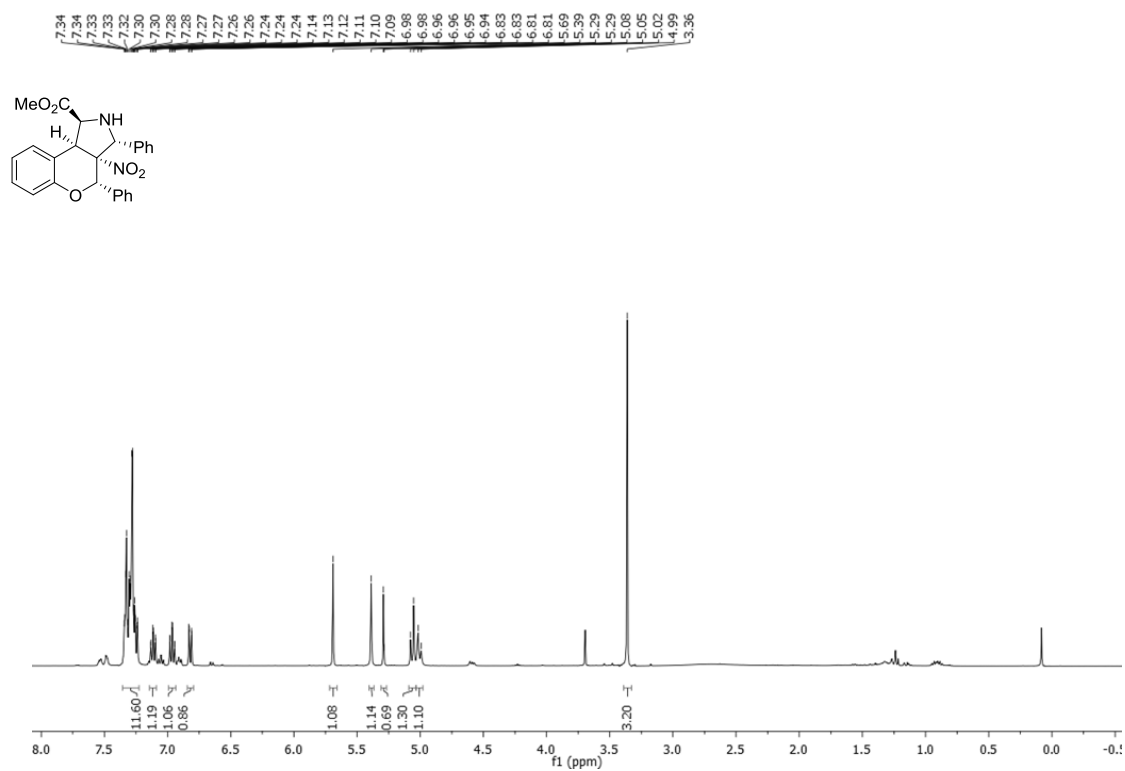
HSQC 2D



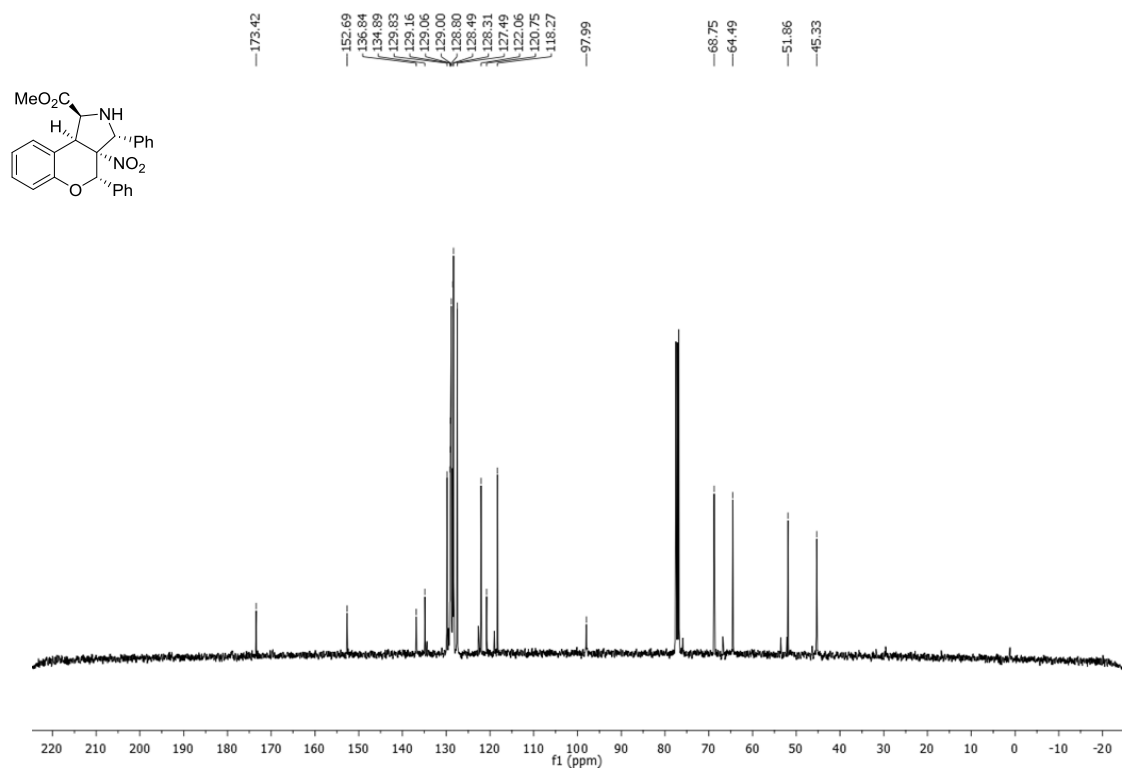
ANNEX I

Compound 130'a

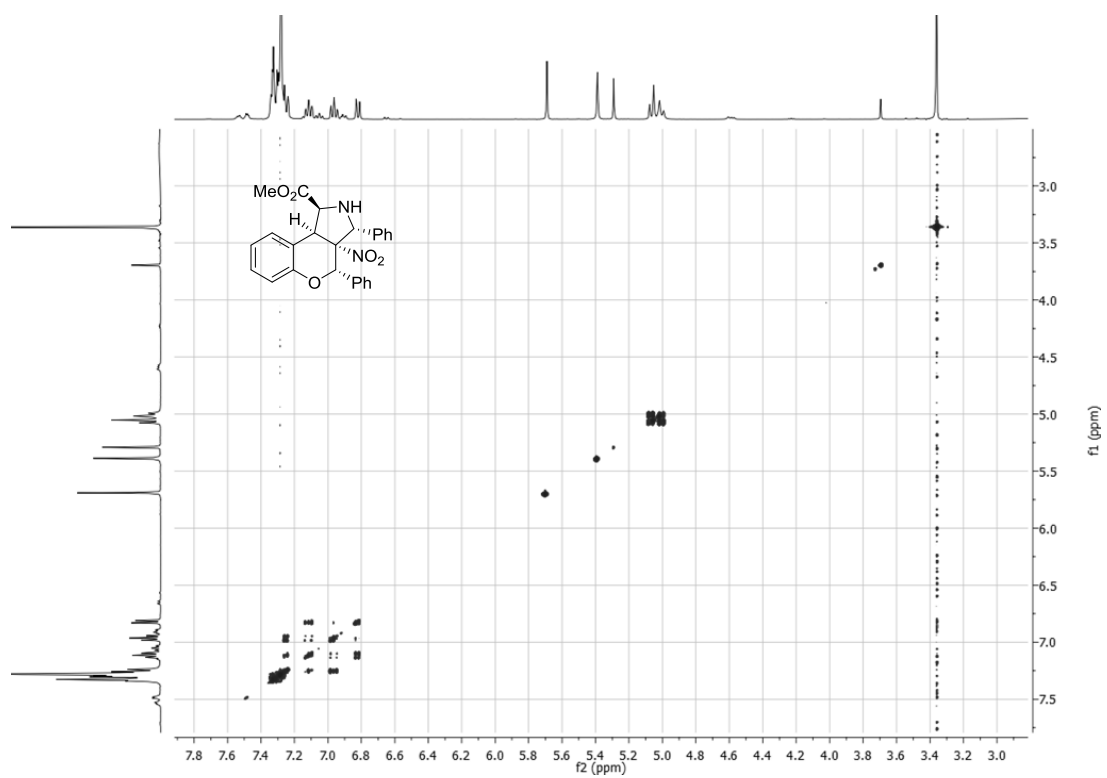
¹H-NMR (CDCl₃) 400 MHz



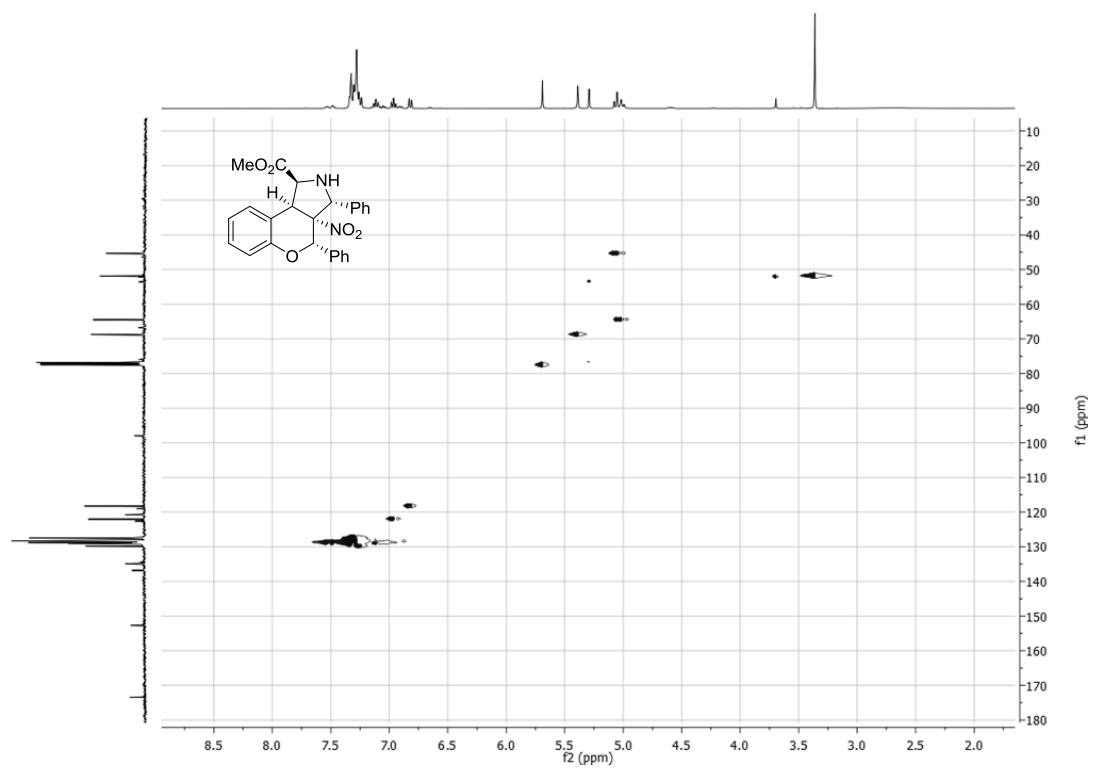
¹³C NMR (CDCl₃) 101 MHz



COSY 2D



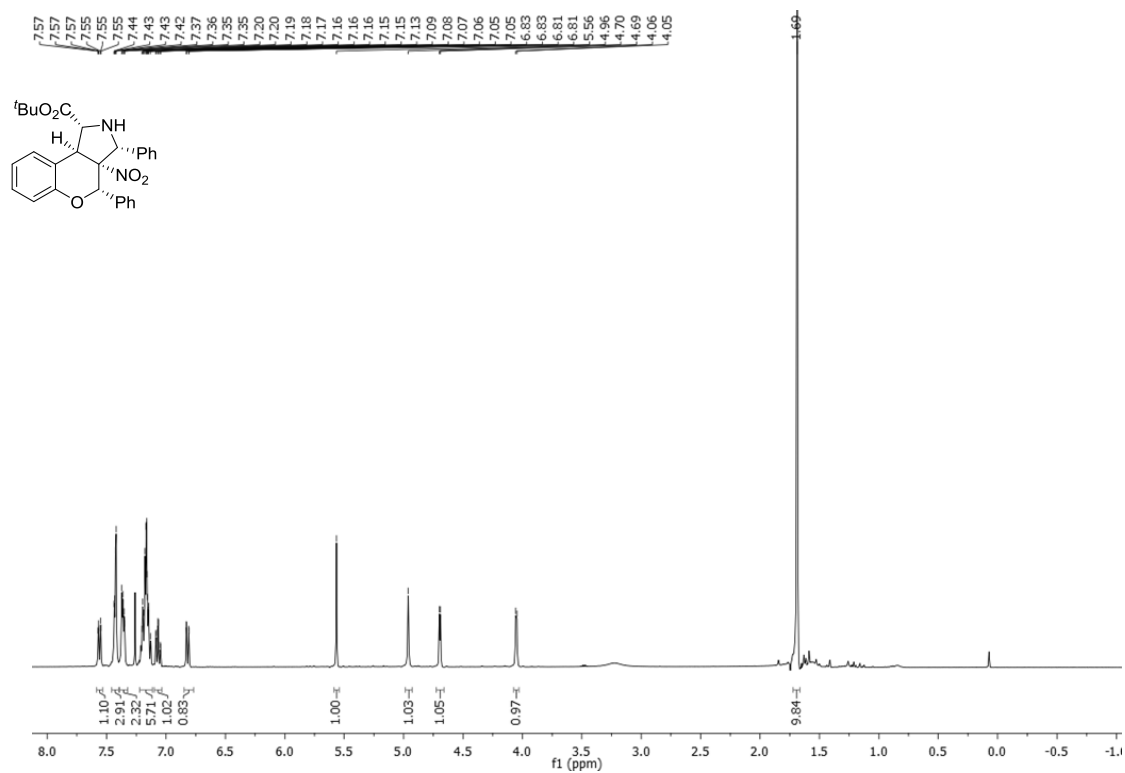
HSQC 2D



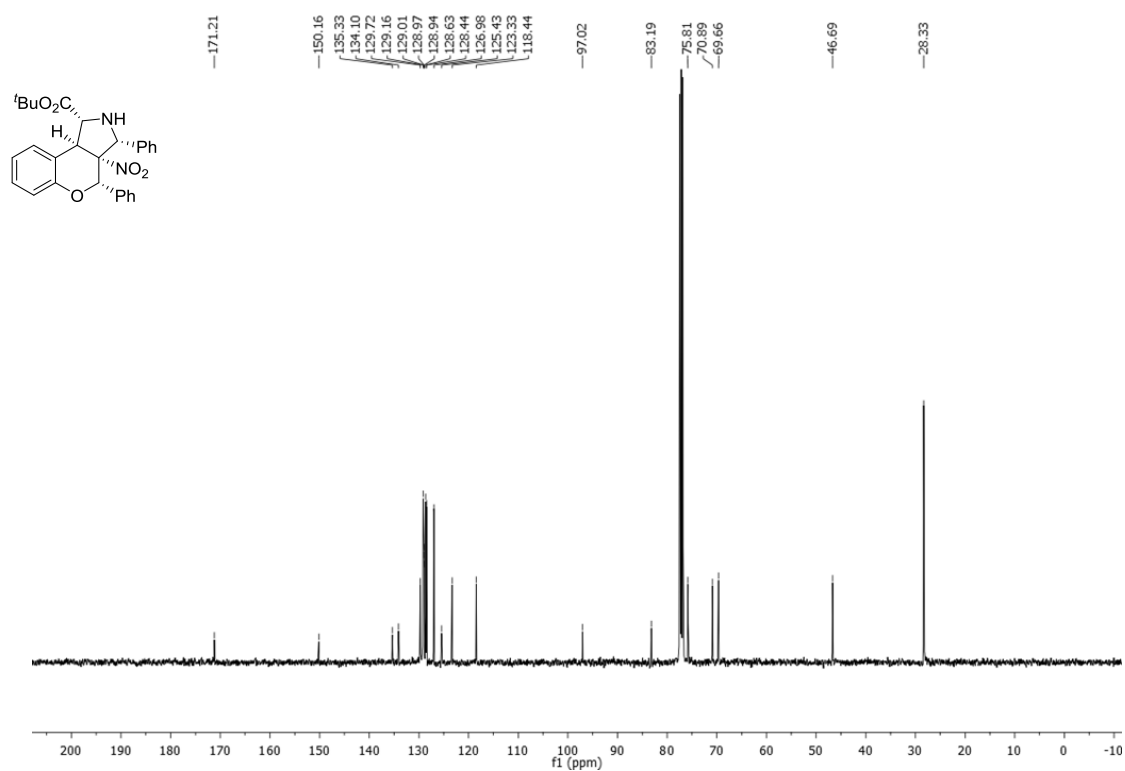
ANNEX I

Compound 130b

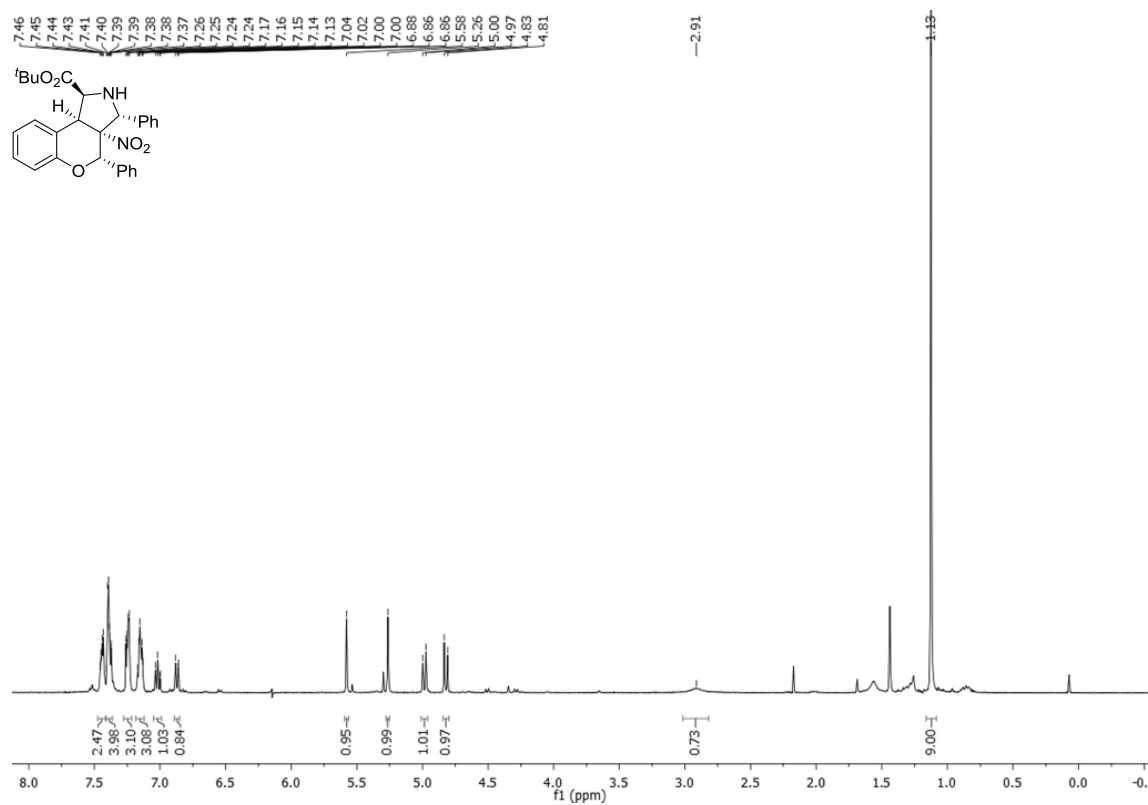
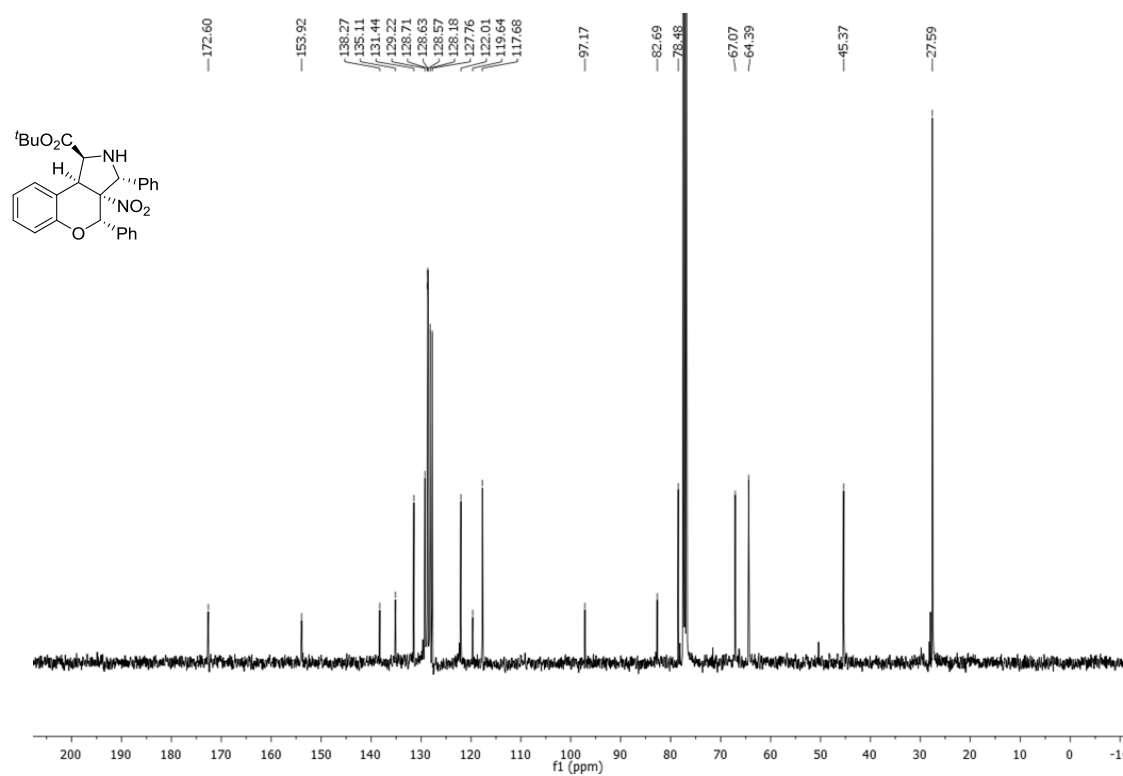
$^1\text{H-NMR}$ (CDCl_3) 400 MHz



$^{13}\text{C NMR}$ (CDCl_3) 101 MHz



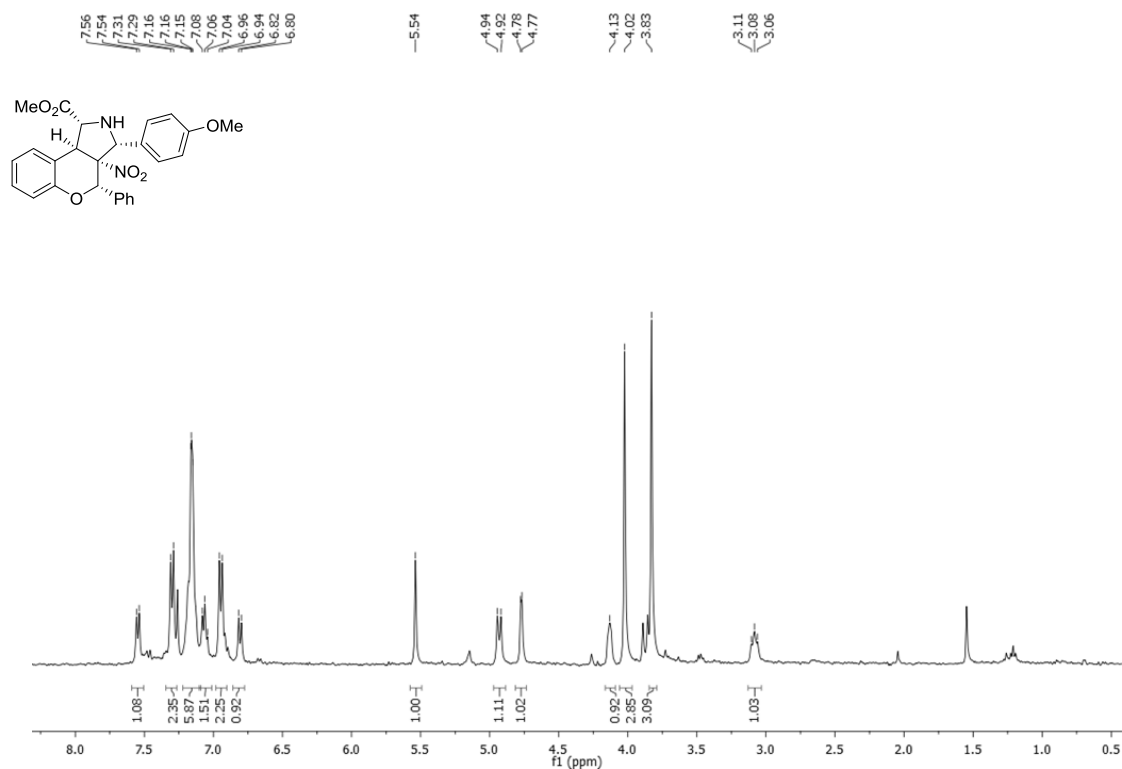
Compound 130'b

 $^1\text{H-NMR}$ (CDCl_3) 400 MHz $^{13}\text{C NMR}$ (CDCl_3) 101 MHz

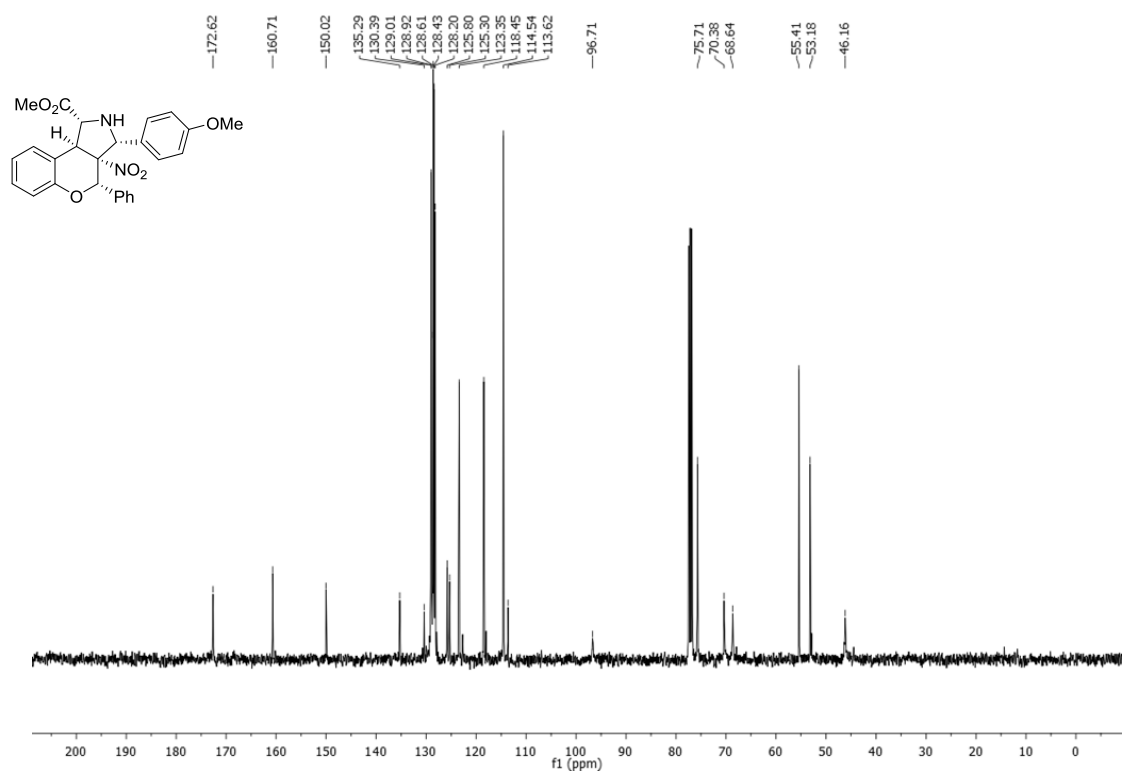
ANNEX I

Compound 130c

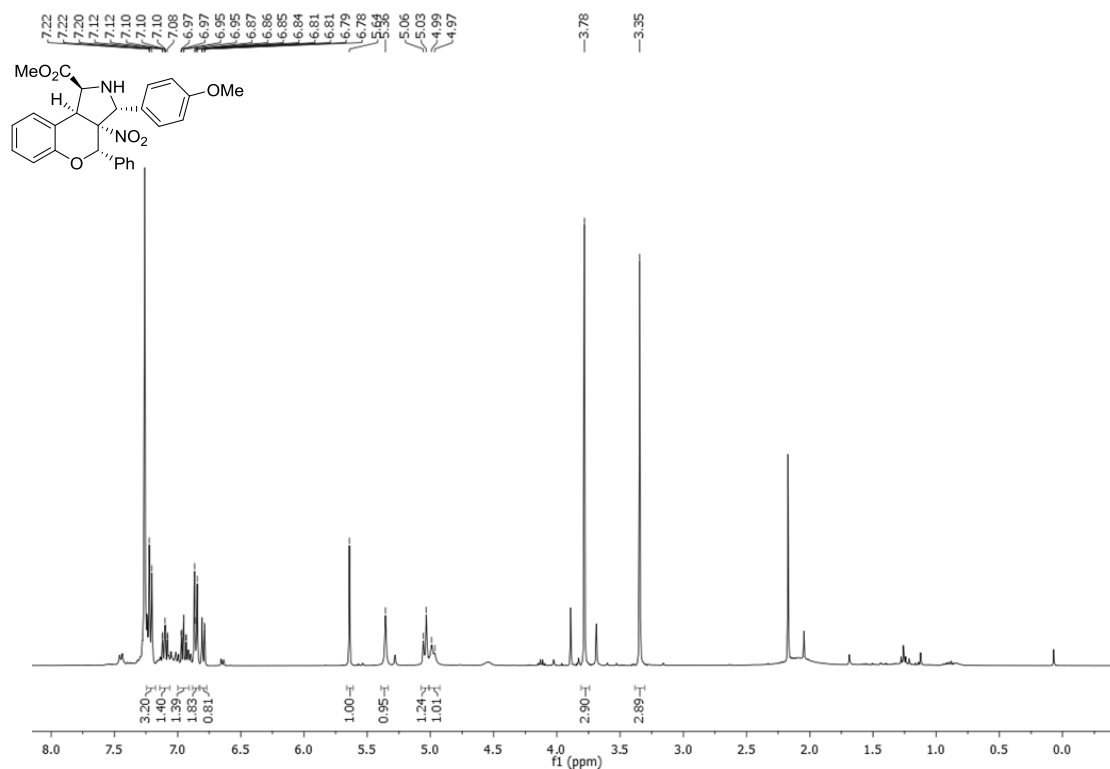
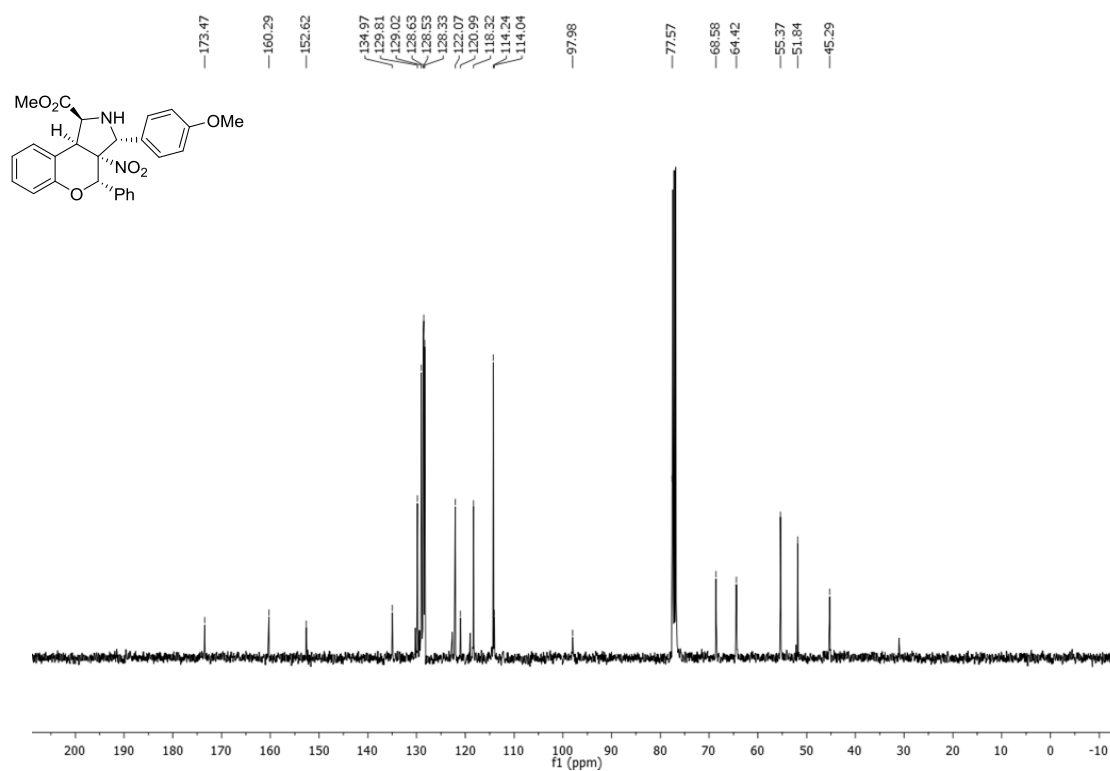
$^1\text{H-NMR}$ (CDCl_3) 400 MHz



$^{13}\text{C NMR}$ (CDCl_3) 101 MHz



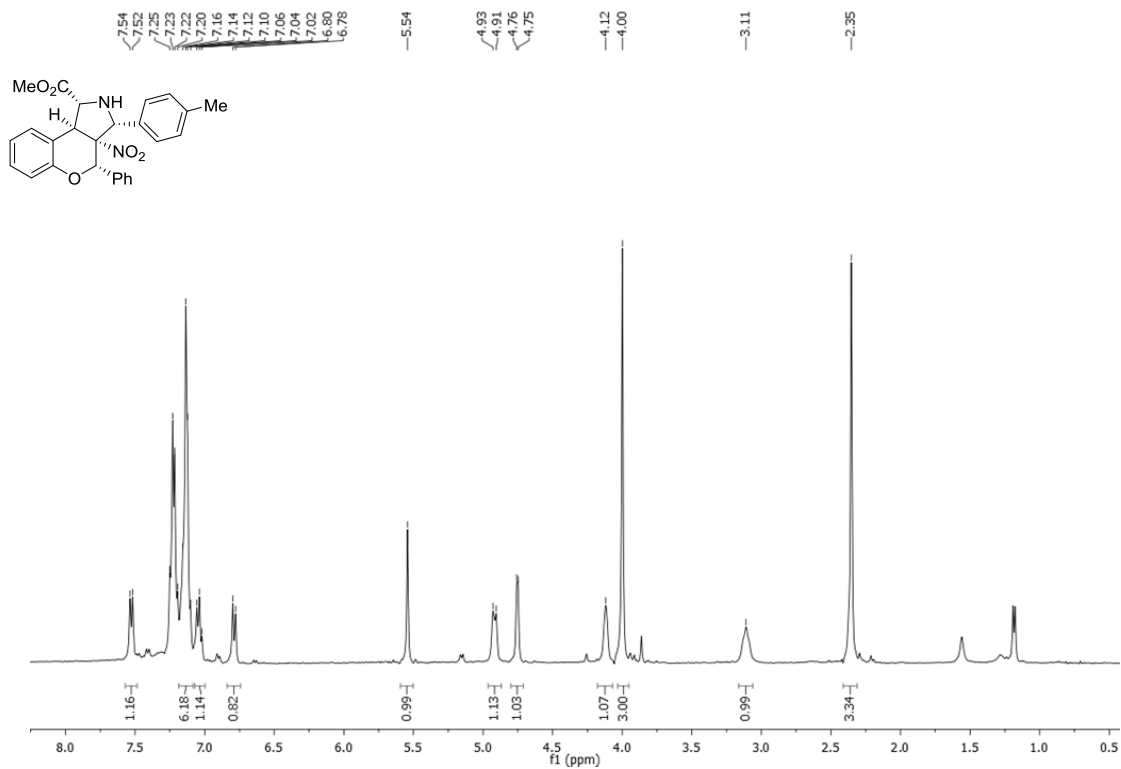
Compound 130'c

 $^1\text{H-NMR}$ (CDCl_3) 400 MHz $^{13}\text{C-NMR}$ (CDCl_3) 101 MHz

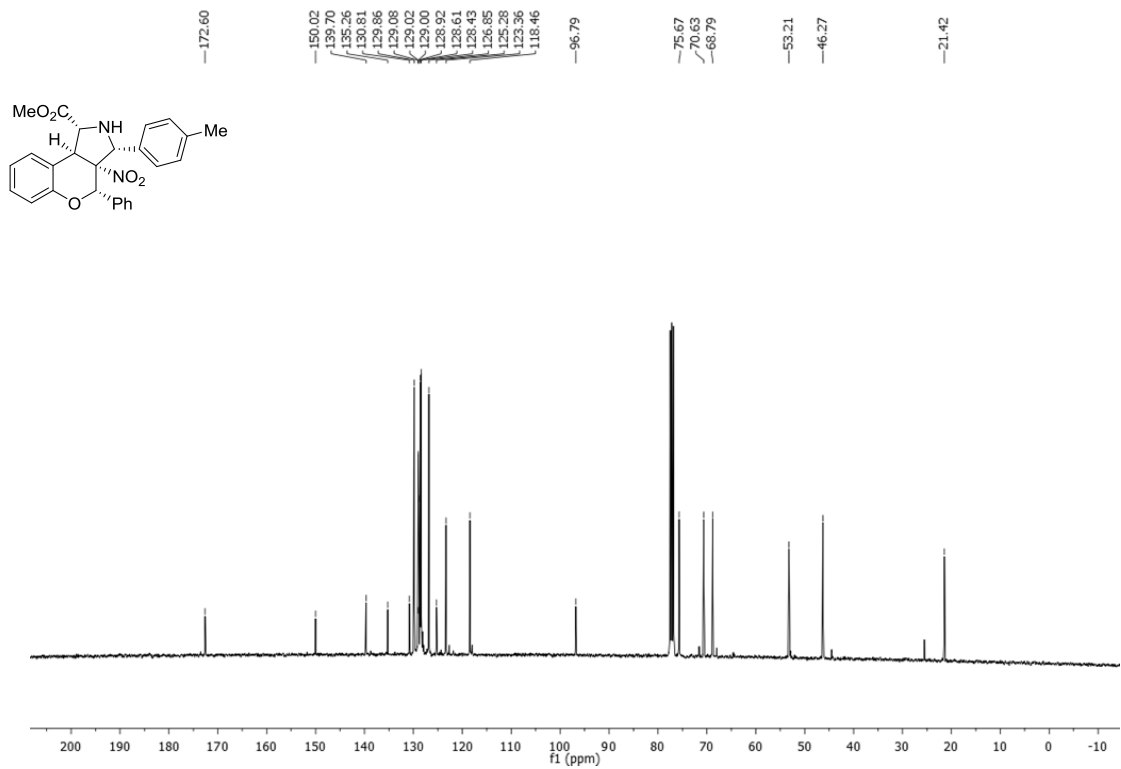
ANNEX I

Compound 130d

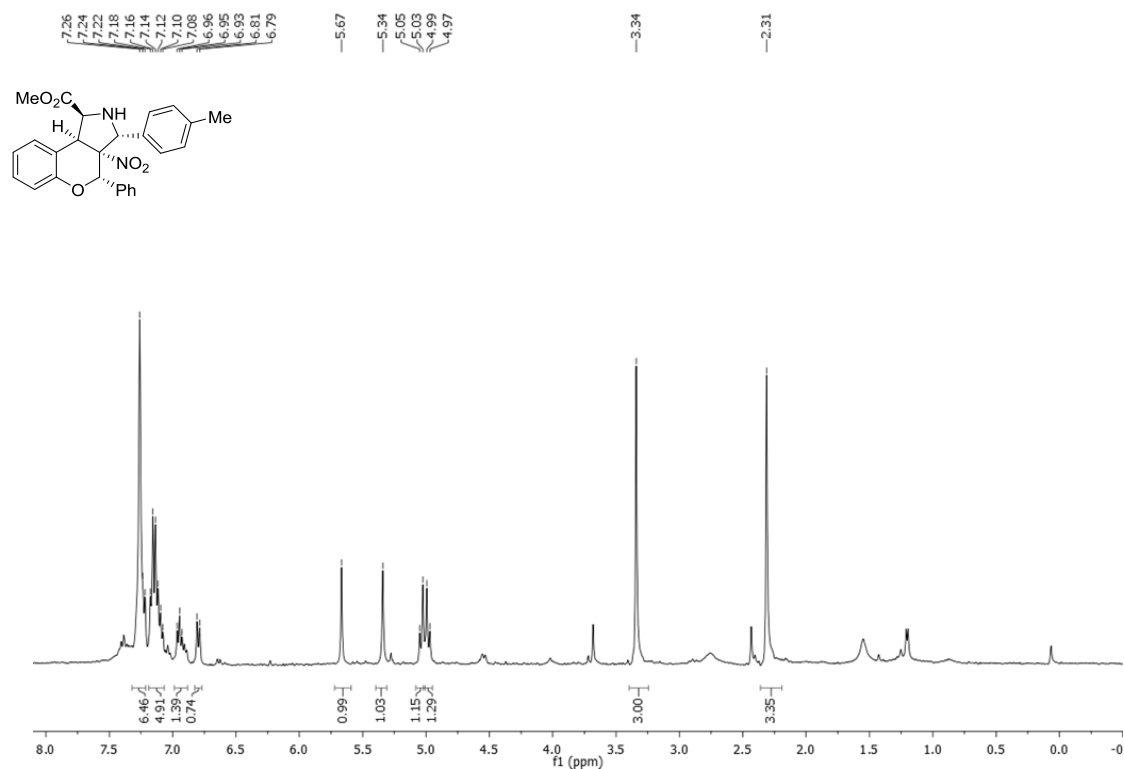
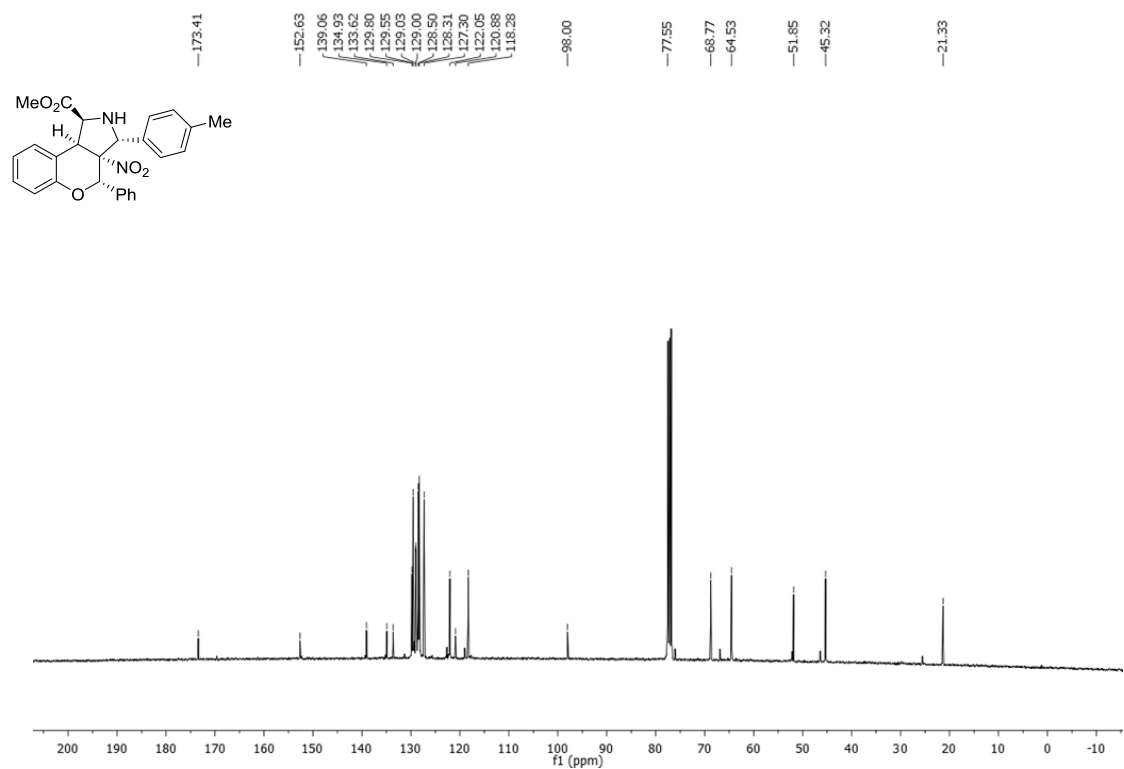
$^1\text{H-NMR}$ (CDCl_3) 400 MHz



$^{13}\text{C NMR}$ (CDCl_3) 101 MHz



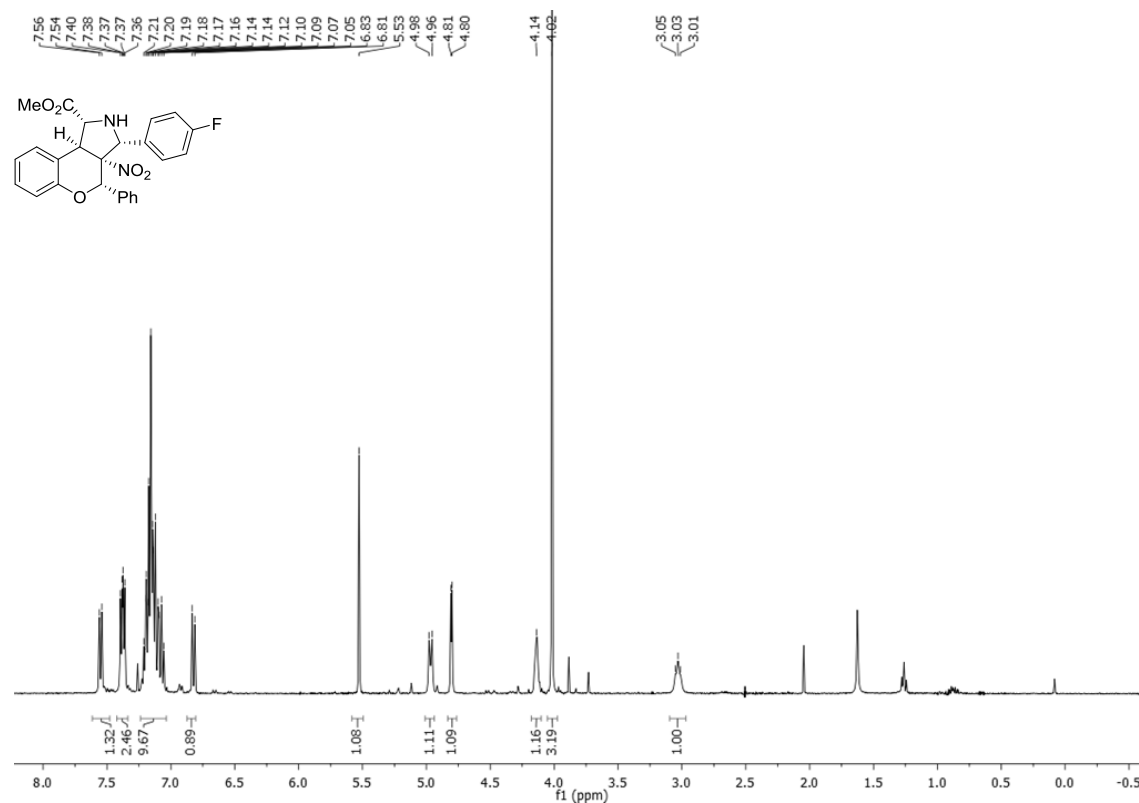
Compound 130'd

 $^1\text{H-NMR}$ (CDCl_3) 400 MHz $^{13}\text{C NMR}$ (CDCl_3) 101 MHz

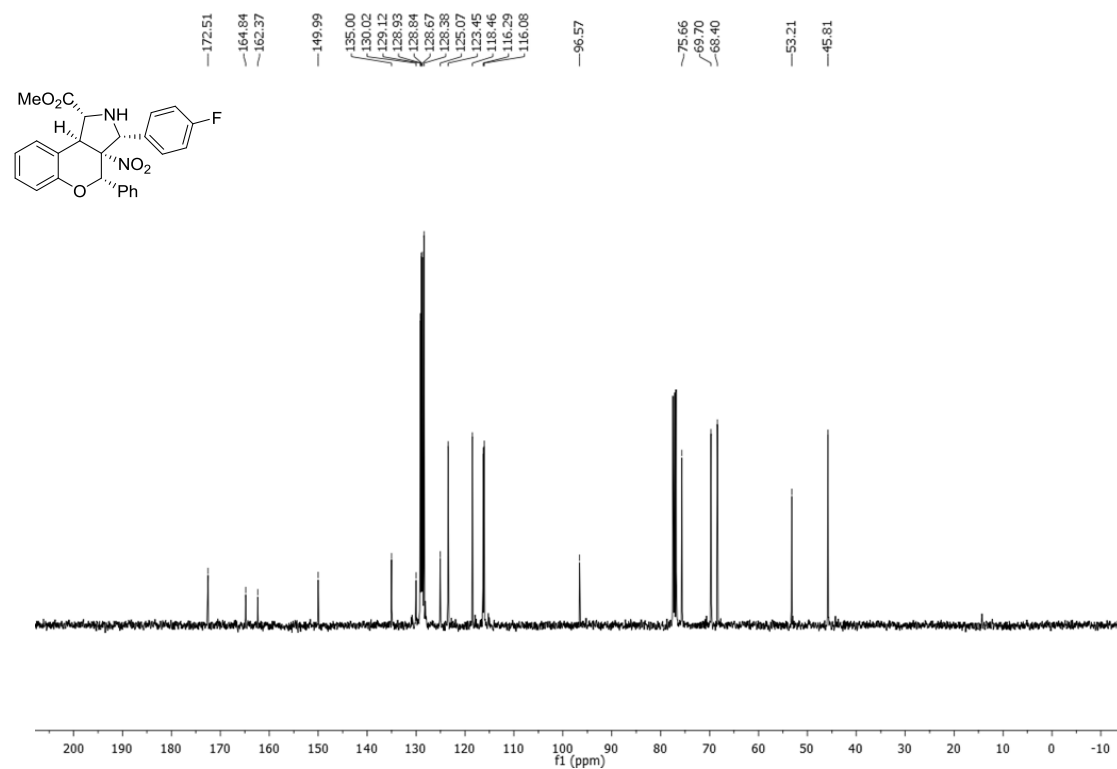
ANNEX I

Compound 130e

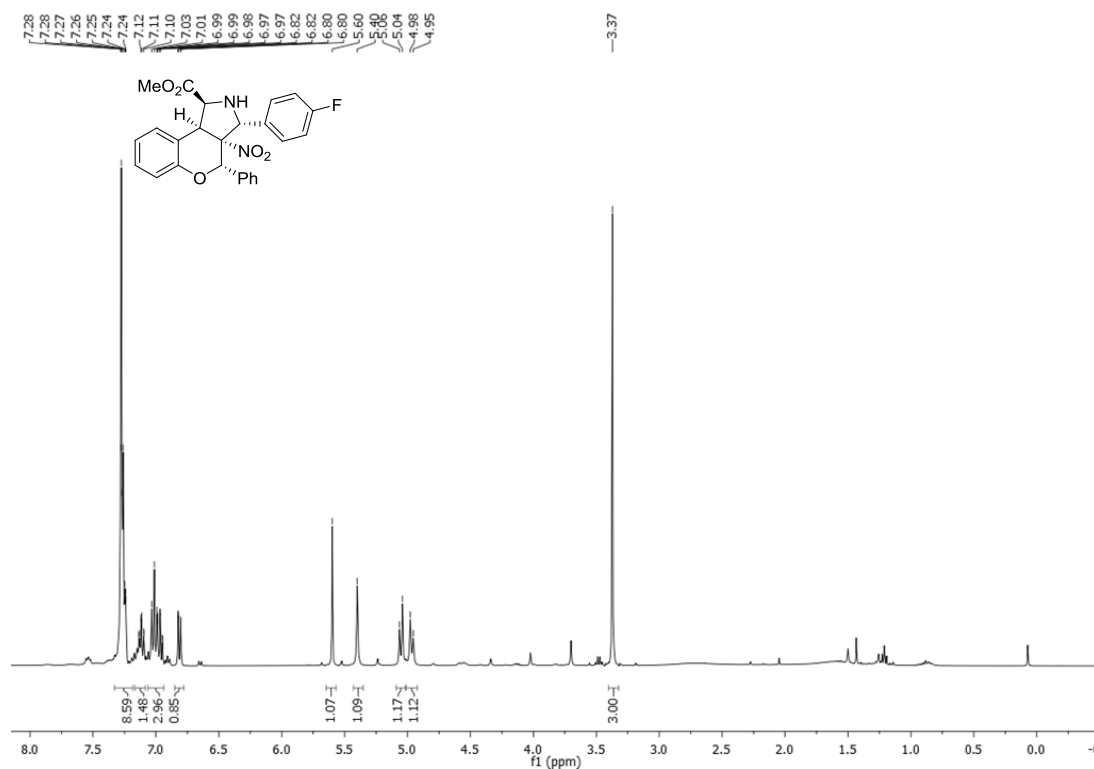
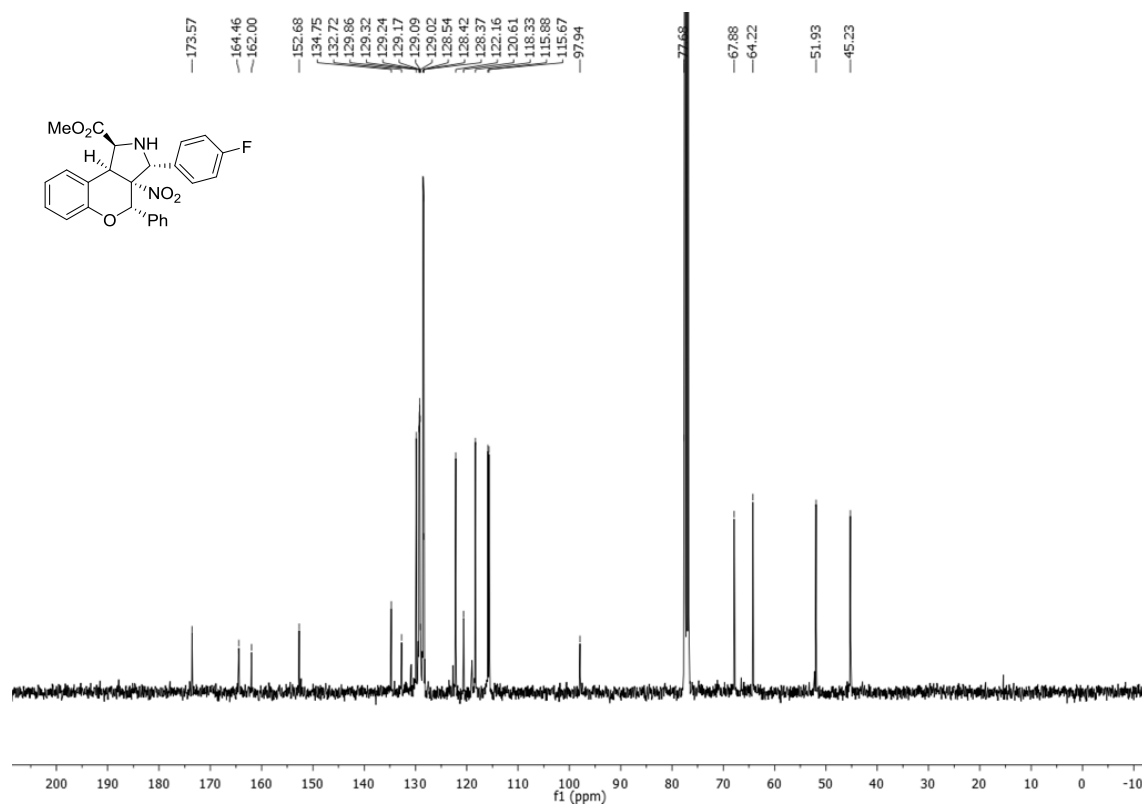
$^1\text{H-NMR}$ (CDCl_3) 400 MHz



$^{13}\text{C-NMR}$ (CDCl_3) 101 MHz



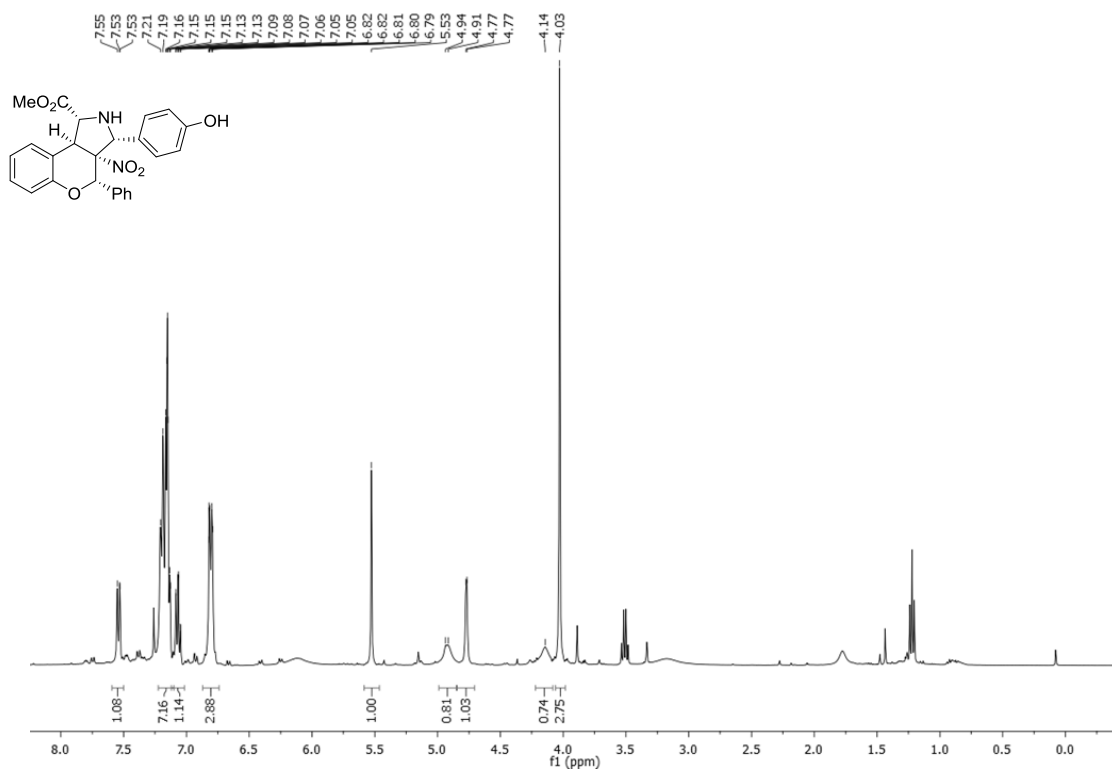
Compound 130'e

 $^1\text{H-NMR}$ (CDCl_3) 400 MHz $^{13}\text{C-NMR}$ (CDCl_3) 101 MHz

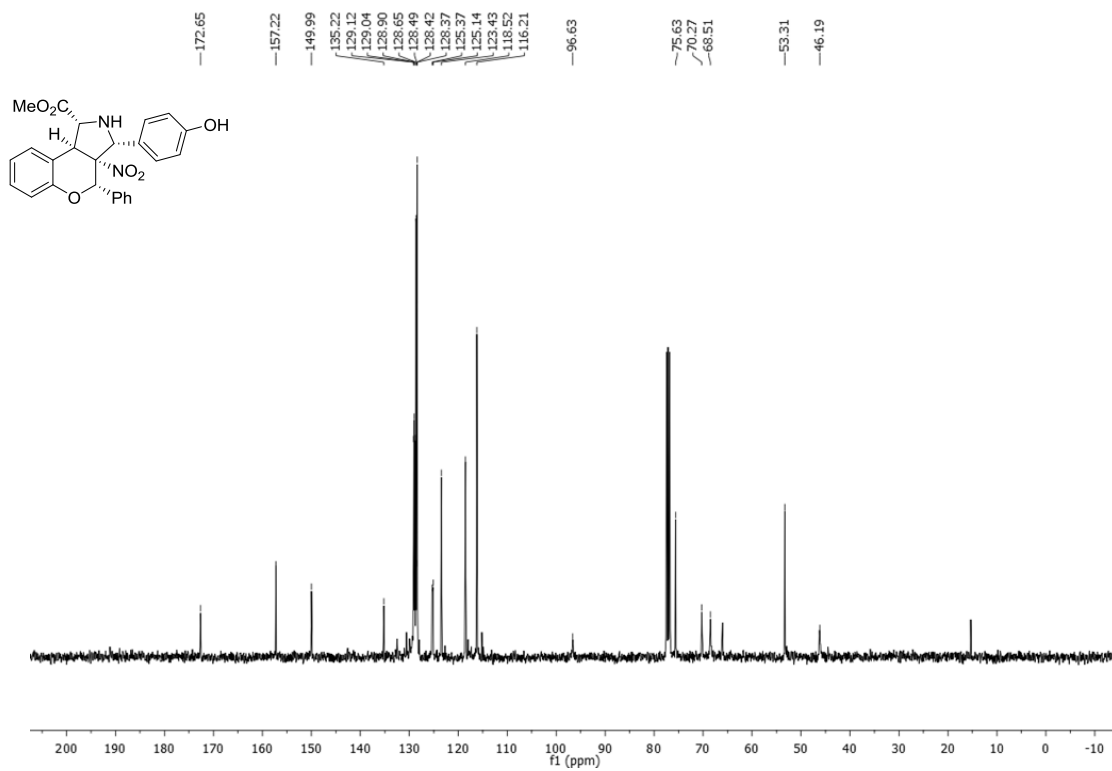
ANNEX I

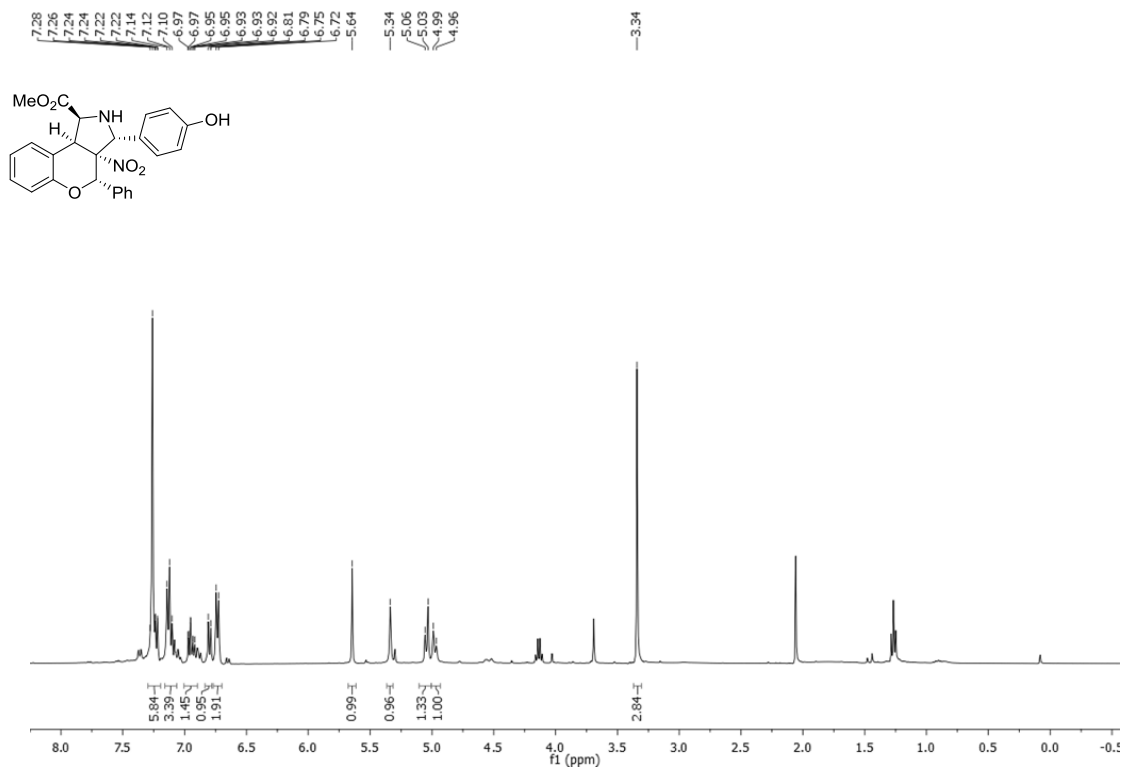
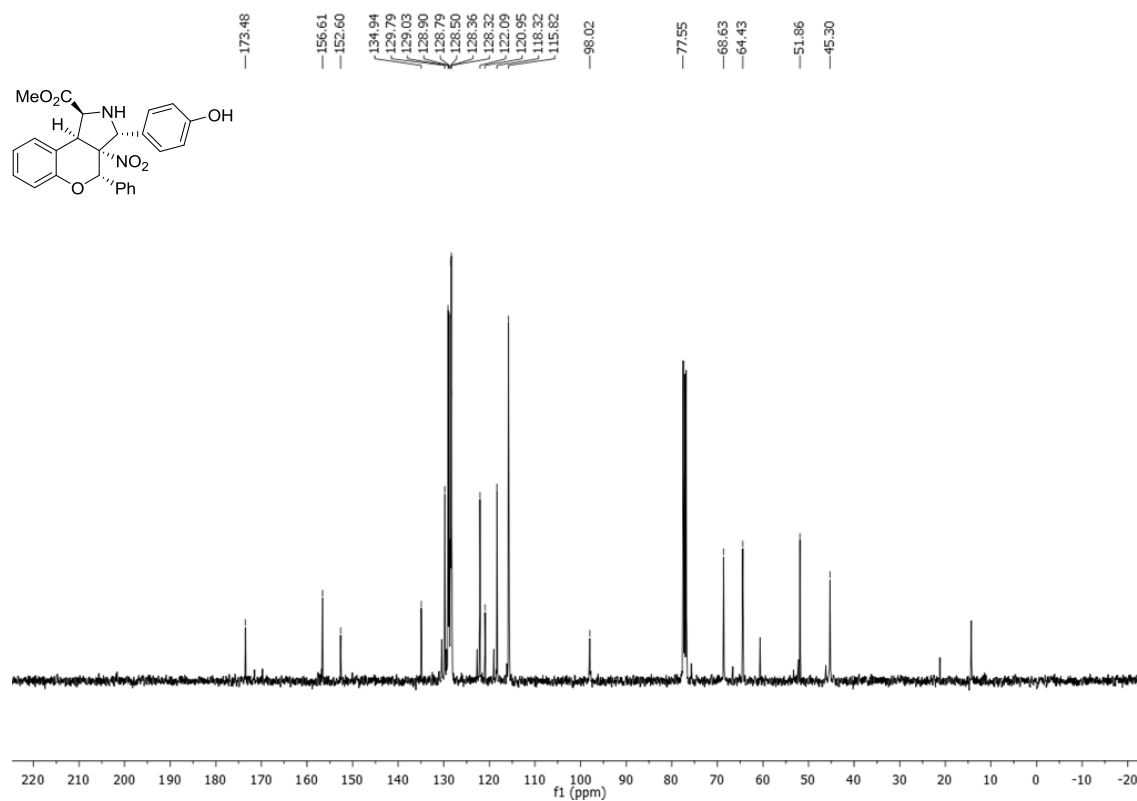
Compound 130f

$^1\text{H-NMR}$ (CDCl_3) 400 MHz



$^{13}\text{C NMR}$ (CDCl_3) 101 MHz

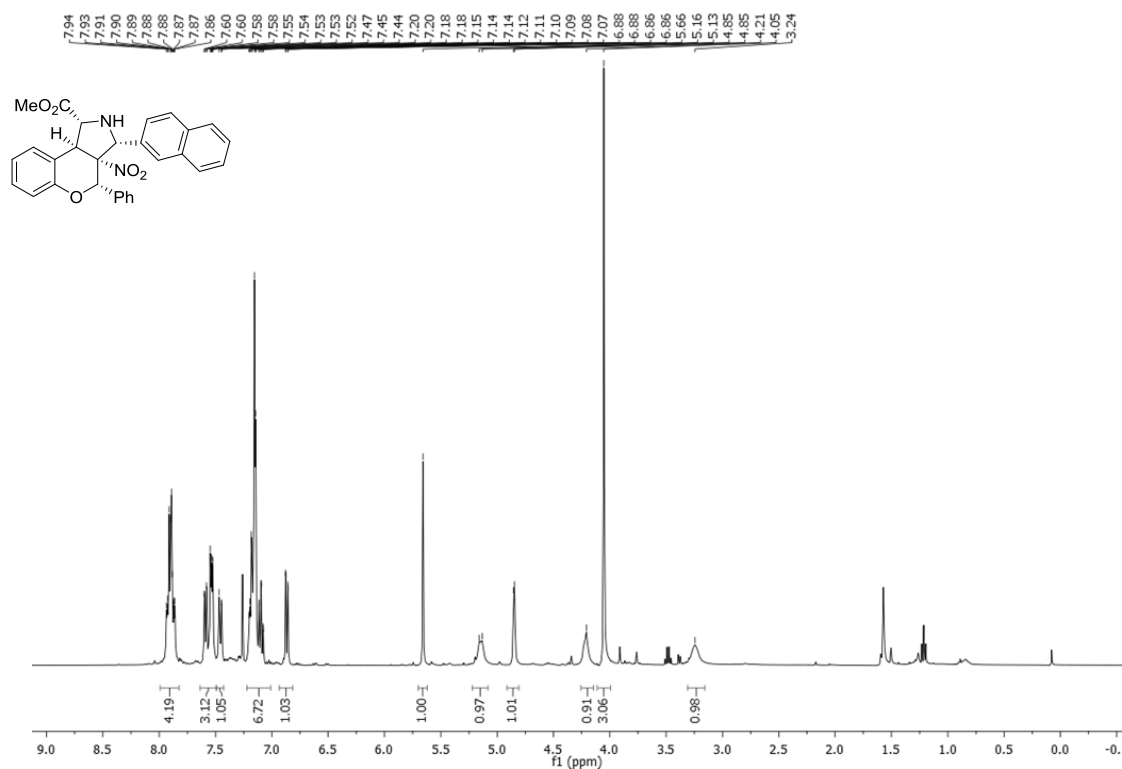


Compound 130^f¹H-NMR (CDCl₃) 400 MHz¹³C NMR (CDCl₃) 101 MHz

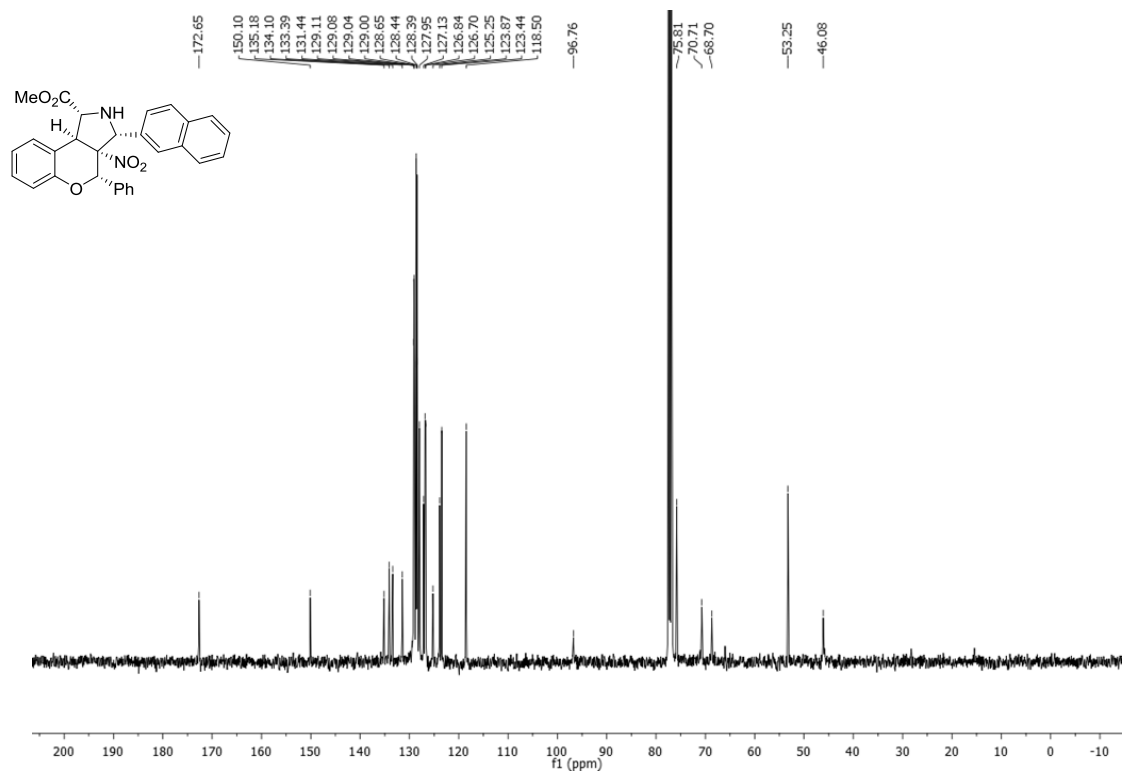
ANNEX I

Compound 130g

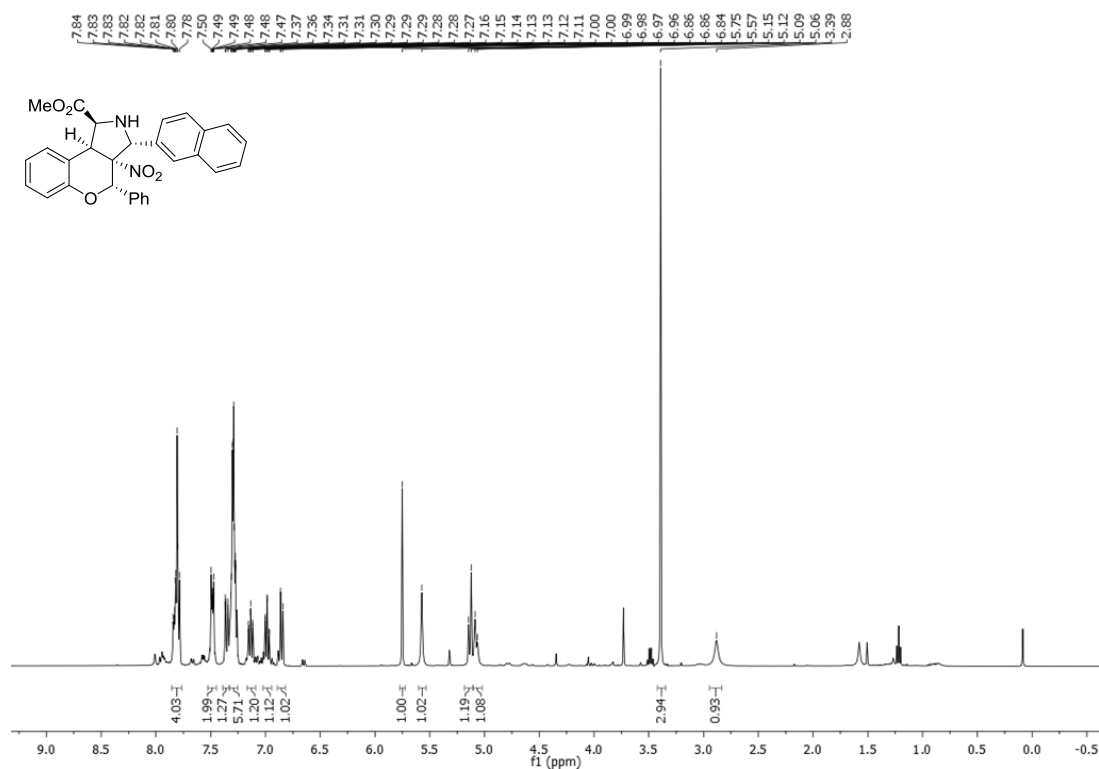
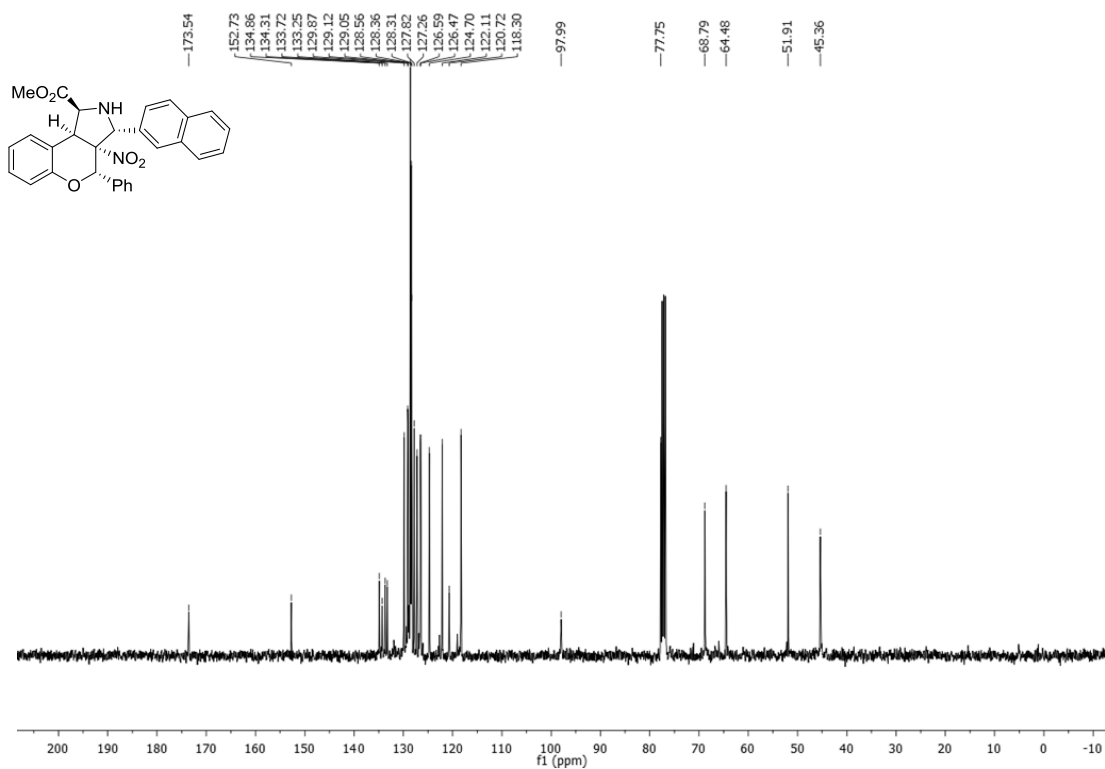
¹H-NMR (CDCl₃) 400 MHz



¹³C NMR (CDCl₃) 101 MHz



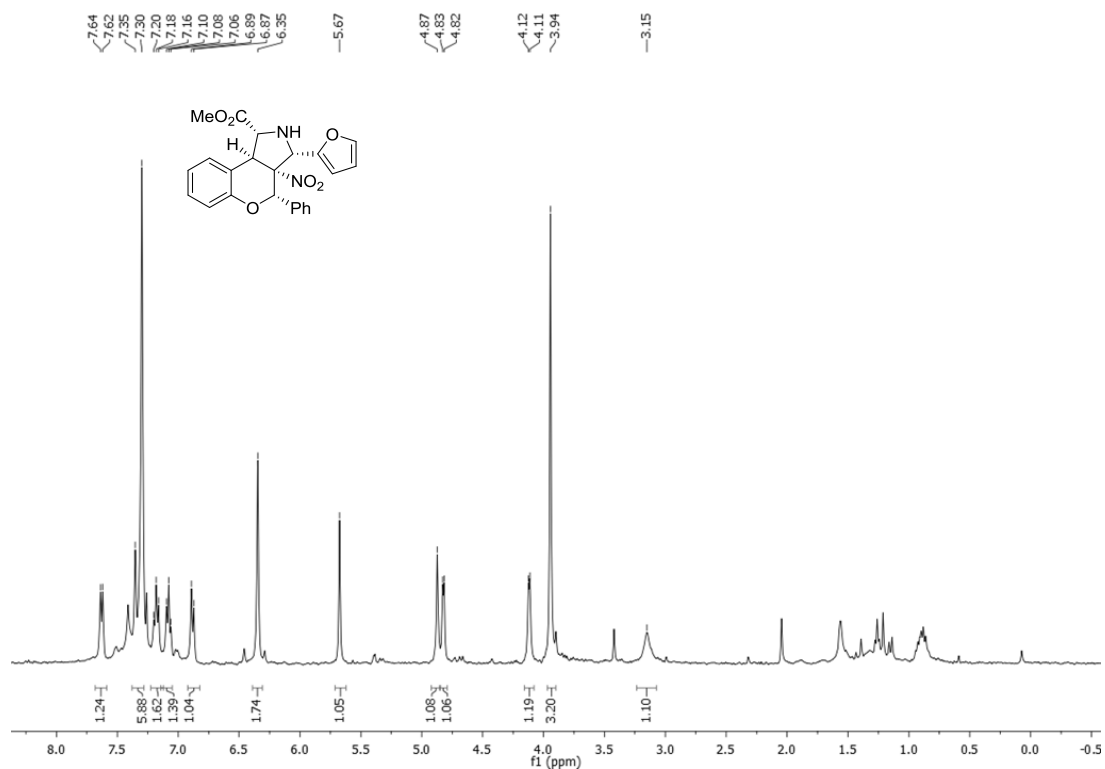
Compound 130'g

 $^1\text{H-NMR}$ (CDCl_3) 400 MHz $^{13}\text{C-NMR}$ (CDCl_3) 101 MHz

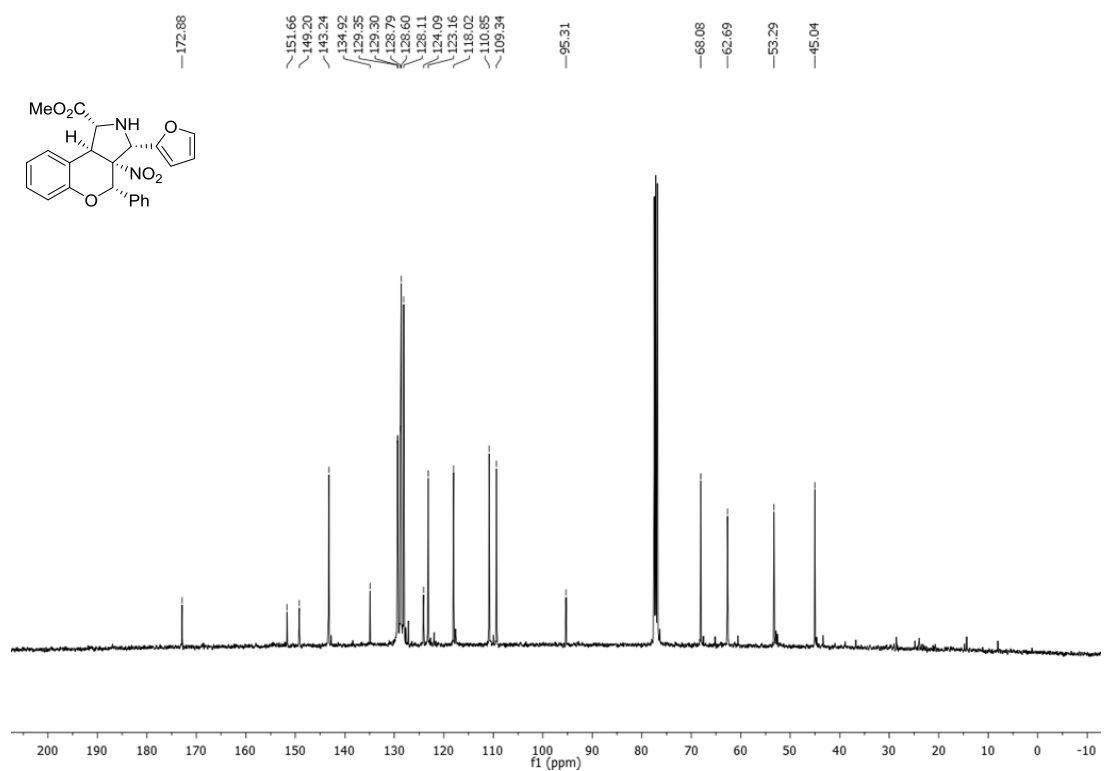
ANNEX I

Compound 130h

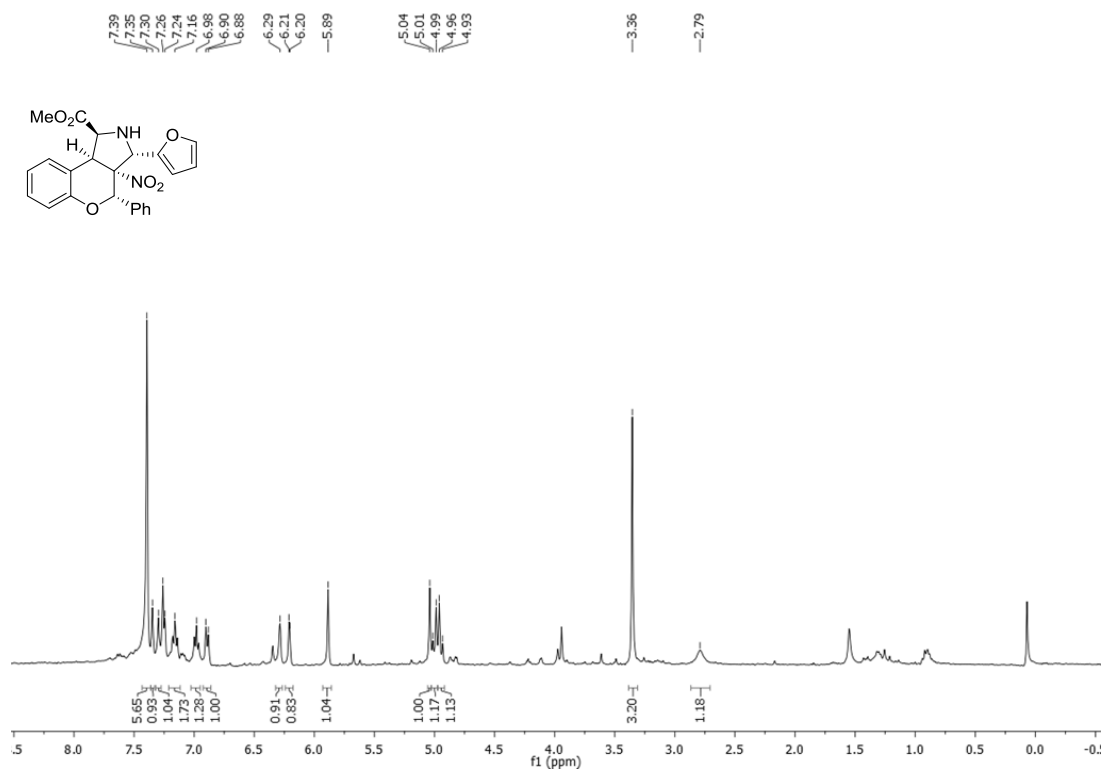
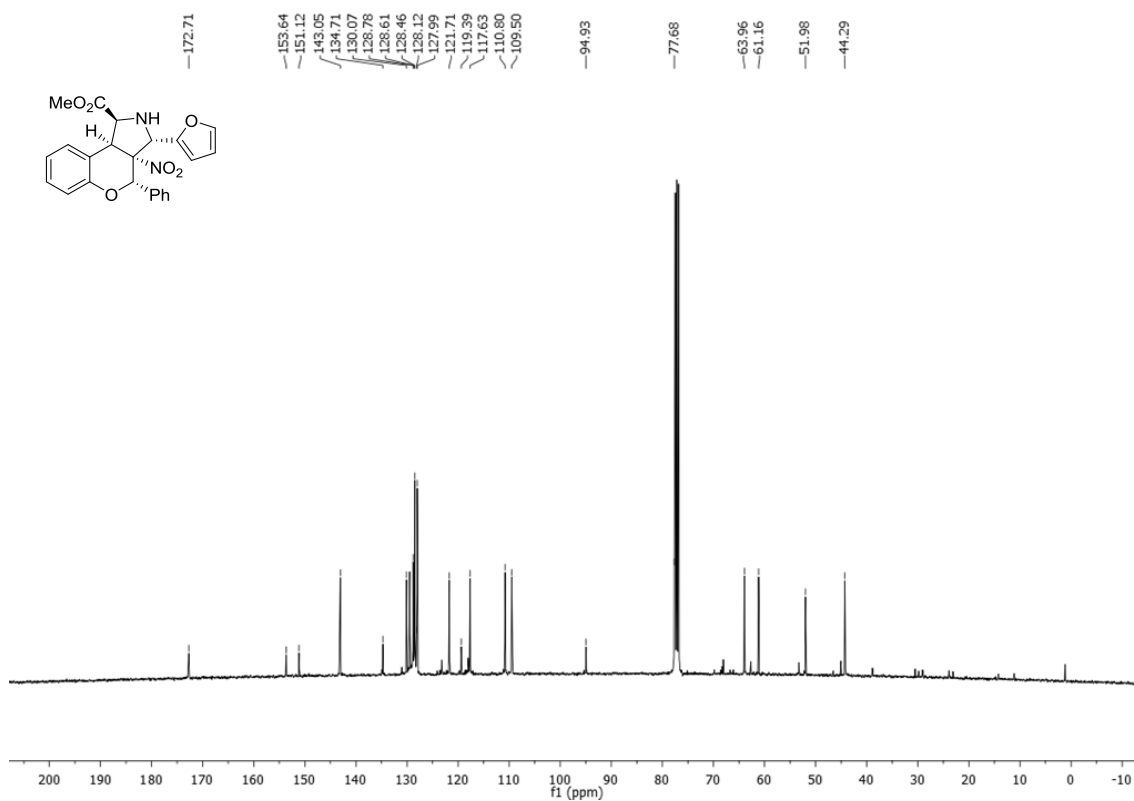
$^1\text{H-NMR}$ (CDCl_3) 400 MHz



$^{13}\text{C-NMR}$ (CDCl_3) 101 MHz



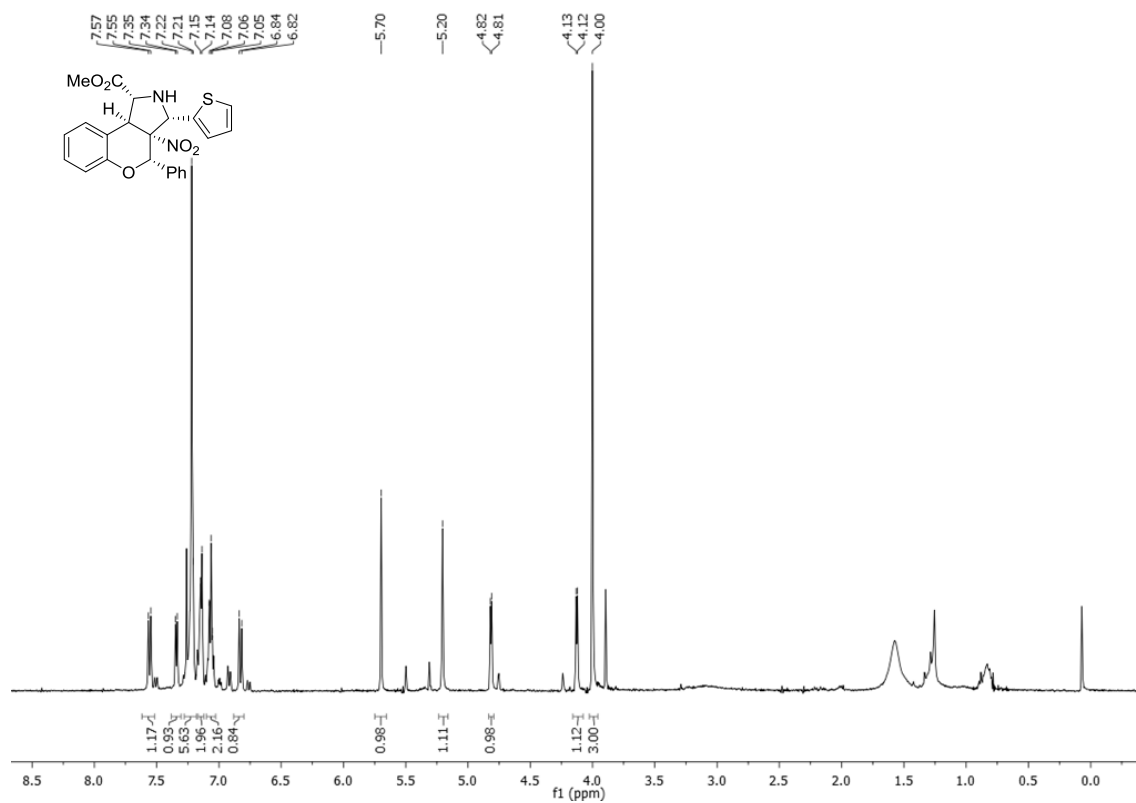
Compound 130'h

 $^1\text{H-NMR}$ (CDCl_3) 400 MHz $^{13}\text{C-NMR}$ (CDCl_3) 101 MHz

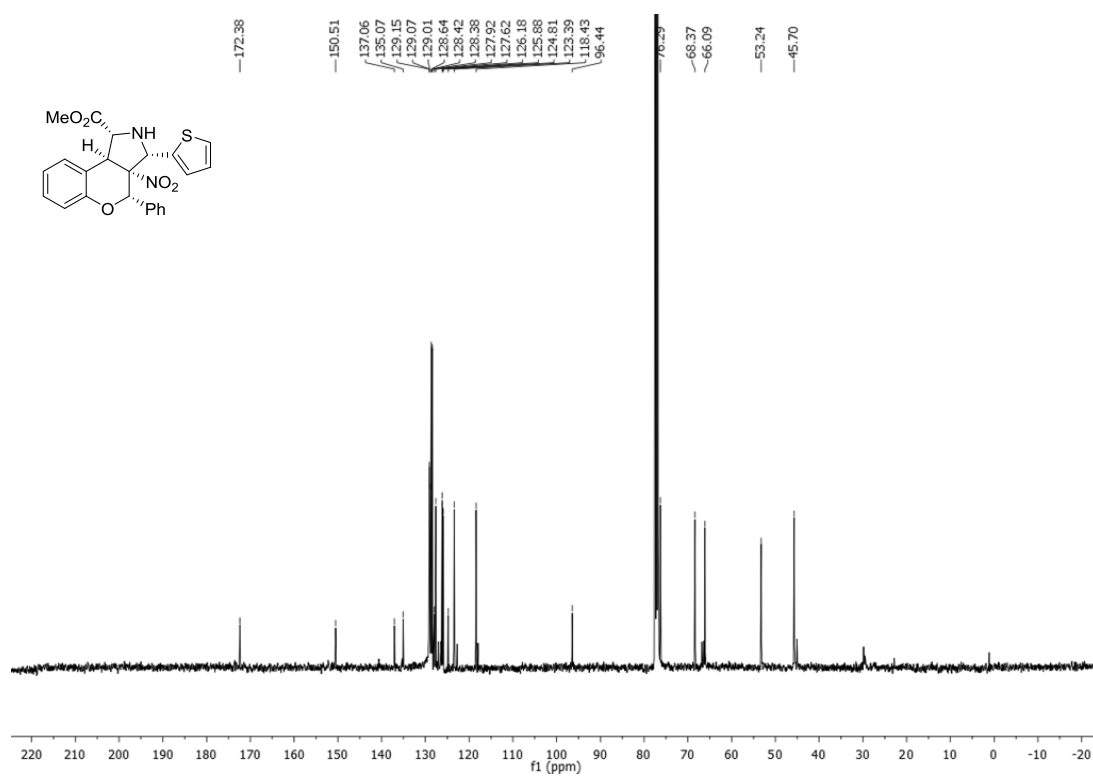
ANNEX I

Compound 130i

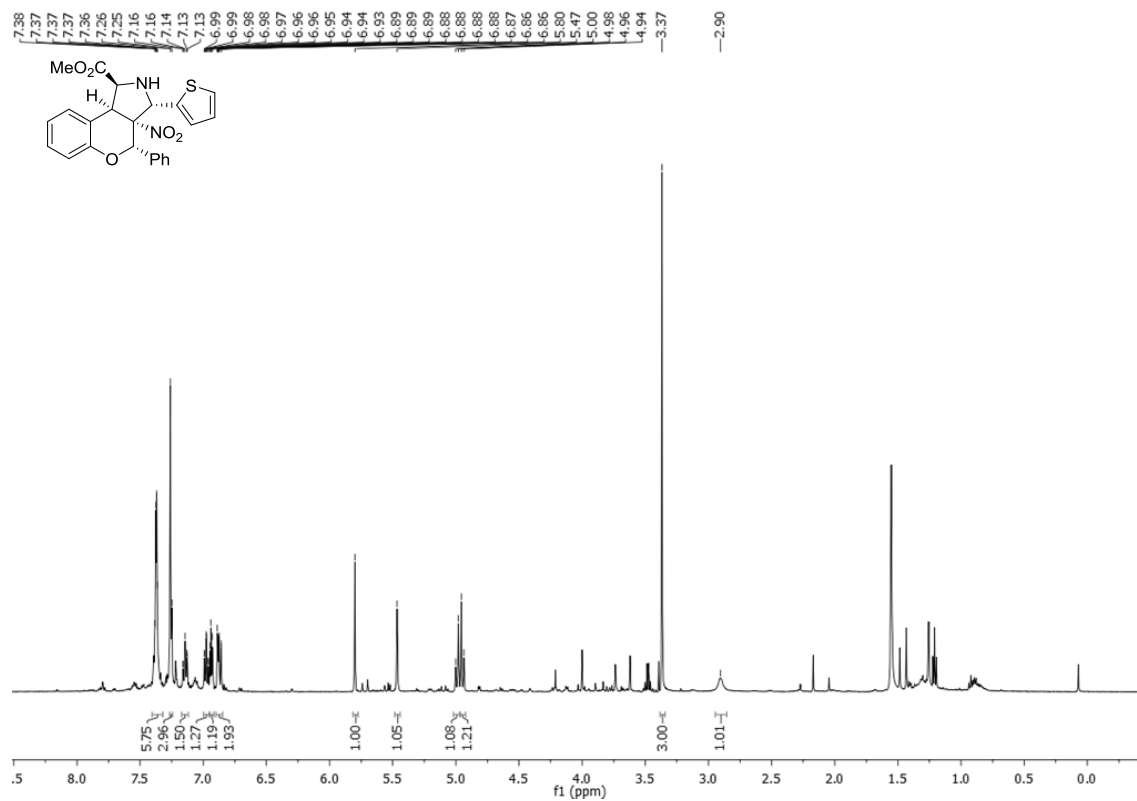
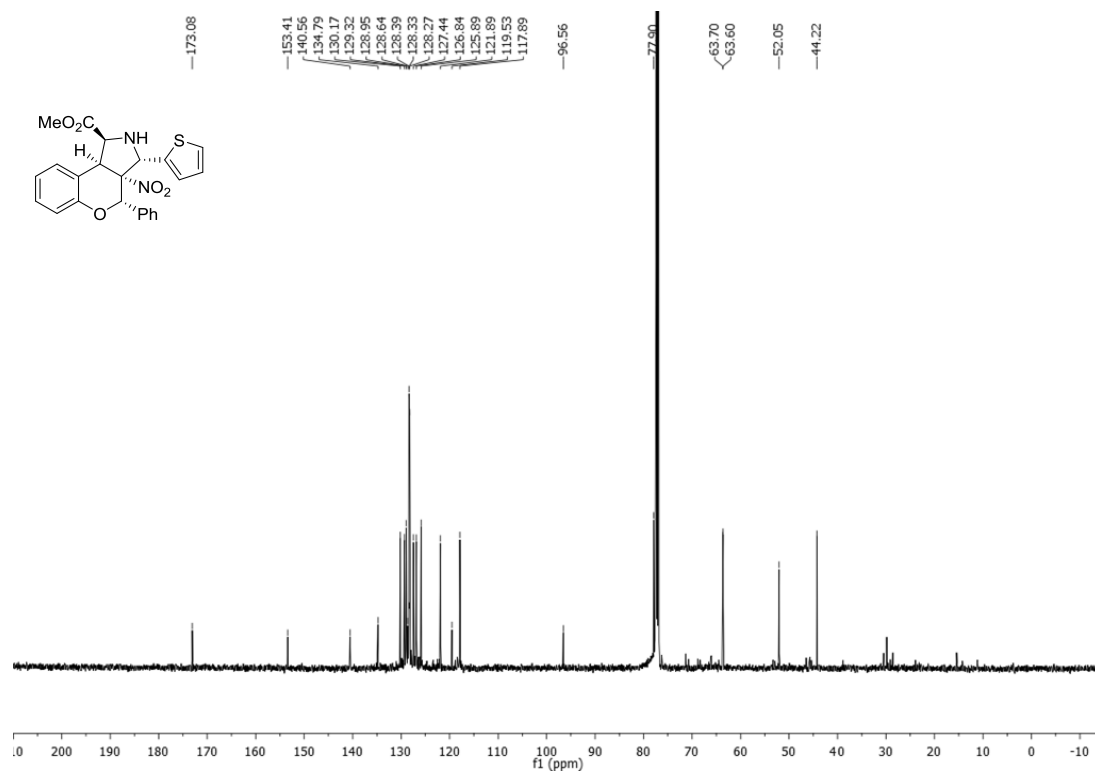
$^1\text{H-NMR}$ (CDCl_3) 400 MHz



$^{13}\text{C-NMR}$ (CDCl_3) 101 MHz



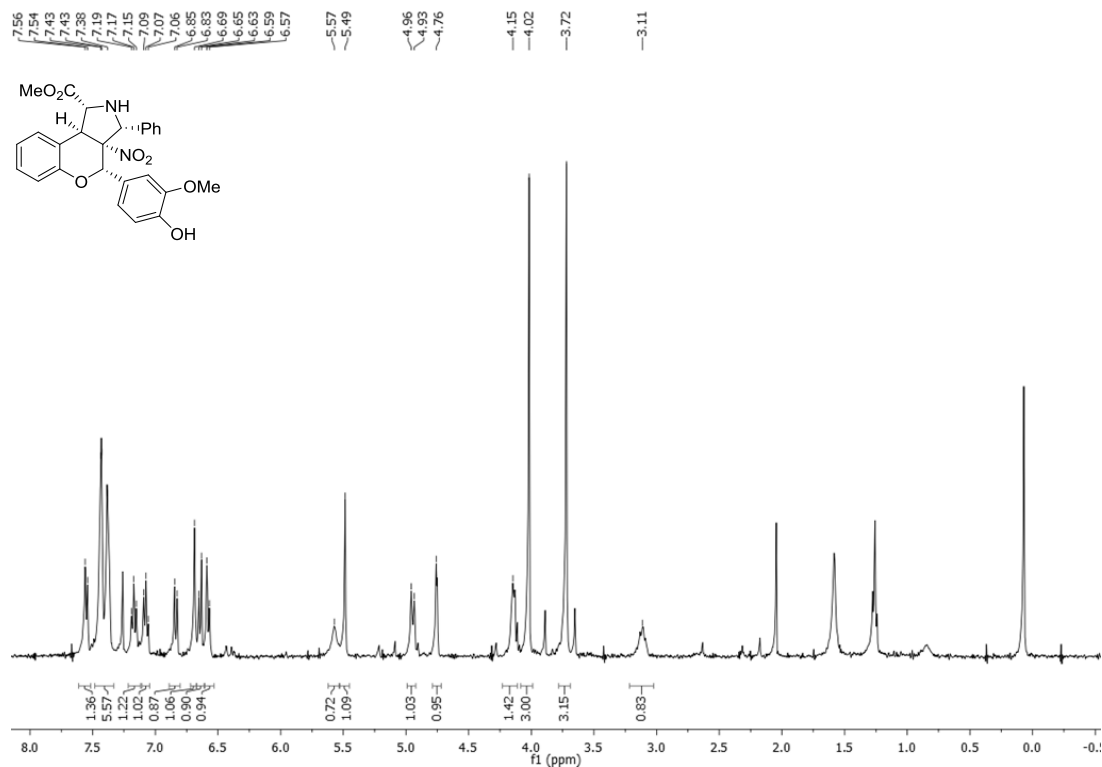
Compound 130'i

¹H-NMR (CDCl₃) 400 MHz¹³C NMR (CDCl₃) 101 MHz

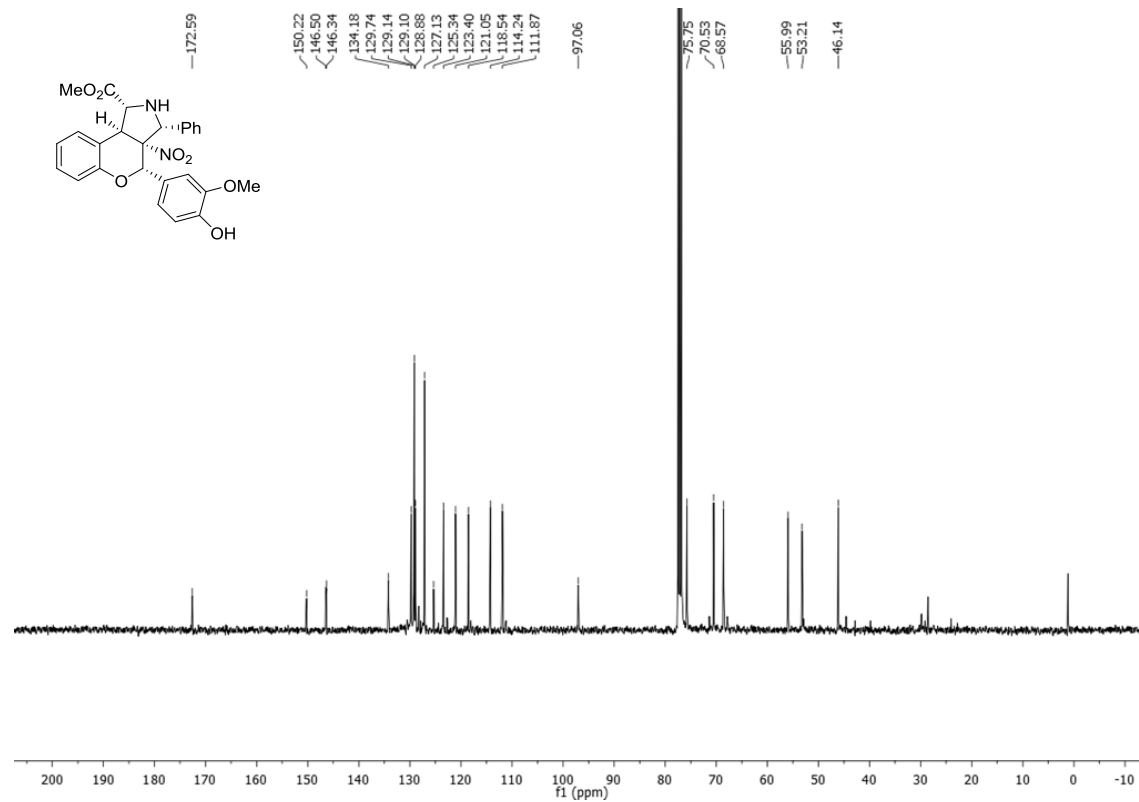
ANNEX I

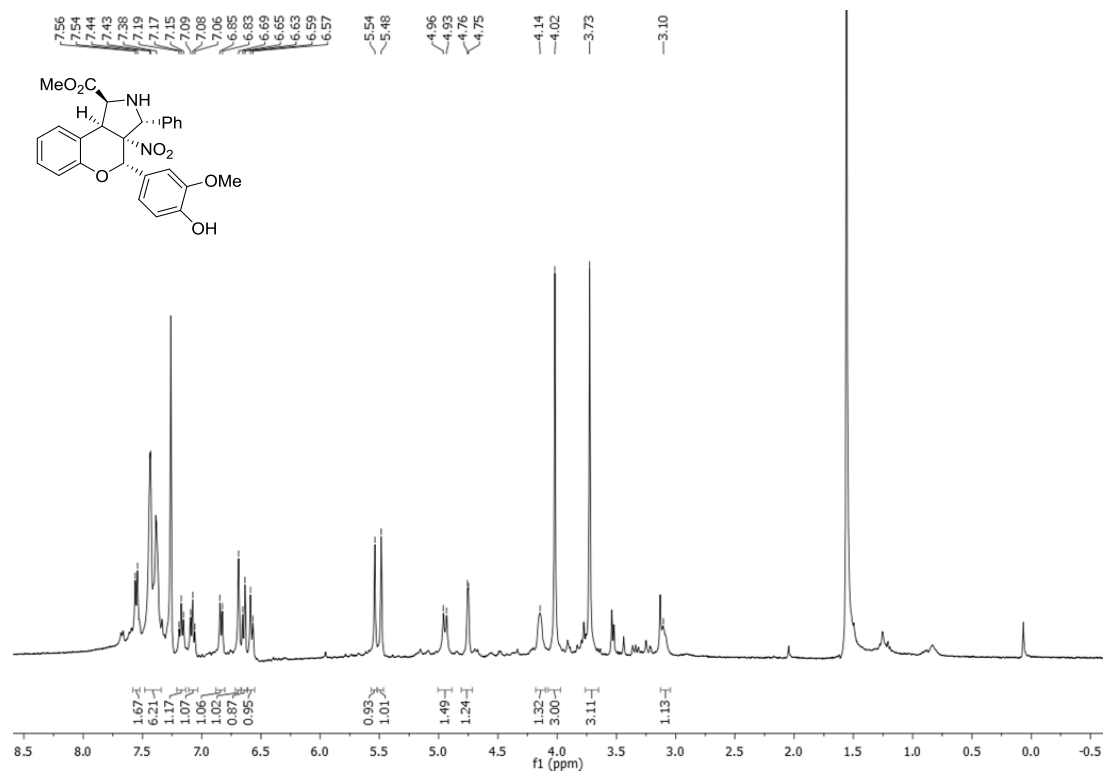
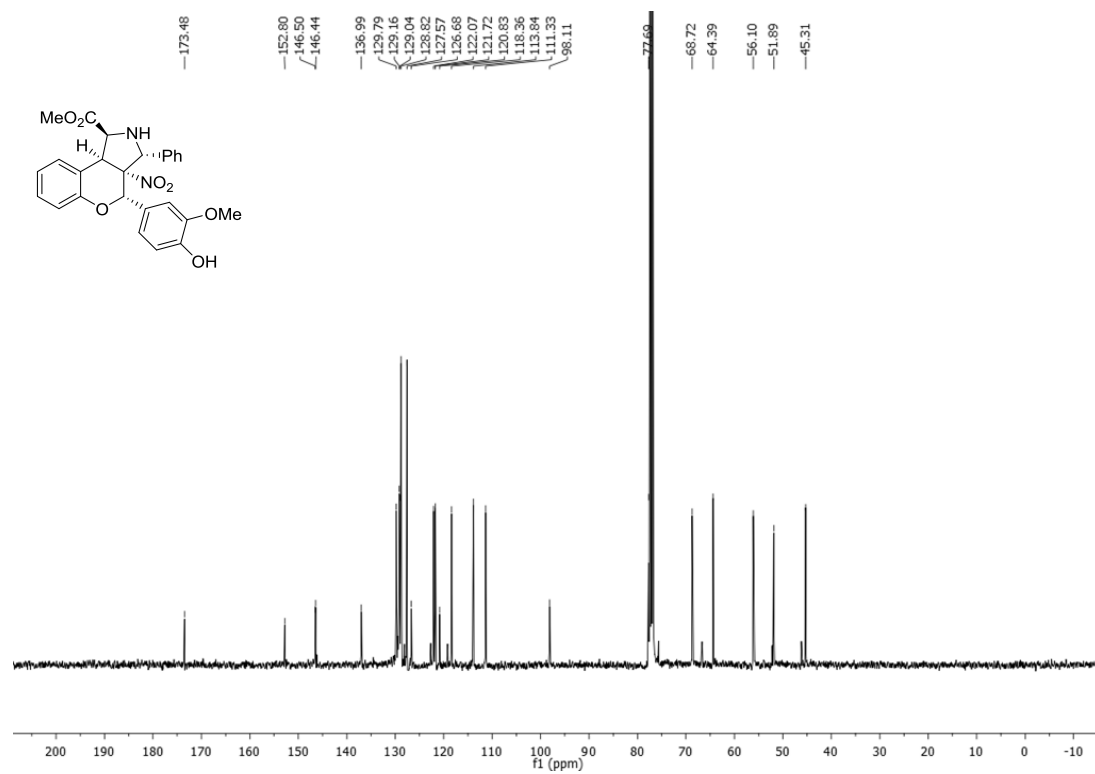
Compound 130j

¹H-NMR (CDCl₃) 400 MHz



¹³C NMR (CDCl₃) 101 MHz

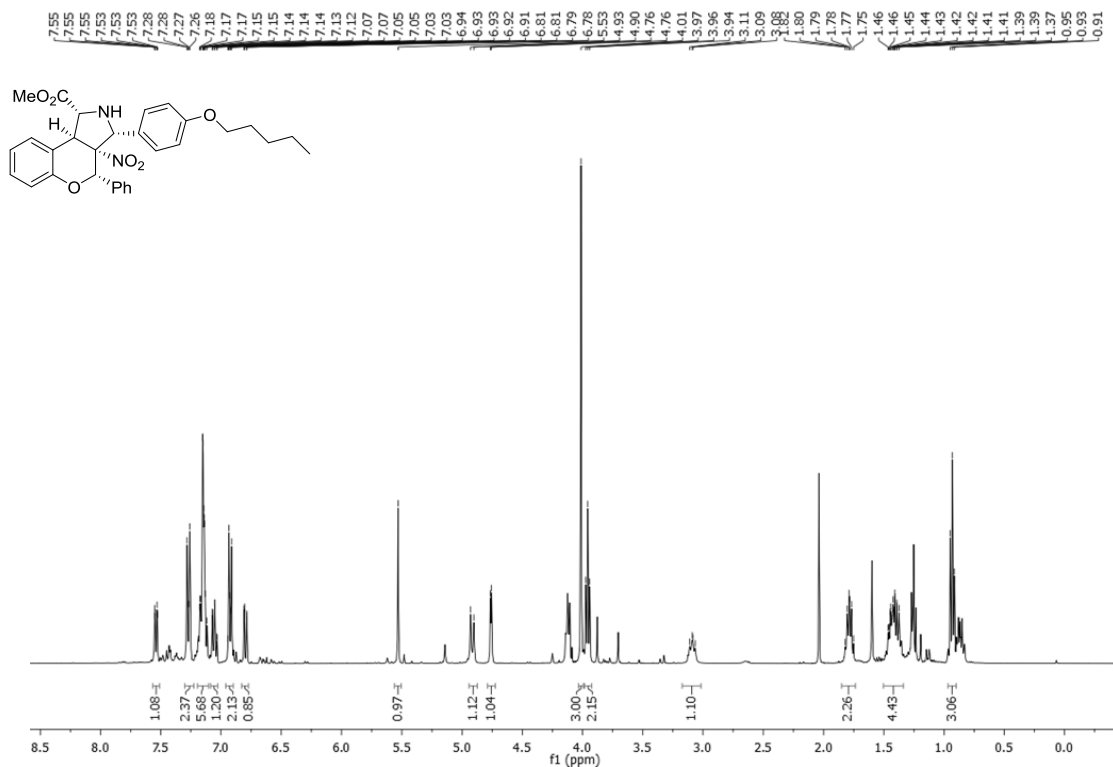


Compound 130'j**¹H-NMR (CDCl₃) 400 MHz****¹³C NMR (CDCl₃) 101 MHz**

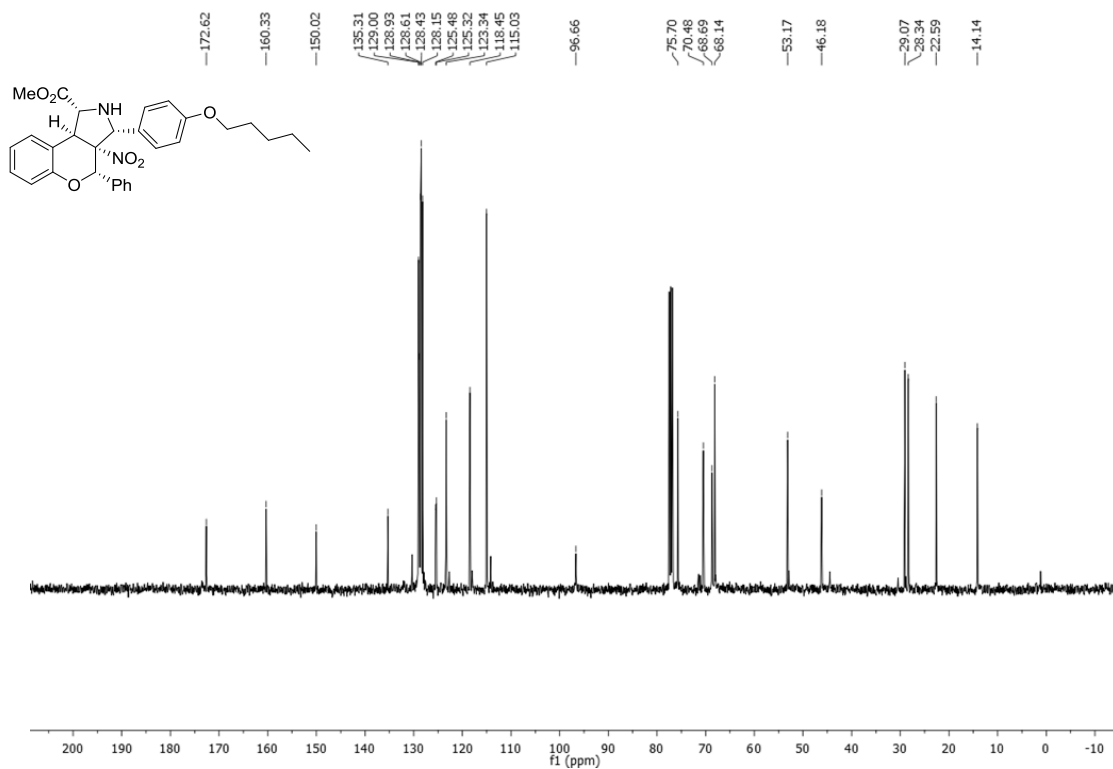
ANNEX I

Compound 130k

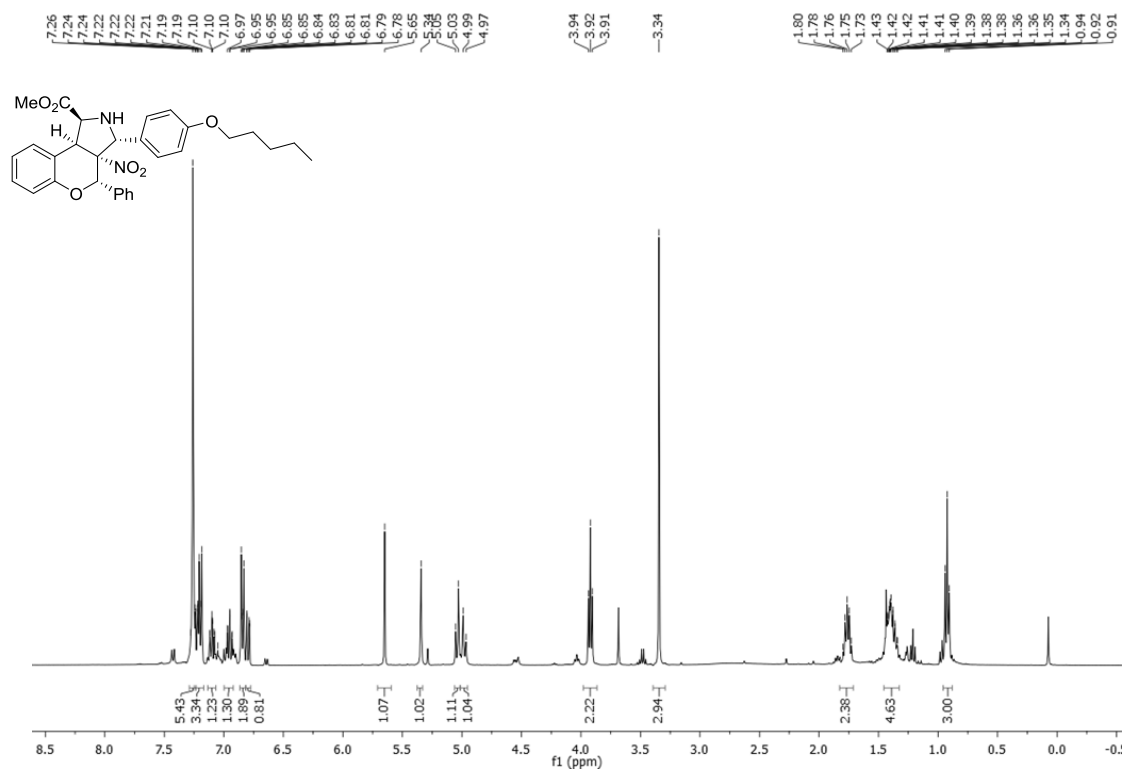
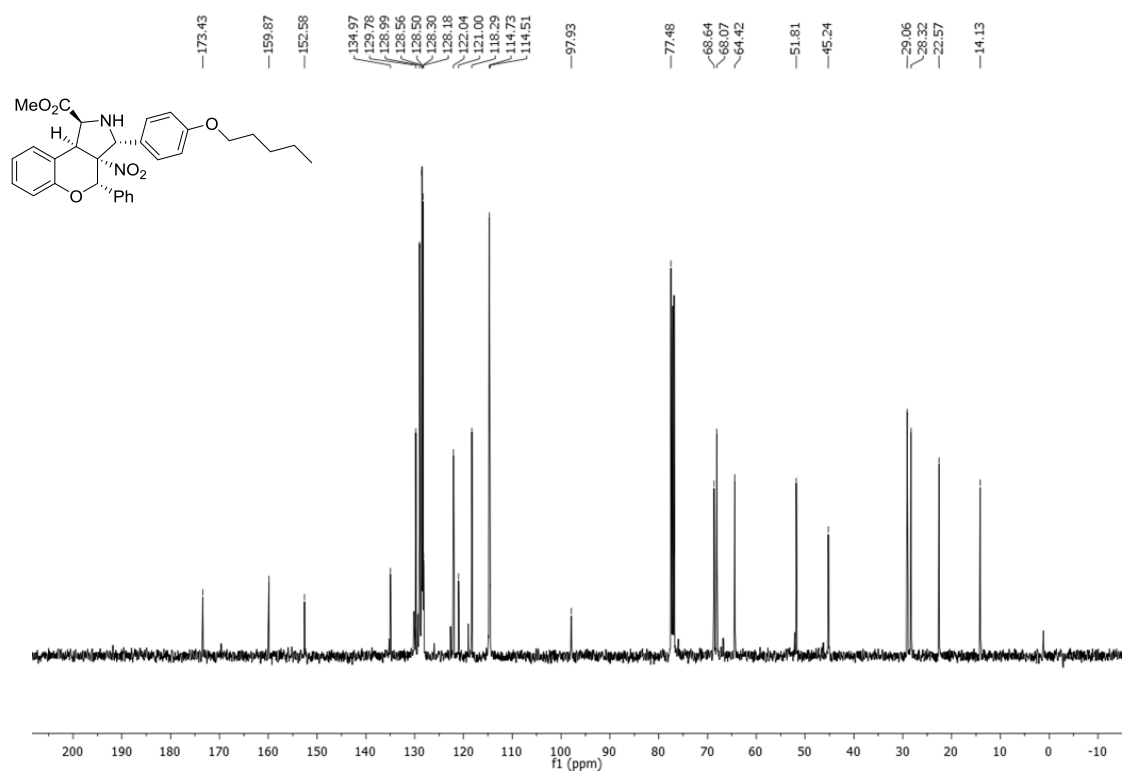
$^1\text{H-NMR}$ (CDCl_3) 400 MHz



$^{13}\text{C-NMR}$ (CDCl_3) 101 MHz



Compound 130'k

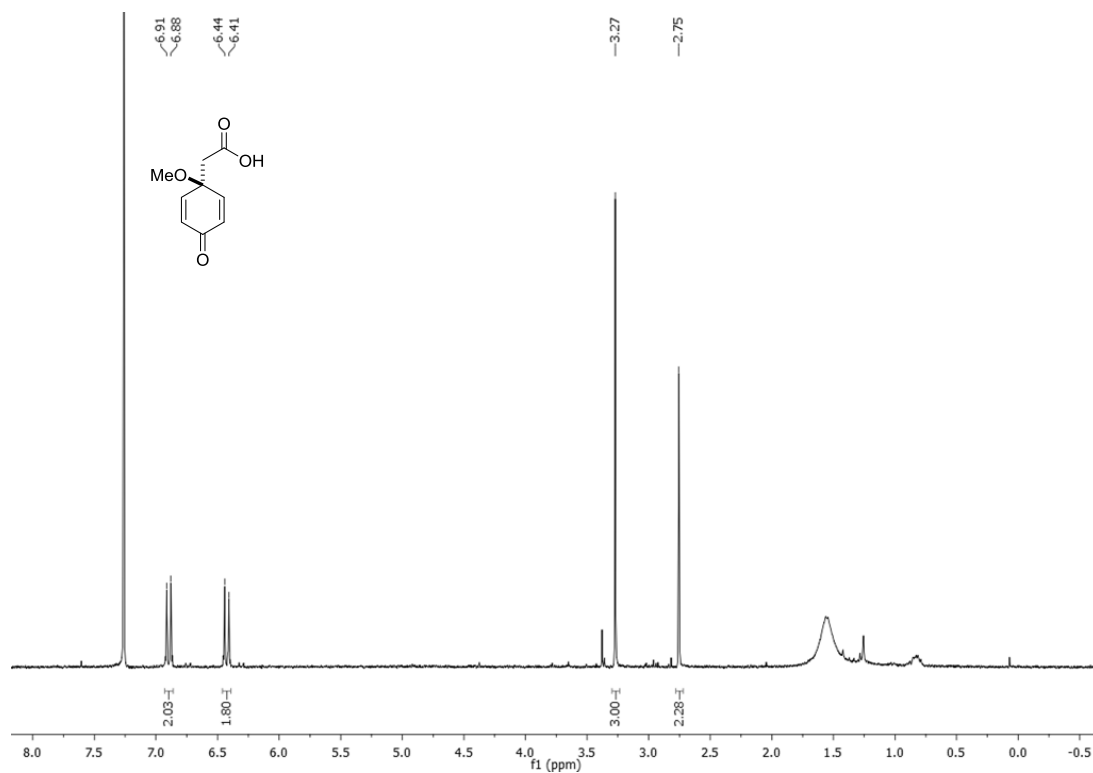
 $^1\text{H-NMR}$ (CDCl_3) 400 MHz $^{13}\text{C NMR}$ (CDCl_3) 101 MHz

ANNEX II

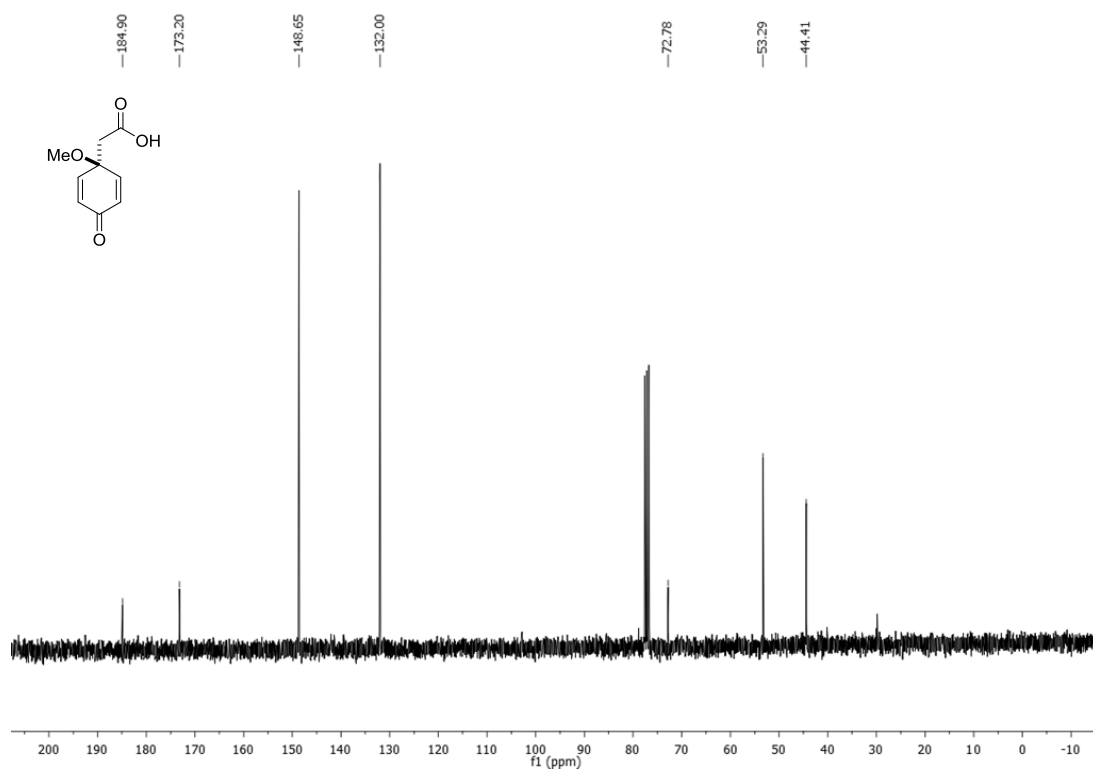
ANNEX II. ^1H , ^{13}C spectra of Chapter 3

Compound 331

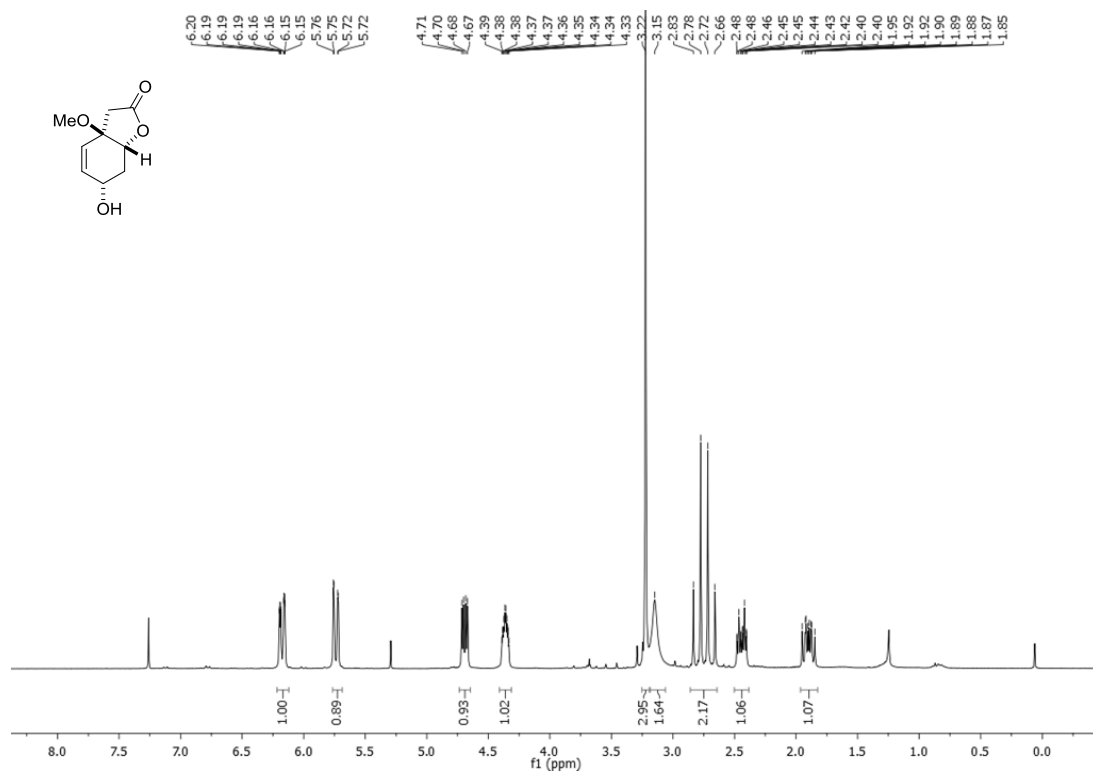
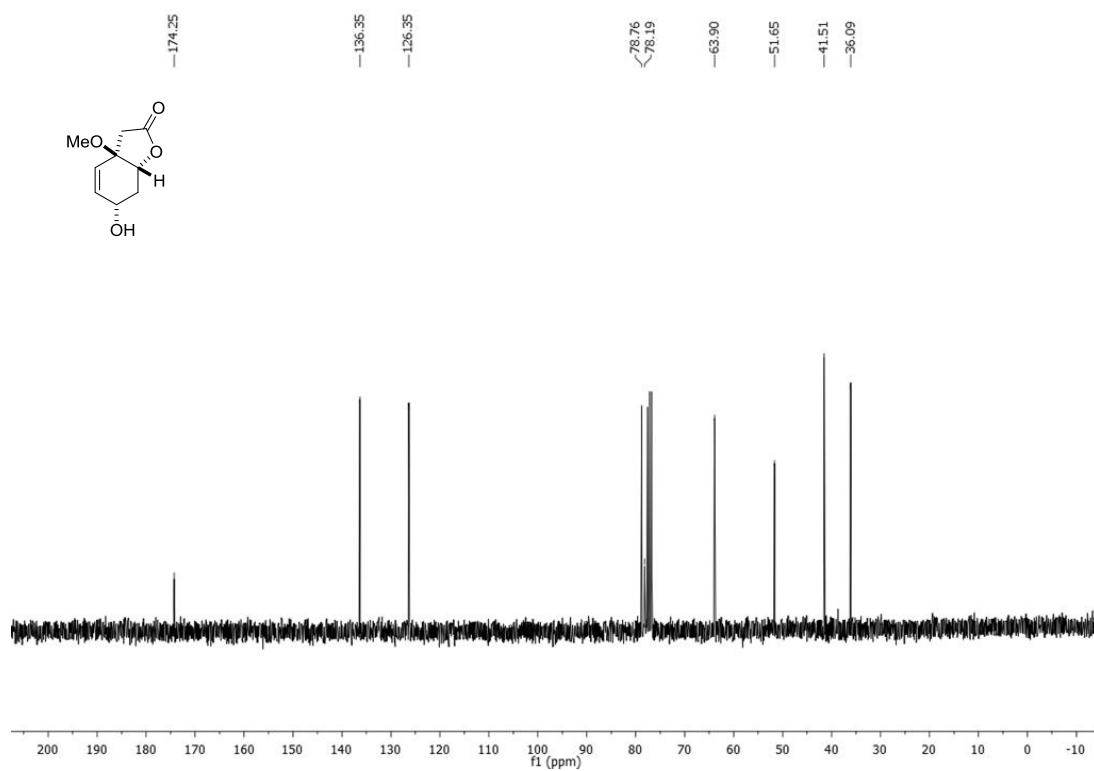
^1H -NMR (CDCl_3) 300 MHz



^{13}C NMR (CDCl_3) 75 MHz



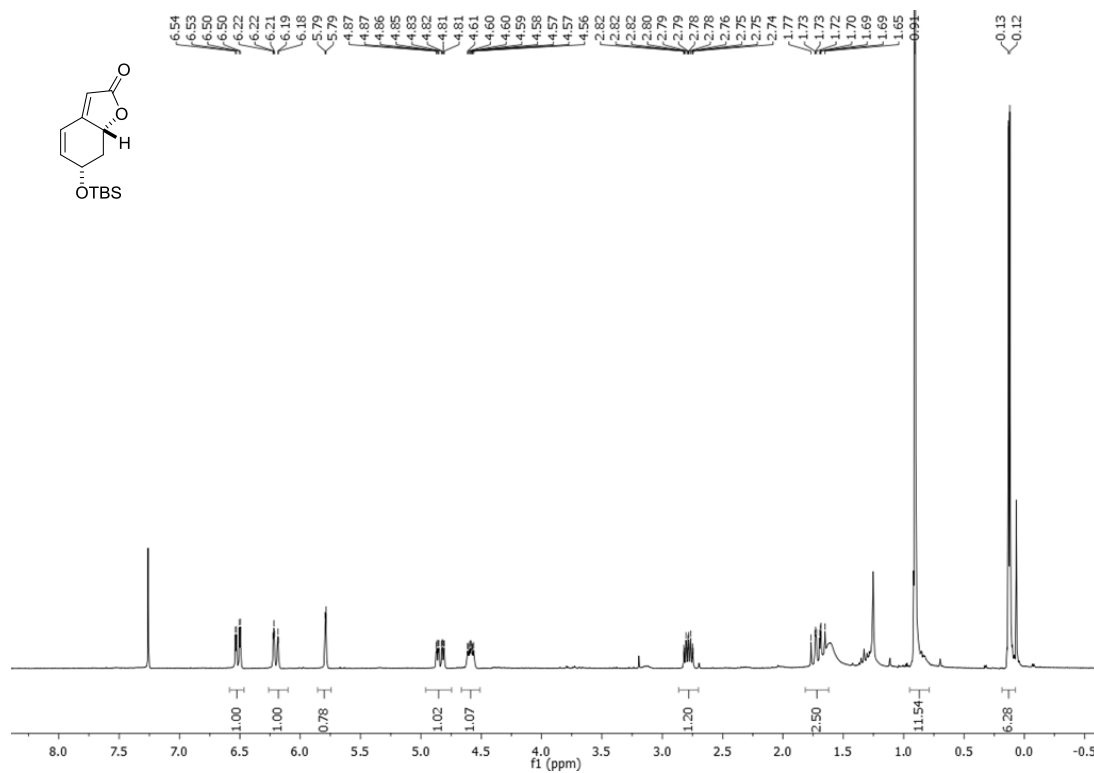
Compound 333

 $^1\text{H-NMR}$ (CDCl_3) 300 MHz $^{13}\text{C NMR}$ (CDCl_3) 75 MHz

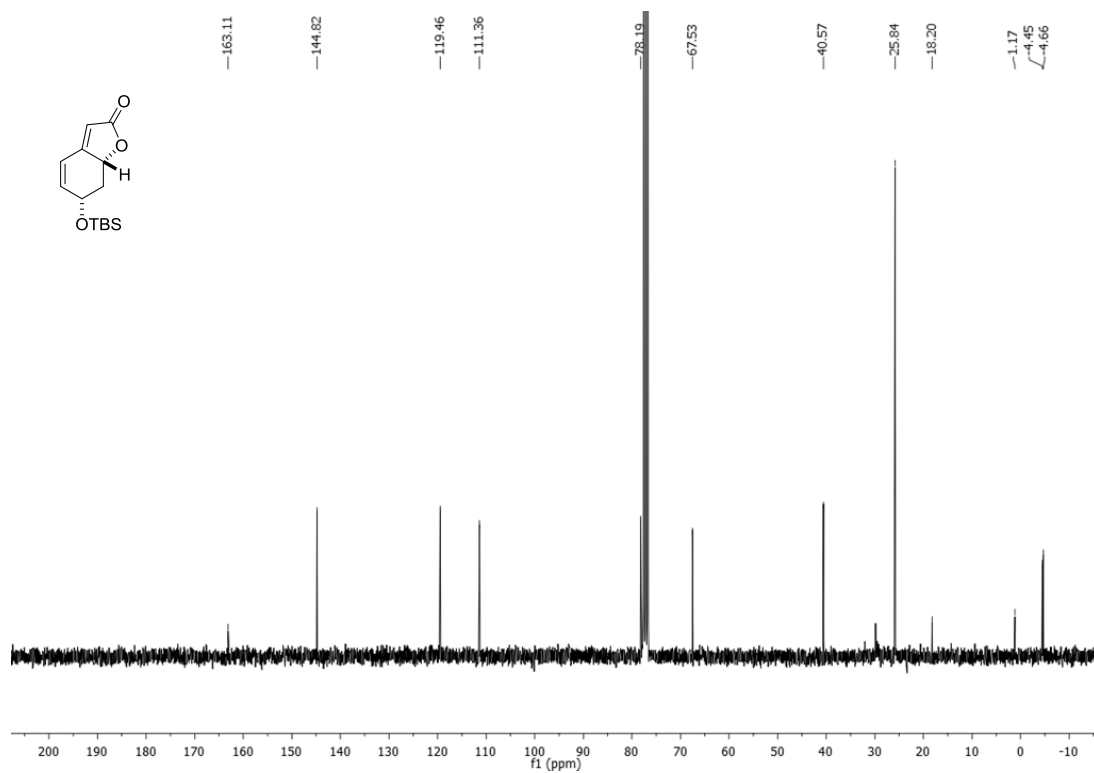
ANNEX II

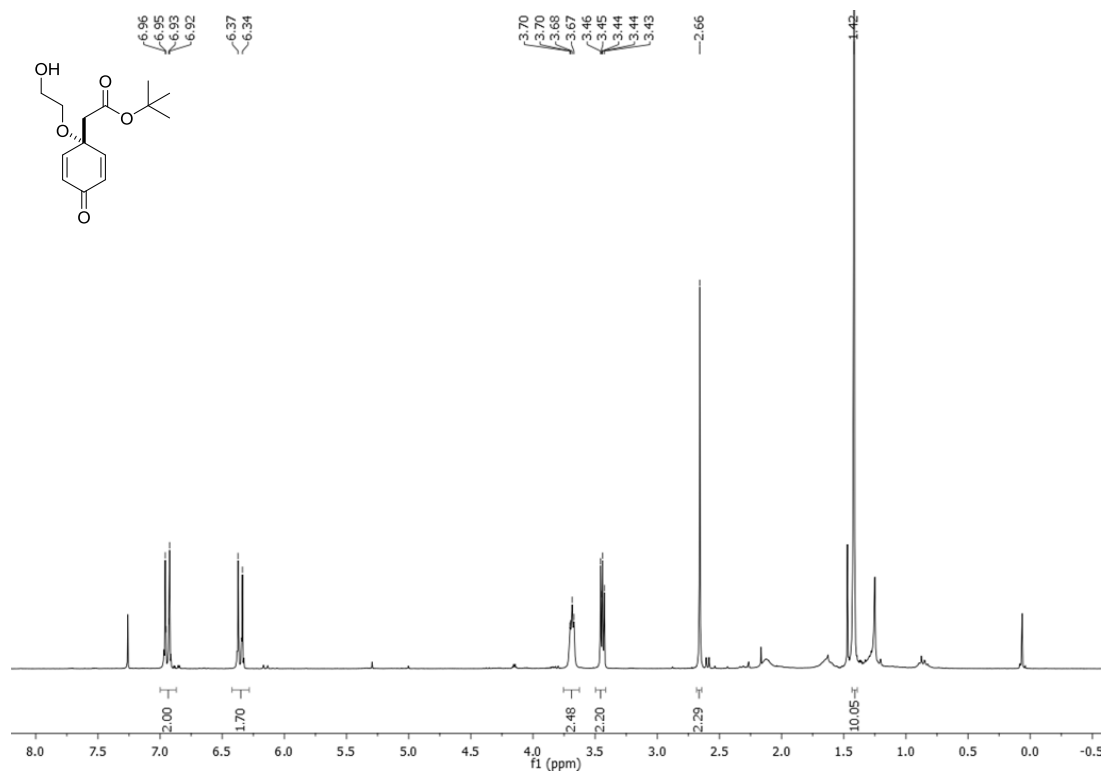
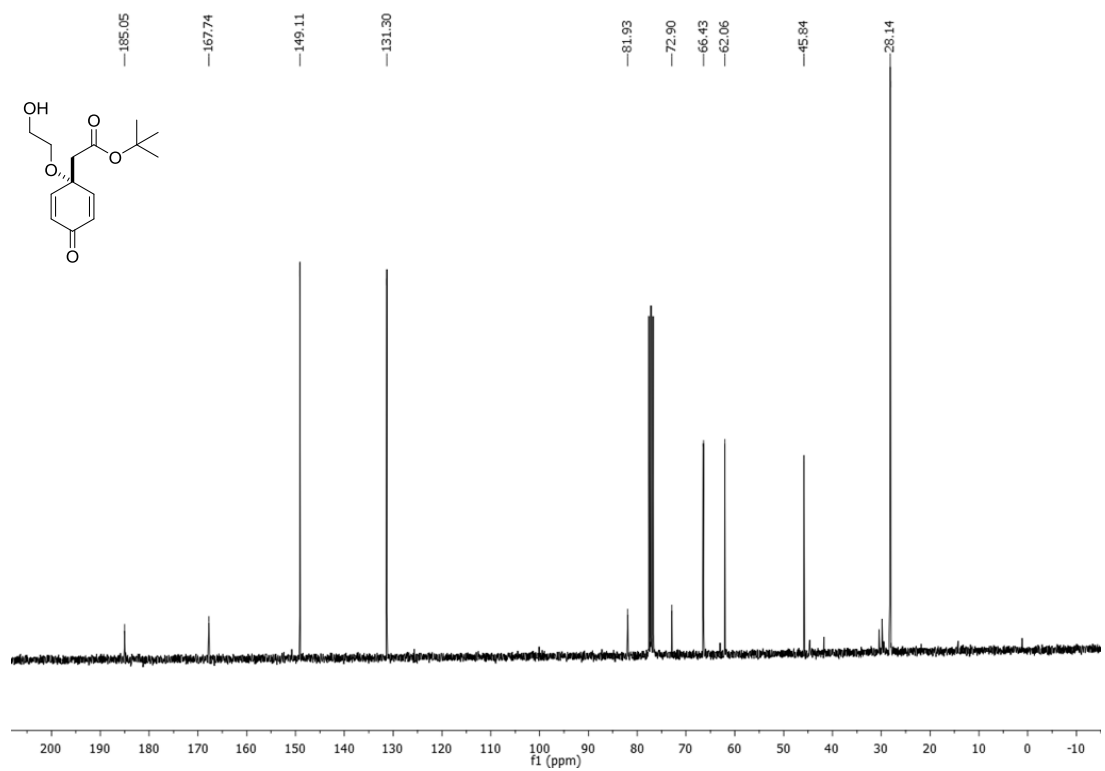
Compound 328

$^1\text{H-NMR}$ (CDCl_3) 300 MHz



$^{13}\text{C NMR}$ (CDCl_3) 75 MHz

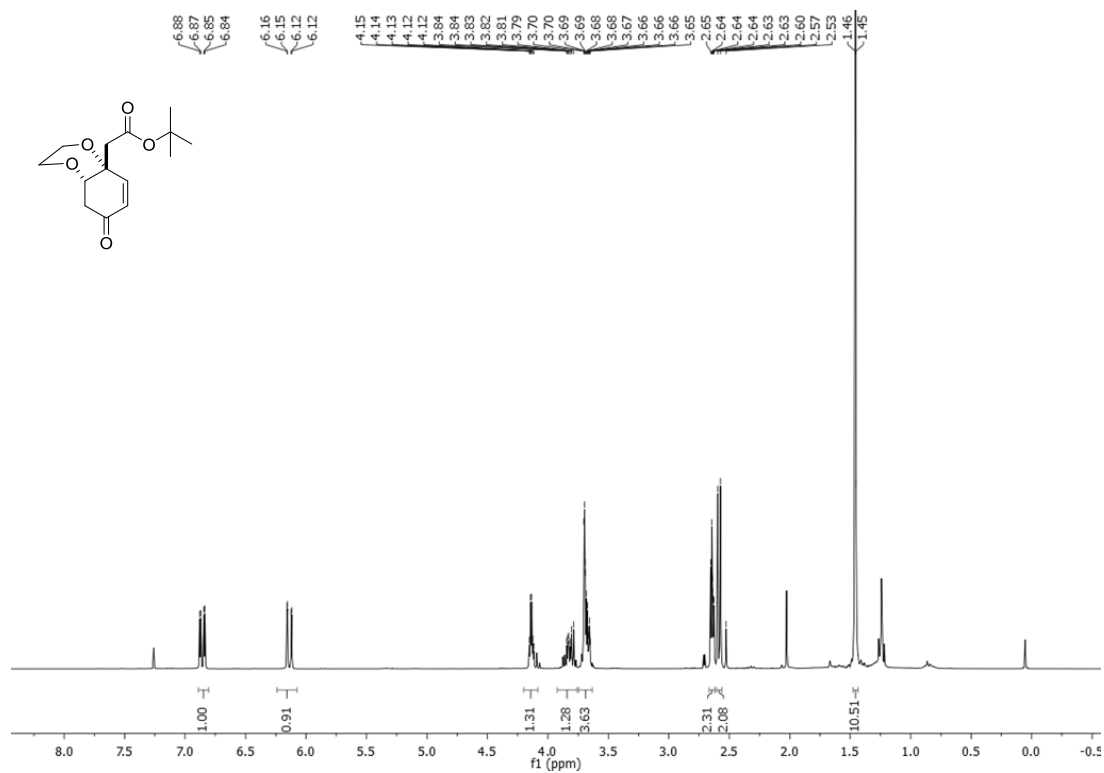


Compound 341 **$^1\text{H-NMR}$ (CDCl_3) 300 MHz** **$^{13}\text{C-NMR}$ (CDCl_3) 75 MHz**

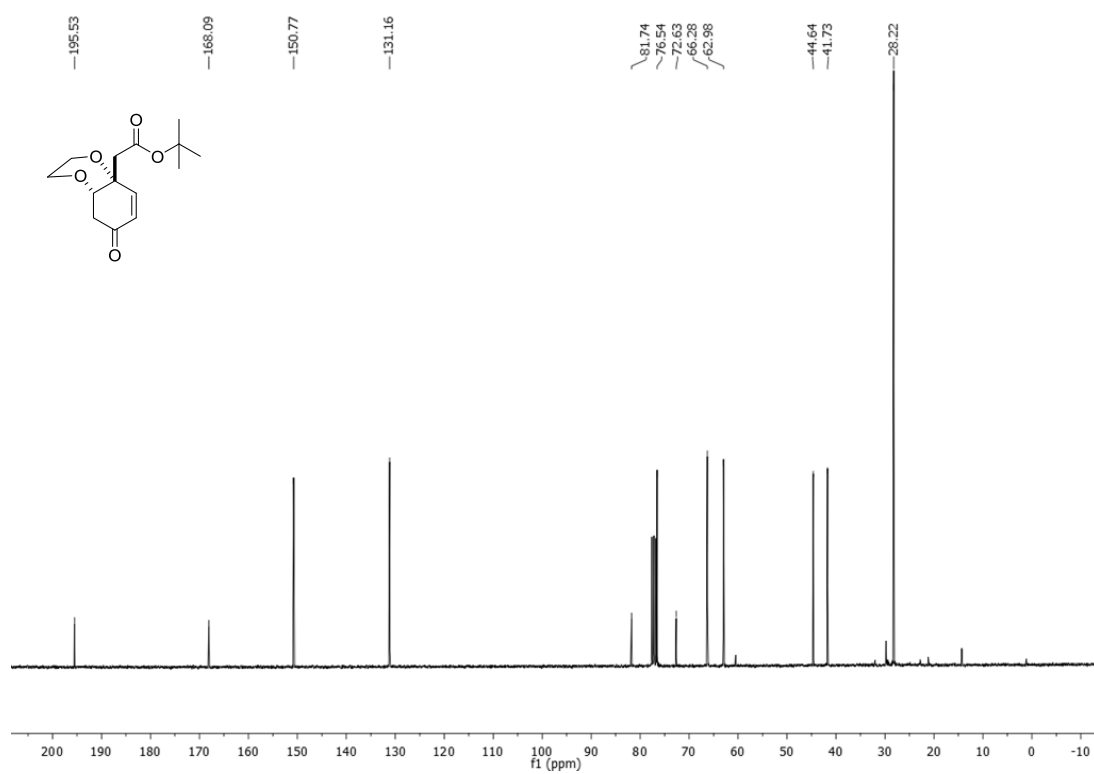
ANNEX II

Compound 342

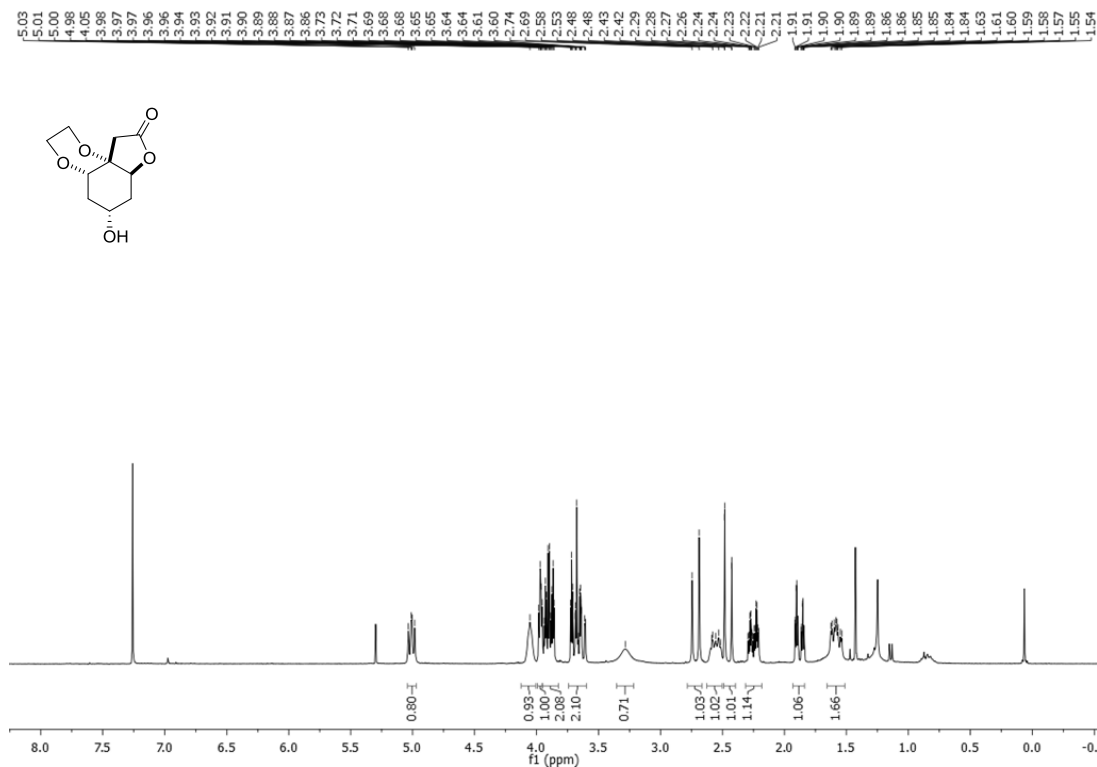
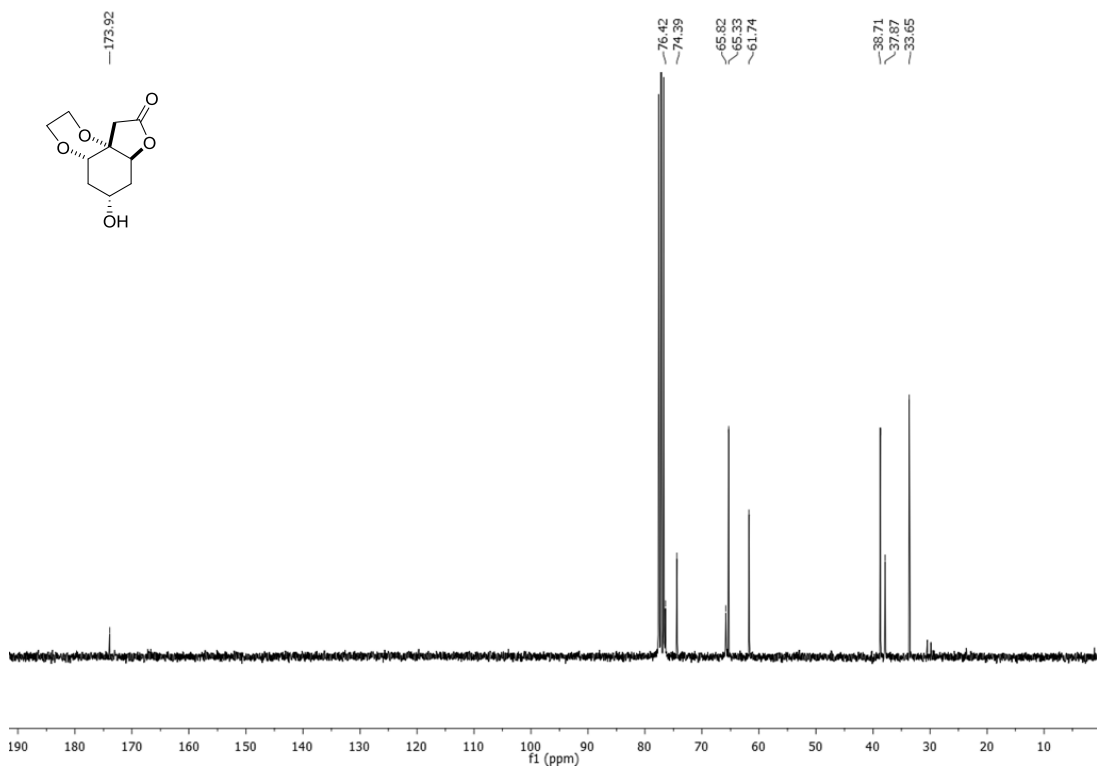
$^1\text{H-NMR}$ (CDCl_3) 300 MHz

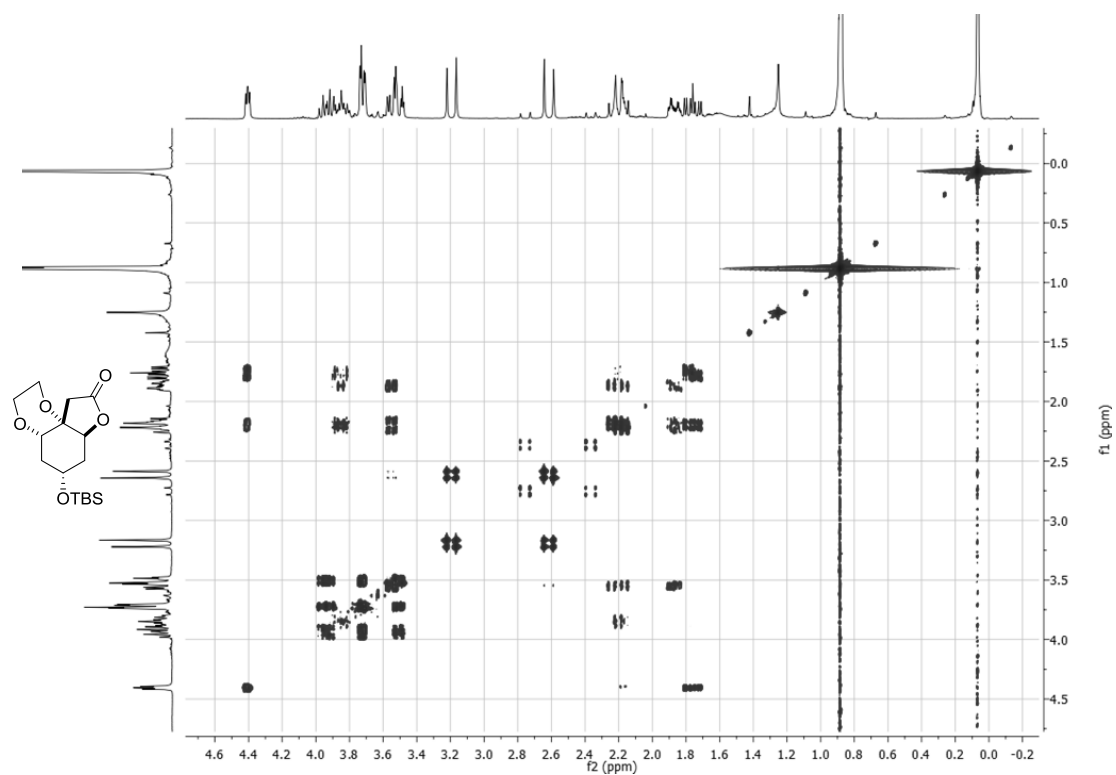
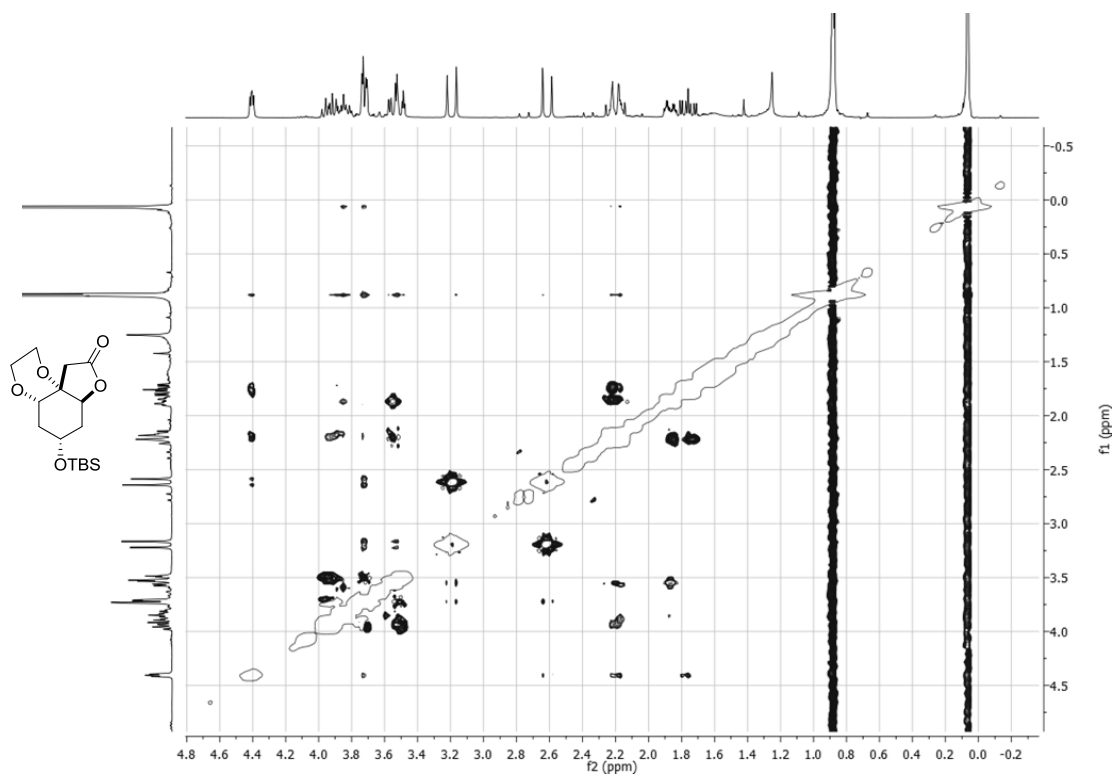


$^{13}\text{C-NMR}$ (CDCl_3) 75 MHz



Compound 344a

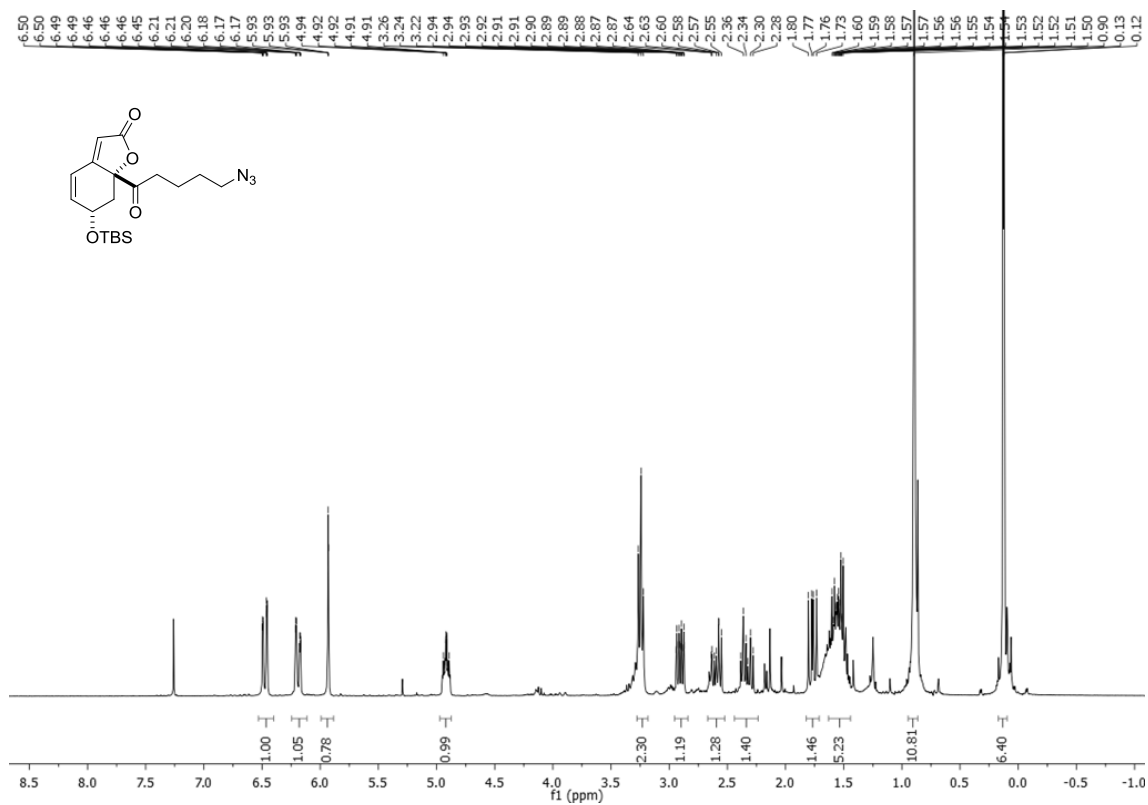
 $^1\text{H-NMR}$ (CDCl_3) 300 MHz $^{13}\text{C-NMR}$ (CDCl_3) 75 MHz

COSY (CDCl₃)NOESY 2D (CDCl₃)

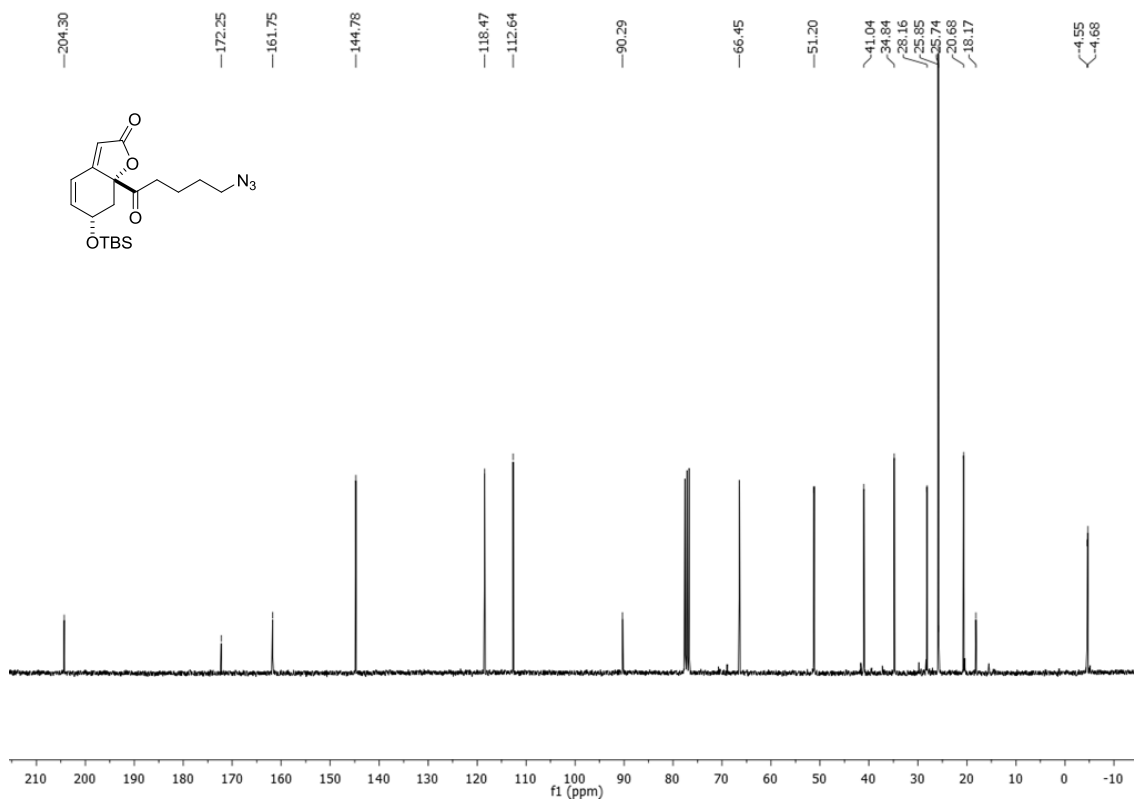
ANNEX II

Compound 352a

¹H-NMR (CDCl₃) 300 MHz



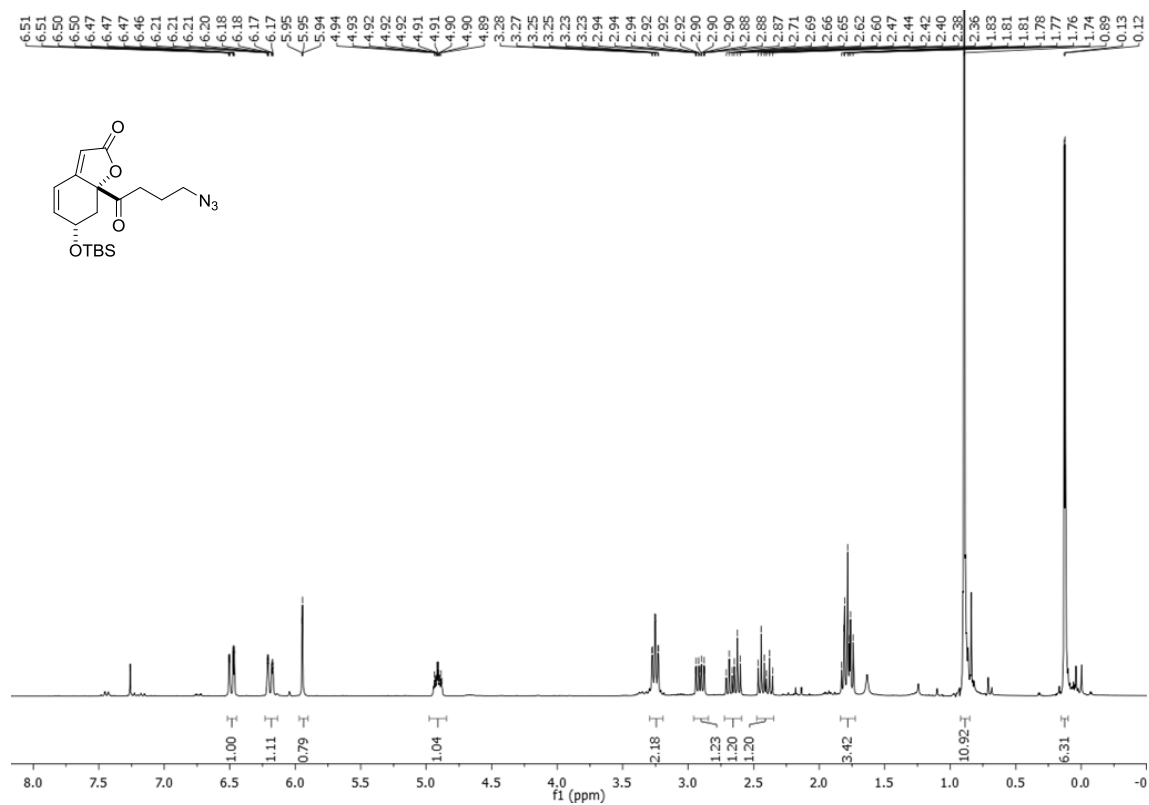
¹³C NMR (CDCl₃) 75 MHz



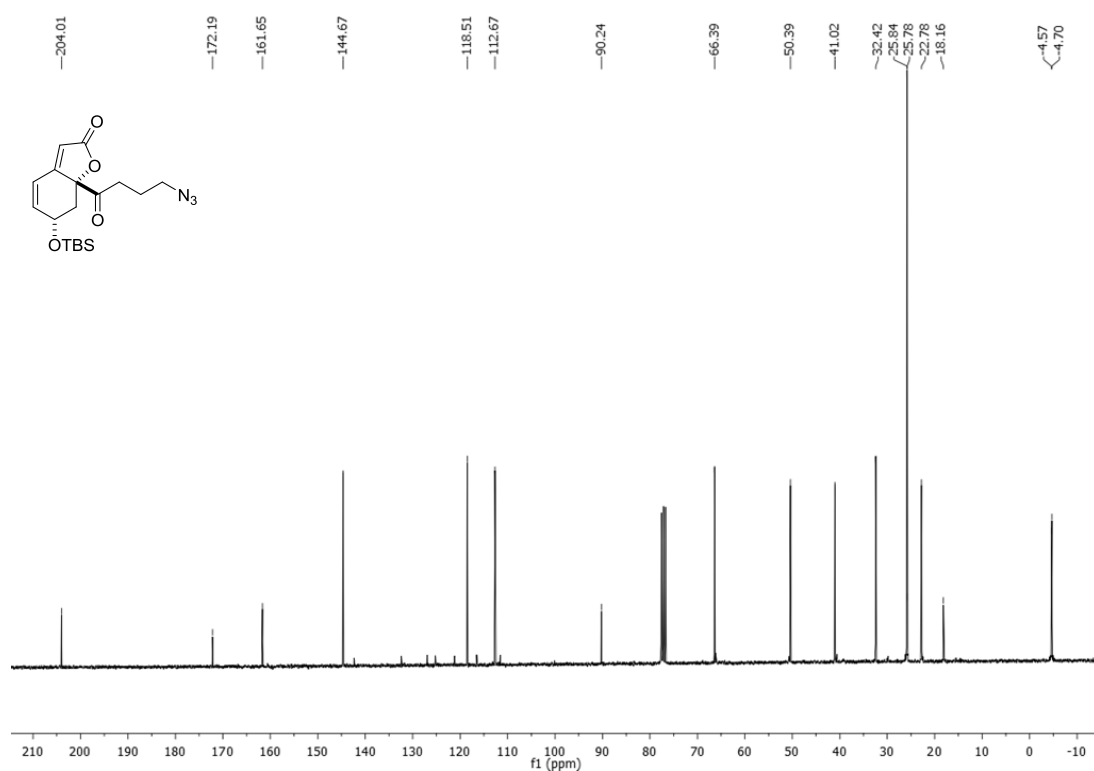
ANNEX II

Compound 354a

$^1\text{H-NMR}$ (CDCl_3) 300 MHz



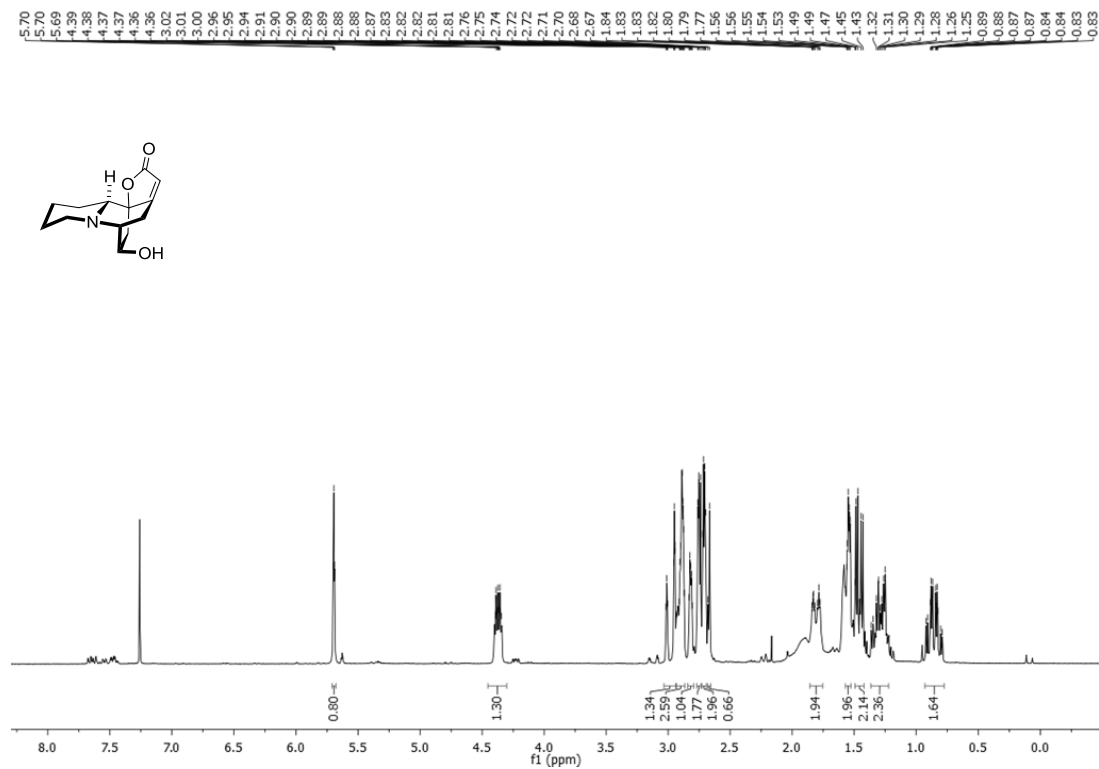
$^{13}\text{C-NMR}$ (CDCl_3) 75 MHz



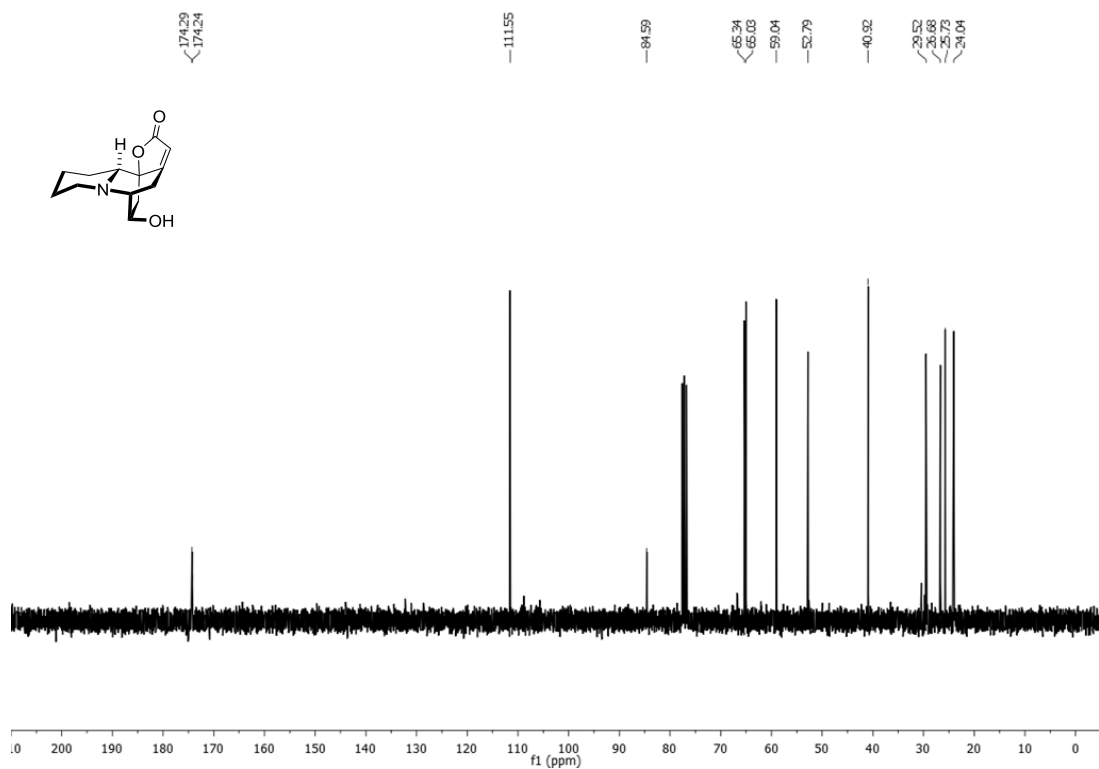
ANNEX II

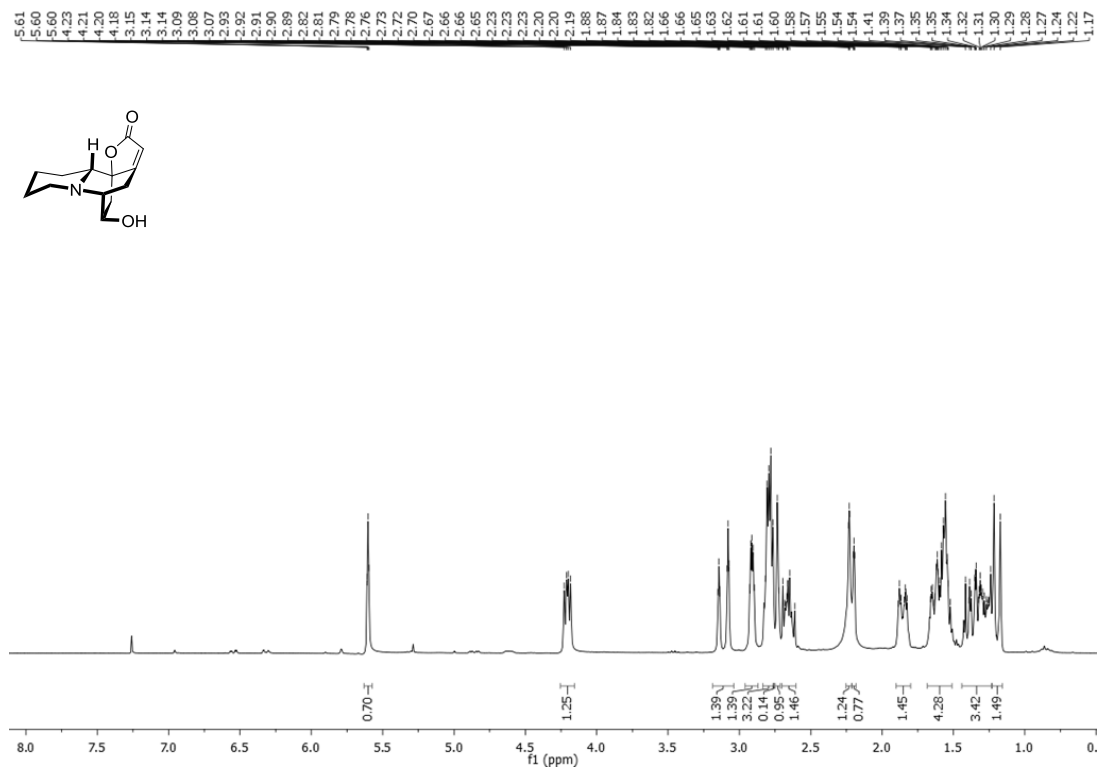
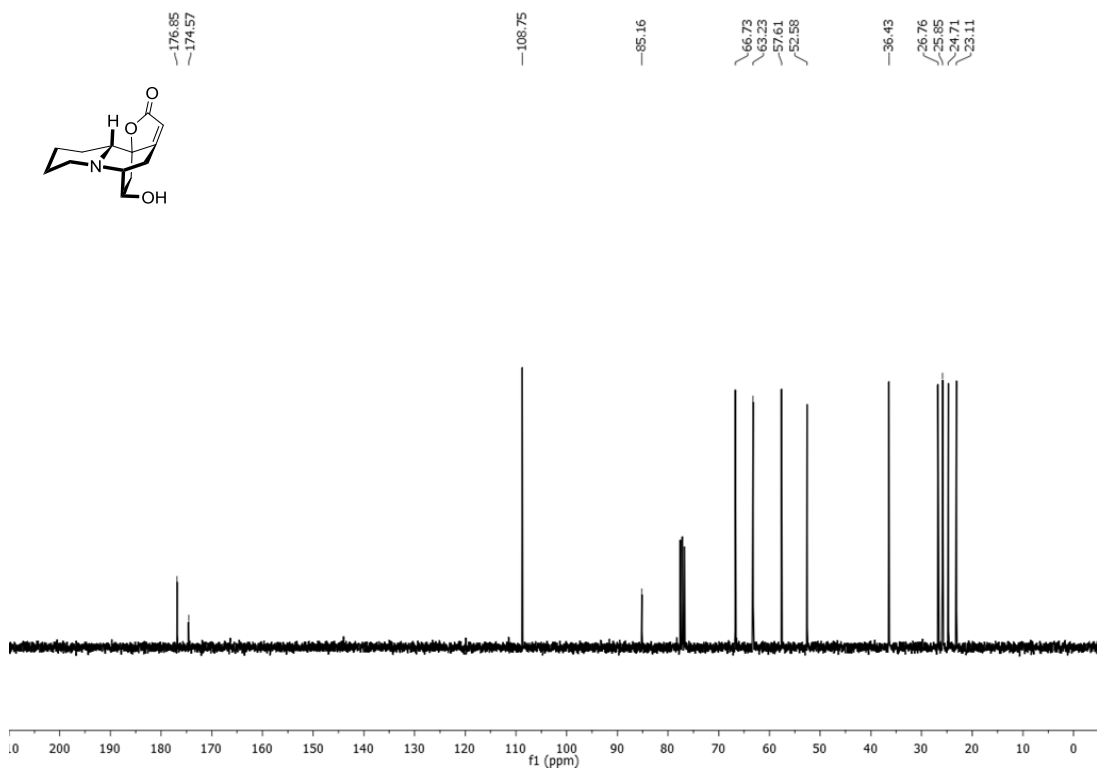
(±)-Virosine A-360

$^1\text{H-NMR}$ (CDCl_3) 300 MHz



$^{13}\text{C-NMR}$ (CDCl_3) 75 MHz

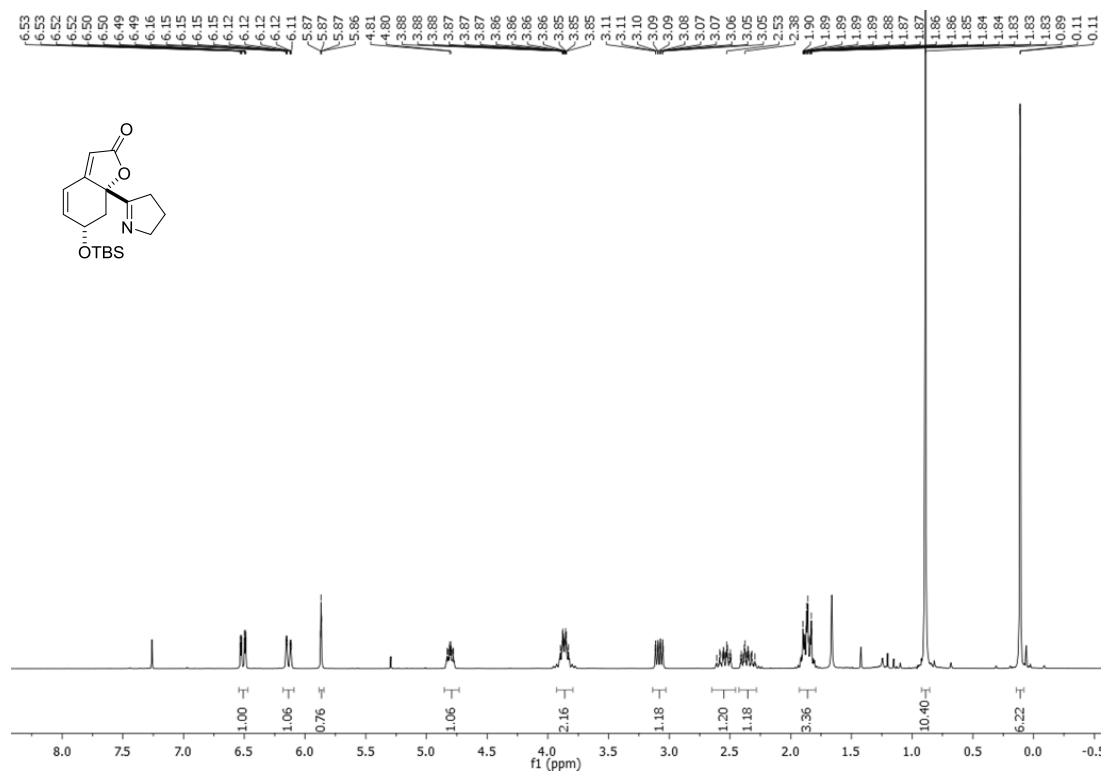


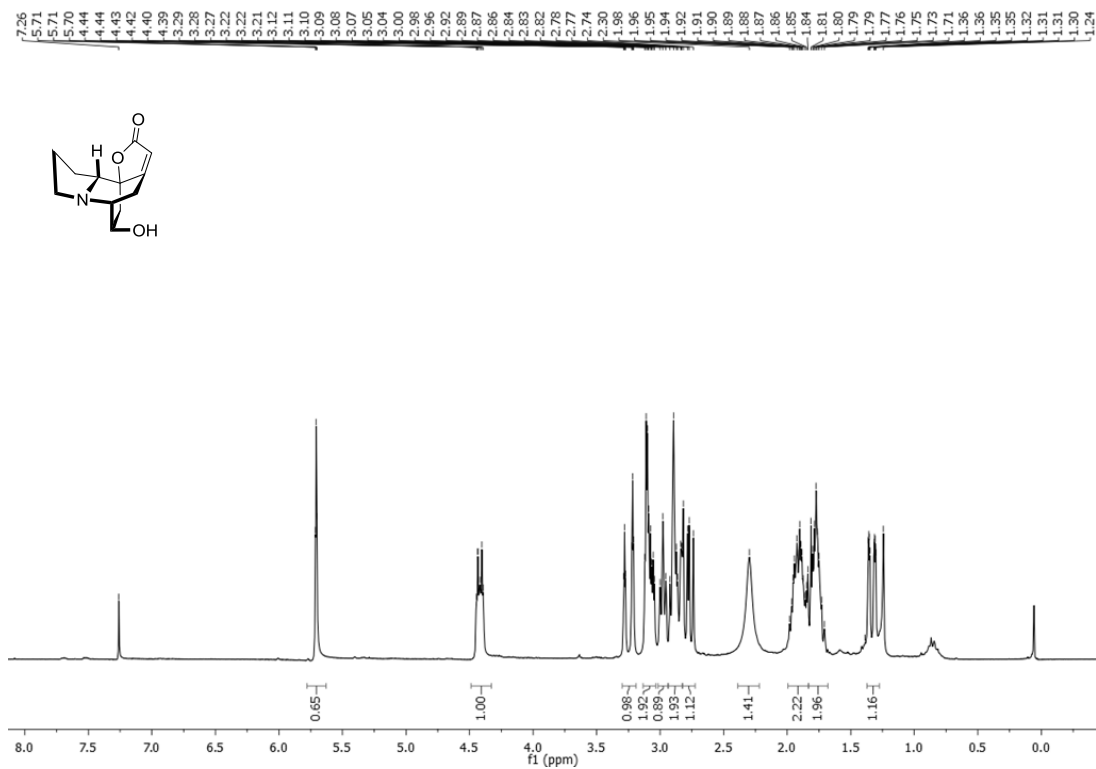
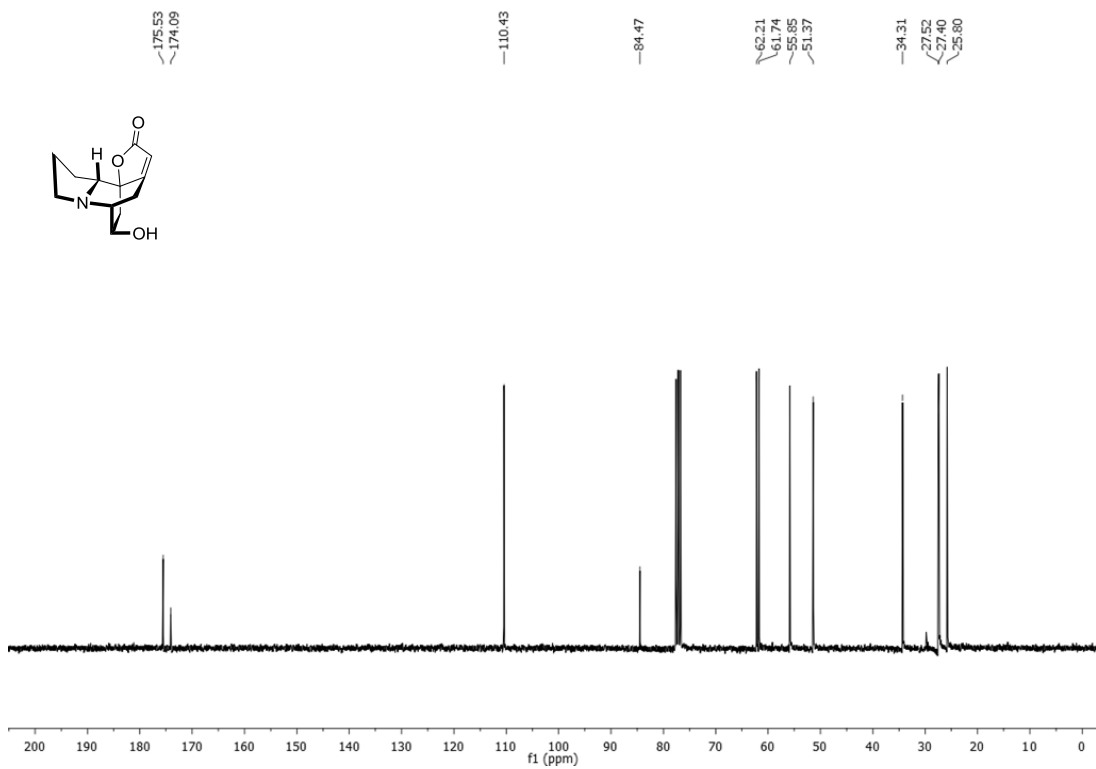
(±)-Virosine B-359**¹H-NMR (CDCl₃) 300 MHz****¹³C NMR (CDCl₃) 75 MHz**

ANNEX II

Compound 361

$^1\text{H-NMR}$ (CDCl_3) 300 MHz

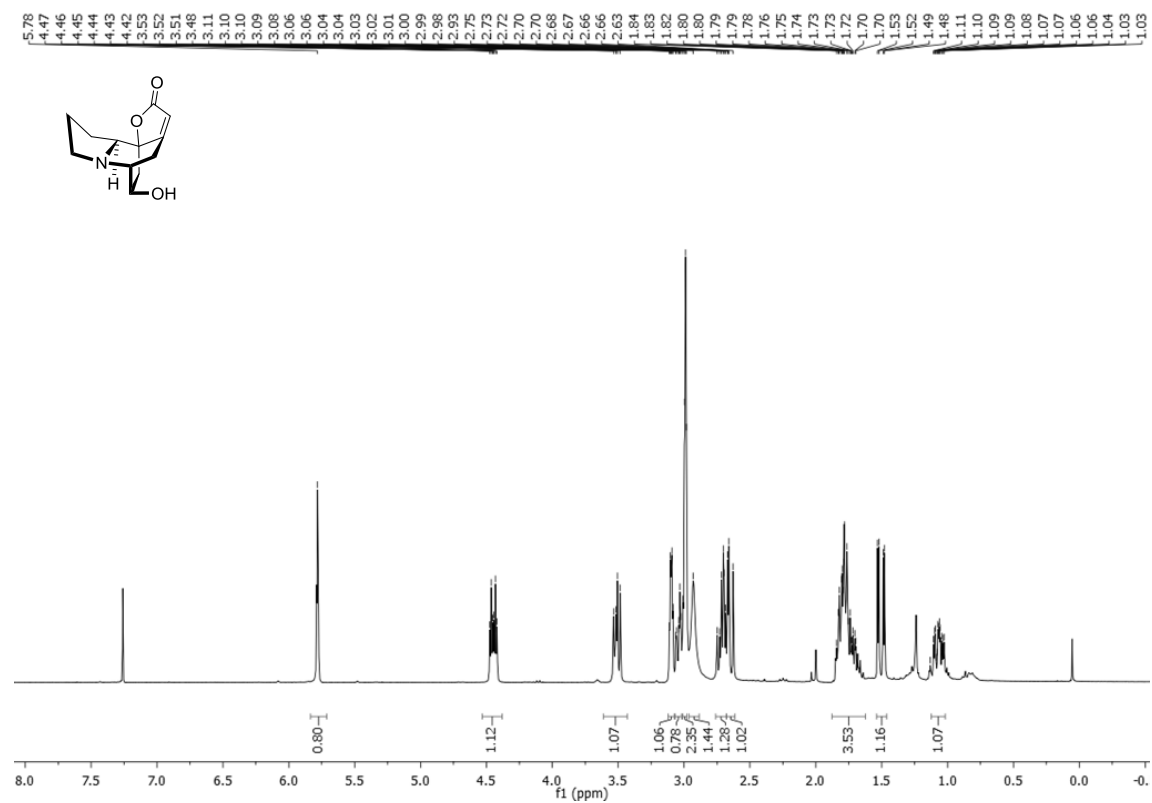


(±)-Niruroidine-272**¹H-NMR (CDCl₃) 300 MHz****¹³C NMR (CDCl₃) 75 MHz**

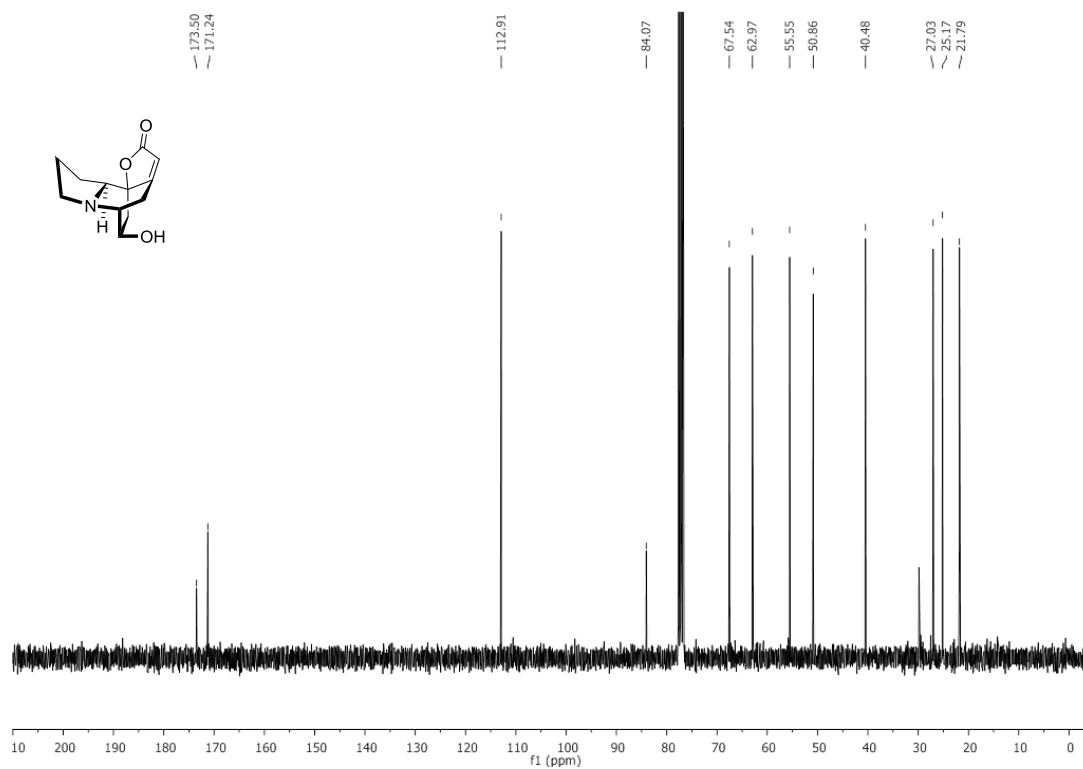
ANNEX II

(±)-Bubbialidine-268

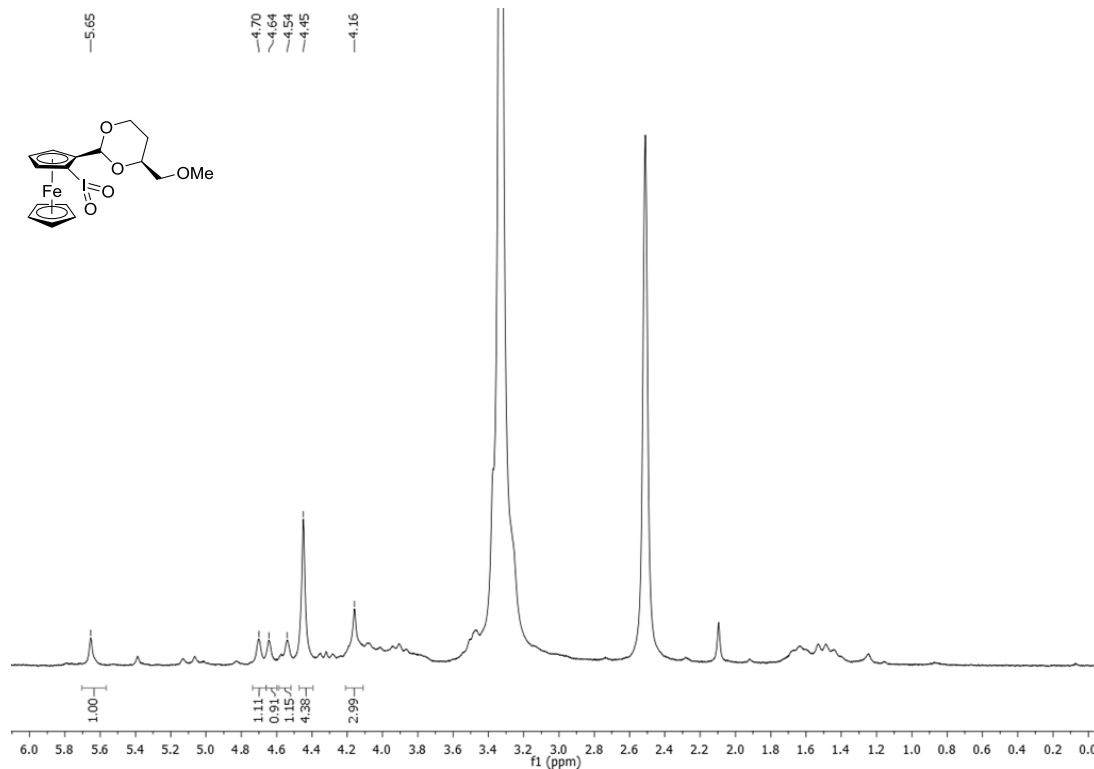
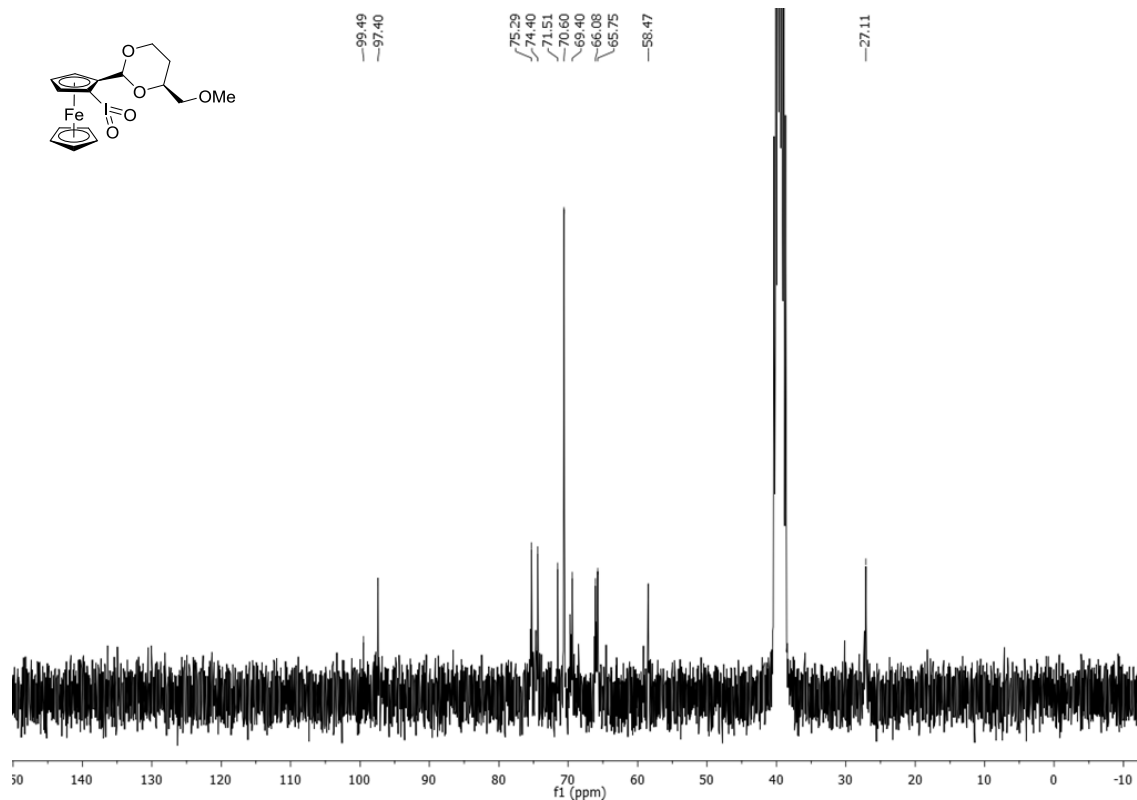
¹H-NMR (CDCl₃) 300 MHz



¹³C NMR (CDCl₃) 75 MHz



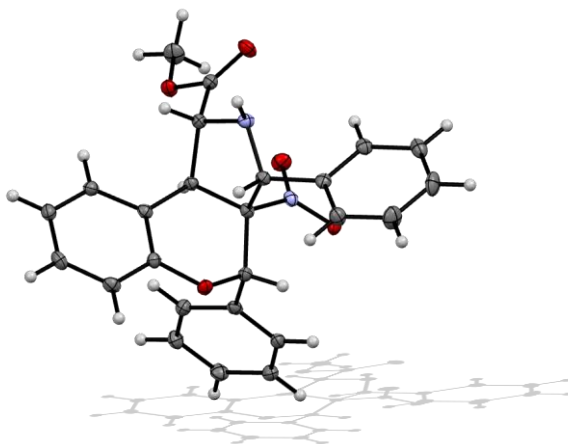
Compound 366

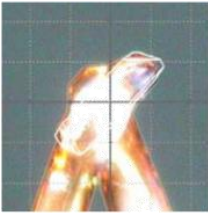
 $^1\text{H-NMR}$ (CDCl_3) 300 MHz $^{13}\text{C-NMR}$ (CDCl_3) 75 MHz

ANNEX III

ANNEX III. X-ray analysis

Compound 130a

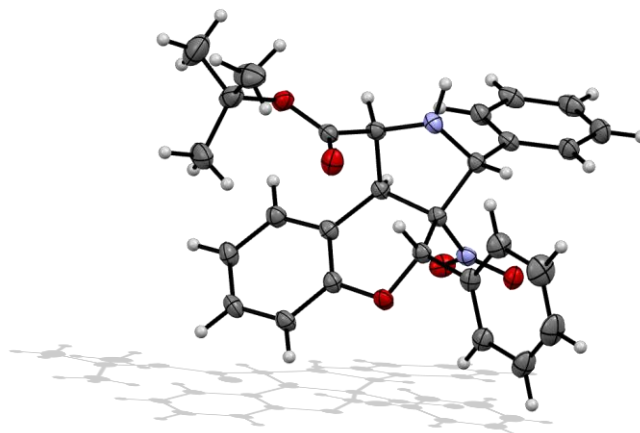


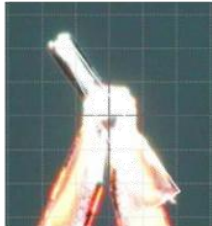
Crystal Data		Data Collection and Refinement	
Formula	C ₂₅ H ₂₂ N ₂ O ₅	Diffractometer	Agilent SuperNova Cu
Formula Weight	430.44	Detector	CCD (Atlas)
Crystal System	monoclinic	Temperature (K)	100(1)°
Space group	P2 ₁ /c (No.14)	λ (CuK α) (Å)	1.54184
a (Å)	8.41448(10)	Monochromator	Óptica multicapa
b (Å)	10.47899(13)	Collimator (mm)	0.2
c (Å)	22.7029(3)	Scan mode	Rotación ω
α (°)	90	Scan width (°)	1.0
β (°)	90.8727(12)	Time per frame (s) (Total, h)	1.5;6 (4)
γ (°)	90	Interval of θ (°)	3.92, 72.50
V (Å ³)	2001.60(4)	(hkl) minimum	(-10 -12 -28)
Z	4	(hkl) maximum	(10 12 22)
D _x (g·cm ⁻³)	1.428	Reflections measures	19033
μ (CuK α) (mm ⁻¹)	0.825	Reflections independent (R_{int})	3965(0.036)
F (000)	904	Reflections observed [$I > 2\sigma(I)$]	3477
Morphology	Prism	Absorption correction	Analytical
Colour	colourless	Solution	OLEX2
Size (mm)	0.08x0.13x0.32	Refinement	SHELXL97(ver.2014)
		Number of parameters	294
		Number of restrictions	0
		Δ/σ maximum	0.000
		Δ/σ medium	0.000
		$\Delta\rho$ maximum (eÅ ⁻³)	0.300
		$\Delta\rho$ minimum (eÅ ⁻³)	-0.251
		S (GOF)	1.039
		Secondary extinction coefficient ^[b]	0
		R(F) ($I > 2\sigma_I$, all)	0.0349, 0.0409
		$R_w(F^2)^{[a]}$ ($I > 2\sigma_I$, all)	0.0843, 0.0890

[a] Esquema de pesado: $1/[\sigma^2(F_o^2) + (0.0395P)^2 + 0.9565P]$ donde $P = [\text{Max}(F_o^2, 0) + 2F_c^2]/3$.

[b] Expresión de extinción secundaria tipo SHELXL: $F_c^* = kF_c[1 + 0.001F_c^2/\lambda^3/\text{sen}(2\theta)]^{-1/4}$

Compound 130'b



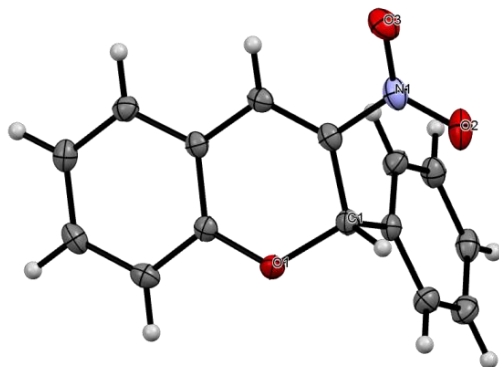
Crystal Data		Data Collection and Refinement	
Formula	C28 H28 N2 O5	Diffractometer	Agilent SuperNova Cu
Formula Weight	472.52	Detector	CCD (Atlas)
Crystal System	Hexagonal	Temperature (K)	100(1)°
Space group	P65 (No.170)	λ (CuK α) (Å)	1.54184
a (Å)	21.1638(4)	Monochromator	Óptica multicapa
b (Å)	21.1638(4)	Collimator (mm)	0.2
c (Å)	9.94418(16)	Scan mode	Rotación ω
α (°)	90	Scan width (°)	1.0
β (°)	90	Time per frame (s) (Total, h)	1.5;6 (4)
γ (°)	120	Interval of θ (°)	4.2, 75.0
V (Å ³)	3857.33(18)	(hkl) minimum	(−25 −26−12)
Z	6	(hkl) maximum	(26 26 12)
D _x (g·cm ^{−3})	1.220	Reflections measures	39648
μ (CuK α) (mm ^{−1})	0.685	Reflections independent (R _{int})	5302(0.081)
F (000)	1500	Reflections observed [$I > 2\sigma(I)$]	4879
Morphology	Plate	Absorption correction	Analytical
Colour	colourless	Solution	OLEX2
Size (mm)	0.05x 0.12x 0.58	Refinement	SHELXL97
		Number of parameters	322
		Number of restrictions	1
		Δ/σ maximum	0.000
		Δ/σ medium	0.000
		$\Delta\rho$ maximum (eÅ ^{−3})	0.468
		$\Delta\rho$ minimum (eÅ ^{−3})	−0.250
Friedel coverage	100%	S (GOF)	1.0609
Flack x	0.01(16)	Secondary extinction coefficient ^[b]	0
Hooft y	0.01(11)	R(F) ($I > 2\sigma_I$, all)	0.0402, 0.0452
P2(wrong)	<10 ^{−18}	R _w (F ²) ^[a] ($I > 2\sigma_I$, all)	0.1002, 0.1034

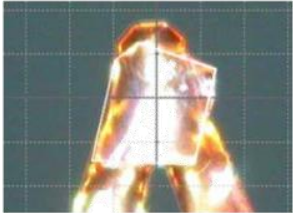
[a] Esquema de pesado: $1/[\sigma^2(F_o^2) + (0.0532P)^2 + 0.5092P]$ donde $P = [\text{Max}(F_o^2, 0) + 2F_c^2]/3$.

[b] Expresión de extinción secundaria tipo SHELXL: $F_c^* = kF_c[1 + 0.001F_c^2/\lambda^3/\sin(2\theta)]^{-1/4}$

ANNEX III

Compound S-129



Crystal Data		Data Collection and Refinement	
Formula	C ₁₅ H ₁₁ N O ₃	Diffractometer	Agilent SuperNova Cu
Formula Weight	253.25	Detector	CCD (Atlas)
Crystal System	Orthorhombic	Temperature (K)	100(1)°
Space group	P2 ₁ 2 ₁ 2 ₁ (No. 19)	λ (CuK α) (Å)	1.54184
a (Å)	5.6901(2)	Monochromator	Óptica multicapa
b (Å)	14.3092(3)	Collimator (mm)	0.2
c (Å)	14.6264(3)	Scan mode	Rotación ω
α (°)	90	Scan width (°)	1.0
β (°)	90	Time per frame (s) (Total, h)	1.5; 6 (4)
γ (°)	90	Interval of θ (°)	4.3, 68.9
V (Å ³)	1190.89(5)	(hkl) minimum	(-6 -17 -17)
Z	4	(hkl) maximum	(6 17 15)
D _x (g·cm ⁻³)	1.413	Reflections measures	13561
μ (CuK α) (mm ⁻¹)	0.820	Reflections independent (R_{int})	2213(0.040)
F (000)	528	Reflections observed [$I > 2\sigma(I)$]	2065
Morphology	Plate	Absorption correction	Analytical
Colour	yellow	Solution	OLEX2
Size (mm)	0.04 x 0.23 x 0.29	Refinement	SHELXL97
		Number of parameters	172
		Number of restrictions	0
		Δ/σ maximum	0.000
		Δ/σ medium	0.000
		$\Delta\rho$ maximum (eÅ ⁻³)	0.135
		$\Delta\rho$ minimum (eÅ ⁻³)	-0.205
Friedel coverage		S (GOF)	1.039
Flack x		Secondary extinction coefficient ^[b]	0
Hooft y		R(F) ($I > 2\sigma_i$, all)	0.0305, 0.0337
P2(wrong)		$R_w(F^2)^{[a]}$ ($I > 2\sigma_i$, all)	0.0735, 0.0759

[a] Esquema de pesado: $1/[\sigma^2(F_o^2) + (0.0423P)^2 + 0.1483P]$ donde $P = [\text{Max}(F_o^2, 0) + 2F_c^2]/3$.

[b] Expresión de extinción secundaria tipo SHELXL: $F_c^* = kF_c[1 + 0.001F_c^2/\lambda^3/\text{sen}(2\theta)]^{-1/4}$

